

Divergent Synthesis of Indolo[3,2-*c*]quinolines, Neocryptolepines and Related Tetracyclic Ring-Systems Containing Promising Biological Activities

By

Katja S. Håheim

Thesis submitted in fulfilment of
the requirements for the degree of
PHILOSOPHIAE DOCTOR
(PhD)



Faculty of Science and Technology
Department of Chemistry, Bioscience and Environmental
Technology 2022

University of Stavanger
NO-4036 Stavanger
NORWAY
www.uis.no

©2022. Katja S. Håheim.

ISBN:978-82-8439-108-3.

ISSN:1 8 9 0 - 1 3 8 7

PhD: Thesis UiS No. 656.

Acknowledgements

First and foremost, I would like to express my deepest gratitude to my main supervisor professor Dr. Magne O. Sydnes for his unrelenting support and excellent guidance throughout my PhD work. Despite having a hectic schedule, you never failed to extend your expertise and support whenever necessary. Secondly, I am eternally grateful for all the support and guidance I received from my co-supervisor associate professor Dr. Emil Lindbäck. You were always there to cheer me up and share your great insights into organic chemistry. I am also forever grateful to associate professor Dr. Kåre B. Jørgensen for always being available to answer any queries and discussing chemistry with me at great lengths. Finally, a sincere thanks to professor Dr. Petra Imhof for teaching me about the world of quantum chemistry and molecular dynamics.

Moreover, I would like to thank current and former members of our research group; Ida T. U. Helgeland, I. Caroline Vaaland, Marianne Bore Haar, Dr. Susana E. Duran, Tereza C. S. Evangelista and Vebjørn Eikemo for making all those hours of lab work pass by in an instant. I would also like to thank fellow PhD students Erik G. Dirdal, Daniel Basiry, Nooshin E. Heravi, Ali H. S. Alkaraly, Abdelrahman T. A. Abdelaal, Monika Moren, Menghour Huy, Hiwot M. Tiryue as well as Dr. Sindhu Kancharla and Dr. Sumit Ganguly for contributing to a great working environment and for all the laughs we have shared together.

Special thanks to the members of our technical staff, in particular Xiaoping Zhang for swiftly handling all our chemical orders (and it was a lot!), including Hans Kristian Brekken, Erling Berge Monsen, Liv Margareth Aksland, Lyudmyla Nilsen and Hong Lin for all your hard work maintaining the laboratories and for providing continuous technical support.

I also extend my sincere thanks to our external collaborators: professor Dr. Vicky Avery and her team for running the antiplasmodial and antiproliferative assays of our prepared compounds, professor Jeanette H. Andersen's group for the antimicrobial evaluations, Dr. Eugene Khaskin and his research group for the fruitful collaboration on the ligand project, professor Dr. Petra Imhof and professor Dr. Ljupco Pejov for their help in running various computational analyses which developed into interesting collaborative projects, Dr. Bjarte Holmelid for collecting HRMS data for us, and finally, Dr. Bjarte A. Lund for running X-ray crystallography analyses on several of our compounds.

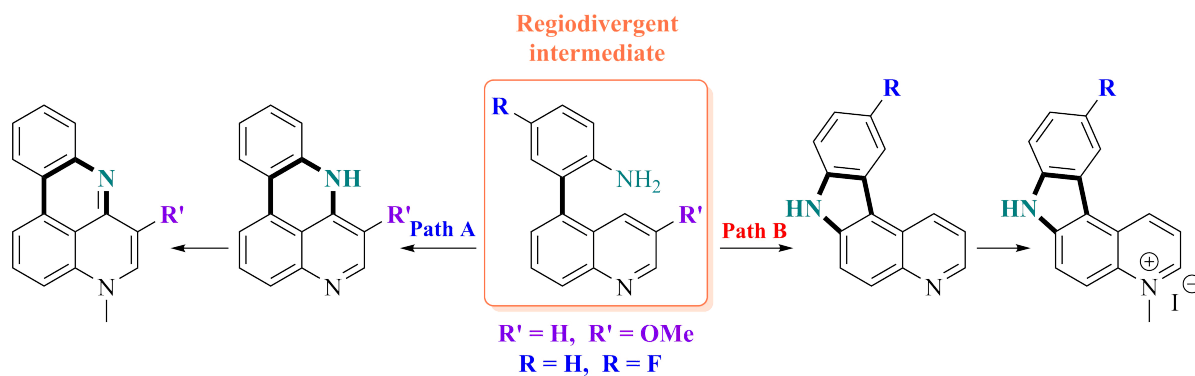
I also want to express my gratitude towards Toppforsk, universitetsfondet and UiS for funding my PhD project. Further, I am thankful for the financial support from both the Norwegian Chemical Society and BioCat, allowing me to attend conferences to expand my knowledge within chemistry. A further thanks to the training received from the BioCat graduate school,

who hosted several useful PhD courses and workshops.

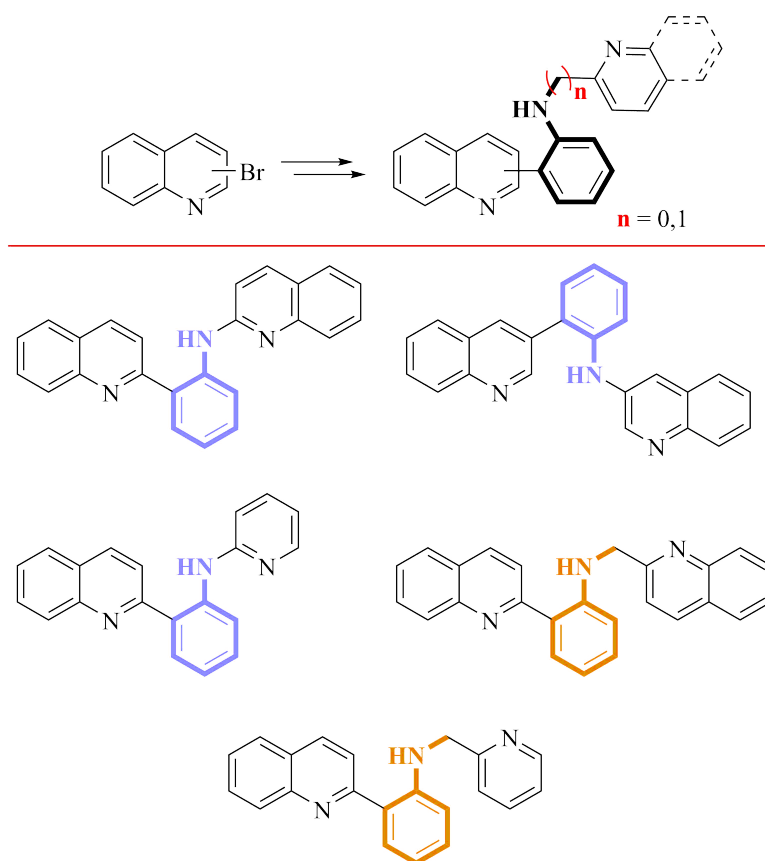
Last but not least, I want to thank my closest friends and family for their continued support during my PhD work. To my best friend, Renate Håland: there are no words which express the magnitude of my appreciation for all the help and encouragement you have shown me in this time. You always believed in me and were always available to listen to me talk extensively about chemistry, despite not even liking the subject. Also, I am forever grateful for your help looking after my cat, Mars, when I was away for conferences. I also want to thank my close friends the Kinden twins, Helge and Håkon, Ådne Tobisen, Kenneth M. Boholm and Elina Alfsvåg for your continued support. Lastly, a special thanks to Dr. Ayman Zakaria and his team for taking a chance on me. This thesis could not be possible without you!

Graphical abstract

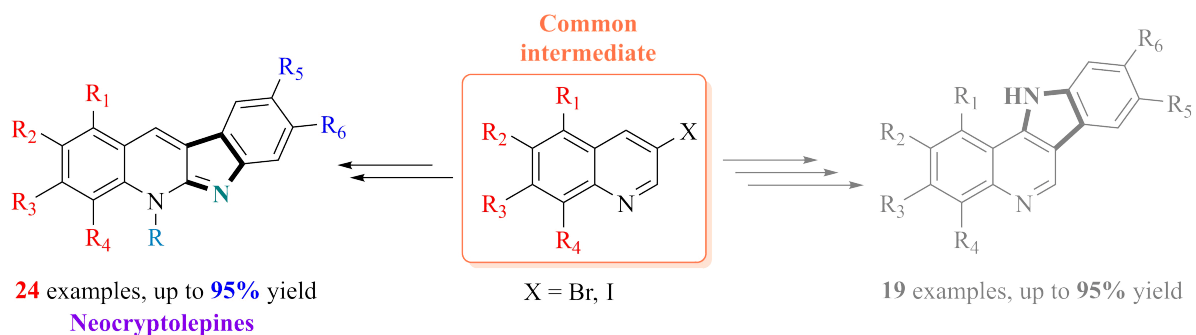
Chapter 2 - Synthesis of isocryptolepine and regioisomers



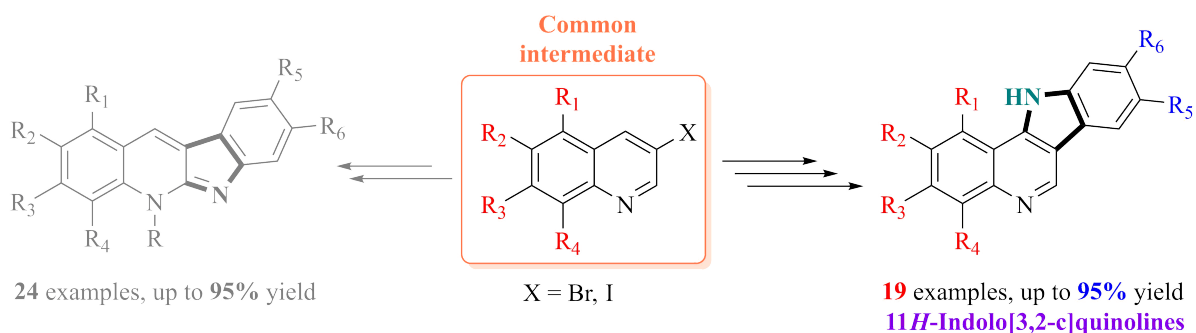
Chapter 3 - Synthesis of quinoline and pyridine N,N,N ligands for catalysis



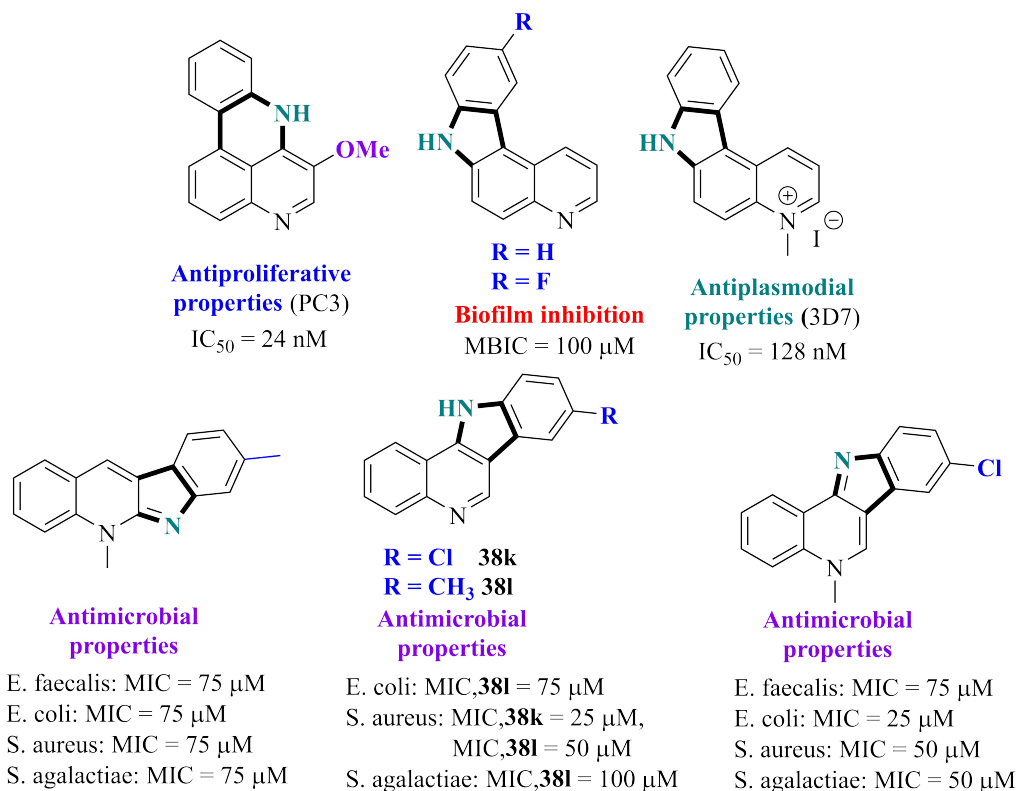
Chapter 4 - Synthesis of neocryptolepines



Chapter 5 - Photochemical synthesis of indoloquinolines



Chapter 6 - Biological evaluation



Abstract

Malaria is a devastating tropical disease, claiming approximately 627 000 lives in 2020. Due to the appearance of resistance towards artemisinin-based therapies, the discovery of novel treatments are of paramount importance. The indoloquinoline natural products cryptolepine, neocryptolepine and isocryptolepine, first discovered in the extracts of the African bush plant *Cryptolepis sanguinolenta*, have been found to exhibit potent antimalarial properties. Moreover, several functionalized derivatives of these compounds have shown great promise as antiplasmodial agents. The indoloquinoline alkaloids have also been found to possess significant antiproliferative and antimicrobial properties, making them ideal targets for the development into novel drug candidates.

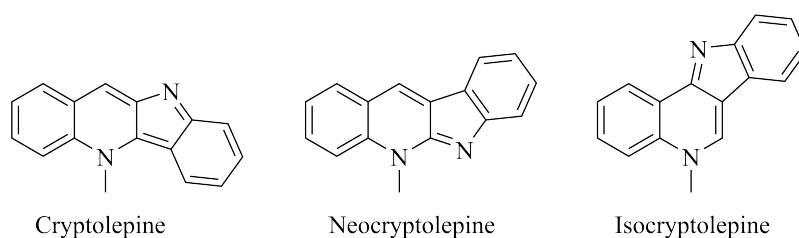
The first project in this work details the application of a synthetic approach first developed by Helgeland and Sydnes to assemble various tetracyclic ring systems. The key synthetic strategies being a Suzuki-Miyaura cross-coupling reaction followed by a palladium-catalyzed intramolecular cyclization. Though the approach was unsuitable to construct all the intended target molecules, it furnished the unexpected pyridophenanthridine scaffold. By further investigating alternative protocols for the construction of indoloquinolines, a regiodivergent intermediate was discovered, which allowed for the synthesis of both novel pyridophenanthridine and pyridocarbazole scaffolds by utilizing two different reaction protocols. By subjecting this common intermediate to a diazotization-azidation-nitrene insertion approach, the novel pyridocarbazoles could be furnished in excellent yields.

The unexpected formation of a biquinoline bridged by an aniline during a Suzuki-Miyaura cross-coupling reaction, was deemed interesting for development into a transition metal complex for catalysis. Through a collaborative effort with Dr. Eugene Khaskin's group at Okinawa Institute of Science and Technology, five quinoline/pyridine N,N,N ligands were designed and synthesized. The key synthetic tools utilized in their construction was either a sequential Suzuki-Miyaura cross-coupling reaction and Buchwald-Hartwig amination or reductive amination.

A novel two-step approach for the synthesis of the natural product neocryptolepine from commercially available bromoquinolines was developed. The key transformations being regioselective *N*-alkylations followed by a cascade Suzuki-Miyaura cross-coupling reaction and intramolecular nucleophilic C-N bond formation. The scope and limitations for the novel protocol was evaluated through the preparation of 24 neocryptolepine derivatives, bearing a diverse range of functional groups, where electron-withdrawing group substitutions were generally superior.

It became apparent that it would also be possible to prepare a library of indolo[3,2-*c*]quinolines from the same starting material as the newly devised strategy to produce neocryptolepines. By utilizing a reaction sequence consisting of a Suzuki-Miyaura cross-coupling reaction, installation of an azido moiety and finally photochemical cyclization, this goal was realized, producing a total of 19 indoloquinolines. This protocol was less robust towards substrate functionalizations than the neocryptolepine approach, with no apparent trend concerning electron-withdrawing and electron-donating groups being apparent. The photochemical cyclization was hypothesized to proceed *via* the formation of a reactive singlet nitrene intermediate.

Finally, a selection of the prepared tetracyclic compounds assembled during this work was evaluated for their antiparasitic, antiproliferative and antimicrobial activities by the help of various external collaborators. The most successful compound was revealed to be the novel pyridophenanthridines, displaying more potent antiproliferative activities than doxorubicin against human prostate cancer ($IC_{50} = 24$ nM). The novel pyridocarbazoles moreover showed excellent inhibition of biofilm formation, with the potential to be developed into a dual anticancer-antimicrobial agent. Of all the tested compounds, only *N*-methylated pyridocarbazole was found to contain any significant activity against the evaluated *Plasmodium falciparum* strain. The antimicrobial assays revealed the importance of the inclusion of a methyl group for activity, but not strictly in the form of an *N*-methyl unit, which is the general consensus in the literature thus far. Further, chlorinated indoloquinolines were revealed to contain excellent antimicrobial activity against both Gram-positive and Gram-negative bacterial cell lines.



Selected abbreviations and acronyms

AMR	Antimicrobial resistance
ACT	Artemisinin-based combination therapy
aq.	Aqueous
IMes	1,3-Bis(2,4,6-trimethylphenyl)-1,3-dihydro-2 <i>H</i> -imidazole-2-ylidene
NBS	<i>N</i> -Bromosuccinimide
COSY	Correlation spectroscopy
DFT	Density functional theory
DCM	Dichloromethane
DME	1,2-Dimethoxyethane
DMF	<i>N,N</i> -Dimethylformamide
DVFC	Dry vacuum flash chromatography
EDG	Electron-donating group
EWG	Electron-withdrawing group
FDA	Food and Drugs Administration
HMBC	Heteronuclear multiple-bond correlation
HSQC	Heteronuclear single-quantum correlation
HRMS	High-resolution mass spectrometry
h	Hour(s)
ISC	Intersystem crossing
LRMS	Low-resolution mass spectrometry
MOF	Metal organic framework
MW	Microwave
MBIC	Minimal biofilm inhibitory concentration
MIC	Minimal inhibitory concentration
min	Minute(s)
MoA	Mode of Action
NMR	Nuclear magnetic resonance
NOESY	Nuclear Overhauser effect

S_NAr	Nucleophilic aromatic substitution
PACT	Photoactivated chemotherapy
PAH	Polycyclic aromatic hydrocarbon
PPA	Polyphosphoric acid
R_f	Retardation factor
sat.	Saturated
THF	Tetrahydrofuran
TLC	Thin-layer chromatography
TLC-LRMS	Thin-layer chromatography-low-resolution mass spectrometry
TFT	α,α,α -Trifluorotoluene
WHO	World Health Organization

Science disseminations

Publications

1. Håheim, K. S.; Lindbäck, E.; Helgeland, I. T. U.; Sydnes, M. O. Mapping the reactivity of the quinoline ring-system - Synthesis of the tetracyclic ring-system of isocryptolepine and regioisomers, *Tetrahedron* **2019**, *75*, 2924-2957.
2. Håheim, K. S.; Lindbäck, E.; Tan, K. N.; Albrigtsen, M.; Helgeland, I. T. U.; Lauga, C.; Matringe, T.; Kennedy, E. K.; Andersen, J. H.; Avery, V. M.; Sydnes, M. O. Synthesis and evaluation of the tetracyclic ring-system of isocryptolepine and regioisomers for antimalarial, antiproliferative and antimicrobial activities, *Molecules* **2021**, *26*, 3268-3290.

Popular science publication

1. Håheim, K. S. The history of malaria and its treatments, *Kjemi* **2020**, *5*, 13-22.

Presentations

1. Håheim, K. S. Synthesis of the tetracyclic ring-system of isocryptolepine and regioisomers - mapping the reactivity of the quinoline ring-system, BioCat conference, Hurdalssjøen, 2019.

Poster and blitz presentation.

2. Håheim, K. S. Synthesis of isocryptolepine and regioisomers, Norwegian Organic Chemistry Winter meeting, Skeikampen, 2020. **Oral presentation.**
3. Håheim, K. S. Synthesis of isocryptolepine and regioisomers, Department PhD presentations, University of Stavanger, 2020. **Oral presentation.**

Contents

1	Introduction	1
1.1	Malaria	2
1.1.1	Antimalarial drugs and emerging resistance	3
1.1.2	The future of antimalarial therapies	7
1.2	Alkaloids as therapeutic agents	8
1.2.1	Alkaloids isolated from <i>Cryptolepis sanguinolenta</i>	9
1.3	Repurposing antimalarial drugs for treating cancer and bacterial infections . . .	11
1.3.1	Cancer	11
1.3.2	Bacterial infections and antibiotic resistance	13
1.4	Project aims	15
2	Synthesis of isocryptolepine and regioisomers	16
2.1	Introduction	17
2.1.1	Synthesis of isocryptolepine in recent literature	17
2.1.2	Synthesis of pyridocarbazoles and pyridophenanthridines in recent literature	19
2.1.3	Project aims	21
2.2	Synthesis of isocryptolepine (25) and regioisomers	22
2.2.1	Introduction	22
2.2.2	Suzuki-Miyaura cross-coupling reactions to give biaryls	24
2.2.3	MW-assisted intramolecular cyclizations to give tetracycles	26
2.3	Divergent synthesis of pyridophenanthridines 54 and pyridocarbazoles 61 . . .	32
2.4	<i>N</i> -Methylations of tetracyclic compounds	36
2.5	Summary and concluding remarks	37
3	Synthesis of quinoline and pyridine N,N,N ligands for catalysis	39
3.1	Introduction	40
3.1.1	Design of biquinoline ligands for catalysis	40
3.1.2	Potential applications	42
3.1.3	Project aims	43
3.2	Synthesis of the quinoline/pyridine N,N,N ligands	44

3.2.1	Synthesis of quinoline/pyridine N,N,N ligands with an aniline bridge	44
3.2.2	Synthesis of quinoline/pyridine N,N,N ligands with an <i>N</i> -methylaniline bridge	49
3.3	Summary and concluding remarks	52
4	Synthesis of neocryptolepines using a novel cascade protocol	54
4.1	Introduction	55
4.1.1	Synthesis of neocryptolepine in recent literature	55
4.1.2	Project aims	58
4.2	Development of a novel synthetic strategy	59
4.2.1	Investigation of substrate scope	61
4.3	Summary and concluding remarks	74
5	Photochemical synthesis of indoloquinolines 38	76
5.1	Introduction	77
5.1.1	Photochemical synthesis of indolo[3,2- <i>c</i>]quinolines 38	77
5.1.2	Chemistry of nitrenes and the photoexcited state	78
5.1.3	Project aims	83
5.2	Development of a novel photochemical approach	84
5.2.1	Investigation of substrate scope	89
5.3	Summary and concluding remarks	105
6	Biological evaluation	107
6.1	Introduction	108
6.2	Antimalarial assay	108
6.3	Antiproliferative assay	110
6.4	Antimicrobial assay	112
6.4.1	Compounds described in Chapter 2	112
6.4.2	Compounds described in Chapter 4	113
6.4.3	Compounds described in Chapter 5	115
6.4.4	Issues with solubility	117
6.5	Summary and concluding remarks	118
6.5.1	Future work	119
7	Experimental	121
7.1	General	122
7.2	Methods	125
7.2.1	Masuda Borylation reactions	125
7.2.2	Synthesis of quinolines	131
7.2.3	Suzuki-Miyaura cross-coupling reactions	134

7.2.4	Diazotization-Azidation	155
7.2.5	Cyclization to form tetracyclic compounds	169
7.2.6	<i>N</i> -Methylations to obtain ringsystems	189
7.2.7	<i>N</i> -Alkylation to obtain pyridinium and quinolinium halides	193
7.2.8	Cascade Suzuki-Miyaura cross coupling and cyclization reactions . . .	202
7.2.9	Buchwald-Hartwig aminations	220
7.2.10	Reductive aminations	222

Chapter 1

Introduction

1.1 Malaria

Malaria is a parasitic blood disease caused by protozoans of the *Plasmodium* genus, with five known strains capable of infecting humans: *P. falciparum*, *P. vivax*, *P. ovale*, *P. malariae* and *P. knowlesi*.^[1-3] There is a wide variety in severity between strains and nearly all malaria-related deaths are caused by infections with *P. falciparum*.^[1] Through considerable global efforts, the number of cases of malaria and accompanying deaths have been steadily declining in the period 2000-2019, however, following the COVID-19 pandemic, a rise in both have been observed (Figure 1.1). Data from the World Health Organization (WHO) estimates the number of malaria cases in 2020 to be 241 million (up 6% from 2019), with 627 000 reported deaths (up 12% from 2019).^[2] The findings from WHO were that the service disruptions during the COVID-19 pandemic were likely responsible for the majority of the observed increases, however, progress in malaria control had begun to stall prior to the emergence of the pandemic^[4] and further, part of the achieved progress has been partially reverted. Resultingly, infection by malaria still poses a serious global health threat, which is exacerbated by the fact that over 90% of all cases occur in the sub-Saharan Africa, home to some of the worlds poorest populations.^[5]

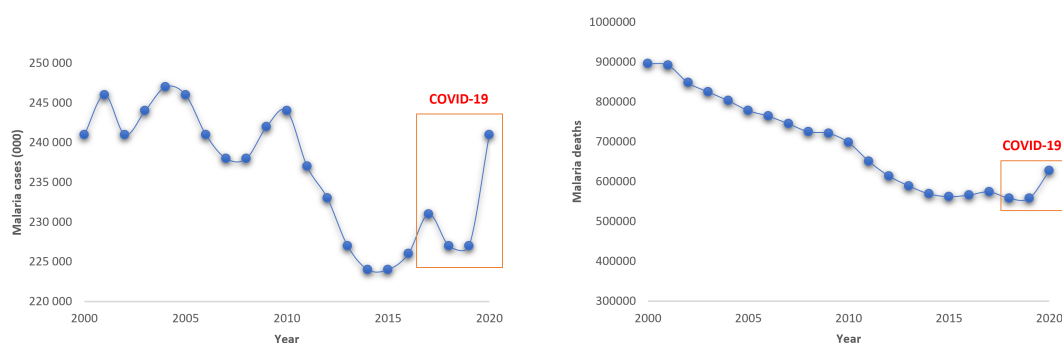


Figure 1.1: Left: Number of malaria cases (in millions) from the year 2000-2020. Right: Number of malaria deaths from the year 2000-2020.^[2]

One of the major aspects contributing to making malaria a major public health concern, is its exceptionally complex life cycle compared to other parasitic species. Due to the complicated nature of the life cycle, only a brief summary will be presented (see Figure 1.2 for a simplified illustration). The life cycle begins by an infected *Anopheles* mosquito delivering the parasitic sporozites to a human through a bite **1**. Then, the sporozites enter the liver where they multiply, a term known as exoerythrocytic shizogony of the liver **2**. The sporozites then form meorozites, which upon bursting spreads the disease into the blood stream **3**. The meorozites multiply in the red blood cells and make gametocytes through a sexual stage, which are taken up by the mosquito **4**. Finally, the cycle is completed by the gametocytes maturing into gamates within the mosquito, eventually forming sporozites, which migrates into the saliva of the insect **5**.^[6,7]

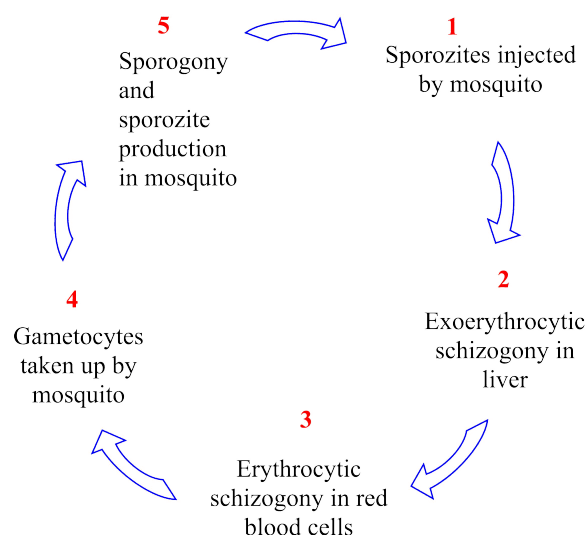


Figure 1.2: The life cycle of the malaria parasite.^[6]

As the mosquitoes thrive in tropical climates, malaria is endemic to the tropical latitudes surrounding the equator. The sporogonic stage (stage **5** in Figure 1.2), or the incubation period, requires sufficiently high temperatures as well as humidity to proceed, explaining the absence of malaria outside tropics.^[8] Being a highly climate sensitive disease, it is feared that the continuing rise in surface air temperatures brought on by climate change will expand the reach of the disease into the currently temperate regions of the world and thus extent the burden onto a larger part of the human population.^[9] Despite being eradicated from Europe in the second half of the 20th century,^[10] several climate models predict favorable conditions for the reintroduction of the disease in the near future.^[11,12]

1.1.1 Antimalarial drugs and emerging resistance

The quinolines

The three major drug classes used to treat malaria clinically today are the quinolines, antifolates and artemisinins.^[13] The first known chemical treatment for malaria belongs to the quinolines, namely the natural product quinine (**1**) (Figure 1.3), which was first isolated from the bark of the cinchona tree in 1820 by Pierre Joseph Pelletier and Joseph Caventhou.^[14] Quinine (**1**) remained the most effective way to treat malaria until it was outclassed by several semi-synthetic derivatives in the 1920s, including the semi-synthetic derivative of quinine (**1**), chloroquine (**2**). Moreover, due to overuse, several parasitic strains had begun to develop resistance against the drug, resulting in quinine (**1**) no longer being recommended for treating malaria.^[15]

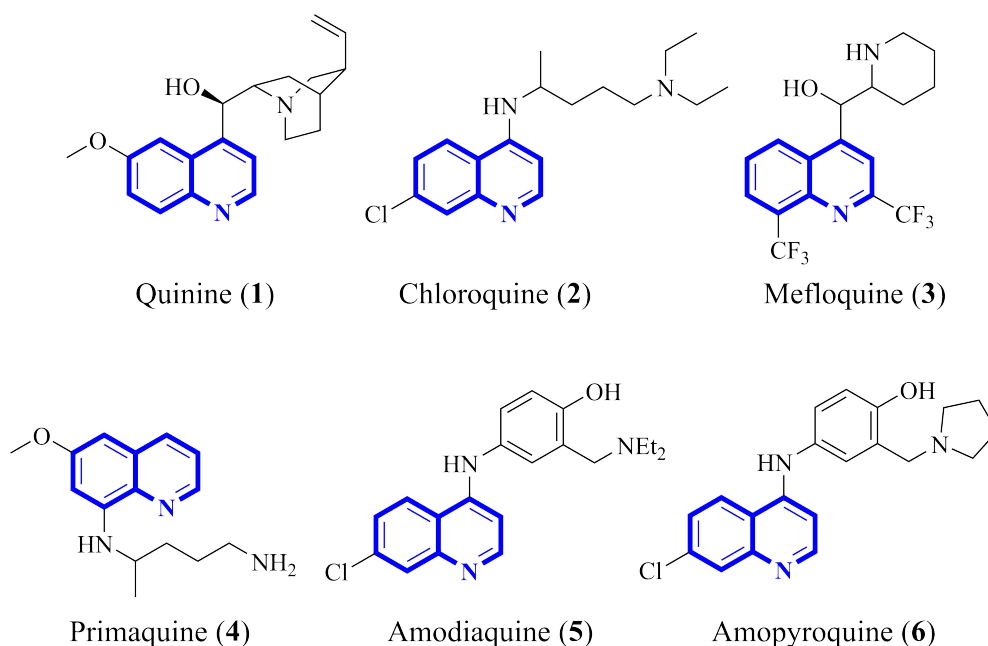


Figure 1.3: The structures of the quinoline-based antimalarials quinine (1), chloroquine (2), mefloquine (3), primaquine (4), amodiaquine (5) and amopyroquine (6).

Soon after its first discovery and development, the semi-synthetic compound chloroquine (2) (Figure 1.3) became the most effective and cheapest treatment available for malaria.^[16] This once successful drug fell victim to the same fate as quinine (1) and the first reports of chloroquine-based resistance surfaced in the 1960s and in the past 60 years, resistant strains of *P. falciparum* has spread to nearly all endemic regions.^[14] Due to the success of quinine (1) and then later chloroquine (2), several quinoline-based antimalarial drugs were subsequently developed, such as mefloquine (3), primaquine (4), amodiaquine (5) and amopyroquine (6) (Figure 1.3) which *P. falciparum* have developed resistance towards.^[2] Moreover, despite the early success of the quinoline antimalarials prior to the emergence and spread of resistance, little is known about their modes of action (MoA) against the parasites.^[14] Contrary to this, the MoA of chloroquine (2) is well understood and the compound acts by inhibiting the hemozoin biocrystallization process of the parasitic life cycle. The formation of hemozoin occurs during both the blood and sexual stages of the life cycle and is an essential process for the parasites survival, and inhibition of these processes swiftly kills it.^[17]

The antifolates

In contrast to the quinoline antimalarials, the antifolates MoA is well understood and acts by inhibiting folate biosynthesis during the blood and sexual stages of the parasites life cycle, which are essential parts of the parasitic DNA synthesis.^[18] The first known antimalarial antifolate agent is proguanil (7) (Figure 1.4), which was discovered during the Second World War. The compound was found to be more potent than quinine (1) against certain strains of the parasite and studies later revealed proguanil (7) to be a prodrug, which is metabolized to the correspond-

ing triazine, cycloguanil (**8**).^[18] This active metabolite then acts by inhibiting a key enzyme in the folate biosynthesis pathway, namely dihydrofolate reductase (DHFR). Antifolates are often used in combination, as is the case with the two antifolates sulfadoxine (**9**) and pyrimethamine (**10**), which are sold under the trade name Metakelfin[®] (Figure 1.4). This combination therapy has been the drug of choice to combat malaria throughout Africa and is still employed in certain parts of western Africa today,^[18] despite the appearance of resistance in the 1980s.^[19] Unfortunately, the whole antifolate drug class has proven to be highly susceptible to resistance, caused by point mutations in two of the key enzymes in the antifolate biosynthesis pathway. This, in addition to high prescription rates, has resulted in resistance to these compounds being common worldwide.^[20]

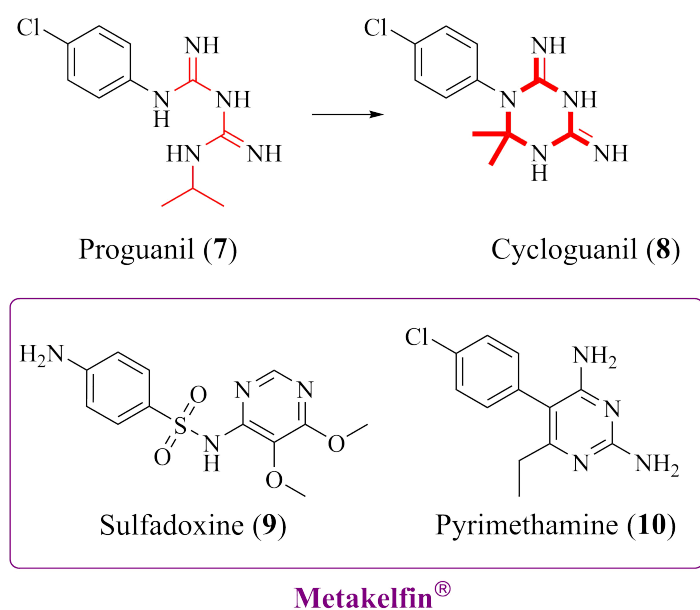


Figure 1.4: The antifolate antimalarials proguanil (**7**) sulfadoxine (**9**) and pyrimethamine (**10**). Top: Proguanil (**7**) is metabolized in the body to cycloguanil (**8**), which is the active metabolite; Bottom: A combination of sulfadoxine (**9**) and pyrimethamine (**10**) is sold as a drug under the name Metakelfin[®].^[18]

The artemisinins and the use of artemisinin-based combination therapy (ACT)

First isolated from the wormwood plant *Artemisia annua* by Tu Youyou in 1971, the natural product artemisinin (**11**) was discovered to exhibit antimalarial properties.^[15] Artemisinin (**11**) is a structurally unique compound and is part of the sesquiterpene lactone class, containing a highly unusual endoperoxide trioxane unit (Figure 1.5). Since its discovery and subsequent introduction as an antimalarial drug, artemisinin (**11**) is believed to be responsible for saving millions of lives from malaria. As a consequence, Youyou was awarded the 2015 Nobel Prize in Medicine and in the announcement of the award, the discovery of artemisinin (**11**) was cited as one of the most monumental advances in modern medicinal chemistry.^[21,22] Following the success of artemisinin (**11**), several synthetic derivatives have been prepared in order to address

and improve a major drawback with artemisinin (**11**); its poor water and oil solubility and thus not able to be administered orally.^[23] Some synthetic derivatives that have been found to be effective against malaria include dihydroartemisinin (**12**), arthemether (**13**), artheether (**14**), artemisone (**15**) and artesunate (**16**).^[24] The MoA of the artemisinins is not yet fully understood, it has however been firmly established that the endoperoxide trioxane is the active pharmacophore, responsible for the compounds biological activities. Recent work by Tilley and coworkers suggests that dihydroartemisinin (**12**), which is the active metabolite of artemisinin (**11**), acts by carrying out a two-pronged attack; firstly by causing protein damage and secondly by compromising the parasite proteasome function, eventually killing the parasites.^[25]

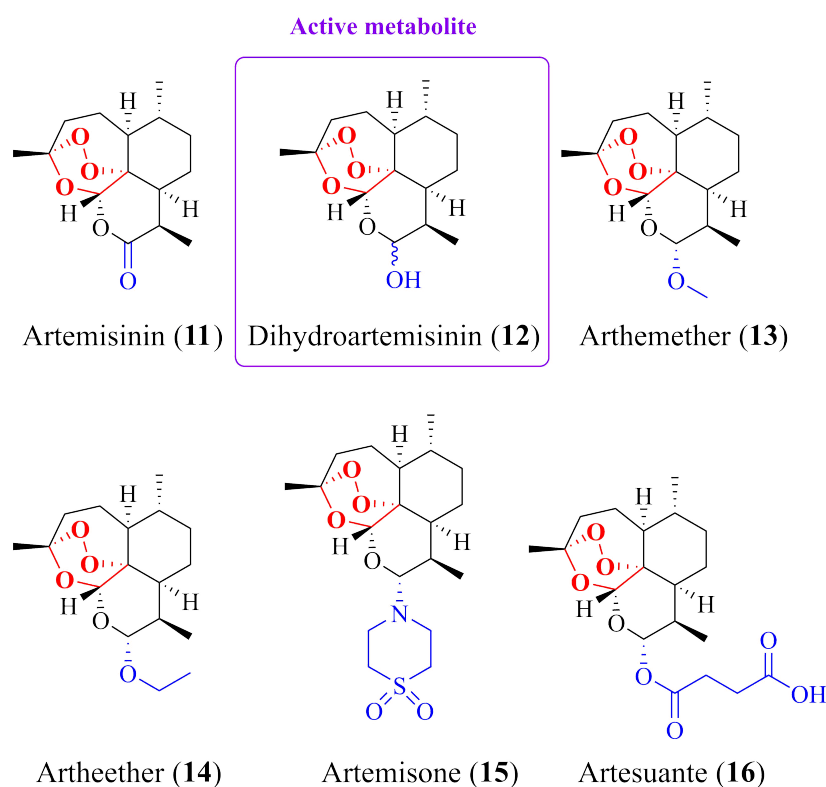


Figure 1.5: Artemisinin (**11**) and some of its synthetic derivatives; dihydroartemisinin (**12**), arthemether (**13**), artheether (**14**), arthemisone (**15**) and artesunate (**16**).

Today, the artemisinins are perhaps the most important drug class which are currently used clinically to treat malaria. The use of artemisinin-based combination therapies (ACTs) represents the gold standard of malaria treatments, where an artemisinin is combined with another antimalarial drug to obtain increased drug efficacy. Additionally, by using drugs in combination, the probability that the parasites will become resistant to two drugs with different MoA will be exponentially reduced.^[26] Some frequently used ACTs consists of dihydroartemisinin (**12**) and piperaquine (**17**), as well as arthemether (**13**) and lumefantrine (**18**) (Figures 1.5 and 1.6).^[2]

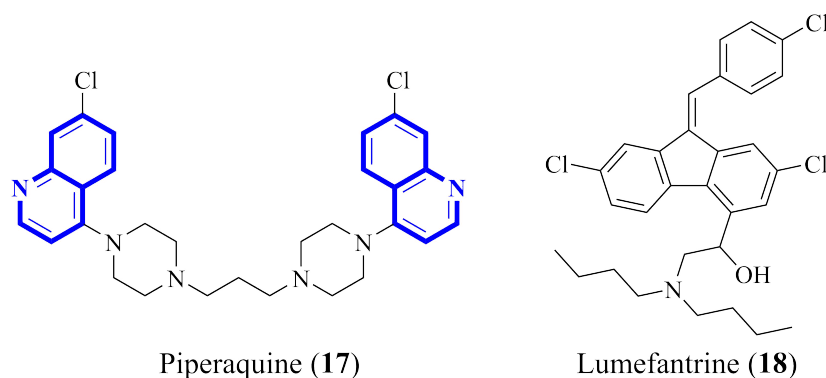


Figure 1.6: Piperaquine (17) and lumefantrine (18), drugs commonly used in combination therapies.

The first reports of artemisinin (11) resistance surfaced in Cambodia in 2008^[27] and in the following ten years, 30 more cases has been documented throughout Southeast Asia.^[28] More ominously, resistance to artemisinin (11) is now being documented in the sub-Saharan Africa, countries already bearing the heaviest malaria burden globally.^[5,29–34] Moreover, due to poor health care infrastructure and economies, these countries are ill-equipped to handle the coming influx of artemisinin (11) resistant parasites. It is believed that if the resistance has not already spread to the entire sub-Saharan region, it is only a matter of time before it reaches every corner of the continent.^[4,35] As a consequence, the discovery of new lead compounds to fight the disease has never been more urgent.

1.1.2 The future of antimalarial therapies

The major obstacle in the global eradication of malaria is resistance to antimalarial drugs and most of the current research into malaria is oriented towards overcoming this challenge.^[36] Complicating such efforts is the complex life cycle of the malaria parasite, making effective treatments particularly difficult to discover.^[6,7] Structural modifications of known malarial drugs has been a common strategy for the development of novel treatments, however, various other strategies are currently under investigation. During the last decades, the pharmaceutical industry has spent considerable efforts on gaining insight into the metabolic and biochemical pathways of the parasites in order to formulate new drugs. This way, the drugs can act as inhibitors of a given metabolic pathway. Some of the biochemical processes currently being investigated include targeting the food vacuole, glycolysis, the fatty acid biosynthesis, NADPH dehydrogenase, inhibition of protease and inhibition of membrane biosynthesis.^[36] Another avenue which has been extensively researched is the possibility of formulating a vaccine against malaria. After spending 30 years in development, the RTS,S vaccine was the first malaria vaccine to show promising results when tested on African children infected with *P. falciparum*. Despite the promising preliminary data obtained in the preclinical trials, the efficacy of the RTS,S vaccine was found to be only 35%.^[37] In 2019, a Phase IV Expanded Programme on

Immunization (EPI)-linked malaria vaccine was underway in Ghana, Kenya and Malawi,^[38] which was unfortunately derailed by the appearance of the COVID-19 pandemic. This resulted in the neglect of malaria control in favor of COVID-19, which has been a catastrophic setback in the global eradication of malaria.^[39]

1.2 Alkaloids as therapeutic agents

Alkaloids are nitrogen-containing compounds and are found in many natural products. Typically derived from plants, but also found in animals and certain microorganisms, natural alkaloids are known for containing a wide array of pharmacological activities, such as anticancer, anti-inflammatory, immunoregulatory,^[40] antibacterial, antiviral, insecticidal, hypoglycemic and antimalarial.^[41] Approximately 40% of all Food and Drugs Administration (FDA) approved drugs were of natural origins as of 2020,^[42] roughly 60 of which belong to the alkaloid sub-class.^[43] Two well known medicinal alkaloids are morphine (**19**) and its prodrug codeine (**20**) (Figure 1.7), widely utilized to induce analgesia, *ie* to treat pain, by interacting directly with the central nervous system. These alkaloids were first isolated from the opium poppy *Papaver somniferum* and references to the poppy plant dates back as far as 6000 BCE.^[44]

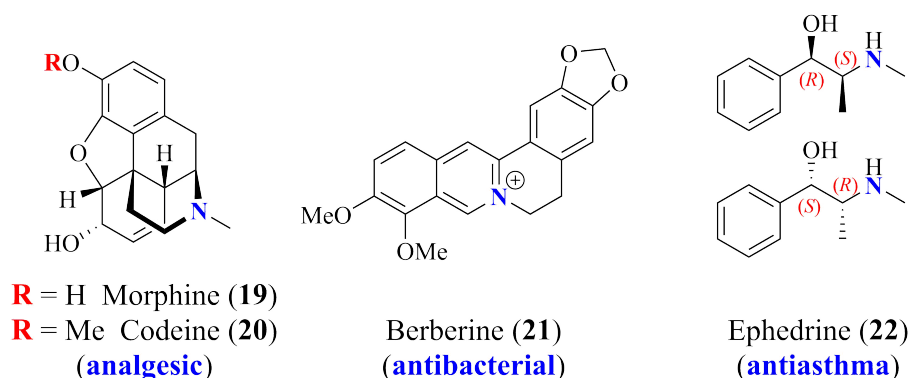


Figure 1.7: Selected examples of naturally occurring alkaloids; morphine (**19**), codeine (**20**), berberine (**21**) and ephedrine (**22**).

The quaternary isoquinolinium alkaloid berberine (**21**) (Figure 1.7) has been widely used as an antibacterial agent and can be found in the root extracts of several medicinal plants, including *Hydrastis canadensis* and *Berberis aristata*. In addition to possessing potent antibacterial properties, berberine (**21**) has also been found to inhibit cell proliferation, making it an ideal target for development of anticancer treatments.^[45] Another natural alkaloid bearing structural similarity to amphetamine, is ephedrine (**22**) (Figure 1.7), typically utilized to treat hypotension, nasal congestion and asthma. Ephedrine (**22**) is one of the oldest medicinal herbs known to mankind and originates from the Chinese plant *Ephedra sinica*.^[46] The alkaloid which is most related to the work conducted in this thesis, however, is the antimalarial compound quinine (**1**),

previously discussed in Section 1.1.1. In the proceeding section, other alkaloids possessing antimalarial properties will be examined.

1.2.1 Alkaloids isolated from *Cryptolepis sanguinolenta*

The West African climbing shrub *Cryptolepis sanguinolenta* has been an essential plant in African traditional medicine. Its water extracts have historically been used to treat malaria along with a variety of other diseases.^[47] The major bioactive component of the extracts was determined to be cryptolepine (**23**) (Figure 1.8) following its isolation and structural elucidation by Gellért and coworkers in 1951.^[48] Cryptolepine (**23**) is a part of the indoloquinoline alkaloids, which are a rare and unique class of *N*-heterocycles composed of a fusion between a quinoline and an indole moiety. The indoloquinolines typically displays planar topology and are further known to exhibit weakly basic properties, with the pK_a of the protonated form of cryptolepine (**23**) estimated to be 11.0 using ^1H NMR spectroscopy.^[49] Cryptolepine (**23**) has received a lot of attention in the literature as a consequence of its numerous biological activities, including antiplasmodial, antimalarial,^[50–55] anti-inflammatory,^[53] antifungal,^[56–58] antimicrobial,^[59–62] antiproliferative,^[63–66] and antiviral.^[60] Cryptolepine (**23**) has also been found to possess high levels of cytotoxicity, impeding its use as a therapeutic agent, likely as a consequence of its linear, planar geometry, allowing it to non-specifically intercalate into DNA and inhibit the topoisomerase II enzyme.^[64,67] In addition to cryptolepine (**23**), the extracts of *Cryptolepis sanguinolenta* was found to contain significant amounts of two other bioactive indoloquinoline alkaloids, namely neocryptolepine^[68] (**24**) and isocryptolepine (**25**) (Figure 1.8).^[69–71] Although studies have ascertained neocryptolepine (**24**) and isocryptolepine (**25**) to display similar biological profiles to those observed for cryptolepine (**23**), they are generally regarded as less potent and moreover, less cytotoxic.^[72]

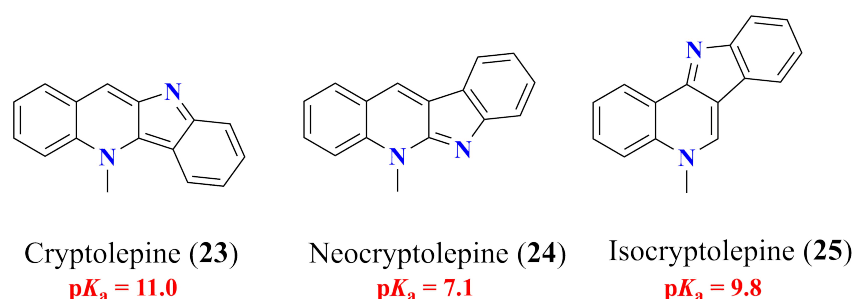


Figure 1.8: Major bioactive alkaloids isolated from *Cryptolepis sanguinolenta*, cryptolepine (**23**), neocryptolepine (**24**) and isocryptolepine (**25**),^[47] with the pK_a of their conjugate acids as determined by ^1H NMR spectroscopy.^[49]

In-depth studies of the extracts of *Cryptolepis sanguinolenta* have shown the plant to contain several other indoloquinoline alkaloids, having been identified as quindoline (**26**), 11-isopropylcryptolepine (**27**), cryptolepinone (**28**), quindolinone (**29**), cryptohepine (**30**), cryp-

tolepicarboline (**31**), biscryptolepine (**32**), cryptoquindoline (**33**), cryptomirisine (**34**) and cryptospirolepine (**35**) (Figure 1.9).^[47,73,74] It is still believed that cryptolepine (**23**), neocryptolepine (**24**) and isocryptolepine (**25**) are the only components with any significant bioactivities, however, there is a large research gap surrounding the other identified alkaloids, some of which could be proven to contain useful biological activities.^[47]

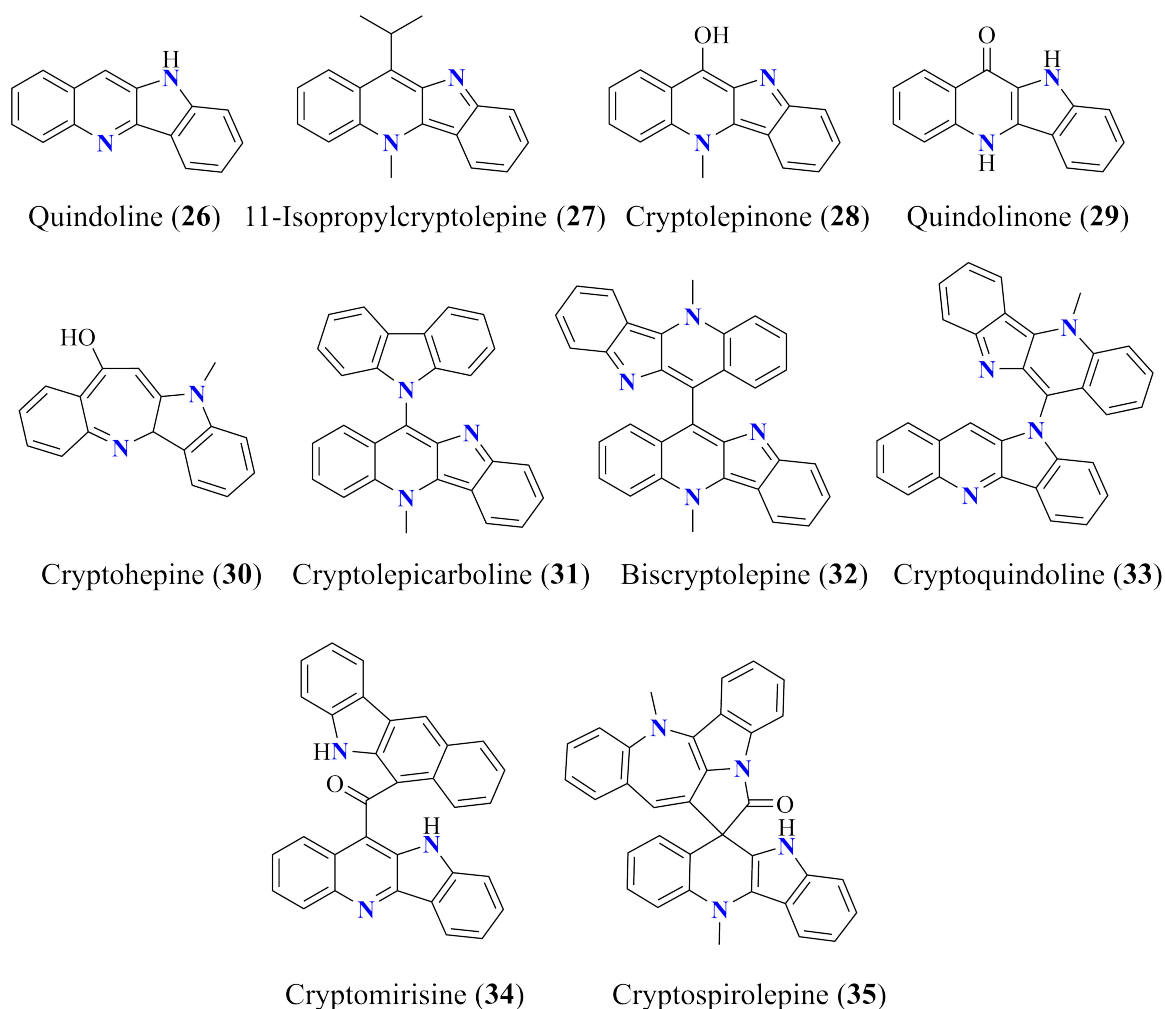


Figure 1.9: Other alkaloids extracted from the roots of *Cryptolepis sanguinolenta*; quindoline (**26**), 11-isopropylcryptolepine (**27**), cryptolepinone (**28**), quindolinone (**29**), cryptohepine (**30**), cryptolepicarboline (**31**), biscryptolepine (**32**), cryptoquindoline (**33**), cryptomirisine (**34**) and cryptospirolepine (**35**).^[47]

The antimalarial MoA of cryptolepine (**23**), neocryptolepine (**24**) and isocryptolepine (**25**) remains largely unknown. Being the most extensively studied of the three indoloquinoline alkaloids, there is support for two different MoAs explaining the antiplasmodial activity of cryptolepine (**23**). Firstly, it is believed to operate in a similar fashion to chloroquine (**2**) and inhibit the formation of the malaria pigment β -hematin. The second proposal involves the ability of cryptolepine (**23**) to intercalate into the base pairs of DNA, which inhibits the parasites DNA synthesis as well as topoisomerase II.^[75,76] A recent study has shown both neocryptolepine (**24**) and isocryptolepine (**25**) to also be capable of binding to DNA,^[77] hinting at

similar MoAs. There is evidence that the inhibition of haem and DNA intercalation are two independent processes, suggesting that the antiplasmodial activity of cryptolepine (**23**) could be the result of more than one distinct MoA.^[76] Nonetheless, further studies into the activities of the indoloquinoline alkaloids could help to clarify the exact MoA(s) and lead to better insight on how to neutralize the malaria parasite.

1.3 Repurposing antimalarial drugs for treating cancer and bacterial infections

In recent years, drug repurposing has become an attractive alternative to novel drug discovery within the pharmaceutical industry. This approach is generally considered as more cost effective and greatly shortens the time a drug has to spend in the "drug pipeline".^[78] In the past, the development of an antimalarial therapy has cost between 150-200 million USD and required 7-10 years to develop. In the future, it is estimated that the development of a novel antimalarial drug may cost on average 124 million USD and spend roughly 29 years in the "drug pipeline" before being finalized.^[79] Natural alkaloids, such as indoloquinolines **23**, **24** and **25** are believed to be effective against multiple diseases through their interaction with multiple biological targets during their evolutionary process,^[80] making them ideal targets for drug repurposing.

1.3.1 Cancer

Cancer is a devastating non-communicable disease characterized by uncontrollable cell proliferation. The 2020 world cancer report published by the WHO estimates 18.1 million cancer cases along with 9.6 million cancer-related deaths in 2018, making it the second leading cause of death worldwide.^[81] Cell proliferation can realistically affect any part of the human body but the five most commonly diagnosed cancers are lung, breast, colorectal, prostate and stomach. Though a variety of cancer treatments are currently available, chemotherapy regimens are most frequently applied, where a drug or combination of several drugs, are utilized to kill cells. These treatments have the unwanted side effect that they also tend to kill healthy cells in addition to the cancerous ones and, moreover, often leave the patients with a compromised immune system.^[82] The most widely administered category of anticancer drugs are the anthracyclines, which are antitumor antibiotics derived from certain *Streptomyces* bacterium.^[83] The potent antineoplastic drug doxorubicin (**36**) belongs to the anthracyclines and is composed of a quinone-hydroquinone aglycone attached through a glycosidic bond to daunosamine (Figure 1.10). Doxorubicin (**36**) is used to treat a multitude of tumors, including breast, prostate, stomach, liver as well as leukaemia.^[83] A recent study has shown doxorubicin (**36**) to also act as an inhibitor to the development of the malaria strain *P. falciparum*, indicating it as a potential

candidate for malaria treatment.^[84]

An alkaloid with significant antitumor properties is the *vica* alkaloid vincristine (**37**) (Figure 1.10), originally isolated from the *Vinca rosea* plant, representing one of the most effective cancer drugs available today. Its use is primarily within paediatric oncology, either as a monotherapy or in combination with other chemotherapeutic agents.^[85]

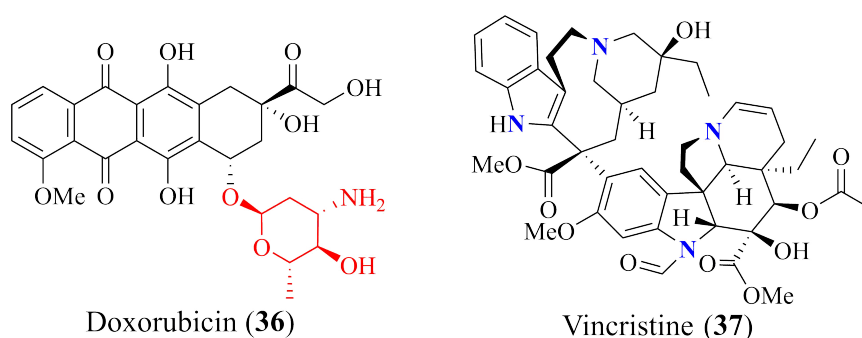
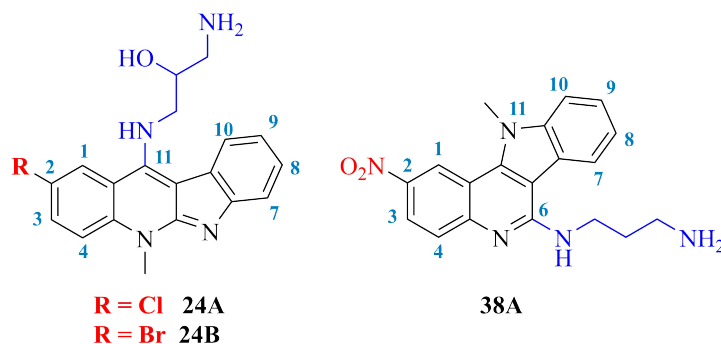


Figure 1.10: The cancer treatments doxorubicin (**36**), with its sugar moiety highlighted, and vincristine (**37**).

Significant antiproliferative activities have been reported for a number of diversely functionalized indoloquinolines, in particular, the inclusion of a basic alkyl amino chain has shown promise, with IC_{50} values similar to those observed for doxorubicin (**36**). Inokuchi and colleagues explored the antiproliferative activities of some C-11 substituted neocryptolepines with branched ω -aminoalkylamino chains.^[86] Their work unveiled neocryptolepines **24A** and **24B** functionalized with a 3-amino-2-hydroxypropylamino group at C-11 to outperform doxorubicin (**36**) ($IC_{50} = 0.33 \mu\text{M}$), the utilized standard, against the non-small cell lung cancer A549 cell line (**24A**: $IC_{50} = 0.197 \mu\text{M}$; **24B**: $IC_{50} = 0.19 \mu\text{M}$) as well as the colon cancer HTC116 cell lines (**24A**: $IC_{50} = 0.138 \mu\text{M}$; **24B**: $IC_{50} = 0.117 \mu\text{M}$) (Table 1.1). The compounds were also tested and showed excellent activity against the human leukaemia MV4-11 cell line, however, being a 10-fold less potent than doxorubicin (**36**). The cytotoxicity was further evaluated against normal BALB/3T3 mice cell fibroblasts, showing the tested compounds to be slightly more toxic than the standard.^[86] In another study, Inokuchi and colleagues showed that the C-6 aminoalkyl substituted 11-methyl-indolo[3,2-*c*]quinoline **38A** to be significantly more active than doxorubicin (**36**) against the lung cancer A549 cell line ($IC_{50} = 0.11 \mu\text{M}$) and the colon cancer HTC116 cell lines ($IC_{50} = 0.010 \mu\text{M}$) (Table 1.1).^[87] Unfortunately, the compound displayed high levels of cytotoxicity ($IC_{50} = 0.080 \mu\text{M}$), which is not optimal for a potential drug candidate. Although enormous efforts have been put into investigating the potential antiproliferative properties of the indoloquinoline alkaloids, they have never made it to human clinical trials, thus further endeavours are required to unlock their full therapeutic potential.^[88]

Table 1.1: Antiproliferative activities of indoloquinolines **24A**, **24B** and **38A** against normal mice cell fibroblasts BALB/3T3 and against cancer cell lines MV4-11, A549 and HCT116.

Compound	BALB/3T3 ^a (μM)	MV4-11 ^a (μM)	A549 ^a (μM)	HCT116 ^a (μM)
24A	0.896 ± 0.042 ^[86]	0.042 ± 0.014 ^[86]	0.197 ± 0.028 ^[86]	0.138 ± 0.050 ^[86]
24B	0.864 ± 0.015 ^[86]	0.057 ± 0.015 ^[86]	0.19 ± 0.027 ^[86]	0.117 ± 0.055 ^[86]
38A	0.080 ± 0.020 ^[87]	0.050 ± 0.010 ^[87]	0.11 ± 0.070 ^[87]	0.010 ± 0.00 ^[87]
Doxorubicin (36)	1.08 ± 0.030 ^[87]	0.0060 ± 0.0020 ^[87]	0.33 ± 0.10 ^[87]	0.39 ± 0.10 ^[87]

^aReported as an IC₅₀ value.

1.3.2 Bacterial infections and antibiotic resistance

What makes bacterial infections so devastating today is not the infection itself but rather that they are difficult, or sometimes impossible, to treat due to antimicrobial resistance (AMR). AMR will naturally occur over time,^[89] however, it is primarily the misuse and overuse of antibiotics which has caused widespread resistance. The WHO has declared AMR as one of the top ten global health threats currently facing humanity, with an estimated 1.27 million deaths directly caused by AMR along with 4.95 million AMR related deaths in 2019. Of these casualties, lower respiratory infections accounted for 1.5 million deaths, while 100 000 was related to the devastating methicillin-resistant *Staphylococcus aureus* (MRSA).^[90] The six pathogens with observed AMR responsible for the most deaths in 2019 was *Escherichia coli*, *Staphylococcus aureus*, *Klebsiella pneumoniae*, *Streptococcus pneumoniae*, *Acinetobacter baumannii* and *Pseudomonas aeruginosa*. Further complicating matters, availability of novel antimicrobial agents is severely lacking, despite more drugs being prepared now than in the past, with the latest antibiotic drug class to be approved by the FDA being the lipopeptide antibiotic daptomycin, made available in 2003.^[91] If the current trends seen in AMR along with the slow rate of novel drugs being discovered and approved for commercial use, it has been estimated that AMR may kill as many as 10 million people per year by 2050.^[92] Bacterial infections can also have a detrimental effect on the treatment of cancer patients, which are often left severely immunosuppressed following chemotherapy, leaving them more prone to contract nosocomial

infections.^[82] Infections caused by drug-resistant *S. aureus* are especially prominent and often seen in combination with the formation of multidrug-resistant biofilms,^[93] which are nearly impossible to treat.^[94,95]

While antibiotics were used long before the dawn of modern medicine, it was Alexander Fleming's accidental discovery of penicillin G (**39**) (Figure 1.11) from the fungi of *S. aureus* in 1928 which truly started the antibiotic era.^[78] The discovery of penicillin **39** is regarded as one of the most pivotal developments in medicinal history and awarded Alexander Fleming the 1945 Nobel Prize in medicine.^[96] Penicillin G (**39**) is a part of the β -lactam antibiotics, containing the characteristic β -lactam moiety (red part in Figure 1.11), fused to a thiazolidine ring (blue part in Figure 1.11) and is one of the standard treatments for infections caused by Gram-positive bacteria.^[78] Another commonly employed antibiotic drug class are the fluoroquinolones, active against a broad spectrum of both Gram-negative and Gram-positive bacteria.^[97] Ciprofloxacin (**40**) (Figure 1.11) is an important member of the fluoroquinolone class, and since its discovery in the 1980s has been the most successful treatment for infections caused by *P. aeruginosa*.^[98] AMR is already observed for both penicillin G (**39**)^[78] and ciprofloxacin (**40**),^[98] making these once potent drugs less effective.

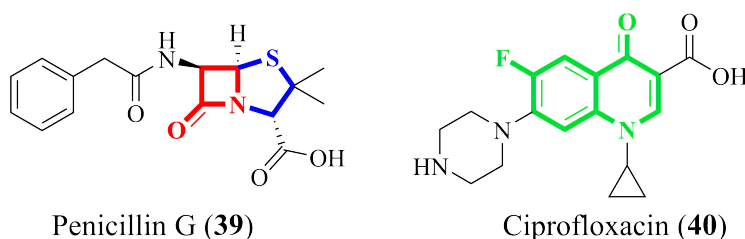
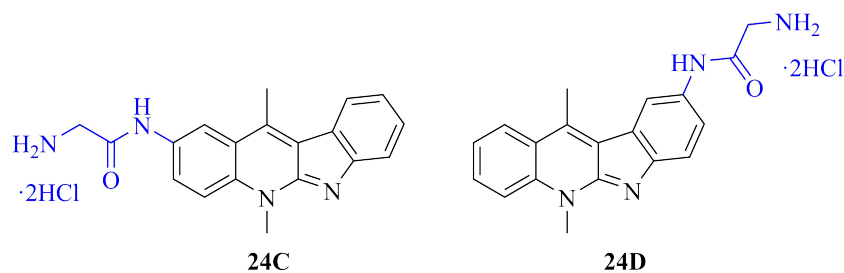


Figure 1.11: Structures of the β -lactam antibiotic penicillin G (**39**) with its β -lactam (in red) and thiazolidine (in blue) units highlighted, and the fluoroquinolone (in green) antibiotic ciprofloxacin (**40**).

The natural products cryptolepine (**23**), neocryptolepine (**24**) and isocryptolepine (**25**) have all been revealed to exhibit some degree of antimicrobial activities.^[72,82] This has sparked several studies into modifications of the core indoloquinoline scaffold in order to improve their antibiotic properties. Work conducted by Sidoryk and coworkers showed glycine-substituted neocryptolepines **24C** and **24D** to exhibit potent antimicrobial activities.^[82] Though not as effective as ciprofloxacin (**40**), the compounds showed impressive minimal inhibitory concentration (MIC) values against *S. aureus* (**24C**: MIC = 12.5 $\mu\text{g/mL}$; **24D**: MIC = 50 $\mu\text{g/mL}$), *Staphylococcus epidermidis* (**24C**: MIC = 12.5 $\mu\text{g/mL}$; **24D**: MIC = 25 $\mu\text{g/mL}$) and *Bacillus subtilis* (**24C**: MIC = 12.5 $\mu\text{g/mL}$; **24D**: MIC = 12.5 $\mu\text{g/mL}$) (Table 1.2). The activity against the biofilm pathogen *S. epidermidis* is especially promising, showing that these compounds, which also contain substantial antiproliferative properties, could serve as a dual antiproliferative-antimicrobial treatment.^[82]

Table 1.2: Antimicrobial activities of neocryptolepines **24C** and **24D** against certain microbial pathogens as presented by Sidoryk and coworkers.^[82]

Compound	<i>S. aureus</i> ^a (μg/mL)	<i>S. epidermis</i> ^b (μg/mL)	<i>B. subtilis</i> ^c (μg/mL)
24C	12.5	12.5	12.5
24D	50	25	12.5
Ciprofloxacin (40)	0.25	0.25	<0.0125

All data given as MIC values; ^aSpecific strain: NCTC 4163; ^bSpecific strain: ATCC 12228; ^cSpecific strain: ATCC 6633.

1.4 Project aims

The overall aim of this PhD project has been the synthesis and description of compounds structurally similar to the indoloquinoline natural products, cryptolepine (**23**), neocryptolepine (**24**) and isocryptolepine (**25**). Moreover, a particular emphasis has been to devise strategies which allow for their construction from common intermediates through regiodivergent reaction protocols. In addition to furnishing novel protocols for the synthesis of the core scaffolds of the indoloquinolines, it was also desirable to prepare a library of diversely functionalized derivatives suitable for biological evaluations. The prepared compounds would be screened for antiplasmodial, antiproliferative and antimicrobial activities. Since the strategies created during this work utilized quite different approaches and conditions, a more in-depth project aims section will be found in each chapter containing the synthetic efforts, detailing the project specific goals.

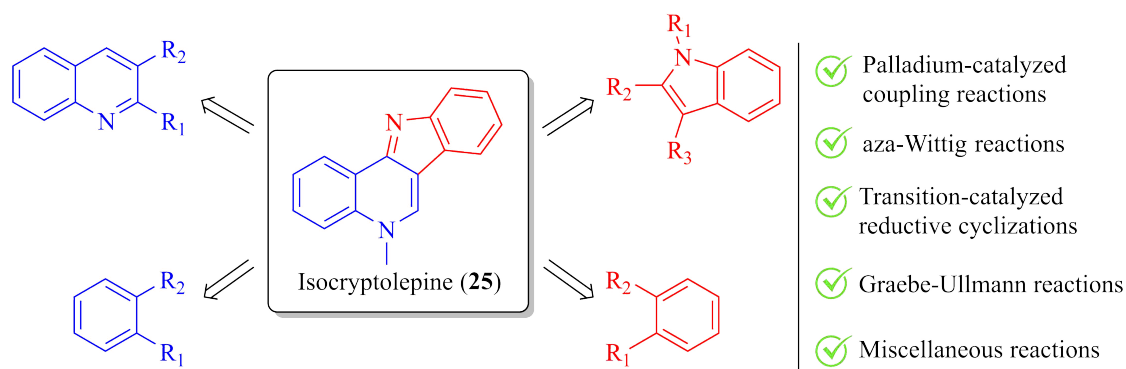
Chapter 2

Synthesis of isocryptolepine and regioisomers

2.1 Introduction

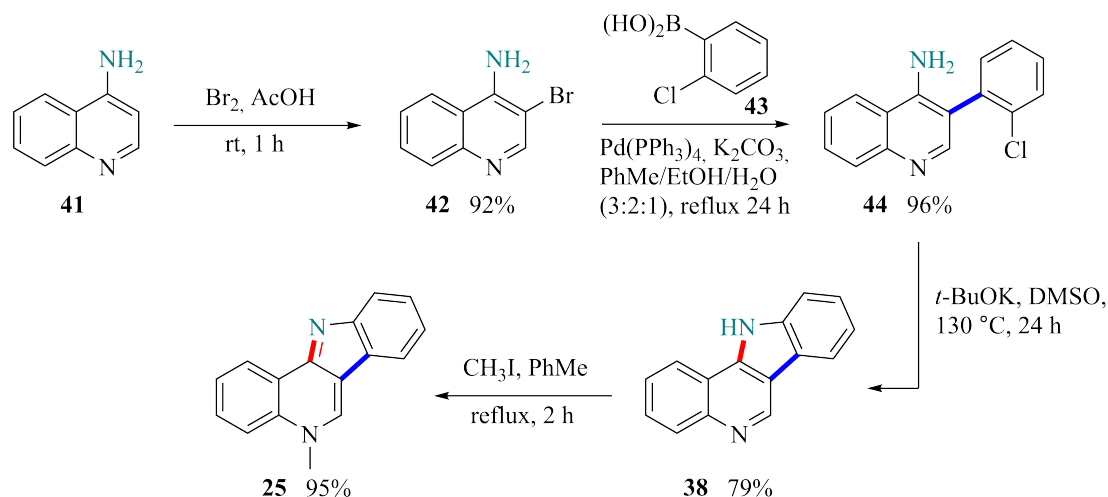
2.1.1 Synthesis of isocryptolepine in recent literature

Due to their impressive library of bioactivities, cryptolepine (**23**) and neocryptolepine (**24**) have been the focus of intense study, while isocryptolepine (**25**) historically has received less attention.^[99] A plethora of synthetic strategies have been reported for all three neutral alkaloids, with major review articles covering all work done up until 2015-2016^[100–103] and one recently published article covering all known methods currently available to prepare the indoloquinoline core.^[104] Consequently, only a small selection of synthetic strategies for the synthesis of isocryptolepine (**25**) will be covered in this thesis. Though a variety of different strategies exist, the synthesis of the indoloquinoline skeleton can be cataloged into six major categories: 1) palladium-catalyzed coupling reactions, 2) aza-Wittig reactions, 3) transition-metal mediated reductive cyclizations, 4) photochemical reactions, 5) Graebe-Ullmann reactions and 6) miscellaneous reactions.^[100–103] The reactions can be generalized as starting from either a functionalized quinoline or indole moiety, although other cyclic starting materials may also be employed (Scheme 1).



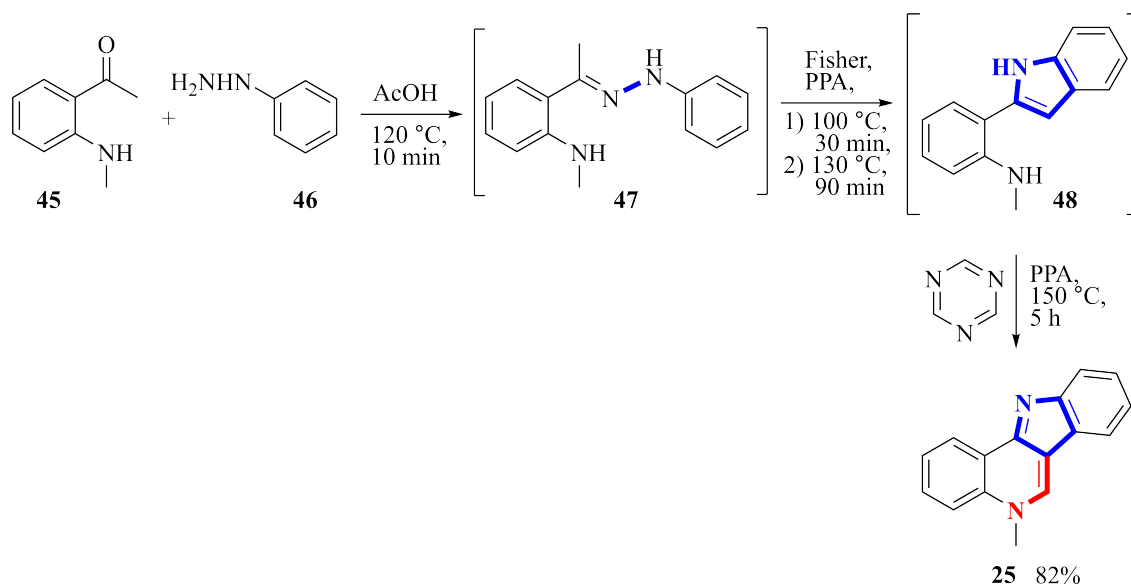
Scheme 1: The most common synthetic strategies to assemble isocryptolepine (**25**).

Tanimori and Sonoda presented a four-step synthesis of isocryptolepine (**25**) from the commercially available 4-aminoquinoline (**41**), where the key transformations involved a Suzuki-Miyaura cross-coupling reaction and a base-induced intramolecular cyclization.^[105] The synthesis was initiated by treating 4-aminoquinoline (**41**) with a small excess of bromine in refluxing acetic acid selectively gave 3-bromo-4-aminoquinoline (**42**) in 92% yield (Scheme 2). Then, bromoquinoline **42** underwent Suzuki-Miyaura cross-coupling with phenylboronic acid **43** in the presence of tetrakis(triphenylphosphine)palladium (0) ($\text{Pd}(\text{PPh}_3)_4$) using K_2CO_3 as the base to give biaryl **44** in excellent yield. The base-induced intramolecular cyclization of biaryl **44** was carried out by the aid of *t*-BuOK to give indoloquinoline **38**, which was readily alkylated using iodomethane to give isocryptolepine (**25**) in an overall yield of 66%.^[105]



Scheme 2: Synthesis of isocryptolepine (**25**) via a Suzuki-Miyaura cross-coupling reaction and base-mediated ring closure strategy as presented by Tanimori and Sonoda.^[105]

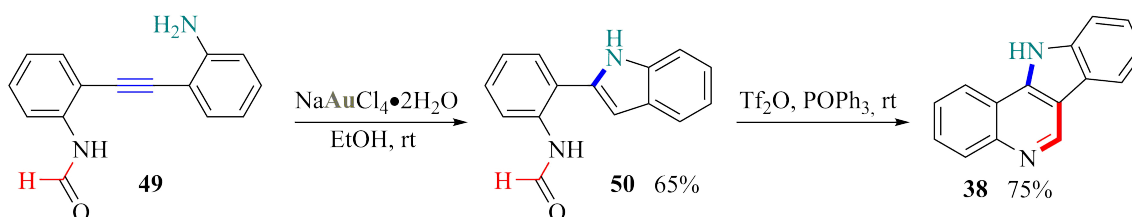
Work conducted by Aksenov and coworkers detailed an efficient one-pot synthesis of isocryptolepine (**25**), perhaps representing the shortest known route to allow for the assembly of this scaffold.^[106] The synthesis commences from the commercially available 2-(methylamino)acetophenone (**45**) and phenylhydrazine (**46**), which when treated with catalytic amounts of acetic acid forms intermediate **47**. Then, subjecting the aforementioned intermediate to an acid-catalyzed Fischer indolization using polyphosphoric acid (PPA) as a catalyst gives indole **48** (Scheme 3). Finally, addition of triazine and further treatment using PPA produces isocryptolepine (**25**) in an overall yield of 82%.



Scheme 3: One-pot synthesis of isocryptolepine (**25**) by Aksenov's group.^[106]

Indoloquinoline **38**, which can act as a precursor to isocryptolepine (**25**), was synthesized by Wang's group using a gold(III) catalyst protocol, operating under relatively mild reaction

conditions (Scheme 4).^[107] By treating acyclic alkyne **49** with sodium tetrachloroaurate(III) at room temperature, indole **50** was obtained in 65% yield through the execution of a 5-*endo-dig*-cyclization. Subjecting the indole to Hendrickson's reagent (POPh₃) and triflic anhydride allowed for a regioselective 6-*endo*-cyclization to furnish indoloquinoline (**38**) in excellent yield. The scope and limitations of the approach was also evaluated, revealing a broad tolerance to a wide selection of functional group substitutions on both sides of the alkyne moiety.



Scheme 4: Gold(III)-catalyzed synthesis of indoloquinoline (**38**) as presented by Wang and coworkers.^[107]

2.1.2 Synthesis of pyridocarbazoles and pyridophenanthridines in recent literature

The pyridocarbazole scaffold is present in several natural products, the two most prominent examples being olivacine (**51**) and ellipticine (**52**) (Figure 2.1).^[108,109] Being regioisomers of the bioactive indoloquinoline compounds, the pyridocarbazoles are also known for possessing a range of biological activities, but are first and foremost known for their potent anticancer properties. First isolated from the tropical evergreen tree *Ochrosia elliptica* in 1959, ellipticine (**52**) was quickly determined to contain significant antiproliferative activities. Since its discovery, several functionalized derivatives of ellipticine (**52**) has reached clinical trials.^[110]

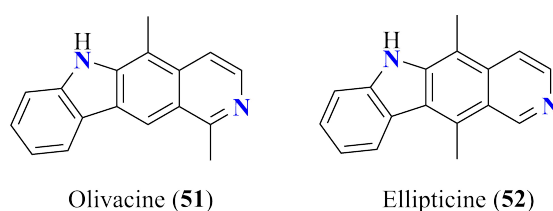
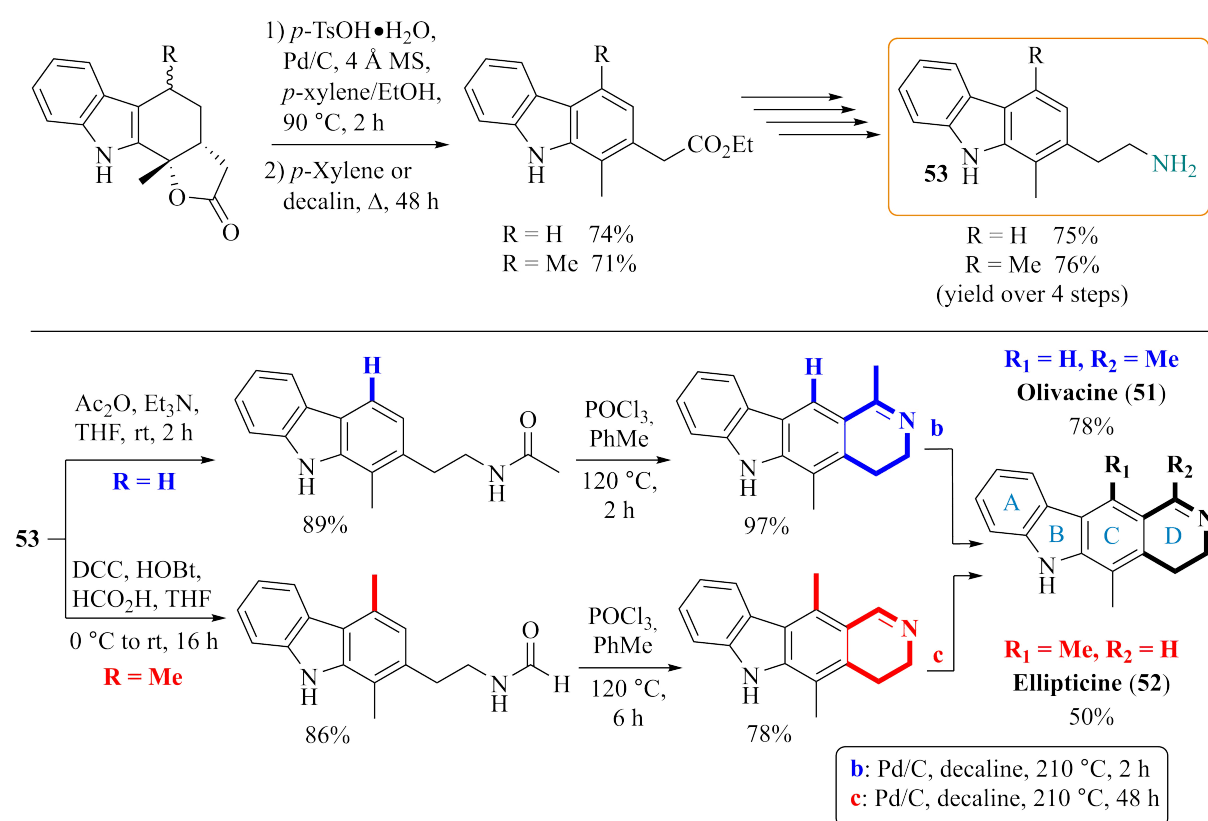


Figure 2.1: The pyridocarbazole natural products olivacine (**51**) and ellipticine (**52**).

Since there exist numerous examples of pyridocarbazoles, ellipticine (**52**) will be used as an example to briefly review common synthetic strategies. Due to its impressive antiproliferative activities, there are several review articles which extensively cover past synthetic endeavours into the construction of ellipticine (**52**).^[111–116] Similarly to isocryptolepine (**25**), the synthetic strategies to assemble such pyridocarbazole scaffolds usually involve palladium-catalyzed cross-coupling reactions, transition-metal catalyzed reactions and Fischer indolizations, though other strategies are also prominent. These include, but are not limited to, the

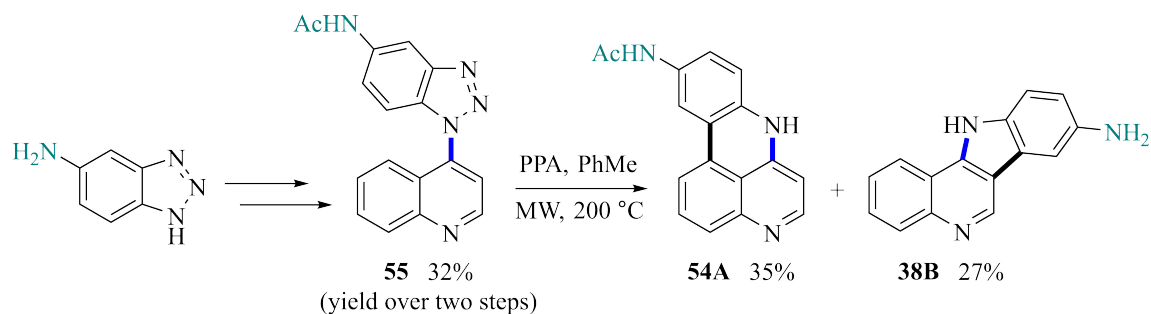
use of a triazole intermediate, nitrene insertion approaches and condensation reactions.^[110] In a relatively recent work, Ertürk's group described the synthesis of both olivacine (**51**) and ellipticine (**52**) from a common lactone intermediate using a high-yielding and practical, though somewhat step-heavy, synthetic cascade (Scheme 5).^[109] The key features required include a trifluoroacetic acid-mediated lactone formation (not included in the reaction scheme), followed by a one-pot two-step lactone ring-opening and finally Pd/C-catalyzed dehydrogenative rearomatization, to give the desired carbazole intermediate **53**. With carbazoles **53** in hand, D-ring cyclizations was realized through application of a previously published reaction sequence,^[117] affording the two natural products olivacine (**51**) and ellipticine (**52**) in 78 and 50% yields, respectively.^[109]



Scheme 5: Synthesis of olivacine (**51**) and ellipticine (**52**) from a common intermediate **53** as presented by Ertürk and coworkers; DCC = *N,N'*-dicyclohexylcarbodiimide; HOBT = 1-hydroxybenzotriazole hydrate.^[109]

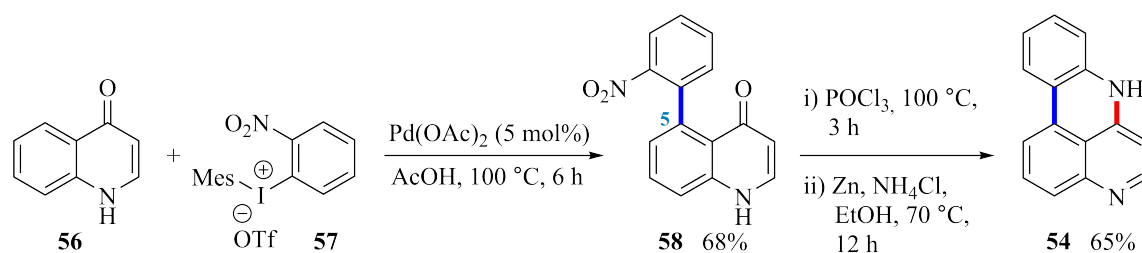
The pyridoacridine scaffold is well detailed in the literature due to its presence in certain natural products,^[118] while its regioisomeric pyridophenanthridines have never been observed naturally and thus remain largely unexplored. To present date, there are only two examples of the synthesis of a pyridophenanthridine in the published literature, the first reported being the accidental synthesis of pyridophenanthridine **54A** by Beauchard and colleagues (Scheme 6).^[119] The unexpected result was the consequence of the teams effort to furnish indoloquinoline **38B** by a microwave-induced thermal decomposition of the benzotriazole-coupled quino-

line **55** in a mixture of PPA and toluene. The procedure follows a classical Graebe-Ullmann cyclization,^[119] likely proceeding *via* a biradical mechanism initiated by the thermal explosion of nitrogen gas.^[120] Kalinowski *et al.* have alternatively suggested an intramolecular electrophilic substitution type mechanism when the reaction is conducted in PPA and a protic solvent.^[121] Subsequent work by Alekseev and coworkers argue this to be an unlikely pathway, as they made observations which contradicted this hypothesis and moreover lend support to the biradical mechanism.^[122]



Scheme 6: Unexpected synthesis of phenanthridine **54A** by Beauchard and coworkers.^[119]

In a more recent work, Kumar and coworkers described the synthesis of pyridophenanthridine **54** through the regioselective arylation of quinolones using diaryliodonium salts (Scheme 7).^[123] By treating quinolone **56** with aryliodonium salt **57** in the presence of palladium(II) acetate ($\text{Pd}(\text{OAc})_2$) in heated acetic acid, regioselective arylation provided aryl nitro quinolone **58** in 68% yield. Subjecting this compound to a standard chlorination reaction followed by a zinc-mediated reduction of the nitro group triggered the intramolecular cyclization into the target pyridophenanthridine **54** in good yield. The regioselectivity is believed to be a consequence of the mechanism by which the arylation occurs, where the palladium complex first adds to the quinolone oxygen, then forming a cyclopalladium species by binding to C-5 of the quinolone ring (C-5 highlighted in Scheme 7).^[123]

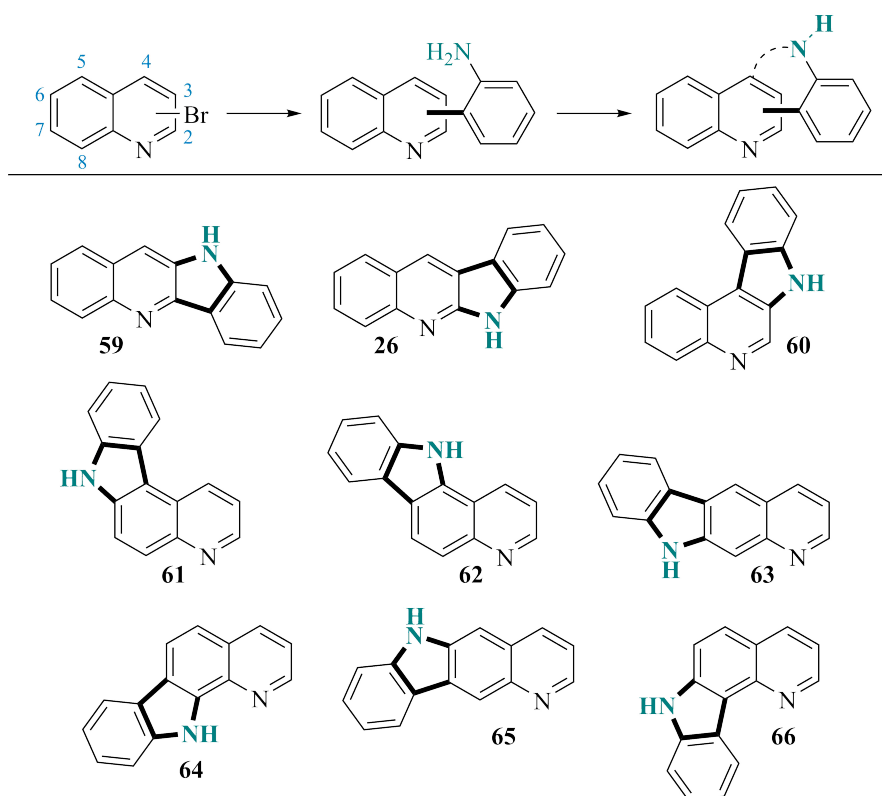


Scheme 7: Synthesis of pyridophenanthridine **54** using diaryliodonium salts by Kumar's group.^[123]

2.1.3 Project aims

As a continuation of the work conducted by Helgeland and Sydnnes, it was envisaged that by simply changing the placement of the bromide on the quinoline starting material, access to a

host of tetracyclic ring-systems could be obtained by following the same synthetic pathway (Scheme 8). Despite the synthesis and characterization of several of these ring systems, in particular the natural products **59** and **26**, already being described in the literature, it would likely be the first time they had been synthesized under the same reaction conditions. Moreover, it was desirable to investigate the various reactivities of these tetracyclic ring-systems to gain better insight into the chemistry of such compounds.



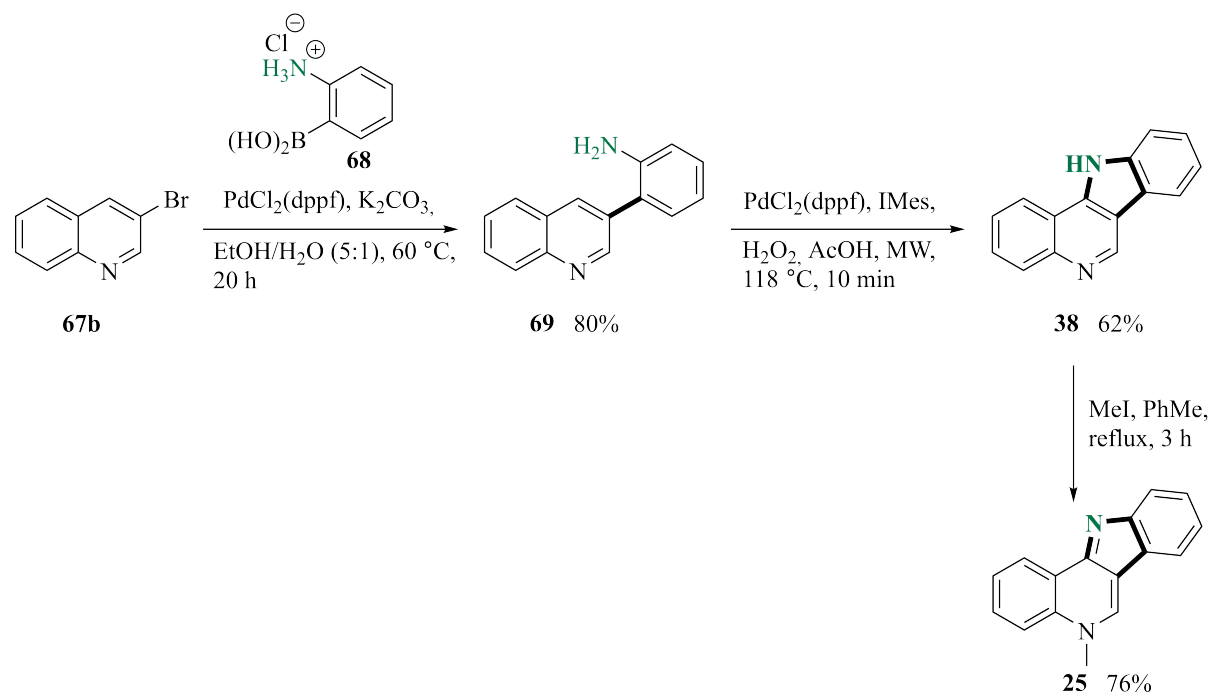
Scheme 8: Projected plan which might grant access to a host of tetracyclic ring-systems; **59**, **26** and **60-66**.

2.2 Synthesis of isocryptolepine (25) and regioisomers

2.2.1 Introduction

Previous work in our laboratories has demonstrated a short and concise synthesis of isocryptolepine (**25**) utilizing readily available starting materials (Scheme 9).^[124] Under optimized Suzuki-Miyaura cross-coupling conditions, 3-bromoquinoline (**67b**) is coupled to 2-aminophenylboronic acid hydrochloride (**68**) to furnish biaryl **69** in good yields (80%). Subsequent intramolecular cyclization by a palladium-catalyzed C-H activation/C-N bond formation gave the tetracyclic ring-system **38**. Finally, regioselective *N*-methylation of indoloquinoline **38** gave isocryptolepine (**25**) in an overall yield of 38%. The two key transformations in this reaction sequence is the Suzuki-Miyaura cross-coupling reaction and the intramolecular cyclization.

While the exact mechanism of the MW-assisted cyclization step is uncertain, the mechanism of the cross-coupling reaction has been extensively studied and is frequently utilized to construct C-C bonds within natural product synthesis.^[125]



Scheme 9: Synthesis of isocryptolepine (**25**) by Helgeland and Sydnes.^[124]

There are several key aspects which makes the Suzuki-Miyaura cross-coupling reaction applicable to many synthetic protocols. The major factors include the availability of a range of commercial starting materials, high reaction yields, broad functional group tolerance, relatively mild reaction conditions and relatively low toxicity of reagents compared to other cross-coupling strategies, in particular the Stille coupling. While the usage of a noble metal such as palladium is certainly not considered environmentally friendly, the Suzuki-Miyaura cross-coupling reaction has the advantage that the often employed boronic acids, or boronic acid pinacol esters, are highly water soluble, allowing for water to be used as a solvent.^[126] The base stability of the boronates requires the use of a sufficiently strong base in order to produce the reactive boronate species. In order to achieve this, bases such as NaOH, Cs₂CO₃, *t*-BuOK and K₃PO₄ are typically used.^[127] A myriade of palladium catalysts are associated with the reaction, using a range of different ligands to aid the catalysis. The main aim of a ligand is to act as a stabilizer to the reaction intermediates, with the choice of ligand further capable of controlling the regioselective outcome of the reaction.^[128] Phosphine ligands are particularly abundant in palladium chemistry, due to their ability to donate σ -electrons from the lone pair electrons of the phosphorous atom, creating a more reactive palladium complex which can more strongly coordinate to the substrate.^[129] The phosphine ligands triphenylphosphine and 1,1'-bis(diphenylphosphino)ferrocene (dppf) are commonly used in the Suzuki-Miyaura cross-coupling, as well as the tris(dibenzylideneacetone) (dba) auxiliary (Figure 2.2).^[127]

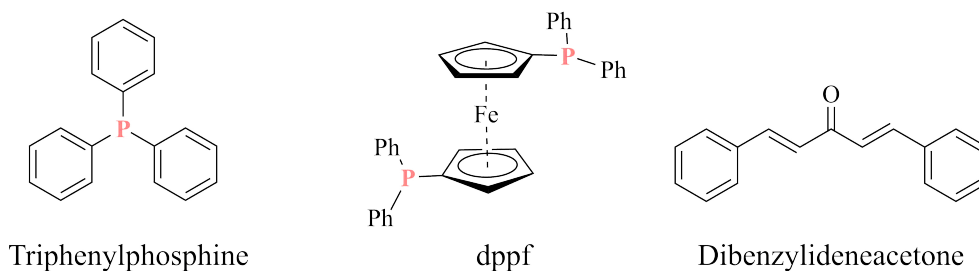
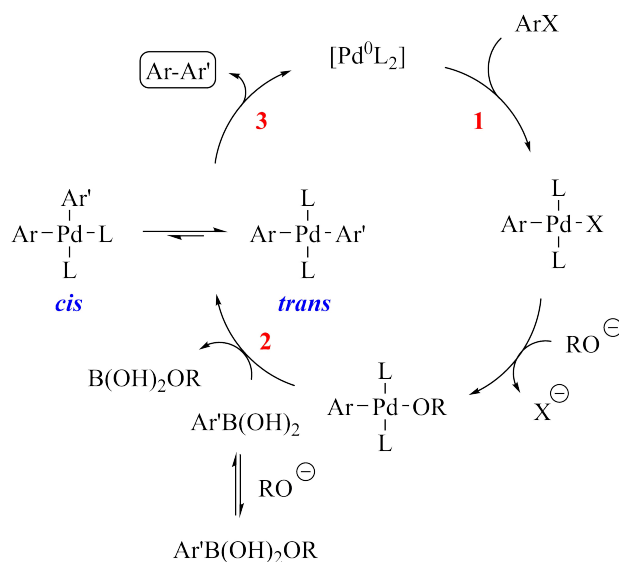


Figure 2.2: Structures of some commonly used ligands in the Suzuki-Miyaura cross-coupling reaction: triphenylphosphine, dppf and dibenzylideneacetone.^[127]

The catalytic cycle of the Suzuki-Miyaura cross coupling has been found to contain three primary steps: **1** oxidative addition, **2** transmetalation and **3** reductive elimination (Scheme 10).^[127] During oxidative addition **1**, the palladium center coordinates to the organohalide (ArX), forming an organopalladium species $[L_2Pd-ArX]$, which upon reacting with the base expels a halide ion, resulting in the formation of $[L_2Pd-ArOH]$. The base has a secondary role in the catalytic cycle, namely to activate the boronic acid to give the more reactive boronate complex $[B(OR)_2OH-Ar']$.^[130] In transmetalation **2**, the boronate complex reacts with the organopalladium species $[L_2Pd-ArOH]$, creating $[L_2Pd-ArAr']$, which exists in an equilibrium between the more favorable *trans* configuration and the sterically demanding *cis* state.^[131] Finally, reductive elimination **3** yields coupling product Ar-Ar' and subsequent regeneration of the palladium catalyst to complete the catalytic cycle.^[127]

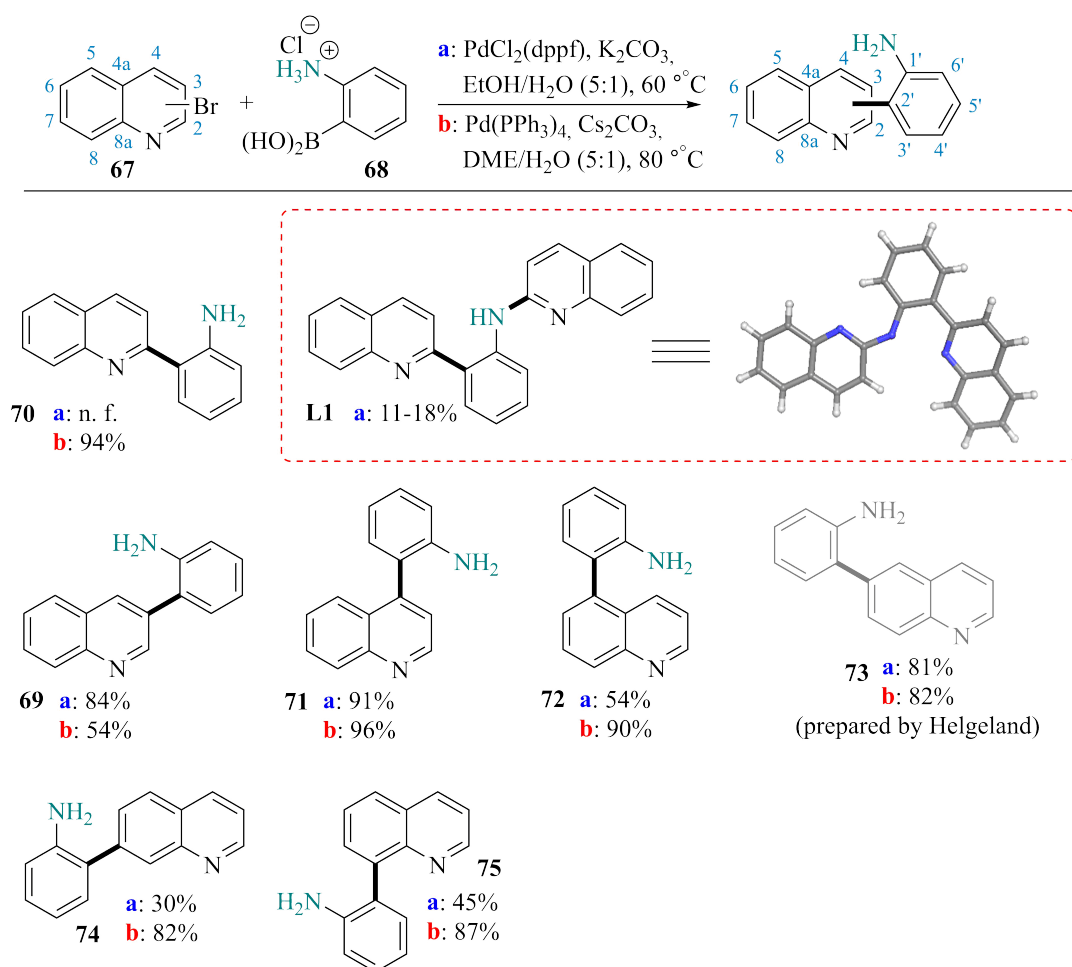


Scheme 10: Catalytic cycle for the Suzuki-Miyaura cross-coupling reaction.^[127]

2.2.2 Suzuki-Miyaura cross-coupling reactions to give biaryls

Serendipitously, all the required bromoquinoline starting materials were readily available from commercial vendors and a natural starting place was the Suzuki-Miyaura cross-coupling reac-

tion of 2-bromoquinoline (**67a**) and 2-aminophenylboronic acid hydrochloride (**68**).^[132] Using the conditions reported by Helgeland and Sydnnes, PdCl₂(dppf) was employed as the catalyst, however, the expected biaryl product **70** was not obtained. Instead, formation of a biquinoline bridged by an aniline moiety (**L1**) was observed. With the help of Dr. Bjarte A. Lund at the University of Tromsø (UiT), this structure was verified by obtaining its X-ray crystal structure (Scheme 11). By switching to a different cross-coupling protocol utilizing Pd(PPh₃)₄ as the catalyst, Cs₂CO₃ as base in a 5:1 solvent mixture of 1,2-dimethoxyethane (DME) and water, the target biaryl **70** was constructed in near quantitative yield (Scheme 11). The divergent results obtained with the two different reaction conditions prompted us to carry out the remaining reactions using both conditions, to study the difference in the reaction outcomes.



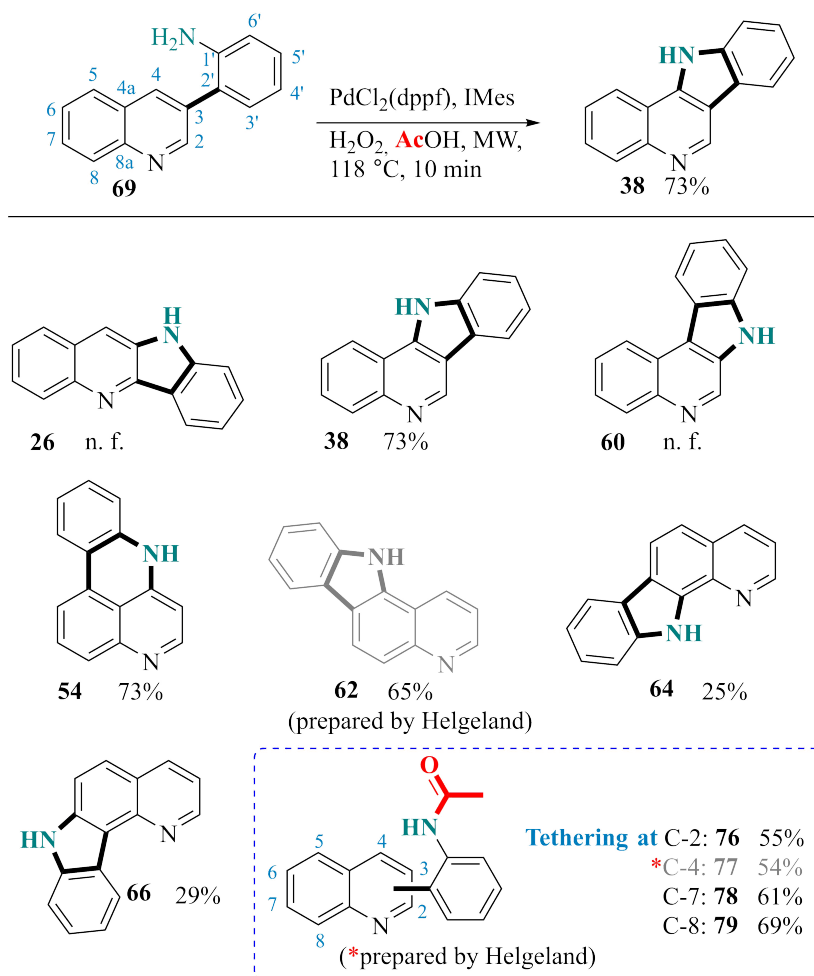
Scheme 11: Suzuki-Miyaura cross-coupling reactions between bromoquinolines **67** and 2-aminophenylboronic acid hydrochloride (**68**) to yield biaryls **69-75** along with biquinoline **L1**; n. f. = not formed.^[132]

Carrying out the remaining Suzuki-Miyaura cross-coupling reactions, it became clear that the conditions employing Pd(PPh₃)₄ performed better overall (Scheme 11). The best results were obtained for the construction of the C-4 tethered biaryl **71**, giving near quantitative yields with both methods (**a**: 91%; **b**: 96%). Compound **73**, which was prepared by former PhD stu-

dent Helgeland, gave nearly identical reaction yields, showing both methods to work equally effectively for this particular compound. The formation of compounds **74** and **75** were relatively sluggish using PdCl₂(dppf) as the catalyst, giving the target products in modest yields (Scheme 11). Based on these results, it appears that the choice of an appropriate catalyst was instrumental for obtaining good yields for the formation of the two aforementioned biaryls.

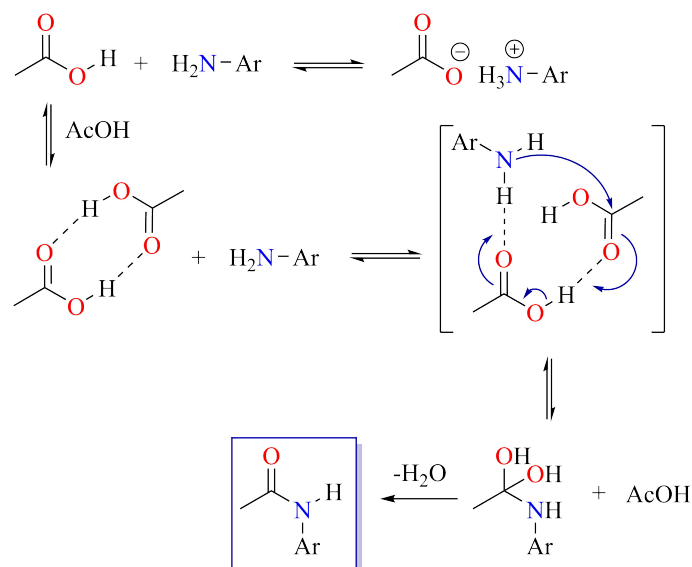
2.2.3 MW-assisted intramolecular cyclizations to give tetracycles

With all the necessary biaryls in hand, they were then subjected to the palladium-catalyzed intramolecular cyclization protocol described by Helgeland and Sydnes (Scheme 12).^[124] While the reaction provided isocryptolepine precursor **38** in excellent yield with a reaction time of only 10 minutes, no formation of indoloquinolines **26** and **60** was detected. Instead, an unwanted acetylation of the starting biaryls had taken place, furnishing acetanilides **76** and **77** in 55 and 54% yields, respectively. The exact mechanism of the acetylation reaction is not known, but it is likely a result of the reaction between the acetic acid utilized as the solvent and the aniline moiety on the biaryls. There has been reports of MW-assisted syntheses in the literature promoting acetylations carried out by acetic acid, though the details surrounding such transformations remains unclear.^[133]



Scheme 12: Summary of the palladium-catalyzed cyclizations of biaryls **69-75** to yield tetracyclic ring-systems **38**, **54**, **62**, **64** and **66** along with the undesired acetylation products **76-79**; n. f. = not formed.^[132]

Based on work supported by both experimental and theoretical endeavours, Whiting and coworkers presented a proposed mechanism for the direct formation of amides from amines *via* the formation of carboxylic acid dimers (Scheme 13).^[134] In the proposal, intermolecular hydrogen bonding supports the formation of a carboxylic acid dimer, enabling nucleophilic attack by the amine onto the carbonyl carbon of one of the acids in the dimer. The second unit of carboxylic acid then acts as a proton acceptor, leading to the formation of a hemiaminal intermediate. Following a concerted proton transfer, water is readily lost to create an acetamide. Additionally, they suggest that the starting amine exists in an equilibrium with its acid salt, acting as a reaction "dead-end". Preliminary computational work carried out by collaborator Professor Dr. Petra Imhof at Friedrich-Alexander-Universität Erlangen-Nürnberg (FAU), Germany, on our biaryls have suggested this mechanism to be a likely source of the observed acetanilides.



Scheme 13: Proposed mechanism for the direct formation of amides from amines by Whiting and coworkers.^[134]

Unexpectedly, the cyclization of biaryl **72** did not furnish the expected pyridocarbazole **61**, but instead ring closure proceeded at C-4, creating a 6-membered ring to give novel pyridophenanthridine **54** in excellent yield (Scheme 12). In order to verify the formation of this compound, its various NMR spectra were analyzed carefully. The presence of two doublets at 8.27 and 6.77 ppm, respectively, with a coupling constant of 6.6 Hz was not compatible with a pyridocarbazole. Through the use of 2D NMR spectrum, in particular NOESY correlations, these signals were determined to belong to H-5 and H-6, respectively (Figure 2.3). The most deshielded signal appearing as a doublet of doublets at 8.33 with corresponding coupling constants of 8.2 Hz and 0.8 Hz fits with H-11, due to the proton experiencing significant anisotropy. The NOESY spectrum further shows H-11 to be spatially close to two signals, belonging to H-1 and H-10, confirming the presence of a "bay-region" and thus the structure of pyridophenanthridine **54**. Additionally, analysis of its ^{13}C NMR spectrum, shows an uncharacteristically shielded aromatic carbon signal at 99.7 ppm, which was found to correspond to the proton at H-6.

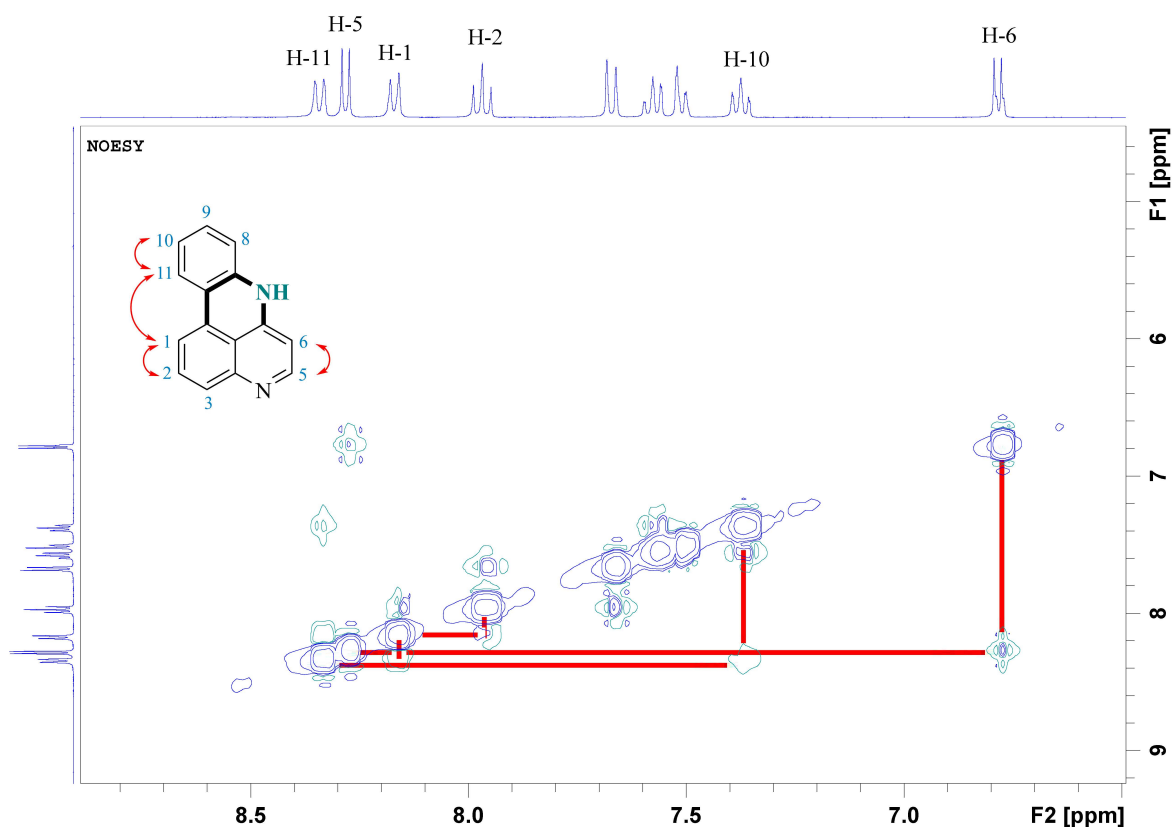
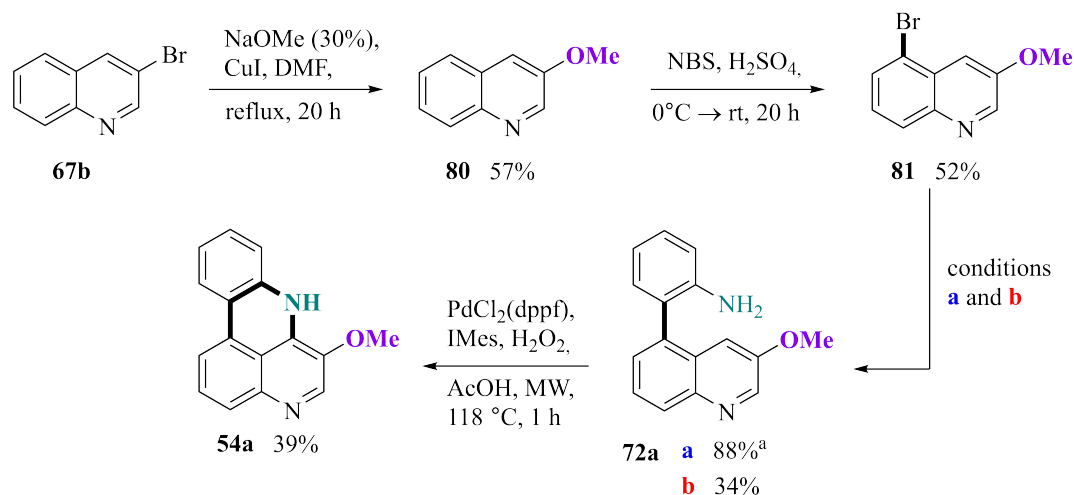


Figure 2.3: NOESY correlation confirming the structure of pyridophenanthridine **54**.

In terms of reaction kinetics, there is generally a preference for the annulation into 5-membered rings over 6-membered rings.^[135] In the study of the ring closure of some diethyl (ω -bromoalkyl)malonates, Galli and Mandolini showed that formation of 5-membered rings is by far the least energetically demanding ring to form, being an order of 10^3 more favorable than the formation of a 6-membered ring.^[136] On the contrary, studying the associated ring-strains, they demonstrated that the 6-membered rings are far less strained than 5-membered rings, with an observed difference in strain energy of roughly 5 kcal/mol. Searching for an explanation for the observed 6-membered ring product **54**, the electron densities of the various carbon atoms were evaluated as a possible cause. The assumption was that the cyclization would proceed at the most electron-deficient carbon site. This was based on the further assumption that the cyclization proceeds *via* and oxidative addition-type mechanism, which was proposed as a likely reaction path by Bjørsvik and Elumalai for the cyclizations of 2-aminobiphenyls to give carbazoles using similar conditions.^[137] If this was the case, it was hypothesized that addition of an EDG at C-3 of biaryl **72** might force the cyclization to occur at C-6 to give a carbazole instead. The installation of a methoxy-substituent would serve this purpose and following a literature procedure, 5-bromo-3-methoxyquinoline (**81**) was prepared in two steps in acceptable yields (Scheme 14).^[138] Subsequent Suzuki-Miyaura cross-coupling reaction be-

tween methoxy quinoline **81** and boronic acid **68** using both protocols resulted in formation of biaryl **72a** in excellent and yields, respectively (**a**: 88%; **b**: 34%, Scheme 14). Carrying out the cyclization of C-3 methoxy-substituted biaryl **72a** gave only 39% of the 6-membered ring product **54a** with traces of what might be the protonated mass of the corresponding carbazole product based on TLC-LRMS (Scheme 11).



Scheme 14: Synthesis of methoxy-substituted pyridophenanthridine **54a** starting from commercially available 3-bromoquinoline (**67b**);^a3.0 equiv. of boronic acid **68**.^[139]

Wanting to explore the notion that the reactivity was to some extent governed by differences in electron densities, some computational analyses were conducted. Obtaining Mulliken charges of biaryl **72**, along with several of the other biaryl starting materials, revealed only minute differences in electron densities (Figure 2.4). Moreover, the difference in the calculated densities were not significant enough to warrant the preferential formation of pyridophenanthridines **54** and other avenues had to be considered.

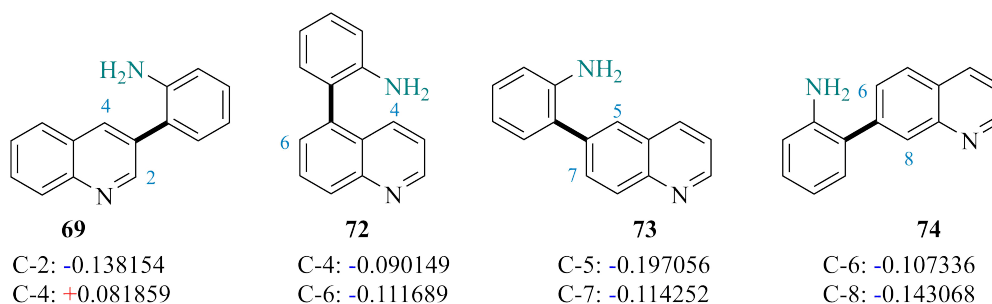
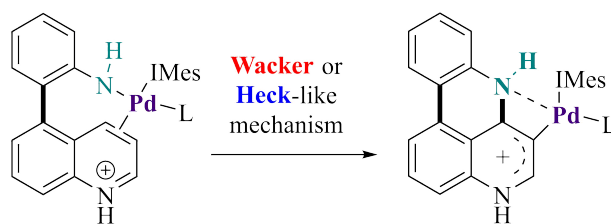


Figure 2.4: Calculated Mulliken charges for biaryls **69**, **72**, **73** and **74** using the B3LYP/6-31G** level of theory.

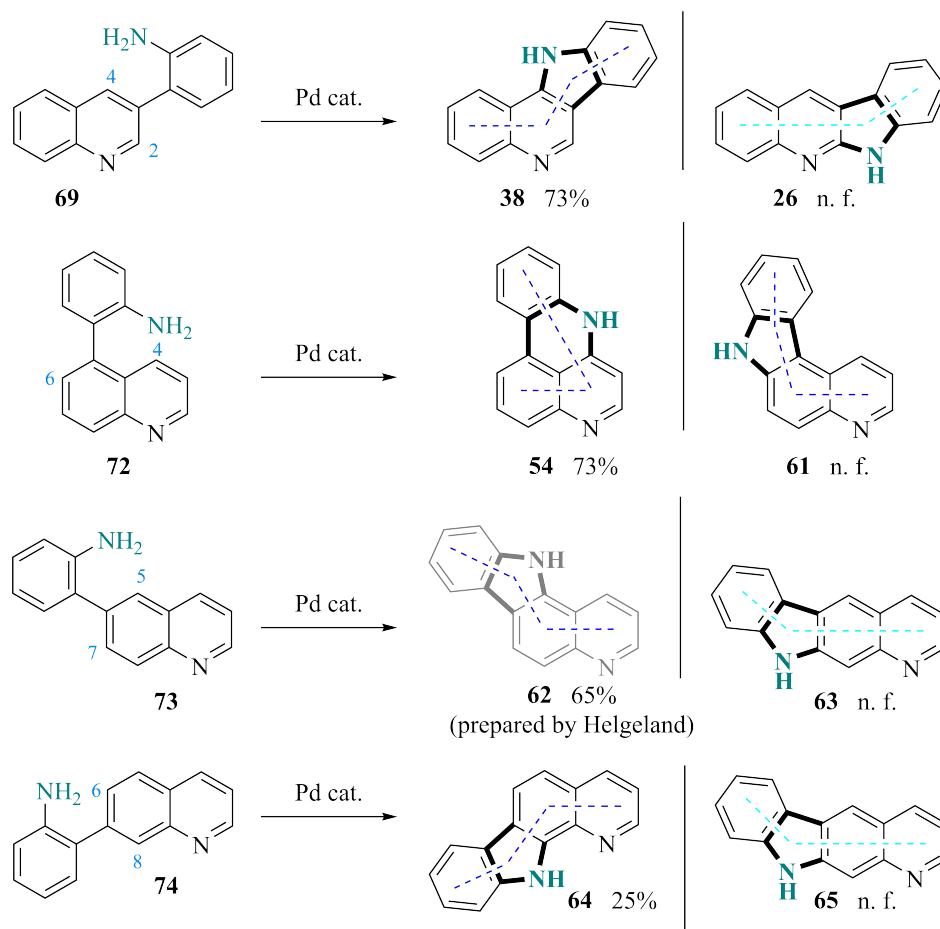
Through a collaboration with Professor Dr. Petra Imhof at FAU, extensive efforts were devoted to understand the formation of the pyridophenanthridine scaffold. As the electron densities had failed to provide a reasonable explanation for our observations, studies into the mechanism of its formation were undertaken. Despite considerable work, no precise catalytic

cycle has been found and it remains uncertain what the precise palladium complex is, though preliminary data suggests it to be a Pd-IMes complex. Two main conclusions have arrived from the computational studies, being the necessity of a protonation site, namely the quinoline nitrogen, and the presence of a carboxylic acid for any reaction to take place. Moreover, the computational data further suggests the mechanism provided by Bjørsvik and Elumalai to be an unlikely pathway for our systems. Taking this into account, the mechanism is more likely to proceed in either a Wacker- or Heck-like manner, where the palladium acts as a nucleophile rather than an electrophile (Scheme 15),^[140,141] which the preliminary computational work supports thus far and efforts to fully resolve this mechanism is still ongoing.



Scheme 15: Proposed Pd-IMes intermediates in the cyclization of biaryl **72**, possibly following a Wacker or Heck-like mechanism.

Of the three remaining biaryls, only indoloquinoline **62** was formed in good yield (65%, Scheme 11). The cyclizations of biaryls **74** and **75** primarily resulted in the formation of acetanilides **78** and **79** in addition to the desired ring closure products. With all the cyclizations reactions having been completed, a clear trend can be observed in terms of the topology of the formed products. Studying the geometries of the tetracyclic compounds, it becomes apparent that given the option between two cyclization sites, the formed product is always the more angular product, with the exception of pyridophenanthridine **54** (Scheme 16). This coincides with previous reports in the literature for the chemistry of polycyclic aromatic hydrocarbons (PAHs), revealing angular systems to generally be more stable than their linear counterparts. This has been particularly well documented in the case of phenanthrene and anthracene, with studies showing phenanthrene to be the more stable regioisomer. The exact nature for this phenomenon is somewhat controversial, with several propositions having been made.^[142–148]

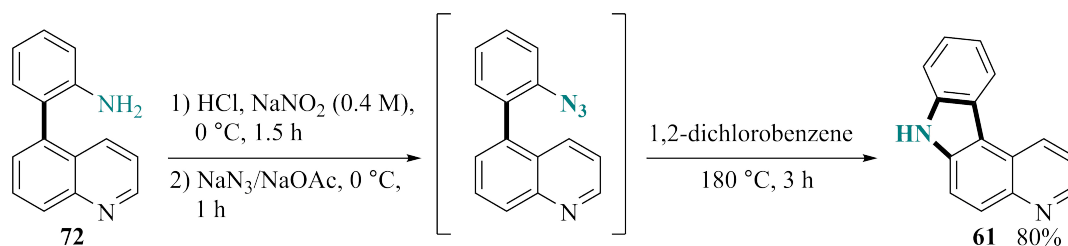


Scheme 16: Observed regioselectivities favoring the more angularly fused products (in dark blue) over linear fusions (in teal). Conditions: PdCl₂(dppf) (20 mol%), IMes (5 mol%), H₂O₂ (35 wt%, 29 mol%), AcOH, MW sealed tube, 118 °C; n. f. = not formed.^[132,149]

2.3 Divergent synthesis of pyridophenanthridines **54** and pyridocarbazoles **61**

While novel pyridophenanthridine **54** was formed in excellent yields using the MW-assisted intramolecular cyclization approach (Scheme 12), the subsequent purification by column chromatography was extremely challenging. In an attempt to avoid this obstacle, other methods for its assembly were considered, which might also lead to greater insight into the chemistry surrounding this novel scaffold. Timári and colleagues have developed a synthetic strategy to furnish isocryptolepine precursor **38** from biaryl **69** using a diazotization-azidation-nitrene insertion approach.^[150] Utilizing this approach, which has later been expanded upon by Maes *et al.*,^[151] indoloquinoline **38** could be formed in high yields with relatively clean reaction crudes. Utilizing the conditions as detailed by Maes and coworkers, biaryl **72** was transformed to the corresponding diazonium salt using concentrated hydrochloric acid and sodium nitrite (Scheme 17). Then, the azido group was installed in an S_NAr-type reaction with sodium azide, giving

an aryl azide intermediate. Subjecting the newly formed aryl azide to thermolysis in boiling 1,2-dichlorobenzene, surprisingly resulted in formation of novel pyridocarbazole **61** and only trace amounts of pyridophenanthridine **54**.^[149]



Scheme 17: Synthesis of the missing pyridocarbazole **61** using a azidation-nitrene-insertion approach.^[149]

The successful formation of pyridocarbazole **61** could be determined by carefully elucidating all the signals of its NMR spectra. Characteristically, the proton at 8.84 ppm ($J = 4.1$ Hz, 1.4 Hz), appearing as a doublet of doublets is easily placed as H-3 based on its proximity to a heteroatom, as evident by its coupling constants (Figure 2.5). The signal at H-3 has a clear COSY correlation to two signals, the doublet of doublets at 9.17 ppm ($J = 8.4$ Hz, 1.4 Hz) belonging to H-1. This signal has a NOESY correlation to the proton located at H-11, revealing the presence of a "bay-like region". Further, the carbazole amine, observed as a broad singlet at 11.92 ppm, correlates to the protons at H-6 and H-8, respectively.

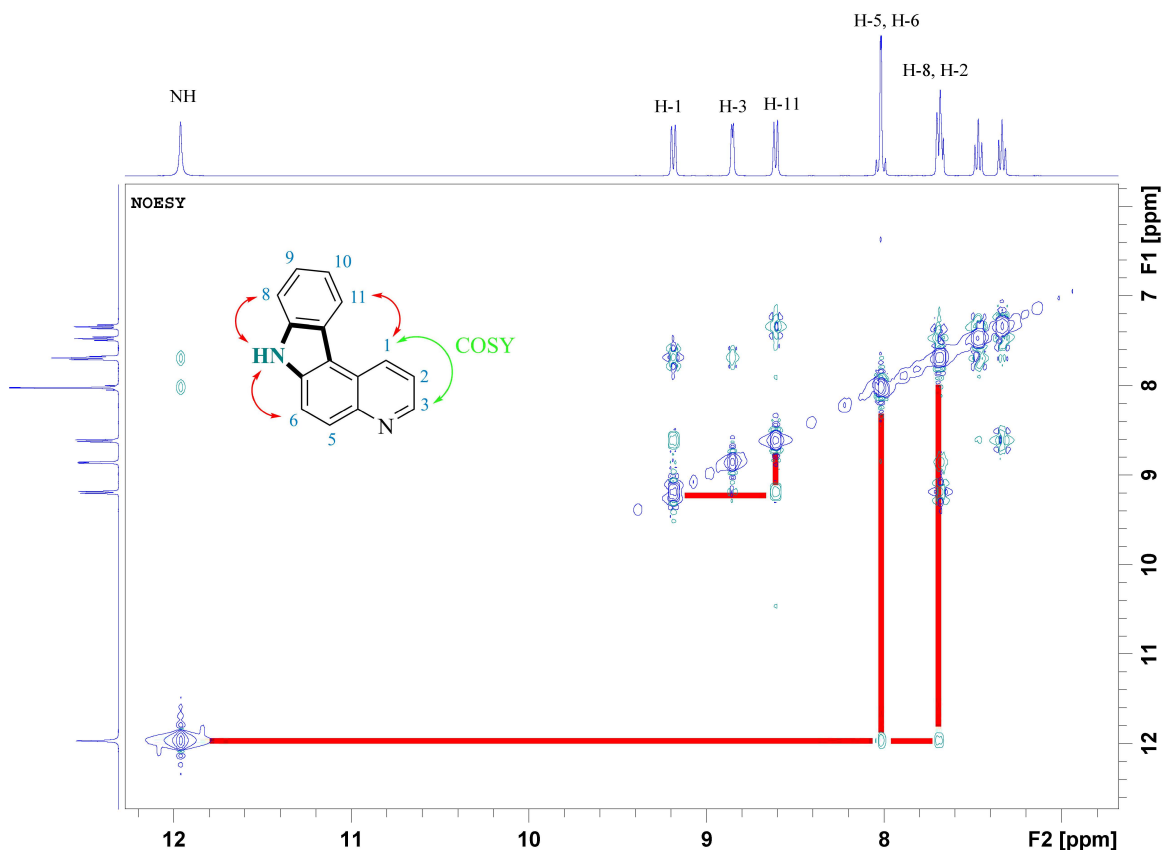
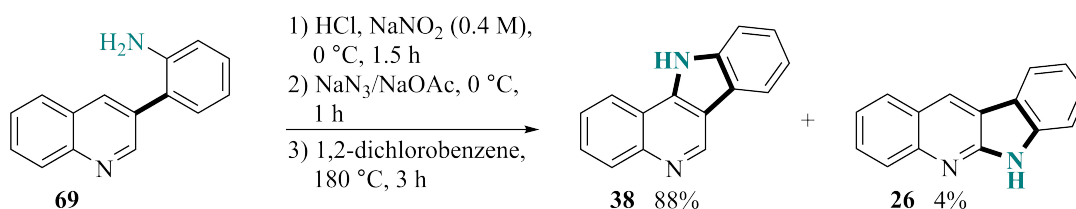


Figure 2.5: NOESY correlation confirming the structure of pyridocarbazole **61**.

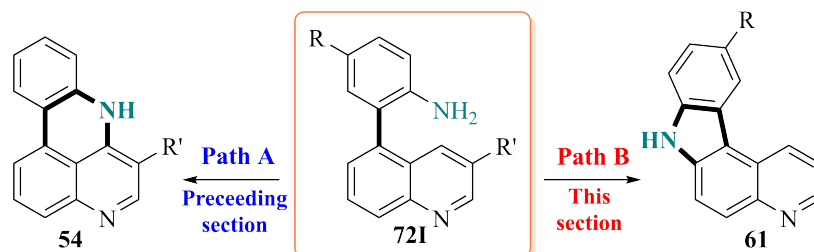
As the thermolysis of aryl azides are believed to proceed *via* the formation of a reactive singlet nitrene species, no direct comparison between this result and the palladium-catalyzed formation of pyridophenanthridine **54** can be made. Nevertheless, this result highlights the important role a metal catalyst has on the outcome of a reaction. Intrigued by the assembly of pyridocarbazole **61**, the approach was also applied to synthesize isocryptolepine precursor **38** in excellent yield (Scheme 18). While Timári and coworkers reported indoloquinoline **38** to be the sole product of the reaction, 4% of its regioisomer, quinindoline (**26**), was also observed.



Scheme 18: Synthesis of indoloquinolines **38** and **26** *via* installation of an azido moiety followed by thermal decomposition.^[149]

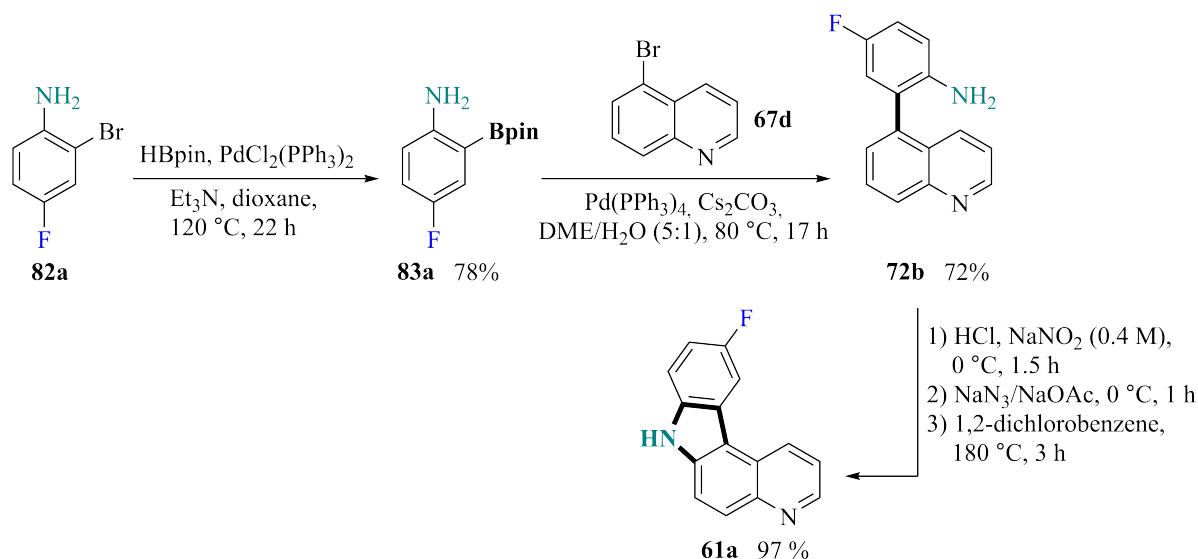
Having discovered conditions which allowed for the formation of pyridocarbazole **61** from biaryl **72**, it was now possible to assemble both this scaffold along with pyridophenanthridine

54 from one common intermediate by using two different sets of reaction conditions, **Path A** and **Path B**, respectively (Scheme 19). Reaction procedures which can grant access to two compounds of interest from a common starting material or intermediate are highly sought after in synthetic chemistry, as they allow for more efficient access to desirable targets in an atom economic fashion.^[152]



Scheme 19: Divergent synthesis of pyridophenanthridine **54** and pyridocarbazole **61** from common intermediate **72I**.^[149]

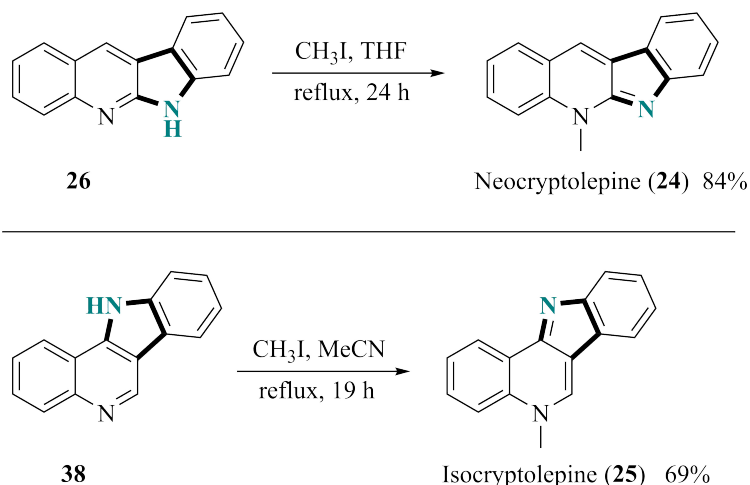
Wanting to also prepare some functionalized derivatives of novel pyridocarbazole **61**, a fluoro-substituted phenyl boronic acid pinacol ester was prepared using a standard Masuda borylation approach (Scheme 20). The obtained boronate was then treated with 5-bromoquinoline (**67d**) using our Suzuki-Miyaura cross-coupling protocol, furnishing biaryl **72b** in excellent yield. Subjecting biaryl **72b** to the diazotization-azidation-nitrene insertion strategy gave novel pyridocarbazole derivative **61a** in near quantitative yield, with no traces of the corresponding pyridophenanthridine observed in the reaction mixture.



Scheme 20: Synthesis of 10-fluoro-substituted pyridocarbazole **61a**.^[149]

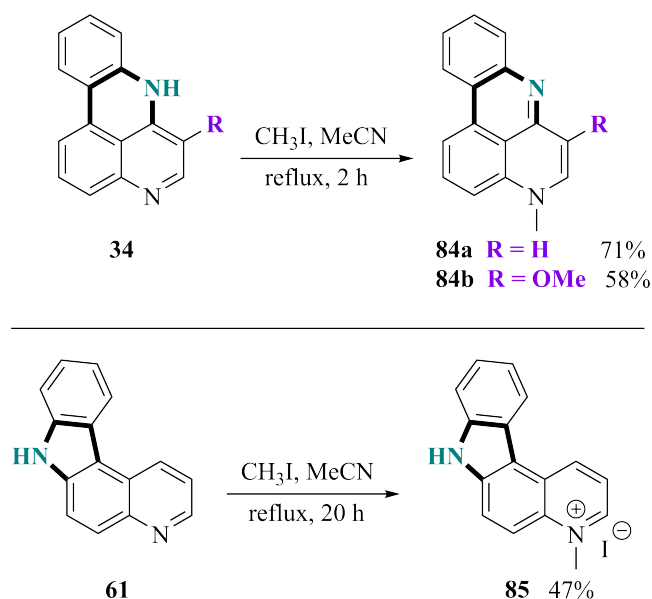
2.4 *N*-Methylations of tetracyclic compounds

Due to *N*-methyl groups being deemed instrumental to biological activities for indoloquinolines,^[72] a selection of the prepared tetracyclic ring systems were subjected to regioselective *N*-methylations as a natural conclusion to this project. Following a literature procedure, neocryptolepine (**24**) was furnished in excellent yield by treating quinindoline (**26**) with iodomethane in refluxing THF (Scheme 21).^[153] The natural product isocryptolepine (**25**) could be prepared in a similar way, however, using acetonitrile as the solvent, to give the target compound in good yield (Scheme 21).^[149] The *N*-methylation observed in these reactions follow a specific S_N2-type mechanism, known as the Menshutkin reaction. Here, an alkyl halide is reacting with a nucleophilic secondary amine, creating an alkylated quaternary ammonium salt as a reaction intermediate, which may be transformed into the free base under basic aqueous conditions.^[154]



Scheme 21: Synthesis of neocryptolepine (**24**) and isocryptolepine (**25**) via regioselective *N*-methylations.^[149]

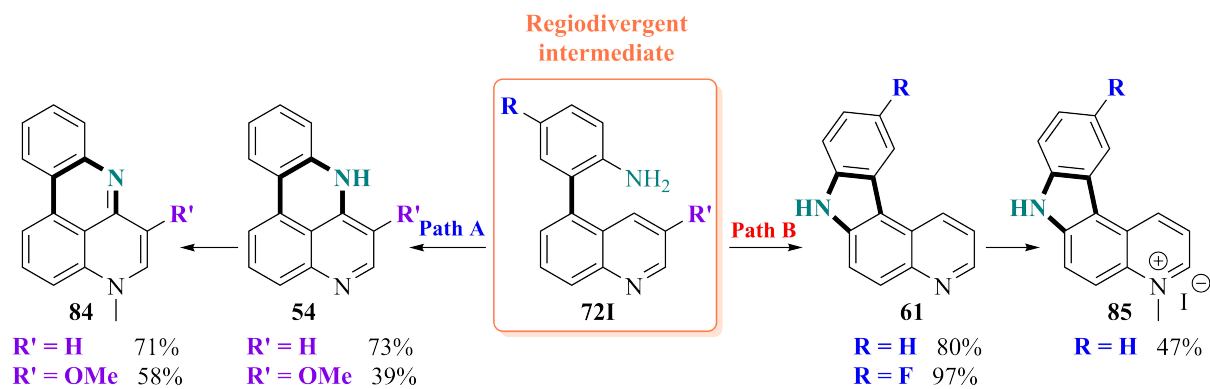
Regioselective *N*-methylation of novel pyridophenanthridines **34** proceeded smoothly, giving the desired products after a reaction time of 2 hours using the same conditions as for the construction of isocryptolepine (**25**) (Scheme 22). Clearly, the quinoline nitrogen of pyridophenanthridines are excellent nucleophiles, readily initiating attack on iodomethane. *N*-Methylation of pyridocarbazole **61** was more sluggish, resulting in only 47% of the target compound being obtained after refluxing the reaction mixture for 20 hours. The placement of the methyl group at the quinoline nitrogen of the compounds depicted in Scheme 22 was readily determined by analysis of their NMR spectra, in particular, examination of their NOESY and ¹H-¹³C HMBC correlations, respectively.



Scheme 22: *N*-Methylations of novel pyridophenanthridines **34** and pyridocarbazole **61**.^[149]

2.5 Summary and concluding remarks

Based on seminal work by Helgeland and Sydnnes,^[124] various tetracyclic ring-systems were prepared from commercially available bromoquinoline starting materials.^[132] The key synthetic strategies involved a Suzuki-Miyaura cross-coupling protocol followed by a palladium-catalyzed intramolecular cyclization reaction to give the target compounds in varying yields. During the Suzuki-Miyaura cross-coupling reactions to obtain biaryls **69-75**, two different protocols were employed, which demonstrated that the choice of catalyst to be vital to the success of the reactions rather than the inherent reactivity of the quinoline ring. While the palladium-catalyzed intramolecular cyclization procedure was excellent to assemble isocryptolepine precursor **38**, it failed to provide all the target tetracyclic systems. In several of the reactions, unwanted acetylation of the biaryl starting materials to yield acetanilides was observed, likely as a result of reaction between the solvent and the amino group. Most surprisingly, cyclization of biaryl **72** provided novel pyridophenanthridine **54** in excellent yield. Extensive efforts were devoted to discover the catalytic cycle of this reaction, however, they were ultimately unsuccessful. In an attempt to optimize the formation of novel pyridophenanthridine **54** using a diazotization-azidation-nitrene insertion approach, novel pyridocarbazole **61** was formed instead. This led to the realization that from common intermediate **72I**, regiodivergent synthesis of pyridophenanthridines **54** and pyridocarbazoles **61** were achievable using two different synthetic strategies (Scheme 23). To conclude this project, some selected tetracycles were subjected to *N*-methylations using a Menshutkin reaction, providing the corresponding *N*-methyl tetracycles in acceptable to excellent yields.^[149]



Scheme 23: Regiodivergent intermediate **72I** granting access to novel pyridophenanthridines **54** and pyridocarbazoles **61**.^[132,149]

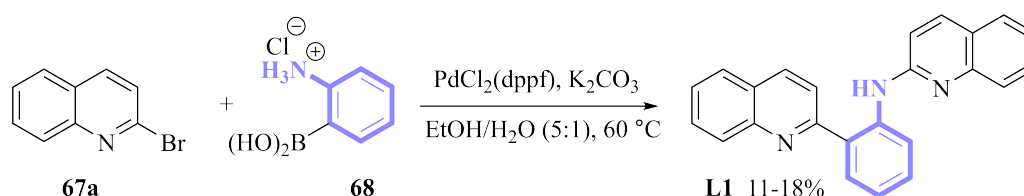
Chapter 3

Synthesis of quinoline and pyridine N,N,N ligands for catalysis

3.1 Introduction

3.1.1 Design of biquinoline ligands for catalysis

The unexpected formation of a biquinoline compound bridged by an aniline group, namely compound **L1**, during the attempted synthesis of biaryl **70** described in Chapter 2 (Scheme 11), opened up the possibility of exploring the chemistry surrounding this quinoline dimer (Scheme 24). One possible application of such a dimer, is the development of a nitrogen-donor chelating ligand for homogeneous and heterogeneous catalysis by complexing compound **L1** with transition metals. Heterocyclic nitrogen ligands are known to be capable of coordinating with a wide variety of metal centers due to their inherent Lewis basic properties. Consequently, in the past few decades, there has been a drastic increase in the popularity of nitrogen-containing ligands for the catalysis of various reactions.^[155,156]



Scheme 24: The unexpected formation of a biquinoline compound bridged by aniline **L1** during the synthesis of biaryl **70** as detailed in Chapter 2.

Some of the most widely studied nitrogen-donor ligands contain a pyridine ring, however, quinoline-based ligands have also received attention in recent literature,^[157,158] though to a lesser extent than their pyridine counterparts. Perhaps the most utilized classes of nitrogen ligands for catalysis are those based around the 2,2'-bipyridine (**86**), 2,2'-biquinoline (**87**) and the 1,10-phenanthroline (**88**) scaffolds (Figure 3.1).^[156,159] These compounds have been found to be capable of coordinating to a range of transition metals, such as cobalt, copper, ruthenium, rhodium, palladium and platinum. Further, the complexes containing such nitrogen-donor ligands have found applications as catalysts for cyclopropanations, allylic substitutions, various C-C and C-N cross-coupling reactions, addition reactions, among others.^[155]

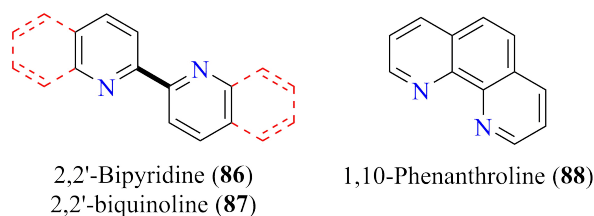
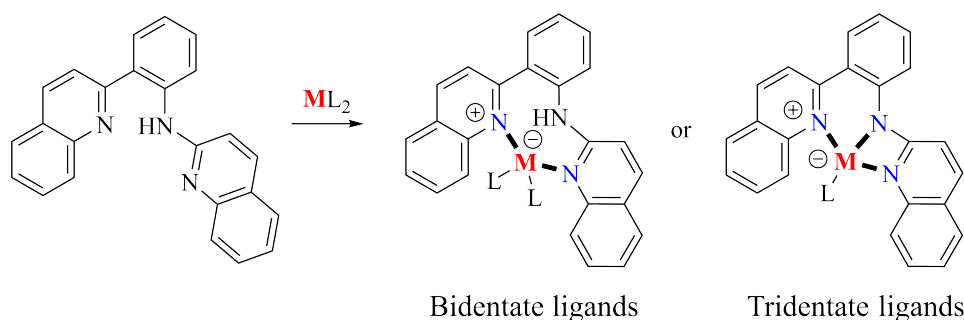


Figure 3.1: Nitrogen-donor chelating ligands 2,2'-bipyridine (**86**), 2,2'-biquinoline (**87**) and 1,10-phenanthroline (**88**).^[155,159]

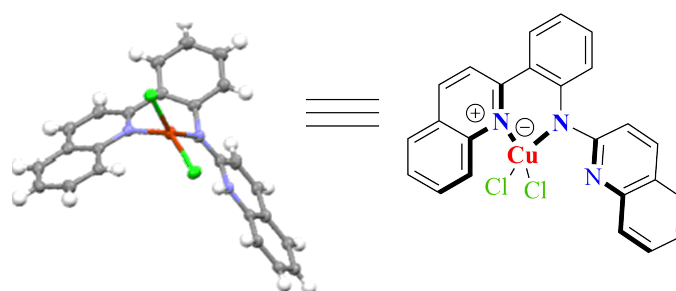
With this in mind, it was envisaged that the prepared biquinoline **L1** could be reacted with a transition metal salt, ML_2 , to give rise to both bidentate and tridentate complexes (Scheme

25). It should be mentioned that a bidentate ligand can have more coordination modes than the one depicted in Scheme 25, however, evaluation of all possible coordination modes is beyond the scope of this thesis.



Scheme 25: Imagined bidentate and tridentate ligands possible to construct from biquinoline **L1**.

Through a collaboration with Dr. Eugene Khaskin's group located at Okinawa Institute of Science and Technology (OIST), Coordination Chemistry and Catalysis Unit, Okinawa, Japan, a brief proof-of-concept study was conducted to ascertain the ability of biquinoline **L1** to form transition metal complexes. By treating biquinoline **L1** with copper(II) chloride, a green solid was formed, which following recrystallization was revealed to be a bidentate copper complex (Figure 3.2). Subsequently, biquinoline **L1** was complexed with various other transition metal salts and employed as a catalyst for certain transformations. The preliminary results of these studies conducted by Khaskin's group show great promise, and the first set of results are currently being prepared for publication. In the following section, two other potential applications for the novel biquinoline scaffold are briefly described.



Conducted by Eugene Khaskin's group at OIST

Figure 3.2: Proof-of-concept shown by complexing compound **L1** with $CuCl_2$ to give its corresponding bidentate copper complex as revealed by its X-ray crystal structure. Complexation and preparation of the sample for X-ray analysis conducted by Eugene Khaskin's group. Used with permission.

3.1.2 Potential applications

Development of metal organic frameworks (MOFs) viable for CO₂ capture

In the past, metal organic frameworks (MOFs) containing heteroaromatics in their organic backbones have shown promise as a means of capturing and storing atmospheric CO₂.^[160] With atmospheric CO₂ levels being at a historic high, the European Union (EU) has set a target of achieving a reduction of 40% in carbon emissions by the year 2030. In addition to being useful within catalysis, biquinoline **L1** could have the potential to be developed into the organic backbone of a MOF which might be capable of capturing atmospheric CO₂. Recently, Qian, Hu and Huang described the preparation of an iridium(III)-coordinated biquinoline MOF, which they demonstrated to selectively adsorb CO₂ (Figure 3.3).^[161]

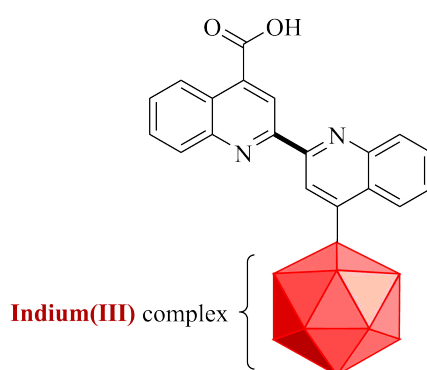


Figure 3.3: The organic backbone of a biquinoline-based indium(III) MOF capable of capturing CO₂ as described by Qian, Hu and Huang.^[161]

Development into photoactivated chemotherapy (PACT) agents

As explained in Section 1.3.1, the development of novel cancer treatments are of paramount importance. A new strategy which has gained attention in recent years, is photoactivated chemotherapy (PACT), in which an inactive drug can be placed near a tumor and then be activated by light.^[162] This allows for more target specific treatments of patients with cancer, as traditional chemotherapy regimens often affect the whole body, causing severe side effects. It is believed that PACT drugs work by ligand photosubstitution, creating an active drug. Then, through interaction with biomolecules, the activated compound causes cell death. In order to be a good candidate for a PACT agent, three main criteria have to be considered: 1) the metal complex needs to be stable in solution in darkness, 2) it needs to be photoactivatable and 3) it needs to display an increase in cytotoxicity following photoactivation. Polypyridyl ruthenium complexes are known for their unique photochemical properties,^[163] and several such complexes have been investigated as potential PACT drugs. One such example is the polypyridyl ruthenium complex prepared by Bonnet and coworkers (Figure 3.4).^[162] Upon testing, the prepared complex was found to fulfill the three criteria for making a good PACT drug candidate. The complex has two quinolyls bridged by an amine, which is somewhat similar to biquinoline

L1 which was prepared in our laboratories. This opens up the possibility that biquinoline **L1** could have potential as a PACT agent, though no studies into this has been conducted thus far.

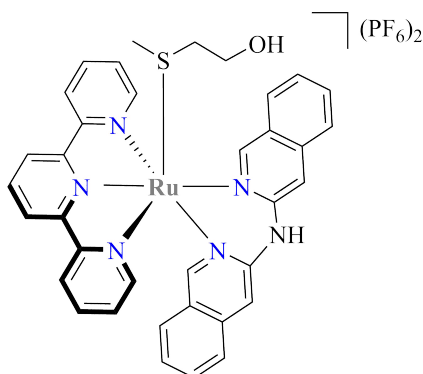


Figure 3.4: Structure of a ruthenium-based biquinoline chelate applicable as a PACT agent.^[162]

3.1.3 Project aims

In collaboration with Dr. Eugene Khaskin at OIST, we designed a total of five quinoline and pyridine *N,N,N* ligands that were of great interest as ligands in their catalytic work. Thus, the aim of this project was to synthesize and detail the synthetic endeavours into five different quinoline and pyridine ligands (Figure 3.5). These can be divided into two categories: ligands with either an aniline (**L1-L3**) or an *N*-methylaniline linker (**L4** and **L5**). Upon having synthesized the target compounds, they would then be sent to OIST for complexation and evaluation of the complexes ability to catalyze some selected reactions.

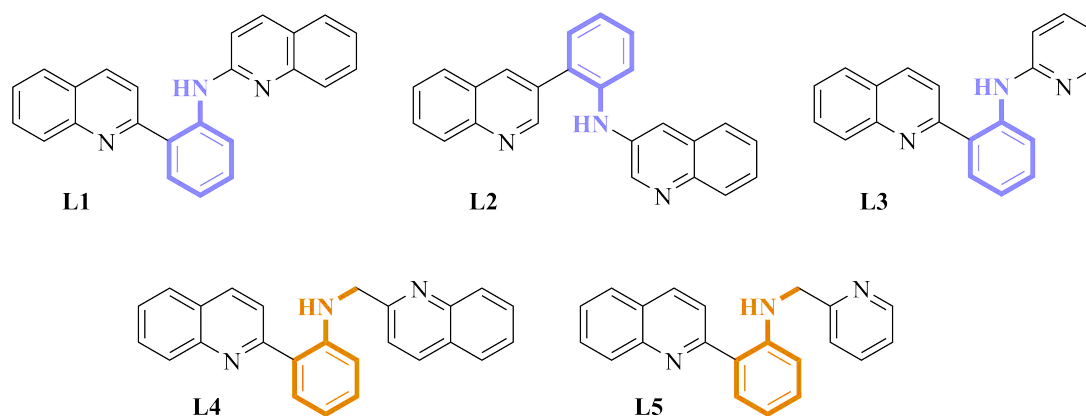


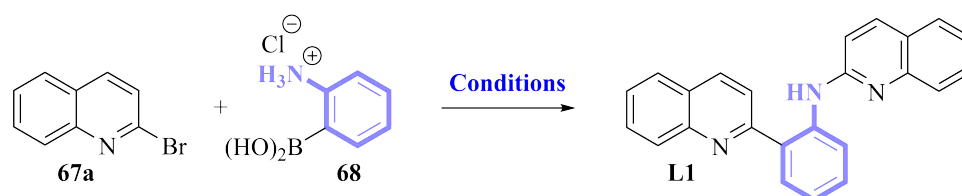
Figure 3.5: Five intended target compounds for this project.

3.2 Synthesis of the quinoline/pyridine N,N,N ligands

3.2.1 Synthesis of quinoline/pyridine N,N,N ligands with an aniline bridge

The unexpected formation of **L1** was hypothesized to be a result of a one-pot sequential Suzuki-Miyaura cross-coupling and a Buchwald-Hartwig amination reaction. As the yield of formation of **L1** was poor, efforts were made to optimize this sequence (Table 3.1). Finding conditions which allowed for both transformations to proceed smoothly proved to be exceedingly difficult, with the highest obtained yield for the target compound remaining at 18%. One-pot cascade reactions such as this has been investigated in the literature, and it has been determined that to find a catalyst which efficiently catalyzes two vastly different catalytic processes, such as the Suzuki-Miyaura cross-coupling reaction and the Buchwald-Hartwig amination, proceeding through different transition states, to be especially demanding.^[164]

Table 3.1: Attempts at optimizing the of constructing **L1** from 2-bromoquinoline (**67a**) and 2-aminophenylboronic acid hydrochloride (**68**) in a one-pot fashion.



Entry	Catalyst	Ligand	Solvent	Base	Temp. (°C)	Yield (%)
1	PdCl ₂ (dppf)	-	EtOH/H ₂ O ^a	K ₂ CO ₃	60	18
2	Pd ₂ (dba) ₃	IMes	Dioxane	<i>t</i> -BuOK	100	17 ^b
3	PdCl ₂ (dppf)	-	EtOH/H ₂ O ^a	K ₂ CO ₃	60	18 ^c
4	PdCl ₂ (dppf)	-	EtOH/H ₂ O ^a	Cs ₂ CO ₃	60	17 ^d
5	Pd(PPh ₃) ₄	-	Dioxane	<i>t</i> -BuOK	100	9 ^e

^a5:1 mixture; ^bAs a mixture of desired product **L1** and biaryl **70** in a 17:83 ratio as determined by their ¹H NMR integrals; ^cMicrowave; ^dAs a mixture of desired product **L1** and biaryl **70** in a 56:44 ratio as determined by their ¹H NMR integrals; ^eAs a mixture of desired product **L1** and homocoupled compound **87** in a 9:91 ratio as determined by their ¹H NMR integrals.

Discouragingly, the aforementioned attempts were more successful at generating the homocoupled byproduct 2,2-biquinoline (**87**) than the desired quinoline dimer **L1**, which was often obtained in a mixture with 2-bromoquinoline (**67a**). Despite obtaining a mixture of two compounds, comparison of the ¹H NMR spectra with a pure sample of 2-bromoquinoline (**67a**) allowed for easy identification of biquinoline **87** *via* observation of some key signals, namely H-3, H-4 and H-8 (Figure 3.6). Characteristically, there was a significant downfield shift in these signals compared to those of 2-bromoquinoline (**67a**). Additional comparison of the observed chemical shifts of biquinoline **87** with reported literature data further indicated this to indeed be the observed compound.^[165]

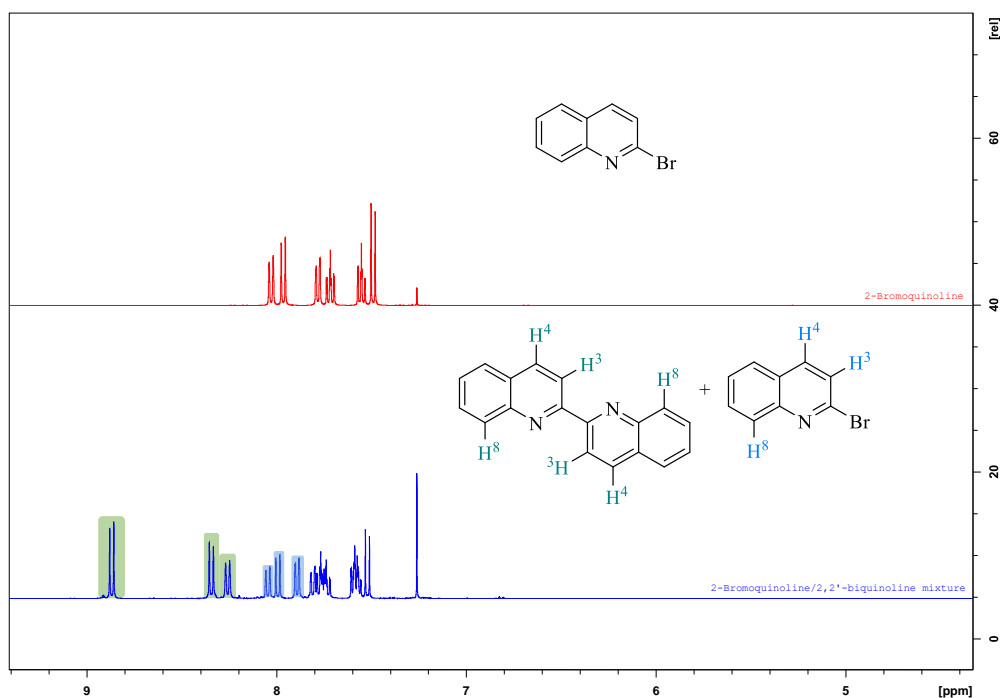
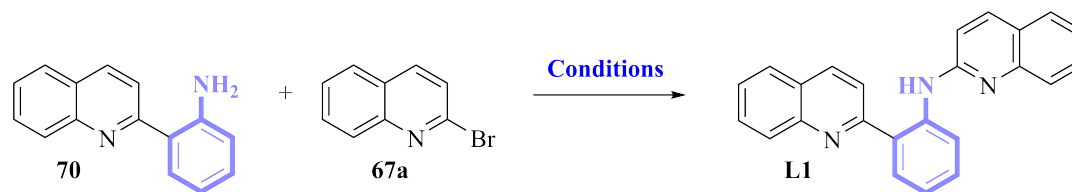


Figure 3.6: ^1H -NMR spectra of 2-bromoquinoline (**67a**) (red) and a 2-bromoquinoline (**67a**)/2,2'-biquinoline (**87**) mixture (blue) in CDCl_3 . The key signals located at H-3, H-4 and H-8 of the biquinoline **87** are highlighted along with H-3, H-4 and H-8 of 2-bromoquinoline (**67a**).

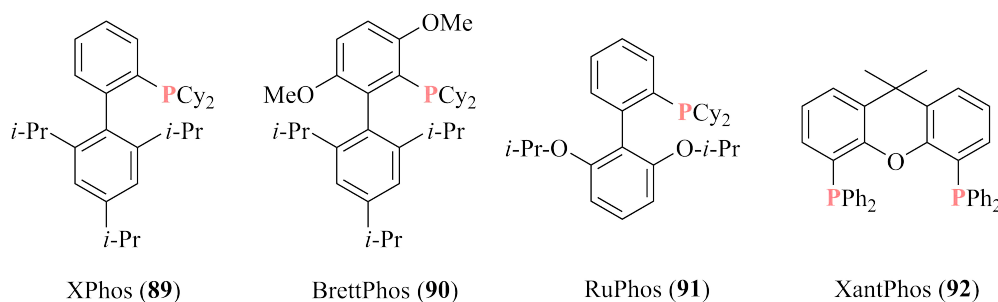
Having already uncovered excellent conditions for the synthesis of biaryl **70**, this compound was then utilized as the starting material in an effort to optimize the Buchwald-Hartwig amination step of the reaction (Table 3.2). Using the same conditions as in the one-pot procedure with Cs_2CO_3 as the base instead of K_2CO_3 , gave a slight increase in yield (Table 3.2, Entry 3), while switching to the weaker base Na_2CO_3 gave no product formation (Table 3.2, Entry 5). Similar results were obtained when employing the powerful base lithium bis(trimethylsilyl)amide (LiHMDS) in THF and tris(dibenzylideneacetone)dipalladium(0) ($\text{Pd}_2(\text{dba})_3$) as the catalyst, giving no traces of the desired product (Table 3.2, Entry 4). A common set of conditions to carry out a Buchwald-Hartwig amination reaction is the use of $\text{Pd}_2(\text{dba})_3$, the bidentate phosphine ligand XantPhos (structure depicted in Figure 3.7) and Cs_2CO_3 in anhydrous THF.^[166] Carrying out the reaction using these conditions delightfully provided the target compound in 80% yield following purification by silica gel column chromatography. Switching the ligand to the monodentate phosphorous ligand RuPhos (Figure 3.7), gave similar results, with **L1** being formed in 78% yield (Table 3.2). Due to the slightly lower cost of commercial XantPhos, these conditions would be used as a standard for the subsequent amination reactions.

Table 3.2: Optimization efforts towards the Buchwald-Hartwig amination between biaryl **70** and 2-bromoquinoline (**67a**) to give ligand **L1**.

Entry	Catalyst	Ligand	Solvent	Base	Temp. (°C)	Yield (%)
1	Pd(OAc) ₂	-	Dioxane	<i>t</i> -BuOK	100	Traces ^a
2	Pd(OAc) ₂	XPhos	PhMe	<i>t</i> -BuOK	80	N/A ^b
3	PdCl ₂ (dppf)	-	EtOH/H ₂ O ^c	Cs ₂ CO ₃	60	20
4	Pd ₂ (dba) ₃	BrettPhos	THF	LiHMDS	65	N/A ^d
5	PdCl ₂ (dppf)	-	EtOH/H ₂ O ^c	Na ₂ CO ₃	60	Traces ^d
6	Pd ₂ (dba) ₃	RuPhos	THF	Cs ₂ CO ₃	reflux	78
7	Pd ₂ (dba) ₃	XantPhos	THF	Cs ₂ CO ₃	reflux	80

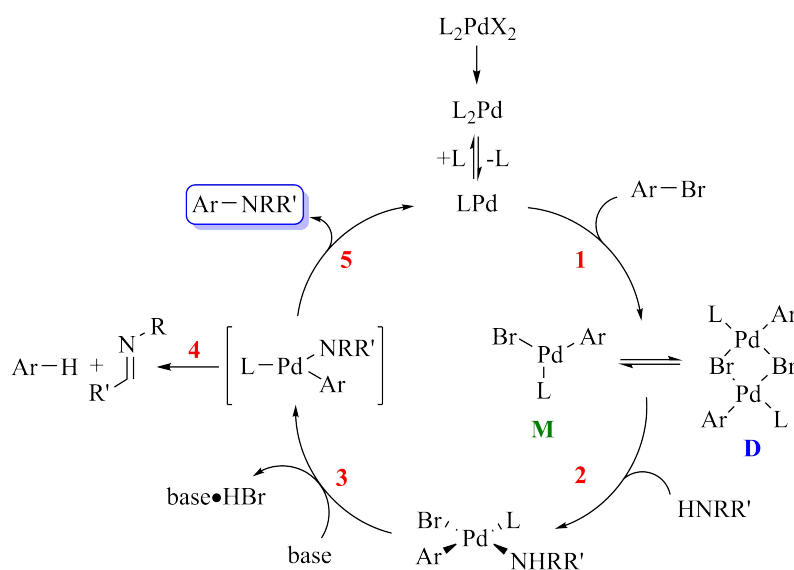
^aAs a mixture of desired product **L1** and biaryl **70**; ^bNo purification as the crude ¹H NMR showed only unreacted starting material and traces of homocoupled product **87**; ^c5:1 mixture; ^dNo workup as crude ¹H NMR showed no reaction.

The Buchwald-Hartwig amination is considered as one of the most powerful approaches available for the formation of C(sp²)-N bonds. The reaction is based on pioneering work done by Buchwald and Hartwig and is defined as the palladium-catalyzed coupling reaction between aryl (pseudo)halides and amines. The method is revered for its broad substrate scope and functional group tolerance, with the possibility of fine-tuning the reaction outcomes by the use of different ligands.^[167] Phosphine-based bidentate ligands are overrepresented in Buchwald-Hartwig amination protocols due to showing excellent efficacy when applied. Some notable phosphine-based ligands commonly employed are XPhos (**89**), BrettPhos (**90**) and the previously mentioned RuPhos (**91**) and XantPhos (**92**) (Figure 3.7).

**Figure 3.7:** Structures of the phosphine ligands XPhos (**89**), BrettPhos (**90**), RuPhos (**91**) and XantPhos (**92**).

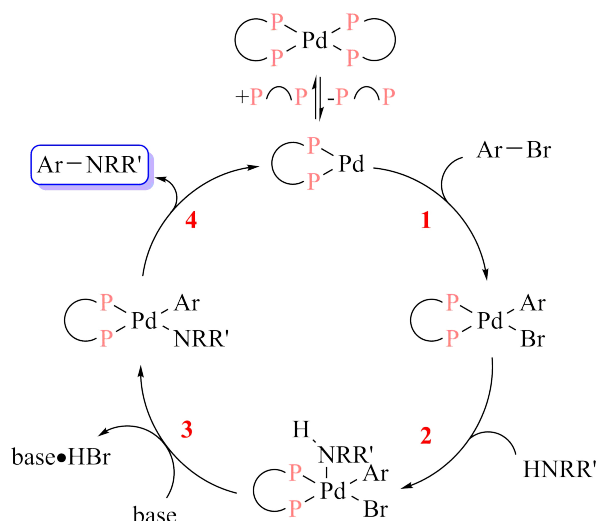
Ever since its conception, the catalytic cycle of the Buchwald-Hartwig amination has been extensively studied.^[168] Interestingly, the catalytic cycle of the reaction has been revealed to

proceed differently based on the nature of the employed ligand. The catalytic cycle which has been proposed for monophosphine ligands, such as RuPhos (**91**), is initiated by the oxidative addition **1** of an aryl halide to a Pd⁰ complex.^[167,169] This creates dimeric species **D**, existing in an equilibrium with its monomer **M**, which through substrate coordination **2** creates a monomeric palladium complex. This complex then undergoes deprotonation **3** to give an amido complex. From this complex, two possible transformations are possible, firstly, it may undergo β-H elimination **4** to give the corresponding elimination products. Alternatively, the amido complex may undergo reductive elimination **5** to furnish the coupled aniline product and subsequent regeneration of the palladium catalyst to complete the catalytic cycle.



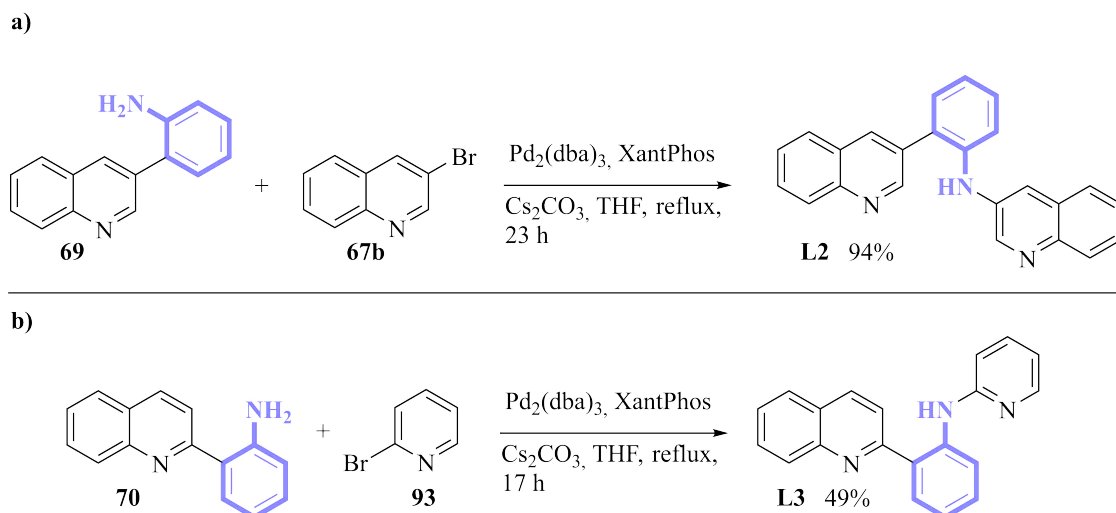
Scheme 26: Proposed catalytic cycle for the Buchwald-Hartwig amination using monophosphine ligands; **1** = oxidative addition, **2** = substrate coordination, **3** = deprotonation = **4** = β-H elimination, **5** = reductive amination.^[167,169]

By utilizing bidentate phosphine ligands with electron-rich, sterically demanding phosphines, the unwanted elimination products occurring as a result of β-H elimination can be avoided.^[170] The catalytic cycle using a biphosphine ligand is proposed to largely follow the same major steps as for the monodentate ligands, namely oxidative addition **1**, substrate coordination **2**, deprotonation **3** and reductive elimination **4** (Scheme 27).^[167]



Scheme 27: Proposed catalytic cycle for the Buchwald-Hartwig amination using biphosphine ligands; **1** = oxidative addition, **2** = substrate coordination, **3** = deprotonation, **4** = reductive elimination.^[167,170]

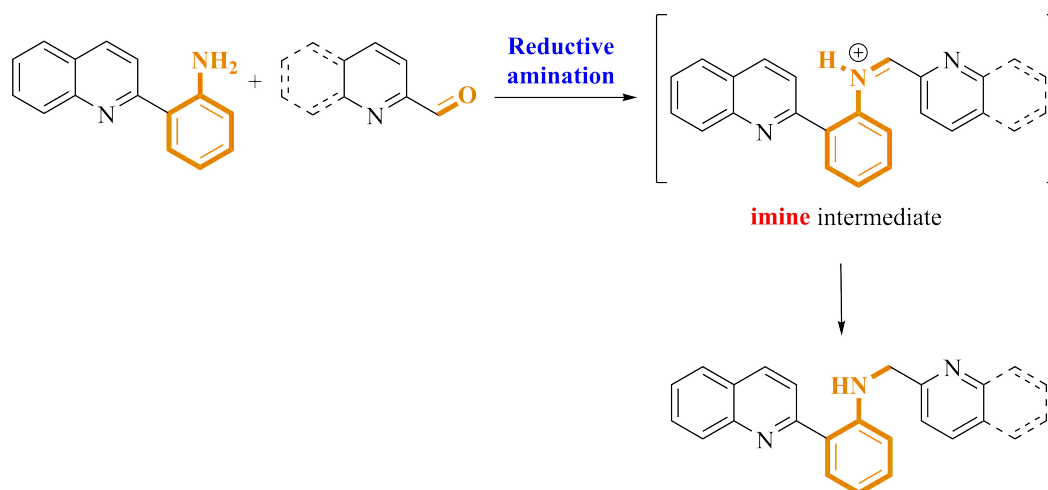
Applying the optimized Buchwald-Hartwig amination conditions (Table 3.2, Entry 7) allowed for the successful construction of ligands **L2** and **L3** from their corresponding biaryls and the relevant heteroaryl halides (Scheme 28). The formation of ligand **L2** was particularly impressive, with a yield of 94% following purification by silica gel column chromatography being obtained when conducting the reaction on a scale of several grams (Scheme 28a). The modest yield obtained for **L3** was somewhat puzzling, as 2-halopyridines are generally considered as excellent electrophilic coupling partners,^[171] more so than their haloquinoline counterparts. Moreover, it appeared that the reaction never went to completion, as the TLC analysis, along with crude ¹H NMR, showed the presence of both starting materials despite allowing the reaction run for up to 48 hours. During the purification of ligand **L3**, 17% unreacted biaryl **70** was also recovered and whilst other fractions contained 2-bromopyridine (**93**) mixed with dba from the catalyst. Nonetheless, attempts at optimizing the yield of formation for ligand **L3** was not undertaken.



Scheme 28: Synthesis of ligands **L2** and **L3** using the optimized Buchwald-Hartwig amination conditions.

3.2.2 Synthesis of quinoline/pyridine *N,N,N* ligands with an *N*-methylaniline bridge

To prepare ligands **L4** and **L5**, reductive amination was chosen as the synthetic strategy over *N*-alkylation (Scheme 29). While *N*-alkylation are widely used in synthetic chemistry and is generally considered as a reliable method to synthesize a variety of compounds, overalkylations remain overrepresented. A way to bypass this issue is the use of *N*-protecting groups, however, this adds an additional two steps to any synthetic pathway,^[172] making this option less attractive. As both the required quinoline and pyridine carboxaldehydes were commercially available at low costs, the reductive amination procedure appeared to be a more feasible option.

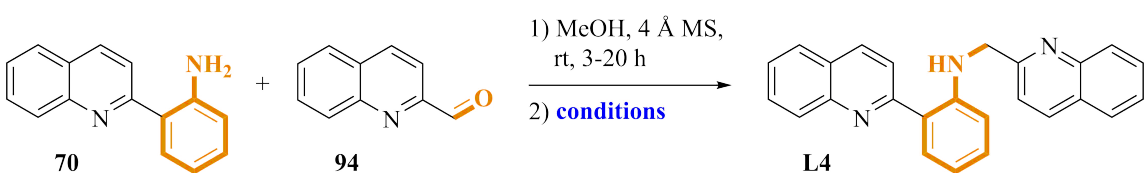


Scheme 29: Reductive amination as a synthetic strategy to furnish ligands **L4** and **L5**.

The preparation of ligand **L4** commenced by carrying out a one-pot reductive amination protocol where biaryl **70** was treated with aldehyde **94** in methanol using 4 Å molecular sieves

(MS) to remove water. The formation of an imine was verified by TLC-LRMS, showing a mass corresponding to the desired intermediate. Subjecting the imine to a standard reduction using $\text{Na}(\text{OAc})_3\text{BH}$ in 1,2-dichloroethane (DCE) with the addition of AcOH as an activator^[173] provided target compound **L4** in poor yield (Table 3.3, Entry 1). Attempts at improving the yield by prolonging the reaction time had no impact on the yield of formation for ligand **L4**. By changing the reducing agent to NaBH_4 resulted in only traces of the desired compound being observed on the crude ^1H NMR spectrum. Wanting to avoid using the exceedingly toxic, but highly efficient, reducing agent NaBH_3CN ,^[173] to prepare the missing ligand, other avenues were explored. Reduction of the imine using palladium on carbon under a hydrogen atmosphere was attempted, giving a meager 6% yield of ligand **L4** (Table 3.3)

Table 3.3: Optimization of the reductive amination to form ligand **L4**.



Entry	Reducing agent	Solvent	Activator	Temp. (°C)	Time (h)	Yield (%)
1	$\text{Na}(\text{OAc})_3\text{BH}$	DCE	AcOH	rt	0.5	29
2	NaBH_4	MeOH	-	rt	20	Traces ^a
3	Pd/C , H_2	MeOH	-	rt	4	6
4	Raney-Ni, H_2	MeOH	-	rt	17	Traces ^a
5	Raney-Ni, H_2	MeOH	-	rt	3	23
6	NaBH_3CN	MeOH	AcOH	0	1.5	72
7	NaBH_3CN	MeOH	AcOH	0	0.3	78

^aDetermined by the crude ^1H NMR spectrum.

Raney-Nickel is generally considered to be capable of reducing a wider selection of functional groups than Pd/C ^[174] and utilizing this strategy, up to 23% yield of the target compound was formed (Table 3.3, Entry 5). However, the Raney-Nickel proved to be a too powerful reagent, and allowing the reaction to run for 17 hours lead to the presumed reduction of the quinoline rings in addition to the imine as determined by TLC-LRMS. The two observed masses is tentatively identified as the protonated mass of a reduction of the carbons adjacent to the nitrogen atom of both quinoline rings ($[\text{M} + \text{H}^+] \approx 366$) and a reduction of the entire pyridine unit within both quinoline rings ($[\text{M} + \text{H}^+] \approx 370$) (Figure 3.8).

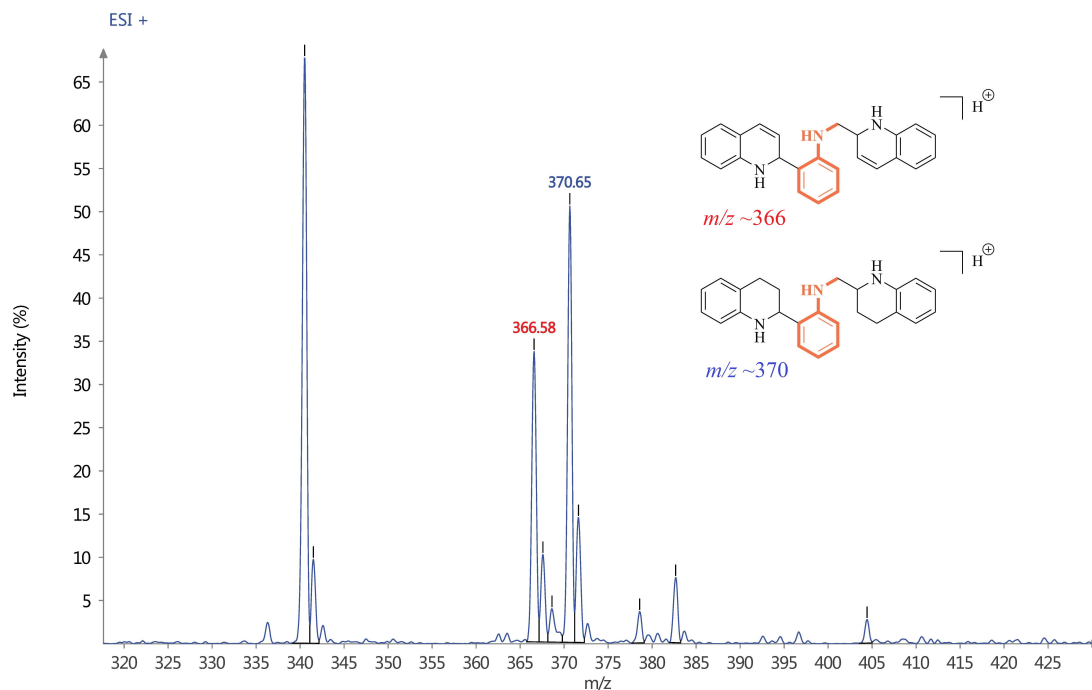
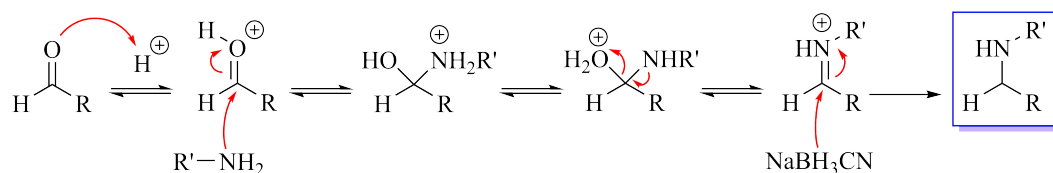


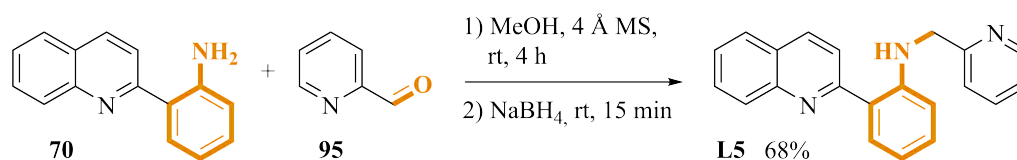
Figure 3.8: Tentative identification of unwanted reduction products based on the observed masses on the TLC-LRMS during the reductive amination to prepare ligand **L4** using Raney-Nickel.

Unsurprisingly, attempting the reduction using NaBH_3CN in methanol allowed for the formation of ligand **L4** in very good yield (Table 3.3, Entries 6 and 7), showing the superior performance of this particular reagents capabilities as a reducing agent. The mechanism for the reductive amination of aldehydes and ketones using borohydrides is only partly understood. The first step in the reaction involves the protonation of the carbonyl oxygen by the activator, increasing the electrophilicity of the carbonyl carbon (Scheme 30).^[173] Then, nucleophilic attack by the amine results in the formation of a hemiaminal, which following a hydrogen transfer leads to the loss of a unit of water. The resulting imine is then subsequently exposed to a hydride anion from the borohydride to give the desired amine product. It is only the details surrounding how the hydride transfer from the borohydride to the amine occurs which is the uncertain aspect of the mechanism.^[175] Despite this, several transition states have been proposed in the years following the widespread usage of borohydrides as reducing agents. One proposal, which is supported by *ab initio* molecular dynamics calculations, suggests that the hydride transfer is preceded by the formation of a unique transition state. Firstly, the NaBH_4 dissolved in methanol presumably exists as a contact ion pair, with three units of methanol stabilizing the sodium cation. Sodium is moreover interacting with the carbonyl oxygen, while the borohydride anion is coordinating to both the sodium cation and the substrate, facilitating the hydride transfer.^[175]



Scheme 30: Proposed reaction mechanism for the reductive amination of aldehydes with NaBH_3CN .^[173]

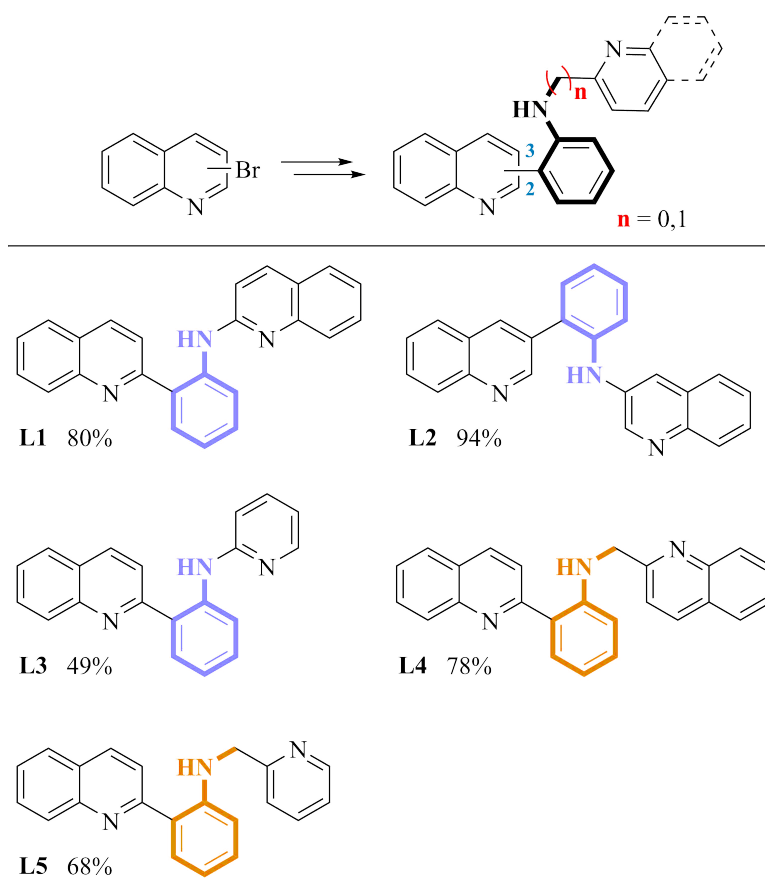
To synthesize the final target product, ligand **L5**, a classical imine formation-reductive sequence was employed. Using NaBH_4 in methanol furnished **L5** in good yield following purification by silica gel column chromatography (Scheme 31). Despite the yield being lower than for ligand **L4**, a 68% yield was satisfactory enough to forego any optimization attempts.



Scheme 31: Synthesis of ligand **L5** using a classical reductive amination protocol.

3.3 Summary and concluding remarks

Through a collaborative effort with Dr. Eugene Khaskin's group at OIST, five novel quinoline and pyridine *N,N,N* ligands were designed and synthesized (Scheme 32). In addition to being employed as catalysts, it is imagined that the designed scaffolds could find applications as MOFs for CO_2 capture as well as development into a PACT drug. The designed compounds can be divided into two categories, where the quinoline/pyridine unit is bridged by either an aniline or an *N*-methylaniline moiety. The three aniline bridged systems were prepared using an optimized Buchwald-Hartwig amination protocol to furnish ligands **L1-L3** in good to excellent yields following purification. To synthesize the two *N*-methylaniline bridged ligands, reductive amination was chosen as the most appropriate strategy, which following reaction optimizations gave the target ligands **L4** and **L5** in good to excellent yields.



Scheme 32: Summary of the prepared nitrogen-donor ligands **L1-L5**.

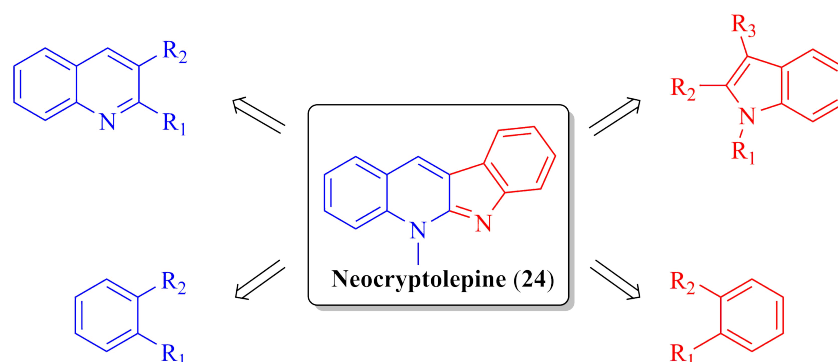
Chapter 4

Synthesis of neocryptolepines using a novel cascade protocol

4.1 Introduction

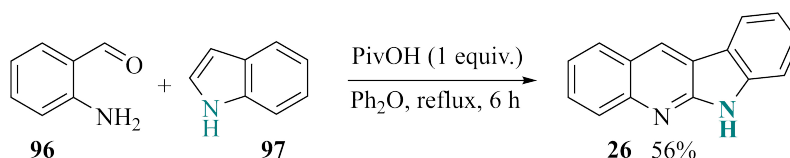
4.1.1 Synthesis of neocryptolepine in recent literature

Similarly to the synthesis of isocryptolepine (**25**) and its regioisomers as discussed in Chapter 2, neocryptolepine (**24**) can be constructed using the same synthetic techniques, with the most common strategies involving functionalized quinolines, indoles or other aryl based starting materials (Scheme 33). Neocryptolepine (**24**) has been the focus of several synthetic works previously and multiple reviews are available covering the endeavours.^[101,102,176,177] Herein, only the most recent and some notable examples will be discussed.



Scheme 33: Starting points for the most common synthetic approaches to neocryptolepine (**24**).

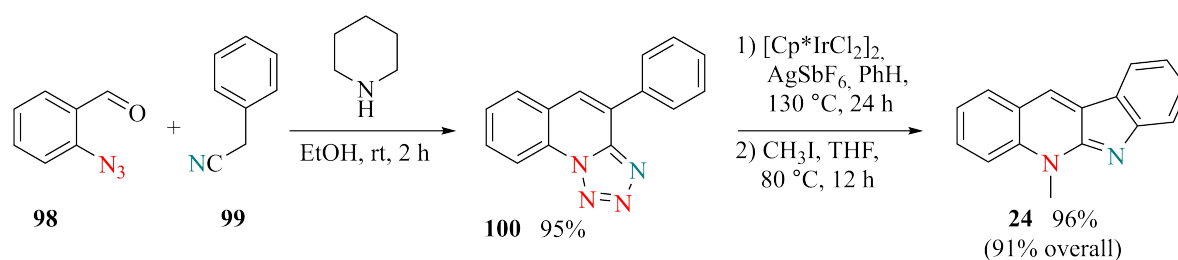
A common drawback in natural product synthesis is step-heavy synthetic routes, leading to low overall yields and poor transferability into commercialization.^[178] The neocryptolepine precursor, quinindoline (**26**), is accessible through a one-step synthesis as presented by Kadam and Tilve. Starting from *o*-aminobenzaldehyde (**96**) and indole (**97**), quinindoline (**26**) was prepared in 56% yield using a one-pot pivalic acid alkylation-dehydration-cyclization-aromatization sequence (Scheme 34). Despite their best efforts, the yield could not be further optimized using the aforementioned conditions. Nonetheless, attempts focusing on step-economy are valuable lessons for future synthetic endeavours of natural products and their derivatives.



Scheme 34: One-pot synthesis of quinindoline (**26**), the precursor to neocryptolepine (**24**), by Tilve and Kadam.^[179]

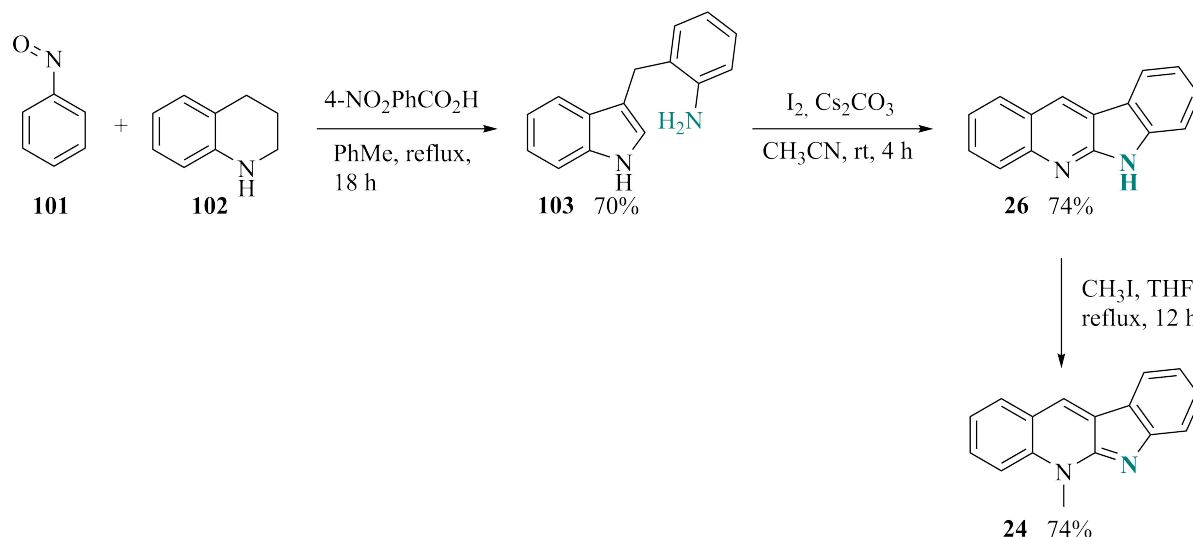
Utilizing an intramolecular denitrogenative transannulation/ $C(sp^2)$ -H amination of an arylated 1,2,3,4-tetrazole, Chattopadhyay and coworkers constructed neocryptolepine (**24**) in an

overall yield of 91% (Scheme 35).^[180] Assembly of the tetrazole intermediate was achieved by following an established literature procedure between 2-azidobenzaldehyde (**98**) and 2-phenylacetonitrile (**99**).^[181] The transannulation was then commenced by treating tetrazole **100** with pentamethylcyclopentadienyliridium(III) chloride dimer ($[\text{Cp}^*\text{IrCl}_2]_2$) and silver hexafluoroantimonate in refluxing benzene. Finally, *N*-methylation using iodomethane in THF was carried out to afford neocryptolepine (**24**).



Scheme 35: Synthesis of neocryptolepine (**24**) by Chattopadhyay's group.^[180]

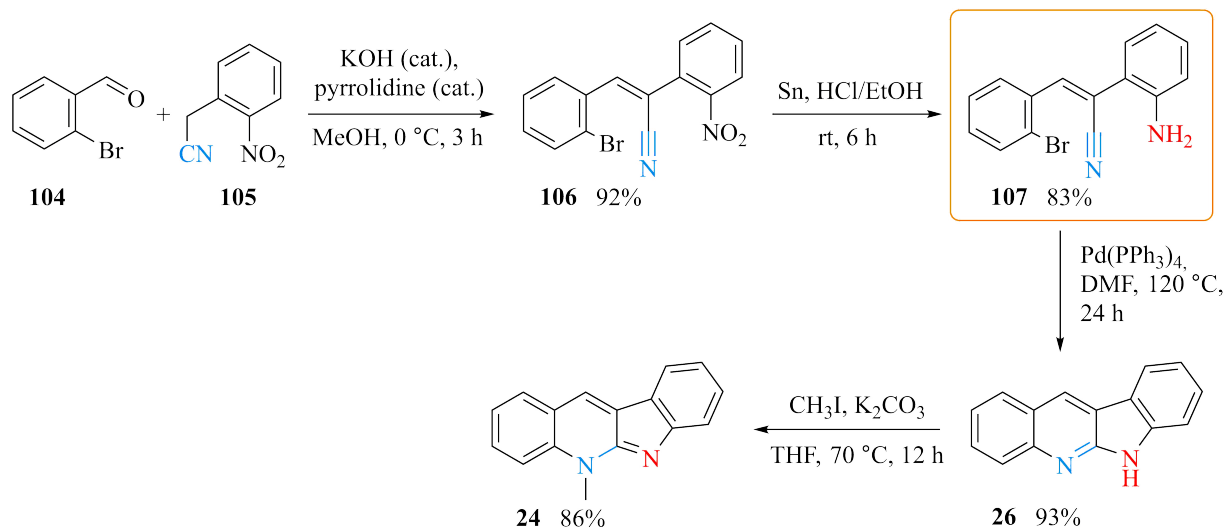
Jana and colleagues describe a novel approach for the construction of indoles by an acid-mediated annulation reaction between aliphatic amines and nitrosoarenes, a strategy which required no pre-functionalization steps. By treating nitrosobenzene (**101**) and tetrahydroquinoline (THQ) (**102**) with 4-nitrobenzoic acid in refluxing toluene, 3-substituted indole **103** could be formed in 70% yield (Scheme 36).^[182] Iodine mediated intramolecular amination yielded quinindoline (**26**) which was further *N*-methylated using iodomethane in THF to yield neocryptolepine (**24**).



Scheme 36: Synthesis of neocryptolepine (**24**) by Jana and coworkers.^[182]

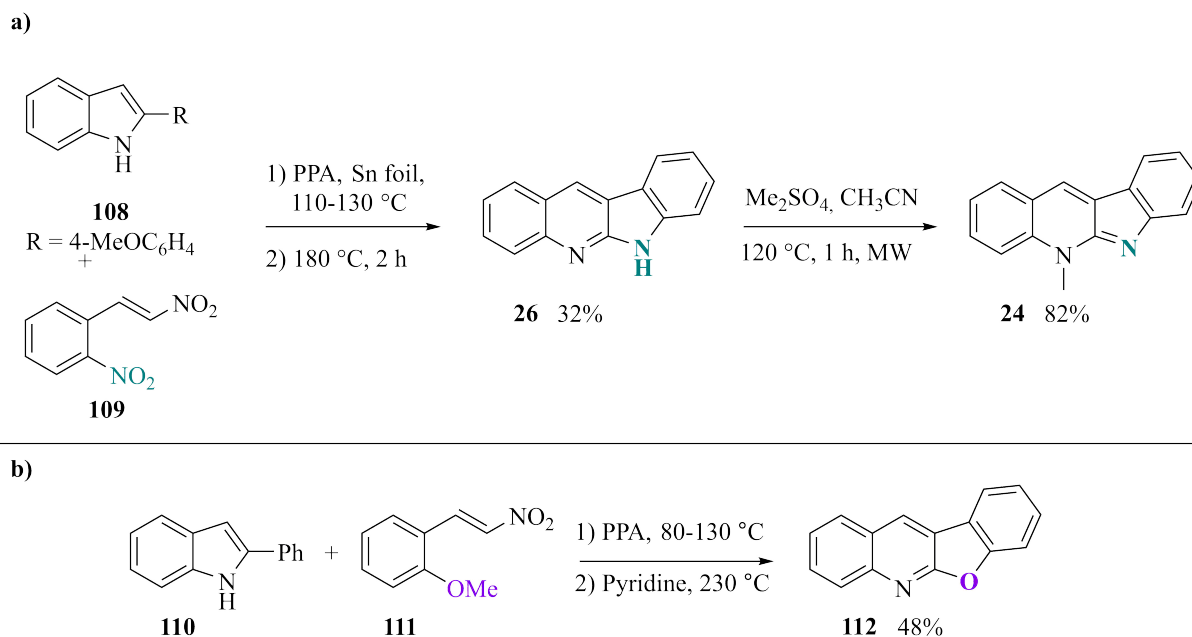
A Pd-catalyzed dual annulation approach to synthesize indolo[2,3-*b*]quinolines from key intermediate **107** was realized by Hsieh's group.^[183] The key intermediate could be assembled by treating 2-bromobenzaldehyde (**104**) and 2-nitrophenylacetonitrile (**105**) with catalytic

amounts of potassium hydroxide and pyrrolidine to give nitro compound **106**. Reduction of the nitro functionality was achieved using tin in ethanolic HCl at room temperature to give key compound **107** in 76% yield over two steps. Following the Pd-catalyzed dual annulation to give quinindoline (**26**), neocryptolepine (**24**) was furnished following a standard alkylation procedure using iodomethane in THF to conclude the synthetic pathway (Scheme 37).



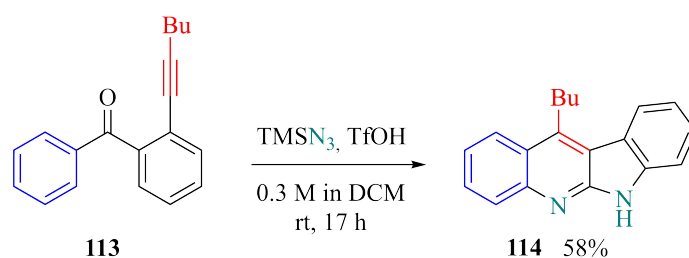
Scheme 37: Synthesis of neocryptolepine (**24**) by Hsieh's group.^[183]

Aksenov *et al.* has reported the total synthesis of neocryptolepine (**24**) using an acid-assisted cascade transformation of certain indoles with 2-nitrostyrenes (scheme 38a). Subjecting indole **108** and 1-nitro-2-nitrostyrene (**109**) to PPA and tin foil at high temperatures furnished quinindoline (**26**) in 32% yield, which could be reacted further to give neocryptolepine (**24**). Considerable efforts were made by Aksenov and coworkers to improve upon the yield of the innovative cascade transformation, however, they were unsuccessful. To their delight, the group was able to extend the conditions to furnish benzofuro[2,3-*b*]quinoline (**112**) by utilizing 1-methoxy-2-nitrostyrene (**111**) in place of the dinitrostyrenen, which also saw an increase in yield (Scheme 38b).



Scheme 38: Strategies described by Aksenov and coworkers for the synthesis of: **a)** neocryptolepine (**24**) and **b)** benzofuro[2,3-*b*]quinoline (**112**).^[184]

Azido compounds are commonly utilized as reactive intermediates in synthetic transformations owing to their high reactivity and ease of preparation. Tummatorn and colleagues have devised a synthesis of various indoloquinolines and carbocycle-fused quinolines using azido complexes as the key intermediates.^[185] Starting from alkenylketone **113**, neocryptolepine derivative **114** was synthesized in 58% yield by treating the substrate with trimethylsilyl azide (TMSN₃) and triflic acid in CH₂Cl₂ at room temperature (Scheme 39). The transformation is believed to proceed *via* N₂-extrusion to generate the carbodiimidium and nitrilium ions *in situ*, which upon cyclization with the alkyne through a domino process provides the target indoloquinolines and quinolines.

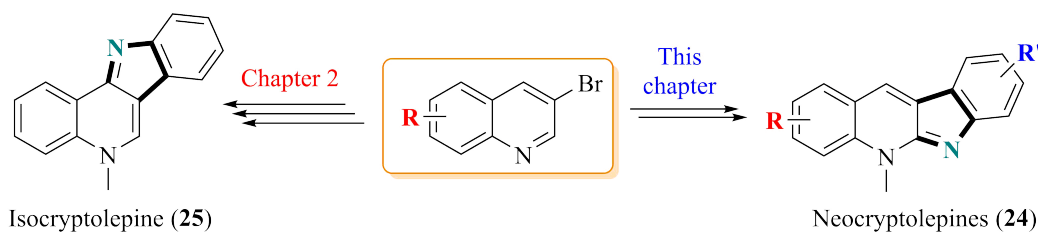


Scheme 39: Domino N₂-extrusion-cyclization approach to the synthesis of quinindoline derivatives as described by Tummatorn and coworkers.^[185]

4.1.2 Project aims

Although a plethora of strategies exist to furnish the indoloquinoline scaffold, scarcely any methods available allow for the direct construction of both neocryptolepine (**24**) and isocryp-

tolepine (**25**) (including their precursors) from a common starting material or key intermediate.^[186–188] Having already described the facile synthesis of isocryptolepine (**25**) starting from commercially available 3-bromoquinoline (**67b**) in Chapter 2, this would serve as a starting material for the development of a novel synthetic pathway towards neocryptolepine (**24**) and functionalized derivatives (Scheme 40).



Scheme 40: The aim of this project was to synthesize neocryptolepine (**24**) and derivatives using 3-bromoquinolines (**67b**) as starting material.

4.2 Development of a novel synthetic strategy

The ability of pyridinium salts to undergo nucleophilic substitutions is well known in the literature and they are often the reagent of choice in the preparation of various natural products.^[189–192] The reactive sites of pyridinium salts are the α or γ positions and addition selectivities are believed to follow the Hard-Soft-Acid-Base (HSAB) model, where soft nucleophiles, such as organocuprates, will add to the γ position while hard nucleophiles, such as Grignard reagents, adds to the α position (Figure 4.1). These selectivities have been most widely studied using organometallic nucleophiles, however, the trends appear extendable to organo nucleophiles.^[193] Despite being the most accepted explanation for the selectivities, the HSAB model has been rejected by others, that believe it should be abandoned in its entirety.^[194]

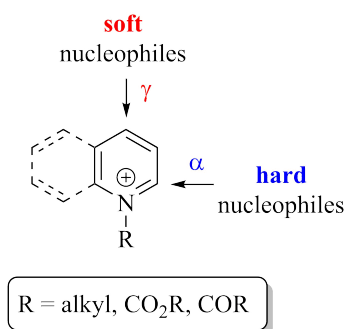
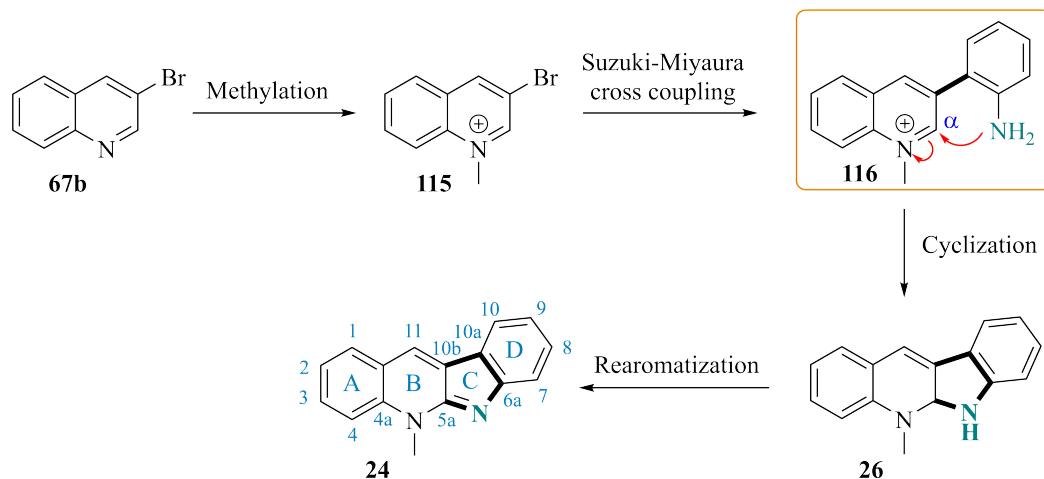


Figure 4.1: Reactive sites of pyridinium and quinolinium salts towards soft and hard nucleophiles.^[190,195]

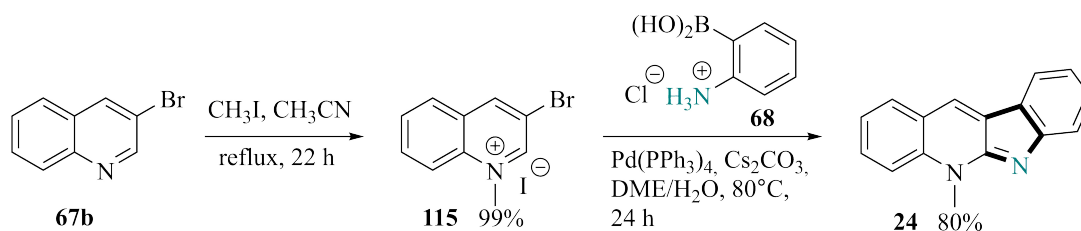
Quinolinium salts behave in a similar manner to pyridinium salts^[195] and nucleophilic additions will proceed following the same principles as outlined above. All nitrogen nucleophiles, excluding rare exceptions, are hard nucleophiles and thus react in an α -selective manner.^[195]

With this in mind, a novel synthetic approach to construct neocryptolepine (**24**) was devised (Scheme 41). The planned synthesis will commence by *N*-methylation of 3-bromoquinoline (**67b**) followed by a Suzuki-Miyaura cross-coupling reaction to yield the key intermediate **116**. Selective α -cyclization of intermediate **116** would produce quinindoline (**26**) which upon rearomatization furnishes neocryptolepine (**24**).



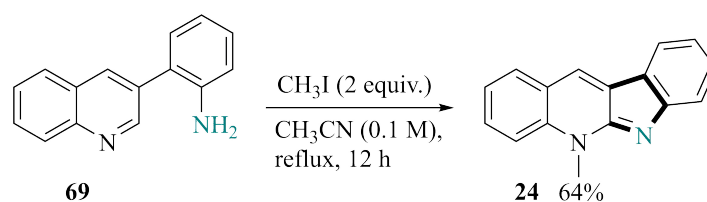
Scheme 41: Proposed synthetic pathway to neocryptolepine (**24**), with its associated nomenclature highlighted.

To test the viability of the strategy, 3-bromoquinoline (**67b**) was *N*-methylated using iodomethane in refluxing acetonitrile to give bromoquinolinium salt **115** in near quantitative yield (Scheme 42). Serendipitously, under the standard Suzuki-Miyaura cross-coupling conditions between bromoquinolinium salt **115** and 2-aminophenylboronic acid hydrochloride (**68**), the regioselective cyclization occurred concurrently to give neocryptolepine (**24**) in excellent yield. It is presumed that the rearomatization is the result of a spontaneous oxidation process, however, investigations into this was never conducted.



Scheme 42: Novel synthetic pathway towards neocryptolepine (**24**).

In a similar approach, Seidel and coworkers describe the synthesis of neocryptolepine (**24**) in 64% yield starting from biaryl **69** using 2 equivalents of iodomethane in refluxing acetonitrile (Scheme 43). Though an interesting strategy indeed, it appears to be beneficial to have the *N*-methyl group installed prior to formation of biaryl **69**, as the iodomethane could be attacked by both intended quinoline nitrogen as well as the amino group and thus hinder product formation.

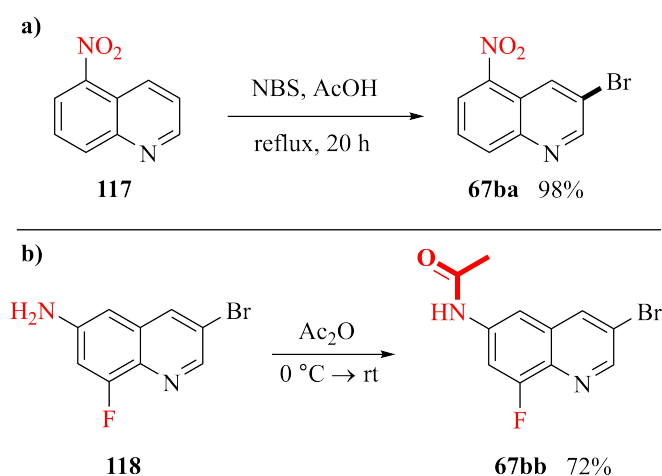


Scheme 43: Neocryptolepine (**24**) synthesis as conducted by Seidel and coworkers.^[186]

4.2.1 Investigation of substrate scope

Preparation of quinoline starting materials

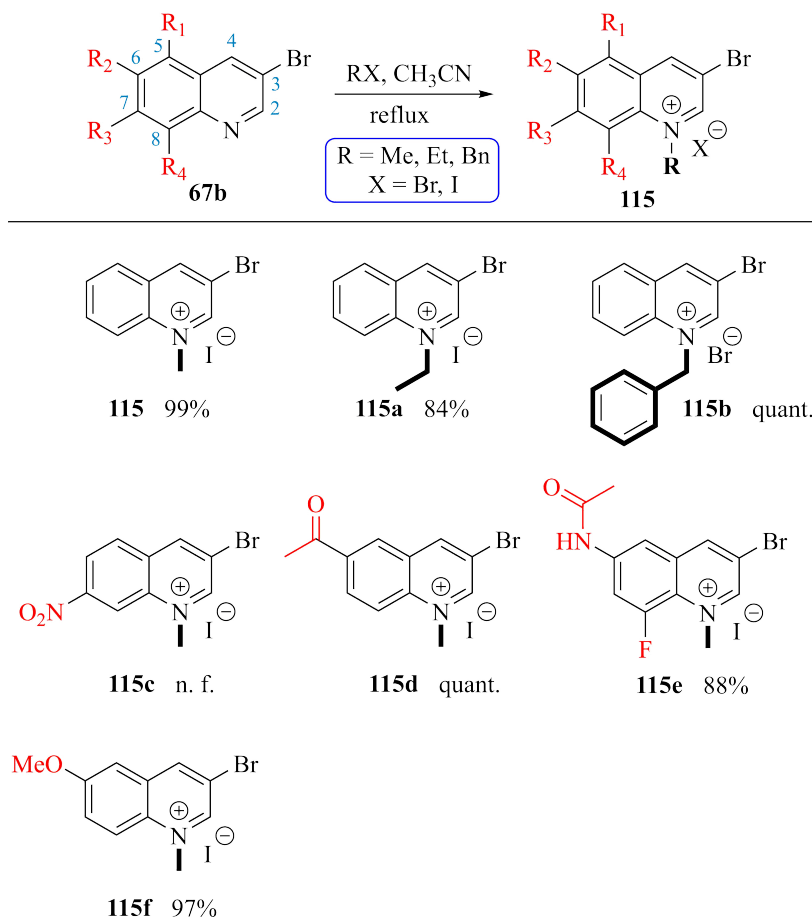
To initiate our investigation of the substrate scope of the novel neocryptolepine (**24**) synthesis, some quinoline starting materials were prepared. To furnish 3-bromo-5-nitroquinoline (**67ba**), a regioselective bromination of 5-nitroquinoline (**117**) using *N*-bromosuccinimide (NBS) in refluxing acetic acid was undertaken, giving the target compound **67ba** in excellent yield (Scheme 44a).^[197] The incorporation of an amide functionality is often associated with biological activity and the same is known for fluorine.^[198] Starting from commercially available bromoquinoline **118**, a compound containing both a fluorine and an amido moiety could be furnished in good yields by treating it with neat Ac_2O (Scheme 44b).



Scheme 44: Synthesis of some quinoline starting materials by following standard literature procedures^[197] to furnish 3-bromo-5-nitroquinoline (**67ba**) and amido compound **67bb**.

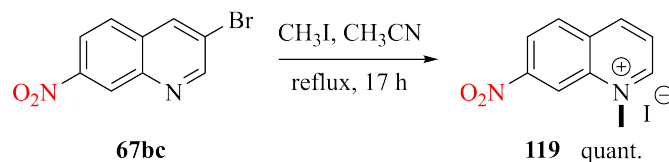
With the prepared bromoquinolines **67ba** and **67bb** in hand along with a variety of commercially available bromoquinolines, the formation of quinolinium salts **115** was the next step. This was achieved by treating the appropriate bromoquinoline with a large excess of alkylating agent in refluxing CH_3CN to give the quinolinium halides **115** in excellent yields (Scheme 45). The primary goal was to prepare *N*-methyl quinolinium salts, but *N*-ethyl and *N*-benzyl quinolinium compounds **115a** and **115b** were also prepared in excellent yields (Scheme 45). While the alkylations overall proceeded smoothly to give the target compounds, unexpectedly, the at-

tempted synthesis of 7-NO₂ substituted bromoquinoline **115c** instead furnished dehalogenation product **119** (Scheme 46).



Scheme 45: Scope of the *N*-alkylations to give quinolinium halides **115**; n. f. = not formed.

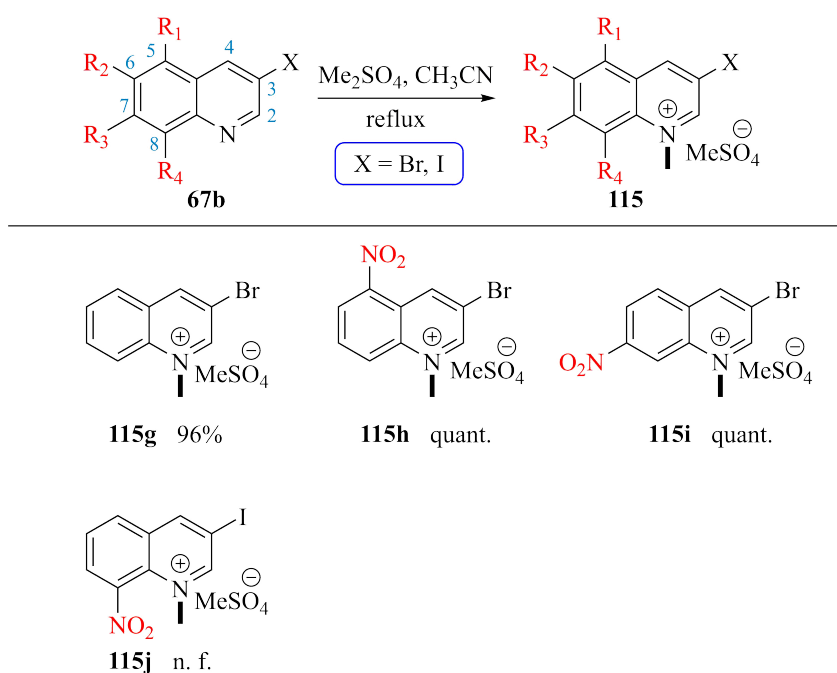
Though puzzling at first, the dehalogenation of compound **67bc** is likely a result of the stabilizer found in the iodomethane. Commercial iodomethane is commonly stabilized by addition of up to 0.5% copper wire. Due to the inductive effect of the nitro group, a large excess of 100 equivalents of iodomethane was required to force a reaction, however in this case not the desired alkylation product. Attempts to avoid this dehalogenation product using fewer equivalents of iodomethane (starting with five and gradually adding up to 75 equivalents over two days) failed to provide any reaction.



Scheme 46: Observed dehalogenation reaction during the *N*-methylation of compound **67bc**.

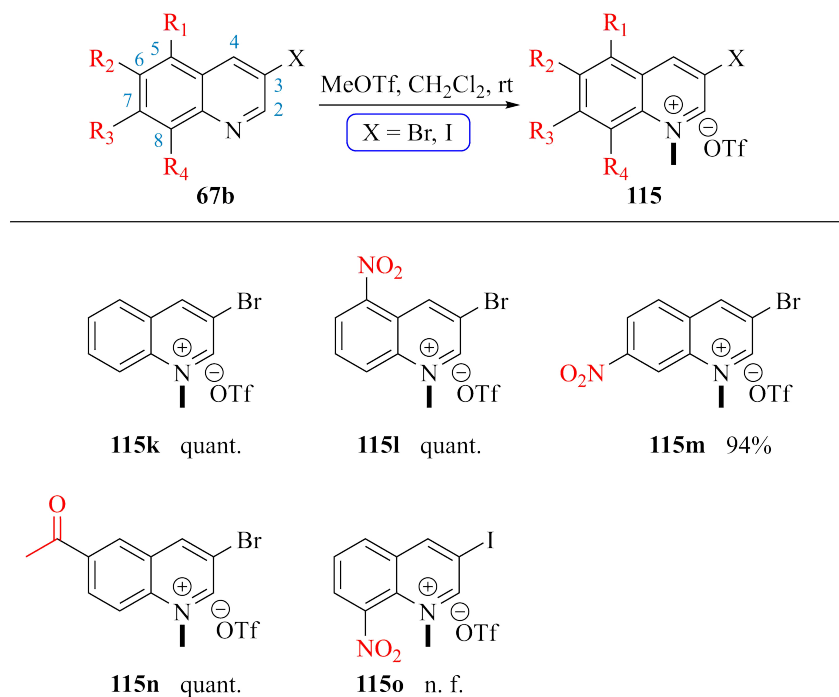
Dehalogenations using metals, such as copper, is well known in the literature, a notable example being the Ullmann coupling.^[199,200] Contrary to the Ullmann reaction, for this de-

halogenation to produce the observed product, the presence of a hydride source is required. Observations made by Hartwig and Fier during the fluorination of aryl iodides showed that the α proton of acetonitrile may serve as a hydride source in copper-mediated reactions. They discovered this after running deuterium labeling experiments, which also revealed water as a potential hydride source.^[201] As the experiments to construct compound **119** were conducted in wet acetonitrile, there are two plausible hydride donors present to explain the observed product. The exact mechanism by which the observed dehalogenation of compound **67bc** occurred is not known and no further investigation into this reaction was conducted. To avoid such hydro-dehalogenation products, any alkylations of nitroquinolines were thus conducted using a different alkylation reagent. Two alkylating reagents which are more powerful than iodomethane is dimethyl sulfate and methyl triflate, both of which were employed under standard conditions to give the corresponding nitro-methyl-quinolinium salts. (Schemes 47 and 48). 3-Bromoquinoline (**67b**) was also subjected to these alkylations protocols, to allow for comparison of the effect of different counter ions on the proceeding cyclization step.



Scheme 47: Scope of the *N*-methylations to give quinolinium salts **115** using Me_2SO_4 ; n. f. = not formed.

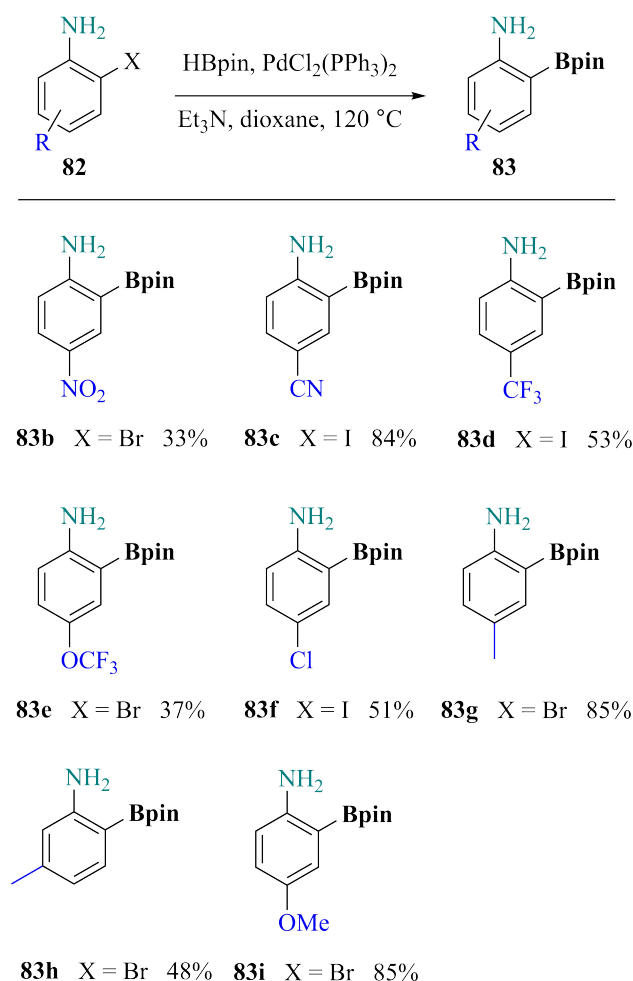
The reactions gave the target compound in up to quantitative yields with the expectation of 3-iodo-8-nitroquinoline (**67bd**), which using both dimethyl sulfate and methyl triflate gave no reaction after nearly three days. The combined electron-withdrawing effect of the nitro and iodo groups must have resulted in such poor nucleophilicity of the quinoline heteroatom resulting in no reaction taking place.



Scheme 48: Scope of the *N*-methylations to give quinolinium salts **115** using MeOTf; n. f. = not formed.

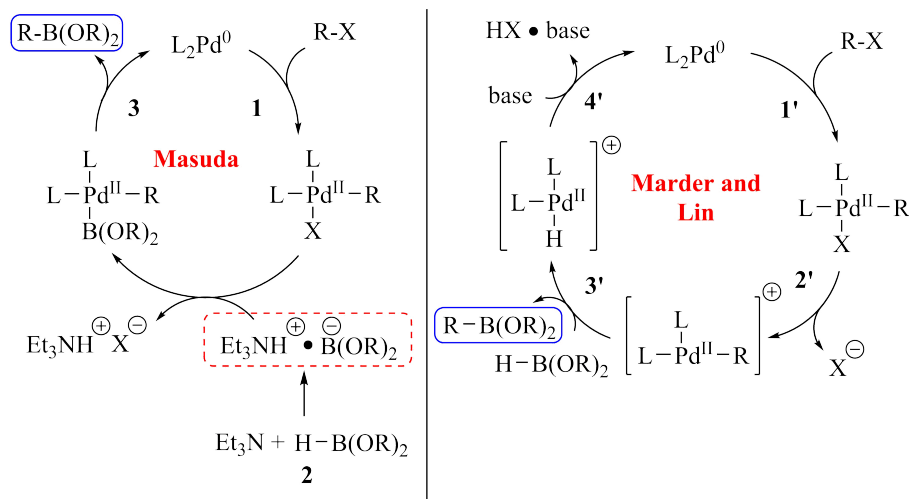
Preparation of 2-aminophenylboronic acid pinacol esters

To prepare the coupling partners needed to construct the C and D rings of neocryptolepine (**24**) (ring numbering shown in Scheme 41), pinacol esters were chosen as the coupling partners due to being less polar than the corresponding acids, and are therefore easier to purify by column chromatography. A selection of 2-aminophenylboronic acid pinacol esters were prepared in poor to excellent yields by reacting halo anilines **82** with pinacolborane (HBpin) in refluxing 1,4-dioxane, using PdCl₂(PPh₃)₂ as catalyst and Et₃N as base (Scheme 49).^[202,203]



Scheme 49: Scope of Masuda borylations to give 2-aminophenylboronic acid pinacol esters **83**.

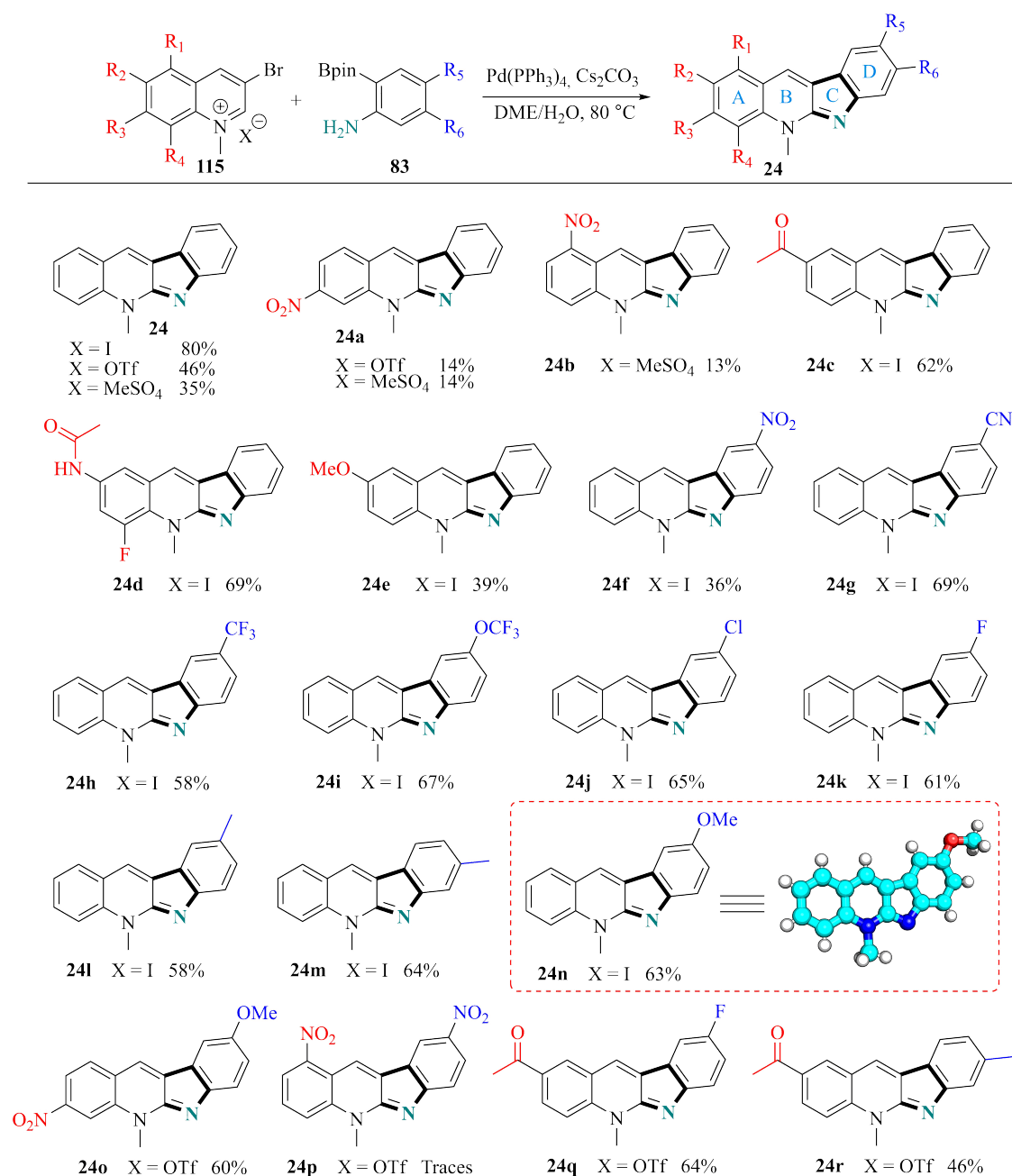
These conditions were initially described by Masuda and coworkers,^[204] where they proposed that the reaction mechanism proceeded through the formation of an ammonium boride ion pair in the transmetalation step (marked in red in Scheme 50).^[205] While the reaction mechanism of the cross coupling between aryl or vinyl halides and bis(pinacolato)diboron (B₂pin₂), first presented by Miyaura and coworkers, is well established,^[206] the mechanism using pinacolboranes is not yet fully understood.^[207] Work conducted by Marder and Lin using density functional theory (DFT) studies showed Masuda's proposal of an ammonium boride ion pair to be highly unfavorable and using their findings, they presented an alternative mechanism (Scheme 50).^[208] In line with Masuda's proposed mechanism, the catalytic cycle is initiated by oxidative addition of Ar-X to Pd(0). Then, a cationic Pd(II) complex is formed *via* the assistance of Et₃N which further reacts through σ -bond metathesis with HBpin to generate the desired R-B(OR)₂ along with the cationic L₂Pd(II)H. The catalytic cycle is then finalized by Et₃N deprotonating the newly formed palladium complex to regenerate Pd(0).



Scheme 50: Left: proposed borylation mechanisms by Masuda;^[204,205] 1 = oxidative addition, 2 = transmetalation and 3 = reductive elimination. Right: proposed borylation mechanism by Merder and Lin;^[208] 1' = oxidative addition, 2' = amine-assisted ionization, 3' = metathesis and 4' = reductive elimination.

Cascade Suzuki-Miyaura cross-coupling and cyclization reactions

With all the starting materials in hand, the scope and limitations of the cascade approach was tested by preparing a selection of functionalized neocryptolepines in up to 69% yield (Scheme 51). The natural product itself was also synthesized using the three different counter ions to ascertain their effect on product formation. It became clear that iodine was the superior counter ion (80%), with OTf (46%) and MeSO₄ (35%) performing poorly, potentially as a result of the presence of sulfur in the two latter, which is known to act as a poison to palladium catalysts.^[209]



Scheme 51: Scope of the cascade Suzuki-Miyaura cross-coupling and cyclization to give neocryptolepines **24**.

Evaluation of A-ring substitution revealed a better tolerance towards EWGs (highest yield observed for compound **24d**) over EDGs (yield of 39% for compound **24e**). The poor yield of 2-methoxy neocryptolepine **24e** is likely explained by the donation of electrons into the aromatic nucleus by the methoxy group, lowering its electrophilicity. Compound **24d** illustrates that dual A-ring functionalizations also proceed smoothly (69% yield). Nitro compounds **24a** and **24b** proceeded in extremely poor yield (14% and 13%, respectively) and in general, of all the five prepared nitro substituted neocryptolepines in the series, compound **24o** is the only entry to be formed in good yield (60%), illustrating the importance of the electron donating

effect of the methoxy group to counter the electron withdrawing nature of the nitro moiety. The markedly higher yield of compound **24f** compared to compounds **24a** and **24b** further demonstrates that it is more detrimental to successful product formation to have the nitro group on the quinoline ring than on the aminophenyl. Compound **24f** turned out to be unstable and decomposed before it could be fully characterized. It was synthesized again and then stored at $-20\text{ }^{\circ}\text{C}$ to avoid decomposition, which, surprisingly, still occurred. Attempts were made to identify the decomposition product(s), however, the ^1H NMR spectra showed a complex mixture which could not be interpreted (Figure 4.2).

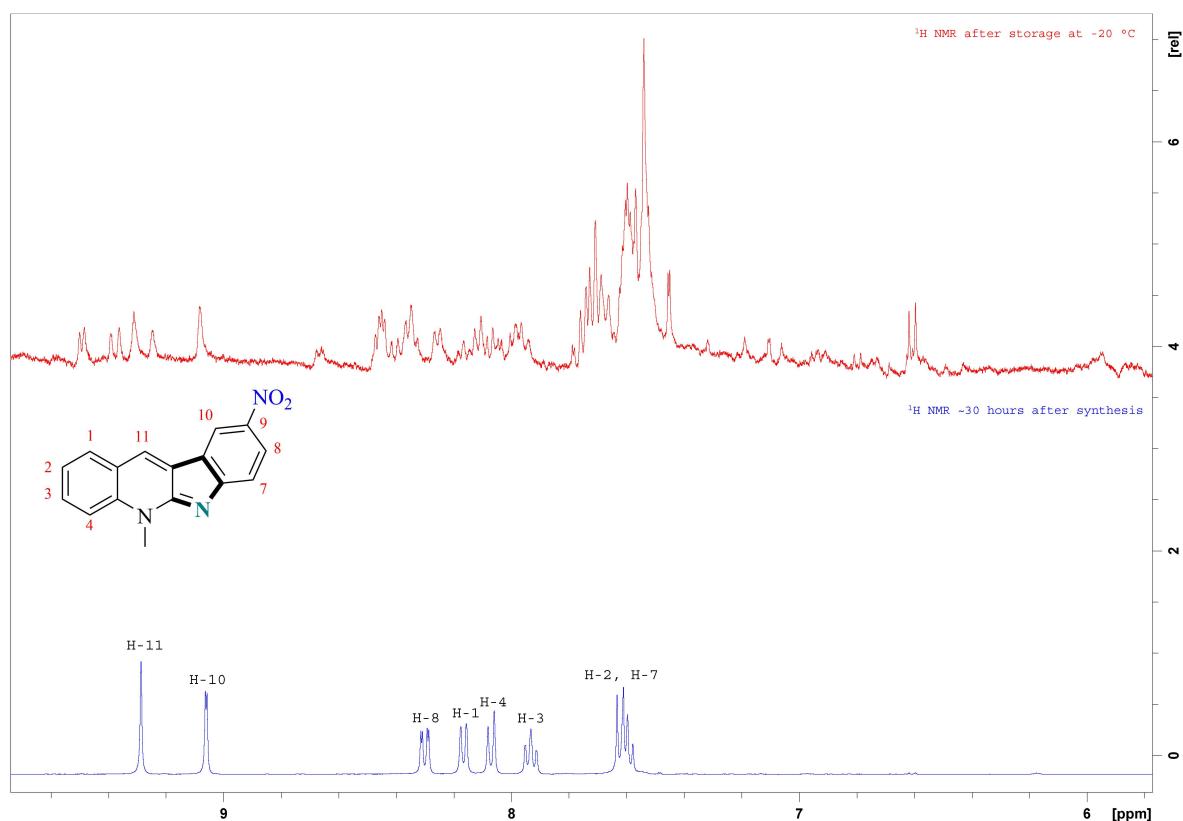


Figure 4.2: ^1H NMR spectra of compound **24f** showing decomposition after storage at $-20\text{ }^{\circ}\text{C}$.

The method tolerated all the tested functionalities on the aminophenyl group, the low yield of compound **24f** likely being due to product decomposition. Being an intramolecular reaction, the close proximity between the nucleophilic and electrophilic sites of key intermediate **116** (Figure 4.3) appears to negate the strong electron withdrawing effect of groups such as cyano and trifluoromethyl (yields 69% and 58%, respectively, for compounds **24g** and **24h**). Dual A- and D-ring functionalizations were also tolerated, with the exception of dinitro neocryptolepine **24p**, where only traces was observed.

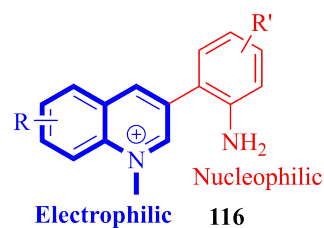


Figure 4.3: Electrophilic and nucleophilic sites of key intermediate **116**.

Delightfully, the α -selective cyclization observed for the natural product itself was further applicable to all the evaluated functionalities. The structures for the prepared neocryptolepines were easily verifiable and distinguished from the δ cyclization products, by examining their characteristic 2D NMR coupling patterns. Using 8-trifluoromethyl neocryptolepine **24h** as an example, the NOESY spectrum clearly shows H-11 to have a correlation with H-1 and H-10 (Figure 4.4). Most of the prepared neocryptolepines were crystalline and therefore highly suitable for analysis by X-ray. Although not strictly necessary for their structural elucidation, the structure of 8-methoxy-neocryptolepine **24n** was confirmed by recrystallizing it and sending it to a collaborator in Tromsø for X-ray analysis (Scheme 51).

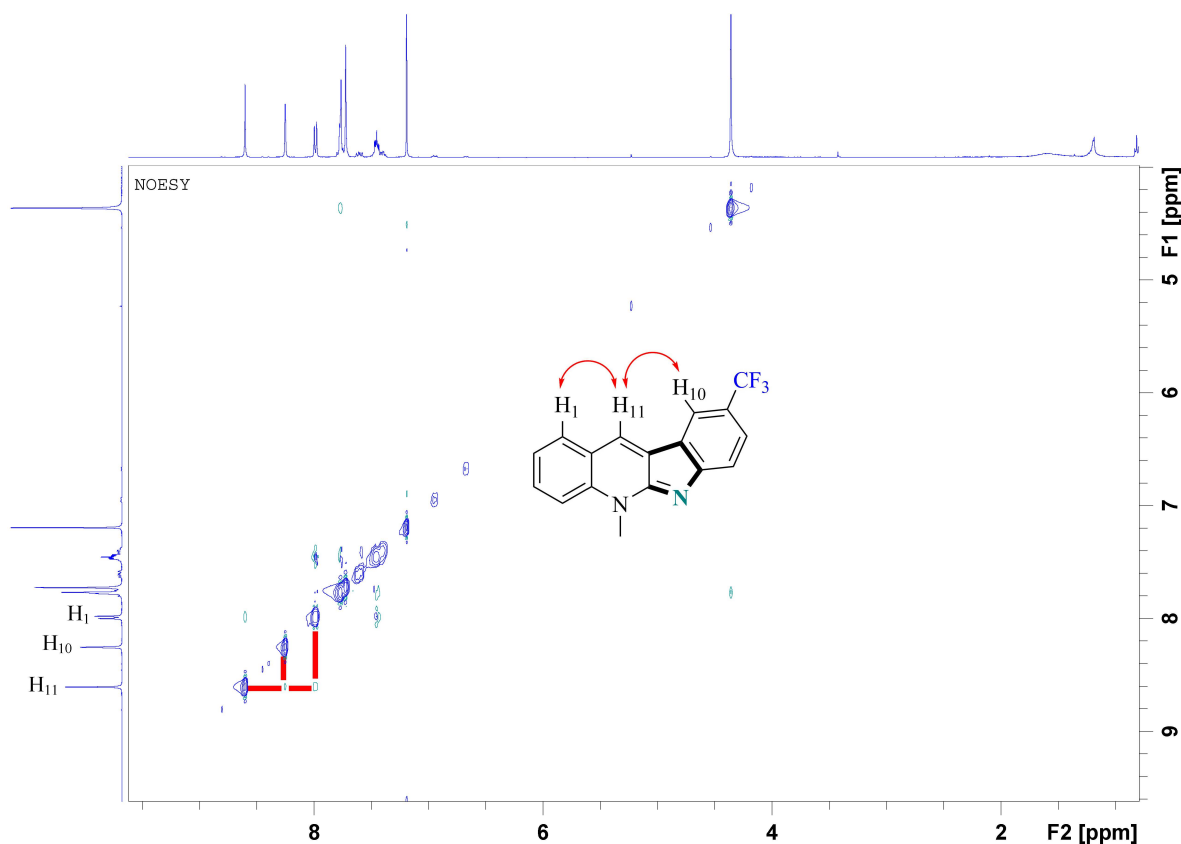
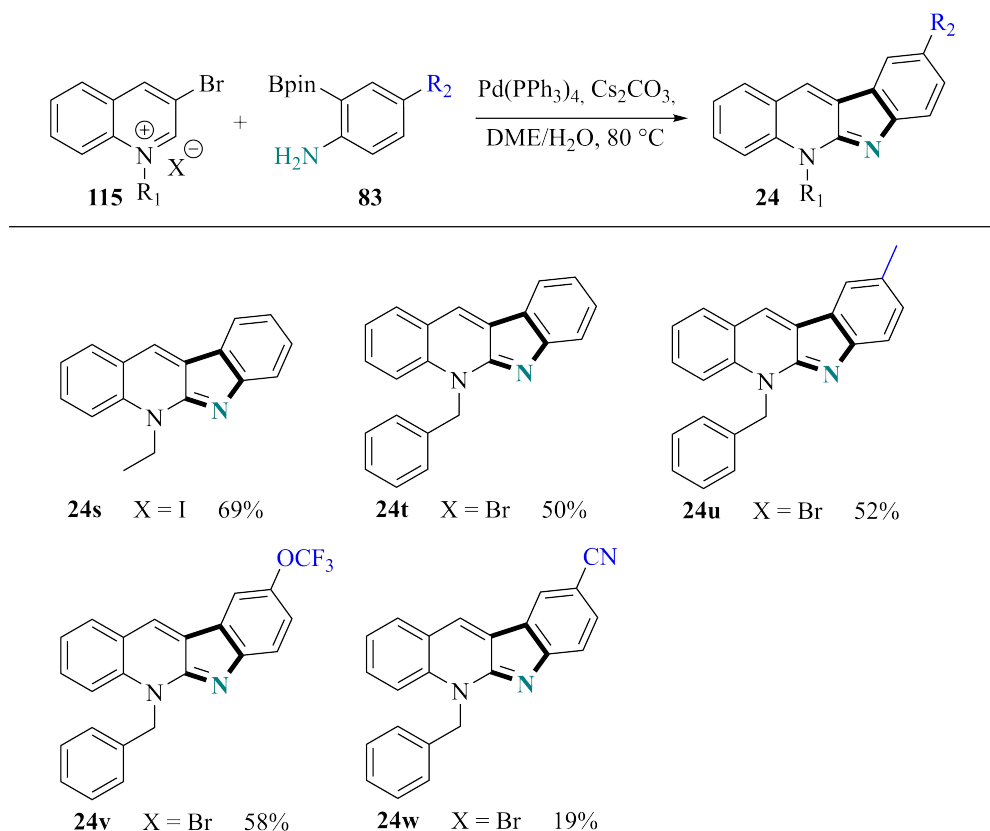


Figure 4.4: NOESY correlations confirming the structure of 8-trifluoromethyl neocryptolepine **24h**.

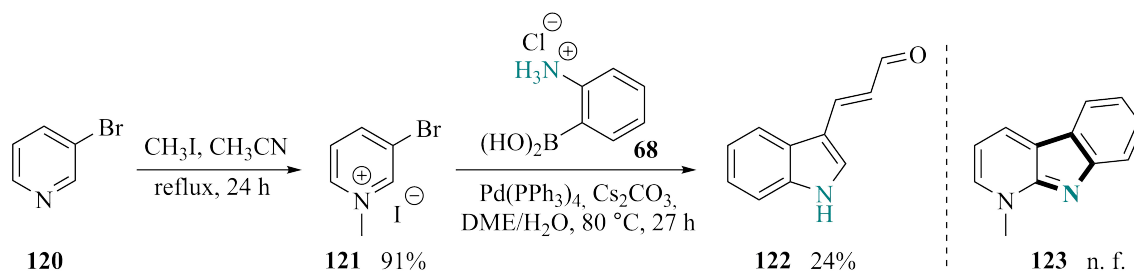
In general, the method appears sensitive to EDG on the A-ring, which when studying the key intermediate **116** in Figure 4.3 is likely due to a lowering of the electrophilicity of the quinoline-ring. It seems reasonable that having a nitro group on the electrophilic quinoline-ring should enhance product formation, however, the contrary was observed. A possible explanation for the poor yields of the quinoline substituted nitro compounds could be that the compounds "overreact", *ie* that the nitro moiety undergoes further transformations. Indeed, nitro aromatics, particularly nitro heteroaromatics, are known to undergo a variety of transformations, including being a precursor for formyl, acyl, cyano and amino groups, as well being susceptible to addition-elimination reactions and allowing for nucleophilic attack of the aromatic ring.^[210] Significant efforts were made to identify any eventual side product(s) formed during the synthesis of compounds **24a** and **24b**, with several spots in addition to the targets isolated during purification. Examining these fractions using both LRMS and ¹H NMR were not fruitful and no structures could be identified.

The effect of replacing the methyl group for an ethyl or benzyl moiety was investigated by synthesizing five alkyl neocryptolepine derivatives (Scheme 4.2.1). Having established that the electron poor nature of the quinoline is key for the intramolecular cyclization, it was expected that this would be reflected in the yields of the benzyl derivatives. Indeed, benzyl neocryptolepines **24t-24w**, and in particular **24w**, were inferior in yield to ethyl neocryptolepine **24s**. The interest in the benzyl derivatives was based on the option to carry out a deprotection reaction to remove the benzyl group, which would grant access quinindolines, another natural product, however, this was never realized.



Scheme 52: Scope of the cascade neocryptolepine protocol when using different alkyl groups.

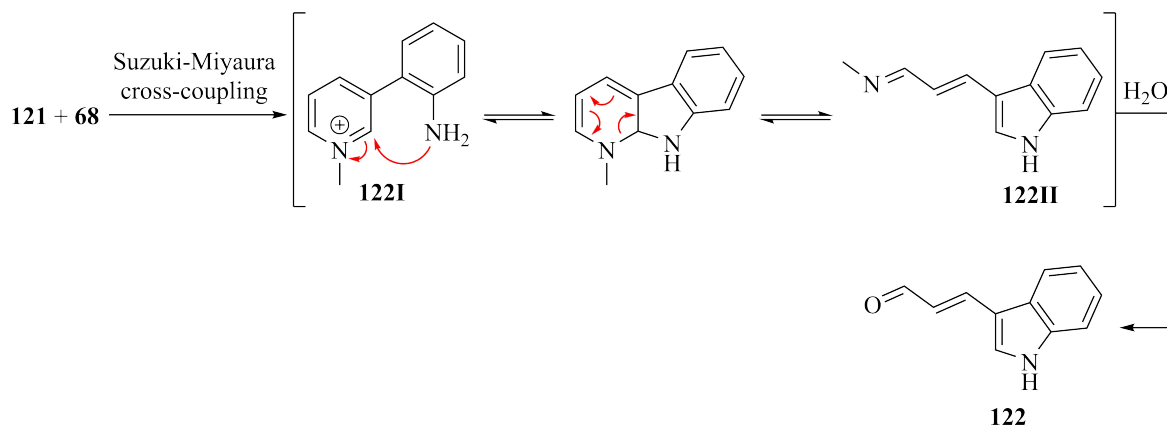
Having completed a large scope study, a clear trend concerning the yields of product formation appeared; the best yields were consistently between 60-69%, possible explanations for which were investigated. The facile ring-opening of pyridinium salts is well documented in the literature,^[212] perhaps the most notable being the Zincke reaction.^[213–215] Indeed, in an attempt to extend our conditions to the synthesis of α carbolines, ring-opening of the pyridinium salt occurred to construct indole **122** (Scheme 53). No traces of the desired carboline **123** was detected and despite isolating several spots, they contained complex mixtures which could not be analyzed by NMR.



Scheme 53: Formation of indole **122** and unsuccessful synthesis of carboline **123**; n. f. = not formed.

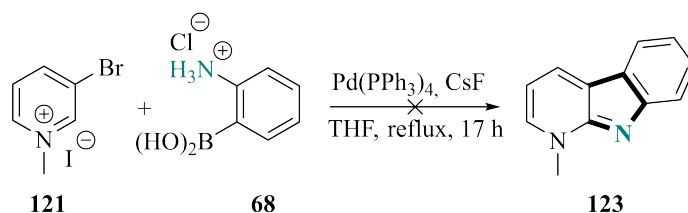
Based on similar work by Kearney and Vanderwal, where they describe the synthesis of various indoles starting from pyridinium salts,^[189] a mechanism for the indole formation may be

proposed; following the Suzuki-Miyaura cross-coupling reaction between pyridinium salt **121** and 2-aminophenylboronic acid hydrochloride (**68**), C-2 of intermediate **122I** becomes sufficiently electrophilic to initiate nucleophilic attack by the amino group. Rather than oxidizing to achieve α carboline (**123**), the cyclic structure ring-opens to give compound **122II**, which due to the presence of water in the reaction is converted to indole **122** (Scheme 54).



Scheme 54: Proposed mechanism for the ring-opening of pyridinium salt **122I** to yield indole **122**.

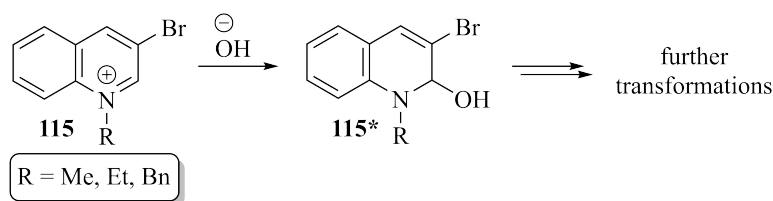
It was natural to try this synthesis under anhydrous conditions to investigate if the equilibria in Scheme 54 would favor the cyclic product in the absence of water. Several anhydrous Suzuki-Miyaura cross-coupling conditions are available^[216] and CsF as base and Pd(PPh₃)₄ as catalyst in anhydrous THF was selected to carry out the reaction (Scheme 55). Disappointingly, no trace of α carboline (**123**) was formed and the crude ¹H NMR showed a complex mixture which despite efforts to purify and analyze did not yield any sensible structure(s) and any further attempts to construct this compound was abandoned.



Scheme 55: Unsuccessful attempt at constructing α carboline (**123**) using anhydrous conditions.

Despite the ring-opening of quinolinium salts being less documented, they are believed to generally follow the same trends and transformations as their corresponding pyridinium salts.^[217] The corresponding indole ring-opening product could not be confirmed as a side product for the synthesis of neocryptolepines and neither could any other structure, despite considerable efforts. A possible route could be that the bromoquinolinium salts in the presence

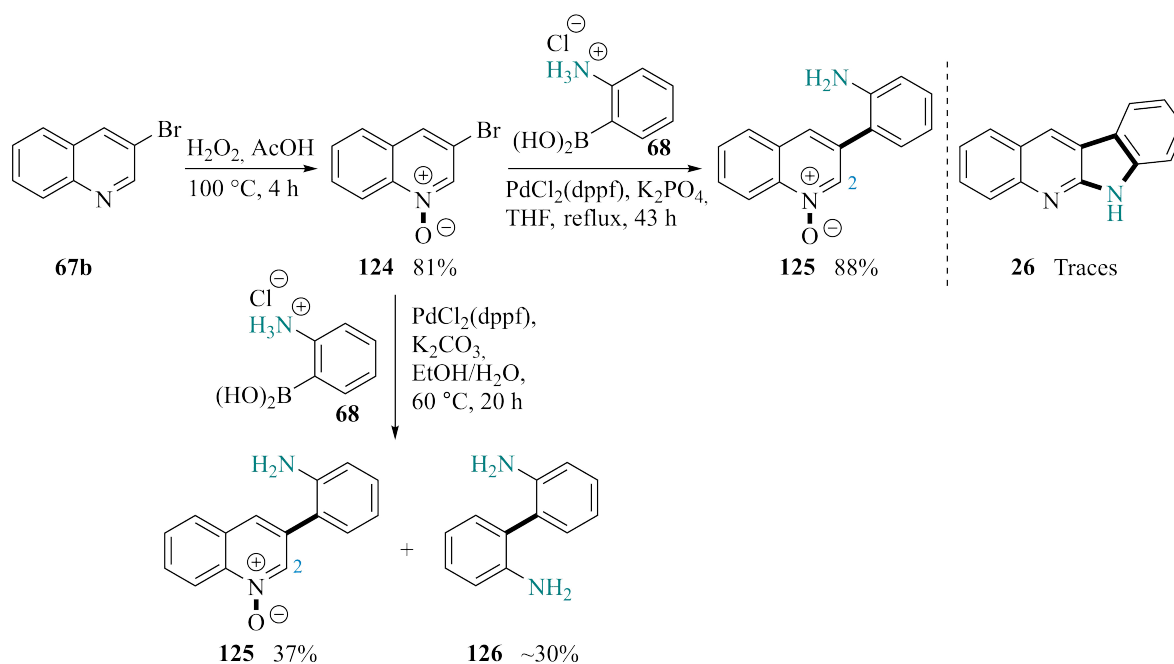
of aqueous base underwent nucleophilic attack by a hydroxyl ion (Scheme 56). A possible reason for the elusiveness of this structure is the fact that it may undergo further transformations, for instance due to the presence of either the base or the palladium in the reaction mixture.



Scheme 56: Proposed side product resulting from the ring-opening of the bromoquinolinium salt **115**.

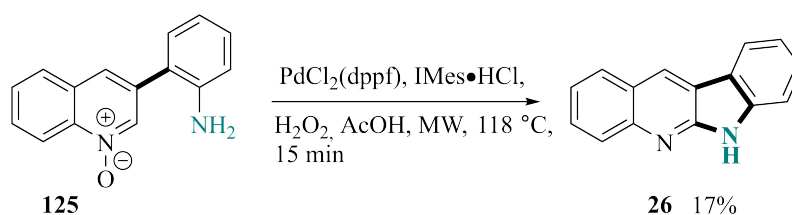
Investigation of quinoline *N*-oxides as intermediates towards quinindoline (**26**)

The successful application of our novel cascade approach to prepare neocryptolepine (**24**) and functionalized derivatives using various *N*-alkyl groups prompted further investigation into the installation of other *N*-functional groups. The use of *N*-oxides as an electrophilic activating group has been demonstrated previously in the literature^[211] and in our own research group. The installation of an *N*-oxide functional group on 3-bromoquinoline (**67b**) in order to activate C-2 for further transformation into quinindoline (**26**) was thus investigated. Carrying out the oxidation of 3-bromoquinoline (**67b**) using H₂O₂ in acetic acid gave the *N*-oxide in good yield (81%, Scheme 57). The use of acetic acid in this reaction has a dual purpose; both as a solvent and as an activating agent for the peroxide. Continuing with our standard Suzuki-Miyaura cross coupling conditions, the hope was that the formed biaryl would spontaneously cyclize to yield quinindoline (**26**). Disappointingly, biaryl **125** was formed in poor yield along with large quantities of homocoupled aniline **126**. Modification of the cross coupling conditions improved the yield of biaryl **125** to 88% with only small amounts of homocoupled product observed. Here, traces of desired compound quinindoline (**26**) was also seen. Despite this, it became clear that the nitroso functionality did not sufficiently activate C-2 to initiate the intramolecular cyclization.



Scheme 57: Synthesis of biaryl **125**, which was not sufficiently electrophilic to initiate intramolecular cyclization to construct quinindoline (**26**).

Subjecting nitroso biaryl **125** to the MW-assisted intramolecular C-H activation/C-N bond formation conditions described in Chapter 2 for the synthesis of various indoloquinolines and pyridocarbazoles, it was possible to improve the yield of quinindoline (**26**) to 17% (Scheme 58). The cyclization appeared to be fully regioselective, as no traces of indoloquinoline **38** was observed in the crude NMR, however, the reaction generated a complicated reaction mixture which despite multiple attempts could not be separated into identifiable fractions through column chromatography. Consequently, no further efforts were put into improving the synthesis of quinindoline (**26**) using this approach.

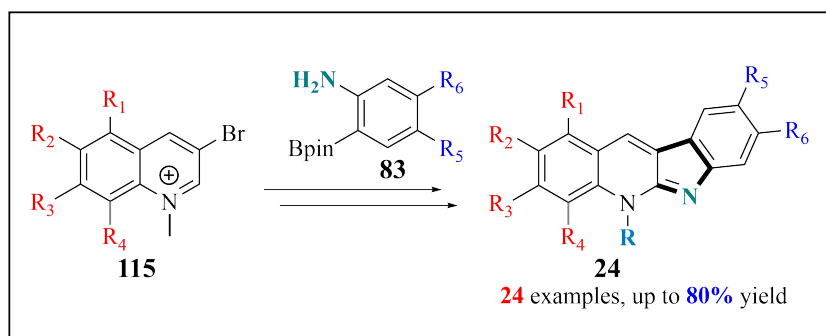


Scheme 58: MW-assisted synthesis of quinindoline (**26**).

4.3 Summary and concluding remarks

The natural product neocryptolepine (**24**) was synthesized in to steps using a novel approach where the key synthetic strategies were a regioselective *N*-alkylation followed by a cascade Suzuki-Miyaura cross-coupling reaction and intramolecular C-N bond formation. The scope and limitations of the method was investigated using diversely functionalized quinolines and

2-aminophenylboronic acid pinacol esters, which were easily prepared following literature procedures or obtained commercially. Through these studies, 24 neocryptolepine derivatives were constructed in up to 80% yield (Scheme 59) and the method showed a high tolerance to most substitution patterns with the exception of nitro functionalities. Moreover, the strategy generally showed a higher robustness towards electron withdrawing substituents on the quinoline ring. Maintaining a high electrophilic character in the quinoline ring of the key reactive intermediate is believed to be the reason for these observations, where EDGs lead to an unfavorable decrease in electrophilicity and EWGs lead to a favorable increase.



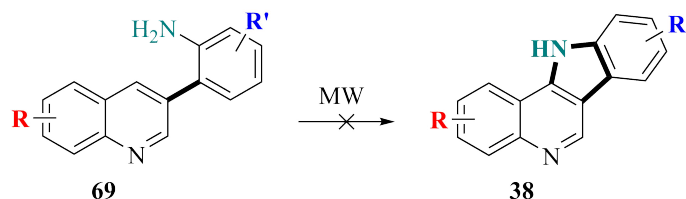
Scheme 59: Summary showcasing the 24 synthesized neocryptolepines utilizing a novel cascade C-C/C-N bond formation strategy.

Chapter 5

Photochemical synthesis of 11*H*-indolo[3,2-*c*]quinolines

5.1 Introduction

Disappointingly, the microwave-induced C-H activation/C-N bond formation strategy developed for the synthesis of compound **38** and certain regioisomers showed no tolerance to substrate functionalizations (Scheme 60). The crude reaction mixtures contained complex signals which could not be elucidated by NMR and up to 12 spots were present on the TLC plates. In order to realize the goal of building a library of indolo[3,2-*c*]quinolines, alternative methods had to be considered. Past endeavours in our laboratories have shown that isocryptolepine precursor **38** is easily prepared *via* a Suzuki-Miyaura cross-coupling-azidation-thermally induced nitrene insertion sequence,^[149] which uses the same quinoline starting material as the neocryptolepine methodology. A major drawback of the thermally-induced nitrene insertion approach is the harsh reaction conditions, requiring temperatures of up to 180 °C for the reaction to proceed. Another classical way of obtaining aryl nitrenes is through the photolysis of the corresponding aryl azides, which are often facile at room temperature.^[218] Thus, the development of a novel photochemical pathway towards indolo[3,2-*c*]quinolines **38** was undertaken. Before venturing into the development of a novel photochemical approach to indolo[3,2-*c*]quinolines **38**, past photochemical endeavours for the synthesis of such compounds will be briefly examined.

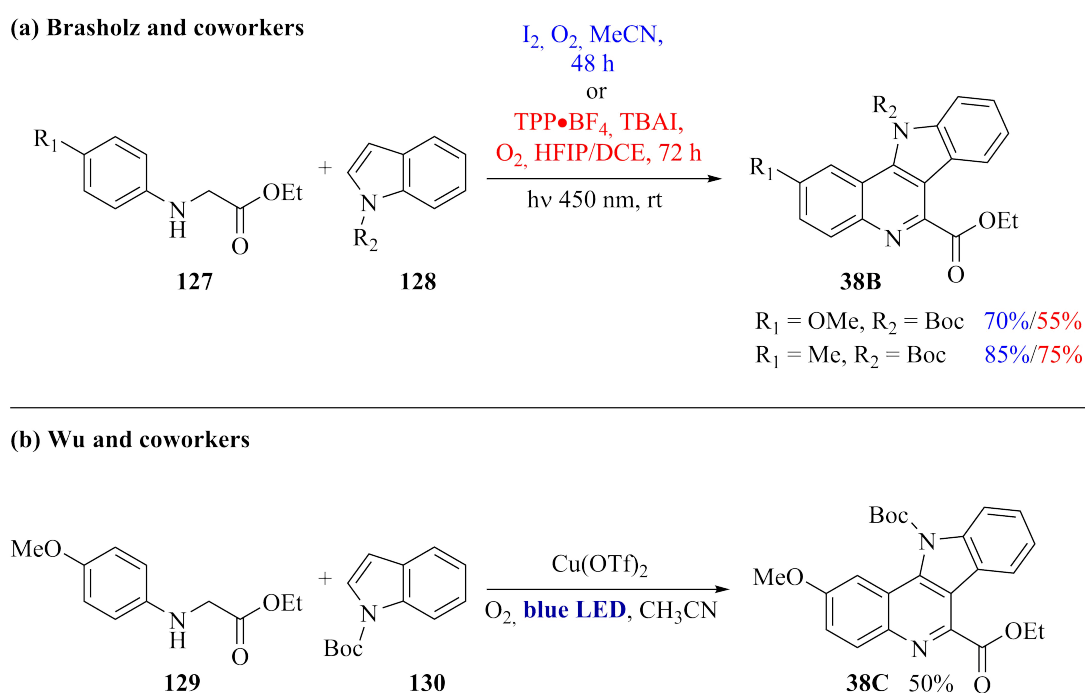


Scheme 60: Unsuccessful MW-assisted synthesis of functionalized indolo[3,2-*c*]quinolines **38**.

5.1.1 Photochemical synthesis of indolo[3,2-*c*]quinolines **38**

Organic photochemistry is a rapidly growing field within synthetic organic chemistry, with the number of publications exploding in the past 10 years.^[219] Some advantages of photochemical reactions, is that they often limit or remove the need for transition metal catalysts and are able to overcome large activation barriers which allows for otherwise inaccessible reactivities compared to conventional methods.^[220] Several photochemical methods for the preparation of indolo[3,2-*c*]quinolines **38** are covered in a review article by Tilve and coworkers, and are thus not included in this section.^[101] Despite the growth of the photochemical field, only two publications presenting the synthesis of indolo[3,2-*c*]quinolines **38** using photochemistry have been published since 2011. Brasholtz and colleagues has presented a metal free light-mediated Povarov reaction, *ie* an aza-Diels Alder reaction, between *N*-aryl glycine esters **127** and indoles **128** to yield diversly functionalized indolo[3,2-*c*]quinolines **38B** (for two examples from their work, see Scheme 61a). Two different approaches were developed for their construction,

the first by treating the *N*-aryl glycine esters **127** and indoles **128** with molecular iodine and oxygen under blue light irradiating. In the second method, they developed a photocatalytic variant and through rigorous screening experiments observed optimal product formation by irradiating the starting materials together with triphenylpyrylium tetrafluoroborate (TPP·BF₄) and tetrabutylammonium iodide (TBAI) using a mixture of hexafluoroisopropanol (HFIP) and 1,2-dichloroethane (DCE) as solvents.^[221] Utilizing the same starting materials, Wu and coworkers have described a copper(II)-catalyzed visible-light-mediated C-H functionalization strategy to yield a range of various indolo[3,2-*c*]quinolines **38C** (one example shown in Scheme 61b).^[222] Despite photochemical synthesis being considered as one of the six major synthetic methods for the construction of the indolo[3,2-*c*]quinoline core,^[101] the aforementioned publications demonstrate a decline in the development of novel synthetic approaches in recent literature. Consequently, by formulating a novel photochemical method for their synthesis, it is hoped that new and interesting chemistry can be uncovered in the process, which might lead to further advancements of natural product synthesis.



Scheme 61: Synthesis of some indolo[3,2-*c*]quinolines **38**; (a) utilizing a visible-light-mediated tandem dehydrogenative Povarov/aromatization reaction as presented by Brasholz and colleagues;^[221] (b) copper(II)-catalyzed C-H activation by Wu and coworkers.^[222]

5.1.2 Chemistry of nitrenes and the photoexcited state

To fully appreciate the photochemical cyclization of aryl azides to yield indoloquinolines, the chemistry of nitrenes has to be considered. Nitrenes are a transient, neutral monovalent species containing six valence electrons and are often considered to be the nitrogen equivalent to carbenes. The reactivity and properties of the various existing nitrenes can vary greatly and thus,

in this thesis, only the transformations and electronic configurations of phenyl nitrenes and *o*-biphenyl nitrene will be considered. Phenyl nitrene is known to have four low-lying spin-states: a triplet, where the non-bonding electrons have parallel spins, an open-shell singlet and two closed-shell singlets, in which the non-bonding electrons have opposite spin.^[223] An illustration of the electron configuration of the triplet ground state and the lowest singlet state of phenyl nitrene can be seen in Figure 5.1.

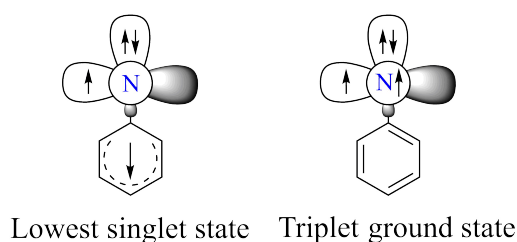
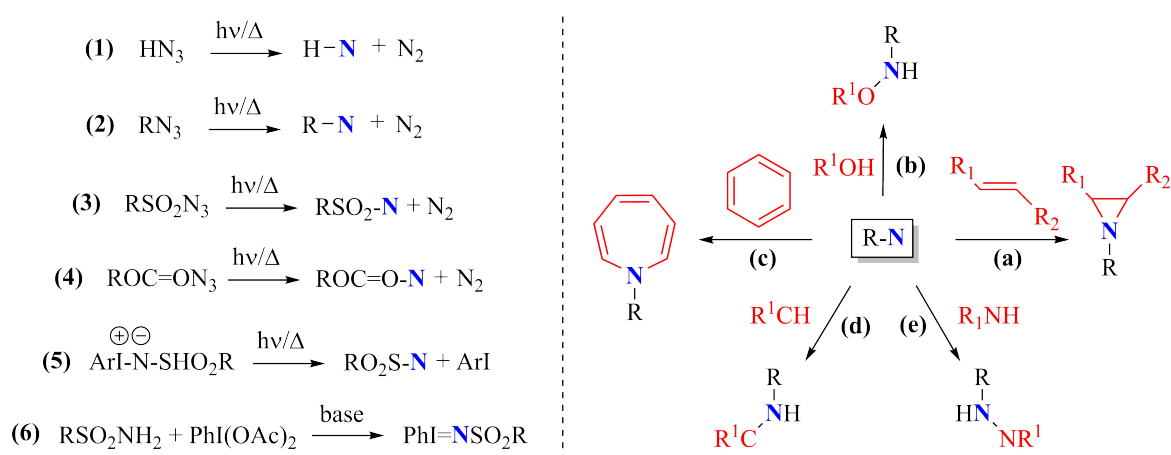


Figure 5.1: Electronic structures of phenyl nitrene displaying the lowest singlet state (left) and the triplet ground state (right).^[224]

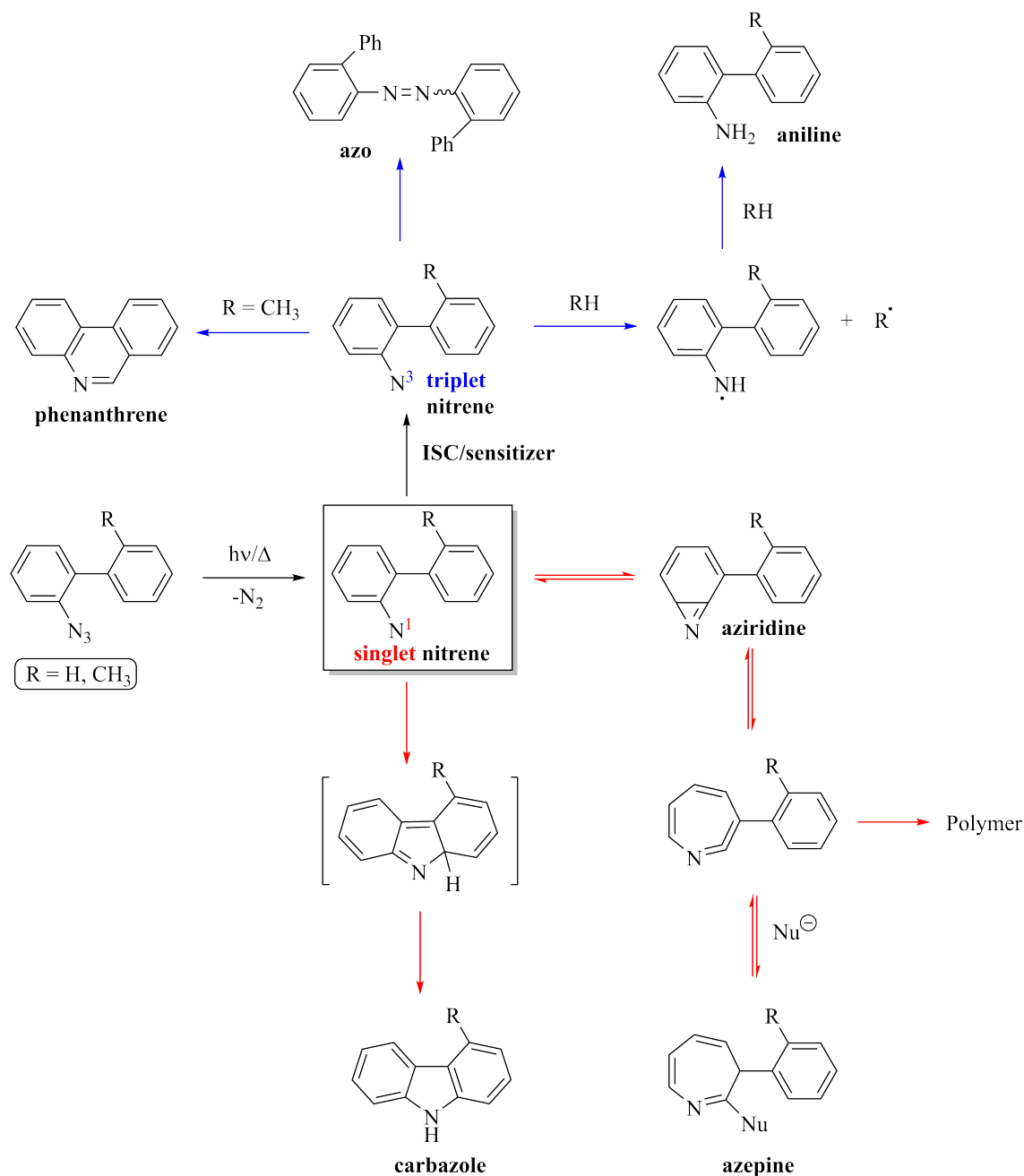
The most classical way to generate nitrenes is through photolysis or thermolysis of azides (Scheme 62, (1) and (2)), but they can also be constructed from sulfonyl azides, azidoformates,^[223,225] iminoiodanes and sulfonamides (Scheme 62, (3)-(6)).^[226,227] Being a highly reactive species, nitrenes smoothly undergo a variety of transformations, such as formation of an aziridine, a hydroxylamine, a ketenimine and C-H and inter- and intramolecular N-H insertion reactions (Scheme 62, (a)-(e)).^[225] Moreover, upon treatment of a sufficiently strong acid, nitrenes can generate nitrenium ions. The reactions of phenyl nitrene is perhaps the most well studied nitrene to this date and the reaction pathways follow the overview given in Scheme 62.^[218,223,227-230]



Scheme 62: Left: some strategies for the construction of nitrenes; Right: common transformations of nitrenes.^[223,225,227]

The photo- and thermochemical transformations of *o*-biphenyl nitrene have also garnered great interest due to its tendency to form carbazoles in great yields.^[223] *o*-Biphenyl nitrene

undergoes several of the same reactions as phenyl nitrene and a generalized summary of its transformations can be seen in Scheme 63. While the ground electronic state of *o*-biphenyl azide is a triplet,^[223] a singlet nitrene is obtained upon expulsion of molecular nitrogen, presumably occurring through the formation of an excited singlet azide.^[218] The singlet nitrene can then follow two distinct pathways, a singlet or a triplet directed path, leading to vastly different products. If the nitrene remains in the first excited singlet state, it can either undergo a nitrene insertion to yield carbazole or it can form a benzaziridine. The aziridine can then undergo a ring-expansion to give a ketenimine, which will polymerize into a black tarry substance. The presence of ketenimines have been established using a nucleophile as a trapping agent, which inhibits polymerization. Alternatively, the singlet nitrene can undergo intersystem crossing into a lower-lying triplet nitrene. This can also be achieved using a sensitizer, to cause a spin inversion from singlet to triplet. From here, the triplet nitrene can dimerize with itself to yield a diazo compound, or it can form a nitrene radical through hydrogen abstraction. This nitrene radical is highly reactive and can easily abstract another hydrogen atom from either the solvent or the substrate to form an aniline. If the given biphenyl has a methyl group *ortho* to the tethering between the two aromatic rings, a ring closure reaction can also take place to provide a phenanthridine.^[218,223,227,228]



Scheme 63: Generalized reaction pathways for some of the photochemical and thermally induced transformations of azidobiphenyl. [218,223,227–230]

The ability of aryl azides to absorb energy in the form of electromagnetic radiation is the key to their capability to produce aryl nitrenes through photolysis. The photophysical journey a compound undergoes following the absorption of energy can be illustrated using a Jablonski state diagram (Figure 5.2). Upon absorption of a photon, a compound will become excited and ascend from the ground state to an excited singlet state, which is higher in vibrational energy. This transformation is typically denoted $S_0 \rightarrow S_m$, where m refers to the order of the energy scale (0, 1, 2, ..., m). Such excitations occur from either a bonding or non-bonding orbital (σ , π , n) to an antibonding orbital (σ^* , π^*), transitions which are defined as $\sigma \rightarrow \sigma^*$, $\pi \rightarrow \pi^*$, $n \rightarrow \sigma^*$

and $n \rightarrow \pi^*$. After reaching an excited singlet state, several further transitions are possible, for instants, energy may be lost as heat through a process termed vibrational cooling (A). Alternatively, energy could be lost *via* emission as fluorescence (B), or it could undergo internal conversion (IC) followed by vibrational cooling back to the ground state, $S_m \rightarrow S_0$.

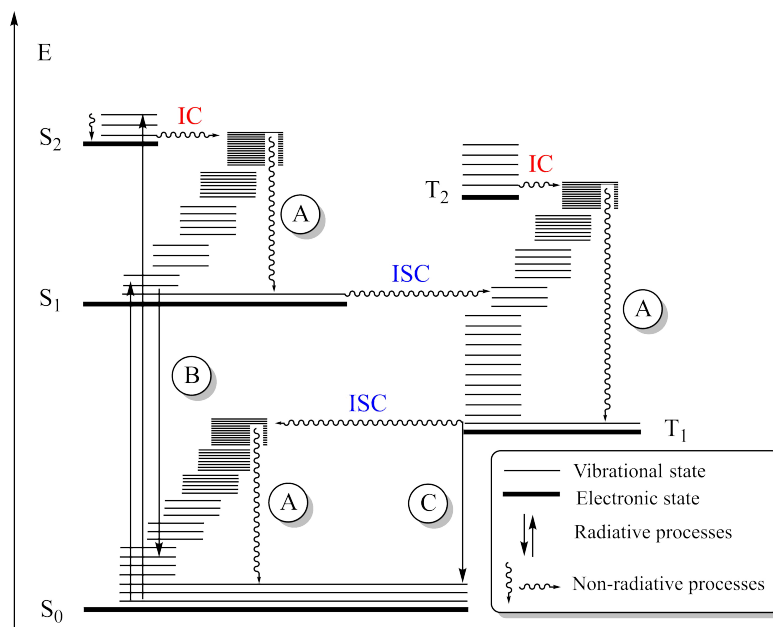
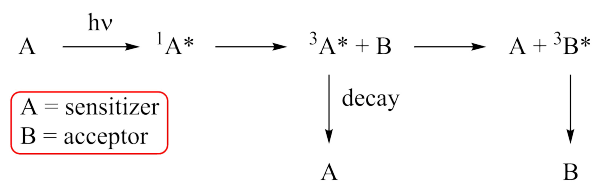


Figure 5.2: State diagram showing the various photophysical processes following excitation of a molecule, where transition A represents vibrational relaxation, B fluorescence and C phosphorescence.^[231]

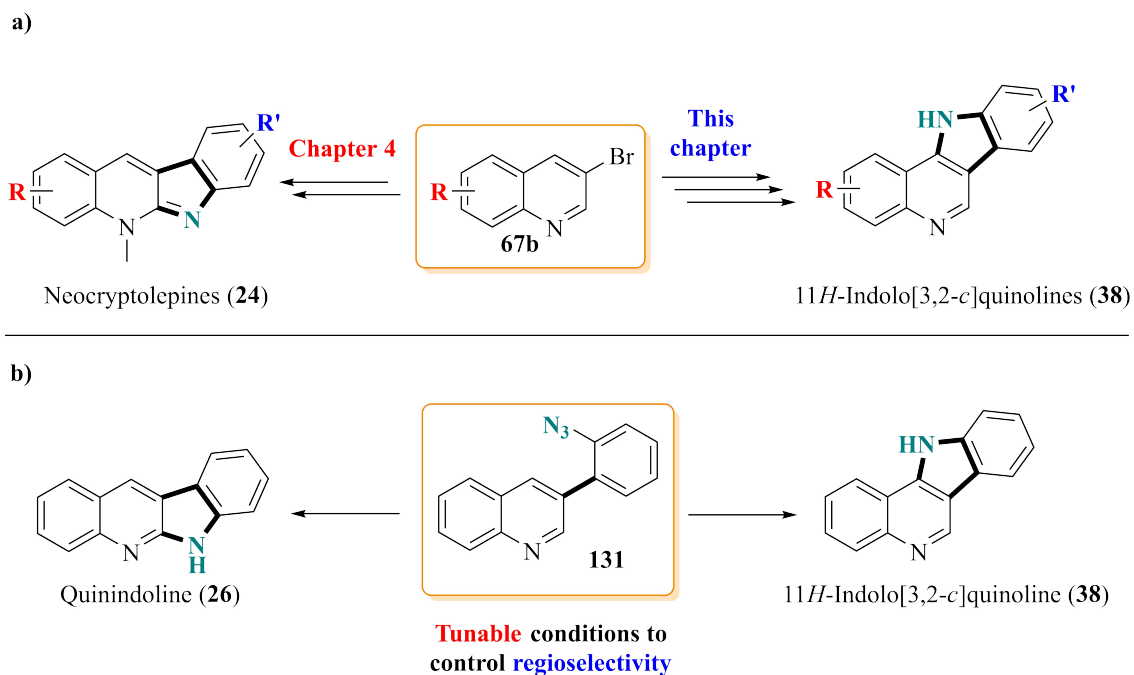
A third option is to undergo the spin forbidden process intersystem crossing (ISC) from an excited singlet state to an excited triplet state, $S_m \rightarrow T_m$, seeing a forbidden inversion in spin. Following ISC, energy may once more be lost as heat through vibrational cooling or emitted as phosphorescence (C).^[231,232] A compound which promotes ISC from a singlet to a triplet state, is known as triplet sensitizer, which acts by absorbing a photon, undergoing vibrational relaxation and ISC. Then, the triplet excited sensitizer transfers triplet energy to an acceptor, converting it from a singlet to a triplet state in the process.^[233] This process is illustrated in Scheme 64, where A is the triplet sensitizer and B the acceptor compound. For a sensitizer to be effective, it should ideally have a triplet energy (E_T) higher than the acceptor compound. Some examples of triplet sensitizers are benzophenone ($E_T = 289$ kJ/kmol), acetophenone ($E_T = 310$ kJ/kmol),^[234] acetone (331-343 kJ/kmol) and diacetal (238 kJ/kmol).^[235]



Scheme 64: Illustration of the triplet sensitization process based on the sensitization of an oxirane using benzophenone, where A is the sensitizer (benzophenone) and B is the energy acceptor (oxirane).^[233]

5.1.3 Project aims

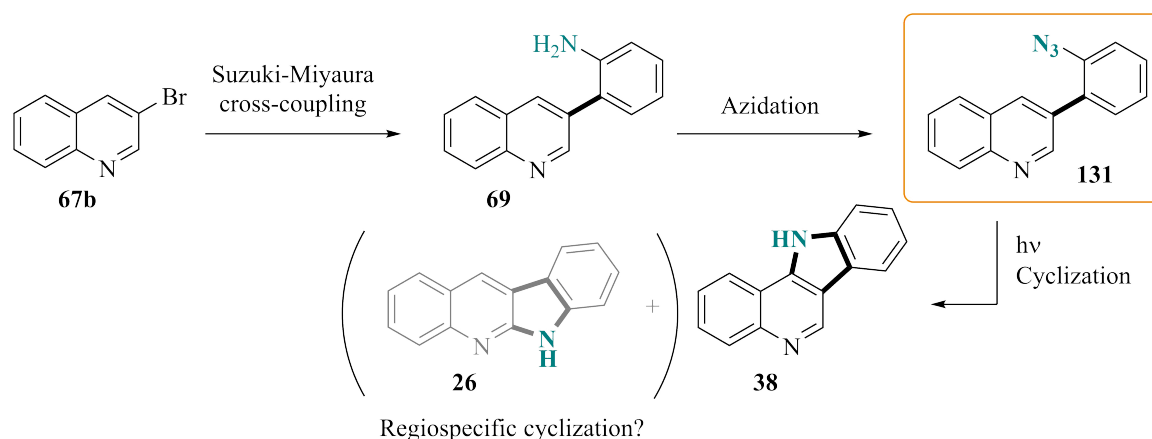
The aim of this part of the thesis was to develop a novel photochemical approach to furnish 11*H*-indolo[3,2-*c*]quinoline (**38**) and subsequently carry out a scope and limitations study to build a library of indoloquinolines viable for biological evaluation. Further, the method would utilize the same starting material, namely 3-bromoquinolines, as the novel neocryptolepine synthesis as outlined in Chapter 4. This would then allow for the synthesis of both neocryptolepine (**24**) and functionalized derivatives and the isocryptolepine precursors **38** from a common starting material (Scheme 65a). Throughout the synthetic process, the involved reactions would be thoroughly investigated to gain a better understanding of the chemistry. A secondary aim was to develop photolytic conditions that can unlock access to the natural product quinindoline **26** by tuning of the reaction conditions which would be employed to synthesize 11*H*-indolo[3,2-*c*]quinoline **38** (Scheme 65b).



Scheme 65: a) The aim of this project was to synthesize 11H-indolo[3,2-c]quinoline (**38**) and derivatives using 3-bromoquinolines **67b** as starting materials. b) A secondary aim was to find tunable conditions which could grant access to both quinindoline (**26**) and 11H-indolo[3,2-c]quinoline (**38**) from the same intermediate **131**.

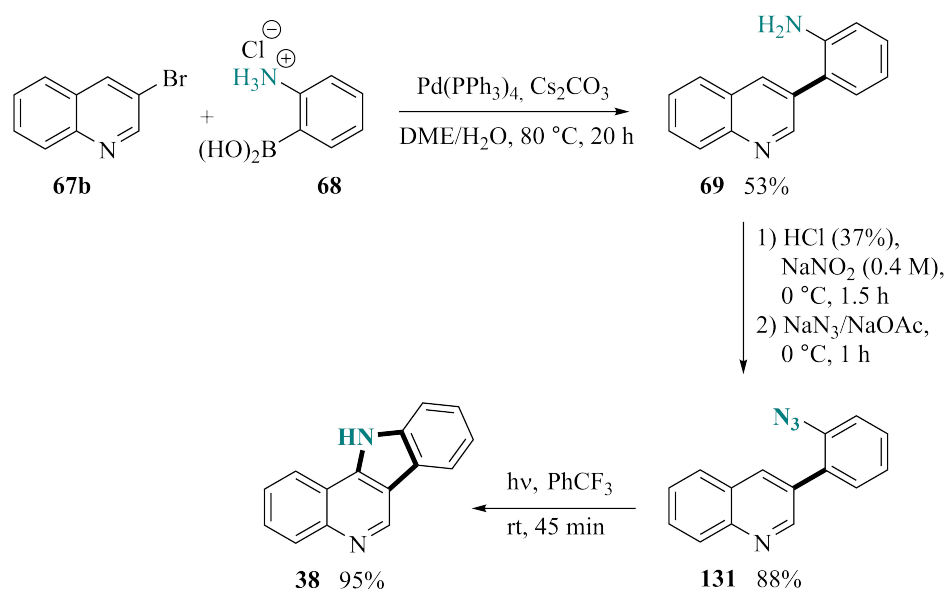
5.2 Development of a novel photochemical approach

Using 3-bromoquinoline (**67b**) as starting material, the novel photochemical pathway would commence with a Suzuki-Miyaura cross-coupling reaction to form biaryl **69**. This would then be subjected to a standard azidation protocol to yield the desired aryl azide **131**, which would finally be photolyzed to give 11H-indolo[3,2-c]quinoline (**38**) (Scheme 66).



Scheme 66: Proposed synthetic pathway to indolo[3,2-c]quinoline (**38**) using a photochemical transformation as the key step.

Although the photochemical cyclization of *o*-biphenyl azide to give carbazole has been intensely studied, photochemical transformations of aryl azide **131** remains unexplored in the currently available literature. Thus, there exists the possibility that the cyclization would not proceed in a regioselective manner, forming a mixture of the two regioisomeric indoloquinolines **38** and **26**. From the study of PAHs, it has been established that regioisomers which can adopt either an angular or linear geometry, are more stable in the angular topology.^[236] If the same trends are applicable to heteroaromatics, the favored product in the photochemical cyclization of aryl azide **131** should be the more angular indoloquinoline **38**. To test the viability of the envisaged synthetic route, a Suzuki-Miyaura cross-coupling reaction between 3-bromoquinoline (**67b**) and 2-aminophenylboronic acid hydrochloride (**68**) was carried out using the same conditions as described in Chapter 4 to give biaryl **69** in 53% yield following purification by silica gel column chromatography (Scheme 67). The obtained biaryl was then transformed to the corresponding diazonium salt using NaNO₂ in ice-cooled concentrated HCl. Then, treatment of the diazonium salt with NaN₃ and NaOAc, acting as a buffer, was used to displace the diazonium salt and furnish the target aryl azide **131** in 88% yield, which after aqueous workup was found to be sufficiently pure by ¹H NMR, ruling out the need for purification by column chromatography. Before subjecting the aryl azide to photolysis, its λ_{max} was determined to be 308 nm using UV-vis spectroscopy (Figure 5.3).



Scheme 67: Novel synthetic pathway towards indolo[3,2-*c*]quinoline (**38**) using photochemistry as the key strategy.

Rigorous screening experiments of suitable solvent systems revealed that photolysis of aryl azide **131** at room temperature furnished isocryptolepine precursor **38** in 95% yield using α,α,α-trifluorotoluene (TFT) as the solvent (Table 5.1, Entry 5). Comparatively, running the reaction in normal toluene was less successful and gave the target compound in a 67% yield following purification by silica gel column chromatography (Table 5.1, Entry 1). Analysis of

the ^1H NMR spectra of the crude mixture showed a complex mixture, presumably due to the formation of polymeric material, which was not observed using TFT. Fluorinated solvents are favored in photochemical transformations due to being more inert than their non-fluorinated counterparts and may thus be less likely to form or react with the formed radicals which contribute to the amount of polymeric tarr being formed.^[237]

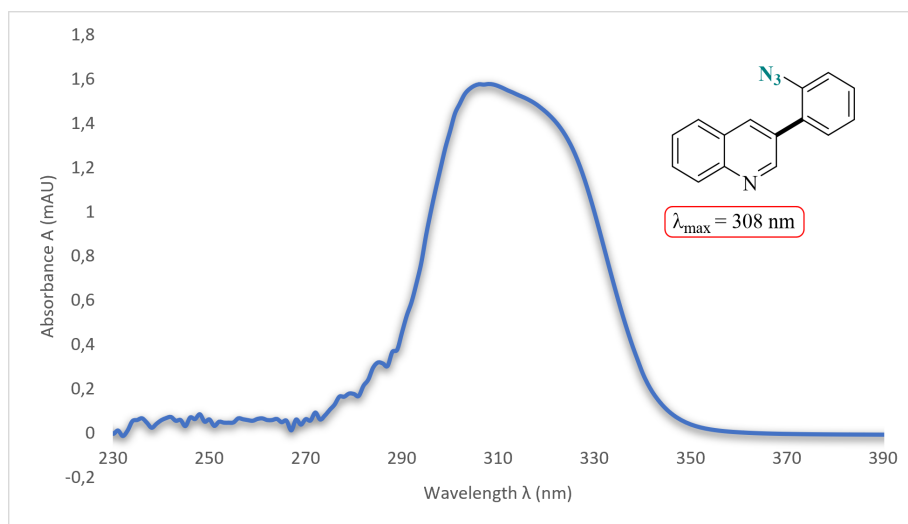
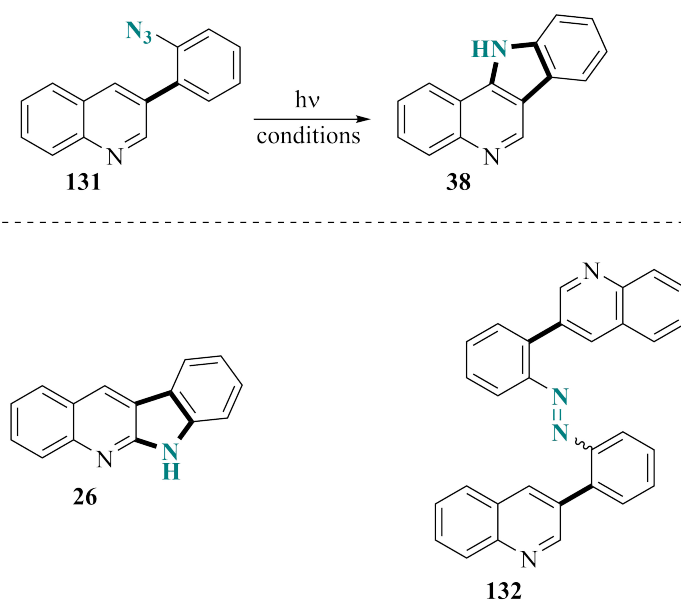


Figure 5.3: UV-vis spectrum of aryl azide **131** showing a λ_{max} of 308 nm in methanol. The solvent profile has been removed by subtracting the background spectrum.

While the photolysis of toluene is known to generate a benzyl radical ($\text{PhCH}_2\cdot$),^[238] a benzodifluoride radical ($\text{PhCF}_2\cdot$) seems unlikely to form due to both the stability of the C-F bond and the instability of such a radical. Since it is believed that the polymeric tarr is derived from a singlet nitrene pathway, by adding a triplet sensitizer, the hope was that this would minimize polymer formation and also potentially give access to indoloquinoline **26** (Table 5.1). Mixing acetophenone and toluene gave a mixture of approximately 47% indoloquinoline **38** and 19% of compound **26** (Table 5.1, Entry 3), while diacetal gave a crude mixture too complex to interpret using NMR. Changing the sensitizer to 10% acetone in toluene gave 92% of indoloquinoline **38**, successfully eliminating the formation of polymers, however not forming any traces of indoloquinoline **26**. By combining TFT with various sensitizers, it was possible to construct indoloquinoline **26** along with diazo compound **132**, however the yields were low (Table 5.1, Entries 6 and 7).

Table 5.1: Solvent screenings for the photocyclization of aryl azide **131**.

Entry	Solvent	Additive (%)	Temp. (°C)	Time (min)	38 (%)	26 (%)	132 (%)
1	PhMe	-	rt	10	67	-	-
2	MeOH	-	rt	15	63	Traces	Traces
3	PhMe	PhAc (10)	rt	15	<47 ^a	19	-
4	PhMe	Diacetal (10)	rt	25	Traces		
5	PhCF ₃	-	rt	45	95 ^b	-	-
6	PhCF ₃	PhAc (10)	rt	45	Traces	5	15
7	PhCF ₃	Ph ₂ CO (0.01 M)	rt	45	24	10 ^c	14 ^c
8	PhMe	Acetone (10)	rt	45	92 ^b	-	-
9	Cyclohexane	Acetone (10)	rt	45	44	<6	-
10	PhCF ₃	-	0	45	quant. ^b	-	-
11	PhMe	PhAc (10)	-10	20	7 ^a	8	13
12	Benzene	Ph ₂ CO (0.01 M)	-10	20	23	14 ^c	9 ^c

All reactions were carried out using 50 mg aryl azide **131** dissolved in 150 mL solvent;^a Contained impurities;^b No purification by silica gel column chromatography required;^c Isolated as a mixture and ratio determined by ¹H NMR integrals.

The formation of diazo compound **132** was easily verified by comparison with the ¹H NMR spectrum of aryl azide **131**, showing the same coupling patterns for all protons, accompanied by a downfield shift of the signals (Figure 5.4). The structure was further corroborated by

HRMS showing a mass of 437.1769, which corresponds well with the protonated mass of diazo compound **c** ($[M + H^+]_{\text{calcd.}} = 437.1761$). The configuration of the azo moiety was not investigated, but it is likely a mixture of both the *cis* and *trans* isomers.

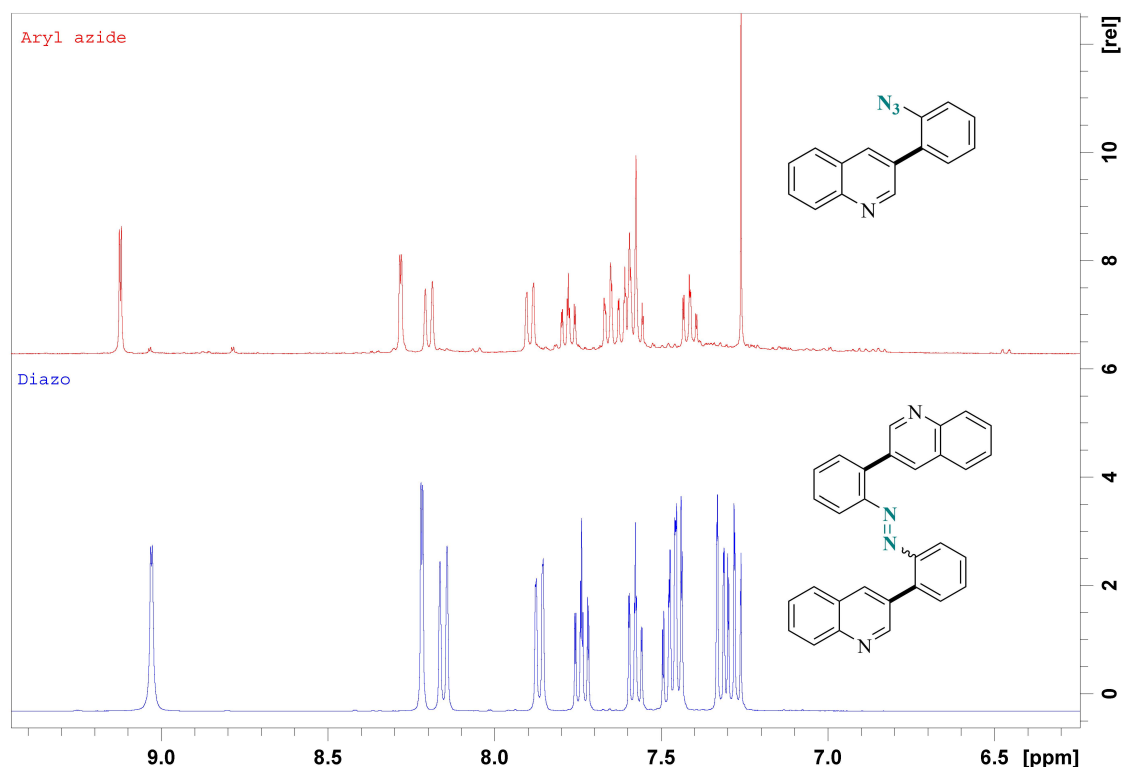
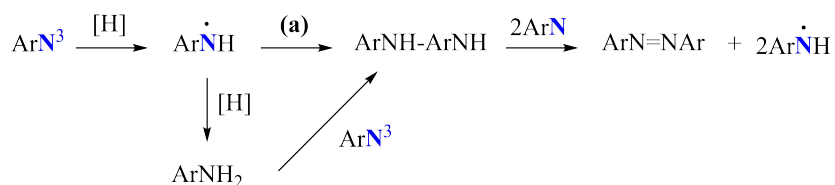


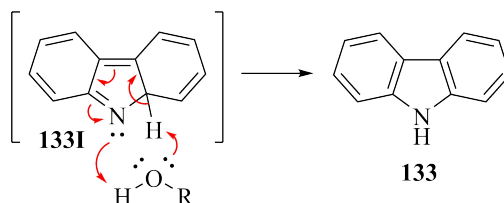
Figure 5.4: ^1H NMR spectra of aryl azide **131** (red) and diazo compound **132** (blue) in CDCl_3 .

Diazo compounds are another triplet derived product,^[223] which is presumed to form following one of two pathways, both of which is initiated by the aryl nitrene abstracting a hydrogen atom from either the solvent, substrate or the product, forming an amino radical ($\text{ArNH}\cdot$) (Scheme 68). The first option is that the newly formed amino radical dimerizes (**a**) to a hydrazobenzene (ArNH-ArNH), which upon oxidation by a nitrene yields the diazo compound (ArN=NAr). The second possibility is for the amino radical to abstract another hydrogen atom to form an aniline, which upon reaction with an aryl nitrene generates the hydrazobenzene, following the same path towards the diazo compound as the first pathway.^[223]



Scheme 68: Proposed mechanism for the formation of diazo compounds from a triplet aryl nitrene.^[223]

In the photochemical synthesis of carbazole from *o*-biphenyl azide, it has been observed that the use of protic solvents, such as water or methanol, greatly accelerate product formation.^[239] This presumably occurs through the solvent catalyzing the 1,5-hydrogen shift from intermediate **133I** to carbazole (**133**), as illustrated in Scheme 69. Attempting the cyclization of aryl azide **131** using methanol disappointingly gave a complex mixture, allowing for the isolation of 63% of indoloquinoline **38** following purification (Table 5.1, Entry 2).



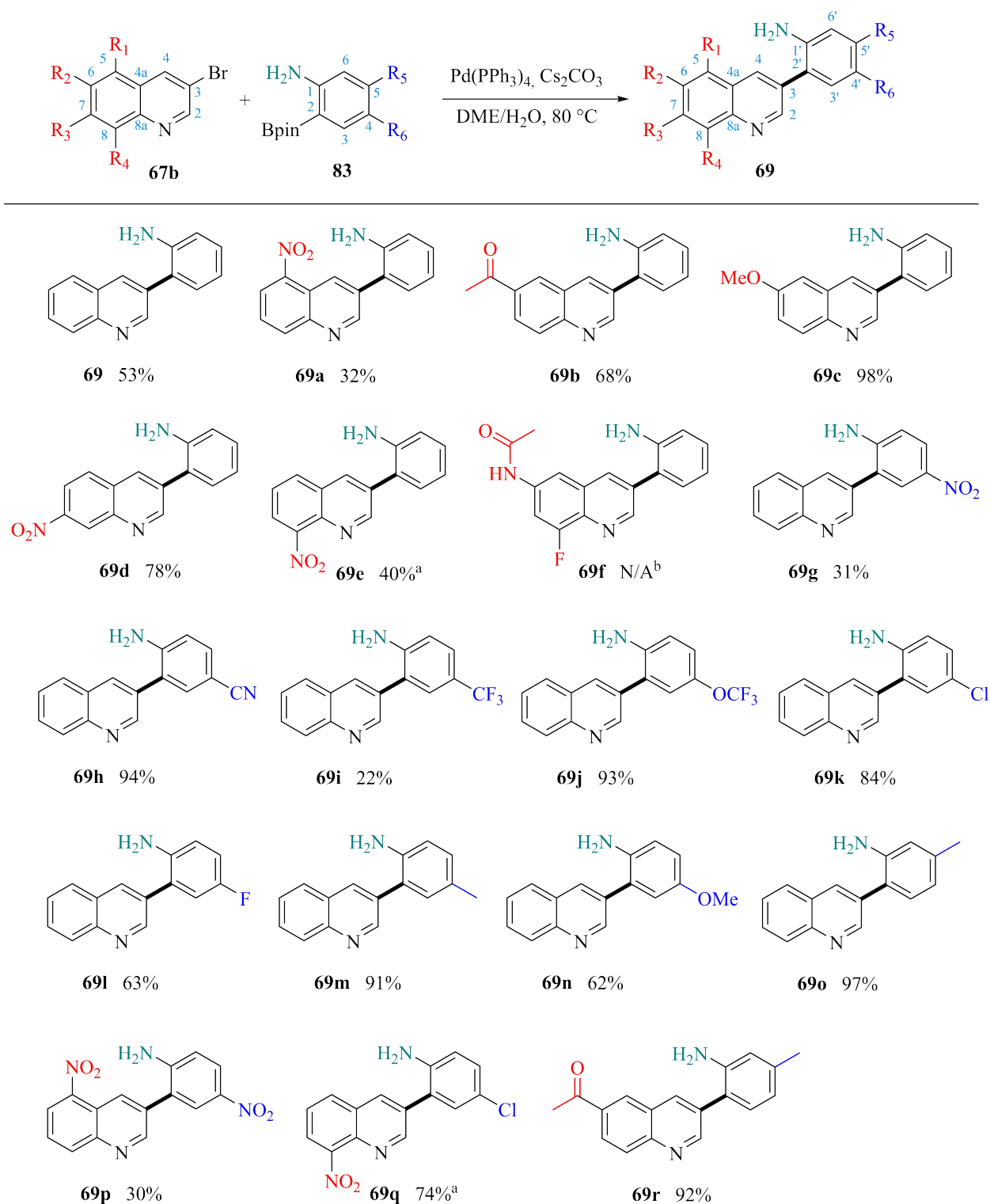
Scheme 69: Proposed mechanism for the solvent promoted cyclization of intermediate **133I** to give carbazole (**133**).^[239]

In an effort to investigate if having lower overall reaction kinetics would affect the outcome of this reaction by increasing the life time of the transient reaction intermediates, some experiments at 0 °C and -10 °C were also attempted (Table 5.1, Entries 10-12). Using toluene and acetophenone at -10 °C resulted in an approximately one-to-one formation of the indoloquinolines **38** and **26**, however, in extremely poor yields, with similar results obtained using benzene and benzophenone. The reaction conducted at 0 °C performed exceedingly well, giving indoloquinoline **38** in quantitative yield (Table 5.1, Entry 10). Despite being the best outcome of the screening experiments, for practical reasons, the reaction at room temperature was chosen as the standard condition moving forward into the scope and limitations study. Despite considerable efforts, the screening experiments did not reveal conditions which allowed for the regioselective synthesis of indoloquinoline **26** in good yield.

5.2.1 Investigation of substrate scope

Synthesis of biaryls **69** using Suzuki-Miyaura cross-coupling reactions

Having prepared 24 neocryptolepine derivatives in Chapter 4 using a specific set of Suzuki-Miyaura cross-coupling reaction conditions, this was used as a template to carry out the cross-coupling reactions to synthesize biaryls **69** in this work, in order to evaluate the efficacy of the method for such systems. The starting quinolines and 2-aminophenylboronic acids/pinacol esters were either obtained commercially or prepared as described previously in Chapter 4, Section 4.2.1. Applying the aforementioned Suzuki-Miyaura cross-coupling conditions, a diverse library of biaryls were prepared in 30-98% yield following purification by column chromatography (Scheme 70). The structure for each biaryl was easily confirmed using ¹H, ¹³C and ¹⁹F NMR, when applicable, along with various 2D NMR spectrum (COSY, NOESY, ¹H-¹³C HSQC and ¹H-¹³C HMBC) for full structure elucidation.



^aUsing 3-iodo-8-nitroquinoline; ^bYield not applicable as the sample was not possible to separate from impurities.

Scheme 70: Scope of the Suzuki-Miyaura cross-coupling reactions to form biaryls **69**.

It is well established in the literature that the Suzuki-Miyaura cross-coupling reaction is tolerant of a broad substrate scope and further has a high level of functional group tolerance.^[127,240,241] With few exceptions, this is well reflected in Scheme 70, where the method

supported both EWG and EDG functionalizations on both the quinoline and aniline moieties. Of the quinoline functionalized biaryls **69a-69f** and **69p-69r**, the three nitro biaryls **69a**, **69e** and **69p** primarily gave poor yields (32, 40, and 30% respectively) due to challenging purifications. In particular, 5-nitro substituted biaryl **69a** could not be purified using silica gel and instead alumina had to be utilized, which made it possible to isolate some pure fractions, albeit, large quantities of product were lost due to overlapping fractions. Compound **69f** was subjected to multiple purification attempts, using both silica gel and alumina, however, a pure sample was never obtained. From the ^1H NMR spectra, it was possible to see that the correct compound had formed, and the product was reacted further in hopes that the impurities would become easier to remove in the next step. Conducting HRMS of compound **69f** showed a mass of 296.1205, corresponding well to its protonated mass ($[\text{M} + \text{H}^+]_{\text{calcd.}} = 296.1194$), along with a plethora of other signals coming from the impurities in the sample.

The preparation of biaryls bearing various substituents on the aniline ring (compounds **69g-69o**) was done with ease. The purification of nitro biaryl **69g** was extremely challenging and is likely the cause for the poor yield of 31%, as the product largely overlapped with unreacted starting material. The poorest yield for this series was obtained for compound **69i**, which suffered from a different issue. Based on the TLC analysis, it should have been a straightforward purification, however, upon analyzing the ^1H NMR spectra, the purified sample contained large amounts of an impurity, which was determined to be pinacol (Figure 5.5, red spectra). The chemical shifts of the methyl groups in pinacol fits perfectly with those observed in the spectra of compound **69i** ($\Delta\delta = 0$ ppm),^[242] while the hydroxyl groups were not visible. The pinacol could easily be removed by dissolving the mixture in CH_2Cl_2 and washing the organic phase multiple times with hot water, resulting in the complete removal of pinacol (Figure 5.5, green spectra and highlighted box). A ^{11}B NMR spectra was also run before the aqueous workup to ensure that the sample contained no traces of boron, which was the case as evident from the flat baseline (Figure 5.5, blue spectra).

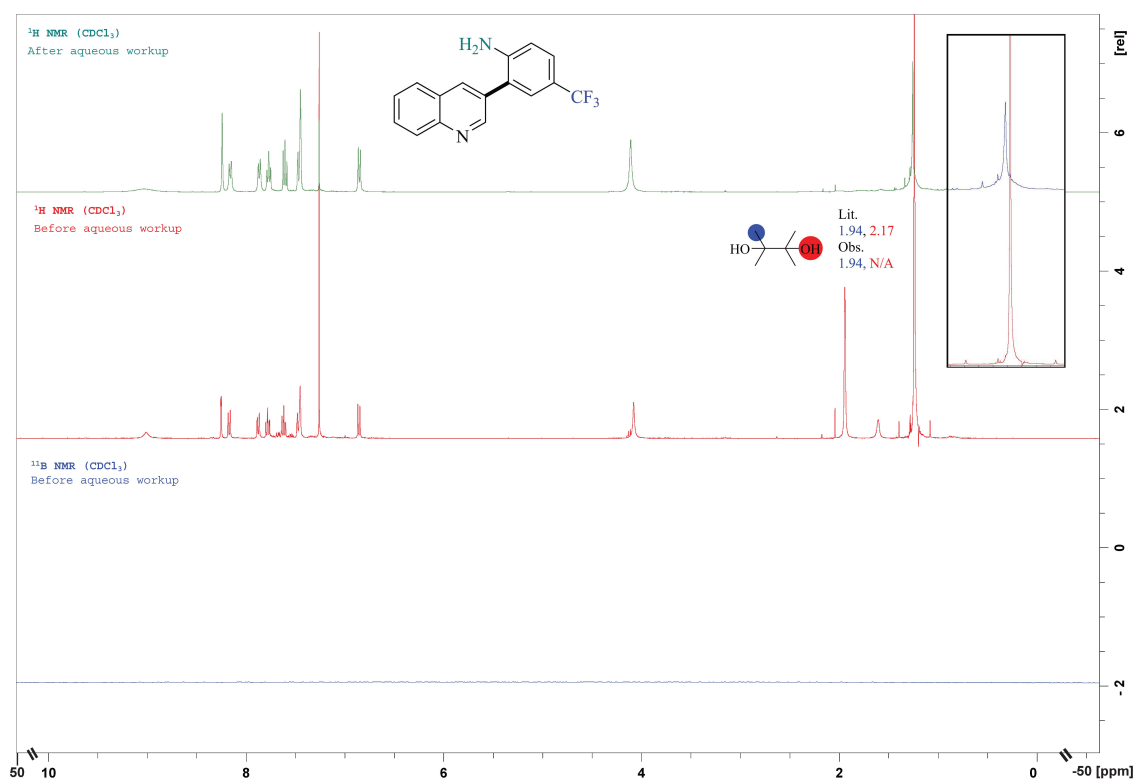
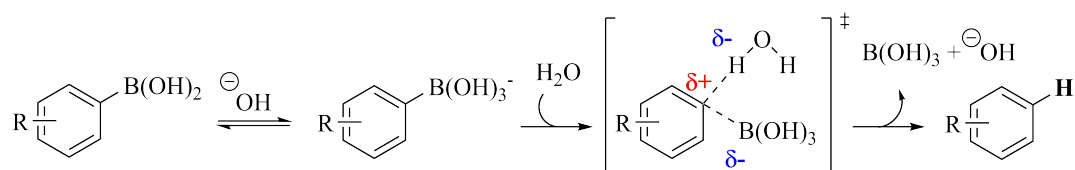


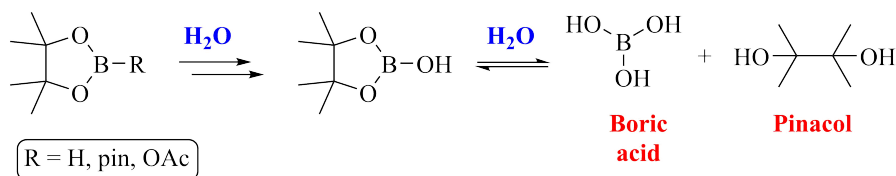
Figure 5.5: ^1H NMR spectrum of compound **69i** before (red) and after (green) workup with hot water, showing the presence of pinacol before the aqueous workup (highlighted box) and ^{11}B NMR confirming that no boron is present in the sample before aqueous workup (blue).

The most obvious source of pinacol in the reaction mixture is pinacol ester **83d**. In addition to being directly catalyzed by water, the protodeboronation of arylboronic acids and arylboronic acid pinacol esters is known to occur under acidic and basic conditions and by reaction with various metal salts.^[243–245] Polyfluorinated and 2-heteroaryl boronic acids have been revealed to be exceptionally unstable and readily undergo deboronation.^[246] The mechanism by which aryl boronic acids undergo base-induced protodeboronation is proposed to commence by the formation of an arylboric acid (Ar-B(OH)_3^-) (Scheme 71). Subsequent direct protonolysis of the benzene ring produces a partially positively charged transition state, which releases the arene along with boric acid and hydroxide. The base-induced protodeboronation of aryl boronic acid pinacol esters is believed to proceed *via* a similar mechanism.^[245]



Scheme 71: Proposed mechanism for the base-induced protodeboronation of arylboronic acids.^[243,244]

The strong electronegative effect exhibited by the trifluoromethyl group of pinacol ester **83d** is presumably sufficient to destabilize the C-B bond, causing deboronation to form 4-(trifluoromethyl)aniline. The reported boiling point of this aniline is 83 °C,^[247] which explains why its presence was never confirmed in the reaction mixture, as the aniline was likely removed when the crude mixture was evaporated onto celite for subsequent purification. The protodeboronation of pinacol ester **83d** alone is not sufficient to directly explain the presence of pinacol in the reaction mixture, as there is no pinacol formed in the proposed mechanism in Scheme 71. In the case of an arylboronic acid pinacol ester, the transition state shown in Scheme 71 would eliminate HO-Bpin instead of boric acid.^[245] Under basic aqueous conditions, *ie* under standard Suzuki-Miyaura cross-coupling conditions, HO-Bpin exists in an equilibrium with boric acid and pinacol (Scheme 72),^[248] providing a probable source for the observed pinacol during the synthesis of biaryl **69i**. The presence of pinacol was also observed in the ¹H NMR spectra of biaryl **69m**, however, in this case it did not negatively impact the yield. Biaryl **69m** was obtained in a 91% yield following both purification by silica gel column chromatography and washing with hot water to finally remove the pinacol. It is not clear why only these two examples resulted in the formation of pinacol, as biaryl **69m** contains no functionalities which are known to destabilize the C-B bond, in fact, the inductive effect of the methyl group in pinacol ester **83g** should help to stabilize the transition state in Scheme 71, making the protodeboronation less favorable.

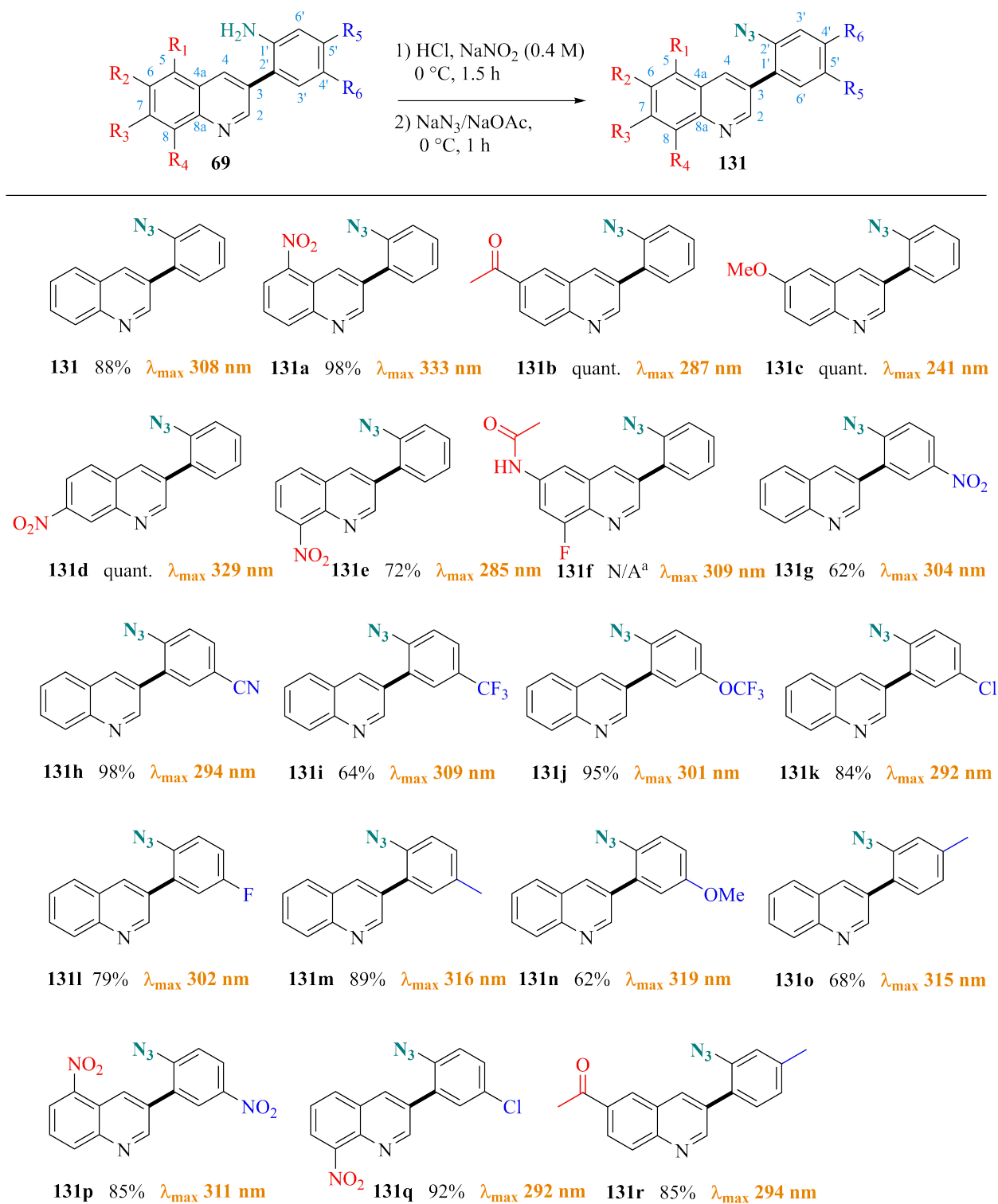


Scheme 72: Proposed formation pathway for boric acid and pinacol from the hydrolysis of some pinacol esters.^[248]

Synthesis of aryl azides **131**

With biaryls **69** in hand, aryl azides **131** were prepared in excellent yields following a diazotization of the amine and subsequent installation of the azido moiety (Scheme 73). Despite the harsh acidic conditions required to carry out this reaction, it has the advantage that following aqueous workup, no purification by silica gel column chromatography was necessary to obtain a sufficiently pure sample to continue the synthetic pathway towards the intended 11*H*-indolo[3,2-*c*]quinolines **38**. Organic azides are widely regarded as unstable and in some cases highly explosive compounds which must be treated with great caution.^[249] The "rule of six" is often employed to assess an azides stability, postulating that if there are six carbon atoms present per one azido group, the compound should be relatively stable.^[250] Having a C-N ratio of on average 15 carbons per one azido functionality, aryl azides **131** should indeed be fairly safe and non-explosive and moreover stable, thus full structure characterizations by ¹H, ¹³C

and ^{19}F NMR, when applicable, were conducted. Perhaps the most straightforward way to confirm the presence of an azide is by analysis of its infrared (IR) spectra. The azide stretch is typically observed as an intense signal in the region of $2160\text{--}2080\text{ cm}^{-1}$. [223,249]



^aYield not obtained as the sample was not possible to separate from impurities.

Scheme 73: Scope of the azidation reactions to form aryl azides **131**. The associated λ_{max} values using methanol as a solvent for all compounds are also shown.

Interestingly, the IR spectra of several of the aryl azides displayed the azide stretch as an intense doublet instead of the expected single peak. Examining the IR spectra of aryl azide **131e**, two distinct signals appear in the azide region, namely at 2125 and 2083 cm^{-1} (Figure 5.6). Studies of the IR spectrum of organic azides have revealed this phenomenon to occur due to Fermi interaction, which is a magnetic interaction between an electron and a nucleus, with combination tones, involving the N_3 symmetric and C-N vibrational stretch.^[249] Typically, the N_3 main band is the most intense and the other signal is an N_3 shoulder band. Consequently, the more intense signal in the IR spectra of compound **131e** is the main azido band, appearing at 2083 cm^{-1} , while the shoulder band represents the signal at 2125 cm^{-1} .

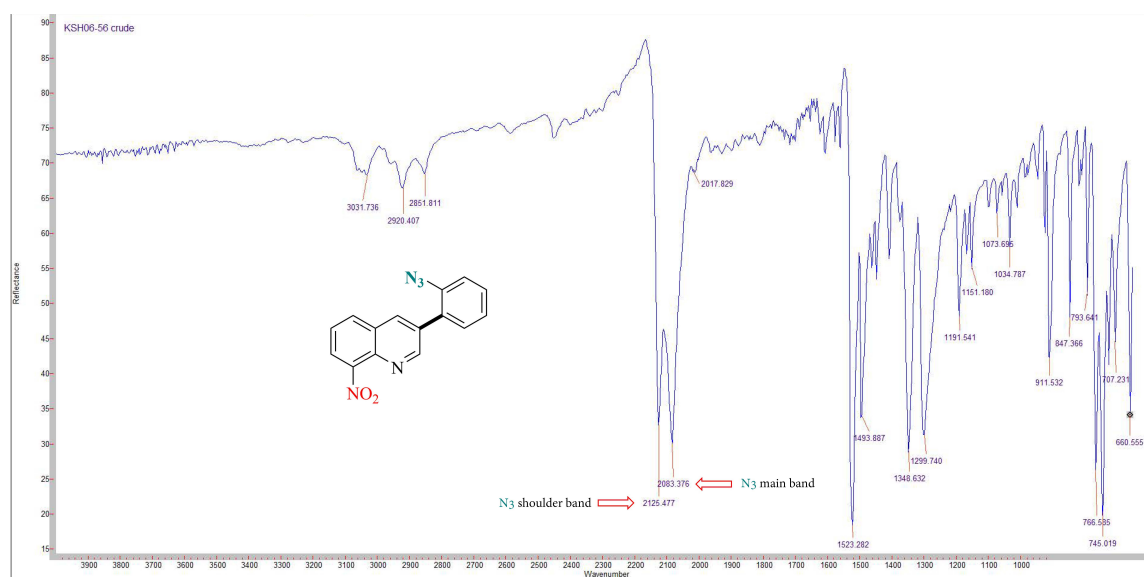
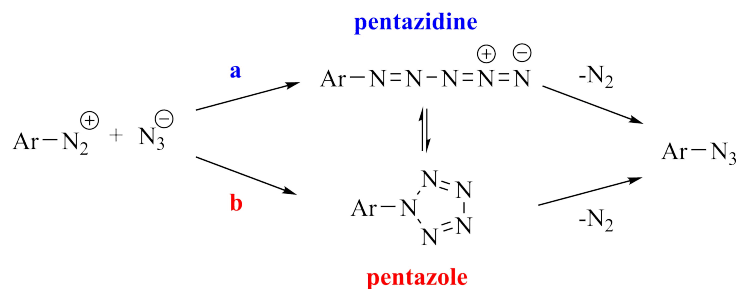


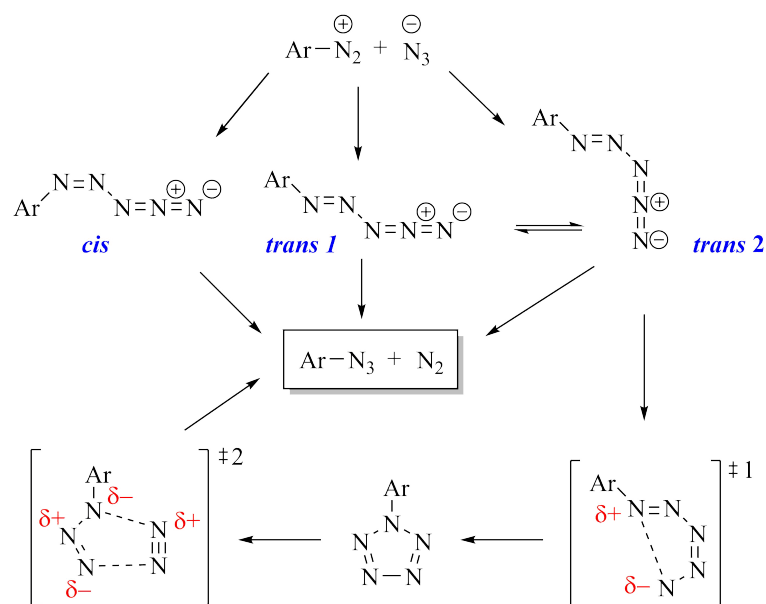
Figure 5.6: IR spectra of aryl azide **131e** showing the azide stretch as a doublet, where one signal is the main azido stretch (2083 cm^{-1}) and the other a shoulder band (2125 cm^{-1}).

Only four of the 19 prepared aryl azides were formed in yields below 70%, namely aryl azides **131g**, **131i**, **131n** and **131o**. There is no immediately apparent rationale for these results being poorer than the rest. Perhaps examining the mechanism by which the azido group is installed might shed some light on these observations. The mechanism by which the amino group in biaryls **69** is transformed into a diazonium salt is well established and proceeds through the amine reacting with the *in situ* generated nitrosonium ion.^[251] From there, two pathways towards the formation of an aryl azide are possible yielding two distinct intermediates: one being a linear dipolar **pentazidine**, which upon loss of the two terminal nitrogen atoms as molecular nitrogen yields the aryl azide (Scheme 74). The second option is the formation of a cyclic intermediate in the form of a **pentazole**, fragmentation of which results in the extrusion of nitrogen gas along with the aryl azide.^[223]



Scheme 74: Two possible pathways for the formation of an aryl azide from a diazonium salt: **a** via a linear dipolar pentazidine intermediate or **b** via a cyclic pentazole.^[223]

The proposal in Scheme 74 does not take into account two important factors; firstly, the configuration of the pentazidine is not considered and secondly, it fails to evaluate how the pentazole is both formed and its fragmentation route. A more comprehensive mechanism was suggested by Butler and coworkers, using a combination of experimental and theoretical work to support their proposal (Scheme 75).^[252] They argue that the pentazidine can exist in three configurations; one *cis* and two *trans* intermediates, which are in an equilibrium. Theoretically, there is a possibility of a second *cis* configuration, not depicted in Scheme 75, which was found to be too sterically congested to be viable. While each of the three pentazidines can then lose molecular nitrogen to form the desired aryl azide, the *trans 2* configuration of pentazidine also undergoes cyclization into the pentazole, through transition state 1. Finally, the pentazole will fragment according to transition state 2 and result in the construction of aryl azide along with extrusion of molecular nitrogen. This proposed reaction pathway has later been supported by correlational analyses by Burke and Fazen, where they also examined substituent effects on the formation of the intermediates.^[253] Their results indicated that both EDGs and EWGs had only minor effects on the overall energetics of the proposed reaction pathway. Of the four poorest performing aryl azides in our study, two examples contain *p*-EWGs (compounds **131g** and **131i**) and the remaining two contain *p,m*-EDGs (compounds **131n** and **131o**). From this it might be fair to speculate that there are other factors affecting the performance of the reaction other than substituent effects, as no clear trend can be established from these examples alone. As the reactions are carried out in concentrated acid, the aryl azides are likely protonated at the quinoline nitrogen during the reaction. Further, no unreacted starting material was ever detected by crude ¹H NMR. A possible explanation for the observed yields could then be that during the workup, the pH of the crude mixture was not made sufficiently basic to facilitate complete deprotonation, resulting in some of the formed product remaining in the aqueous phase.



Scheme 75: Detailed proposition for the formation of aryl azides from diazonium salts, supported by a combination of experimental and theoretical work conducted by Butler and coworkers.^[252]

After obtaining all aryl azides, the next step in the synthesis was the photochemical cyclizations. In order to carry this reaction out successfully, the UV-vis spectrum of all aryl azides **131** were obtained (results in Scheme 73). All analyses were conducted using methanol as the solvent owing to its low UV cut-off value of 205 nm,^[254] subtracting the solvent signals through the use of background scans. The λ_{max} values for the prepared aryl azides were in the range of 241–333 nm. Nitroaromatics, in particular *o*-nitrobenzyls, are known to be photolabile groups and it was thus not surprising to see a large range of λ_{max} values for the nitro functionalized aryl azides (compounds **131a**, **131d**, **131e**, **131g** and **131p**).^[255] Aryl azides **131b** and **131r**, containing a carbonyl functionality at C-6 of the quinoline ring (nomenclature shown in Scheme 73) had very similar absorption spectrum, displaying maximum absorbance at 287 and 294 nm, respectively (Figure 5.7).

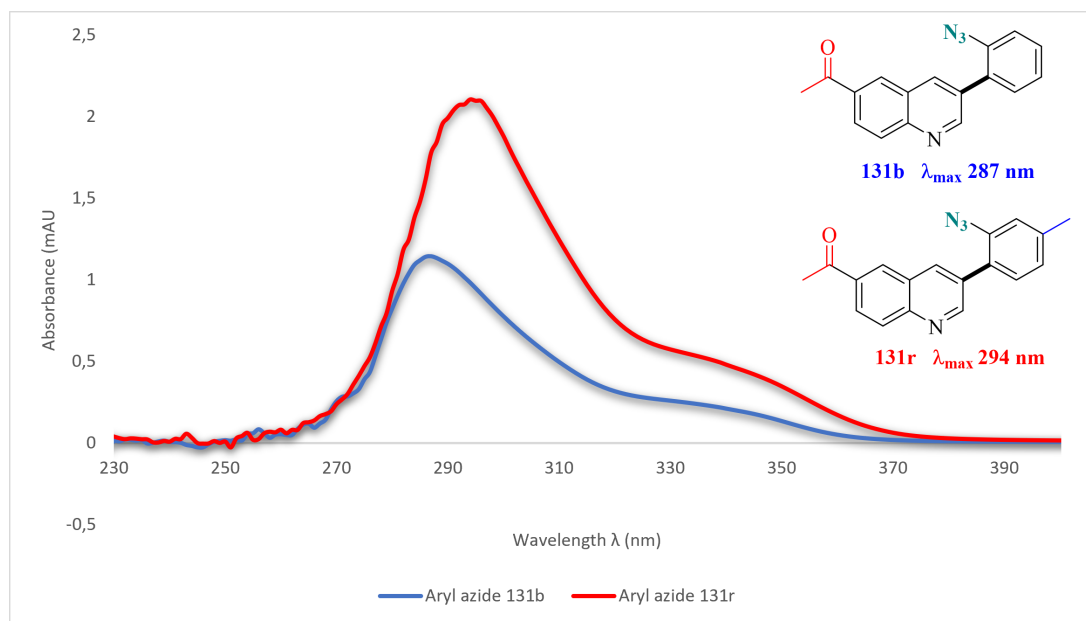
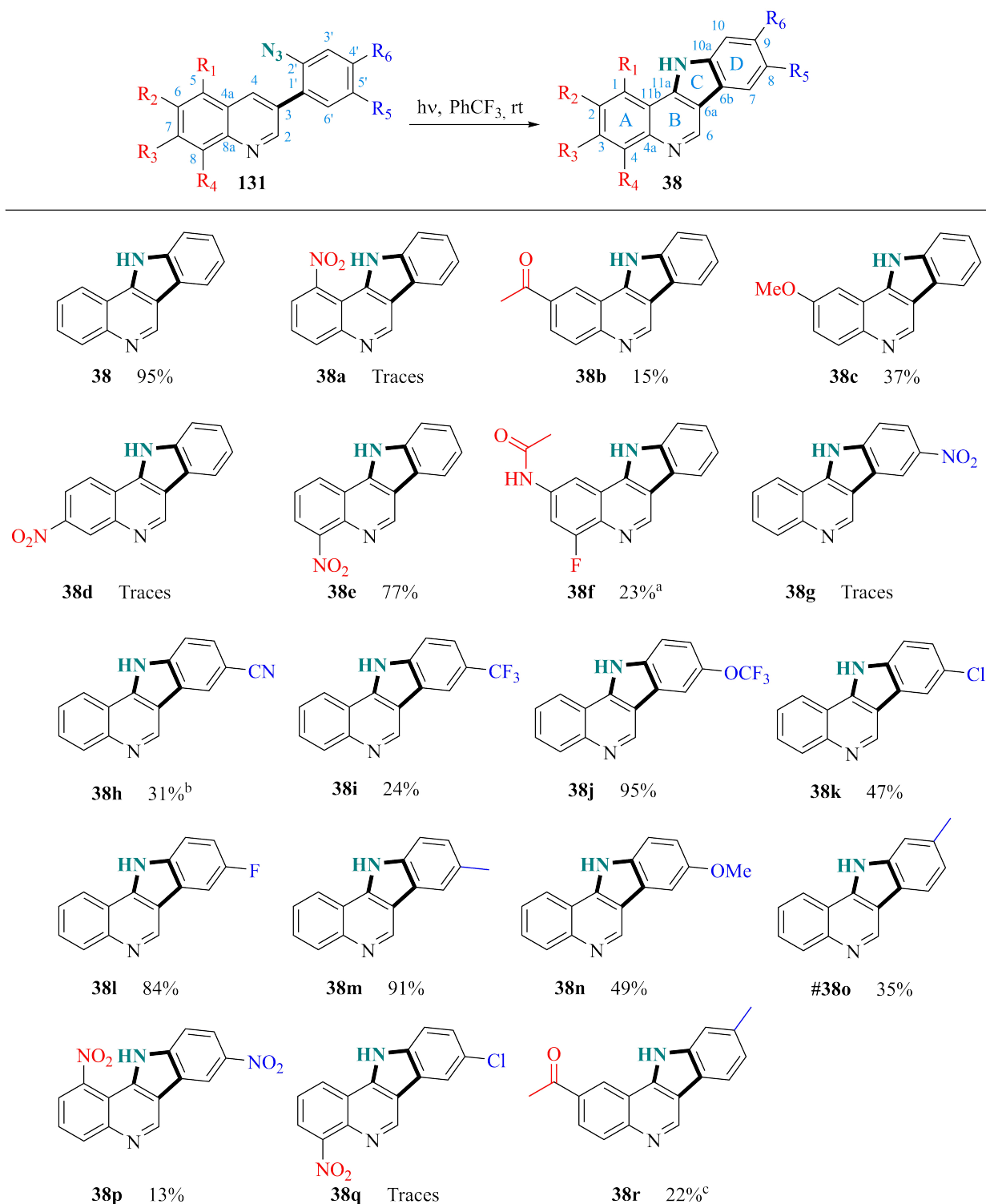


Figure 5.7: UV-vis spectrum of aryl azides **131b** in blue and **131r** in red using methanol as solvent. The solvent signals have been subtracted by using background scans.

Photochemical synthesis of 11H-indolo[3,2-c]quinolines 38

With an arsenal of aryl azides in hand, it was time to subject them to the photochemical cyclization procedure. Given that the observed absorbances of aryl azides **131** were generally in the range of 254–366 nm, a 125 W medium-pressure mercury-vapor lamp, which emits radiation at 254, 265, 270, 289, 297, 302, 313, 334 and 366 nm, was chosen to carry out the reactions. The lamp also emits significant amounts of radiation within the visible region, between 405–580 nm. The glassware utilized was a Pyrex immersion well and cold finger, filtering out minimal amounts of light. Irradiation of aryl azides **131** under optimized photochemical conditions proceeded in a regiospecific manner to give 11H-indolo[3,2-c]quinolines **38** in variable yields (Scheme 76). The structure of all formed compounds were verified and distinguished from the corresponding 6H-indolo[2,3-b]quinolines **26** by ^1H , ^{13}C and ^{19}F NMR, when applicable, and further analyses by 2D NMR spectrum, such as COSY, NOESY, ^1H - ^{13}C HSQC and ^1H - ^{13}C HMBC, allowed for full structural elucidation.



^aYield over 3 steps; ^b6*H*-indolo[2,3-*b*]quinoline-9-carbonitrile (**26a**) was also formed; ^cDiazo compound **132a** also formed.

Scheme 76: Scope of the photochemical cyclizations of aryl azides **131** to yield 11*H*-indolo[3,2-*c*]quinolines **38**.

A-ring substitutions generally performed poorly, with the only exception being compound **38e**, bearing a nitro functionality at C-4 on the indoloquinoline core (nomenclature displayed in Scheme 76), achieving a yield of 77%. Examining the NOESY spectra for compound **38e**

showed correlations between the characteristic H-6 proton and just one other signal, namely H-7, which would be expected for such a geometry (Figure 5.8).^[256] Further, the indole proton shows two correlations on opposing sides of the ring system, belonging to H-1 and H-10, respectively. Having identified these signals, it is then trivial to elucidate the remaining signals to confirm the structure.

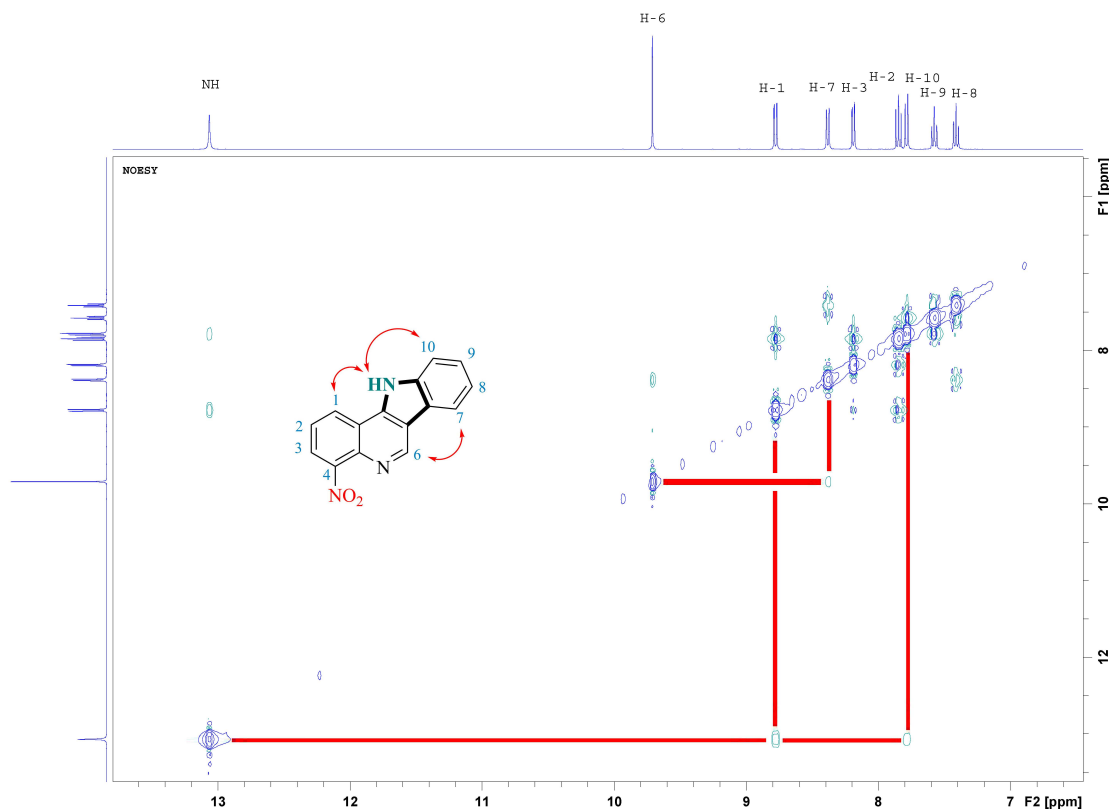
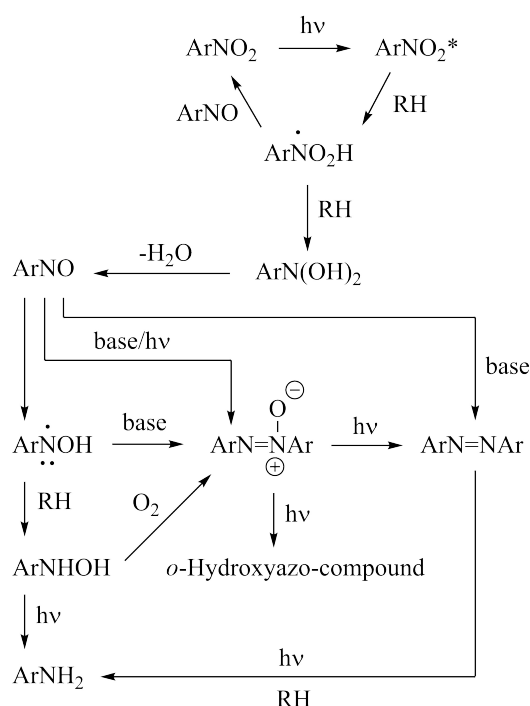


Figure 5.8: NOESY correlations confirming the structure of 4-nitro-11*H*-indolo[3,2-*c*]quinoline (**38e**).

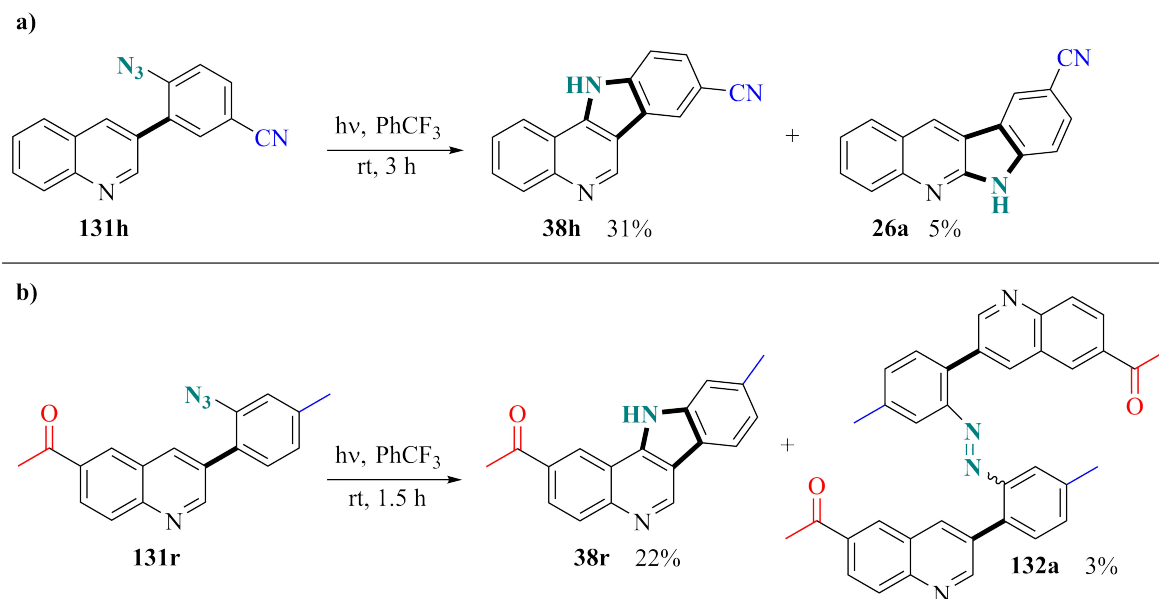
The excellent yield of indoloquinoline **38e** is in stark contrast to all other nitro functionalized compounds in the evaluated series (compounds **38a**, **38d**, **38g**, **38p** and **38q**), resulting in only traces of the desired compound being formed, or at best, the 13% yield observed for compound **38p**. Analysis of the crude ¹H NMR spectrum of the reactions bearing nitro substituents contained complex mixtures, however, some characteristic signals belonging to the desired products could be spotted, namely H-6 and the NH. The TLC plates contained up to 10 spots and by the aid of TLC-LRMS, the spot most likely belonging to the products were tentatively identified. Attempts at isolating these spots through chromatography were carried out, however, the isolated fractions still gave complex NMR spectrum which no structure(s) could be elucidated from.

The photolysis of aromatic nitro compounds in organic solvents containing abstractable hydrogen atoms are known to give rise to a series of reduction products, such as nitroso and azo compounds as well as hydroxylamines and anilines (Scheme 77).^[257] A detailed examination of the transformations in Scheme 77 is beyond the scope of this thesis, however, it serves as a perfect illustration of the photosensitive nature of the nitro group. Further, the intricacy of these transformations along with the observations made in this work makes it apparent that nitro functionalized aryl azides are unsuitable for this type of photochemical cyclization reaction. No concrete explanation has been found for the successful formation of nitro compound **38e**. One might speculate that the placement of the nitro group at C-8 of the aryl azide makes the nitro group a poor chromophore, leaving all the absorbed radiation to transform the azido group into a reactive nitrene, instead of reactions taking place at the nitro group itself. Indeed, the observed λ_{max} for compound **38e** at 285 nm is significantly lower than other nitro substituted aryl azides, all having maximum absorbances above 300 nm, illustrating that the placement of the nitro group on the quinoline ring is important for the outcome of the photocyclizations.



Scheme 77: Overview of the light-induced transformations of aromatic nitro compounds.^[257]

Studying the results of the D-ring functionalizations as presented in Scheme 76 it is hard to establish a clear trend in regards to the effects of the various substituents. The method does not appear to be more tolerant towards EWGs over EDGs, or vice versa, and both categories contain excellent and poor yields. Interestingly, in the cyclization of cyano substituted compound **131h** two cyclic products were formed: the expected 11*H*-indolo[3,2-*c*]quinoline **38h** in 31% yield along with 5% of its regioisomer, quinindoline **26a** (Scheme 78a).



Scheme 78: a) Formation of quinindoline **26a** in addition to the expected 11*H*-indolo[3,2-*c*]quinoline **38h**; b) Formation of diazo compound **132a** during the synthesis of compound **38r**.

This represents the only entry in the series where formation of a quinindoline was detected and isolated, albeit in poor yield. Having a cyano group *para* to an azide is known to retard the rate of cyclization and rate of reaction significantly and further increases the life time of the excited state nitrene.^[218] Indeed, the cyclization of aryl azide **131h** was extremely sluggish and a reaction time of 3 hours was necessary for all starting material to be consumed. Assuming formation of quinindolines from this reaction is rather unfavorable as the nitrene is naturally in near proximity to C-4 of the quinoline ring, perhaps the slow rate of cyclization and longer nitrene life time allowed for the rotation of the biaryl to position the nitrene in near proximity to the C-2 of the quinoline ring to eventually form quinindoline **26a**. The formation of quinindoline **26a** was verified by studying its NOESY correlations, showing the characteristic correlation between the indole proton and the closest proton on the neighbouring ring, namely H-7 (Figure 5.9). It also further displays H-11 to be in spatial proximity to two signals, which were identified as H-1 and H-10 by tracking their respective correlations.

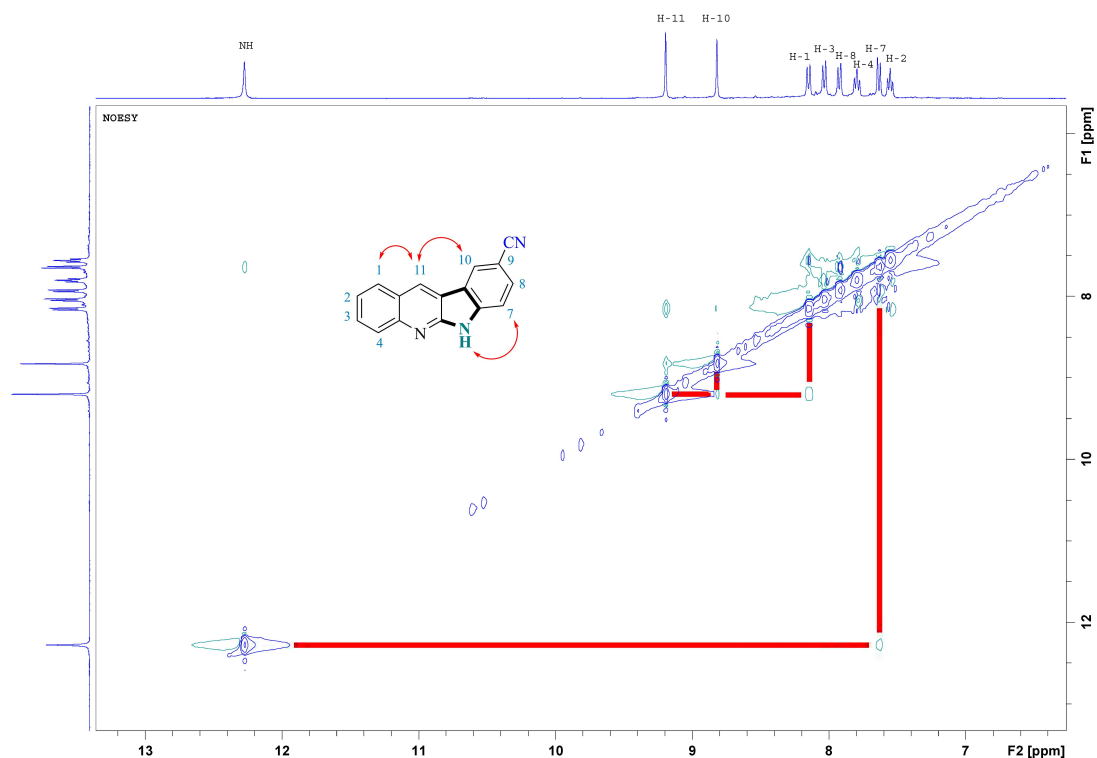


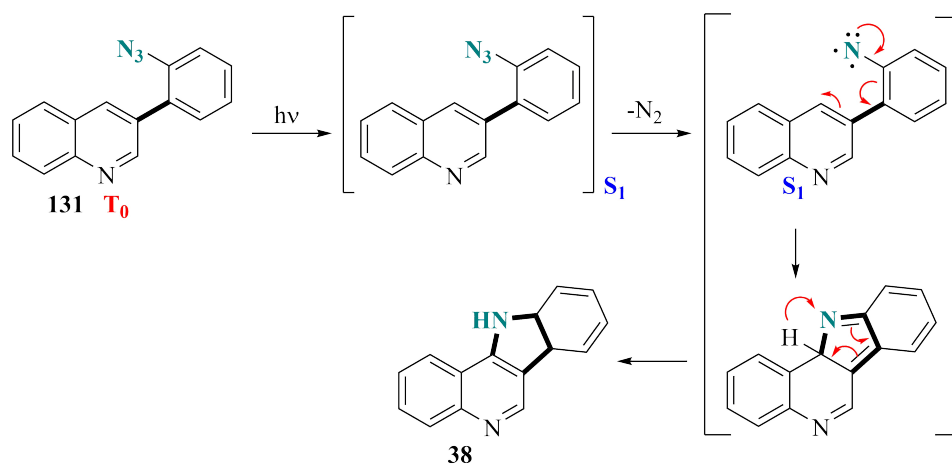
Figure 5.9: NOESY correlations confirming the structure of quinindoline **26a**.

Another factor which appears to be of low significance is the substrate concentration, *ie* the concentration of aryl azide, in the reaction mixture. The concentration of aryl azides **131** was kept between 0.90–7.0 M, to minimize the risk of products forming through intermolecular processes, such as diazo compounds, which are known to more favorably form at high substrate concentrations.^[223] Nonetheless, the reaction which was performed at the highest substrate concentration was the cyclization of aryl azide **131m**, where $C \approx 7.0$ M, which gave a clean reaction mixture giving only indoloquinoline **38m** in 91% yield following aqueous workup. The cyclization of aryl azide **131r** was carried out at a concentration of 0.40 M, nearly 18 times lower than the concentration of aryl azide **131m**, and yet the target compound was only formed in a yield of 22% and moreover, 3% of diazo compound **132a** was isolated (Scheme 78b). The formation of a diazo compound was not detected in any of the other reaction mixtures, despite several of the reactions being carried out at similar or higher substrate concentrations.

Perhaps one of the most relevant factor to the success in the photochemical cyclization study was the ability of TFT to solubilize the target indoloquinolines. All the prepared aryl azides were readily solubilized in TFT, however, during several of the reactions, specifically during the photolysis of aryl azides **131b**, **131c**, **131h**, **131k**, **131o** and **131r**, a thick, dark yellow to orange film was produced along the entire surface of the glassware during the reaction,

presumably belonging to the target products. 11*H*-Indolo[3,2-*c*]quinolines **38** are highly polar and to run NMR analyses, DMSO-*d*₆ is typically required to solubilize the sample. Indeed, to remove the formed layer of film, the glassware had to be thoroughly washed with DMSO. Moreover, the solution in the reaction mixture itself transformed from a clear to an opaque liquid, which appeared to act as a filter for the light emitted by the lamp, consequently leading to poor conversion of the aryl azide into the target indoloquinolines.

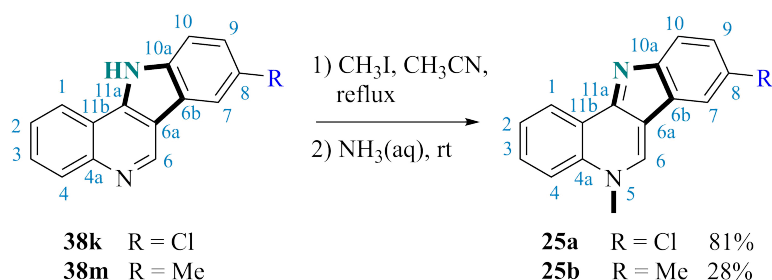
As briefly mentioned in Section 5.2, photochemical transformations of aryl azides **131** to yield indoloquinolines **38** remains unexplored in the literature and by extension so does the mechanism by which the transformation proceeds through. In the photochemical decomposition of a generalized aryl azide, it is believed that the decomposition is initiated by absorption of light by the aromatic nucleus, followed by the absorbed energy being vibrationally transmitted to the azido moiety, extruding molecular nitrogen and forming the reactive nitrene.^[258,259] The ground electronic state of aryl azides have been further established to be a triplet configuration.^[223] With this in mind, a mechanism may be proposed for the photolytic conversion of aryl azides **131** to 11*H*-indolo[3,2-*c*]quinolines **38**: the triplet ground state aryl azide firstly transforms into an excited singlet azide, which upon loss of nitrogen gas furnishes the corresponding singlet state nitrene (Scheme 79). Finally, annulation facilitated by a nitrene insertion followed by a 1,5-hydrogen shift results in formation of the target 11*H*-indolo[3,2-*c*]quinoline **38**. This proposal is based on the assumption that it is in fact the singlet nitrene which is the key intermediate, and not the triplet species. Work to resolve this matter is currently underway by an external collaborator, where computational chemistry is being employed to study and describe such systems.



Scheme 79: Proposed mechanism for the photochemical cyclization of aryl azides **131** to give 11*H*-indolo[3,2-*c*]quinolines **38**.

The 11*H*-indolo[3,2-*c*]quinolines **38** obtained in this study are all relevant for biological evaluation and are further just one simple transformation away from the natural product

isocryptolepine (**25**). The synthetic strategy employed to obtain isocryptolepine (**25**) was described in Chapter 2 and the same approach was utilized to synthesize two isocryptolepine derivatives viable for biological testing (Scheme 80). While the 8-chloro-substituted analogue **38k** proceeded smoothly to give the target compound in excellent yield (81%), the 8-methyl-substituted isocryptolepine **25b** was obtained in only 28% yield following purification. The difference in yield could be the result of the inductive effect exhibited by the methyl group decreasing the nucleophilicity of the quinoline nitrogen towards the electrophile, in this case, the methyl iodide. As the aim of these reactions was simply to prepare samples for biological screenings, attempts at improving the sluggish reaction was never attempted.

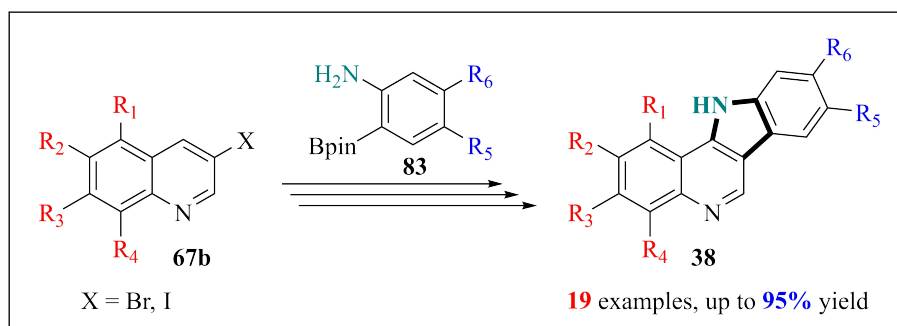


Scheme 80: Synthesis of two functionalized isocryptolepines **25**.

5.3 Summary and concluding remarks

The isocryptolepine precursor, 11*H*-indolo[3,2-*c*]quinoline (**38**), was prepared in excellent yield *via* three steps using a novel approach where the key synthetic strategies were a Suzuki-Miyaura cross-coupling reaction, a diazotization-azidation reaction and finally a photolytic intramolecular cyclization. It was envisaged that by tuning the reaction conditions of the photolytic step, this strategy could also grant access to the natural product quinindoline (**26**). Attempts at realizing this vision through various sensitization experiments were ultimately unsuccessful. A scope and limitations study for the novel pathway towards 11*H*-indolo[3,2-*c*]quinolines **38** was carried out using a selection of diversely functionalized quinolines and 2-aminophenylboronic acids/pinacol esters, which were either obtained commercially or prepared following various literature procedures. The approach allowed for construction of 19 examples in up to 95% yield (Scheme 81), where the electronic nature of the substituents seemed to have little impact on product formation. With the puzzling exception of nitro substituted product **38e**, the method was incompatible with nitro functionalizations owing to the innate photosensitive nature of the nitro moiety leading to a cascade of unwanted reduction products.^[210] The biggest challenge observed through the scope and limitations study, however, was that several of the target compounds were mostly insoluble in TFT, leading to buildup of a thick film on the glassware in the photoreactor, blocking out the radiation emitted by the lamp and essentially terminating the reaction. Addition of small amounts of a highly polar aprotic solvent such as

DMSO in the reaction mixture is a potential solution to this problem and should be considered for future optimization endeavours. Based on the observations made in the study along with consideration of the available literature concerning the photolysis of aryl azides,^[218,223] the reaction was proposed to proceed *via* a singlet nitrene as the key reactive intermediate.



Scheme 81: Summary showcasing the 19 synthesized 11*H*-indolo[3,2-*c*]quinolines **38** using a novel photochemical cyclization method.

Chapter 6

Biological evaluation

6.1 Introduction

A selection of the compounds prepared in Chapter 2, Chapter 4 and Chapter 5 were chosen to undergo various biological tests. Antiplasmodial and antiproliferative data were only obtained for certain compounds prepared in Chapter 2, however, antimicrobial data were obtained for selected compounds prepared in all three aforementioned chapters. The biological testing were conducted externally by various collaborators. The antiplasmodial and antiproliferative evaluations were conducted by Professor Avery's research team at Griffith Institute for Drug Discovery at Griffith University, Australia, while the antimicrobial assays were conducted by Professor Andersen and coworkers at Marbio, UiT, The Arctic University of Norway.

6.2 Antimalarial assay

Some of the compounds prepared in Chapter 2 (overview in Figure 6.1) were tested for their *in vitro* antiplasmodial activities against the *P. falciparum* 3D7 (Pf3D7) strain. To examine the associated cytotoxicities of the evaluated compounds, they were also tested for their *in vitro* cytotoxicity against the HEK293 (human embryonic kidney) cell line and this data was further used to calculate their selectivity indices (SI). To serve as positive controls for the experiments, chloroquine (**2**), dihydroartemisinin (DHA) (**12**) and puromycin were chosen. The evaluated compounds showed diverse activities against the Pf3D7 cell line and the results of the assay can be seen in Table 6.1.^[149] To the best of our knowledge, this study represents the first instance of the antiplasmodial activity of neocryptolepine (**24**) against this particular cell line, showing modest potency ($IC_{50} = 7249$ nM). Comparably, isocryptolepine (**25**) performed better ($IC_{50} = 1211$ nM) although was revealed to be roughly ten times more cytotoxic. Isocryptolepine precursor **38** was found to be somewhat more potent than the natural product itself ($IC_{50} = 977$ nM) and significantly less cytotoxic, while the neocryptolepine precursor **26** displayed no antiplasmodial inhibition. The lack of activity in indoloquinoline **26** demonstrates the importance of the inclusion of the *N*-5 methyl unit for antimalarial performance, a fact which has been observed by other research groups previously.^[260]

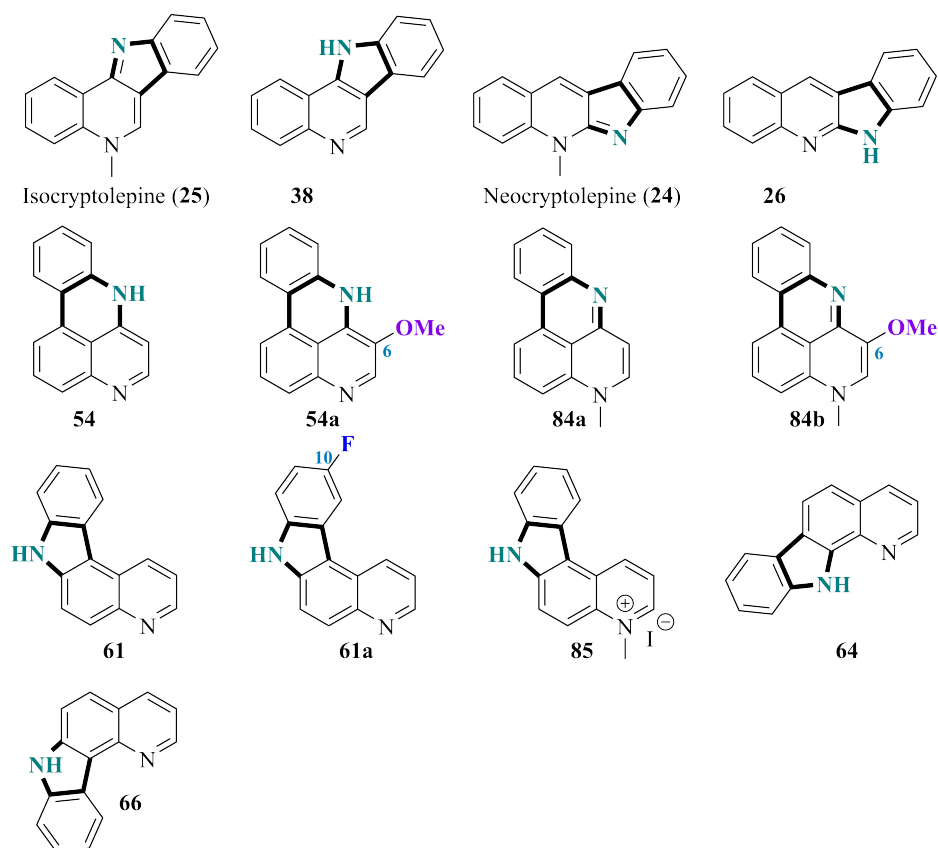


Figure 6.1: Compounds described in Chapter 2 which were evaluated for antiplasmodial, antiproliferative and antimicrobial activities.^[132,149]

Interestingly, the *N*-methyl group has the opposite effect on the antiplasmodial inhibition for the novel pyridophenanthridines **54**, **54a**, **84a** and **84b**. Here, the non-methyl containing pyridophenanthridines **54** ($IC_{50} = 548$ nM) and **54a** ($IC_{50} = 866$ nM) both show a drastic decrease in plasmodial inhibition following addition of the *N*-methyl unit (**84a**: $IC_{50} = 1698$ nM; **84b**: $IC_{50} = 1546$ nM). The presence of an *N*-methyl group is considered instrumental for the activities observed in all of the indoloquinoline natural products,^[72] while this is clearly not applicable to the pyridophenanthridine scaffold. This suggests the possibility that the pyridophenanthridines contains a novel mode of action against *P. falciparum*, which could allow for this scaffold to be developed into a novel lead compound through strategic functionalizations.

Table 6.1: *In vitro* antiplasmodial activities of certain tetracycles against the 3D7 *Plasmodium falciparum* strain, cytotoxicity against HEK293 cells and selectivity indices (SI).^[149]

Entry	Compound	3D7 IC ₅₀ (nM)	Cytotoxicity IC ₅₀ (nM)	SI ^a
1	Isocryptolepine (25)	1211 ± 84	2074 ± 70	1.7
2	Neocryptolepine (24)	7249 ± 6	>20 000	2.8
3	38	977 ± 11	18 460 ± 183	18.9
4	26	NA ^b	NA ^b	-
5	54	548 ± 3	2834 ± 92	5.2
6	54a	866 ± 2	3657 ± 2	4.2
7	84a	1698 ± 5	7410 ± 207	4.4
8	84b	1546 ± 27	5057 ± 45	3.3
9	61	6825 ± 61	>80 000	11.7
10	61a	NT ^c	NT ^c	-
11	85	128 ± 2	NA ^b	213.9
12	64	NA ^b	NA ^b	-
13	66	2414 ± 42	NA ^b	16.6
14	Chloroquine (2)	24 ± 1	>4000	165
15	DHA (12)	1 ± 0.07	NA ^b	74
16	Puromycin	93 ± 2	3 ± 3	0.03

Data are presented as the mean ± standard deviation from two separate experiments. The IC₅₀ values were determined using non-linear dose-response curves in GraphPad Prism. ^aSI = cytotoxicity in HEK293 cells/activity in 3D7 cells; ^b NA = not active; ^c NT = not tested.

The most prominent result from the biological assay belonged to the novel hydroiodide salt **85** (IC₅₀ = 128 nM). Again, its precursor **61** showed little activity, highlighting the crucial role the *N*-methyl functionality might play in obtaining malarial inhibition. Conducting biological tests on the protonated form of indoloquinolines is often done in order to maximize its solubility in aqueous media,^[261] increasing the biological availability of the compound.

6.3 Antiproliferative assay

Selected compounds prepared in Chapter 2 (Figure 6.1) were evaluated for their *in vitro* activity against the cancer cell lines HCT116 (human color cancer), MDA-MB-231 (human breast adenocarcinoma) and PC-3 (human prostate cancer). The results were obtained by running a resazurin assay using puromycin and doxorubicin (**36**) as positive controls for the observed IC₅₀ values (Table 6.2).^[149]

Table 6.2: *In vitro* antiproliferative activities of certain tetracycles against the HCT116, MDA-MB-231 and PC-3 cell lines. All data are given as IC₅₀ values. The associated cytotoxicities against HEK293 cells can be seen in Table 6.1.^[149]

Entry	Compound	HTC116 (nM)	MDA-MB-231 (nM)	PC-3 (nM)
1	Isocryptolepine (25)	667 ± 45	695 ± 130	1821 ± 7
2	Neocryptolepine (24)	6218 ± 90	10 435 ± 375	27% at 80 μM
3	38	3573 ± 309	36% at 80 μM	30% at 80 μM
4	26	NA ^a	NA ^a	NA ^a
5	54	721 ± 27	594 ± 140	1630 ± 173
6	54a	166 ± 16	1002 ± 297	24 ± 3
7	84a	444 ± 52	360 ± 51	2571 ± 114
8	84b	871 ± 172	814 ± 162	4539 ± 361
9	61	20 015 ± 1665	21 540 ± 2480	17 790 ± 1640
10	61a	NT ^b	NT ^b	NT ^b
11	85	38% at 40 μM	24% at 40 μM	36% at 40 μM
12	64	NT ^b	NT ^b	NT ^b
13	66	12% at μM	16 415 ± 2305	47% at 40 μM
14	Puromycin	85	300	270
15	Doxorubicin (36)	150	590	830

Data are presented as the mean ± sem (= standard error of the mean) from two separate experiments. The IC₅₀ values were determined using non-linear dose-response curves in GraphPad Prism.^a NA = not active;^b NT = not tested.

Neocryptolepine (24) displayed poor activities against all three cancer cell lines, while isocryptolepine (25) performed relatively well against the HTC116 (IC₅₀ = 667 nM) and MDA-MB-231 (IC₅₀ = 695 nM) cultures. Several of the tested compounds showed little to no activity against the evaluated cell lines, including the natural product quinindoline (26), as well as compounds 61, 64 and 66. As discussed in Section 1.2.1, neocryptolepine (24) and isocryptolepine (25) are DNA intercalators,^[77] and the lack of activity in compounds 26, 61, 64 and 66 indicate the necessity of the *N*-methyl functional group in this process. This is further demonstrated by comparing the activities for pyridophenanthridines 54 and *N*-methyl pyridophenanthridine (84a) against the HCT116 and MDA-MB-231 cell lines, with the latter being more active. Delightfully, methoxy-substituted compound 54a displayed potent antiproliferative activity against the prostate cancer cell line (IC₅₀ = 24 nM). Compared to the two positive controls, puromycin and doxorubicin (36), methoxy compound 54a exhibited a 10- and 35-fold increase in activity, respectively. The unsubstituted pyridophenanthridine 54 showed only minor antiproliferation of the same cell line, demonstrating the significance of the methoxy

group. Work conducted by Inokuchi and colleagues detailed the strategic functionalization of some indolo[2,3-*b*]quinoline with the aim of increasing antiproliferation.^[262] They remarked that installation of an ester group at certain sites of the indoloquinoline core yielded potent anticarcinogenic properties in comparison to the low inhibition of cell growth as observed for neocryptolepine (**24**). *N*-methyl pyridophenanthridine **84a** was also revealed to be more potent than doxorubicin (**36**) against the human breast adenocarcinoma cell cultures, further showing the potential of developing this novel scaffold into a new anticancer therapy. Naturally, the MoA of the pyridophenanthridines against cancer proliferation is not known at this point in time, giving proceeding studies the opportunity to potentially discover a new MoA. This may be regarded as one of the most sought after fields within drug discovery, as a novel MoA is less likely to be the subject of drug resistance.^[263]

6.4 Antimicrobial assay

Compounds prepared in Chapters 2, 4 and 5 were evaluated for their *in vitro* antimicrobial activities against certain microbial pathogens. The compounds were tested at concentrations of 100, 75, 50, 25, 12.5, 10, 6.3, 3.1 and 1.6 μM to obtain their minimal inhibitory concentrations (MIC). To serve as a positive control for the observed MIC values, the antibiotic gentamycin was employed. Five bacterial strains were investigated, being the Gram-positive pathogens *E. faecalis* (ATCC 29122), *S. aureus* (ATCC 25923) and *S. agalactiae* (ATCC 12386) and the Gram-negative bacteria *E. coli* (ATCC 159233) and *P. aeruginosa* (ATCC 27853). Some of the compounds were further tested for biofilm inhibition using *S. epidermis* (ATCC 35984) and the activity is given in terms of the minimal biofilm inhibitory concentrations (MBIC).

6.4.1 Compounds described in Chapter 2

The MIC values obtained against the five bacterial cell cultures for the compounds prepared in Chapter 2 can be seen in Table 6.3.^[149] Of the 13 compounds evaluated, only six showed antimicrobial activity, two of which were the natural products isocryptolepine (**25**) and neocryptolepine (**24**), with the latter only active against *S. agalactiae* (MIC = 100 μM). Similarly, novel pyridocarbazole **61** only displayed activity against *S. aureus*, at the same MIC value as neocryptolepine (**24**). The poor antimicrobial activities observed for neocryptolepine (**24**) is in accordance with previous reports, suggesting it to solely contain bacteriostatic properties against certain Gram-positive bacteria and no activity against Gram-negative bacteria.^[60,263] The assay showed isocryptolepine (**25**) to be active at a MIC value of 100 μM for all five bacterial pathogens with the exception of the Gram-negative bacterium *P. aeruginosa*.

Table 6.3: Antimicrobial activities of certain tetracycles against five bacterial cell lines. All data are given as MIC values.^[149]

Entry	Compound	<i>E. faecalis</i> (μM)	<i>E. coli</i> (μM)	<i>P. aeruginosa</i> (μM)	<i>S. aureus</i> (μM)	<i>S. agalactiae</i> (μM)
1	Isocryptolepine (25)	100	100	I ^a	100	100
2	Neocryptolepine (24)	I ^a	I ^a	I ^a	I ^a	100
3	54	100	I ^a	I ^a	100	I ^a
4	54a	I ^a	50	I ^a	I ^a	75
5	84a	75	I ^a	I ^a	75	I ^a
6	61	I ^a	I ^a	I ^a	I ^a	100
7	Gentamycin	8	0.13	0.25	0.06	4

MIC values determined and processed using the GraphPad Prism 8 software.^aI = inactive.

Pyridophanthridines **54** and **84a** were both active against the Gram-positive bacteria *E. faecalis* (**54**: MIC = 100 μM; **84a**: MIC = 75 μM) and *S. aureus* (**54**: MIC = 100 μM; **84a**: MIC = 75 μM), but showed no activity against the three other strains. These results show that the inclusion of an *N*-methyl group in addition to being important for antiplasmodial and antiproliferative activities, is also vital for antimicrobial inhibition. The most successful compound in the evaluated series was methoxy-substituted compound **54a**, being active against the Gram-negative bacterium *E. coli* (MIC = 50 μM) and *S. aureus* (MIC = 75 μM). Surprisingly, *N*-methyl methoxy-substituted compound **84b** was inactive against all five bacteria, indicating that the MoA for the methoxy-substituted **54a** and **84b** could be divergent from their non-substituted relatives **54** and **84a**.

In addition to being screened against the aforementioned bacteria, the compounds depicted in Figure 6.1 were also tested for biofilm inhibition against *S. epidermis*. While most of the compounds were unable to inhibit biofilm formation, isocryptolepine (**25**) and compounds **61** and **61a** showed MBIC values of 100 μM.^[149] The novel pyridocarbazoles **61** and **61a** moreover showed poor antiproliferation (Table 6.2), making them ideal compounds for the investigation of a dual anticancer-antimicrobial therapy to fight nosocomial infections.^[82,93]

6.4.2 Compounds described in Chapter 4

Of the compounds prepared in Chapter 4, 18 were subjected to the antimicrobial assay (Figure 6.2) and was additionally tested against the HepG2 (human liver) and MRC-5 (human fetal lung fibroblasts) cell lines to ascertain their cytotoxicity. Naturally, it is undesirable for a potential antibiotic therapy to be highly cytotoxic, and fortunately, only six of the prepared compounds were determined to be toxic to the two employed cell cultures (Table 6.4).

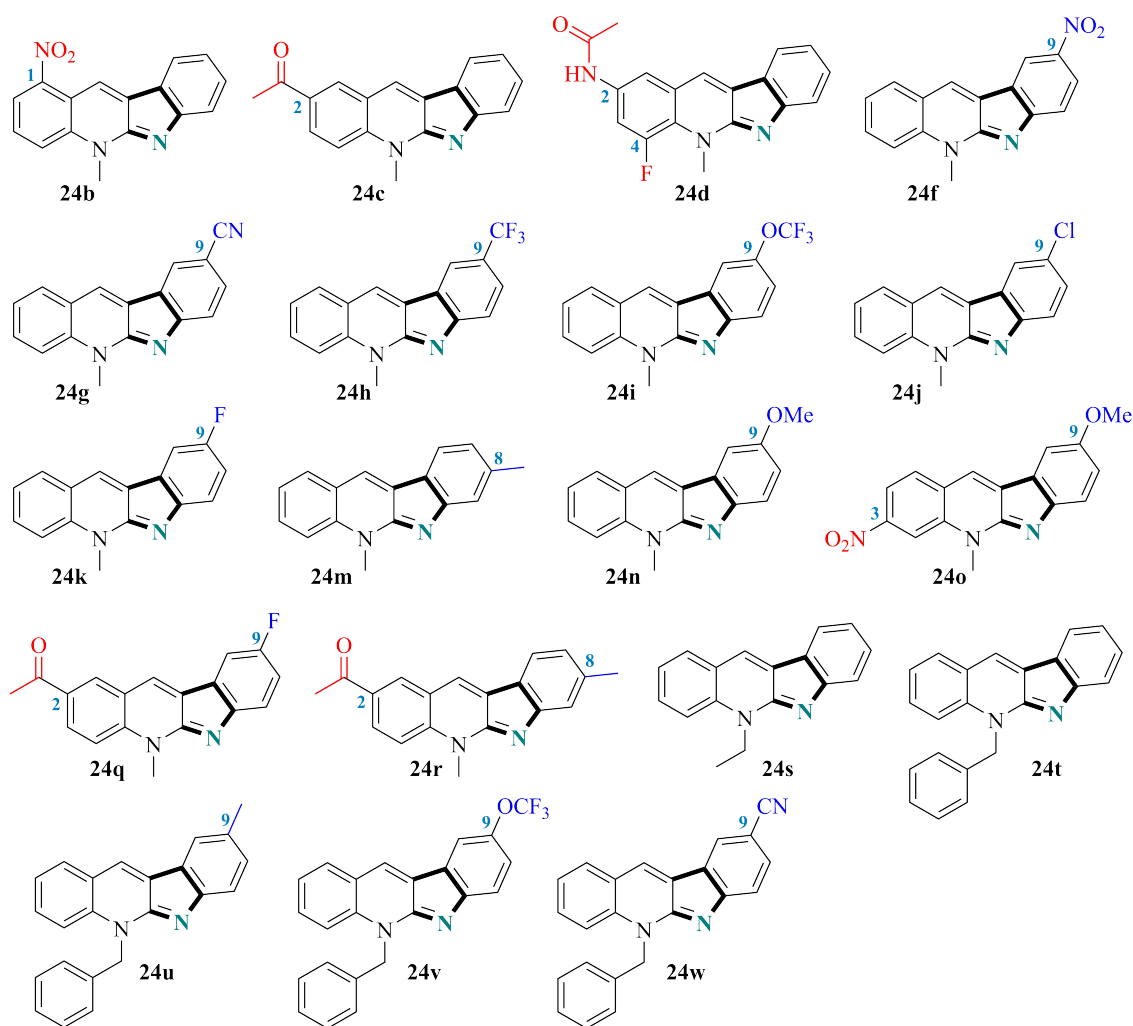


Figure 6.2: Compounds described in Chapter 4 which were evaluated for cytotoxicity and antimicrobial activities.

8-Methyl-substituted compound **24m** was revealed to be significantly cytotoxic, with MIC values of 25 and 12.5 μM against the HepG2 and MRC-5 cell lines, respectively. Though not as toxic towards the liver cultures, compound **24n** also displayed high toxicity towards the MRC-5 cell line (MIC = 12.5 μM), indicating that both of these compounds would be unsuitable for the development of a novel antimicrobial agent.

Table 6.4: Viability assay of certain tetracycles against the HepG2 and MRC-5 cell lines.

Entry	Compound	HepG2 MIC (μM)	MRC-5 MIC (μM)
1	24b	I ^a	50
2	24c	I ^a	75
3	24d	I ^a	50
4	24m	25	12.5
5	24n	100	12.5
6	24o	I ^a	75

MIC values determined and processed using the GraphPad Prism 8 software.^aI = inactive.

Ironically, it was the two highly cytotoxic compounds which displayed activity against the five bacterial pathogens, while the remaining compounds were all inactive (Table 6.5). Compound **24m** had MIC values of 75 μM against all cell lines except *P. aeruginosa*, towards which it was inactive. Though less potent, the same trend was observed for compound **24n**, having MIC values of 100 μM against the same cell lines as well as being inactive towards *P. aeruginosa*. The vitality assay which was conducted is not directly comparable to an antiproliferative screening, however, the data presented in Table 6.4 does indicate that these two compounds could potentially represent interesting targets for the study of novel anticancer therapies rather than antimicrobial agents.

Table 6.5: Antimicrobial activities of neocryptolepines **24m** and **24n** against five bacterial cell lines. All data are given as MIC values.

Entry	Compound	<i>E. faecalis</i> (μM)	<i>E. coli</i> (μM)	<i>P. aeruginosa</i> (μM)	<i>S. aureus</i> (μM)	<i>S. agalactiae</i> (μM)
1	24m	75	75	I ^a	75	75
2	24n	100	100	I ^a	100	100
3	Gentamycin	8	0.13	0.25	0.06	4

MIC values determined and processed using the GraphPad Prism 8 software.^aI = inactive.

6.4.3 Compounds described in Chapter 5

Despite synthesizing a library of indoloquinolines in Chapter 5, nine of the prepared compounds containing diverse functionalizations were selected for evaluation against the five bacterial strains (Figure 6.3). In order to further determine if the tested compounds would be suitable for development into antimicrobial agents, their cytotoxicity was also investigated against the same cell lines as for the compounds prepared in Chapter 4.

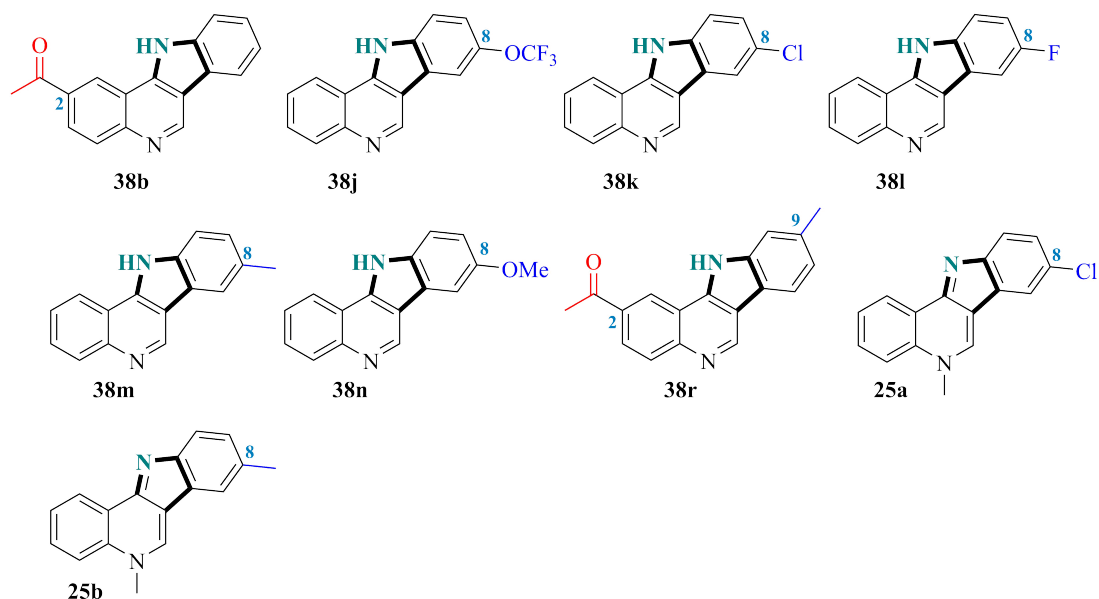


Figure 6.3: Compounds described in Chapter 5 which were evaluated for cytotoxicity and antimicrobial activities.

Nearly all of the compounds were revealed to contain some degree of cellular toxicity, with isocryptolepine derivative **25a** being exceptionally cytotoxic against both cell lines (HepG2: MIC = 6.25 μ M; MRC-5: MIC = 12 μ M). Interestingly, its chlorinated precursor **38k** was inactive against the HepG2 cell line and displayed lower toxicity towards the MRC-5 cells (MIC = 25 μ M).

Table 6.6: Viability assay of certain tetracyclines against the HepG2 and MRC-5 cell lines.

Entry	Compound	HepG2 MIC (μ M)	MRC-5 MIC (μ M)
1	38k	I ^a	25
2	38m	75	25
3	38n	50	50
4	25a	6.25	12
5	25b	75	75

MIC values determined and processed using the GraphPad Prism 8 software.^aI = inactive.

Consistent with the previously evaluated tetracyclines, none of the compounds prepared in Chapter 5 were active against *P. aeruginosa* (Table 6.7). Chlorinated compound **38k** showed excellent inhibition of *S. aureus* (MIC = 25 μ M), while its *N*-methylated counterpart **25a** was highly effective against *E. coli* (MIC = 25 μ M). 8-Chloro isocryptolepine (**25a**) has also been demonstrated to possess significant antiplasmodial activities.^[261] Comparing the results for the two chloro compounds, shows the activity against *S. aureus* to decrease with the inclusion of an *N*-methyl group, while the activity against *E. coli* increases. The other evaluated isocryptolepine derivative **25b** also showed poorer antimicrobial activity than chlorinated isocryp-

tolepine **25a** against the same bacteria. As mentioned several times previously, the *N*-methyl group is deemed pivotal to certain biological activities seen in the indoloquinoline natural products,^[72] however, 8-methyl-substituted compound **38m** also showed significant activity against *S. aureus* (MIC = 75 μ M), *E. coli* (MIC = 75 μ M) and *S. agalactiae* (MIC = 100 μ M). This illustrates that the methyl group functionalization in itself is important, not necessarily the presence of an *N*-methyl. Similar data was also obtained for the 8-methoxy-substituted compound **38n**, further corroborating the significance of any methyl group for antimicrobial activity.

Table 6.7: Antimicrobial activities of certain tetracycles against five bacterial cell lines. All data are given as MIC values.

Entry	Compound	<i>E. faecalis</i> (μ M)	<i>E. coli</i> (μ M)	<i>P. aeruginosa</i> (μ M)	<i>S. aureus</i> (μ M)	<i>S. agalactiae</i> (μ M)
1	38k	I ^a	I ^a	I ^a	25	I ^a
2	38m	I ^a	75	I ^a	50	100
3	38n	I ^a	75	I ^a	75	75
4	25a	75	25	I ^a	50	50
5	25b	75	50	I ^a	75	50
6	Gentamycin	8	0.13	0.25	0.06	4

MIC values determined and processed using the GraphPad Prism 8 software.^aI = inactive.

6.4.4 Issues with solubility

During the preparation of the 40 mM H₂O/DMSO (98:2 v/v) stock solutions used for the antimicrobial assays with, solubility issues were observed for several of the synthesized compounds (Table 6.8). The polyaromatic nature of the evaluated compounds makes it reasonable to assume that the compounds would be largely insoluble in aqueous media, however, all of the prepared samples were readily soluble in DMSO-*d*₆. Consequently, the poor overall solubility of the affected samples lead to precipitation in the stock solution, resulting in a discrepancy between the intended and the actual substrate concentration. In principal, this leads to the substrate being of lower concentration in the sample well than what is intended. As evident from Table 6.8, precipitation of the substrate was more prominent for the neocryptolepine derivatives which were prepared in Chapter 4 than the indolo[3,2-*c*]quinolines. Notably, the presence of functional groups such as nitro, acetyl or halides appeared to be associated with poor solubilities. Compound **24o** containing both a nitro and a methoxy substituent was particularly insoluble (Table 6.8, Entry 8), showing enormous amounts of precipitation. For the indoloquinoline compounds, it was the inclusion of alkyl groups which lead to poor solubilities (Table 6.8, Entries 13-15), with the remaining functionalizations being readily soluble in the stock solution.

Table 6.8: Compounds which precipitated in the 40 mM H₂O/DMSO (98:2 v/v) stock solution.

Entry	Compound	Functional group
1	24b	1-NO ₂
2	24c	2-Acetyl
3	24d	2-NHC ₂ O, 4-F
4	24f	9-NO ₂
5	24g	9-CF ₃
6	24i	9-OCF ₃
7	24j	9-Cl
8	24o	3-NO ₂ , 9-OCH ₃
9	24q	2-Acetyl, 9-F
10	24r	2-Acetyl, 8-CH ₃
11	24u	<i>N</i> -Benzyl, 9-CH ₃
12	24v	<i>N</i> -Benzyl, 9-OCF ₃
13	24w	<i>N</i> -Benzyl, 9-CN
13	38b	2-Acetyl
14	38r	2-Acetyl, 8-CH ₃
15	25a	<i>N</i> -methyl, 8-Cl

6.5 Summary and concluding remarks

Of the compounds which were evaluated for antiplasmodial activity against the Pf3D7 strain, the hydroiodide salt of the novel pyridocarbazole **85** showed most promise (Figure 6.4). The antiproliferative assay revealed novel methoxy-substituted pyridophenanthridine **54a** to be significantly more potent against the human prostate cancer cell line than the clinically used treatments purmycin and doxorubicin (**36**). Notably, this potency was not observed for the naked pyridophenanthridine **54**, indicating the methoxy unit to be paramount to antiproliferation. The novel pyridocarbazoles **61** and **61a** showed moderate efficacy against all evaluated cancer cell lines, but more interestingly, they contained excellent biofilm inhibition. This opens up the possibility of developing this scaffold to a lead compound within dual anticancer-antimicrobial therapies, which could be utilized to treat cancer patients suffering from nosocomial infections. Further, the survey of a library of indoloquinoline derivatives which were prepared in Chapter 4 and 5 revealed the inclusion of a methyl functionality to be paramount to antimicrobial activity (Figure 6.4). Methyl-substituted neocryptolepine **24m** was the most potent of the studied compounds, showing good activities against all the five investigated bacterial strains. Isocryptolepine precursors **38k** and **38m** further demonstrated the potency of methyl substitution, but also unveiled the importance of the presence of a halogen, namely chlorine. In particular, com-

pound **38k** showed excellent inhibition of *S. aureus*. Chloro-isocryptolepine **25a** was the most potent of the evaluated series, showing potent activity against all strains, in particular against the Gram-negative bacteria *E. coli*. This compound has previously also displayed excellent antiplasmodial activities^[261] and represents an interesting target for further studies.

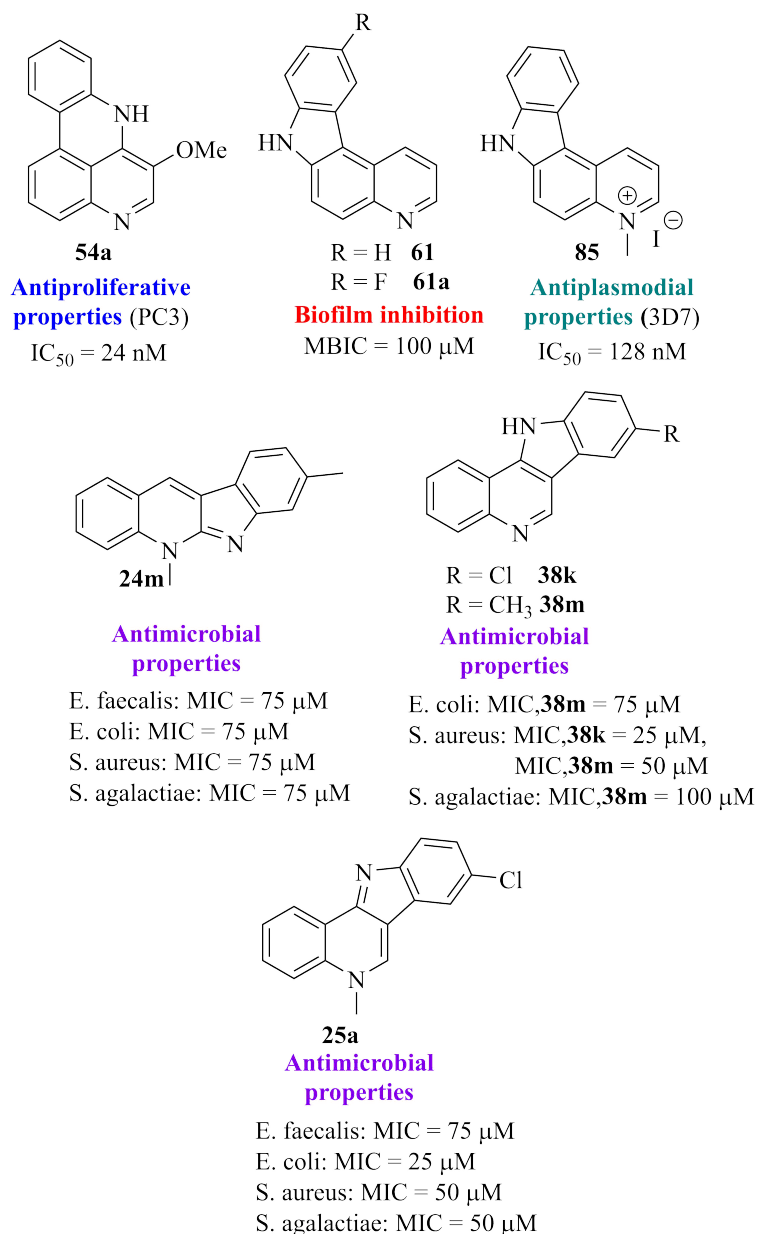


Figure 6.4: Summary of the most successful compounds unraveled in the biological testings.

6.5.1 Future work

Naturally, all the compounds shown in Figure 6.4 is a good starting point for further work into the biological activities of the indoloquinoline, pyridocarbazole and pyridophenanthridine scaffolds. The only prepared and tested variant of the novel pyridophenanthridine scaffold is methoxy-substituted compound **54a**. Further studies into various substitution patterns could

lead to even more potent anticancer properties and should be investigated. Moreover, efforts should be put into discovering and describing such compounds MoA against cancerous cells, as this may provide useful information for the development of future cancer therapies. Additionally, the same strategy could be employed to investigate pyridocarbazole **61**, which might result in a compound containing more potent inhibition of biofilm growth. These compounds also displayed potent antiplasmodial properties, which any analogues of compound **61** could reasonably also be screened for. Efforts into adding a methyl functionality to this core scaffold could provide interesting results, based on the data obtained in this work.

The evaluation of the compound prepared in 4 and 5 revealed significant solubility issues, which should needs to be resolved in the quest to obtain better biological activities. Studies have shown the addition of various basic alkyl amino chains to be favorable for biological activities, which should be considered for future endeavours (some examples in Figure 6.5). Such functional groups further are known to increase a compounds overall polar surface area, allowing for the creation of more H-bonds, leading to increase aqueous solubility.^[86]

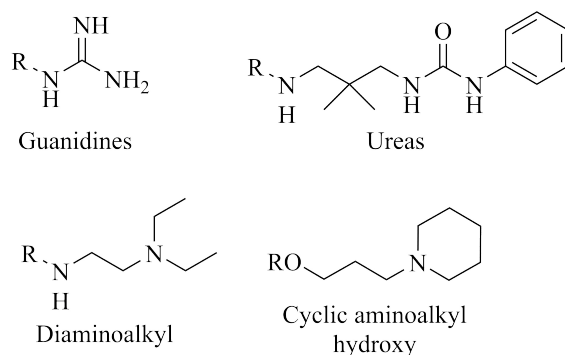


Figure 6.5: Some basic alkyl amino groups associated with increased water solubility when placed on the indoloquinoline scaffold.^[86]

Chapter 7

Experimental

7.1 General

Solvents and reagents

All chemicals were obtained from Merck, VWR or Sigma Aldrich and used as supplied. When specified, dichloromethane (DCM), 1,4-dioxane, Et₃N and *N,N*-dimethyl formamide (DMF) was dried by storing over 4 Å molecular sieves. Tetrahydrofuran (THF) and diethyl ether were distilled using sodium benzophenone ketyl and stored over 4 Å MS.

Spectroscopic and spectrometric analysis

Nuclear magnetic resonance (NMR) spectra were recorded on a Bruker Ascend™ 400 series, operating at 400 MHz for ¹H and ¹¹B, 376 MHz for ¹⁹F and 100 MHz for ¹³C, respectively. The chemical shifts (δ) are expressed in ppm relative to residual chloroform-*d* (¹H, 7.26 ppm; ¹³C, 77.16 ppm), DMSO-*d*₆ (¹H, 2.50 ppm; ¹³C, 39.52 ppm), methanol-*d*₄ (¹H, 3.31 ppm; ¹³C, 49.00 ppm), acetone-*d*₆ (¹H, 2.09 ppm; ¹³C, 30.60 ppm)^[264] or DCM-*d*₂ (¹H, 5.32 ppm; ¹³C, 53.84 ppm). Calibration for ¹⁹F NMR is done using α,α,α -trifluorotoluene as an internal standard in chloroform-*d* (-62.61 ppm), DMSO-*d*₆ (-60.94 ppm) or acetone-*d*₆ (-63.22 ppm).^[265] Coupling constants (*J*) are given in Hertz (Hz) and the multiplicity is reported as: singlet (s), doublet (d), triplet (t), doublet of doublets (dd), doublet of doublet of doublets (ddd), triplet of doublets (td), doublet of triplets (dt), multiplet (m) and broad singlet (bs). The assignments of signals in NMR spectra was assisted by conducting heteronuclear single-quantum correlation spectroscopy (HSQC), heteronuclear multiple bond correlation spectroscopy (HMBC), correlation spectroscopy (COSY) and nuclear Overhauser effect spectroscopy (NOESY).

Infrared (IR) spectra were recorded on an Agilent Cary 630 FTIR spectrophotometer. Samples were analyzed either as a thin film on NaCl plates or by placing the sample directly onto the crystal of an attenuated total reflectance (ATR) module. Samples were analyzed neat using ATR and the absorption frequencies are given in wave numbers (cm⁻¹).

UV-vis spectra were obtained on a VWR UV-1600PC single-beam UV-vis spectrophotometer with a deuterium-discharge lamp for the UV range and a tungsten lamp for the visible wavelength range. Samples were analysed in an Agilent open-top UV quartz cell (10 mm, 2.0 mL) with methanol as the solvent, and the solvent signals were subtracted using background scans. The observed wavelengths (λ) were reported in nm.

Melting points (mp) were determined on a Stuart SMP20 melting point apparatus and are uncorrected.

Low resolution mass spectra were obtained on an Advion *expression*^s CMS mass spectrometer operating at 3.5 kV in electrospray ionization (ESI) mode. Samples were analyzed using a Plate Express[®]. A solution of ammonium acetate (3.0 mM) and formic acid (0.05%) in CH₃CN and H₂O (95:5) was used as the mobile phase for both positive and negative ESI modes. The low resolution mass spectrometer (LRMS) was routinely used to monitor reactions and identify the various components of reaction mixtures.

High resolution mass spectrometry (HRMS) were conducted externally at the University of Bergen (UiB) using a JEOL AccuTOF[™] T100GC mass spectrometer. The instrument was operated with an orthogonal electrospray ionization source (ESI), an orthogonal accelerated time of flight (TOF) single stage reflectron mass analyzer and a dual micro channel plate (MCP) detector at the following instrumental settings/conditions; ionization mode: positive, desolvating temperature/ion source temperature = 250 °C, needle voltage = 3000 V, desolvation gas flow = 2.0 L/min, nebulizing gas flow = 1.0 L/min, orifice1 temperature = 120 °C, orifice1 voltage = 24 V, ring lens voltage = 12 V, orifice2 voltage = 6 V, ion gauge peak voltage = 800 V, detector voltage = 2300 V, acquisition range = 4-1000 *m/z*, spectral recording interval = 0.5 s, wait time = 0.03 ns and data sampling interval = 0.5 ns. Mass calibrations were performed using the internal standard method and mass drift compensation was performed in each acquisition.

Chromatography

Thin-layer chromatography (TLC) was carried out using aluminum backed 0.2 mm thick silica gel plates from Merck (type: 60 F₂₅₄). The spots were detected with ultraviolet (UV) (extinction at $\lambda = 254$ nm or fluorescent at $\lambda = 366$ nm). Flash chromatography (FC) was carried out with silica gel (particle size 40-63 μm), with solvent gradients as indicated in the experimental procedures. Dry vacuum flash chromatography^[266] (DVFC) was carried out by dry-packing the column with approximately 5 cm of silica gel (particle size 19-37 μm). The crude mixture, which had previously been evaporated onto celite, was then added on top of the silica layer. The column was eluted by the addition of 20 mL of the eluent system as indicated by the experimental procedures. The polarity of the eluent was usually increased by 0.5-1% in increments of 4 fractions.

Automated flash chromatography was carried out using an Interchim *puriFlash*[®] 215 chromatography system. The sample was evaporated onto celite and then dry-loaded into a specialized column. This was then attached to a second column filled with 40 μm silica gel particles. The eluent was flushed through the columns using an applied pressure of 26 bar.

Reactions

The microwave (MW) assisted experiments were performed in a CEM Focused MicrowaveTM Synthesis System, model type Discover that operated at 0-300 W at a temperature of 118 °C, a pressure range of 0-290 psi, with reactor vial volumes of 10 or 35 mL.

The photochemical experiments were conducted using a 125 W medium-pressure mercury lamp (model 3010, Photochemical Reactors Ltd.), irradiating the sample at $254 \leq \lambda \leq 579$ nm. The lamp was immersed in a Pyrex tube which was kept in a water-cooled quartz well. The progress of the reaction was monitored carefully by TLC and TLC-LRMS at regular intervals.

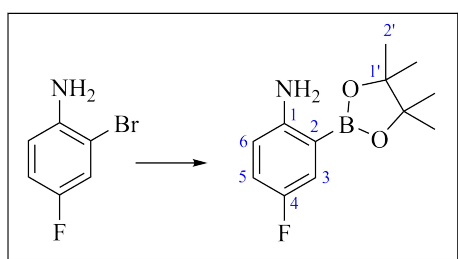
7.2 Methods

7.2.1 Masuda Borylation reactions

General procedures

To a mixture of haloaniline **82** (1 equiv.), anhydrous Et₃N (4 equiv.), Pd(0) (10 mol%) in an appropriate amount of anhydrous 1,4-dioxane under an argon atmosphere, was added 4,4,5,5-tetramethyl-1,3,2-dioxaborolane (3 equiv.) dropwise. The resulting reaction mixture was refluxed until completion as indicated by TLC analysis. The crude mixture was then allowed to cool to rt and quenched by addition of suitable amounts of sat. aq. NH₄Cl and subsequently extracted with CH₂Cl₂ (3 x 10 mL). The combined organic phases were washed (1 x 10 mL H₂O, 1 x 10 mL brine), dried (MgSO₄), filtered and concentrated *in vacuo*. The concentrate was then evaporated onto celite and purified by column chromatography using the eluent indicated in the specific description in order to give target compounds **83**.

4-Fluoro-2-(4,4,5,5-tetramethyl-1,3,2-dioxaborolan-2-yl)aniline (**83a**)^[203]



Following the general procedure, the title compound was prepared from 2-bromo-4-fluoroaniline (**82a**) (1.00 g, 5.26 mmol), 4,4,5,5-tetramethyl-1,3,2-dioxaborolane (2.30 mL, 15.79 mmol), Et₃N (2.93 mL, 21.04 mmol), PdCl₂(PPh₃)₂ (0.37 g, 0.53 mmol) in dioxane (20 mL). After a reaction time of 22 hours, workup was carried out according to the general procedure. Subsequent purification by silica gel column chromatography (pet. ether/EtOAc, 9:1 v/v) and concentration of the relevant fractions [*R*_f = 0.33 (pet. ether/EtOAc, 9:1 v/v)] gave the target compound **83a** as a red solid (0.97 g, 78%).

mp: 49-50 °C (lit.^[203] 50-52 °C).

IR (ATR): ν_{max} 3481, 3388, 2978, 2931, 1621, 1431, 1137, 854 cm⁻¹.

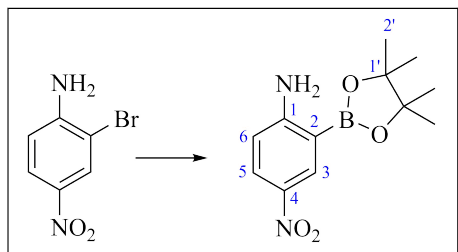
¹H NMR (400 MHz, CDCl₃): δ 7.28 (dd, *J* = 9.1 Hz, 3.1 Hz, 1H, H-5), 6.92 (ddd, *J* = 8.6 Hz, 8.3 Hz, 3.1 Hz, 1H, H-3), 6.53 (dd, *J* = 8.8 Hz, 4.3 Hz, 1H, H-6), 4.55 (bs, 2H, NH₂), 1.34 (s, 12H, C-2').

¹³C NMR (100 MHz, CDCl₃): δ 155.3 (d, *J*_{CF} = 235.0 Hz, C-4), 149.9 (C-1), 121.6 (d, *J*_{CF} = 20.3 Hz, C-5), 119.8 (d, *J*_{CF} = 23.0 Hz, C-3), 116.1 (d, *J*_{CF} = 6.9 Hz, C-6), 83.9 (C-1'), 25.0 (C-2'). C-2 was obscured or overlapping.

^{19}F NMR (376 MHz, CDCl_3): δ -129.0.

In accordance with previously reported data.^[203]

4-Nitro-2-(4,4,5,5-tetramethyl-1,3,2-dioxaborolan-2-yl)aniline (**83b**)



Following the general procedure, the title compound was prepared from 2-bromo-4-nitroaniline (**82b**) (1.00 g, 3.79 mmol), 4,4,5,5-tetramethyl-1,3,2-dioxaborolane (1.65 mL, 11.36 mmol), Et_3N (2.10 mL, 15.16 mmol) and $\text{PdCl}_2(\text{PPh}_3)_2$ (0.27 g, 0.38 mmol) in dioxane (20 mL). After a reaction time of 16 hours, workup was carried out according to the general procedure. Subsequent purification by silica gel column chromatography (pet. ether/EtOAc, 8:2 v/v) and concentration of the relevant fractions [$R_f = 0.26$ (pet. ether/EtOAc, 8:2 v/v)] gave the target compound **83b** as a yellow solid (0.34 g, 33%).

mp: 176-178 °C (lit.^[268] 159-160 °C).

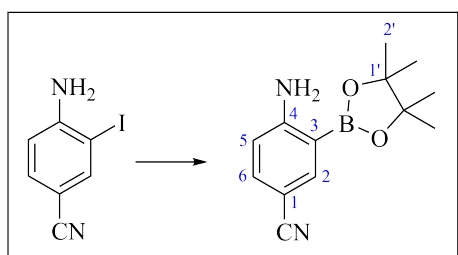
IR (ATR): ν_{max} 3470, 3359, 3233, 3007, 2975, 1603, 1295, 1254, 1114, 850, 831 cm^{-1} .

^1H NMR (400 MHz, CDCl_3): δ 8.53 (d, $J = 2.5$ Hz, 1H, H-3), 8.06 (dd, $J = 9.0$ Hz, 2.7 Hz, 1H, H-5), 6.52 (d, $J = 9.0$ Hz, 1H, H-6), 5.52 (bs, 2H, NH_2).

^{13}C NMR (100 MHz, CDCl_3): δ 158.8 (C-1), 138.1 (C-4), 134.3 (C-3), 128.9 (C-5), 113.9 (C-6), 84.5 (C-1'), 25.0 (C-2'). C-2 was obscured or overlapping.

In accordance with previously reported data.^[268]

4-Amino-3-(4,4,5,5-tetramethyl-1,3,2-dioxaborolan-2-yl)benzotrile (**83c**)



Following the general procedure, the title compound was prepared from 4-amino-3-iodobenzotrile (**82c**) (1.00 g, 4.10 mmol), 4,4,5,5-tetramethyl-1,3,2-dioxaborolane (1.80 mL, 12.30

mmol), Et₃N (2.30 mL, 16.40 mmol) and PdCl₂(PPh₃)₂ (0.29 g, 0.41 mmol) in dioxane (20 mL). After a reaction time of 18 hours, workup was carried out according to the general procedure. Subsequent purification by silica gel column chromatography (pet. ether/EtOAc, 8:1 v/v) and concentration of the relevant fractions [*R*_f = 0.33 (pet. ether/EtOAc, 8:2 v/v)] gave the target compound **83c** as a white solid (842.4 mg, 84%).

mp: 112-115 °C (lit.^[267] 96-97 °C).

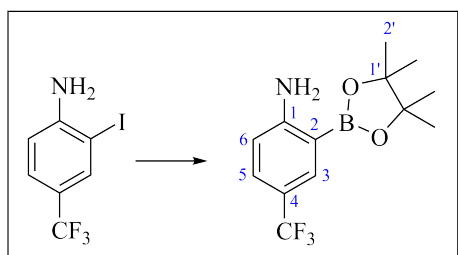
IR (ATR): ν_{\max} 3483, 3369, 3228, 2981, 2923, 2210, 1633, 1604, 1369, 815 cm⁻¹.

¹H NMR (400 MHz, CDCl₃): δ 7.88 (d, *J* = 2.1 Hz, 1H, H-2), 7.39 (dd, *J* = 8.5 Hz, 2.1 Hz, 1H, H-6), 6.54 (d, *J* = 8.5 Hz, 1H, H-5), 5.28 (bs, 2H, NH₂), 1.33 (s, 12H, H-2').

¹³C NMR (100 MHz, CDCl₃): δ 156.7 (C-4), 142.0 (C-2), 136.0 (C-6), 120.4 (CN), 114.6 (C-5), 98.9 (C-1), 84.3 (C-1'), 24.9 (C-2'). C-3 was obscured or overlapping.

In accordance with previously reported data.^[267]

2-(4,4,5,5-Tetramethyl-1,3,2-dioxaborolan-2-yl)-4-(trifluoromethyl)aniline (**83d**)



Following the general procedure, the title compound was prepared from 2-iodo-4-(trifluoromethyl)aniline (**82d**) (500.0 mg, 1.74 mmol), 4,4,5,5-tetramethyl-1,3,2-dioxaborolane (0.76 mL, 5.23 mmol), Et₃N (0.97 mL, 6.96 mmol) and PdCl₂(PPh₃)₂ (122.1 mg, 0.17 mmol) in dioxane (25 mL). After a reaction time of 19 hours, workup was carried out according to the general procedure. Subsequent purification by silica gel column chromatography (pet. ether/EtOAc, 9:1 v/v) and concentration of the relevant fractions [*R*_f = 0.35 (pet. ether/EtOAc, 9:1 v/v)] gave the target compound **83d** as white crystals (267.2 mg, 53%).

mp: 117-119 °C (lit.^[267] 110-113 °C).

IR (ATR): ν_{\max} 3473, 3376, 2978, 2935, 1622, 1368, 1302, 1095, 1072, 833 cm⁻¹.

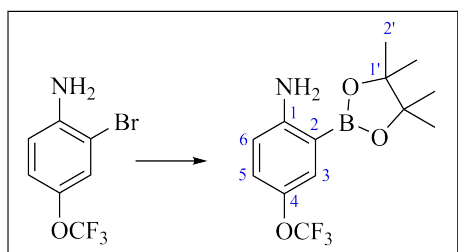
¹H NMR (400 MHz, CDCl₃): δ 7.85 (d, *J* = 1.5 Hz, 1H, H-3), 7.40 (ddd, *J* = 8.6 Hz, 2.3 Hz, 0.4 Hz, 1H, H-5), 6.59 (d, *J* = 8.5 Hz, 1H, H-6), 5.06 (bs, 2H, NH₂), 1.35 (s, 12H, H-2').

¹³C NMR (100 MHz, CDCl₃): δ 156.2 (C-1), 134.4 (q, *J*_{CF} = 3.9 Hz, C-3), 129.6 (d, *J*_{CF} = 3.6 Hz, C-5), 126.4 (C-2), 123.8 (C-4), 118.7 (q, *J*_{CF} = 32.3 Hz, CF₃), 114.3 (C-6), 84.1 (C-1'), 25.0 (C-2').

^{19}F NMR (376 MHz, CDCl_3): δ -61.0.

In accordance with previously reported data.^[267]

2-(4,4,5,5-Tetramethyl-1,3,2-dioxaborolan-1-yl)-4-(trifluoromethoxy)aniline (83e)



Following the general procedure, the title compound was prepared from 2-bromo-4-(trifluoromethoxy)aniline (**82e**) (0.59 mL, 3.90 mmol), 4,4,5,5-tetramethyl-1,3,2-dioxaborolane (1.70 mL, 11.72 mmol), Et_3N (2.17 mL, 15.60 mmol) and $\text{PdCl}_2(\text{dppf})$ (285.4 mg, 0.39 mmol) in dioxane (15 mL). After a reaction time of 18 hours, workup was carried out according to the general procedure. Subsequent purification by silica gel column chromatography (pet. ether/EtOAc, 9:1 v/v) and concentration of the relevant fractions [$R_f = 0.24$ (pet. ether/EtOAc, 9:1 v/v)] gave the target compound **83e** as pink crystals (438.7 mg, 37%).

mp: 72-73 °C (lit.^[202] 63-67 °C).

IR (ATR): ν_{max} 3478, 3376, 2983, 2933, 1627, 1492, 1435, 1210, 1136 cm^{-1} .

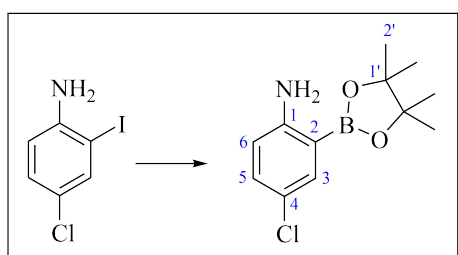
^1H NMR (400 MHz, CDCl_3): δ 7.43 (d, $J = 2.6$ Hz, 1H, H-3), 7.07-7.04 (m, 1H, H-5), 6.55 (d, $J = 8.8$ Hz, 1H, H-6), 4.78 (bs, 2H, NH_2), 1.34 (s, 12H, H-2').

^{13}C NMR (100 MHz, CDCl_3): δ 152.5 (C-1), 140.1 (d, $J_{\text{CF}} = 1.5$ Hz, C-4), 129.2 (C-6), 126.2 (C-5), 120.8 (q, $J_{\text{CF}} = 254.7$ Hz, OCF_3), 115.6 (C-3), 84.1 (C-1'), 25.0 (C-2'). C-2 was obscured or overlapping.

^{19}F NMR (376 MHz, CDCl_3): δ -58.2.

In accordance with previously reported data.^[202]

4-Chloro-2-(4,4,5,5-tetramethyl-1,3,2-dioxaborolan-2-yl)benzeneamine (83f)



Following the general procedure, the title compound was prepared from 4-chloro-2-iodoaniline (**82f**) (1.00 g, 3.94 mmol), 4,4,5,5-tetramethyl-1,3,2-dioxaborolane (1.70 mL, 11.83 mmol), Et₃N (2.20 mL, 15.76 mmol) and PdCl₂(PPh₃)₂ (0.28 g, 0.39 mmol) in dioxane (25 mL). After a reaction time of 18 hours, workup was carried out according to the general procedure. Subsequent purification by silica gel column chromatography (pet. ether/EtOAc, 95:5 v/v) and concentration of the relevant fractions [*R*_f = 0.28 (pet. ether/EtOAc, 95:5 v/v)] gave the target compound **83f** as a white fused mass (0.51 g, 51%).

mp: 87-90 °C (lit.^[267] 91-93 °C).

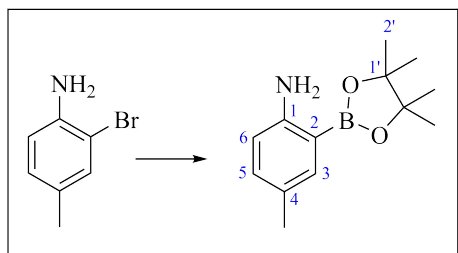
IR (ATR): ν_{\max} 3475, 3375, 2973, 2928, 1414, 1345, 1139, 827 cm⁻¹.

¹H NMR (400 MHz, CDCl₃): δ 7.54 (d, *J* = 2.6 Hz, 1H, H-3), 7.13 (dd, *J* = 8.6 Hz, 2.6 Hz, 1H, H-5), 6.52 (d, *J* = 8.6 Hz, 1H, H-6), 4.73 (bs, 2H, NH₂).

¹³C NMR (100 MHz, CDCl₃): δ 152.2 (C-1), 135.9 (C-3), 132.6 (C-5), 121.7 (C-4), 116.3 (C-6), 84.0 (C-1'), 25.0 (C-2'). C-2 was obscured or overlapping.

In accordance with previously reported data.^[267]

4-Methyl-2-(4,4,5,5-tetramethyl-1,3,2-dioxaborolan-2-yl)aniline (**83g**)^[203]



Following the general procedure, the title compound was prepared from 2-bromo-4-methylaniline (**82g**) (1.00 mg, 5.37 mmol), 4,4,5,5-tetramethyl-1,3,2-dioxaborolane (2.34 mL, 16.12 mmol), Et₃N (3.00 mL, 21.48 mmol), PdCl₂(PPh₃)₂ (0.38 g, 0.54 mmol) in dioxane (20 mL). After a reaction time of 19 hours, workup was carried out according to the general procedure. Subsequent purification by silica gel column chromatography (*n*-hexanes/EtOAc, 95:5 v/v) and concentration of the relevant fractions [*R*_f = 0.16 (*n*-hexanes/EtOAc, 95:5 v/v)] gave the target compound **83g** as a pale red fused mass (1.06 g, 85%).

mp: 72-73 °C (lit.^[203] 60 °C).

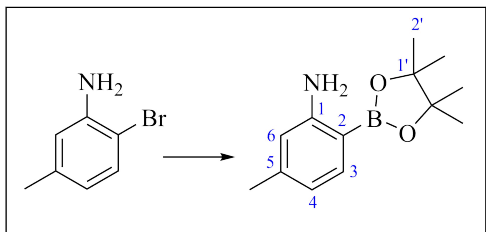
IR (ATR): ν_{\max} 3496, 3398, 2976, 2920, 2859, 1613, 1348, 1136, 852, 819 cm⁻¹.

¹H NMR (400 MHz, CDCl₃): δ 7.42 (d, *J* = 2.1 Hz, 1H, H-3), 7.03 (ddd, *J* = 8.2 Hz, 2.2 Hz, 0.5 Hz, 1H, H-5), 6.53 (d, *J* = 8.2 Hz, 1H, H-6), 4.60 (bs, 2H, NH₂), 2.21 (s, 3H, CH₃), 1.34 (s, 12H, H-2').

¹³C NMR (100 MHz, CDCl₃): δ 151.5 (C-1), 136.8 (C-3), 133.7 (C-5), 126.0 (C-4), 115.1 (C-6), 83.6 (C-1'), 25.0 (C-2'), 20.3 (CH₃). C-2 was obscured or overlapping.

In accordance with previously reported data.^[203]

5-Methyl-2-(4,4,5,5-tetramethyl-1,3,2-dioxaborolan-2-yl)aniline (**83h**)



Following the general procedure, the title compound was prepared from 2-bromo-5-methylaniline (**82h**) (1.00 g, 5.37 mmol), 4,4,5,5-tetramethyl-1,3,2-dioxaborolane (2.30 mL, 16.12 mmol), Et₃N (3.0 mL, 21.48 mmol) and PdCl₂(PPh₃)₂ (0.38 g, 0.54 mmol) in dioxane (20 mL). After a reaction time of 20 hours, workup was carried out according to the general procedure. Subsequent purification by silica gel column chromatography (pet. ether/EtOAc, 1:0 → 95:5 v/v) and concentration of the relevant fractions [*R*_f = 0.17 (pet. ether)] gave the target compound **83h** as a clear oil (0.60 g, 48%).

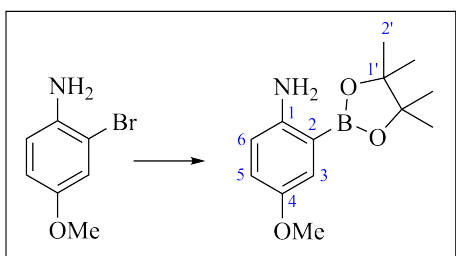
IR (ATR): ν_{max} 3483, 3387, 2977, 2924, 1611, 1355, 1140, 857 cm⁻¹.

¹H NMR (400 MHz, CDCl₃): δ 7.50 (d, *J* = 7.6 Hz, 1H, H-3), 6.52-6.50 (m, 1H, H-4), 6.43 (s, 1H, H-6), 4.65 (bs, 2H, NH₂), 2.24 (s, 3H, CH₃), 1.33 (s, 12H, H-2').

¹³C NMR (100 MHz, CDCl₃): δ 153.9 (C-1), 143.2 (C-5), 136.9 (C-3), 118.3 (C-4), 115.5 (C-6), 83.5 (C-1'), 25.0 (C-2'), 21.8 (CH₃). C-2 was obscured or overlapping.

In accordance with previously reported data.^[203]

4-Methoxy-2-(4,4,5,5-tetramethyl-1,3,2-dioxaborolan-2-yl)aniline (**83i**)



Following the general procedure, the title compound was prepared from 2-bromo-4-methoxyaniline (**82i**) (100.0 mg, 0.50 mmol), 4,4,5,5-tetramethyl-1,3,2-dioxaborolane (0.21 mL, 1.48 mmol), Et₃N (0.28 mL, 2.00 mmol) and PdCl₂(PPh₃)₂ (35.1 mg, 0.050 mmol) in dioxane (5

mL). After a reaction time of 19 hours, workup was carried out according to the general procedure. Subsequent purification by silica gel column chromatography (pet. ether/EtOAc, 9:1 → v/v) and concentration of the relevant fractions [$R_f = 0.14$ (pet. ether/EtOAc, 9:1 v/v)] gave the target compound **83i** as a red solid (106.3 mg, 85%).

mp: 60-63 °C (lit.^[267] 73-74 °C).

IR (ATR): ν_{\max} 3114, 2967, 2932, 1489, 1147, 1005 cm^{-1} .

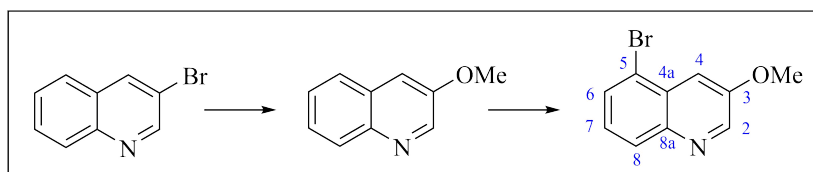
^1H NMR (400 MHz, CDCl_3): δ 7.14 (d, $J = 3.1$ Hz, 1H, H-3), 6.85 (dd, $J = 8.7$ Hz, 3.1 Hz, 1H, H-5), 6.57 (d, $J = 8.7$ Hz, 1H, H-6), 3.76 (s, 3H, OCH_3), 1.34 (s, 12H, H-2').

^{13}C NMR (100 MHz, CDCl_3): δ 151.5 (C-4), 148.0 (C-1), 120.7 (C-5), 119.7 (C-3), 116.6 (C-6), 83.7 (C-1'), 56.1 (OCH_3), 25.0 (C-2'). C-2 was obscured or overlapping.

In accordance with previously reported data.^[267]

7.2.2 Synthesis of quinolines

5-Bromo-3-methoxyquinoline (**81**)^[139]



Step 1: To a solution of 3-bromoquinoline (**67b**) (0.65 mL, 4.80 mmol) in DMF (5 mL) were added NaOMe (30%, 2.7 mL, 14.4 mmol) and CuI (45.7 mg, 0.24 mmol, 5 mol%). The mixture was then refluxed for 20 hours under an argon atmosphere, hydrolyzed and extracted with Et_2O (1 x 20 mL). The organic layer was washed with water (3 x 20 mL), brine (2 x 20 mL), dried (MgSO_4), filtered and concentrated *in vacuo* to give 3-methoxyquinoline (**80**) as a dark yellow oil (434.7 mg, 57%). Spectroscopic data were in accordance with previously reported data.^[139]

Step 2: To a stirred solution of 3-methoxyquinoline (**80**) (434.7 mg, 2.73 mmol) in conc. H_2SO_4 (5 mL) was added NBS (486.0 mg, 2.73 mmol) portionwise at 0 °C. The mixture was then allowed to warm to rt and after stirring for 20 hours the pH was adjusted to 10 by addition of suitable amounts of 1 M NaOH. The formed precipitate was redissolved in CH_2Cl_2 and the filtrate extracted using CH_2Cl_2 (3 x 30 mL). The combined organic phases were washed with water (2 x 15 mL), brine (1 x 15 mL), dried (MgSO_4), filtered and evaporated onto celite. Purification by silica gel column chromatography (pet. ether/EtOAc, 85:15 v/v) and concentration of the relevant fractions [$R_f = 0.18$ (pet. ether/EtOAc, 9:1 v/v)] gave the target compound **81** as off-white crystals (337.7 mg, 52%).

mp: 76-77 °C (lit.^[139] 81-83 °C).

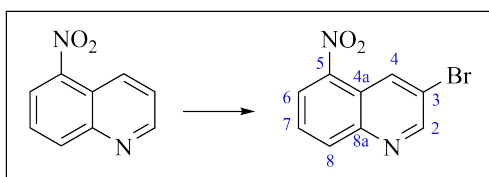
IR (ATR): ν_{\max} 3067, 3004, 2995, 2964, 2853, 1599, 1407, 1161, 859 cm^{-1} .

$^1\text{H NMR}$ (400 MHz, CD_3OD): δ 8.61 (d, $J = 2.8$ Hz, 1H, H-2), 7.99-7.96 (m, 1H, H-8), 7.87 (dd, $J = 7.6$ Hz, 1.0 Hz, 1H, H-6), 7.84 (d, $J = 2.6$ Hz, 1H, H-3), 7.48 (dd, $J = 8.4$ Hz, 7.6 Hz, 1H, H-7), 4.02 (s, 3H, OCH_3).

$^{13}\text{C NMR}$ (100 MHz, CD_3OD): δ 155.9 (C-3), 146.2 (C-2), 144.6 (C-8a), 132.3 (C-6), 129.7 (C-4a), 129.3 (C-8), 128.3 (C-7), 121.5 (C-5), 113.2 (C-4), 56.3 (OCH_3).

In accordance with previously reported data.^[139]

3-Bromo-5-nitroquinoline (67ba)^[197]



5-Nitroquinoline (**117**) (1.00 g, 5.74 mmol) and NBS (1.53 g, 8.61 mmol) were dissolved in glacial AcOH (20 mL) and refluxed under an argon atmosphere for 20 hours. The reaction mixture was allowed to cool to rt and roughly half the solvent was removed under reduced pressure before addition of H_2O (10 mL) and the pH adjusted to 10 by addition of suitable amounts of 5 M NaOH. The product was then extracted using CH_2Cl_2 (5 x 10 mL) and the combined organic layers were washed (1 x 10 mL brine), dried (MgSO_4), filtered and concentrated *in vacuo* to give the crude product as a yellow solid (1.41 g, 98%), which was essentially pure by NMR.

mp: 123-126 $^\circ\text{C}$ (lit.^[197] 135 $^\circ\text{C}$).

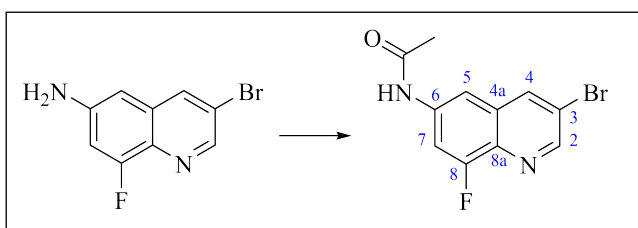
IR (ATR): ν_{\max} 3089, 3055, 3014, 1514, 1319, 736 cm^{-1} .

$^1\text{H NMR}$ (400 MHz, CDCl_3): δ 9.24 (dd, $J = 2.2$ Hz, 0.8 Hz, 1H, H-4), 9.02 (d, $J = 2.2$ Hz, 1H, H-2), 8.44 (dd, $J = 7.7$ Hz, 1.1 Hz, 1H, H-8), 8.41-8.39 (m, 1H, H-6), 7.28 (dd, $J = 8.4$ Hz, 7.8 Hz, 1H, H-6).

$^{13}\text{C NMR}$ (100 MHz, CDCl_3): δ 153.0 (C-2), 146.5 (C-5), 144.5 (C-8a), 136.9 (C-6), 133.7 (C-4), 127.9 (C-7), 125.9 (C-8), 122.1 (C-3), 121.4 (C-4).

In accordance with previously reported data.^[197]

N-(3-Bromo-8-fluoroquinolin-6-yl)acetamide (67bb)



3-Bromo-8-fluoroquinolin-6-amino (**118**) (1.00 g, 4.15 mmol) was cooled to 0 °C using an ice bath before dropwise addition of ice-cooled Ac₂O (50 mL) under an argon atmosphere. The resulting mixture was allowed to warm to rt and stirred for 23 hours. The crude mixture was then diluted with CH₂Cl₂, quenched (sat. aq. Na₂CO₃) and extracted using CH₂Cl₂ (2 x 50 mL). The combined organic phases were washed with water (1 x 30 mL), brine (1 x 30 mL), dried (MgSO₄), filtered and evaporated onto celite. Purification by silica gel column chromatography (pet. ether/EtOAc, 1:1 → 4:6 v/v) and concentration of the relevant fractions [*R_f* = 0.16 (pet. ether/EtOAc, 1:1 v/v)] gave the target compound **67bb** as an off-white solid (0.85 g, 72%).

mp: 197-200 °C.

IR (ATR): ν_{\max} 3291, 3271, 3098, 3047, 1662 (C=O), 1492, 1356, 1097, 781 cm⁻¹.

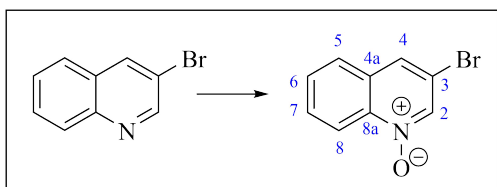
¹H NMR (400 MHz, CD₃OD): δ 8.73 (d, *J* = 2.1 Hz, 1H, H-2), 8.44 (t, *J* = 1.7 Hz, 1H, H-4), 7.92-7.91 (m, 1H, H-5), 7.68 (dd, *J* = 12.4 Hz, 2.2 Hz, 1H, H-7), 2.18 (s, 3H, CH₃).

¹³C NMR (100 MHz, CD₃OD): δ 171.9 (C=O), 158.7 (d, *J_{CF}* = 255.3 Hz, C-8), 150.9 (C-2), 139.7 (d, *J_{CF}* = 10.3 Hz, C-6), 138.5 (d, *J_{CF}* = 3.0 Hz, C-4), 134.2 (d, *J_{CF}* = 12.5 Hz, C-8a), 132.7 (d, *J_{CF}* = 2.5 Hz, C-4a), 119.9 (C-3), 111.5 (d, *J_{CF}* = 4.2 Hz, C-5), 109.4 (d, *J_{CF}* = 23.1 Hz, C-7), 24.0 (CH₃).

¹⁹F NMR (376 MHz, CD₃OD): δ -125.6.

HRMS (ESI): calcd. for C₁₁H₈BrFN₂O [M + Na⁺] 336.9958; 338.9938, found 336.9933; 338.9946.

3-Bromoquinoline *N*-oxide (**124**)



3-Bromoquinoline (**67b**) (3.3 mL, 24.0 mmol) and H₂O₂ (35 wt%, 6.0 mL, 24.0 mmol) in AcOH (35 mL) was stirred at 100 °C for 4 hours. Sat. aq. K₂CO₃ (30 mL) was then added and the mixture was extracted with CHCl₃ (3 x 15 mL). The combined organic layers were dried (MgSO₄), filtered and concentrated *in vacuo*. The concentrate was subsequently evaporated onto celite and purified by silica gel column chromatography (pet. ether/EtOAc, 8:2 → 7:3 v/v) and concentration of the relevant fractions [*R_f* = 0.25 (pet. ether/EtOAc, 1:1 v/v)] gave the target compound **124** as an off-white solid (4.30 g, 81%).

mp: 108-110 °C (lit.^[269] 97-99 °C).

IR (NaCl): ν_{\max} 3102, 3054, 2926, 1555, 1497, 1078, 841, 769 cm⁻¹.

$^1\text{H NMR}$ (400 MHz, CDCl_3): δ 8.61 (d, $J = 8.9$ Hz, 1H, H-8), 8.57 (s, 1H, H-2), 7.84 (s, 1H, H-4), 7.74-7.69 (m, 2H, H-5 and H-7), 7.63-7.59 (m, 1H, H-6).

$^{13}\text{C NMR}$ (100 MHz, CDCl_3): δ 140.6 (C-2), 137.3 (C-8a), 130.6 (C-7), 130.2 (C-5), 129.8 (C-6), 128.0 (C-4a), 127.4 (C-4), 119.9 (C-8), 114.3 (C-3).

In accordance with previously reported data.^[269]

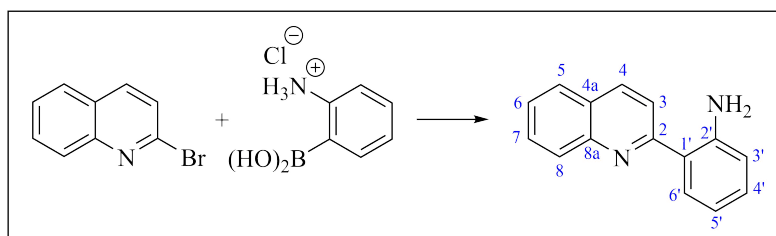
7.2.3 Suzuki-Miyaura cross-coupling reactions

General procedures

Method 1 - using $\text{PdCl}_2(\text{dppf})$ as catalyst: To a solution of haloquinoline (1 equiv.) in an appropriate amount of EtOH under an argon atmosphere was added boronic acid (1.5 equiv.), an aq. solution of K_2CO_3 (3.5 equiv. in an appropriate amount of H_2O) and $\text{PdCl}_2(\text{dppf})$ (5 mol%). The resulting reaction mixture was stirred at 60 °C until completion as indicated by TLC analysis. The crude mixture was then allowed to cool to rt and the volatiles were removed under reduced pressure. The concentrate was evaporated onto celite and purified by column chromatography using the chromatographic technique and eluent as indicated in the specific description in order to give target compounds.

Method 2 - using $\text{Pd}(\text{PPh}_3)_4$ as catalyst: To a solution of haloquinoline (1 equiv.) in an appropriate amount of DME under an argon atmosphere was added boronic acid (1.5 equiv.), an aq. solution of Cs_2CO_3 (3.5 equiv. in an appropriate amount of H_2O) and $\text{Pd}(\text{PPh}_3)_4$ (5 mol%). The resulting reaction mixture was stirred at 80 °C until completion as indicated by TLC analysis. The crude mixture was then allowed to cool to rt and the volatiles were removed under reduced pressure. The concentrate was evaporated onto celite and purified by column chromatography using the chromatographic technique and eluent as indicated in the specific description in order to give target compounds.

2-(Quinolin-2-yl)aniline (70)



Method 1: Following the general procedure, the title compound was prepared from 2-bromoquinoline (**67a**) (50.0 mg, 0.24 mmol), 2-aminophenylboronic acid hydrochloride (**68**) (62.5 mg, 0.36 mmol), an aq. solution of K_2CO_3 (116.1 mg, 0.84 mmol, in 1 mL H_2O) and $\text{PdCl}_2(\text{dppf})$ (8.8 mg, 0.012 mmol) in EtOH (5 mL). After a reaction time of 1 hour, the crude was purified

by an Interchim puriFlash chromatography system (pet. ether/EtOAc, 95:5 \rightarrow 1:1 v/v) and concentration of the relevant fractions [$R_f = 0.17$ (pet. ether/EtOAc, 9:1 v/v)] followed by recrystallization using boiling *n*-hexanes/EtOAc (9:1 v/v) gave the target compound **70** as bright yellow crystals (25.7 mg, 65%).

Method 2: Following the general procedure, the title compound was prepared from 2-bromoquinoline (**67a**) (100.0 mg, 0.48 mmol), 2-aminophenylboronic acid hydrochloride (**68**) (125.0 mg, 0.72 mmol), an aq. solution of Cs₂CO₃ (547.4 mg, 1.68 mmol in 1 mL H₂O) and Pd(PPh₃)₄ (27.7 mg, 0.024 mmol) in DME (5 mL). After a reaction time of 19 hours, the crude was purified by silica gel column chromatography (pet. ether/EtOAc, 9:1 v/v) and concentration of the relevant fractions [$R_f = 0.17$ (pet. ether/EtOAc, 9:1 v/v)] gave the target compound **70** as bright yellow crystals (99.2 mg, 94%).

mp: 152-155 °C (lit.^[270] 153 °C).

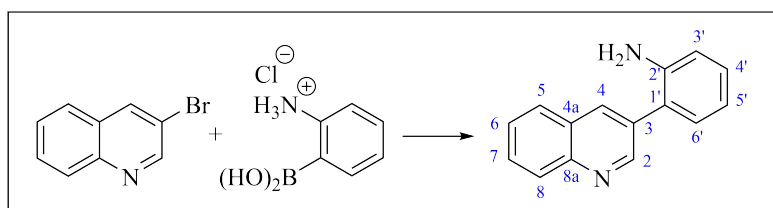
IR (ATR): ν_{\max} 2922, 2852, 1718, 1465, 759 cm⁻¹.

¹H NMR (400 MHz, CDCl₃): δ 8.20 (d, $J = 8.7$ Hz, 1H, H-4), 8.06 (d, $J = 8.4$ Hz, 1H, H-8), 7.84 (d, $J = 8.7$ Hz, 1H, H-3), 7.82-7.80 (m, 1H, H-5), 7.73-7.69 (m, 2H, H-7 and H-6'), 7.54-7.49 (m, 1H, H-6), 7.24-7.19 (m, 1H, H-4'), 6.85-6.82 (m, 2H, H-3' and H-6').

¹³C NMR (100 MHz, CDCl₃): δ 159.2 (C-2), 147.2 (C-2'), 146.9 (C-8a), 136.9 (C-4), 130.5 (C-4'), 129.9 (C-7), 129.8 (C-6'), 128.9 (C-8), 127.5 (C-5), 126.4 (C-4a), 126.3 (C-6), 121.8 (C-1'), 120.6 (C-3), 117.9 (C-5'), 117.7 (C-3').

In accordance with previously reported data.^[271]

2-(Quinolin-3-yl)aniline (**69**)



Method 1: Following the general procedure, the title compound was prepared from 3-bromoquinoline (**67b**) (1.3 mL, 9.61 mmol), 2-aminophenylboronic acid hydrochloride (**68**) (2.00 g, 11.53 mmol), an aq. solution of K₂CO₃ (4.25 g, 30.75 mmol in 12 mL H₂O) and PdCl₂(dppf) (0.35 g, 0.48 mmol) in EtOH (60 mL). After a reaction time of 16 hours, the crude was purified by silica gel column chromatography (pet. ether/diethyl ether, 2:8 \rightarrow 1:9 v/v) and concentration of the relevant fractions [$R_f = 0.31$ (pet. ether/diethyl ether, 2:8 v/v)] gave the target compound **69** as orange crystals (1.77 g, 84%).

Method 2: Following the general procedure, the title compound was prepared from 3-bromoquinoline (**67b**) (0.030 mL, 0.24 mmol), 2-aminophenylboronic acid hydrochloride (**68**)

(45.8 mg, 0.26 mmol), an aq. solution of Cs_2CO_3 (234.9 mg, 0.72 mmol in 0.2 mL H_2O) and $\text{Pd}(\text{PPh}_3)_4$ (13.9 mg, 0.012 mmol) in DME (1.2 mL). After a reaction time of 20 hours, the crude was purified by silica gel column chromatography (pet. ether/EtOAc, 6:4 v/v) and concentration of the relevant fractions [$R_f = 0.46$ (pet. ether/EtOAc, 6:4 v/v)] gave the target compound **69** as a yellow crystalline solid (27.8 mg, 53%).

mp: 132-135 °C (lit.^[124] 130-132 °C).

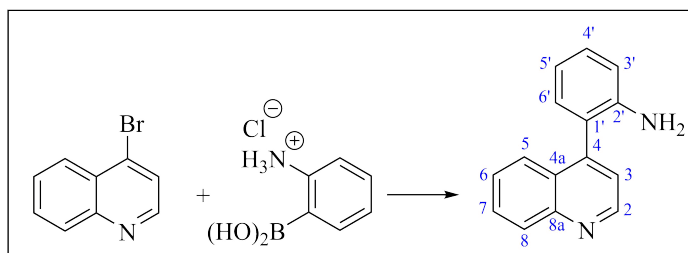
IR (ATR): ν_{max} 3438, 3331, 3208, 3061, 1619, 1575, 1497, 1452 cm^{-1} .

^1H NMR (400 MHz, CDCl_3): δ 9.03 (d, $J = 2.0$ Hz, 1H, H-2), 8.25 (d, $J = 2.0$ Hz, 1H, H-4), 8.14 (d, $J = 8.4$ Hz, 1H, H-8), 7.83-7.81 (m, 1H, H-5), 7.75-7.71 (m, 1H, H-7), 7.59-7.55 (m, 1H, H-6), 7.25-7.19 (m, 2H, H-4' and H-6'), 6.92-6.88 (m, 1H, H-5'), 6.84-6.82 (m, 1H, H-3'), 3.80 (bs, 2H, NH_2).

^{13}C NMR (100 MHz, CDCl_3): δ 151.6 (C-2), 147.1 (C-8a), 144.1 (C-2'), 135.5 (C-4), 132.5 (C-3), 130.9 (C-6'), 129.6 (C-4'), 129.5 (C-7), 129.2 (C-8), 128.0 (C-4a), 127.9 (C-5), 127.1 (C-6), 123.7 (C-1'), 119.1 (C-5'), 116.0 (C-3').

In accordance with previously reported data.^[124]

2-(Quinolin-4-yl)aniline (**71**)



Method 1: Following the general procedure, the title compound was prepared from 4-bromoquinoline (50.0 mg, 0.24 mmol), 2-aminophenylboronic acid hydrochloride (**68**) (62.4 mg, 0.36 mmol), an aq. solution of K_2CO_3 (116.1 mg, 0.84 mmol in 1 mL H_2O) and $\text{PdCl}_2(\text{dppf})$ (8.9 mg, 0.012 mmol) in EtOH (5 mL). After a reaction time of 21 hours, the crude was purified by an Interchim puriFlash chromatography system (pet. ether/EtOAc, 95:5 \rightarrow 55:45 v/v) and concentration of the relevant fractions [$R_f = 0.29$ (pet. ether/EtOAc, 1:1 v/v)] gave the target compound **71** as a yellow solid (48.1 mg, 91%).

Method 2: Following the general procedure, the title compound was prepared from 4-bromoquinoline (246.0 mg, 1.18 mmol), 2-aminophenylboronic acid hydrochloride (**68**) (410.1 mg, 2.36 mmol), an aq. solution of Cs_2CO_3 (1.54 g, 4.72 mmol in 1.4 mL H_2O) and $\text{Pd}(\text{PPh}_3)_4$ (68.2 mg, 0.059 mmol) in DME (7 mL). After a reaction time of 1.75 hours, the crude was purified by an Interchim puriFlash chromatography system (pet. ether/EtOAc, 95:5 \rightarrow 55:45 v/v) and concentration of the relevant fractions [$R_f = 0.29$ (pet. ether/EtOAc, 1:1 v/v)] gave the

target compound **71** as a yellow solid (250.3 mg, 96%).

mp: 128-129 °C (lit.^[272] 119 °C).

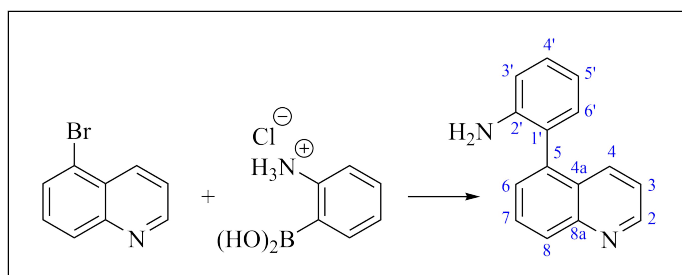
IR (NaCl): ν_{\max} 3454, 3328, 3210, 3061, 3033, 1617, 1494, 1451, 752 cm^{-1} .

¹H NMR (400 MHz, CDCl₃): δ 8.94 (d, $J = 4.4$ Hz, 1H, H-2), 8.18-8.15 (m, 1H, H-8), 7.74-7.69 (m, 2H, H-6 and H-7), 7.50-7.46 (m, 1H, H-5), 7.37 (d, $J = 4.4$ Hz, 1H, H-3), 7.28 (ddd, $J = 7.5$ Hz, 1.6 Hz, 0.6 Hz, 1H, H-4'), 7.12 (dd, $J = 7.5$ Hz, 1.5 Hz, 1H, H-6'), 6.88 (td, $J = 7.4$ Hz, 1.0 Hz, 1H, H-5'), 6.83 (dd, $J = 8.1$ Hz, 0.8 Hz, 1H, H-3'), 3.83 (bs, 2H, NH₂).

¹³C NMR (100 MHz, CDCl₃): δ 150.4 (C-2), 148.7 (C-8a), 146.2 (C-4), 143.9 (C-2'), 130.6 (C-1'), 129.9 (C-8), 129.8 (C-4'), 129.7 (C-7), 126.9 (2C, C-4a and C-5), 126.1 (C-6), 122.9 (C-6'), 122.3 (C-3), 118.5 (C-5'), 115.8 (C-3').

In accordance with previously reported data.^[272]

2-(Quinolin-5-yl)aniline (**72**)



Method 2: Following the general procedure, the title compound was prepared from 5-bromoquinoline (**67d**) (1.00 g, 4.81 mmol), 2-aminophenylboronic acid hydrochloride (**68**) (1.25 g, 7.21 mmol), an aq. solution of Cs₂CO₃ (5.48 g, 16.83 mmol in 10 mL H₂O) and Pd(PPh₃)₄ (0.28 g, 0.24 mmol) in DME (50 mL). After a reaction time of 19 hours, the crude was purified by silica gel column chromatography (pet. ether/EtOAc, 1:1 → 3:7 v/v) and concentration of the relevant fractions [$R_f = 0.23$ (pet. ether/EtOAc, 1:1 v/v)] gave the target compound **72** as light brown crystals (0.95 g, 90%).

mp: 163-165 °C (lit.^[132] 163-166 °C).

IR (ATR): ν_{\max} 3410, 3318, 3209, 2924, 1618, 1491, 959, 803, 754 cm^{-1} .

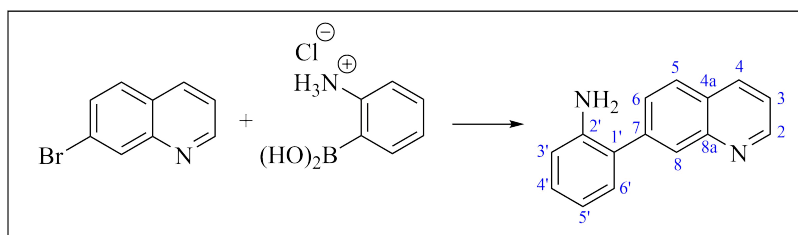
¹H NMR (400 MHz, CDCl₃): δ 8.93 (dd, $J = 4.1$ Hz, 1.7 Hz, 1H, H-2), 8.16-8.14 (m, 1H, H-8), 8.02-7.99 (m, 1H, H-4), 7.81-7.77 (m, 1H, H-7), 7.53 (dd, $J = 6.9$ Hz, 0.9 Hz, 1H, H-6), 7.35 (dd, $J = 8.5$ Hz, 4.2 Hz, 1H, H-3), 7.30-7.25 (m, 1H, H-4'), 7.13 (dd, $J = 7.5$ Hz, 1.5 Hz, 1H, H-6'), 6.88 (td, $J = 7.5$ Hz, 1.1 Hz, 1H, H-5'), 6.84 (dd, $J = 8.0$ Hz, 0.7 Hz, 1H, H-3'), 3.44 (bs, 2H, NH₂).

^{13}C NMR (100 MHz, CDCl_3): δ 150.6 (C-2), 148.7 (C-8a), 144.4 (C-2'), 137.5 (C-5), 134.9 (C-4), 131.4 (C-6'), 129.6 (C-7), 129.5 (C-4'), 129.3 (C-8), 128.2 (C-6), 127.1 (C-4a), 124.4 (C-1'), 121.4 (C-3), 118.5 (C-5'), 115.6 (C-3').

HRMS (ESI): calcd. for $\text{C}_{15}\text{H}_{12}\text{N}_2$ [$\text{M} + \text{H}^+$] 221.1073, found 221.1071.

In accordance with previously reported data.^[132]

2-(Quinolin-7-yl)aniline (74)



Method 1: Following the general procedure, the title compound was prepared from 7-bromoquinoline (50.0 mg, 0.24 mmol), 2-aminophenylboronic acid hydrochloride (**68**) (45.8 mg, 0.26 mmol), an aq. solution of K_2CO_3 (99.5 mg, 0.72 mmol in 0.2 mL H_2O) and $\text{PdCl}_2(\text{dppf})$ (8.8 mg, 0.012 mmol) in EtOH (1 mL). After a reaction time of 29 hours, the crude was purified by silica gel column chromatography (pet. ether/EtOAc, 6:4 v/v) and concentration of the relevant fractions [$R_f = 0.21$ (pet. ether/EtOAc, 6:4 v/v)] gave the target compound **74** as a pale yellow oil (15.0 mg, 30%).

Method 2: Following the general procedure, the title compound was prepared from 7-bromoquinoline (500.0 mg, 2.40 mmol), 2-aminophenylboronic acid hydrochloride (**68**) (624.3 mg, 3.60 mmol), an aq. solution of Cs_2CO_3 (2.74 g, 8.40 mmol in 2 mL H_2O) and $\text{Pd}(\text{PPh}_3)_4$ (138.7 mg, 0.12 mmol) in DME (10 mL). After a reaction time of 20 hours, the crude was purified by silica gel column chromatography (pet. ether/EtOAc, 6:4 v/v) and concentration of the relevant fractions [$R_f = 0.21$ (pet. ether/EtOAc, 6:4 v/v)] gave the target compound **74** as a green oil (433.0 mg, 82%).

IR (ATR): ν_{max} 3453, 3330, 3200, 3050, 3019, 2923, 2858, 1618, 1488, 1301, 839, 749 cm^{-1} .

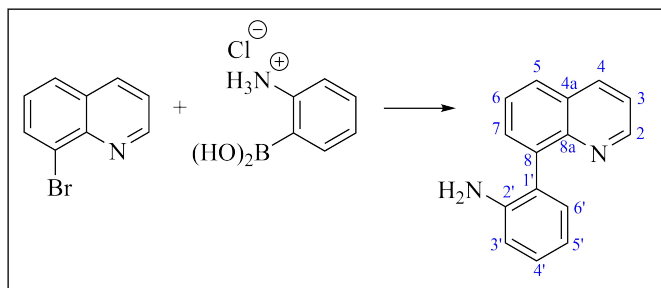
^1H NMR (400 MHz, CDCl_3): δ 8.93 (d, $J = 3.1$ Hz, 1H, H-2), 8.22 (s, 1H, H-8), 8.17 (d, $J = 8.3$ Hz, 1H, H-4), 7.87 (d, $J = 8.4$ Hz, 1H, H-5), 7.68 (dd, $J = 8.4$ Hz, 1.6 Hz, 1H, H-6), 7.40 (dd, $J = 8.2$ Hz, 4.2 Hz, 1H, H-3), 7.24 (dd, $J = 7.6$ Hz, 1.5 Hz, 1H, H-6'), 7.20 (td, $J = 7.9$ Hz, 1.5 Hz, 1H, H-4'), 6.87 (td, $J = 7.4$ Hz, 1.0 Hz, 1H, H-5'), 6.80 (dd, $J = 8.0$ Hz, 0.8 Hz, 1H, H-3'), 3.73 (bs, 2H, NH_2).

^{13}C NMR (100 MHz, CDCl_3): δ 150.8 (C-2), 148.5 (C-8a), 143.7 (C-2'), 141.2 (C-7), 135.9 (C-4), 130.7 (C-6'), 129.1 (C-4'), 129.0 (C-8), 128.4 (C-5), 128.3 (C-6), 127.3 (C-4a), 126.6 (C-1'), 121.2 (C-3), 118.9 (C-5'), 115.9 (C-3').

HRMS (ESI): calcd. for $C_{15}H_{12}N_2$ [$M + H^+$] 221.1073, found 221.1073.

In accordance with previously reported data.^[132]

2-(Quinolin-8-yl)aniline (**75**)



Method 2: Following the general procedure, the title compound was prepared from 8-bromoquinoline (540.0 mg, 2.59 mmol), 2-aminophenylboronic acid hydrochloride (**68**) (673.7 mg, 3.88 mmol), an aq. solution of Cs_2CO_3 (2.95 g, 9.06 mmol in 1 mL H_2O) and $Pd(PPh_3)_4$ (149.6 mg, 0.13 mmol) in DME (6 mL). After a reaction time of 16 hours, the crude was purified by silica gel column chromatography ($CH_2Cl_2/EtOAc$, 9:1 v/v) and concentration of the relevant fractions [$R_f = 0.21$ ($CH_2Cl_2/EtOAc$, 9:1 v/v)] gave the target compound **75** as pale red crystals (497.3 mg, 87%).

mp: 103-105 °C (lit.^[273] 100-102 °C).

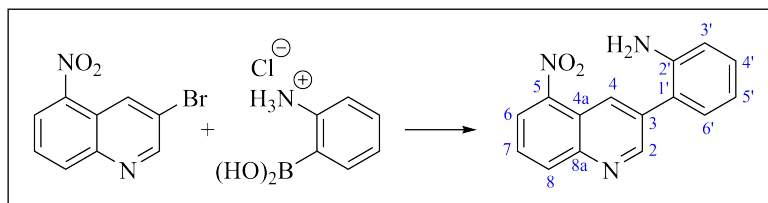
IR (ATR): ν_{max} 3424, 3330, 3206, 3026, 1615, 1491, 793, 743 cm^{-1} .

1H NMR (400 MHz, $CDCl_3$): δ 9.00 (dd, $J = 4.2$ Hz, 1.7 Hz, 1H, H-2), 8.27 (dd, $J = 8.2$ Hz, 1.7 Hz, 1H, H-4), 7.90 (dd, $J = 8.1$ Hz, 1.4 Hz, 1H, H-5), 7.76 (dd, $J = 7.1$ Hz, 1.5 Hz, 1H, H-7), 7.67 (dd, $J = 8.0$ Hz, 7.3 Hz, 1H, H-6), 7.46 (dd, $J = 8.3$ Hz, 4.1 Hz, 1H, H-3), 7.32-7.27 (m, 2H, H-4' and H-6'), 6.96 (dt, $J = 7.4$ Hz, 0.9 Hz, 1H, H-5'), 6.91 (dd, $J = 8.0$ Hz, 0.7 Hz, 1H, H-3'), 3.84 (bs, 2H, NH_2).

^{13}C NMR (100 MHz, $CDCl_3$): δ 150.7 (C-2), 146.3 (C-8a), 144.8 (C-2'), 139.5 (C-8), 136.8 (C-4), 131.8 (C-7), 131.7 (C-6'), 129.0 (C-4'), 128.7 (C-5), 128.0 (C-4a), 127.0 (C-1'), 126.9 (C-6), 121.2 (C-3), 119.0 (C-5'), 116.5 (C-3').

In accordance with previously reported data.^[273]

2-(5-Nitroquinolin-3-yl)aniline (69a)



Method 2: Following the general procedure, the title compound was prepared from 3-bromo-5-nitroquinoline (**67ba**) (100.0 mg, 0.40 mmol), 2-aminophenylboronic acid hydrochloride (**68**) (89.5 mg, 0.52 mmol), an aq. solution of Cs_2CO_3 (430.1 mg, 1.32 mmol in 1 mL H_2O) and $\text{Pd}(\text{PPh}_3)_4$ (23.1 mg, 0.020 mmol) in DME (5 mL). After a reaction time of 22 hours, the crude was purified by alumina gel column chromatography (pet. ether/EtOAc, 75:25 \rightarrow 7:3 v/v) and concentration of the relevant fractions [$R_f = 0.23$ (pet. ether/EtOAc, 75:25 v/v)] gave the target compound **69a** as a bright orange crystalline solid (34.1 mg, 32%).

mp: 139-142 °C.

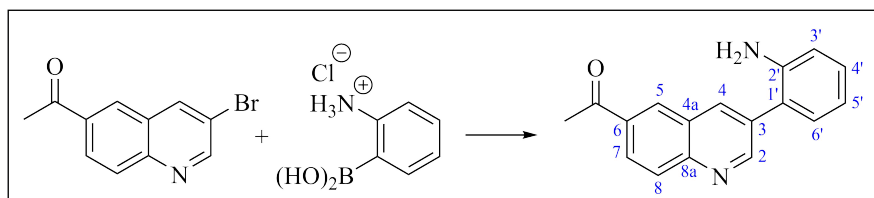
IR (ATR): ν_{max} 3444, 3364, 3339, 3212, 3054, 2922, 2853, 1518, 1326, 734 cm^{-1} .

$^1\text{H NMR}$ (400 MHz, CDCl_3): δ 9.17 (d, $J = 2.1$ Hz, 1H, H-2), 9.08 (d, $J = 1.9$ Hz, 1H, H-4), 8.44-8.42 (m, 1H, H-6), 8.39 (dd, $J = 7.7$ Hz, 1.0 Hz, 1H, H-8), 7.80 (t, $J = 8.2$ Hz, 1H, H-7), 7.29-7.25 (m, 1H, H-6'), 7.23 (dd, $J = 7.6$ Hz, 1.5 Hz, 1H, H-4'), 6.92 (td, $J = 7.4$ Hz, 0.8 Hz, 1H, H-5'), 6.85 (dt, $J = 8.0$ Hz, 0.5 Hz, 1H, H-3'), 3.85 (bs, 2H, NH_2).

$^{13}\text{C NMR}$ (100 MHz, CDCl_3): δ 153.1 (C-2), 147.2 (C-8a), 145.6 (C-5), 144.1 (C-2'), 136.4 (C-6), 135.9 (C-3), 131.1 (C-4), 131.0 (C-4'), 130.2 (C-6'), 127.4 (C-7), 125.1 (C-8), 122.9 (C-4a), 121.2 (C-1'), 119.4 (C-5'), 116.4 (C-3').

HRMS (ESI): samples sent to UiB for analysis.

2-(6-Acetylquinolin-3-yl)aniline (69b)



Method 2: Following the general procedure, the title compound was prepared from 6-acetyl-3-bromoquinoline (200.0 mg, 0.80 mmol), 2-aminophenylboronic acid hydrochloride (**68**) (180.3 mg, 1.04 mmol), an aq. solution of Cs_2CO_3 (860.2 mg, 2.64 mmol in 5 mL H_2O) and $\text{Pd}(\text{PPh}_3)_4$ (46.2 mg, 0.040 mmol) in DME (10 mL). After a reaction time of 21 hours, the

crude was purified by silica gel column chromatography (pet. ether/EtOAc, 1:1 v/v) and concentration of the relevant fractions [$R_f = 0.17$ (pet. ether/EtOAc, 1:1 v/v)] gave the target compound **69b** as an orange solid (143.7 mg, 68%).

mp: 173-175 °C.

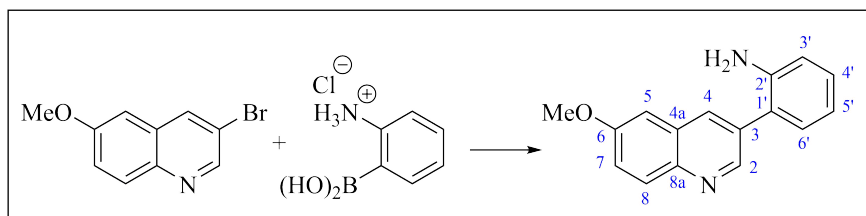
IR (ATR): ν_{\max} 3392, 3318, 3211, 3061, 3023, 2961, 2920, 2854, 1667 (C=O), 1364, 833, 751 cm^{-1} .

^1H NMR (400 MHz, CDCl_3): δ 9.11 (d, $J = 2.2$ Hz, 1H, H-2), 8.43 (d, $J = 1.9$ Hz, 1H, H-5), 8.35 (d, $J = 2.1$ Hz, 1H, H-4), 8.24 (dd, $J = 8.8$ Hz, 2.0 Hz, 1H, H-7), 8.17-8.14 (m, 1H, H-8), 7.25 (ddd, $J = 8.0$ Hz, 7.5 Hz, 1.6 Hz, 1H, H-6'), 7.20 (dd, $J = 7.6$ Hz, 1.5 Hz, 1H, H-4'), 6.90 (td, $J = 7.5$ Hz, 1.2 Hz, 1H, H-5'), 6.84 (dd, $J = 8.0$ Hz, 0.9 Hz, 1H, H-3'), 3.83 (bs, 2H, NH_2), 2.73 (s, 3H, CH_3).

^{13}C NMR (100 MHz, CDCl_3): δ 197.5 (C=O), 153.9 (C-2), 149.0 (C-8a), 144.1 (C-2'), 136.8 (C-4), 135.3 (C-6), 133.6 (C-3), 130.9 (C-6'), 129.9 (C-5), 129.9 (C-4'), 129.8 (C-8), 127.8 (C-7), 127.3 (C-4a), 123.2 (C-1'), 119.3 (C-5'), 116.3 (C-3'), 26.9 (CH_3).

HRMS (ESI): calcd. for $\text{C}_{17}\text{H}_{14}\text{N}_2\text{O}$ [$\text{M} + \text{H}^+$] 263.1179, found 263.1180.

2-(6-Methoxyquinolin-3-yl)aniline (**69c**)



Method 2: Following the general procedure, the title compound was prepared from 3-bromo-6-methoxyquinoline (300.0 mg, 1.26 mmol), 2-aminophenylboronic acid hydrochloride (**68**) (285.4 mg, 1.64 mmol), an aq. solution of Cs_2CO_3 (1.35 g, 4.16 mmol in 4 mL H_2O) and $\text{Pd}(\text{PPh}_3)_4$ (72.8 mg, 0.063 mmol) in DME (20 mL). After a reaction time of 22 hours, the crude was purified by silica gel column chromatography (pet. ether/EtOAc, 7:3 \rightarrow 1:1 v/v) and concentration of the relevant fractions [$R_f = 0.27$ (pet. ether/EtOAc, 7:3 v/v)] gave the target compound **69c** as a puffy red solid (307.6 mg, 98%).

mp: 140-141 °C.

IR (ATR): ν_{\max} 3410, 3306, 2959, 2923, 1571, 1493, 828, 756 cm^{-1} .

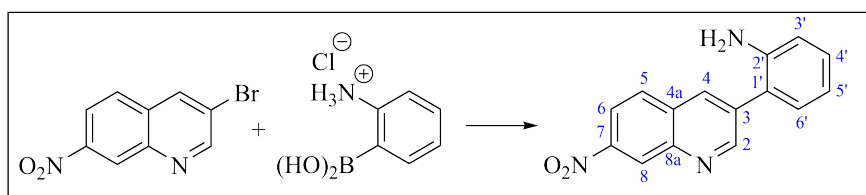
^1H NMR (400 MHz, CDCl_3): δ 8.86 (d, $J = 2.1$ Hz, 1H, H-2), 8.14 (d, $J = 1.9$ Hz, 1H, H-4), 8.02 (d, $J = 9.2$ Hz, 1H, H-8), 7.38 (dd, $J = 9.2$ Hz, 2.8 Hz, 1H, H-7), 7.25-7.19 (m, 2H,

H-4' and H-6'), 7.08 (d, $J = 2.8$ Hz, 1H, H-5), 6.89 (td, $J = 7.4$ Hz, 1.1 Hz, 1H, H-5'), 6.82 (dd, $J = 8.0$ Hz, 0.8 Hz, 1H, H-3'), 3.94 (s, 3H, OCH₃), 3.79 (bs, 2H, NH₂).

¹³C NMR (100 MHz, CDCl₃): δ 158.3 (C-6), 149.1 (C-2), 144.1 (C-2'), 143.5 (C-8a), 134.4 (C-4), 132.8 (C-3), 130.9 (C-4'), 130.8 (C-8), 129.5 (C-6'), 129.1 (C-1'), 124.1 (C-4a), 122.4 (C-7), 119.1 (C-5'), 116.0 (C-3'), 105.3 (C-6), 55.7 (OCH₃).

HRMS (ESI): calcd. for C₁₆H₁₄N₂O [M + H⁺] 251.1179, found 251.1179.

2-(7-Nitroquinolin-3-yl)aniline (69d)



Method 2: Following the general procedure, the title compound was prepared from 3-bromo-7-nitroquinoline (**67bc**) (100.0 mg, 0.39 mmol), 2-aminophenylboronic acid hydrochloride (**68**) (89.1 mg, 0.51 mmol), an aq. solution of Cs₂CO₃ (419.3 mg, 1.29 mmol in 1 mL H₂O) and Pd(PPh₃)₄ (22.5 mg, 0.019 mmol) in DME (5 mL). After a reaction time of 23 hours, the crude was purified by silica gel column chromatography (pet. ether/EtOAc, 9:1 → 7:3 v/v) and concentration of the relevant fractions [$R_f = 0.38$ (pet. ether/EtOAc, 7:3 v/v)] gave the target compound **69d** as an orange crystalline solid (80.4 mg, 78%).

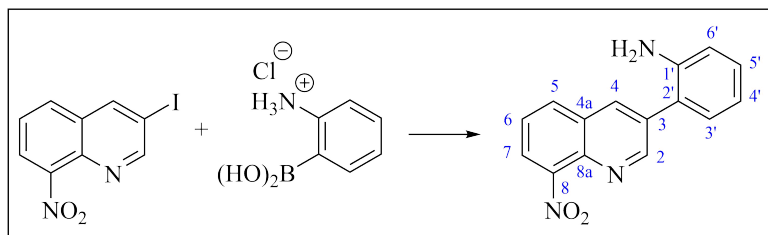
mp: 169-170 °C.

IR (ATR): ν_{\max} 3361, 3064, 2998, 1519, 1493, 1338, 743 cm⁻¹.

¹H NMR (400 MHz, CDCl₃): δ 9.22 (d, $J = 2.2$ Hz, 1H, H-2), 9.04 (d, $J = 2.2$ Hz, 1H, H-8), 8.37 (d, $J = 1.9$ Hz, 1H, H-4), 8.35 (d, $J = 2.3$ Hz, 1H, H-6), 7.99 (d, $J = 8.9$ Hz, 1H, H-5), 7.30-7.26 (m, 2H, H-6'), 7.23 (dd, $J = 7.6$ Hz, 1.5 Hz, 1H, H-4'), 6.93 (td, $J = 7.5$ Hz, 0.8 Hz, 1H, H-5'), 6.87-6.85 (m, 1H, H-3'), 3.80 (bs, 2H, NH₂).

¹³C NMR (100 MHz, CDCl₃): δ 154.2 (C-2), 148.1 (C-7), 146.1 (C-8a), 144.1 (C-2'), 135.9 (C-3), 135.0 (C-4), 131.4 (C-4a), 130.9 (C-4'), 130.3 (C-6'), 129.5 (C-5), 125.8 (C-8), 122.7 (C-1'), 120.7 (C-6), 119.6 (C-5'), 116.5 (C-3').

HRMS (ESI): calcd. for C₁₅H₁₁N₃O₂ [M + H⁺] 266.0924, found 266.0921.

2-(8-Nitroquinolin-3-yl)aniline (69e)

Method 2: Following the general procedure, the title compound was prepared from 3-iodo-8-nitroquinoline (300.0 mg, 0.99 mmol), 2-aminophenylboronic acid hydrochloride (**68**) (225.4 mg, 1.29 mmol), an aq. solution of Cs_2CO_3 (1.06 g, 3.27 mmol in 6 mL H_2O) and $\text{Pd}(\text{PPh}_3)_4$ (57.2 mg, 0.049 mmol) in DME (30 mL). After a reaction time of 20 hours, the crude was purified by silica gel column chromatography (pet. ether/EtOAc, 6:4 v/v) and concentration of the relevant fractions [$R_f = 0.32$ (pet. ether/EtOAc, 6:4 v/v)] gave the target compound **69e** as an orange crystalline solid (103.8 mg, 40%).

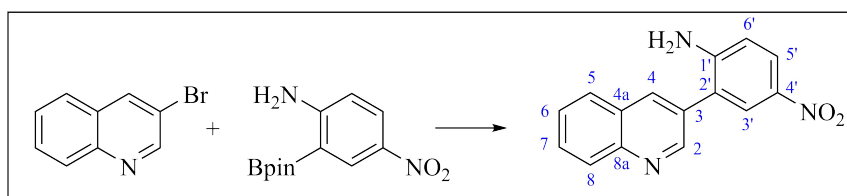
mp: 163-165 °C (decomp.).

IR (ATR): ν_{max} 3434, 3343, 3221, 3053, 2920, 1518, 1337, 760 cm^{-1} .

$^1\text{H NMR}$ (400 MHz, CDCl_3): δ 9.21 (d, $J = 2.1$ Hz, 1H, H-2), 8.37 (d, $J = 2.2$ Hz, 1H, H-4), 8.08-8.06 (m, 2H, H-5 and H-7), 7.65 (t, $J = 7.9$ Hz, 1H, H-6), 7.27 (ddd, $J = 9.0$ Hz, 7.4 Hz, 1.5 Hz, 1H, H-3'), 7.20 (dd, $J = 7.6$ Hz, 1.5 Hz, 1H, H-5'), 6.92 (td, $J = 7.5$ Hz, 1.1 Hz, 1H, H-4'), 6.85 (dd, $J = 8.0$ Hz, 0.9 Hz, 1H, H-6'), 3.78 (bs, 2H, NH_2).

$^{13}\text{C NMR}$ (100 MHz, CDCl_3): δ 154.1 (C-2), 148.4 (C-8), 144.1 (C-1'), 138.5 (C-8a), 135.4 (C-4), 134.7 (C-3), 132.2 (C-5), 130.9 (C-5'), 130.2 (C-3'), 129.1 (C-4a), 125.9 (C-6), 123.8 (C-7), 122.7 (C-2'), 119.5 (C-4'), 116.4 (C-6').

In accordance with previously reported data.^[275]

4-Nitro-2-(quinolin-3-yl)aniline (69g)

Method 2: Following the general procedure, the title compound was prepared from 3-bromoquinoline (**67b**) (0.20 mL, 1.44 mmol), 4-nitro-2-(4,4,5,5-tetramethyl-1,3,2-dioxaborolan-2-yl)aniline (**83b**) (494.4 mg, 1.87 mmol), an aq. solution of Cs_2CO_3 (1.64 g, 5.04 mmol in 6 mL

H₂O) and Pd(PPh₃)₄ (83.2 mg, 0.072 mmol) in DME (30 mL). After a reaction time of 21 hours, the crude was purified by silica gel column chromatography (pet. ether/EtOAc, 1:1 → 4:6 v/v) and concentration of the relevant fractions [*R*_f = 0.12 (pet. ether/EtOAc, 1:1 v/v)] gave the target compound **69g** as a dark yellow solid (117.1 mg, 31%).

mp: 228-230 °C.

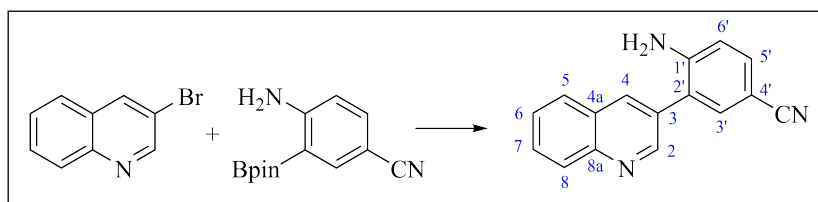
IR (ATR): ν_{\max} 2955, 2865, 1599, 1464, 883, 796, 756 cm⁻¹.

¹H NMR (400 MHz, CDCl₃): δ 8.99 (d, *J* = 2.1 Hz, 1H, H-2), 8.25 (d, *J* = 1.9 Hz, 1H, H-4), 8.18-8.13 (m, 3H, H-8, H-3' and H-5'), 7.88 (d, *J* = 8.1 Hz, 1H, H-5), 7.82-7.78 (m, 1H, H-7), 7.65-7.61 (m, 1H, H-6), 6.81 (dd, *J* = 7.1 Hz, 2.4 Hz, 1H, H-6'), 4.53 (bs, 2H, NH₂).

¹³C NMR (100 MHz, CDCl₃): δ 150.6 (C-2), 150.2 (C-4'), 147.9 (C-8a), 139.7 (C-1'), 136.2 (C-4), 130.5 (C-7), 130.1 (C-3), 129.6 (C-8), 128.0 (C-4a), 127.9 (C-5), 127.7 (C-6), 127.5 (C-5'), 126.1 (C-3'), 122.8 (C-2'), 114.6 (C-6').

HRMS (ESI): calcd. for C₁₅H₁₁N₃O₂ [*M* + H⁺] 266.0924, found 266.0934.

4-Amino-3-(quinolin-3-yl)benzonitrile (**69h**)



Method 2: Following the general procedure, the title compound was prepared from 3-bromoquinoline (**67b**) (0.20 mL, 1.44 mmol), 4-amino-3-(4,4,5,5-tetramethyl-1,3,2-dioxaborolan-2-yl)benzonitrile (**83c**) (457.0 mg, 1.87 mmol), an aq. solution of Cs₂CO₃ (1.55 g, 4.75 mmol in 6 mL H₂O) and Pd(PPh₃)₄ (83.2 mg, 0.072 mmol) in DME (30 mL). After a reaction time of 24 hours, the crude was purified by silica gel column chromatography (pet. ether/EtOAc, 1:1 v/v) and concentration of the relevant fractions [*R*_f = 0.19 (pet. ether/EtOAc, 1:1 v/v)] gave the target compound **69h** as a pink solid (330.9 mg, 94%).

mp: 228-230 °C.

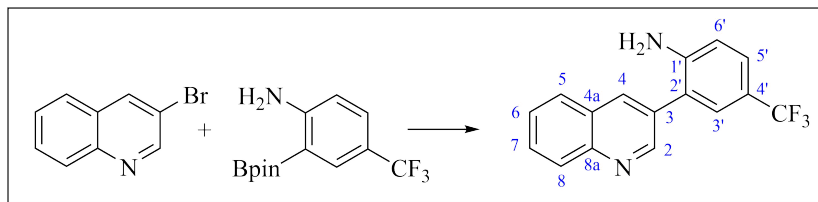
IR (ATR): ν_{\max} 3433, 3306, 3196, 2979, 2209 (CN), 1368, 1103, 946, 828 cm⁻¹.

¹H NMR (400 MHz, CD₃OD): δ 8.89 (s, 1H, H-2), 8.42 (d, *J* = 1.7 Hz, 1H, H-4), 8.08 (d, *J* = 8.4 Hz, 1H, H-8), 8.01 (d, *J* = 8.1 Hz, 1H, H-5), 7.83-7.79 (m, 1H, H-7), 7.68-7.64 (m, 1H, H-6), 7.49-7.45 (m, 2H, H-3' and H-5'), 6.90 (d, *J* = 8.4 Hz, 1H, H-6').

¹³C NMR (100 MHz, CD₃OD): δ 151.8 (C-2), 147.9 (C-8a), 138.0 (C-4), 136.1 (C-5'), 134.4 (C-3'), 132.7 (C-3), 131.4 (C-7), 129.7 (C-4a), 129.5 (C-5), 129.0 (C-8), 128.5 (C-6), 124.0 (C-2'), 121.0 (C-1'), 116.6 (C-6'), 116.3 (CN), 99.7 (C-4').

HRMS (ESI): calcd. for $C_{16}H_{11}N_3$ [$M + H^+$] 246.1026, found 246.1037.

2-(Quinolin-3-yl)-4-(trifluoromethyl)aniline (**69i**)



Method 2: Following the general procedure, the title compound was prepared from 3-bromoquinoline (**67b**) (0.15 mL, 1.13 mmol), 2-(4,4,5,5-tetramethyl-1,3,2-dioxaborolan-2-yl)-4-(trifluoromethyl)aniline (**83d**) (421.8 mg, 1.47 mmol), an aq. solution of Cs_2CO_3 (1.21 g, 3.73 mmol in 6 mL H_2O) and $Pd(PPh_3)_4$ (65.3 mg, 0.056 mmol) in DME (30 mL). After a reaction time of 17 hours, the crude was purified by silica gel column chromatography (pet. ether/EtOAc, 6:4 \rightarrow 1:1 v/v) and concentration of the relevant fractions [$R_f = 0.2$ (pet. ether/EtOAc, 6:4 v/v)] gave the target compound **69i** as a dark red oil. 1H NMR of the obtained oil showed a mixture of the desired compound **69i** and pinacol, which was removed by the oil subsequently being dissolved in CH_2Cl_2 and washed with hot water (4 x 5 mL), dried ($MgSO_4$), filtered and concentrated *in vacuo* to give the target compound **69i** as a red crystalline solid (72.1 mg, 22%).

mp: 137-139 °C.

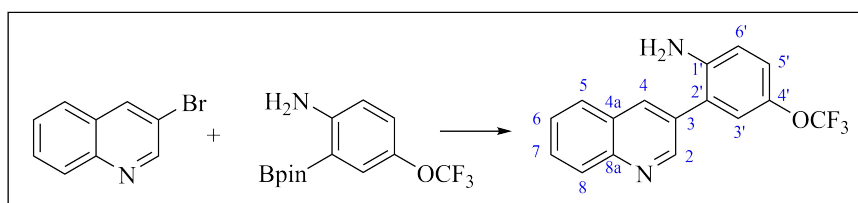
IR (ATR): ν_{max} 3467, 3312, 3208, 2919, 2850, 1635, 1309, 1105, 1075, 824, 743 cm^{-1} .

1H NMR (400 MHz, $CDCl_3$): δ 9.04 (bs, 1H, H-2), 8.23 (d, $J = 1.6$ Hz, 1H, H-4), 8.14 (d, $J = 8.4$ Hz, 1H, H-8), 7.84 (d, $J = 8.1$ Hz, 1H, H-5), 7.77-7.73 (m, 1H, H-7), 7.61-7.57 (m, 1H, H-6), 7.46-7.43 (m, 2H, H-3' and H-5'), 6.84 (d, $J = 8.3$ Hz, 1H, H-6'), 4.14 (bs, 2H, NH_2).

^{13}C NMR (100 MHz, $CDCl_3$): δ 150.9 (C-2), 147.7 (C-8a), 135.9 (C-4), 130.1 (C-6), 129.5 (C-8), 128.8 (C-3), 128.2 (q, $J_{CF} = 3.7$ Hz, C-3'), 128.0 (C-5), 127.4 (C-7), 126.7 (q, $J_{CF} = 3.6$ Hz, C-5'), 126.1 (C-1'), 123.4 (C-4a), 123.3 (C-2'), 120.9 (q, $J_{CF} = 33.0$ Hz, C-4'), 115.4 (C-6') (CF₃ was obscured or overlapping).

^{19}F NMR (376 MHz, $CDCl_3$): δ -61.1.

2-(Quinolin-3-yl)-4-(trifluoromethoxy)aniline (**69j**)



Method 2: Following the general procedure, the title compound was prepared from 3-bromoquinoline (**67b**) (0.10 mL, 0.69 mmol), 2-(3,3,4,4-tetramethyl-1,3,2-dioxaborolan-1-yl)-4-(trifluoromethoxy)aniline (**83e**) (272.4 mg, 0.90 mmol), an aq. solution of Cs_2CO_3 (741.8 mg, 2.28 mmol in 1 mL H_2O) and $\text{Pd}(\text{PPh}_3)_4$ (39.9 mg, 0.034 mmol) in DME (5 mL). After a reaction time of 22 hours, the crude was purified by silica gel column chromatography (pet. ether/EtOAc, 6:4 v/v) and concentration of the relevant fractions [$R_f = 0.20$ (pet. ether/EtOAc, 6:4 v/v)] gave the target compound **69j** as a light brown solid (196.1 mg, 93%).

mp: 118-121 °C.

IR (ATR): ν_{max} 3455, 3310, 3208, 3062, 2922, 1637, 1244, 1213, 1159, 752 cm^{-1} .

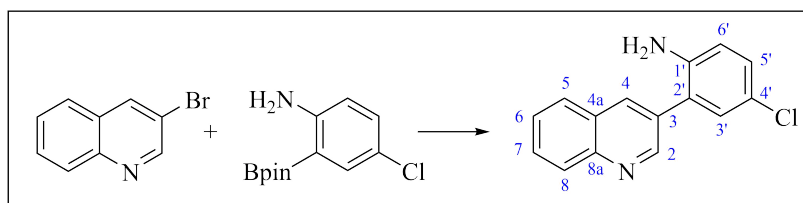
^1H NMR (400 MHz, CDCl_3): δ 9.00 (d, $J = 1.9$ Hz, 1H, H-2), 8.24 (d, $J = 1.5$ Hz, 1H, H-4), 8.15 (d, $J = 8.4$ Hz, 1H, H-8), 7.86 (d, $J = 8.1$ Hz, 1H, H-5), 7.78-7.74 (m, 1H, H-7), 7.62-7.51 (m, 1H, H-6), 7.11-7.09 (m, 2H, H-3' and H-6'), 6.81-6.78 (m, 1H, H-5'), 3.84 (bs, 2H, NH_2).

^{13}C NMR (100 MHz, CDCl_3): δ 151.1 (C-2), 147.6 (C-8a) 143.0 (C-1'), 141.6 (q, $J_{\text{CF}} = 2.0$ Hz, C-4'), 135.8 (C-4), 131.3 (C-3), 130.0 (C-7), 129.5 (C-8), 128.0 (C-5), 127.9 (C-6), 127.4 (C-4a), 124.5 (C-2'), 123.8 (C-3'), 122.1 (C-6'), 120.9 (q, $J_{\text{CF}} = 256.9$ Hz, OCF_3), 116.5 (C-5').

^{19}F NMR (376 MHz, CDCl_3): δ -58.3.

HRMS (ESI): calcd. for $\text{C}_{16}\text{H}_{11}\text{F}_3\text{N}_2\text{O}$ [$\text{M} + \text{H}^+$] 305.0896, found 305.0905.

4-Chloro-2-(quinolin-3-yl)aniline (**69k**)



Method 2: Following the general procedure, the title compound was prepared from 3-bromoquinoline (**67b**) (0.20 mL, 1.44 mmol), 4-chloro-2-(4,4,5,5-tetramethyl-1,3,2-dioxaborolan-2-yl)benzeneamine (**83f**) (474.4 mg, 1.87 mmol), an aq. solution of Cs_2CO_3 (1.55 g, 4.75 mmol in 6 mL H_2O) and $\text{Pd}(\text{PPh}_3)_4$ (83.2 mg, 0.072 mmol) in DME (30 mL). After a reaction time of 19 hours, the crude was purified by silica gel column chromatography (pet. ether/EtOAc, 7:3 v/v) and concentration of the relevant fractions [$R_f = 0.24$ (pet. ether/EtOAc, 7:3 v/v)] gave the target compound **69k** as a light brown solid (306.7 mg, 84%).

mp: 165-166 °C (lit.^[274] 123-125 °C).

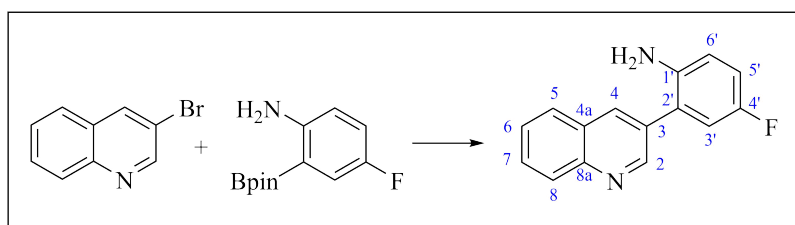
IR (ATR): ν_{\max} 3429, 3296, 3192, 1635, 1486, 808, 753 cm^{-1} .

^1H NMR (400 MHz, CDCl_3): δ 9.00 (d, $J = 2.1$ Hz, 1H, H-2), 8.23 (d, $J = 1.9$ Hz, 1H, H-4), 8.15 (d, $J = 8.5$ Hz, 1H, H-8), 7.85 (dd, $J = 8.3$ Hz, 1.0 Hz, 1H, H-5), 7.78-7.74 (m, 1H, H-7), 7.62-7.58 (m, 1H, H-6), 7.19-7.17 (m, 2H, H-3' and H-5'), 6.76 (dd, $J = 7.0$ Hz, 2.0 Hz, 1H, H-6'), 3.78 (bs, 2H, NH_2).

^{13}C NMR (100 MHz, CDCl_3): δ 151.1 (C-2), 147.5 (C-8a), 142.8 (C-1'), 135.7 (C-4), 131.4 (C-3), 130.4 (C-5'), 129.9 (C-7), 129.5 (C-8), 129.3 (C-3'), 128.0 (C-5), 127.9 (C-4a), 127.3 (C-6), 125.2 (C-2'), 123.7 (C-4-), 117.2 (C-6').

In accordance with previously reported data.^[274]

4-Fluoro-2-(quinolin-3-yl)aniline (**69I**)



Method 2: Following the general procedure, the title compound was prepared from 3-bromoquinoline (**67b**) (0.13 mL, 0.96 mmol), 4-fluoro-2-(4,4,5,5-tetramethyl-1,3,2-dioxaborolan-2-yl)aniline (**82a**) (295.9 mg, 1.25 mmol), an aq. solution of Cs_2CO_3 (1.03 g, 3.17 mmol in 2 mL H_2O) and $\text{Pd}(\text{PPh}_3)_4$ (55.5 mg, 0.048 mmol) in DME (10 mL). After a reaction time of 22 hours, the crude was purified by silica gel column chromatography (pet. ether/EtOAc, 1:1 v/v) and concentration of the relevant fractions [$R_f = 0.44$ (pet. ether/EtOAc, 1:1 v/v)] gave the target compound **69I** as a pink solid (145.2 mg, 63%).

mp: 160-161 $^\circ\text{C}$.

IR (ATR): ν_{\max} 3437, 3307, 3211, 1499, 747 cm^{-1} .

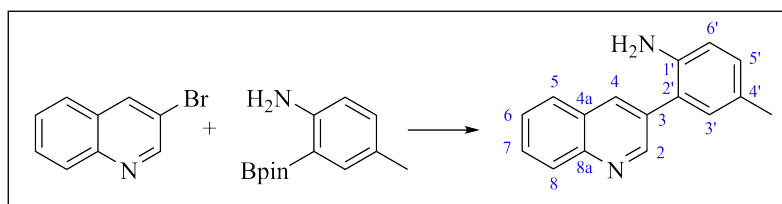
^1H NMR (400 MHz, CDCl_3): δ 9.01 (d, $J = 2.0$ Hz, 1H, H-2), 8.25 (d, $J = 2.0$ Hz, 1H, H-4), 8.15 (d, $J = 8.4$ Hz, 1H, H-8), 7.85 (dd, $J = 8.1$ Hz, 1.0 Hz, 1H, H-5), 7.77-7.73 (m, 1H, H-6), 7.61-7.57 (m, 1H, H-7), 6.97-6.92 (m, 2H, H-3' and H-5'), 6.76 (dd, $J = 9.5$ Hz, 4.8 Hz, 1H, H-6'), 3.64 (bs, 2H, NH_2).

^{13}C NMR (100 MHz, CDCl_3): δ 156.6 (d, $J_{\text{CF}} = 237.8$ Hz, C-4'), 151.2 (C-2), 147.5 (C-8a), 140.2 (d, $J_{\text{CF}} = 2.0$ Hz, C-1'), 135.7 (C-4), 131.7 (C-3), 129.9 (C-6), 129.4 (C-8), 128.0 (C-5), 127.9 (C-4a), 127.3 (C-7), 124.9 (d, $J_{\text{CF}} = 7.2$ Hz, C-2'), 117.2 (d, $J_{\text{CF}} = 9.6$ Hz, C-6'), 117.0 (d, $J_{\text{CF}} = 5.3$ Hz, C-3'), 116.1 (d, $J_{\text{CF}} = 22.1$ Hz, C-5').

^{19}F NMR (376 MHz, CDCl_3): δ -126.2.

HRMS (ESI): calcd. for $\text{C}_{15}\text{H}_{11}\text{FN}_2$ [$\text{M} + \text{H}^+$] 239.0979, found 239.0987.

4-Methyl-2-(quinolin-3-yl)aniline (**69m**)



Method 2: Following the general procedure, the title compound was prepared from 3-bromoquinoline (**67b**) (0.20 mL, 1.44 mmol), 4-methyl-2-(4,4,5,5-tetramethyl-1,3,2-dioxaborolan-2-yl)aniline (**83g**) (436.5 mg, 1.87 mmol), an aq. solution of Cs_2CO_3 (1.55 g, 4.75 mmol in 6 mL H_2O) and $\text{Pd}(\text{PPh}_3)_4$ (83.2 mg, 0.072 mmol) in DME (30 mL). After a reaction time of 21 hours, the crude was purified by silica gel column chromatography (pet. ether/EtOAc, 7:3 \rightarrow 1:1 v/v) and concentration of the relevant fractions [$R_f = 0.16$ (pet. ether/EtOAc, 7:3 v/v)] gave the target compound **69m** as a dark yellow oil. ^1H NMR of the obtained oil showed a mixture of the desired compound and pinacol, which was removed by the oil subsequently being dissolved in CH_2Cl_2 and washed with hot water (5 x 30 mL), dried (MgSO_4), filtered and concentrated *in vacuo* to give the target compound **69m** as a yellow oil (307.2 mg, 91%).

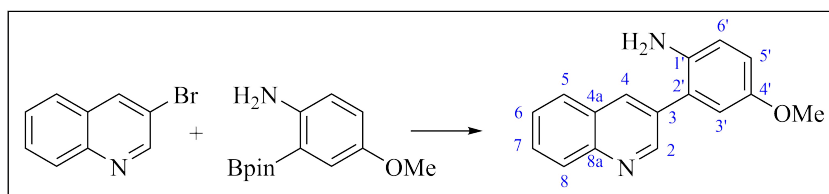
IR (ATR): ν_{max} 3437, 3324, 3203, 3016, 2918, 2857, 1618, 1504, 1488, 726 cm^{-1} .

^1H NMR (400 MHz, CDCl_3): δ 9.02 (d, $J = 2.1$ Hz, 1H, H-2), 8.24 (d, $J = 1.9$ Hz, 1H, H-4), 8.14 (d, $J = 8.5$ Hz, 1H, H-8), 7.83 (dd, $J = 8.1$ Hz, 1.0 Hz, 1H, H-5), 7.75-7.71 (m, 1H, H-7), 7.59-7.55 (m, 1H, H-6), 7.06-7.04 (m, 2H, H-3' and H-5'), 6.75 (d, $J = 7.8$ Hz, 1H, H-6'), 3.66 (bs, 2H, NH_2), 2.32 (s, 3H, CH_3).

^{13}C NMR (100 MHz, CDCl_3): δ 151.7 (C-2), 147.2 (C-8a), 141.6 (C-1'), 135.5 (C-4), 132.7 (C-3), 131.3 (C-5'), 130.1 (C-3'), 129.5 (C-6), 129.3 (C-8), 128.4 (C-4'), 128.0 (C-2'), 127.9 (C-7), 127.0 (C-5), 123.9 (C-4a), 116.3 (C-6'), 20.5 (CH_3).

HRMS (ESI): calcd. for $\text{C}_{16}\text{H}_{14}\text{N}_2$ [$\text{M} + \text{H}^+$] 235.1230, found 235.1239.

4-Methoxy-2-(quinolin-3-yl)aniline (**69n**)



Method 2: Following the general procedure, the title compound was prepared from 3-bromoquinoline (**67b**) (0.065 mL, 0.48 mmol), 4-methoxy-2-(4,4,5,5-tetramethyl-1,3,2-dioxaborolan-2-yl)aniline (**83i**) (155.7 mg, 0.62 mmol), an aq. solution of Cs_2CO_3 (516.1 mg, 1.58 mmol in

1 mL H₂O) and Pd(PPh₃)₄ (27.7 mg, 0.024 mmol) in DME (5 mL). After a reaction time of 26 hours, the crude was purified by silica gel column chromatography (pet. ether/EtOAc, 1:1 v/v) and concentration of the relevant fractions [*R*_f = 0.31 (pet. ether/EtOAc, 1:1 v/v)] gave the target compound **69n** as an orange solid (74.6 mg, 62%).

mp: 147-150 °C (lit.^[274] 145-147 °C).

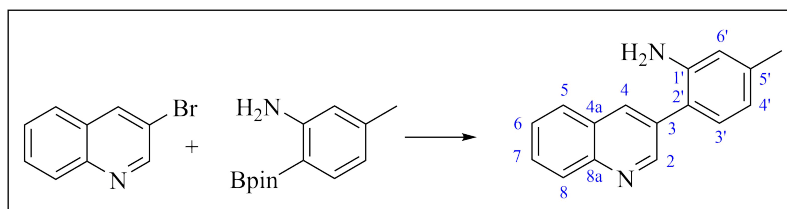
IR (ATR): ν_{\max} 3424, 3393, 3322, 3224, 3036, 3001, 2953, 2923, 1486, 1282, 1042, 747 cm⁻¹.

¹H NMR (400 MHz, CDCl₃): δ 9.04 (d, *J* = 2.1 Hz, 1H, H-2), 8.27 (dd, *J* = 2.3 Hz, 0.5 Hz, 1H, H-4), 8.16-8.14 (m, 1H, H-8), 7.86 (dd, *J* = 8.2 Hz, 1.3 Hz, 1H, H-5), 7.77-7.72 (m, 1H, H-7), 7.61-7.57 (m, 1H, H-6), 6.85 (dd, *J* = 8.6 Hz, 2.9 Hz, 1H, H-6'), 6.81 (d, *J* = 2.5 Hz, 1H, H-3'), 6.79 (dd, *J* = 8.6 Hz, 0.4 Hz, 1H, H-5'), 3.79 (s, 3H, OCH₃), 3.52 (bs, 2H, NH₂).

¹³C NMR (100 MHz, CDCl₃): δ 153.2 (C-4'), 151.6 (C-2), 147.4 (C-8a), 137.8 (C-1'), 135.6 (C-4), 132.6 (C-3), 129.7 (C-7), 129.4 (C-8), 128.0 (C-5), 128.0 (C-4a), 127.2 (C-6), 125.0 (C-2'), 117.5 (C-6'), 116.2 (C-3'), 115.5 (C-5'), 56.0 (OCH₃).

In accordance with previously reported data.^[274]

5-Methyl-2-(quinolin-3-yl)aniline (**69o**)



Method 2: Following the general procedure, the title compound was prepared from 3-bromoquinoline (**67b**) (0.20 mL, 1.44 mmol), 5-methyl-2-(4,4,5,5-tetramethyl-1,3,2-dioxaborolan-2-yl)aniline (**83h**) (436.5 mg, 1.87 mmol), an aq. solution of Cs₂CO₃ (1.55 g, 4.75 mmol in 6 mL H₂O) and Pd(PPh₃)₄ (83.2 mg, 0.072 mmol) in DME (30 mL). After a reaction time of 24 hours, the crude was purified by silica gel column chromatography (pet. ether/EtOAc, 7:3 → 6:4 → 1:1 v/v) and concentration of the relevant fractions [*R*_f = 0.24 (pet. ether/EtOAc, 7:3 v/v)] gave the target compound **69o** as a grey solid (327.3 mg, 97%).

mp: 134-138 °C.

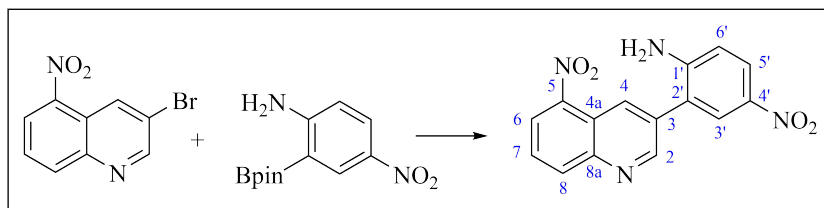
IR (ATR): ν_{\max} 3323, 3203, 3011, 2918, 1617, 1489, 786, 732 cm⁻¹.

¹H NMR (400 MHz, CDCl₃): δ 9.02 (d, *J* = 2.0 Hz, 1H, H-2), 8.24 (d, *J* = 2.0 Hz, 1H, H-4), 8.14 (d, *J* = 8.5 Hz, 1H, H-8), 7.84 (dd, *J* = 8.2 Hz, 1.1 Hz, 1H, H-5), 7.75-7.71 (m, 1H, H-7), 7.59-7.55 (m, 1H, H-6), 7.11 (d, *J* = 7.7 Hz, 1H, H-3'), 6.73 (ddd, *J* = 8.4 Hz, 7.8 Hz, 0.7 Hz, 1H, H-4'), 6.67 (d, *J* = 0.5 Hz, 1H, H-6'), 3.74 (bs, 2H, NH₂), 2.34 (s, 3H, CH₃).

^{13}C NMR (100 MHz, CDCl_3): δ 151.8 (C-2), 147.2 (C-8a), 143.9 (C-1'), 139.6 (C-5'), 135.4 (C-4), 132.6 (C-3), 130.9 (C-3'), 129.5 (C-7), 129.4 (C-8), 128.1 (C-4a), 127.9 (C-5), 127.1 (C-6), 121.2 (C-2'), 120.2 (C-4'), 116.7 (C-6'), 21.4 (CH_3).

HRMS (ESI): calcd. for $\text{C}_{16}\text{H}_{14}\text{N}_2$ [$\text{M} + \text{H}^+$] 235.1230, found 235.1230.

4-Nitro-2-(5-nitroquinolin-3-yl)aniline (69p)



Method 2: Following the general procedure, the title compound was prepared from 3-bromo-5-nitroquinoline (**67ba**) (250.0 mg, 0.99 mmol), 4-nitro-2-(4,4,5,5-tetramethyl-1,3,2-dioxaborolan-2-yl)aniline (**83b**) (339.2 mg, 1.28 mmol), an aq. solution of Cs_2CO_3 (1.06 g, 3.27 mmol in 5 mL H_2O) and $\text{Pd}(\text{PPh}_3)_4$ (57.2 mg, 0.049 mmol) in DME (25 mL). After a reaction time of 22 hours, the crude was purified by silica gel column chromatography (pet. ether/EtOAc, 1:1 \rightarrow 4:6 v/v) and concentration of the relevant fractions [$R_f = 0.15$ (pet. ether/EtOAc, 1:1 v/v)] gave the target compound **69p** as an orange solid (91.1 mg, 30%).

mp: 238 °C (decomp.).

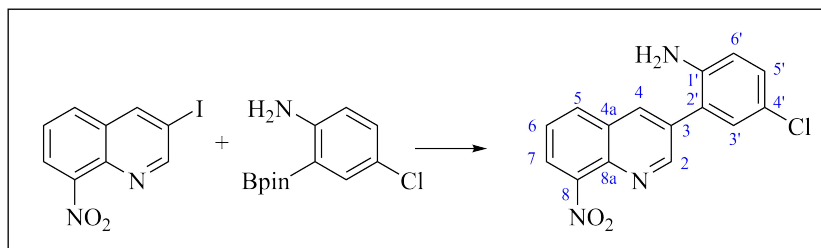
IR (ATR): ν_{max} 3476, 3377, 3222, 2921, 2851, 1478, 1301, 1261, 826, 737 cm^{-1} .

^1H NMR (400 MHz, $\text{DMSO}-d_6$): δ 9.10 (d, $J = 2.0$ Hz, 1H, H-2), 8.88 (d, $J = 1.4$ Hz, 1H, H-4), 8.50-8.47 (m, 2H, H-6 and H-8), 8.07-8.05 (m, 2H, H-7 and H-3'), 8.00-7.96 (m, 1H, H-4), 6.88 (dd, $J = 7.7$ Hz, 1.7 Hz, 1H, H-6'), 6.74 (bs, 2H, NH_2).

^{13}C NMR (100 MHz, $\text{DMSO}-d_6$): δ 153.0 (C-2), 152.3 (C-5), 146.6 (C-8a), 145.4 (C-1'), 136.5 (C-4'), 135.7 (C-6), 133.0 (C-3), 131.1 (C-4), 128.3 (C-5'), 127.5 (C-7), 126.1 (C-3'), 125.1 (C-8), 120.1 (C-2'), 120.0 (C-4a), 114.5 (C-6').

HRMS (ESI): sample sent to UiB for analysis.

4-Chloro-2-(8-nitroquinolin-3-yl)aniline (**69q**)



Method 2: Following the general procedure, the title compound was prepared from 3-iodo-8-nitroquinoline (300.0 mg, 1.00 mmol), 4-chloro-2-(4,4,5,5-tetramethyl-1,3,2-dioxaborolan-2-yl)benzeneamine (**83f**) (328.9 mg, 1.30 mmol), an aq. solution of Cs_2CO_3 (1.07 g, 3.30 mmol in 6 mL H_2O) and $\text{Pd}(\text{PPh}_3)_4$ (57.8 mg, 0.050 mmol) in DME (30 mL). After a reaction time of 19 hours, the crude was purified by silica gel column chromatography (pet. ether/EtOAc, 7:3 \rightarrow 1:1 v/v) and concentration of the relevant fractions [$R_f = 0.22$ (pet. ether/EtOAc, 7:3 v/v)] gave the target compound **69q** as a light brown solid (221.6 mg, 74%).

mp: 212-215 °C.

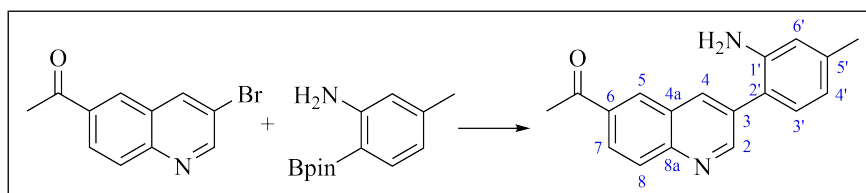
IR (ATR): ν_{max} 3467, 3338, 3052, 2923, 1626, 1525, 766 cm^{-1} .

^1H NMR (400 MHz, CDCl_3): δ 9.16 (d, $J = 2.1$ Hz, 1H, H-2), 8.33 (d, $J = 2.1$ Hz, 1H, H-4), 8.08-8.05 (m, 2H, H-5 and H-7), 7.69-7.65 (m, 1H, H-6), 7.21 (dd, $J = 8.5$ Hz, 2.4 Hz, 1H, H-5'), 7.17 (d, $J = 2.4$ Hz, 1H, H-3'), 6.77 (d, $J = 8.6$ Hz, 1H, H-6'), 3.78 (bs, 2H, NH_2).

^{13}C NMR (100 MHz, CDCl_3): δ 153.5 (C-2), 148.4 (C-8), 142.7 (C-1'), 138.7 (C-8a), 135.7 (C-4), 133.5 (C-3), 132.2 (C-5), 130.4 (C-3'), 129.9 (C-5'), 128.9 (C-4a), 126.1 (C-6), 124.1 (C-7), 124.0 (C-4'), 123.9 (C-2'), 117.6 (C-6').

HRMS (ESI): calcd. for $\text{C}_{15}\text{H}_{10}\text{ClN}_3\text{O}_2$ [$\text{M} + \text{Na}^+$] 322.0354, found 322.0353.

2-(6-Acetylquinolin-3-yl)-5-methylaniline (**69r**)



Method 2: Following the general procedure, the title compound was prepared from 6-acetyl-3-bromoquinoline (213.6 mg, 0.85 mmol), 5-methyl-2-(4,4,5,5-tetramethyl-1,3,2-dioxaborolan-2-yl)aniline (**83h**) (258.9 mg, 1.11 mmol), an aq. solution of Cs_2CO_3 (913.9 mg, 2.80 mmol in 4 mL H_2O) and $\text{Pd}(\text{PPh}_3)_4$ (49.1 mg, 0.042 mmol) in DME (20 mL). After a reaction time of

20 hours, the crude was purified by silica gel column chromatography (pet. ether/EtOAc, 1:1 → 4:6 v/v) and concentration of the relevant fractions [$R_f = 0.35$ (pet. ether/EtOAc, 4:6 v/v)] gave the target compound **69r** as a dark yellow solid (215.1 mg, 92%).

mp: 179-182 °C.

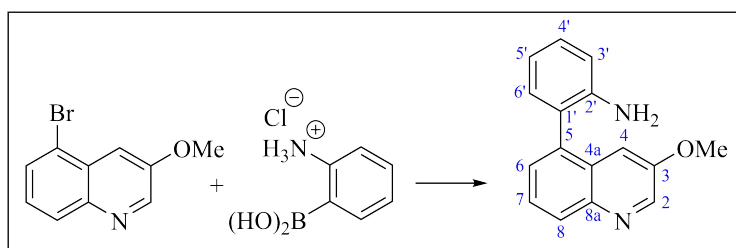
IR (ATR): ν_{\max} 3432, 3355, 3219, 3007, 2920, 2861, 1679 (C=O), 1620 (C=O), 1258, 840 cm^{-1} .

$^1\text{H NMR}$ (400 MHz, CDCl_3): δ 9.10 (d, $J = 2.1$ Hz, 1H, H-2), 8.43 (d, $J = 1.6$ Hz, 1H, H-5), 8.34 (d, $J = 1.7$ Hz, 1H H-4), 8.25 (dd, $J = 8.8$ Hz, 1.8 Hz, 1H, H-7), 8.16 (d, $J = 8.7$ Hz, 1H, H-8), 7.11 (d, $J = 7.7$ Hz, 1H, H-3'), 6.75-6.73 (m, 1H, H-4'), 6.68 (s, 1H, H-6'), 3.76 (bs, 2H, NH_2), 2.74 (s, 3H, $\text{CH}_3\text{-CO}$), 2.34 (s, 3H, CH_3).

$^{13}\text{C NMR}$ (100 MHz, CDCl_3): δ 197.5 (C=O), 154.1 (C-2), 148.9 (C-8a), 143.9 (C-1'), 140.0 (C-5'), 136.6 (C-4), 135.3 (C-6), 133.7 (C-3), 130.8 (C-3'), 130.0 (C-8), 129.9 (C-5), 127.7 (C-7), 127.4 (C-4a), 120.6 (C-2'), 120.4 (C-4'), 116.9 (C-6'), 26.9 ($\text{CH}_3\text{-CO}$), 21.4 (CH_3).

HRMS (ESI): calcd. for $\text{C}_{18}\text{H}_{16}\text{N}_2\text{O}$ [$\text{M} + \text{H}^+$] 277.1335, found 277.1345.

2-(3-Methoxyquinolin-5-yl)aniline (**72a**)



Method 1: Following the general procedure, the title compound was prepared from 5-bromo-3-methoxyquinoline (**81**) (330.0 mg, 1.39 mmol), 2-aminophenylboronic acid hydrochloride (**68**) (724.7 mg, 4.18 mmol), an aq. solution of K_2CO_3 (960.5 mg, 6.95 mmol in 2 mL H_2O) and $\text{PdCl}_2(\text{dppf})$ (50.8 mg, 0.069 mmol) in EtOH (10 mL). After a reaction time of 22 hours, the crude was purified by silica gel column chromatography (pet. ether/EtOAc, 1:1 v/v) followed by alumina gel column chromatography (CH_2Cl_2 /pet. ether, 8:2 v/v) and concentration of the relevant fractions [$R_f = 0.33$ (CH_2Cl_2 /pet. ether, 8:2 v/v)] gave the target compound **72a** as an orange solid (304.7 mg, 88%).

Method 2: Following the general procedure, the title compound was prepared from 5-bromo-3-methoxyquinoline (**81**) (50.0 mg, 0.21 mmol), 2-aminophenylboronic acid hydrochloride (**68**) (54.9 mg, 0.32 mmol), an aq. solution of Cs_2CO_3 (239.5 mg, 0.73 mmol in 0.4 mL H_2O) and $\text{Pd}(\text{PPh}_3)_4$ (12.1 mg, 0.010 mmol) in DME (2 mL). After a reaction time of 23.5 hours, the crude was purified by silica gel column chromatography (pet. ether/EtOAc, 1:1 v/v)

followed by alumina gel column chromatography ($\text{CH}_2\text{Cl}_2/\text{pet. ether}$, 8:2 v/v) and concentration of the relevant fractions [$R_f = 0.33$ ($\text{CH}_2\text{Cl}_2/\text{pet. ether}$, 8:2 v/v)] gave the target compound **72a** as a yellow oily solid (17.8 mg, 34%) along with recovered starting material **81** as white crystals (9.3 mg, 18%).

mp: 142-144 °C.

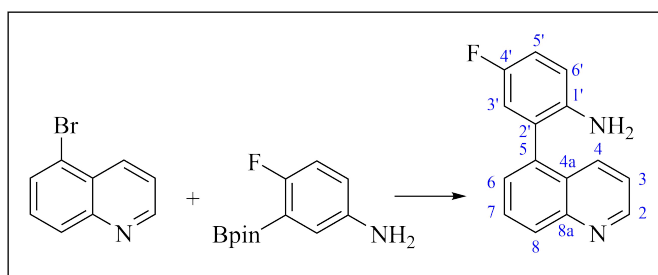
IR (ATR): ν_{max} 3059, 3018, 2957, 2933, 2857, 1604, 1249, 819 cm^{-1} .

^1H NMR (400 MHz, CDCl_3): δ 8.68 (d, $J = 2.9$ Hz, 1H, H-2), 8.11-8.08 (m, 1H, H-8), 7.62 (dd, $J = 8.4$ Hz, 7.1 Hz, 1H, H-7), 7.49 (dd, $J = 7.0$ Hz, 1.2 Hz, 1H, H-6), 7.27 (ddd, $J = 7.9$ Hz, 7.5 Hz, 1.6 Hz, 1H, H-4'), 7.21 (d, $J = 2.8$ Hz, 1H, H-4), 7.14 (dd, $J = 7.5$ Hz, 1.5 Hz, 1H, H-6'), 6.88 (dt, $J = 7.4$ Hz, 1.1 Hz, 1H, H-5'), 6.84 (dd, $J = 8.0$ Hz, 0.8 Hz, 1H, H-3'), 3.79 (s, 3H, OCH_3), 3.58 (bs, 2H, NH_2).

^{13}C NMR (100 MHz, CDCl_3): δ 153.4 (C-3), 144.3 (C-2'), 144.0 (C-2), 143.6 (C-8a), 136.2 (C-5), 131.3 (C-6'), 129.3 (C-4'), 128.9 (C-6), 128.8 (C-8), 127.6 (C-4a), 126.8 (C-7), 124.6 (C-1'), 118.5 (C-5'), 115.6 (C-3'), 111.4 (C-4), 55.6 (OCH_3).

HRMS (ESI): calcd. for $\text{C}_{16}\text{H}_{14}\text{N}_2\text{O}$ [$\text{M} + \text{H}^+$] 251.1179, found 251.1188.

4-Fluoro-2-(quinolin-5-yl)aniline (**72b**)



Method 1: Following the general procedure, the title compound was prepared from 5-bromoquinoline (**67d**) (50.0 mg, 0.24 mmol), 4-fluoro-2-(4,4,5,5-tetramethyl-1,3,2-dioxaborolan-2-yl)aniline (**83a**) (85.5 mg, 0.36 mmol), an aq. solution of K_2CO_3 (116.1 mg, 0.85 mmol in 1 mL H_2O) and $\text{PdCl}_2(\text{dppf})$ (8.8 mg, 0.012 mmol) in EtOH (5 mL). After a reaction time of 18 hours, the crude was purified by silica gel column chromatography (pet. ether/EtOAc, 1:1 \rightarrow 3:7 v/v) and concentration of the relevant fractions [$R_f = 0.10$ (pet. ether/EtOAc, 1:1 v/v)] gave the target compound **72b** as a light brown solid (18.5 mg, 32%).

Method 2: Following the general procedure, the title compound was prepared from 5-bromoquinoline (**67d**) (512.3 mg, 2.46 mmol), 4-fluoro-2-(4,4,5,5-tetramethyl-1,3,2-dioxaborolan-2-yl)aniline (**83a**) (875.7 mg, 3.69 mmol), an aq. solution of Cs_2CO_3 (2.80 g, 8.61 mmol in 5 mL H_2O) and $\text{Pd}(\text{PPh}_3)_4$ (142.1 mg, 0.12 mmol) in DME (25 mL). After a reaction time of 17 hours, the crude was purified by silica gel column chromatography (pet. ether/EtOAc, 1:1 v/v) and concentration of the relevant fractions [$R_f = 0.10$ (pet. ether/EtOAc, 1:1 v/v)] gave the

target compound **72b** as an orange solid (419.5 mg, 72%).

mp: 196-197 °C.

IR (ATR): ν_{\max} 3041, 2921, 2852, 1635, 1490, 1192, 900, 792 cm^{-1} .

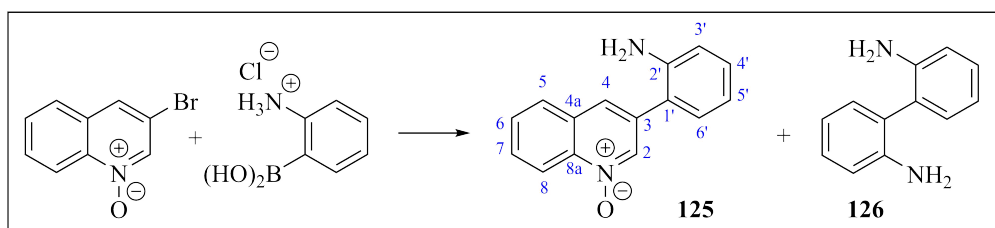
^1H NMR (400 MHz, CD_2Cl_2): δ 8.90 (dd, $J = 4.1$ Hz, 1.7 Hz, 1H, H-2), 8.14-8.12 (m, 1H, H-8), 7.96 (ddd, $J = 8.5$ Hz, 1.6 Hz, 0.8 Hz, 1H, H-4), 7.79 (dd, $J = 8.5$ Hz, 7.1 Hz, 1H, H-7), 7.51 (dd, $J = 7.0$ Hz, 1.1 Hz, 1H, H-6), 7.36 (dd, $J = 8.5$ Hz, 4.2 Hz, 1H, H-3), 7.00 (td, $J = 8.6$ Hz, 3.0 Hz, 1H, H-5'), 6.88 (dd, $J = 9.0$ Hz, 3.0 Hz, 1H, H-3'), 6.79 (dd, $J = 8.8$ Hz, 4.8 Hz, 1H, H-6'). 3.42 (bs, 2H, NH_2).

^{13}C NMR (100 MHz, CD_2Cl_2): δ 156.4 (d, $J_{\text{CF}} = 235.8$ Hz, C-4'), 151.0 (C-2), 149.1 (C-8a), 141.4 (C-1'), 136.8 (C-5), 134.5 (C-4), 130.1 (C-8), 129.6 (C-7), 128.3 (C-6), 127.0 (C-4a), 125.7 (d, $J_{\text{CF}} = 7.2$ Hz, C-2'), 121.8 (C-3), 117.7 (d, $J_{\text{CF}} = 22.1$ Hz, C-6'), 116.6 (d, $J_{\text{CF}} = 8.0$ Hz, C-3'), 115.9 (d, $J_{\text{CF}} = 22.1$ Hz, C-5').

^{19}F NMR (376 MHz, CD_2Cl_2): δ -128.0.

HRMS (ESI): calcd. for $\text{C}_{15}\text{H}_{11}\text{FN}_2$ [$\text{M} + \text{H}^+$] 239.0979, found 239.0988.

3-(2-Aminophenyl)quinoline *N*-oxide (**125**)



To a solution of 3-bromoquinoline *N*-oxide (**124**) (100.0 mg, 0.45 mmol) in THF (5 mL) under an argon atmosphere was added 2-aminophenylboronic acid hydrochloride (**68**) (171.1 mg, 0.99 mmol), an aq. solution of K_2PO_4 (401.2 mg, 1.89 mmol in 1 mL H_2O) and $\text{PdCl}_2(\text{dppf})$ (16.5 mg, 0.022 mmol). The resulting reaction mixture was stirred at reflux for 43 hours and allowed to cool to rt. The volatiles were then removed under reduced pressure and the concentrate was evaporated onto celite. Purification by silica gel column chromatography (EtOAc) and concentration of the relevant fractions [$R_f = 0.17$ (EtOAc)] gave homocoupled product **126** as yellow needles (38.9 mg, 37%) along with the target compound **125** as yellow crystals (93.1 mg, 88%).

Characterization of compound **125**:

mp: 114-116 °C.

IR (ATR): ν_{\max} 3324, 3206, 3049, 2961, 1361, 1216, 730 cm^{-1} .

^1H NMR (400 MHz, CDCl_3): δ 8.75 (d, $J = 8.8$ Hz, 1H, H-8), 8.68 (d, $J = 1.4$ Hz, 1H, H-2), 7.88-7.87 (m, 1H, H-5), 7.84 (s, 1H, H-4) 7.79-7.74 (m, 1H, H-7), 7.69-7.65 (m, 1H,

H-6), 7.26-7.22 (m, 1H, H-6'), 7.18 (dd, $J = 7.6$ Hz, 1.5 Hz, 1H, H-4'), 6.88 (td, $J = 7.5$ Hz, 1.1 Hz, 1H, H-5'), 6.82 (dd, $J = 8.0$ Hz, 0.8 Hz, 1H, H-3'), 3.83 (bs, 2H, NH₂).

¹³C NMR (100 MHz, CDCl₃): δ 144.0 (C-2'), 140.6 (C-8a), 136.6 (C-2), 133.5 (C-3), 130.6 (C-4'), 130.5 (C-4a), 130.4 (C-7), 130.2 (C-6'), 129.2 (C-6), 128.3 (C-5), 125.8 (C-4), 121.9 (C-1'), 119.9 (C-8), 119.3 (C-5'), 116.4 (C-3').

HRMS (ESI): calcd. for C₁₅H₁₂N₂O [M + H⁺] 237.1022, found 237.1031.

Characterization of compound **126**:

¹H NMR (400 MHz, DMSO-*d*₆): δ 7.07 (ddd, $J = 8.8$ Hz, 7.3 Hz, 1.6 Hz, 2H), 6.94 (dd, $J = 7.5$ Hz, 1.5 Hz, 2H), 6.78 (dd, $J = 8.0$ Hz, 1.0 Hz, 2H), 6.65 (td, $J = 7.3$ Hz, 1.1 Hz, 2H), 4.57 (bs, 4H).

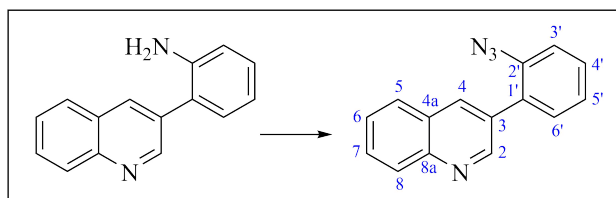
In accordance with previously reported data^[276,277] and is readily available commercially.

7.2.4 Diazotization-Azidation

General procedure^[278]

Biaryl (1 equiv.) was dissolved in an appropriate amount of aq. HCl (37%) and the mixture was cooled to 0 °C using an ice bath. Then, ice-cooled aq. NaNO₂ (0.4 M) was added dropwise and the resulting mixture was stirred at 0 °C for 1.5 hours. An ice-cooled aq. solution of NaN₃/NaOAc (2.1 equiv.:14 equiv. in an appropriate amount of H₂O) was added dropwise and the mixture stirred for 1 hour while keeping the temperature at 0 °C. The reaction mixture was quenched by addition of appropriate amounts of sat. aq. K₂CO₃ and subsequently extracted with CH₂Cl₂ (3 x 20 mL). The combined organic phases were washed (1 x 20 mL H₂O, 1 x 20 mL brine), dried (MgSO₄), filtered and concentrated *in vacuo*. The concentrate was then evaporated onto celite and purified by column chromatography using the chromatographic technique and eluent as indicated in the specific description to give target compounds.

3-(2-Azidophenyl)quinoline (131)



Following the general procedure, the title compound was prepared from 2-(quinolin-3-yl)aniline (**69**) (626.5 mg, 2.85 mmol), HCl (10 mL), NaNO₂ (0.4 M), NaN₃ (389.0 mg, 5.98 mmol) and NaOAc (3.27 g, 39.90 mmol in 15 mL H₂O). The crude was purified by silica gel column chromatography (pet. ether/EtOAc 7:3 → 1:1 v/v) and concentration of the relevant fractions

[$R_f = 0.68$ (pet. ether/EtOAc, 1:1 v/v)] gave the target compound **131** as a yellow solid (462.3 mg, 66%).

mp: 105-107 °C.

IR (ATR): ν_{\max} 3049, 3021, 2923, 2118 (N₃), 2075 (N₃), 1275, 730 cm⁻¹.

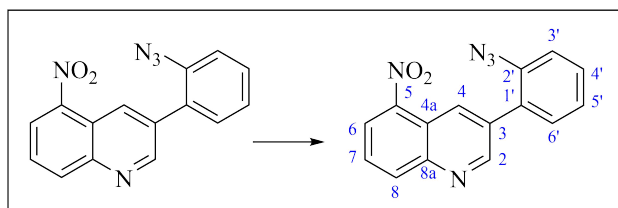
¹H NMR (400 MHz, CDCl₃): δ 9.03 (d, $J = 2.0$ Hz, 1H, H-2), 8.22 (d, $J = 2.0$ Hz, 1H, H-4), 8.16-8.14 (m, 1H, H-8), 7.86 (dd, $J = 8.1$ Hz, 1.2 Hz, 1H, H-5), 7.76-7.72 (m, 1H, H-7), 7.60-7.56 (m, 1H, H-6), 7.50-7.44 (m, 2H, H-4' and H-6'), 7.33-7.31 (m, 1H, H-5'), 7.28 (td, $J = 7.4$ Hz, 1.1 Hz, 1H, H-3').

¹³C NMR (100 MHz, CDCl₃): δ 151.5 (C-2), 147.3 (C-8a), 137.8 (C-2'), 135.9 (C-4), 131.5 (C-6'), 131.3 (C-3), 130.2 (C-4a), 129.7 (2C, C-7 and C-4'), 129.4 (C-8), 128.1 (C-5), 127.7 (C-1'), 127.0 (C-6), 125.4 (C-3'), 119.0 (C-5').

UV (MeOH): λ_{\max} 308 nm.

In accordance with previously reported data.^[150]

3-(2-Azidophenyl)-5-nitroquinoline (131a)



Following the general procedure, the title compound was prepared from 2-(5-nitroquinolin-3-yl)aniline (**69a**) (92.4 mg, 0.35 mmol), HCl (4 mL), NaNO₂ (0.4 M), NaN₃ (47.8 mg, 0.73 mmol) and NaOAc (401.9 mg, 4.90 mmol in 5 mL H₂O). Workup was carried out according to the general procedure to give the target compound **131a** as an orange solid (100.4 mg, 98%).

mp: 199-200 °C.

IR (ATR): ν_{\max} 2923, 2853, 2127 (N₃), 2086 (N₃), 1517, 1327, 743 cm⁻¹.

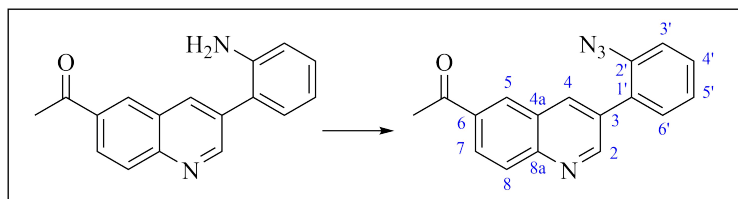
¹H NMR (400 MHz, CDCl₃): δ 9.16 (d, $J = 2.1$ Hz, 1H, H-2), 9.04 (dd, $J = 2.1$ Hz, 0.8 Hz, 1H, H-4), 8.47-8.45 (m, 1H, H-8), 8.42 (dd, $J = 7.8$ Hz, 1.2 Hz, 1H, H-6), 7.82 (dd, $J = 8.3$ Hz, 7.8 Hz, 1H, H-7), 7.53 (ddd, $J = 8.1$ Hz, 7.4 Hz, 1.6 Hz, 1H, H-5'), 7.48 (dd, $J = 7.7$ Hz, 1.4 Hz, 1H, H-6'), 7.36-7.30 (m, 2H, H-3' and H-4').

¹³C NMR (100 MHz, CDCl₃): δ 152.9 (C-2), 147.2 (C-8a), 145.8 (C-5), 138.0 (C-1'), 136.5 (C-8), 134.5 (C-3), 131.6 (C-5'), 130.5 (C-6'), 129.3 (C-2'), 127.6 (C-7), 125.6 (C-6), 125.1 (C-4'), 120.9 (C-4a), 119.1 (C-3'). The presence of C-5' was confirmed by ¹H-¹³C HSQC and ¹H-¹³C HMBC.

UV (MeOH): λ_{\max} 333 nm.

HRMS (ESI): sample sent to UiB for analysis.

3-(2-Azidophenyl)-6-acetylquinoline (131b)



Following the general procedure, the title compound was prepared from 2-(6-acetylquinolin-3-yl)aniline (**69b**) (100.0 mg, 0.38 mmol), HCl (5 mL), NaNO₂ (0.4 M), NaN₃ (52.1 mg, 0.80 mmol) and NaOAc (436.4 mg, 5.32 mmol in 10 mL H₂O). Workup was carried out according to the general procedure to give the target compound **131b** as a pale orange solid (109.9 mg, quant.).

mp: 159-162 °C.

IR (ATR): ν_{\max} 3007, 2959, 2919, 2850, 2126 (N₃), 2082 (N₃), 1671 (C=O), 742 cm⁻¹.

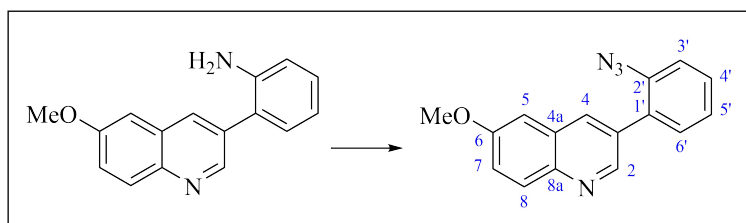
¹H NMR (400 MHz, CDCl₃): δ 9.10 (s, 1H, H-2), 8.48 (d, J = 1.4 Hz, 1H, H-5), 8.33 (d, J = 1.5 Hz, 1H, H-4), 8.27 (dd, J = 8.8 Hz, 1.7 Hz, 1H, H-7), 8.18 (d, J = 8.8 Hz, 1H, H-8), 7.52-7.47 (m, 1H, H-6'), 7.45 (dd, J = 7.6 Hz, 1.2 Hz, 1H, H-5'), 7.34-7.27 (m, 2H, H-3' and H-4'), 2.74 (s, 3H, CH₃).

¹³C NMR (100 MHz, CDCl₃): δ 197.4 (C=O), 153.7 (C-2), 149.1 (C-8a), 137.9 (C-1'), 137.3 (C-4), 135.3 (C-6), 132.2 (C-3), 131.4 (C-5'), 130.2 (C-5), 129.9 (C-6'), 129.5 (C-2'), 127.9 (C-7), 126.9 (C-4a), 125.5 (C-3'), 119.1 (C-4'), 26.9 (CH₃).

UV (MeOH): λ_{\max} 287 nm.

HRMS (ESI): sample sent to UiB for analysis.

3-(2-Azidophenyl)-6-methoxyquinoline (131c)



Following the general procedure, the title compound was prepared from 2-(6-methoxyquinolin-3-yl)aniline (**69c**) (200.0 mg, 0.80 mmol), HCl (10 mL), NaNO₂ (0.4 M), NaN₃ (109.1 mg, 1.68 mmol) and NaOAc (918.7 mg, 11.20 mmol in 10 mL H₂O). Workup was carried out according to the general procedure to give the target compound **131c** as a red wax (220.7 mg, quant.).

IR (ATR): ν_{\max} 3059, 3003, 2929, 2125 (N₃), 2097 (N₃), 1623, 1495, 1294, 1216 cm⁻¹.

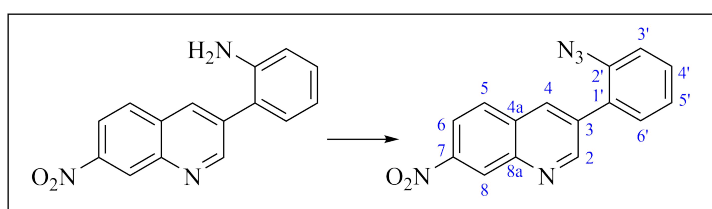
¹H NMR (400 MHz, CDCl₃): δ 8.56 (bs, 1H, H-2), 8.12 (d, J = 1.9 Hz, 1H, H-4), 8.03 (d, J = 9.2 Hz, 1H, H-8), 7.50-7.43 (m, 2H, H-4' and H-5'), 7.39 (dd, J = 9.2 Hz, 2.8 Hz, 1H, H-7), 7.32 (dd, J = 8.0 Hz, 0.6 Hz, 1H, H-3'), 7.30-7.26 (m, 1H, H-6'), 7.12 (d, J = 2.7 Hz, 1H, H-5), 3.95 (s, 3H, OCH₃).

¹³C NMR (100 MHz, CDCl₃): δ 158.2 (C-6), 148.9 (C-2), 143.5 (C-8a), 137.9 (C-1'), 134.9 (C-4), 131.5 (C-4'), 130.8 (C-8), 130.4 (C-2'), 129.7 (C-5'), 128.8 (C-4a), 125.4 (C-6'), 122.6 (C-7), 119.0 (C-3'), 105.5 (C-5), 55.7 (OCH₃).

UV (MeOH): λ_{\max} 241 nm.

HRMS (ESI): calcd. for C₁₆H₁₂N₄O [M + H⁺] 277.1084, found 277.1084.

3-(2-Azidophenyl)-7-nitroquinoline (131d)



Following the general procedure, the title compound was prepared from 2-(7-nitroquinolin-3-yl)aniline (**69d**) (150.0 mg, 0.56 mmol), HCl (5 mL), NaNO₂ (0.4 M), NaN₃ (77.2 mg, 1.19 mmol) and NaOAc (643.1 mg, 7.84 mmol in 10 mL H₂O). Workup was carried out according to the general procedure to give the target compound **131d** as a light yellow solid (165.2 mg, quant.).

mp: 117-119 °C.

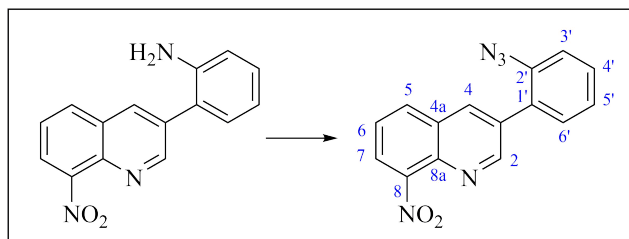
IR (ATR): ν_{\max} 3111, 3022, 2924, 2856, 2127 (N₃), 2083 (N₃), 1526, 1345, 1287, 911, 743 cm⁻¹.

¹H NMR (400 MHz, CDCl₃): δ 9.19 (d, J = 1.6 Hz, 1H, H-2), 9.05 (d, J = 1.5 Hz, 1H, H-8), 8.37 (dd, J = 8.9 Hz, 2.0 Hz, 1H, H-5), 8.32 (d, J = 1.5 Hz, 1H, H-4), 8.02 (d, J = 8.9 Hz, 1H, H-6), 7.56-7.52 (m, 1H, H-6'), 7.49-7.47 (m, 1H, H-5'), 7.37-7.31 (m, 2H, H-3' and H-4').

¹³C NMR (100 MHz, CDCl₃): δ 154.0 (C-2), 148.2 (C-7), 146.1 (C-8a), 138.0 (C-1'), 135.6 (C-4), 134.4 (C-3), 131.5 (C-5'), 131.0 (C-4a), 130.6 (C-6'), 129.7 (C-6), 129.0 (C-2'), 125.8 (C-3'), 125.6 (C-8), 120.6 (C-5), 119.2 (C-4').

UV (MeOH): λ_{\max} 329 nm.

HRMS (ESI): sample sent to UiB for analysis.

3-(2-Azidophenyl)-8-nitroquinoline (131e)

Following the general procedure, the title compound was prepared from 2-(8-nitroquinolin-3-yl)aniline (**69e**) (95.0 mg, 0.36 mmol), HCl (5 mL), NaNO₂ (0.4 M), NaN₃ (48.9 mg, 0.75 mmol) and NaOAc (413.4 mg, 5.04 mmol in 10 mL H₂O). Workup was carried out according to the general procedure to give the target compound **131e** as an orange solid (75.5 mg, 72%).

mp: 168-170 °C.

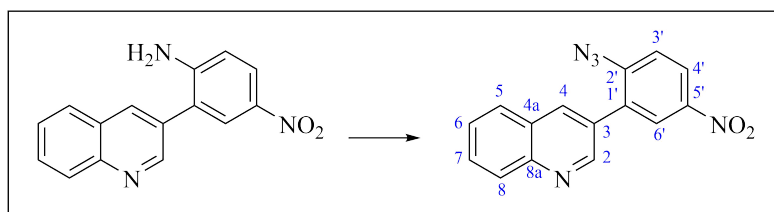
IR (ATR): ν_{\max} 3032, 2920, 2852, 2125 (N₃), 2083 (N₃), 1523, 1349, 766, 745 cm⁻¹.

¹H NMR (400 MHz, CDCl₃): δ 9.18 (d, J = 2.1 Hz, 1H, H-2), 8.32 (d, J = 2.1 Hz, 1H, H-4), 8.10-8.06 (m, 2H, H-5 and H-7), 7.67-7.63 (m, 1H, H-6), 7.52 (ddd, J = 8.0 Hz, 7.5 Hz, 1.5 Hz, 1H, H-6'), 7.45 (dd, J = 7.6 Hz, 1.4 Hz, 1H, H-5'), 7.35 (dd, J = 8.0 Hz, 0.8 Hz, 1H, H-4'), 7.31 (td, J = 7.5 Hz, 1.0 Hz, 1H, H-3').

¹³C NMR (100 MHz, CDCl₃): δ 153.9 (C-2), 148.3 (C-8), 138.5 (C-8a), 138.0 (C-1'), 135.8 (C-4), 133.2 (C-3), 132.4 (C-5), 131.4 (C-5'), 130.4 (C-6'), 128.9 (C-2'), 128.7 (C-4a), 125.8 (C-6), 125.6 (C-3'), 124.0 (C-7), 119.1 (C-4').

UV (MeOH): λ_{\max} 285 nm.

HRMS (ESI): calcd. for C₁₅H₉N₅O₂ [M + H⁺] 292.0829, found 292.0829.

3-(2-Azido-5-nitrophenyl)quinoline (131g)

Following the general procedure, the title compound was prepared from 3-(2-azido-5-nitrophenyl)quinoline (**69g**) (100.0 mg, 0.38 mmol), HCl (5 mL), NaNO₂ (0.4 M), NaN₃ (51.5 mg, 0.79 mmol) and NaOAc (436.4 mg, 5.32 mmol in 10 mL H₂O). Workup was carried out according to the general procedure to give the target compound **131g** as an off-white solid (68.7 mg 62%).

mp: 178-179 °C.

IR (ATR): ν_{\max} 3070, 3026, 2920, 2851, 2118 (N₃), 1519, 1348, 1274, 740 cm⁻¹.

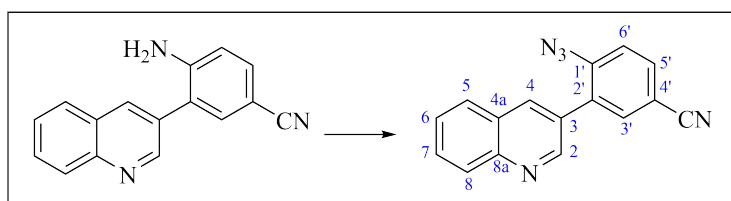
¹H NMR (400 MHz, CDCl₃): δ 9.04 (bs, 1H, H-2), 8.37-8.33 (m, 2H, H-4' and H-6'), 8.27 (d, J = 1.5 Hz, 1H, H-4), 8.18 (d, J = 8.4 Hz, 1H, H-8), 7.91 (d, J = 8.1 Hz, 1H, H-5), 7.81-7.78 (m, 1H, H-7), 7.65-7.61 (m, 1H, H-6), 7.44 (dt, J = 9.8 Hz, 1.6 Hz, 1H, H-3').

¹³C NMR (100 MHz, CDCl₃): δ 150.6 (C-2), 147.7 (C-8a), 144.9 (C-1'), 144.6 (C-5'), 136.4 (C-4), 131.1 (C-2'), 130.5 (C-7), 129.5 (C-8), 128.3 (C-5), 127.5 (C-6), 127.3 (C-4a), 126.3 (C-4'), 125.6 (C-3), 124.9 (C-6'), 119.4 (C-3').

UV (MeOH): λ_{\max} 304 nm.

HRMS (ESI): calcd. for C₁₅H₉N₅O₂ [M + H⁺] 292.0829, found 292.0829.

4-Azido-3-(quinolin-3-yl)benzonitrile (**131h**)



Following the general procedure, the title compound was prepared from 4-amino-3-(quinolin-3-yl)benzonitrile (**69h**) (200.0 mg, 0.82 mmol), HCl (10 mL), NaNO₂ (0.4 M), NaN₃ (111.4 mg, 1.71 mmol) and NaOAc (941.7 mg, 11.48 mmol in 15 mL H₂O). Workup was carried out according to the general procedure to give the target compound **131h** as a light pink solid (218.0 mg, 98%).

mp: 199 °C (decomp.).

IR (ATR): ν_{\max} 3060, 2915, 2849, 2121 (CN/N₃), 1485, 1278, 745 cm⁻¹.

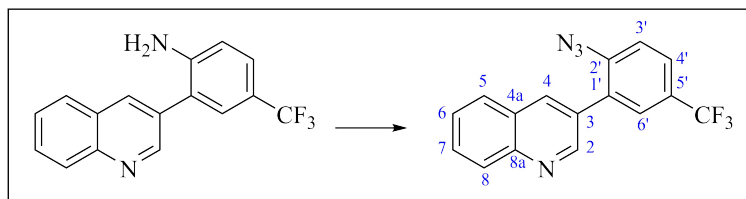
¹H NMR (400 MHz, DMSO-*d*₆): δ 9.05 (d, J = 2.2 Hz, 1H, H-2), 8.53 (d, J = 2.0 Hz, 1H, H-4), 8.09 (d, J = 1.9 Hz, 1H, H-3'), 8.07 (d, J = 8.8 Hz, 1H, H-8), 8.04 (dd, J = 8.2 Hz, 0.9 Hz, 1H, H-5), 8.00 (dd, J = 8.4 Hz, 2.0 Hz, 1H, H-7), 7.85-7.81 (m, 1H, H-6), 7.70-7.65 (m, 2H, H-5' and H-6').

¹³C NMR (100 MHz, DMSO-*d*₆): δ 150.8 (C-2), 146.7 (C-8a), 142.4 (C-2'), 136.2 (C-4), 135.1 (C-3'), 133.5 (C-7), 130.2 (C-6), 129.1 (C-4a), 128.6 (C-5), 128.4 (C-8), 127.1 (C-5'), 120.8 (C-6'), 118.3 (CN), 107.6 (C-4'). The presence of C-3 and C-1' were confirmed by ¹H-¹³C HSCQ and ¹H-¹³C HMBC.

UV (MeOH): λ_{\max} 294 nm.

HRMS (ESI): sample sent to UiB for analysis.

3-(2-Azido-5-(trifluoromethyl)phenyl)quinoline (131i)



Following the general procedure, the title compound was prepared from 2-(quinolin-3-yl)-4-(trifluoromethyl)aniline (**69i**) (70.0 mg, 0.24 mmol), HCl (5 mL), NaNO₂ (0.4 M), NaN₃ (32.7 mg, 0.50 mmol) and NaOAc (275.6 mg, 3.36 mmol in 5 mL H₂O). Workup was carried out according to the general procedure to give the target compound **131i** as a red oil (48.2 mg, 64%).

IR (ATR): ν_{\max} 2924, 2852, 2107 (N₃), 1323, 1271, 1113, 730 cm⁻¹.

¹H NMR (400 MHz, DMSO-*d*₆): δ 9.06 (bs, 1H, H-2), 8.53 (d, J = 1.4 Hz, 1H, H-4), 8.08-8.05 (m, 2H, H-6 and H-8), 7.91-7.88 (m, 2H, H-4' and H-6'), 7.84-7.80 (m, 1H, H-7), 7.70 (d, J = 8.9 Hz, 1H, H-5), 7.65 (d, J = 7.6 Hz, 1H, H-3').

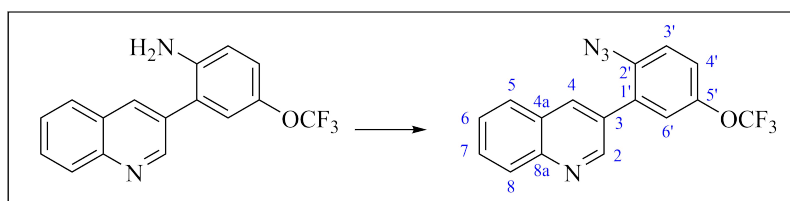
¹³C NMR (100 MHz, DMSO-*d*₆): δ 150.9 (C-2), 146.7 (C-8a), 141.5 (C-1'), 136.2 (C-4), 130.1 (C-7), 130.0 (C-4a), 128.6 (C-8), 128.4 (C-6), 128.1 (q, J_{CF} = 3.5 Hz, C-4'), 127.0 (C-3'), 126.6 (q, J_{CF} = 3.6 Hz, C-6'), 125.6 (q, J_{CF} = 32.5 Hz, C-5'), 125.3 (C-3), 122.6 (C-2'), 120.5 (C-5). CF₃ was obscured or overlapping.

¹⁹F NMR (376 MHz, DMSO-*d*₆): δ -60.3.

UV (MeOH): λ_{\max} 309 nm.

HRMS (ESI): calcd. for C₁₆H₉F₃N₄ [M + H⁺] 315.0852, found 315.0851.

3-(2-Azido-5-(trifluoromethoxy)phenyl)quinoline (131j)



Following the general procedure, the title compound was prepared from 2-(quinolin-3-yl)-4-(trifluoromethoxy)aniline (**69j**) (150.0 mg, 0.49 mmol), HCl (5 mL), NaNO₂ (0.4 M), NaN₃ (67.3 mg, 1.03 mmol) and NaOAc (562.7 mg, 6.86 mmol in 10 mL H₂O). Workup was carried out according to the general procedure to give the target compound **131j** as a dark orange solid (153.3 mg, 95%).

mp: 54-56 °C.

IR (ATR): ν_{\max} 3063, 2923, 2853, 2114 (N₃), 2085 (N₃), 1488, 1246, 1210, 1159, 786, 753 cm⁻¹.

¹H NMR (400 MHz, CDCl₃): δ 9.01 (s, 1H, H-2), 8.22 (d, J = 2.1 Hz, 1H, H-4), 8.16 (d, J = 8.5 Hz, 1H, H-8), 7.88 (dd, J = 8.1 Hz, 0.9 Hz, 1H, H-5), 7.79-7.75 (m, 1H, H-7), 7.62-7.58 (m, 1H, H-6), 7.36-7.31 (m, 3H, H-3', H-4' and H-6').

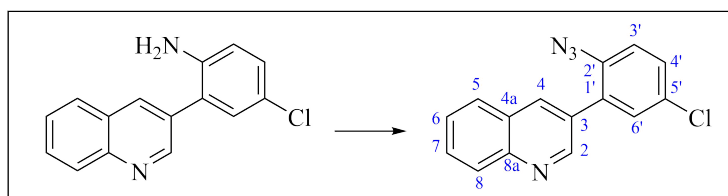
¹³C NMR (100 MHz, CDCl₃): δ 150.9 (C-2), 147.6 (C-8a), 146.2 (q, J_{CF} = 2.0 Hz, C-5'), 136.7 (C-1'), 136.2 (C-4), 131.7 (C-3), 130.2 (C-7), 129.9 (C-4a), 129.5 (C-8), 128.2 (C-5), 127.6 (C-2'), 127.3 (C-6), 124.1 (C-3'), 122.3 (C-4'), 120.6 (q, J_{CF} = 257.7 Hz, OCF₃), 120.2 (C-6').

¹⁹F NMR (376 MHz, CDCl₃): δ -57.9.

UV (MeOH): λ_{\max} 301 nm.

HRMS (ESI): calcd. for C₁₆H₉F₃N₄O [M + H⁺] 331.0801, found 331.0801.

3-(2-Azido-5-chlorophenyl)quinoline (131k)



Following the general procedure, the title compound was prepared from 4-chloro-2-(quinolin-3-yl)aniline (**69k**) (200.0 mg, 0.79 mmol), HCl (10 mL), NaNO₂ (0.4 M), NaN₃ (107.8 mg, 1.66 mmol) and NaOAc (907.2 mg, 11.06 mmol in 10 mL H₂O). Workup was carried out according to the general procedure to give the target compound **131k** as a bright orange crystalline solid (186.3 mg, 84%).

mp: 138-139 °C.

IR (ATR): ν_{\max} 3078, 2921, 2852, 2122 (N₃), 2092 (N₃), 1482, 1283, 742 cm⁻¹.

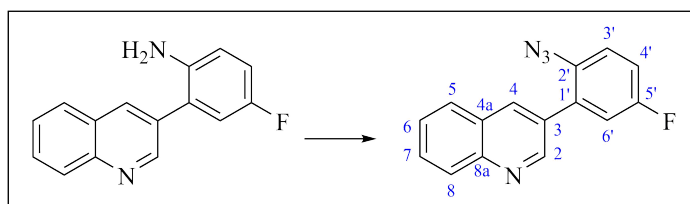
¹H NMR (400 MHz, CDCl₃): δ 8.99 (bs, 1H, H-2), 8.19 (d, J = 1.9 Hz, 1H, H-4), 8.15 (d, J = 8.4 Hz, 1H, H-8), 7.86 (dd, J = 8.2 Hz, 0.9 Hz, 1H, H-5), 7.77-7.73 (m, 1H, H-7), 7.61-7.57 (m, 1H, H-6), 7.44-7.41 (m, 2H, H-4' and H-6'), 7.23 (dd, J = 6.4 Hz, 2.8 Hz, 1H, H-3').

¹³C NMR (100 MHz, CDCl₃): δ 150.9 (C-2), 147.5 (C-8a), 136.5 (C-1'), 136.1 (C-4), 131.7 (C-3), 131.3 (C-6'), 130.6 (C-5'), 130.1 (C-7), 129.6 (C-4'), 129.4 (C-8), 128.2 (C-5), 127.6 (C-4a), 127.2 (C-6), 120.2 (C-3'). C-2' was obscured or overlapping.

UV (MeOH): λ_{\max} 292 nm.

HRMS (ESI): sample sent to UiB for analysis.

3-(2-Azido-5-fluorophenyl)quinoline (131l)



Following the general procedure, the title compound was prepared from 4-fluoro-2-(quinolin-3-yl)aniline (**69l**) (145.0 mg, 0.61 mmol), HCl (5 mL), NaNO₂ (0.4 M), NaN₃ (83.3 mg, 1.28 mmol) and NaOAc (700.5 mg, 8.54 mmol in 10 mL H₂O). Workup was carried out according to the general procedure to give the target compound **131l** as a pale yellow solid (127.6 mg, 79%).

mp: 151-154 °C (decomp.).

IR (ATR): ν_{\max} 3220, 3056, 3019, 2919, 2852, 2112 (N₃), 2067 (N₃), 1487, 1238, 803, 743 cm⁻¹.

¹H NMR (400 MHz, CDCl₃): δ 9.00 (d, $J = 2.2$ Hz, 1H, H-2), 8.22 (d, $J = 2.0$ Hz, 1H, H-4), 8.16-8.14 (m, 1H, H-8), 7.88 (dd, $J = 8.1$ Hz, 1.1 Hz, 1H, H-5), 7.78-7.74 (m, 1H, H-7), 7.62-7.58 (m, 1H, H-6), 7.28-7.27 (m, 1H, H-6'), 7.21-7.17 (m, 2H, H-3' and H-4').

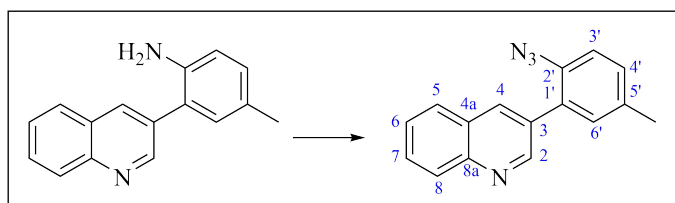
¹³C NMR (100 MHz, CDCl₃): δ 160.0 (d, $J_{\text{CF}} = 245.7$ Hz, C-5'), 151.0 (C-2), 147.5 (C-8a), 136.1 (C-4), 133.7 (d, $J_{\text{CF}} = 3.0$ Hz, C-2'), 131.8 (d, $J_{\text{CF}} = 7.7$ Hz, C-1'), 130.3 (C-3), 130.1 (C-7), 129.5 (C-8), 128.2 (C-5), 127.6 (C-4a), 127.2 (C-6), 120.4 (d, $J_{\text{CF}} = 8.5$ Hz, C-6'), 118.2 (d, $J_{\text{CF}} = 23.3$ Hz, C-4'), 116.5 (d, $J_{\text{CF}} = 23.2$ Hz, C-3').

¹⁹F NMR (376 MHz, CDCl₃): δ -116.9.

UV (MeOH): λ_{\max} 302 nm.

HRMS (ESI): sample sent to UiB for analysis.

3-(2-Azido-5-methylphenyl)quinoline (131m)



Following the general procedure, the title compound was prepared from 4-methyl-2-(quinolin-3-yl)aniline (**69m**) (300.0 mg, 1.28 mmol), HCl (20 mL), NaNO₂ (0.4 M), NaN₃ (174.7 mg, 2.69 mmol) and NaOAc (1.47 g, 17.92 mmol in 20 mL H₂O). Workup was carried out according to the general procedure to give the target compound **131m** as a dark yellow oil (287.8 mg,

89%).

IR (ATR): ν_{\max} 3022, 2921, 2855, 2107 (N₃), 2065 (N₃), 1487, 1290, 748 cm⁻¹.

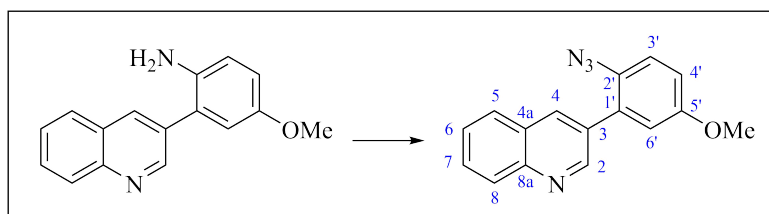
¹H NMR (400 MHz, CDCl₃): δ 9.01 (s, 1H, H-2), 8.21 (d, J = 2.0 Hz, 1H, H-4), 8.14 (d, J = 8.4 Hz, 1H, H-8), 7.86 (dd, J = 8.1 Hz, 0.8 Hz, 1H, H-5), 7.76-7.72 (m, 1H, H-7), 7.60-7.56 (m, 1H, H-6), 7.29-7.25 (m, 2H, H-4' and H-6'), 7.21 (d, J = 8.1 Hz, 1H, H-3'), 2.42 (s, 3H, CH₃).

¹³C NMR (100 MHz, CDCl₃): δ 151.6 (C-2), 147.3 (C-8a), 135.9 (C-4), 135.2 (C-5'), 135.1 (C-1'), 132.1 (C-6'), 131.4 (C-3), 130.4 (C-4'), 130.0 (C-2'), 129.7 (C-7), 129.4 (C-8), 128.1 (C-5), 127.8 (C-4a), 127.0 (C-6), 118.9 (C-3'), 21.0 (CH₃).

UV (MeOH): λ_{\max} 316 nm.

HRMS (ESI): calcd. for C₁₆H₁₂N₄ [M + H⁺] 261.1135, found 261.1136.

3-(2-Azido-5-methoxyphenyl)quinoline (131n)



Following the general procedure, the title compound was prepared from 4-methoxy-2-(quinolin-3-yl)aniline (**69n**) (60.0 mg, 0.24 mmol), HCl (5 mL), NaNO₂ (0.4 M), NaN₃ (32.8 mg, 0.50 mmol) and NaOAc (275.6 mg, 3.36 mmol in 5 mL H₂O). Workup was carried out according to the general procedure to give the target compound **131n** as a brown oil (41.4 mg, 62%).

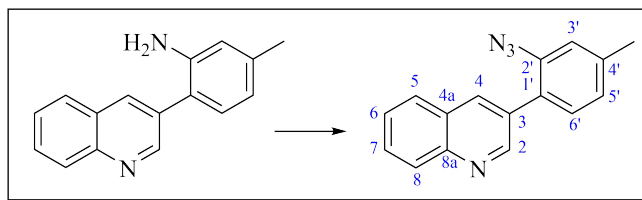
IR (ATR): ν_{\max} 3059, 3002, 2927, 2851, 2110 (N₃), 1498, 1288, 1239, 753 cm⁻¹.

¹H NMR (400 MHz, CDCl₃): δ 9.02 (d, J = 2.0 Hz, 1H, H-2), 8.22 (d, J = 2.1 Hz, 1H, H-4), 8.15-8.13 (m, 1H, H-8), 7.87 (dd, J = 8.3 Hz, 3.0 Hz, 1H, H-5), 7.76-7.72 (m, 1H, H-7), 7.60-7.56 (m, 1H, H-6), 7.23 (d, J = 8.6 Hz, 1H, H-3'), 7.02 (dd, J = 8.7 Hz, 3.0 Hz, 1H, H-4'), 6.98 (d, J = 2.8 Hz, 1H, H-6'), 3.58 (s, 3H, OCH₃).

¹³C NMR (100 MHz, CDCl₃): δ 157.2 (C-5'), 151.4 (C-2), 147.3 (C-8a), 135.9 (C-4), 131.2 (C-3), 131.2 (C-2'), 130.2 (C-1'), 129.8 (C-7), 129.4 (C-8), 128.2 (C-5), 127.7 (C-4a), 120.1 (C-3'), 116.8 (C-6'), 115.2 (C-4'), 55.8 (OCH₃).

UV (MeOH): λ_{\max} 319 nm.

HRMS (ESI): calcd. for C₁₆H₁₂N₄O [M + H⁺] 277.1084, found 277.1083.

3-(2-Azido-4-methylphenyl)quinoline (131o)

Following the general procedure, the title compound was prepared from 5-methyl-2-(quinolin-3-yl)aniline (**69o**) (100.0 mg, 0.43 mmol), HCl (5 mL), NaNO₂ (0.4 M), NaN₃ (58.3 mg, 0.90 mmol) and NaOAc (493.8 mg, 6.02 mmol in 10 mL H₂O). Workup was carried out according to the general procedure to give the target compound **131o** as a dark yellow solid (75.8 mg, 68%).

mp: 87-89 °C.

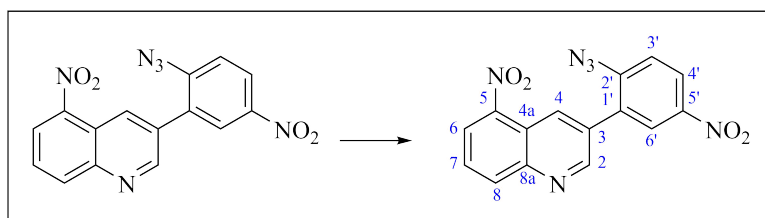
IR (ATR): ν_{\max} 3055, 3022, 2928, 2850, 2104 (N₃), 1297, 815, 741 cm⁻¹.

¹H NMR (400 MHz, CDCl₃): δ 9.01 (bs, 1H, H-2), 8.19 (d, $J = 2.0$ Hz, 1H, H-4), 8.14 (d, $J = 8.4$ Hz, 1H, H-8), 7.85 (dd, $J = 8.2$ Hz, 1.0 Hz, 1H, H-5), 7.74-7.70 (m, 1H, H-7), 7.58-7.54 (m, 1H, H-6), 7.33 (d, $J = 7.7$ Hz, 1H, H-5'), 7.11 (s, 1H, H-3'), 7.09-7.07 (m, 1H, H-6'), 2.45 (s, 3H, CH₃).

¹³C NMR (100 MHz, CDCl₃): δ 151.6 (C-2), 147.1 (C-8a), 140.1 (C-4'), 137.5 (C-1'), 135.8 (C-4), 131.3 (C-2'), 131.3 (C-5'), 129.6 (C-6), 129.3 (C-8), 128.1 (C-5), 127.8 (C-4a), 127.3 (C-3), 126.9 (C-6), 126.3 (C-3'), 119.5 (C-6'), 21.3 (CH₃).

UV (MeOH): λ_{\max} 315 nm.

HRMS (ESI): calcd. for C₁₆H₁₂N₄ [M + H⁺] 261.1135, found 261.1133.

3-(2-Azido-5-nitrophenyl)-5-nitroquinoline (131p)

Following the general procedure, the title compound was prepared from 4-nitro-2-(5-nitroquinolin-3-yl)aniline (**69p**) (61.9 mg, 0.20 mmol), HCl (2 mL), NaNO₂ (0.4 M), NaN₃ (27.3 mg, 0.42 mmol) and NaOAc (229.7 mg, 2.80 mmol in 5 mL H₂O). Workup was carried out according to the general procedure to give the target compound **131p** as a green solid (57.2 mg, 85%).

mp: 153 °C (decomp.).

IR (ATR): ν_{\max} 3102, 3023, 2917, 2853, 2125 (N₃), 2092 (N₃), 1511, 1303, 826, 733 cm⁻¹.

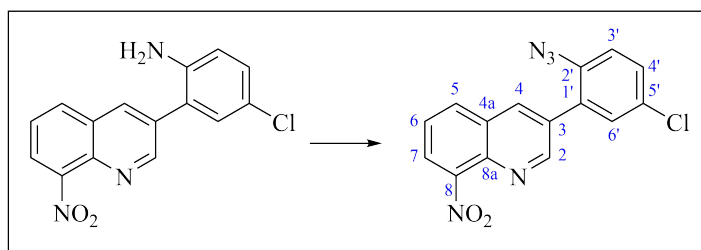
¹H NMR (400 MHz, CDCl₃): δ 9.13-9.11 (m, 2H, H-2 and H-4), 8.51-8.48 (m, 1H, H-6), 8.47 (dd, J = 7.8 Hz, 1.2 Hz, 1H, H-8), 8.40 (dd, J = 8.7 Hz, 2.6 Hz, 1H, H-4'), 8.38 (dd, J = 2.5 Hz, 0.4 Hz, 1H, H-6'), 7.88 (dd, J = 8.4 Hz, 7.8 Hz, 1H, H-7), 7.47 (dd, J = 8.6 Hz, 0.4 Hz, 1H, H-3').

¹³C NMR (100 MHz, CDCl₃): δ 152.0 (C-2), 147.6 (C-8a), 145.7 (C-5), 144.9 (C-5'), 144.8 (C-1'), 136.7 (C-6), 132.4 (C-4), 132.3 (C-2'), 130.1 (C-3), 128.4 (C-7), 127.0 (C-6'), 125.6 (C-4'), 120.7 (C-4a), 119.5 (C-3'). The presence of C-8 was confirmed by ¹H-¹³C HSQC.

UV (MeOH): λ_{\max} 311 nm.

HRMS (ESI): sample decomposed before the analysis could be completed.

3-(2-Azido-5-chlorophenyl)-8-nitroquinoline (131q)



Following the general procedure, the title compound was prepared from 4-chloro-2-(8-nitroquinolin-3-yl)aniline (**69q**) (200.0 mg, 0.67 mmol), HCl (10 mL), NaNO₂ (0.4 M), NaN₃ (91.3 mg, 1.40 mmol) and NaOAc (769.4 mg, 9.38 mmol in 10 mL H₂O). Workup was carried out according to the general procedure to give the target compound **131q** as a red solid (201.2 mg, 92%).

mp: 182-183 °C.

IR (ATR): ν_{\max} 2922, 2851, 2127 (N₃), 2099 (N₃), 1519, 1339, 1291, 766 cm⁻¹.

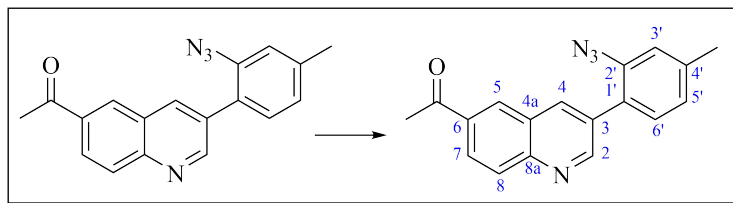
¹H NMR (400 MHz, CDCl₃): δ 9.15 (d, J = 2.2 Hz, 1H, H-2), 8.30 (d, J = 2.2 Hz, 1H, H-4), 8.10-8.08 (m, 2H, H-5 and H-7), 7.67 (t, J = 7.9 Hz, 1H, H-6), 7.48 (dd, J = 8.5 Hz, 2.4 Hz, 1H, H-4'), 7.43 (d, J = 2.4 Hz, 1H, H-6'), 7.28 (d, J = 8.6 Hz, 1H, H-3').

¹³C NMR (100 MHz, CDCl₃): δ 153.4 (C-2), 148.3 (C-8), 138.7 (C-8a), 136.7 (C-5'), 135.9 (C-4), 132.4 (C-5), 132.0 (C-3), 131.2 (C-6'), 130.9 (C-1'), 130.4 (C-2'), 130.3 (C-4'), 128.6 (C-4a), 126.0 (C-6), 124.3 (C-7), 120.4 (C-3').

UV (MeOH): λ_{\max} 292 nm.

HRMS (ESI): calcd. for C₁₅H₈ClN₅O₂ [M + Na⁺] 348.0259, found 348.0260.

3-(2-Azido-4-methylphenyl)-6-acetylquinoline (131r)



Following the general procedure, the title compound was prepared from 2-(6-acetylquinolin-3-yl)-5-methylaniline (**69r**) (200.0 mg, 0.72 mmol), HCl (10 mL), NaNO₂ (0.4 M), NaN₃ (98.9 mg, 1.52 mmol) and NaOAc (826.9 mg, 10.08 mmol in 10 mL H₂O). Workup was carried out according to the general procedure to give the target compound **131r** as a pale yellow solid (184.7 mg, 85%).

mp: 163-165 °C.

IR (ATR): ν_{\max} 2922, 2852, 2107 (N₃), 1670 (C=O), 1295, 813 cm⁻¹.

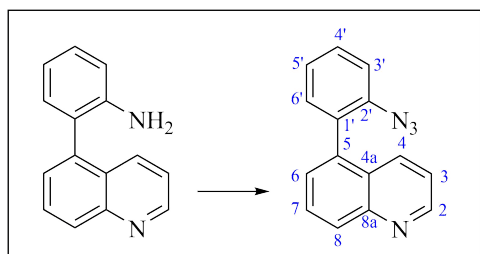
¹H NMR (400 MHz, CDCl₃): δ 9.09 (s, 1H, H-2), 8.48 (d, J = 1.7 Hz, 1H, H-5), 8.32 (d, J = 2.0 Hz, 1H, H-4), 8.26 (dd, J = 8.9 Hz, 1.9 Hz, 1H, H-7), 8.17 (d, J = 1.7 Hz, 1H, H-8), 7.34 (d, J = 7.7 Hz, 1H, H-6'), 7.13 (s, 1H, H-3'), 7.11-7.09 (m, 1H, H-5'), 2.75 (s, 3H, CO-CH₃), 2.46 (s, 3H, CH₃).

¹³C NMR (100 MHz, CDCl₃): δ 197.5 (C=O), 153.9 (C-2), 148.9 (C-8a), 140.5 (C-4'), 137.5 (C-1'), 137.1 (C-4), 135.3 (C-6), 132.3 (C-3), 131.2 (C-6'), 130.2 (C-5), 129.9 (C-8), 127.8 (C-7), 127.1 (C-4a), 126.7 (C-2'), 126.5 (C-5'), 119.6 (C-3'), 26.9 (CO-CH₃), 21.4 (CH₃).

UV (MeOH): λ_{\max} 294 nm.

HRMS (ESI): sample sent to UiB for analysis.

5-(2-Azidophenyl)quinoline (134)



Following the general procedure, the title compound was prepared from 2-(quinolin-5-yl)aniline (**72**) (500.0 mg, 2.27 mmol), HCl (15 mL), NaNO₂ (0.4 M), NaN₃ (309.8 mg, 4.77 mmol) and NaOAc (2.61 g, 31.78 mmol in 15 mL H₂O). The crude was purified by silica gel column chromatography (pet. ether/EtOAc, 1:1 v/v) and concentration of the relevant fractions [R_f =

0.60 (pet. ether/EtOAc, 1:1 v/v)] gave the target compound **134** as yellow crystals (443.2 mg, 79%).

mp: 110-112 °C.

IR (ATR): ν_{\max} 3053, 3034, 2111 (N₃), 2078 (N₃), 1278, 1261, 803, 753 cm⁻¹.

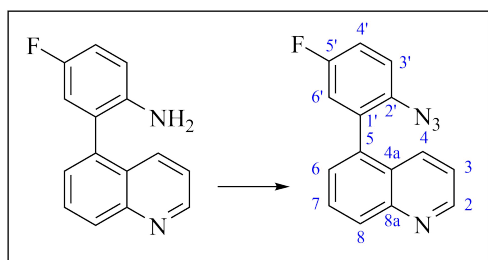
¹H NMR (400 MHz, CDCl₃): δ 8.93 (dd, $J = 4.0$ Hz, 1.4 Hz, 1H, H-2), 8.17-8.15 (m, 1H, H-8), 7.86 (ddd, $J = 8.5$ Hz, 1.5 Hz, 0.7 Hz, 1H, H-4), 7.77 (dd, $J = 8.5$ Hz, 7.1 Hz, 1H, H-7), 7.52 (ddd, $J = 9.1$ Hz, 7.1 Hz, 1.9 Hz, 1H, H-4'), 7.44 (dd, $J = 7.1$ Hz, 1.1 Hz, 1H, H-6), 7.36-7.25 (m, 4H, H-3, H-3', H-5' and H-6').

¹³C NMR (100 MHz, CDCl₃): δ 150.5 (C-2), 148.3 (C-8a), 138.8 (C-2'), 136.6 (C-5), 134.5 (C-4), 132.4 (C-6'), 131.1 (C-1'), 129.8 (C-8), 129.7 (C-4'), 128.9 (C-7), 128.0 (C-6), 127.2 (C-4a), 125.0 (C-5'), 121.3 (C-3), 118.7 (C-3').

UV (MeOH): λ_{\max} 234 nm.

HRMS (ESI): calcd. for C₁₅H₁₀N₄ [M + H⁺] 247.0978, found 247.0987.

5-(2-Azido-5-fluorophenyl)quinoline (135)



Following the general procedure, the title compound was prepared from 4-fluoro-2-(quinolin-5-yl)aniline (**72b**) (419.5 mg, 1.76 mmol), HCl (8 mL), NaNO₂ (0.4 M), NaN₃ (240.5 mg, 3.70 mmol) and NaOAc (2.02 g, 24.64 mmol in 15 mL H₂O). The crude was essentially pure by NMR and the target compound **135** was obtained as an orange solid (393.5 mg, 85%).

mp: 113-114 °C.

IR (ATR): ν_{\max} 3031, 2923, 2853, 2106 (N₃), 2065 (N₃), 1488, 1199, 801, 773 cm⁻¹.

¹H NMR (400 MHz, CDCl₃): δ 8.94 (dd, $J = 3.9$ Hz, 1.1 Hz, 1H, H-2), 8.20-8.17 (m, 1H, H-8), 7.85 (ddd, $J = 8.5$ Hz, 1.6 Hz, 0.8 Hz, 1H, H-4), 7.77 (dd, $J = 8.5$ Hz, 7.1 Hz, 1H, H-7), 7.43 (dd, $J = 7.1$ Hz, 1.1 Hz, 1H, H-6), 7.37 (dd, $J = 8.5$ Hz, 4.2 Hz, 1H, H-3), 7.28-7.20 (m, 2H, H-3' and H-6'), 7.06 (ddd, $J = 8.6$ Hz, 2.8 Hz, 0.4 Hz, 1H, H-4').

¹³C NMR (100 MHz, CDCl₃): δ 159.7 (d, $J_{\text{CF}} = 246.7$ Hz, C-5'), 150.6 (C-2), 148.2 (C-8a), 135.3 (d, $J_{\text{CF}} = 1.1$ Hz, C-5), 134.7 (d, $J_{\text{CF}} = 2.9$ Hz, C-1'), 134.1 (C-4), 132.7 (d, $J_{\text{CF}} = 8.0$ Hz, C-2'), 130.2 (C-8), 128.9 (C-7), 128.0 (C-6), 126.8 (C-4a), 121.5 (C-3), 120.0 (d, $J_{\text{CF}} = 8.6$ Hz, C-3'), 119.2 (d, $J_{\text{CF}} = 23.1$ Hz, C-4'), 116.5 (d, $J_{\text{CF}} = 23.1$ Hz, C-6').

^{19}F NMR (376 MHz, CDCl_3): δ -117.3.

UV (MeOH): λ_{max} 302 nm.

HRMS (ESI): calcd. for $\text{C}_{15}\text{H}_9\text{FN}_4$ [$\text{M} + \text{H}^+$] 265.0884, found 265.0890.

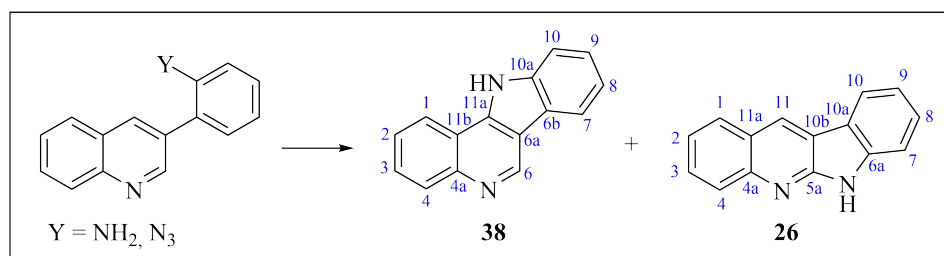
7.2.5 Cyclization to form tetracyclic compounds

General procedures

Method 1 - palladium-catalyzed intramolecular C-H activation/C-N bond formation: Biaryl (1 equiv.) in an appropriate amount of glacial acetic acid was added to a premixed solution of $\text{PdCl}_2(\text{dppf})$ (20 mol%), 1,3-bis(2,4,6-trimethylphenyl)imidazolium (IMes) (5 mol%), H_2O_2 (35 wt%, 29 mol%) and a suitable amount of glacial acetic acid. The reaction mixture was placed in a sealed reactor tube and immersed into the cavity of a microwave oven and heated at 118 °C until completion as indicated by TLC analysis. The reaction mixture was then transferred to a round-bottom flask with the aid of $\text{EtOAc}/\text{CHCl}_3$ and the volatiles were removed under reduced pressure. The reaction mixture was evaporated onto celite and purified by column chromatography using the eluent as indicated in the specific description to give target compounds.

Method 2 - one-pot nitrene insertion:^[278] Biaryl (1 equiv.) was dissolved in an appropriate amount of aq. HCl (37%) and the mixture was cooled to 0 °C using an ice bath. Then, ice-cooled aq. NaNO_2 (0.4 M) was added dropwise and the resulting mixture was stirred at 0 °C for 1.5 hours. An ice-cooled aq. solution of $\text{NaN}_3/\text{NaOAc}$ (2.1 equiv.:14 equiv. in an appropriate amount of H_2O) was added dropwise and the mixture stirred for 1 hour while keeping the temperature at 0 °C. The reaction mixture was quenched by addition of appropriate amounts of sat. aq. K_2CO_3 and subsequently extracted with CH_2Cl_2 (3 x 20 mL). The combined organic phases were washed (1 x 20 mL H_2O , 1 x 20 mL brine), dried (MgSO_4), filtered and concentrated *in vacuo*. The residue was subsequently dissolved in a suitable amount of 1,2-dichlorobenzene and flushed with argon. The resulting mixture was stirred at 180 °C for 3 hours under an argon atmosphere. The crude mixture was then allowed to cool to rt and the solvent was removed under reduced pressure. Finally, the concentrate was evaporated onto celite and purified by column chromatography using eluent as indicated in the specific description to give target compounds.

Method 3 - photocyclization: Aryl azide (1 equiv.) in 150 mL of the appropriate solvent was bubbled with a steady flow of argon as the mixture was irradiated at ambient temperature with a 125 W medium-pressure (254-579 nm) mercury-vapor lamp until completion as indicated by TLC analysis. The volatiles were then removed under reduced pressure and the concentrate was evaporated onto celite. Finally, the crude mixture was purified by column chromatography using the eluent as indicated in the specific description to give target compounds.

11H-Indolo[3,2-c]quinoline (38)

Method 1: Following the general procedure, the title compound was prepared from 2-(quinolin-3-yl)aniline (**69**) (70.0 mg, 0.32 mmol), PdCl₂(dppf) (46.3 mg, 0.063 mmol), IMes (4.8 mg, 0.016 mmol), H₂O₂ (0.075 mL, 0.092 mmol) in AcOH (2 mL). After a reaction time of 10 minutes, the crude was purified by silica gel column chromatography (CH₂Cl₂/EtOAc, 8:2 → 6:4 v/v) and concentration of the relevant fractions [*R_f* = 0.25 (CH₂Cl₂/EtOAc, 1:1 v/v)] gave the target compound **38** as an off-white solid (50.3 mg, 73%).

Method 2: Following the general procedure, the title compound was prepared from 2-(quinolin-3-yl)aniline (**69**) (100.0 mg, 0.45 mmol), HCl (3 mL), NaNO₂ (0.4 M), NaN₃ (61.4 mg, 0.94 mmol) and NaOAc (516.8 mg, 6.30 mmol in 5 mL H₂O). After formation of the azide was confirmed by IR, the cyclization was carried out using 1,2-dichlorobenzene (3 mL). The crude was purified by silica gel column chromatography (CH₂Cl₂/EtOAc, 8:2 → 0:1 v/v) and concentration of the relevant fractions [*R_f* = 0.25 (CH₂Cl₂, 1:1 v/v)] gave the target compound **38** as an off-white solid (86.4 mg, 88%) along with compound **26** as off-white crystals (4.2 mg, 4%).

Method 3: Following the general procedure, the title compound was prepared by irradiating 3-(2-azidophenyl)quinoline (**131**) (50.0 mg, 0.20 mmol) in α-α-α-trifluorotoluene (150 mL) for 45 minutes. The volatiles were removed under reduced pressure to give the target compound **38** as an off-white powder (41.3 mg, 95%).

Characterization of compound **38**:

mp: 333-336 °C (lit.^[124] 340-341 °C).

IR (NaCl): ν_{max} 3060, 2958, 2854, 1682, 1582, 1515, 1493 cm⁻¹.

¹H NMR (400 MHz, DMSO-*d*₆): δ 12.74 (bs, 1H, NH), 9.60 (s, 1H, H-6), 8.52 (dd, *J* = 7.8 Hz, 1.1 Hz, 1H, H-1), 8.33-8.31 (m, 1H, H-7), 8.14 (dd, *J* = 8.4 Hz, 1.1 Hz, 1H, H-4), 7.77-7.68 (m, 3H, H-2, H-3 and H-10), 7.52-7.48 (m, 1H, H-9), 7.37-7.33 (m, 1H, H-8).

¹³C NMR (100 MHz, DMSO-*d*₆): δ 145.3 (C-4a), 144.7 (C-6), 139.8 (C-11a), 138.8 (C-10a), 129.4 (C-4), 128.1 (C-3), 125.7 (C-2), 125.6 (C-9), 122.1 (C-1), 121.9 (C-6b), 120.6 (C-8), 120.1 (C-7), 117.1 (C-11b), 114.3 (C-6a), 111.9 (C-10).

In accordance with previously reported data.^[124]

Characterization of compound **26**:

mp: 341-342 °C (lit.^[279] 342-346 °C).

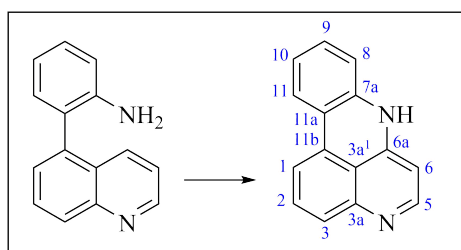
IR (ATR): ν_{\max} 3139, 2923, 2849, 1402, 725 cm^{-1} .

¹H NMR (400 MHz, DMSO-*d*₆): δ 11.72 (bs, 1H, NH), 9.06 (s, 1H, H-11), 8.26 (d, *J* = 7.7 Hz, 1H, H-10), 8.11 (dd, *J* = 8.1 Hz, 1.3 Hz, 1H, H-1), 7.99-7.97 (m, 1H, H-4), 7.75-7.70 (m, 1H, H-3), 7.55-7.46 (m, 3H, H-2, H-7 and H-8), 7.29-7.25 (m, 1H, H-9).

¹³C NMR (100 MHz, DMSO-*d*₆): δ 152.7 (C-4a), 146.1 (C-5a), 141.4 (C-6a), 128.7 (C-1), 128.6 (C-3), 128.2 (C-2), 127.7 (C-11), 126.8 (C-4), 123.6 (C-11a), 122.8 (C-8), 121.8 (C-10), 120.3 (C-10a), 119.7 (C-9), 118.0 (C-10b), 110.9 (C-7).

In accordance with previously reported data.^[183]

7*H*-Pyrido[4,3,2-*gh*]phenanthridine (**54**)



Method 1: Following the general procedure, the title compound was prepared from 2-(quinolin-5-yl)aniline (**72**) (100.0 mg, 0.45 mmol), PdCl₂(dppf) (66.5 mg, 0.091 mmol), IMes (6.8 mg, 0.022 mmol), H₂O₂ (11 μ L, 0.13 mmol) in AcOH (2 mL). After a reaction time of 30 minutes, the crude was purified by silica gel column chromatography (CH₂Cl₂/EtOH, 1:1 \rightarrow 0:1 v/v) and concentration of the relevant fractions [*R*_f = 0.19 (EtOH)] gave the target compound **54** as a yellow gel (72.0 mg, 73%).

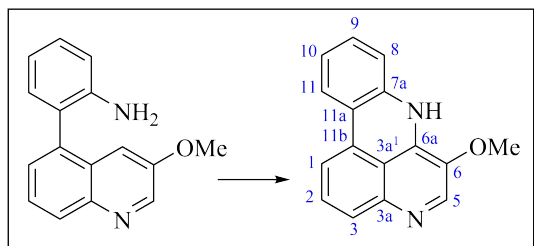
IR (NaCl): ν_{\max} 3274, 3167, 3112, 3049, 2919, 2851, 2762, 1614, 1576, 1460, 669 cm^{-1} .

¹H NMR (400 MHz, DMSO-*d*₆): δ 8.33 (dd, *J* = 8.2 Hz, 0.8 Hz, 1H, H-11), 8.27 (d, *J* = 6.6 Hz, 1H, H-5), 8.16 (d, *J* = 7.8 Hz, 1H, H-1), 7.96 (t, *J* = 8.0 Hz, 1H, H-2), 7.66 (dd, *J* = 8.4 Hz, 0.6 Hz, 1H, H-3), 7.59-7.55 (m, 1H, H-9), 7.50 (dd, *J* = 8.1 Hz, 0.8 Hz, 1H, H-8), 7.39-7.34 (m, 1H, H-10), 6.77 (d, *J* = 6.6 Hz, 1H, H-6).

¹³C NMR (100 MHz, DMSO-*d*₆): δ 149.2 (C-3a), 143.3 (C-5), 141.1 (C-6a), 135.5 (C-7a), 134.1 (C-2), 131.6 (C-11b), 130.9 (C-9), 124.9 (C-10), 123.8 (C-11), 120.4 (C-11a), 118.1 (C-8), 117.2 (C-3a'), 115.9 (C-3), 115.0 (C-1), 99.7 (C-6).

HRMS (ESI): calcd. for C₁₅H₁₀N₂ [M + H⁺] 219.0917, found 219.0917.

6-Methoxy-7H-pyrido[4,3,2-gh]phenanthridine (54b)



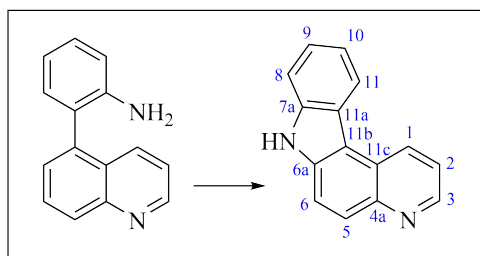
Method 1: Following the general procedure, the title compound was prepared from 2-(3-methoxyquinolin-5-yl)aniline (**72a**) (100.0 mg, 0.40 mmol), PdCl₂(dppf) (58.5 mg, 0.080 mmol), IMes (6.1 mg, 0.020 mmol), H₂O₂ (10 μL, 0.12 mmol) in AcOH (2 mL). After a reaction time of 1 hour, the crude was purified by silica gel column chromatography (CH₂Cl₂/EtOAc/EtOH, 1:1:0 → 1:0:1 → 0:0:1 v/v) followed by a second purification by silica gel (CH₂Cl₂/EtOH, 7:3 → 1:1 v/v) and concentration of the relevant fractions [*R*_f = 0.33 (CH₂Cl₂/EtOH, 7:3 v/v)] gave the target compound **54b** as a bright yellow gel (38.4 mg, 39%).

¹H NMR (400 MHz, DMSO-*d*₆): δ 8.42 (bs, 1H, H-5), 8.30 (dd, *J* = 8.4 Hz, 1.0 Hz, 1H, H-11), 8.08 (d, *J* = 7.7 Hz, 1H, H-1), 7.88 (t, *J* = 8.0 Hz, 1H, H-2), 7.80 (dd, *J* = 8.2 Hz, 0.8 Hz, 1H, H-3), 7.71 (d, *J* = 8.4 Hz, 1H, H-8), 7.56-7.52 (m, 1H, H-9), 7.38-7.34 (m, 1H, H-10), 4.07 (s, 3H, OCH₃).

¹³C NMR (100 MHz, DMSO-*d*₆): δ 140.2 (C-3a), 138.3 (C-6a), 135.5 (C-6), 132.8 (C-2), 131.0 (C-7a), 130.8 (C-9), 127.0 (C-5), 127.0 (C-11b), 125.2 (C-10), 123.6 (C-11), 120.7 (C-3a¹), 118.8 (C-3), 116.5 (C-11a), 115.7 (C-8), 113.8 (C-1), 57.8 (OCH₃).

HRMS (ESI): calcd. for C₁₆H₁₃N₂O [M + H⁺] 249.1022, found 249.1029.

7H-Pyrido[2,3-*c*]carbazole (61)



Method 2: Following the general procedure, the title compound was prepared from 2-(quinolin-5-yl)aniline (**72**) (100.0 mg, 0.45 mmol), HCl (3 mL), NaNO₂ (0.4 M), NaN₃ (61.4 mg, 0.94 mmol) and NaOAc (516.8 mg, 6.30 mmol in 5 mL H₂O). After formation of the azide was confirmed by IR, the cyclization was carried out using 1,2-dichlorobenzene (3 mL). The crude was

purified by silica gel column chromatography ($\text{CH}_2\text{Cl}_2/\text{EtOAc}$, 95:5 \rightarrow 9:1 v/v) and concentration of the relevant fractions [$R_f = 0.22$ ($\text{CH}_2\text{Cl}_2/\text{EtOAc}$, 95:5 v/v)] gave the target compound **61** as a light brown solid (78.8 mg, 80%).

mp: 204-205 °C.

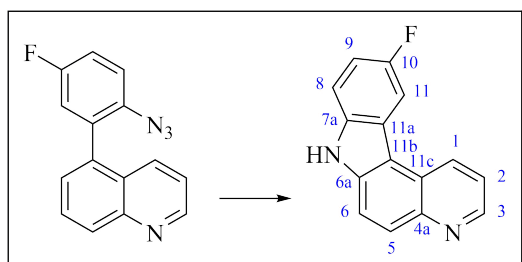
IR (ATR): ν_{max} 3045, 2919, 2842, 1523, 1274, 956, 804, 728 cm^{-1} .

^1H NMR (400 MHz, $\text{DMSO}-d_6$): δ 11.92 (bs, 1H, NH), 9.17 (dd, $J = 8.4$ Hz, 1.4 Hz, 1H, H-1), 8.84 (dd, $J = 4.1$ Hz, 1.4 Hz, 1H, H-3), 8.60 (d, $J = 8.0$ Hz, 1H, H-11), 8.03-7.98 (m, 2H, H-5 and H-6), 7.69-7.65 (m, 2H, H-2 and H-8), 7.47-7.44 (m, 1H, H-9), 7.34-7.31 (m, 1H, H-10).

^{13}C NMR (100 MHz, $\text{DMSO}-d_6$): δ 146.4 (C-3), 144.3 (C-4a), 139.0 (C-7a), 136.9 (C-6a), 130.8 (C-1), 127.7 (C-5), 124.5 (C-9), 124.3 (C-11c), 122.9 (C-11a), 121.6 (C-2), 121.5 (C-11), 119.8 (C-10), 116.8 (C-6), 113.6 (C-11b), 111.9 (C-8).

HRMS (ESI): calcd. for $\text{C}_{15}\text{H}_{10}\text{N}_2$ 219.0917, found 219.0927.

10-Fluoro-7H-pyrido[2,3-c]carbazole (**61a**)



Method 2: 5-(2-Azido-5-fluorophenyl)quinoline (**135**) (100.0 mg, 0.38 mmol) was dissolved in 1,2-dichlorobenzene (2 mL) and flushed with argon. The resulting mixture was stirred at 180 °C for 3 hours under an argon atmosphere. The crude mixture was allowed to cool to rt and the solvent was removed under reduced pressure. The crude was essentially pure by NMR and the target compound **61a** was obtained as a dark green solid (87.3 mg, 97%).

mp: 256-257 °C.

IR (ATR): ν_{max} 3137, 2974, 2746, 1460, 1149, 789 cm^{-1} .

^1H NMR (400 MHz, CD_3OD): δ 9.07 (ddd, $J = 8.4$ Hz, 1.6 Hz, 0.8 Hz, 1H, H-1), 8.74 (dd, $J = 4.4$ Hz, 1.6 Hz, 1H, H-3), 8.18-8.15 (m, 1H, H-11), 7.98 (dd, $J = 9.1$ Hz, 0.7 Hz, 1H, H-6), 7.91 (d, $J = 9.1$ Hz, 1H, H-5), 7.67 (dd, $J = 8.4$ Hz, 4.4 Hz, 1H, H-2), 7.58 (ddd, $J = 8.8$ Hz, 4.5 Hz, 0.5 Hz, 1H, H-9), 7.25-7.20 (m, 1H, H-8).

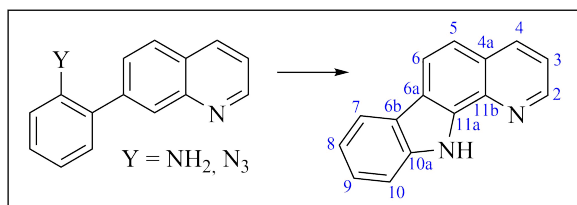
^{13}C NMR (100 MHz, CD_3OD): δ 159.2 (d, $J_{\text{CF}} = 234.5$ Hz, C-10), 146.9 (C-3), 145.1 (C-4a), 139.8 (C-6a), 137.3 (C-7a), 132.9 (C-1), 127.9 (C-6), 126.4 (C-11c), 124.7 (d, $J_{\text{CF}} =$

9.5 Hz, C-11a), 122.7 (C-2), 118.3 (C-5), 115.1 (d, $J_{CF} = 5.3$ Hz, C-11b), 113.7 (d, $J_{CF} = 24.0$ Hz, C-9), 113.5 (d, $J_{CF} = 7.2$ Hz, C-8), 107.6 (d, $J_{CF} = 24.8$ Hz, C-11).

^{19}F NMR (376 MHz, CD_3OD): δ -123.6.

HRMS (ESI): calcd. for $\text{C}_{15}\text{H}_9\text{FN}_2$ [$\text{M} + \text{H}^+$] 237.0823, found 237.0830.

11H-Pyrido[2,3-a]carbazole (64)



Method 1: Following the general procedure, the title compound was prepared from 2-(quinolin-7-yl)aniline (**74**) (160.0 mg, 0.73 mmol), $\text{PdCl}_2(\text{dppf})$ (106.4 mg, 0.14 mmol), IMes (11.1 mg, 0.036 mmol), H_2O_2 (0.017 mL, 0.21 mmol) in AcOH (2.2 mL). After a reaction time of 10 minutes, the crude was purified by silica gel column chromatography (pet. ether/EtOAc, 1:1 + 0.2% $\text{Et}_3\text{N} \rightarrow 2:8$ v/v) and concentration of the relevant fractions [$R_f = 0.27$ (pet. ether/ CH_2Cl_2 , 1:1 v/v)] gave the target compound **64** as pale yellow crystals (40.1 mg, 25%).

Method 2: Following the general procedure, the title compound was prepared from 2-(quinolin-7-yl)aniline (**74**) (100.0 mg, 0.45 mmol), HCl (3 mL), NaNO_2 (0.4 M), NaN_3 (61.4 mg, 0.94 mmol) and NaOAc (516.8 mg, 6.30 mmol in 3 mL H_2O). After formation of the azide was confirmed by IR, the cyclization was carried out using 1,2-dichlorobenzene (3 mL). The crude was purified by silica gel column chromatography ($\text{CH}_2\text{Cl}_2/\text{EtOAc}$, 9:1 v/v) and concentration of the relevant fractions [$R_f = 0.36$ ($\text{CH}_2\text{Cl}_2/\text{EtOAc}$, 9:1 v/v)] gave the target compound **64** as off-white crystals (40.0 mg, 41%).

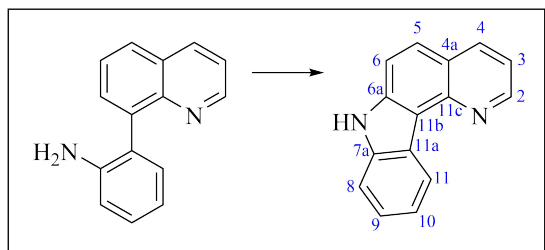
mp: 165-167 °C (lit.^[280] 164-165 °C).

IR (ATR): ν_{max} 3263, 3043, 2923, 2854, 1523, 1369, 820, 734 cm^{-1} .

^1H NMR (400 MHz, CDCl_3): δ 10.20 (bs, 1H, NH), 8.92 (dd, $J = 4.4$ Hz, 1.5 Hz, 1H, H-2), 8.35 (dd, $J = 8.3$ Hz, 1.5 Hz, 1H, H-4), 8.24 (d, $J = 8.5$ Hz, 1H, H-5), 8.19-8.17 (m, 1H, H-7), 7.62-7.60 (m, 2H, H-6 and H-10), 7.51-7.47 (m, 2H, H-3 and H-9), 7.35-7.31 (m, 1H, H-8).

^{13}C NMR (100 MHz, CDCl_3): δ 147.8 (C-2), 139.2 (C-10a), 137.4 (C-4), 136.8 (C-11b), 134.9 (C-11a), 127.3 (C-4a), 125.9 (C-3), 123.8 (C-6b), 121.7 (C-6a), 120.8 (C-5), 120.5 (C-9), 120.4 (C-7), 120.2 (C-8), 118.8 (C-6), 111.8 (C-10).

In accordance with previously reported data.^[280]

7H-Pyrido[3,2-c]carbazole (66)

Method 1: Following the general procedure, the title compound was prepared from 2-(quinolin-8-yl)aniline (**75**) (50.0 mg, 0.23 mmol), PdCl₂(dppf) (33.6 mg, 0.046 mmol), IMes (3.5 mg, 0.011 mmol), H₂O₂ (5.5 μL, 0.067 mmol) in AcOH (1 mL). After a reaction time of 30 minutes, the crude was purified by silica gel column chromatography (pet. ether/EtOAc, 1:1 + 0.2% Et₃N v/v) and concentration of the relevant fractions [*R_f* = 0.06 (pet. ether/EtOAc, 6:4 v/v)] gave the target compound **66** as a pale yellow solid (4.9 mg, 10%).

Method 2: Following the general procedure, the title compound was prepared from 2-(quinolin-8-yl)aniline (**75**) (450.0 mg, 2.04 mmol), HCl (10 mL), NaNO₂ (0.4 M), NaN₃ (278.5 mg, 4.28 mmol) and NaOAc (2.34 g, 28.56 mmol in 10 mL H₂O). After formation of the azide was confirmed by IR, the cyclization was carried out using 1,2-dichlorobenzene (5 mL). The crude was purified by silica gel column chromatography (pet. ether/EtOAc, 1:1 v/v) and concentration of the relevant fractions [*R_f* = 0.85 (pet. ether/EtOAc, 1:1 v/v)] gave the target compound **66** as a dark red oily solid (195.9 mg, 44%).

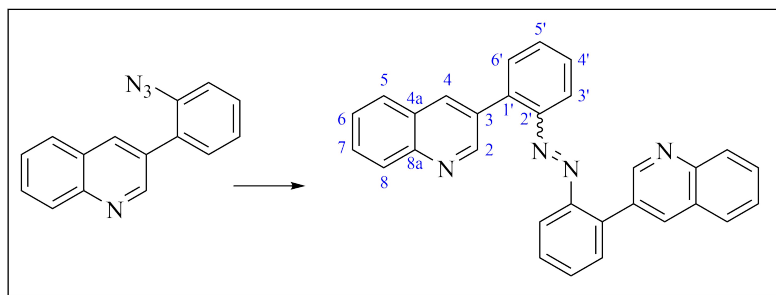
mp: 150-152 °C (lit.^[281] 173-174 °C).

IR (ATR): ν_{\max} 3207, 2976, 2919, 2850, 2740, 2605, 2499 cm⁻¹.

¹H NMR (400 MHz, DMSO-*d*₆): δ 11.92 (bs, 1H, NH), 9.02 (dd, *J* = 4.4 Hz, 1.8 Hz, 1H, H-2), 8.90-8.88 (m, 1H, H-11), 8.46 (dd, *J* = 8.1 Hz, 1.4 Hz, 1H, H-4), 7.92 (d, *J* = 8.8 Hz, 1H, H-5), 7.84 (d, *J* = 8.8 Hz, 1H, H-6), 7.66-7.64 (m, 1H, H-8), 7.49 (dd, *J* = 8.0 Hz, 4.3 Hz, 1H, H-3), 7.46-7.42 (m, 1H, H-9), 7.33-7.29 (m, 1H, H-10).

¹³C NMR (100 MHz, DMSO-*d*₆): δ 149.8 (C-2), 145.3 (C-4a), 139.6 (C-6a), 138.5 (C-7a), 136.5 (C-4), 126.0 (C-5), 124.5 (C-9), 123.1 (C-11), 122.9 (C-11c), 122.8 (C-11a), 119.7 (C-10), 118.3 (C-3), 115.3 (C-11b), 114.2 (C-6), 111.4 (C-8).

1,2-Bis(2-(quinolin-3-yl)phenyl)diazene (132)



Method 3: Following the general procedure, the title compound was prepared by irradiating 3-(2-azidophenyl)quinoline (**131**) (50.0 mg, 0.20 mmol) in α,α,α -trifluorotoluene (135 mL) and acetophenone (15 mL) for 45 minutes. Purification by silica gel column chromatography (pet. ether/EtOAc, 7:3 \rightarrow 1:1 v/v) and concentration of the relevant fractions [$R_f = 0.15$ (pet. ether/EtOAc, 1:1 v/v)] gave the target compound **132** as an orange solid (6.7 mg, 15%).

mp: 116-117 °C.

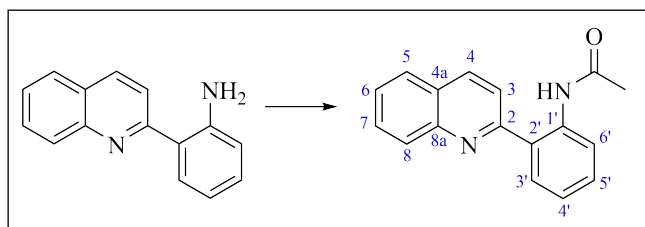
IR (ATR): ν_{\max} 3059, 2925, 2854, 1492, 756 cm^{-1} .

$^1\text{H NMR}$ (400 MHz, CDCl_3): δ 9.12 (d, $J = 2.2$ Hz, 2H, H-2), 8.28 (d, $J = 2.0$ Hz, 2H, H-4), 8.20-8.18 (m, 2H, H-8), 7.89 (dd, $J = 8.1$ Hz, 1.2 Hz, 2H, H-6'), 7.80-7.75 (m, 2H, H-7), 7.67-7.62 (m, 4H, H-6 and H-3'), 7.61-7.55 (m, 4H, H-5 and H-5'), 7.43-7.39 (m, 2H, H-4').

$^{13}\text{C NMR}$ (100 MHz, CDCl_3): δ 152.7 (C-2), 149.7 (C-2'), 147.0 (C-8a), 138.7 (C-4a), 136.8 (C-4), 132.5 (C-1'), 131.7 (C-6), 131.3 (C-5), 129.8 (C-7), 129.4 (C-4'), 129.3 (C-8), 128.2 (C-6'), 127.9 (C-3), 127.1 (C-5'), 116.4 (C-3').

HRMS (ESI): calcd. for $\text{C}_{30}\text{H}_{20}\text{N}_4$ [$\text{M} + \text{H}^+$] 437.1761, found 437.1769.

N-(2-(Quinolin-2-yl)phenyl)acetamide (76)



Method 1: Following the general procedure, the title compound was prepared from 2-(quinolin-2-yl)aniline (**70**) (50.0 mg, 0.23 mmol), $\text{PdCl}_2(\text{dppf})$ (33.6 mg, 0.046 mmol), IMes (3.5 mg, 0.011 mmol), H_2O_2 (5.6 μL , 0.067 mmol) in AcOH (1 mL). After a reaction time of 1 hour, the crude was purified by silica gel column chromatography (pet. ether/EtOAc, 9:1 \rightarrow 7:3 v/v) and concentration of the relevant fractions [$R_f = 0.24$ (pet. ether/EtOAc, 9:1 v/v)] gave the target

compound **76** as orange crystals (27.0 mg, 55%).

mp: 124-125 °C.

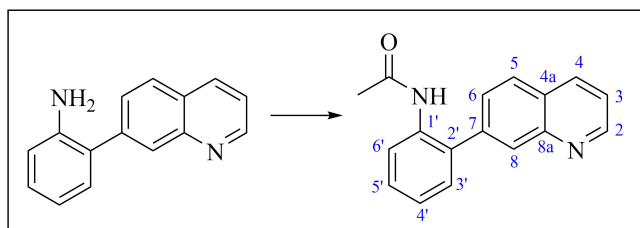
IR (NaCl): ν_{\max} 3054, 2958, 2925, 2852, 1677 (C=O), 1587, 1422, 1234, 765 cm^{-1} .

^1H NMR (400 MHz, CDCl_3): δ 12.97 (bs, 1H, NH), 8.65 (d, $J = 8.2$ Hz, 1H, H-3'), 8.28 (d, $J = 8.7$ Hz, 1H, H-4), 8.06-8.04 (m, 1H, H-8), 7.89 (d, $J = 8.7$ Hz, 1H, H-3), 7.86 (dd, $J = 8.2$ Hz, 1.0 Hz, 1H, H-6'), 7.83 (dd, $J = 7.9$ Hz, 1.5 Hz, 1H, H-5), 7.80-7.76 (m, 1H, H-7), 7.61-7.57 (m, 1H, H-6), 7.48-7.43 (m, 1H, H-4'), 7.20 (td, $J = 7.9$ Hz, 1.2 Hz, 1H, H-5'), 2.26 (s, 3H, CH_3).

^{13}C NMR (100 MHz, CDCl_3): δ 168.8 (C=O), 158.2 (C-2), 146.2 (C-8a), 138.6 (C-1'), 137.7 (C-4), 130.7 (C-4'), 130.5 (C-7), 129.4 (C-4), 128.4 (C-8), 127.8 (C-6'), 127.1 (C-6), 126.6 (C-4a), 124.9 (C-2'), 123.4 (C-5'), 121.8 (C-3'), 120.9 (C-3), 25.5 (CH_3).

HRMS (ESI): calcd. for $\text{C}_{17}\text{H}_{14}\text{N}_2$ [$\text{M} + \text{H}^+$] 263.1179, found 263.1182.

N-(2-(Quinolin-7-yl)phenyl)acetamide (**78**)



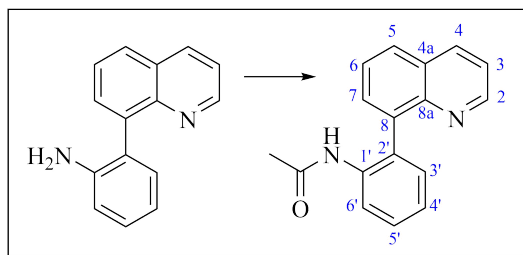
Method 1: Following the general procedure, the title compound was prepared from 2-(quinolin-7-yl)aniline (**74**) (50.0 mg, 0.23 mmol), $\text{PdCl}_2(\text{dppf})$ (33.6 mg, 0.045 mmol), IMes (3.5 mg, 0.011 mmol), H_2O_2 (5.6 μL , 0.067 mmol) in AcOH (3 mL). After a reaction time of 5 hours, the crude was purified by silica gel column chromatography (pet. ether/EtOAc, 1:1 + 0.2% Et_3N v/v) and concentration of the relevant fractions [$R_f = 0.16$ (pet. ether/EtOAc, 8:2 v/v)] gave the target compound **78** as a red oil (30.4 mg, 61%).

IR (NaCl): ν_{\max} 3418, 3249, 3051, 2966, 2924, 2852, 1676 (C=O), 1526, 1301, 840, 758 cm^{-1} .

^1H NMR (400 MHz, CD_3OD): δ 8.87 (d, $J = 3.0$ Hz, 1H, H-2), 8.41 (d, $J = 8.1$ Hz, 1H, H-4), 8.05 (s, 1H, H-8), 8.01 (d, $J = 8.4$ Hz, 1H, H-5), 7.65 (dd, $J = 8.3$ Hz, 1.2 Hz, 1H, H-6), 7.56 (dd, $J = 8.3$ Hz, 4.3 Hz, 1H, H-3), 7.53-7.37 (m, 4H, H-3', H-4', H-5' and H-6'), 1.93 (s, 3H, CH_3).

^{13}C NMR (100 MHz, CD_3OD): δ 172.4 (C=O), 151.5 (C-2), 148.6 (C-8a), 142.9 (C-7), 138.4 (C-4), 138.1 (C-1'), 135.7 (C-2'), 131.7, 129.7, 129.5 (C-6), 129.2 (C-5), 129.0 (C-4a), 128.6 (C-8), 128.4, 128.0, 122.7 (C-3), 22.8 (CH_3).

HRMS (ESI): calcd. for $\text{C}_{17}\text{H}_{14}\text{N}_2\text{O}$ [$\text{M} + \text{H}^+$] 263.1179, found 263.1181.

***N*-(2-(Quinolin-8-yl)phenyl)acetamide (79)**

Method 1: Following the general procedure, the title compound was prepared from 2-(quinolin-8-yl)aniline (**75**) (200.0 mg, 0.91 mmol), PdCl₂(dppf) (132.9 mg, 0.18 mmol), IMes (13.8 mg, 0.045 mmol), H₂O₂ (0.021 mL, 0.26 mL) in AcOH (3 mL). After a reaction time of 2.5 hours, the crude was purified by silica gel column chromatography (pet. ether/EtOAc, 9:1 → 4:6 + 1% Et₃N v/v) and concentration of the relevant fractions [*R*_f = 0.21 (pet. ether/EtOAc, 1:1 v/v)] gave the target compound **79** as dark yellow crystals (136.6 mg, 69%).

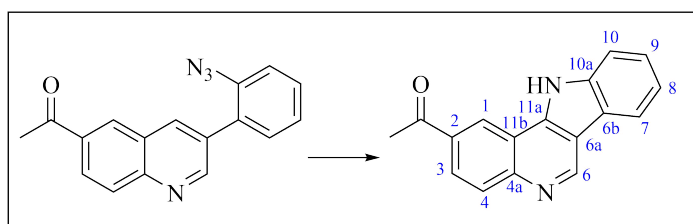
mp: 128-130 °C.

IR (ATR): ν_{\max} 3247, 3195, 3059, 3026, 2926, 2854, 1678 (C=O), 1522, 1439, 1295, 789, 748 cm⁻¹.

¹H NMR (400 MHz, CDCl₃): δ 8.97 (dd, *J* = 4.0 Hz, 1.5 Hz, 1H, H-2), 8.49 (bs, 1H, NH), 8.31 (dd, *J* = 8.3 Hz, 1.4 Hz, 1H, H-4), 8.00 (d, *J* = 8.1 Hz, 1H, H-3'), 7.93 (dd, *J* = 7.9 Hz, 1.3 Hz, 1H, H-5), 7.73 (dd, *J* = 7.1 Hz, 1.4 Hz, 1H, H-6), 7.69-7.66 (m, 1H, H-7), 7.50 (dd, *J* = 8.5 Hz, 4.2 Hz, 1H, H-3), 7.47-7.45 (m, 1H, H-6'), 7.35 (dd, *J* = 7.5 Hz, 1.1 Hz, 1H, H-5'), 7.29-7.25 (m, 1H, H-4'), 1.77 (s, 3H, CH₃).

¹³C NMR (100 MHz, CDCl₃): δ 168.3 (C=O), 150.6 (C-2), 145.7 (C-8a), 138.7 (C-1'), 137.8 (C-4), 135.7 (C-2'), 133.1 (C-6), 132.9 (C-8), 132.0 (C-5'), 128.9 (C-6'), 128.6 (C-5), 128.5 (C-4a), 127.3 (C-7), 125.3 (C-4'), 124.5 (C-3'), 121.4 (C-3), 24.4 (CH₃).

HRMS (ESI): calcd. for C₁₇H₁₄N₂O [M + H⁺] 263.1179, found 263.1183.

2-Acetyl-11*H*-indolo[3,2-*c*]quinoline (38b)

Method 3: Following the general procedure, the title compound was prepared by irradiating 3-(2-azidophenyl)-6-acetylquinoline (**131b**) (100.0 mg, 0.35 mmol) in α,α,α -trifluorotoluene

(150 mL) for 30 minutes. Purification by silica gel column chromatography ($\text{CH}_2\text{Cl}_2/\text{EtOAc}$, 1:1 v/v) and concentration of the relevant fractions [$R_f = 0.26$ ($\text{CH}_2\text{Cl}_2/\text{EtOAc}$, 1:1 v/v)] gave the target compound **38b** as a yellow solid (13.6 mg, 15%).

mp: > 350 °C.

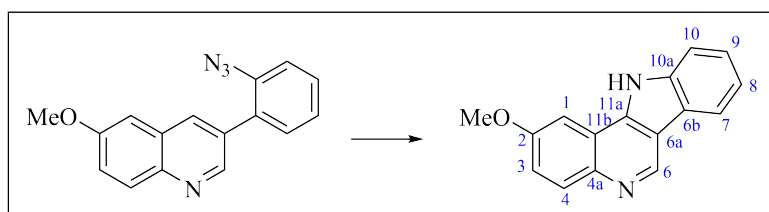
IR (ATR): ν_{max} 3053, 2923, 2852, 1678 (C=O), 1362, 1253, 736 cm^{-1} .

^1H NMR (400 MHz, DMSO- d_6): δ 13.01 (bs, 1H, NH), 9.69 (s, 1H, H-6), 9.29 (s, 1H, H-5), 8.35 (d, $J = 7.8$ Hz, 1H, H-7), 8.21-8.20 (m, 2H, H-3 and H-4), 7.76 (d, $J = 8.3$ Hz, 1H, H-10), 7.56-7.52 (m, 1H, H-9), 7.40-7.36 (m, 1H, H-8), 2.78 (s, 3H, CH_3).

^{13}C NMR (100 MHz, DMSO- d_6): δ 197.3 (C=O), 147.1 (C-4a), 146.8 (C-6), 140.6 (C-11a), 138.8 (C-10a), 133.4 (C-2), 129.6 (C-4), 126.1 (C-3), 125.9 (C-9), 124.6 (C-1), 121.7 (C-6b), 120.9 (C-7), 120.3 (C-8), 116.3 (C-11b), 114.9 (C-6a), 112.0 (C-10), 26.8 (CH_3).

HRMS (ESI): calcd. for $\text{C}_{17}\text{H}_{12}\text{N}_2\text{O}$ [$\text{M} + \text{H}^+$] 261.1022, found 261.1021.

2-Methoxy-11H-indolo[3,2-c]quinoline (38c)



Method 3: Following the general procedure, the title compound was prepared by irradiating 3-(2-azidophenyl)-6-methoxyquinoline (**131b**) (212.7 mg, 0.77 mmol) in α,α,α -trifluorotoluene (150 mL) for 1.5 hours. Purification by silica gel column chromatography (pet. ether/EtOAc, 1:1 \rightarrow 0:1 v/v) and concentration of the relevant fractions [$R_f = 0.12$ (pet. ether/EtOAc, 1:1 v/v)] gave the target compound **38c** as a dark red solid (74.3 mg, 37%).

mp: 307-309 °C (lit.^[284] 312-314 °C).

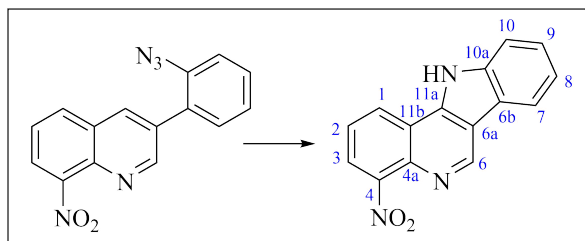
IR (ATR): ν_{max} 3046, 2982, 2838, 1518, 1457, 1234 cm^{-1} .

^1H NMR (400 MHz, DMSO- d_6): δ 12.57 (bs, 1H, NH), 9.45 (s, 1H, H-6), 8.29 (d, $J = 7.8$ Hz, 1H, H-7), 8.04 (d, $J = 9.1$ Hz, 1H, H-4), 7.97 (dd, $J = 9.1$ Hz, 2.7 Hz, 1H, H-3), 7.73-7.71 (m, 1H, H-10), 7.51-7.47 (m, 1H, H-9), 7.36 (dd, $J = 9.1$ Hz, 2.7 Hz, 1H, H-3), 7.34-7.30 (m, 1H, H-8), 3.98 (s, 3H, OCH_3).

^{13}C NMR (100 MHz, DMSO- d_6): δ 156.9 (C-2), 142.2 (C-6), 141.0 (C-4a), 139.4 (C-11b), 138.7 (C-10a), 131.0 (C-4), 125.5 (C-9), 121.9 (C-6b), 120.4 (C-8), 120.1 (C-7), 119.4 (C-3), 117.7 (C-11a), 114.3 (C-6a), 111.8 (C-10), 101.3 (C-1), 55.5 (OCH_3).

In accordance with previously reported data.^[284]

4-Nitro-11H-indolo[3,2-c]quinoline (38e)



Method 3: Following the general procedure, the title compound was prepared by irradiating 3-(2-azidophenyl)-8-nitroquinoline (**131e**) (71.5 mg, 0.24 mmol) in α,α,α -trifluorotoluene (150 mL) for 1 hour. Purification by silica gel column chromatography (pet. ether/EtOAc, 6:4 \rightarrow 1:1 v/v) and concentration of the relevant fractions [$R_f = 0.24$ (pet. ether/EtOAc, 6:4 v/v)] gave the target compound **38e** as an orange solid (48.8 mg, 77%).

mp: 244 °C (decomp.).

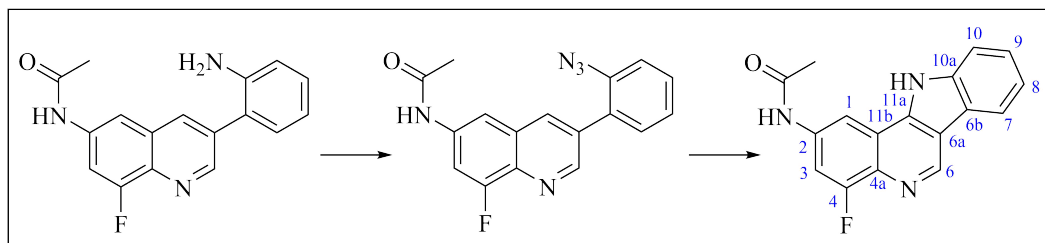
IR (ATR): ν_{\max} 3150, 3079, 2922, 2853, 1515, 1337, 1235, 770, 737 cm^{-1} .

^1H NMR (400 MHz, DMSO- d_6): δ 13.05 (bs, 1H, NH), 9.70 (s, 1H, H-6), 8.77 (dd, $J = 8.3$ Hz, 1.3 Hz, 1H, H-1), 8.37 (d, $J = 7.9$ Hz, 1H, H-7), 8.18 (dd, $J = 7.5$ Hz, 1.3 Hz, 1H, H-3), 7.84 (dd, $J = 8.1$ Hz, 7.7 Hz, 1H, H-2), 7.79-7.77 (m, 1H, H-10), 7.59-7.55 (m, 1H, H-9), 7.42-7.38 (m, 1H, H-8).

^{13}C NMR (100 MHz, DMSO- d_6): δ 148.9 (C-4), 146.7 (C-6), 139.1 (C-11a), 139.0 (C-4a), 135.9 (C-10a), 126.4 (C-9), 125.6 (C-1), 124.9 (C-2), 121.5 (C-11b), 121.2 (C-8), 121.0 (C-3), 120.5 (C-7), 118.1 (C-6a), 115.5 (C-6b).

HRMS (ESI): sample sent to UiB for analysis.

N-(4-Fluoro-11H-indolo[3,2-c]quinolin-2-yl)acetamide (38f)



Method 3: Step 1: Following the general procedure for the Suzuki-Miyaura cross-couplings, the desired compound was prepared from *N*-(3-bromo-8-fluoroquinolin-6-yl)acetamide (**67bb**) (300.0 mg, 1.06 mmol), 2-aminophenylboronic acid hydrochloride (**68**) (239.8 mg, 1.38 mmol), an aq. solution of Cs_2CO_3 (1139.7 mg, 3.50 mmol in 6 mL H_2O) and $\text{Pd}(\text{PPh}_3)_4$ (61.2 mg, 0.053 mmol) in DME (30 mL). After a reaction time of 23 hours, the crude was purified by

silica gel column chromatography (pet. ether/EtOAc, 4:6 \rightarrow 0:1 v/v) and concentration of the relevant fractions [$R_f = 0.38$ (EtOAc)] gave the target compound **69f** as red crystals (231.0 mg, 74%). The sample contained impurities and was used in the next step without any further purification.

Step 2: Following the general procedure for the diazotization-azidations, the desired compound was prepared from *N*-(3-(2-aminophenyl)-8-fluoroquinolin-6-yl)acetamide (**69f**) (200.0 mg, 0.68 mmol), HCl (5 mL), NaNO₂ (0.4 M), NaN₃ (92.5 mg, 1.42 mmol) and NaOAc (780.9 mg, 9.52 mmol in 10 mL H₂O). Workup was carried out according to the general procedure to give the target compound **131f** as a dark yellow solid (127.0 mg, 58%). The impurity from the previous step was still present and the next step was carried out without attempting purification.

Step 3: Following the general procedure, the title compound was prepared by irradiating *N*-(3-(2-azidophenyl)-8-fluoroquinolin-6-yl)acetamide (**131f**) (100.0 mg, 0.31 mmol) in α,α,α -trifluorotoluene (150 mL) for 2 hours. Purification by silica gel column chromatography (EtOAc) and concentration of the relevant fractions [$R_f = 0.17$ (EtOAc)] gave the target compound **38f** as a yellow solid (25.6 mg, 28%).

mp: > 350 °C.

IR (ATR): ν_{\max} 3052, 2987, 2818, 1694 (C=O), 1519, 1363, 1240, 1006, 744 cm⁻¹.

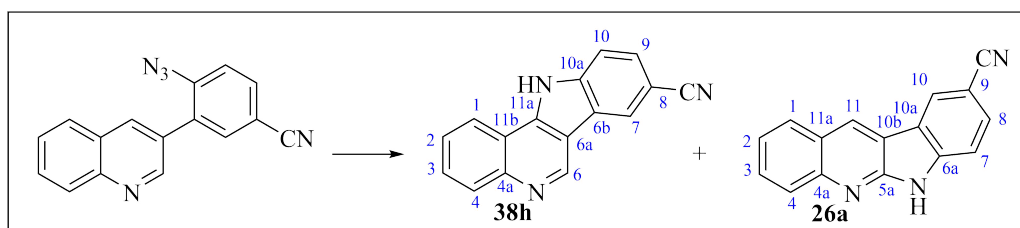
¹H NMR (400 MHz, DMSO-*d*₆): δ 12.88 (bs, 1H, NH), 10.41 (bs, 1H, NH-COCH₃), 9.52 (s, 1H, H-6), 8.72 (d, $J = 1.1$ Hz, 1H, H-1), 8.31 (d, $J = 7.8$ Hz, 1H, H-7), 7.71 (d, $J = 8.1$ Hz, 1H, H-10), 7.61-7.54 (m, 1H, H-3), 7.52-7.48 (m, 1H, H-9), 7.36-7.32 (m, 1H, H-8), 2.17 (s, 3H, CH₃).

¹³C NMR (100 MHz, DMSO-*d*₆): δ 168.0 (C=O), 157.9 (d, $J_{CF} = 252.6$ Hz, C-4), 143.3 (C-6), 139.1 (C-10a), 136.5 (d, $J_{CF} = 10.8$ Hz, C-4a), 132.0 (d, $J_{CF} = 2.6$ Hz, C-2), 130.1 (dd, $J_{CF} = 274.9$ Hz, 10.0 Hz, C-3), 125.9 (C-9), 121.7 (C-11a), 120.7 (C-8), 120.3 (C-7), 119.0 (d, $J_{CF} = 3.8$ Hz, C-11b), 115.2 (C-6b), 112.1 (C-10), 106.1 (d, $J_{CF} = 23.0$ Hz, C-6a), 105.8 (d, $J_{CF} = 3.3$ Hz, C-1), 21.2 (CH₃).

¹⁹C NMR (376 MHz, DMSO-*d*₆): δ -121.5.

HRMS (ESI): sample sent to UiB for analysis.

11*H*-Indolo[3,2-*c*]quinoline-8-carbonitrile (**38h**)



Method 3: Following the general procedure, the title compounds were prepared by irradiating 4-azido-3-(quinolin-3-yl)benzotrile (**131h**) (100.0 mg, 0.37 mmol) in α,α,α -trifluorotoluene (150 mL) for 3 hours. Purification by silica gel column chromatography (pet. ether/EtOAc, 1:1 \rightarrow 4:6 v/v) and concentration of the relevant fractions [$R_f = 0.18$ and 0.32 (pet. ether/EtOAc, 1:1 v/v) for compounds **38h** and **26a**, respectively] gave the target compound **38h** as a yellow solid (28.2 mg, 31%) along with compound **26a** as an off-white solid (4.7 mg, 5%).

Characterization of compound **38h**:

mp: > 350 °C (lit.^[285] 397-398 °C).

IR (ATR): ν_{\max} 2957, 2921, 2850, 2220 (CN), 1567, 1244, 1218, 751 cm^{-1} .

^1H NMR (400 MHz, DMSO- d_6): δ 13.25 (bs, 1H, NH), 9.69 (s, 1H, H-6), 8.93 (t, $J = 1.0$ Hz, 1H, H-7), 8.55-8.53 (m, 1H, H-1), 8.18 (dd, $J = 8.4$ Hz, 0.9 Hz, 1H, H-3), 7.87 (d, $J = 1.1$ Hz, 2H, H-9 and H-10), 7.83-7.79 (m, 1H, H-4), 7.77-7.73 (m, 1H, H-2).

^{13}C NMR (100 MHz, DMSO- d_6): δ 145.8 (C-4a), 145.1 (C-6), 141.0 (C-11a), 140.7 (C-10a), 129.6 (C-3), 128.8 (C-4), 128.4 (C-9), 126.3 (C-2), 125.7 (C-7), 122.2 (C-1), 122.0 (CN), 120.1 (C-6b), 116.8 (C-11b), 113.7 (C-6a), 113.1 (C-10), 102.6 (C-8).

In accordance with previously reported data.^[285]

Characterization of compound **26a**:

mp: 263 °C (decomp.).

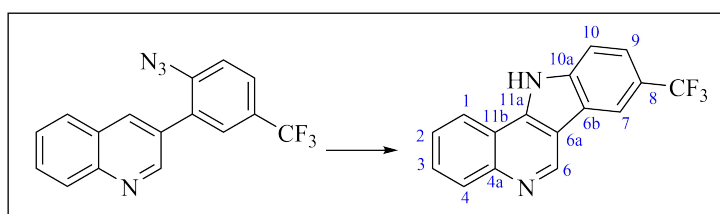
IR (ATR): ν_{\max} 2922, 2850, 2718 (CN), 1610, 746 cm^{-1} .

^1H NMR (400 MHz, DMSO- d_6): δ 12.26 (bs, 1H, NH), 9.18 (s, 1H, H-11), 8.81 (d, $J = 1.1$ Hz, 1H, H-10), 8.14 (d, $J = 7.5$ Hz, 1H, H-1), 8.02 (d, $J = 8.5$ Hz, 1H, H-3), 7.91 (dd, $J = 8.4$ Hz, 1.5 Hz, 1H, H-8), 7.81-7.76 (m, 1H, H-4), 7.62 (d, $J = 8.4$ Hz, 1H, H-7), 7.56-7.52 (m, 1H, H-2).

^{13}C NMR (100 MHz, DMSO- d_6): δ 152.9 (C-5a), 148.6 (C-4a), 143.9 (C-6a), 131.5 (C-4), 129.5 (C-8), 129.2 (C-1), 128.9 (C-11), 127.3 (C-3), 126.6 (C-10), 123.9 (CN), 123.5 (C-2), 120.8 (C-10b), 120.0 (C-11a), 116.6 (C-10a), 111.9 (C-7), 101.4 (C-9).

HRMS (ESI): sample sent to UiB for analysis.

8-(Trifluoromethyl)-11H-indolo[3,2-c]quinoline (**38i**)



Method 3: Following the general procedure, the title compound was prepared by irradiating 3-(2-azido-5-(trifluoromethyl)phenyl)quinoline (**131i**) (40.0 mg, 0.13 mmol) in α,α,α -trifluorotoluene (150 mL) for 30 minutes. Purification by silica gel column chromatography ($\text{CH}_2\text{Cl}_2/\text{EtOAc}$, 9:1 v/v) gave the target compound **38i** as a pink solid (8.8 mg, 24%).

mp: 347-348 °C.

IR (ATR): ν_{max} 3033, 2937, 2849, 2671, 1327, 1102, 753 cm^{-1} .

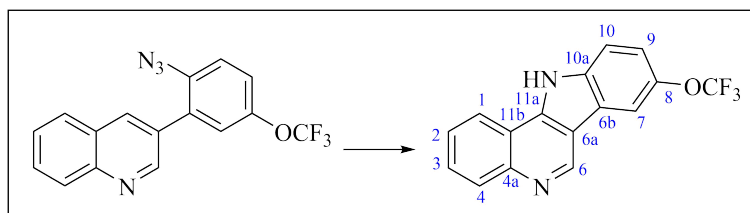
^1H NMR (400 MHz, DMSO- d_6): δ 13.12 (bs, 1H, NH), 9.75 (s, 1H, H-6), 8.81 (s, 1H, H-7), 8.54 (dd, $J = 7.8$ Hz, 1.1 Hz, 1H, H-1), 8.17 (d, $J = 8.2$ Hz, 1H, H-3), 7.89 (d, $J = 8.5$ Hz, 1H, H-10), 7.81-7.77 (m, 2H, H-4 and H-9), 7.75-7.71 (m, 1H, H-2).

^{13}C NMR (100 MHz, DMSO- d_6): δ 146.2 (C-4a), 145.7 (C-6), 141.5 (C-11a), 140.9 (C-10a), 130.1 (C-3), 129.1 (C-4), 126.5 (C-2), 125.7 (q, $J_{\text{CF}} = 271.8$ Hz, CF_3), 122.6 (C-1), 122.4 (q, $J_{\text{CF}} = 3.7$ Hz, C-9), 122.1 (C-11b), 121.7 (q, $J_{\text{CF}} = 31.5$ Hz, C-8), 118.5 (q, $J_{\text{CF}} = 4.2$ Hz, C-7), 117.4 (C-6b), 114.6 (C-6a), 113.0 (C-10).

^{19}F NMR (376 MHz, DMSO- d_6): δ -58.2.

HRMS (ESI): sample sent to UiB for analysis.

8-(Trifluoromethoxy)-11H-indolo[3,2-c]quinoline (**38j**)



Method 3: Following the general procedure, the title compound was prepared by irradiating 3-(2-azido-5-(trifluoromethoxy)phenyl)quinoline (**131j**) (150.0 mg, 0.45 mmol) in α,α,α -trifluorotoluene (150 mL) for 30 minutes to give the target compound **38j** as an orange solid (129.7 mg, 95%), which was essentially pure by NMR.

mp: 313 °C (decomp.).

IR (ATR): ν_{max} 3036, 2926, 2851, 2752, 1277, 1240, 1206, 1145, 754 cm^{-1} .

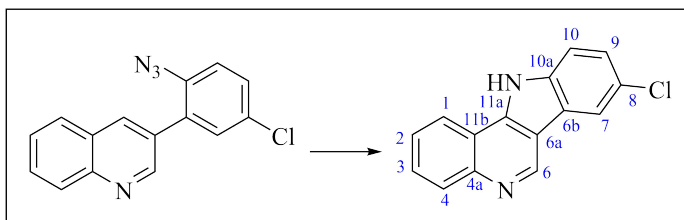
^1H NMR (400 MHz, DMSO- d_6): δ 12.97 (bs, 1H, NH), 9.67 (s, 1H, H-6), 8.53 (dd, $J = 8.1$ Hz, 1.0 Hz, 1H, H-1), 8.41 (d, $J = 0.9$ Hz, 1H, H-7), 8.15 (d, $J = 8.1$ Hz, 1H, H-3), 7.81-7.70 (m, 3H, H-2, H-4 and H-10), 7.47 (dd, $J = 8.7$ Hz, 1.2 Hz, 1H, H-9).

^{13}C NMR (100 MHz, DMSO- d_6): δ 145.5 (C-4a), 145.1 (C-6), 142.6 (q, $J_{\text{CF}} = 1.6$ Hz, C-8), 141.1 (C-10a), 137.2 (C-11a), 129.5 (C-3), 128.5 (C-4), 125.9 (C-2), 122.4 (C-11b), 122.1 (C-1), 120.4 (q, $J_{\text{CF}} = 255.1$ Hz, OCF_3), 119.0 (C-9), 116.9 (C-6a), 114.1 (C-6b), 113.1 (C-10), 113.0 (C-7).

^{19}F NMR (376 MHz, DMSO- d_6): δ -56.7.

HRMS (ESI): sample sent to UiB for analysis.

8-Chloro-11H-indolo[3,2-c]quinoline (38k)



Method 3: Following the general procedure, the title compound was prepared by irradiating 3-(2-azido-5-chlorophenyl)quinoline (**131k**) (180.0 mg, 0.64 mmol) in α,α,α -trifluorotoluene (150 mL) for 2 hours. Purification by silica gel column chromatography ($\text{CH}_2\text{Cl}_2/\text{EtOAc}$, 1:1 \rightarrow 0:1 v/v) and concentration of the relevant fractions [$R_f = 0.33$ ($\text{CH}_2\text{Cl}_2/\text{EtOAc}$, 1:1 v/v)] gave the target compound **38k** as an off-white solid (75.5 mg, 47%).

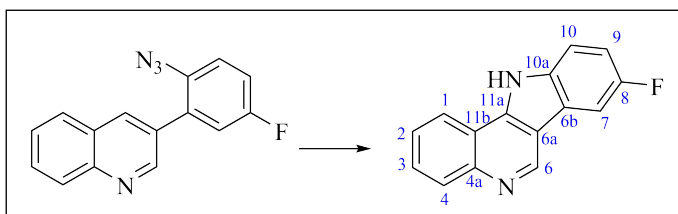
mp: 346 °C (lit. ^[284] > 300 °C).

IR (ATR): ν_{max} 2954, 2926, 2865, 1598, 1458, 796, 756 cm^{-1} .

^1H NMR (400 MHz, DMSO- d_6): δ 12.87 (bs, 1H, NH), 9.62 (s, 1H, H-6), 8.50 (dd, $J = 7.9$ Hz, 1.1 Hz, 1H, H-1), 8.44 (d, $J = 2.0$ Hz, 1H, H-7), 8.14 (dd, $J = 8.4$ Hz, 0.9 Hz, 1H, H-3), 7.78-7.74 (m, 1H, H-4), 7.73-7.68 (m, 2H, H-2 and H-10), 7.49 (dd, $J = 8.6$ Hz, 2.1 Hz, 1H, H-9).

^{13}C NMR (100 MHz, DMSO- d_6): δ 145.6 (C-4a), 145.1 (C-6), 140.5 (C-11a), 137.2 (C-10a), 129.6 (C-3), 128.4 (C-4), 125.9 (C-2), 125.3 (C-9), 125.0 (C-8), 123.2 (C-11b), 122.1 (C-1), 119.8 (C-7), 116.9 (C-6b), 113.6 (C-6a), 113.3 (C-10).

8-Fluoro-11H-indolo[3,2-c]quinoline (38l)



Method 3: Following the general procedure, the title compound was prepared by irradiating 3-(2-azido-5-fluorophenyl)quinoline (**131l**) (50.0 mg, 0.21 mmol) in α,α,α -trifluorotoluene (150 mL) for 30 minutes. Purification by silica gel column chromatography (CHCl_3) and concentration of the relevant fractions [$R_f = 0.30$ (CHCl_3)] gave the target compound **38l** as a pale yellow

solid (41.6 mg, 84%).

mp: > 350 °C (lit.^[282] 376-377 °C).

IR (ATR): ν_{\max} 3114, 3038, 2922, 2751, 1507, 1457, 1150, 755 cm^{-1} .

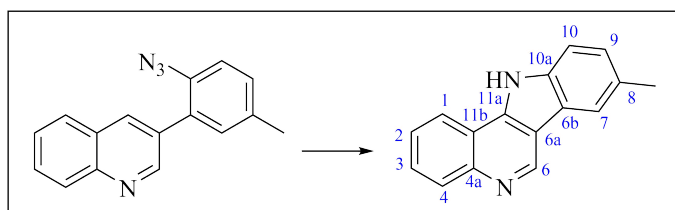
¹H NMR (400 MHz, DMSO-*d*₆): δ 12.82 (bs, 1H, NH), 9.59 (s, 1H, H-6), 8.51 (dd, $J = 7.9$ Hz, 1.1 Hz, 1H, H-1), 8.17 (dd, $J = 9.5$ Hz, 2.5 Hz, 1H, H-7), 8.15-8.13 (m, 1H, H-3), 7.78-7.74 (m, 1H, H-4), 7.73-7.68 (m, 2H, H-2 and H-10), 7.35 (td, $J = 9.3$ Hz, 2.6 Hz, 1H, H-9).

¹³C NMR (100 MHz, DMSO-*d*₆): δ 157.5 (d, $J_{\text{CF}} = 234.8$ Hz, C-8), 145.4 (C-4a), 145.1 (C-6), 140.9 (C-11a), 135.3 (C-10a), 129.5 (C-3), 128.4 (C-4), 125.9 (C-2), 122.5 (d, $J_{\text{CF}} = 10.5$ Hz, C-6b), 122.1 (C-1), 117.1 (C-11b), 114.2 (d, $J_{\text{CF}} = 4.4$ Hz, C-6a), 113.4 (d, $J_{\text{CF}} = 25.6$ Hz, C-10), 113.0 (d, $J_{\text{CF}} = 9.5$ Hz, C-9), 105.7 (d, $J_{\text{CF}} = 24.4$ Hz, C-7).

¹⁹F NMR (376 MHz, DMSO-*d*₆): δ -122.1.

In accordance with previously reported data.^[282]

8-Methyl-11*H*-indolo[3,2-*c*]quinoline (38m)



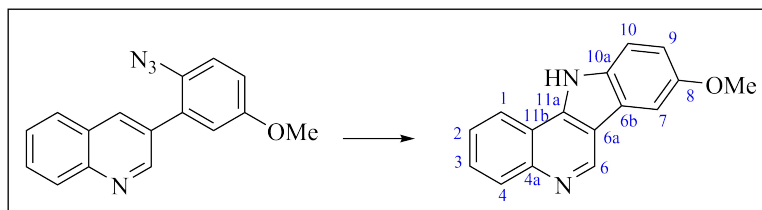
Method 3: Following the general procedure, the title compound was prepared by irradiating 3-(2-azido-5-methylphenyl)quinoline (**131m**) (272.9 mg, 1.05 mmol) in α,α,α -trifluorotoluene (150 mL) for 1.5 hours. The crude was filtered through a Celite pad using CH_2Cl_2 to give the target compound **38m** as a dark orange solid (221.1 mg, 91%).

mp: 304-306 °C (lit.^[106] 305-311 °C).

¹H NMR (400 MHz, DMSO-*d*₆): δ 12.60 (bs, 1H, NH), 8.50 (dd, $J = 7.9$ Hz, 1.1 Hz, 1H, H-1), 8.13-8.10 (m, 2H, H-4 and H-7), 7.74-7.65 (m, 2H, H-2 and H-3), 7.60 (d, $J = 8.3$ Hz, 1H, H-10), 7.32 (dd, $J = 8.3$ Hz, 1.2 Hz, 1H, H-9), 2.51 (s, 3H, CH_3).

¹³C NMR (100 MHz, DMSO-*d*₆): δ 145.2 (C-4a), 144.6 (C-6), 139.9 (C-11a), 137.0 (C-10a), 129.5 (C-8), 129.4 (C-4), 127.9 (C-2), 126.9 (C-9), 125.6 (C-3), 122.0 (C-1), 119.7 (C-7), 117.1 (C-6a), 114.1 (C-11b), 111.5 (C-10), 21.2 (CH_3). C-6b was obscured or overlapping.

In accordance with previously reported data.^[106]

8-Methoxy-11H-indolo[3,2-c]quinoline (38n)

Method 3: Following the general procedure, the title compound was prepared by irradiating 3-(2-azido-5-methoxyphenyl)quinoline (**131n**) (40.0 mg, 0.14 mmol) in α,α,α -trifluorotoluene (150 mL) for 30 minutes. Purification by silica gel column chromatography ($\text{CH}_2\text{Cl}_2/\text{EtOAc}$, 1:1 v/v) and concentration of the relevant fractions [$R_f = 0.12$ ($\text{CH}_2\text{Cl}_2/\text{EtOAc}$, 1:1 v/v)] gave the target compound **38n** as a light brown solid (16.9 mg, 49%).

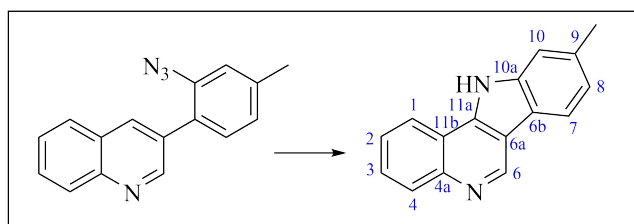
mp: 275-278 °C (lit.^[282] 327-328 °C).

IR (ATR): ν_{max} 3028, 2922, 2825, 2779, 1627, 1578, 1474, 1206, 799, 753 cm^{-1} .

$^1\text{H NMR}$ (400 MHz, $\text{DMSO}-d_6$): δ 12.59 (bs, 1H, NH), 9.59 (s, 1H, H-6), 8.50 (dd, $J = 7.8$ Hz, 0.8 Hz, 1H, H-1), 8.12 (d, $J = 8.1$ Hz, 1H, H-3), 7.90 (d, $J = 2.4$ Hz, 1H, H-7), 7.75-7.71 (m, 1H, H-4), 7.69-7.65 (m, 1H, H-2), 7.61 (d, $J = 8.8$ Hz, 1H, H-10), 7.12 (dd, $J = 8.7$ Hz, 2.5 Hz, 1H, H-9), 3.89 (s, 3H, OCH_3).

$^{13}\text{C NMR}$ (100 MHz, $\text{DMSO}-d_6$): δ 154.5 (C-8), 145.1 (C-4a), 144.8 (C-6), 140.1 (C-11a), 133.5 (C-10a), 129.3 (C-3), 127.9 (C-4), 125.6 (C-2), 122.4 (C-6a), 122.0 (C-1), 117.2 (C-11b), 115.1 (C-9), 114.4 (C-6b), 112.5 (C-10), 102.5 (C-7), 55.6 (OCH_3).

In accordance with previously reported data.^[282]

9-Methyl-11H-indolo[3,2-c]quinoline (38o)

Method 3: Following the general procedure, the title compound was prepared by irradiating 3-(2-azido-4-methylphenyl)quinoline (**131o**) (70.0 mg, 0.27 mmol) in α,α,α -trifluorotoluene (150 mL) for 1 hour. Purification by silica gel column chromatography ($\text{CH}_2\text{Cl}_2/\text{EtOAc}$, 1:1 \rightarrow 0:1 v/v) and concentration of the relevant fractions [$R_f = 0.24$ ($\text{CH}_2\text{Cl}_2/\text{EtOAc}$, 1:1 v/v)] gave the target compound **38o** as a yellow solid (21.7 mg, 35%).

mp: > 350 °C (lit.^[283] 310 °C).

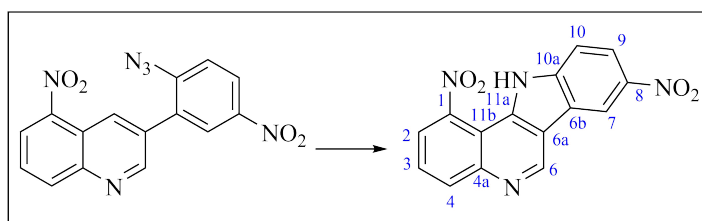
IR (ATR): ν_{\max} 3048, 2916, 2853, 1566, 1508, 1237, 755 cm^{-1} .

¹H NMR (400 MHz, DMSO-*d*₆): δ 12.57 (bs, 1H, NH), 9.54 (s, 1H, H-6), 8.50 (dd, *J* = 7.8 Hz, 1.1 Hz, 1H, H-1), 8.17 (d, *J* = 8.0 Hz, 1H, H-7), 8.13-8.11 (m, 1H, H-4), 7.74-7.65 (m, 2H, H-2 and H-3), 7.50 (s, 1H, H-10), 7.16 (d, *J* = 8.0 Hz, 1H, H-9), 2.53 (s, 3H, CH₃).

¹³C NMR (100 MHz, DMSO-*d*₆): δ 145.2 (C-4a), 144.5 (C-6), 139.6 (C-11a), 139.3 (C-10a), 135.2 (C-9), 129.5 (C-4), 127.7 (C-2), 125.5 (C-3), 122.2 (C-8), 121.9 (C-1), 119.7 (C-7), 117.1 (C-6a), 114.3 (C-6b), 111.7 (C-10), 21.6 (CH₃).

In accordance with previously reported data.^[283]

1,8-Dinitro-11*H*-indolo[3,2-*c*]quinoline (38p)



Method 3: Following the general procedure, the title compound was prepared by irradiating 3-(2-azido-5-nitrophenyl)-5-nitroquinoline (**131p**) (56.3 mg, 0.17 mmol) in α,α,α -trifluorotoluene (150 mL) for 1.5 hours. Purification by silica gel column chromatography (pet. ether/EtOAc, 1:1 v/v) and concentration of the relevant fractions [R_f = 0.46 (pet. ether/EtOAc, 1:1 v/v)] gave the target compound **38p** as an orange solid (6.6 mg, 13%).

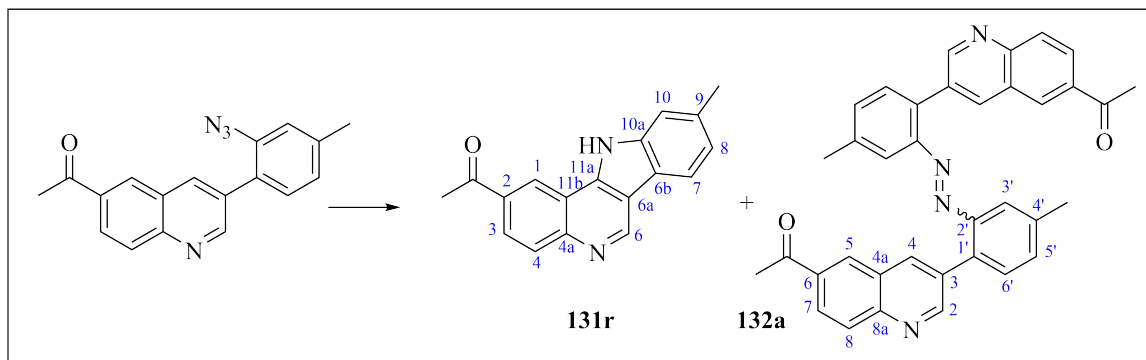
mp: >350 °C.

IR (ATR): ν_{\max} 3381, 3086, 3051, 2919, 1506, 1332, 732 cm^{-1} .

¹H NMR (100 MHz, DMSO-*d*₆): δ 12.17 (bs, 1H, NH), 10.00 (s, 1H, H-6), 9.44 (d, *J* = 2.2 Hz, 1H, H-7), 8.52 (d, *J* = 7.9 Hz, 1H, H-2), 8.39-8.36 (m, 2H, H-4 and H-9), 7.97 (d, *J* = 9.1 Hz, 1H, H-10), 7.95-7.92 (m, 1H, H-3).

¹³C NMR (100 MHz, DMSO-*d*₆): δ 147.1 (C-6), 146.5 (C-1), 144.7 (C-10a), 142.2 (C-11a), 142.0 (C-11b), 136.4 (C-8), 136.2 (C-2), 127.4 (C-3), 124.3 (C-4), 121.7 (C-9), 120.3 (C-6b), 117.5 (C-6a), 117.5 (C-7), 113.4 (C-10), 109.4 (C-11b).

HRMS (ESI): sample sent to UiB for analysis.

2-Acetyl-9-methyl-11Hindolo[3,2-c]quinoline (38r)

Method 3: Following the general procedure, the title compounds were prepared by irradiating 3-(2-azido-4-methylphenyl)-6-acetylquinoline (**131r**) (182.7 mg, 0.60 mmol) in α,α,α -trifluorotoluene (150 mL) for 1.5 hours. Purification by silica gel column chromatography (pet. ether/EtOAc, 1:1 \rightarrow 4:6 v/v) and concentration of the relevant fractions [$R_f = 0.21$ and 0.55 (pet. ether/EtOAc, 4:6 v/v) for compounds **38r** and **132a**] gave target compound **38r** as an orange solid (35.9 mg, 22%) along with compound **132a** as a yellow solid (5.9 mg, 3%).

Characterization of compound **38r**:

mp: 319-320 °C.

IR (ATR): ν_{\max} 3059, 2955, 2920, 2853, 1677 (C=O), 1361, 1322, 1232, 825 cm^{-1} .

$^1\text{H NMR}$ (400 MHz, DMSO- d_6): δ 12.83 (bs, 1H, NH), 9.64 (s, 1H, H-6), 9.27 (d, $J = 0.9$ Hz, 1H, H-1), 8.22-8.18 (m, 3H, H-3, H-4 and H-7), 7.54 (s, 1H, H-10), 7.20 (d, $J = 8.0$ Hz, 1H, H-8), 2.78 (s, 3H, CO-CH₃), 2.55 (s, 3H, CH₃).

$^{13}\text{C NMR}$ (100 MHz, DMSO- d_6): δ 197.3 (C=O), 147.1 (C-4a), 146.6 (C-6), 140.4 (C-11a), 139.3 (C-10a), 135.7 (C-2), 133.3 (C-9), 129.7 (C-6b), 111.8 (C-10), 26.8 (CO-CH₃), 21.6 (CH₃).

HRMS (ESI): calcd. for C₁₈H₁₄N₂O [$M + H^+$] 275.1179, found 275.1180.

Characterization of compound **132a**:

mp: 159-161 °C.

IR (ATR): ν_{\max} 3049, 2923, 2855, 1680 (C=O), 1527, 1357, 840 cm^{-1} .

$^1\text{H NMR}$ (400 MHz, DMSO- d_6): δ 8.86 (d, $J = 2.3$ Hz, 2H, H-2), 8.78 (d, $J = 1.8$ Hz, 2H, H-5), 8.55 (d, $J = 2.1$ Hz, 2H, H-4), 8.26 (dd, $J = 8.8$ Hz, 2.0 Hz, 2H, H-7), 8.14 (d, $J = 8.8$ Hz, 2H, H-8), 8.03 (s, 2H, H-3'), 7.72-7.70 (m, 2H, H-5'), 7.62 (d, $J = 7.8$ Hz, 2H, H-6'), 2.73 (s, 6H, CO-CH₃), 2.50 (s, 7H, CH₃).

^{13}C NMR (100 MHz, DMSO- d_6): δ 197.4 (C=O), 152.0 (C-2), 148.3 (C-8a), 148.1 (C-2'), 140.3 (C-4'), 135.9 (C-4), 134.9 (C-6), 134.3 (C-5'), 132.4 (C-6'), 131.7 (C-3), 130.7 (C-5), 129.3 (C-1'), 129.1 (C-8), 127.7 (C-7), 126.6 (C-4a), 124.9 (C-3'), 26.8 (CO-CH₃), 20.3 (CH₃).

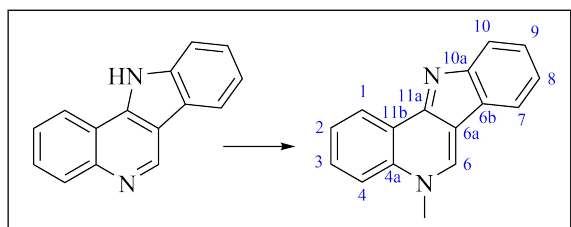
HRMS (ESI): sample sent to UiB for analysis.

7.2.6 N-Methylations to obtain ringsystems

General procedure

To a solution of tetracycle (1 equiv.) in an appropriate amount of CH₃CN, CH₃I (100 equiv.) was added and the resulting mixture refluxed until completion as determined by TLC analysis. The volatiles were then removed under reduced pressure and the concentrate was evaporated onto celite. Purification by the column chromatography using the eluent as indicated gave the hydroiodide salt of the target compounds. To obtain the free base, the hydroiodide salt was dissolved in a 1:1 mixture of CH₂Cl₂ and NH_{3(aq)} (20%) and stirred at rt for 15-45 minutes. The organic layer was separated and the aqueous layers were extracted with CHCl₃ (3 x 15 mL) and the combined organic layers were washed with water (1 x 15 mL), brine (1 x 15 mL), dried (MgSO₄), filtered and concentrated *in vacuo* to give the target tetracycle.

Isocryptolepine (25)



Following the general procedure, isocryptolepine (**25**) was prepared from 11*H*-indolo[3,2-*c*]quinoline (**38**) (34.0 mg, 0.20 mmol), CH₃I (1.0 mL, 15.6 mmol) in CH₃CN (2 mL). After a reaction time of 19 hours, the crude was purified by silica gel DVFC (CHCl₃/MeOH, 95:5 v/v) and concentration of the relevant fractions [R_f = 0.18 (CHCl₃/MeOH, 95:5 v/v)] to give the hydroiodide salt of isocryptolepine. The free base was obtained according to the general procedure to give the target compound **25** as a pale yellow crystalline solid (24.3 mg, 69%).

mp: 188-192 °C (lit.^[124] 185-187 °C).

IR (NaCl): ν_{max} 3049, 2923, 2852, 1638, 1598, 1455, 1351 cm⁻¹.

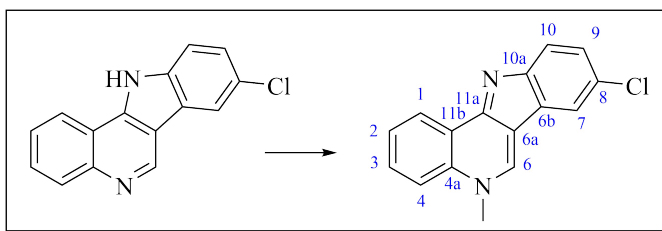
^1H NMR (400 MHz, DMSO- d_6): δ 9.38 (s, 1H, H-6), 8.77 (dd, J = 8.0 Hz, 1.4 Hz, 1H, H-1), 8.14-8.11 (m, 1H, H-7), 8.07 (d, J = 8.6 Hz, 1H, H-4), 7.86 (ddd, J = 8.6 Hz, 7.0 Hz, 1.6

Hz, 1H, H-3), 7.80-7.78 (m, 1H, H-10), 7.74-7.70 (m, 1H, H-2), 7.42 (ddd, $J = 8.2$ Hz, 7.1 Hz, 1.2 Hz, 1H, H-9), 7.25-7.21 (m, 1H, H-8), 4.28 (s, 3H, NCH₃).

¹³C NMR (100 MHz, DMSO-*d*₆): δ 154.1 (C-10a), 152.3 (C-11a), 138.4 (C-6), 135.5 (C-4a), 129.6 (C-3), 129.3 (C-6b), 125.5 (C-9), 125.3 (C-2), 123.9 (C-1), 120.9 (C-11b), 119.8 (C-8), 119.5 (C-7), 118.3 (C-10), 117.6 (C-4), 116.1 (C-6a), 42.2 (NCH₃).

In accordance with previously reported data.^[124]

8-Chloro-5-methyl-5H-indolo[3,2-*c*]quinoline (25a)



Following the general procedure, the title compound was prepared from 8-chloro-11H-indolo[3,2-*c*]quinoline (**38k**) (50.0 mg, 0.20 mmol), CH₃I (1.23 mL, 20.0 mmol) in CH₃CN (5 mL). After a reaction time of 20 hours, the crude was purified by silica gel column chromatography (CHCl₃/MeOH, 9:1 → 9:1 + 2% NH_{3(aq)} v/v) and concentration of the relevant fractions [$R_f = 0.05$ (CHCl₃/MeOH, 9:1 v/v)] gave the hydroiodide salt of compound **25a** as a bright yellow powder. The free base was liberated following the general procedure to obtain the target compound **25a** as a bright yellow solid (43.2 mg, 81%).

mp: 264-265 °C (lit.^[261] 257-259 °C).

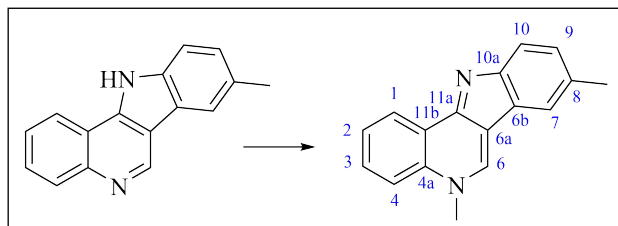
IR (ATR): ν_{\max} 3339, 3251, 2916, 2848, 1637, 1439, 808, 745, 718 cm⁻¹.

¹H NMR (400 MHz, DMSO-*d*₆): δ 9.39 (s, 1H, H-6), 8.75 (d, $J = 7.7$ Hz, 1H, H-1), 8.15 (d, $J = 2.1$ Hz, 1H, H-4), 8.05 (d, $J = 8.5$ Hz, 1H, H-4), 7.89-7.83 (m, 1H, H-3), 7.76 (d, $J = 8.5$ Hz, 1H, H-10), 7.74-7.70 (m, 1H, H-2), 7.41 (dd, $J = 8.5$ Hz, 2.1 Hz, 1H, H-9), 4.24 (s, 3H, NCH₃).

¹³C NMR (100 MHz, DMSO-*d*₆): δ 152.9 (C-10a), 152.4 (C-11a), 139.5 (C-6), 135.5 (C-4a), 129.6 (C-3), 126.8 (C-11b), 125.6 (C-2), 125.2 (C-9), 124.0 (C-8), 123.9 (C-1), 121.0 (C-6b), 119.4 (C-10), 119.2 (C-7), 117.8 (C-4), 115.3 (C-6a), 42.5 (NCH₃).

In accordance with previously reported data.^[261]

5,8-Dimethyl-5*H*-indolo[3,2-*c*]quinoline (25b)



Following the general procedure, the title compound was prepared from 8-methyl-11*H*-indolo[3,2-*c*]quinoline (**38m**) (100.0 mg, 0.43 mmol), CH₃I (2.68 mL, 43.08 mmol) in CH₃CN (20 mL). After a reaction time of 25 hours, the crude was purified by silica gel column chromatography (CHCl₃/MeOH, 9:1 v/v) and concentration of the relevant fractions [*R*_f = 0.05 (CHCl₃/MeOH, 9:1 v/v)] gave the hydroiodide salt of compound **25b** as a light brown solid. The free base was liberated following the general procedure to obtain the target compound **25b** as an orange oil (29.4 mg, 28%).

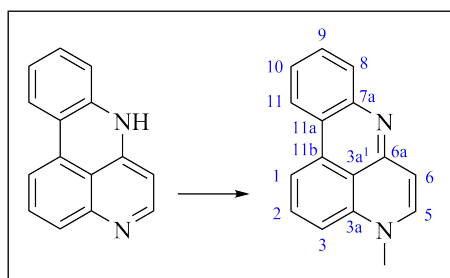
IR (ATR): ν_{\max} 3051, 2924, 2855, 1640, 1605, 1449, 1337, 1220, 756 cm⁻¹.

¹H NMR (400 MHz, DMSO-*d*₆): δ 9.25 (s, 1H, H-6), 8.73 (dd, *J* = 8.0 Hz, 1.3 Hz, 1H, H-1), 8.01 (d, *J* = 8.5 Hz, 1H, H-4), 7.89-7.88 (m, 1H, H-7), 7.83-7.79 (m, 1H, H-3), 7.69-7.65 (m, 2H, H-2 and H-10), 7.25-7.23 (m, 1H, H-9), 4.23 (s, 3H, NCH₃), 2.50 (s, 3H, CH₃).

¹³C NMR (100 MHz, DMSO-*d*₆): δ 152.6 (C-11a), 152.2 (C-10a), 137.9 (C-6), 135.4 (C-4a), 129.0 (C-3), 128.5 (C-8), 126.9 (C-9), 125.8 (C-6b), 125.0 (C-2), 123.8 (C-1), 121.1 (C-11b), 119.4 (C-7), 118.0 (C-10), 117.4 (C-4), 116.1 (C-6a), 42.0 (NCH₃), 21.4 (CH₃).

In accordance with previously reported data.^[106]

4-Methyl-4*H*-pyrido[4,3,2-*gh*]phenanthridine (84a)



Following the general procedure, the title compound # was prepared from 7*H*-pyrido[4,3,2-*gh*]phenanthridine (**54**) (70.0 mg, 0.32 mmol), CH₃I (2.0 mL, 32.0 mmol) in CH₃CN (2 mL). After a reaction time of 2 hours, the crude was purified by silica gel column chromatography (CHCl₃/MeOH, 95:5 + 0.3% NH₃(aq) v/v) and concentration of the relevant fractions [*R*_f = 0.33 (CHCl₃/MeOH, 95:5 + 0.3% NH₃(aq) v/v)] to give the hydroiodide salt of compound **84a**. The

free base was obtained according to the general procedure, take for Et₂O being used for the extractions instead of CHCl₃, to give the target compound **84a** as dark yellow crystals (52.8 mg, 71%).

mp: 182-183 °C.

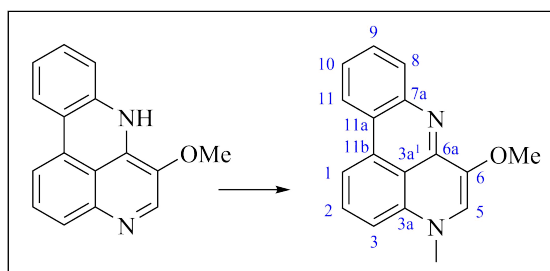
IR (ATR): ν_{\max} 3485, 3051, 2922, 2851, 2574, 1601, 1327, 820, 748 cm⁻¹.

¹H NMR (400 MHz, DMSO-*d*₆): δ 8.29 (dd, *J* = 8.1 Hz, 1.1 Hz, 1H, H-11), 7.97 (d, *J* = 7.9 Hz, 1H, H-1), 7.71 (t, *J* = 8.1 Hz, 1H, H-2), 7.56 (dd, *J* = 8.2 Hz, 1.2 Hz, 1H, H-8), 7.51-7.47 (m, 2H, H-5 and H-10), 7.30-7.26 (m, 1H, H-9), 7.05 (d, *J* = 8.1 Hz, 1H, H-3), 6.18 (d, *J* = 7.6 Hz, 1H, H-6), 3.45 (s, 3H, NCH₃).

¹³C NMR (100 MHz, DMSO-*d*₆): δ 152.9 (C-3a), 145.9 (C-7a), 141.0 (C-11b), 140.9 (C-5), 133.8 (C-6a), 131.6 (C-2), 129.2 (C-10), 127.0 (C-8), 123.2 (C-9), 122.9 (C-11), 121.3 (C-11a), 119.6 (C-3a¹), 112.2 (C-1), 108.8 (C-3), 106.2 (C-6), 39.6 (NCH₃).

HRMS (ESI): calcd. for C₁₆H₁₂N₂ [M + H⁺] 233.1073, found 233.1073.

6-Methoxy-4-methyl-4*H*-pyrido[4,3,2-*gh*]phenanthridine (**84b**)



Following the general procedure, the title compound was prepared from 6-methoxy-7*H*-pyrido[4,3,2-*gh*]phenanthridine (**54a**) (90.0 mg, 0.36 mmol), CH₃I (2.25 mL, 36.3 mmol) in CH₃CN (10 mL). After a reaction time of 2 hours, the crude was purified by silica gel column chromatography (EtOH + 0.1-5% NH₃(aq) v/v) and concentration of the relevant fractions [*R*_f = 0.23 (EtOH)] gave the hydroiodide salt of compound **84b**. The free base was obtained according to the general procedure to give the target compound **84b** as a dark yellow gel (55.1 mg, 58%).

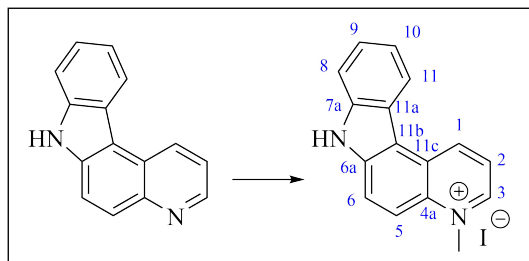
IR (ATR): ν_{\max} 2918, 2850, 1600, 1255, 1059, 745 cm⁻¹.

¹H NMR (400 MHz, CD₂Cl₂): δ 8.19 (dd, *J* = 8.2 Hz, 1.3 Hz, 1H, H-11), 7.79 (dd, *J* = 8.2 Hz, 1.0 Hz, 1H, H-2), 7.72 (d, *J* = 7.9 Hz, 1H, H-1), 7.57-7.51 (m, 2H, H-3 and H-9), 7.34-7.30 (m, 1H, H-10), 6.74-6.72 (m, 2H, H-5 and H-8), 3.85 (s, 3H, OCH₃), 3.34 (s, 3H, NCH₃).

¹³C NMR (100 MHz, CD₂Cl₂): δ 148.1 (C-6a), 146.3 (C-7a), 140.8 (C-6), 139.9 (C-3a), 134.8 (C-11b), 130.9 (C-3), 129.4 (C-9), 128.6 (C-2), 124.1 (C-10), 122.7 (C-11), 122.5 (C-8), 119.9 (C-3a¹), 110.6 (C-1), 107.7 (C-5), 57.1 (OCH₃), 40.4 (NCH₃). C-11a was obscured or overlapping.

HRMS (ESI): calcd. for C₁₇H₁₄N₂O [M + H⁺] 263.1179, found 263.1188.

4-Methyl-7H-pyrido[2,3-*c*]carbazolium iodide (**85**)



Following the general procedure, the title compound was prepared from 7H-pyrido[2,3-*c*]carbazole (**61**) (40.7 mg, 0.19 mmol), CH₃I (1.20 mL, 19.6 mmol) in CH₃CN (5 mL). After a reaction time of 20 hours, the crude was purified by silica gel column chromatography (CHCl₃/MeOH, 9:1 v/v + 1% NH₃(aq)) and concentration of the relevant fractions [*R*_f = 0.12 (CHCl₃/MeOH, 9:1 v/v + 2% NH₃(aq))] gave the target compound **85** as a bright yellow solid (20.9 mg, 47%).

mp: 284-286 °C.

IR (ATR): ν_{\max} 3353, 3043, 3006, 2960, 2921, 2853, 1556, 1370, 1326, 741 cm⁻¹.

¹H NMR (400 MHz, DMSO-*d*₆): δ 12.84 (bs, 1H, NH), 9.99 (d, *J* = 8.4 Hz, 1H, H-1), 9.39 (d, *J* = 5.6 Hz, 1H, H-3), 8.76 (d, *J* = 8.1 Hz, 1H, H-11), 8.50 (d, *J* = 9.3 Hz, 1H, H-6), 8.43 (d, *J* = 9.4 Hz, 1H, H-5), 8.22 (dd, *J* = 8.5 Hz, 5.7 Hz, 1H, H-2), 7.82 (d, *J* = 8.2 Hz, 1H, H-8), 7.64-7.60 (m, 1H, H-9), 7.48-7.44 (m, 1H, H-10), 4.74 (s, 3H, NCH₃).

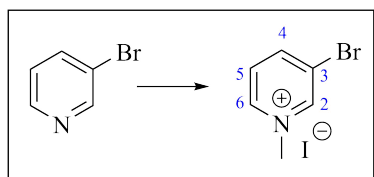
¹³C NMR (100 MHz, DMSO-*d*₆): δ 145.0 (C-3), 140.8 (C-1), 139.8 (C-7a), 137.5 (C-6a), 134.5 (C-4a), 126.6 (C-9), 125.8 (C-11c), 122.4 (C-6), 122.1 (C-11), 121.9 (C-2), 121.6 (C-11a), 121.1 (C-10), 116.0 (C-5), 114.3 (C-11b), 112.8 (C-8), 46.3 (NCH₃).

HRMS (ESI): calcd. for C₁₆H₁₃N₂I [M - I⁻] 233.1073, found 233.1073.

7.2.7 *N*-Alkylation to obtain pyridinium and quinolinium halides

General procedure

To a solution of either 3-bromopyridine (**120**) or 3-bromoquinoline (**67b**) in an appropriate amount of solvent, the alkylation reagent (5-10 equiv.) was added and the resulting mixture stirred at the relevant temperature under an argon atmosphere until completion as indicated by TLC analysis. The formed precipitate was thoroughly washed with *n*-hexanes, filtered and dried to give the target pyridinium or quinolinium salts **115**.

3-Bromo-*N*-methylpyridinium iodide (121)

Following the general procedure, the title compound was prepared from 3-bromopyridine (**120**) (0.31 mL, 3.16 mmol), CH₃I (0.98 mL, 15.80 mmol) in CH₃CN (20 mL). After refluxing for 24 hours, workup was carried out according to the general procedure to give the target compound **121** as yellow crystals (864.6 mg, 91%).

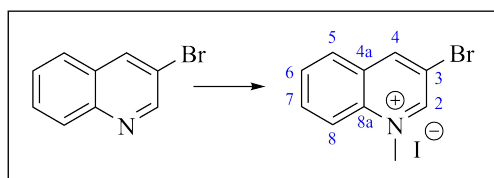
mp: 163-165 °C (lit.^[286] 163-164 °C).

IR (ATR): ν_{\max} 3016, 2980, 1627, 1459, 1318, 721 cm⁻¹.

¹H NMR (400 MHz, DMSO-*d*₆): δ 9.43 (s, 1H, H-2), 9.03 (d, $J = 6.0$ Hz, 1H, H-6), 8.85 (d, $J = 8.4$ Hz, 1H, H-4), 8.09 (dd, $J = 8.3$ Hz, 6.0 Hz, 1H, H-5), 4.34 (s, 3H, NCH₃).

¹³C NMR (100 MHz, DMSO-*d*₆): δ 147.3 (C-4), 146.8 (C-2), 144.6 (C-6), 128.3 (C-5), 121.4 (C-3), 48.1 (NCH₃).

In accordance with previously reported data.^[286]

3-Bromo-*N*-methylquinolinium iodide (115)

Following the general procedure, the title compound was prepared from 3-bromoquinoline (**67b**) (0.33 mL, 2.40 mmol), CH₃I (0.75 mL, 12.00 mmol) in CH₃CN (25 mL). After refluxing for 22 hours, workup was carried out according to the general procedure to give the target compound **115** as a bright yellow powder (835.3 mg, 99%).

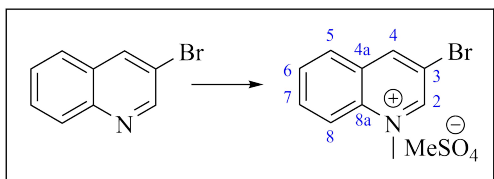
mp: 345-347 °C (lit.^[286] 288-289 °C).

IR (ATR): ν_{\max} 3423, 3033, 2923, 2852, 1515, 1215, 771 cm⁻¹.

¹H NMR (400 MHz, DMSO-*d*₆): δ 9.90 (d, $J = 1.6$ Hz, 1H, H-2), 9.64 (d, $J = 1.6$ Hz, 1H, H-4), 8.51-8.49 (m, 1H, H-8), 8.39 (dd, $J = 8.2$ Hz, 1.3 Hz, 1H, H-5), 8.33-8.28 (m, 1H, H-7), 8.11-8.07 (m, 1H, H-6), 4.62 (s, 3H, NCH₃).

¹³C NMR (100 MHz, DMSO-*d*₆): δ 151.3 (C-2), 148.1 (C-4), 137.2 (C-8a), 135.6 (C-7), 130.8 (C-6), 129.6 (C-4a), 129.5 (C-5), 119.2 (C-8), 114.4 (C-3), 45.3 (NCH₃).

In accordance with previously reported data.^[286]

3-Bromo-*N*-methylquinolinium methyl sulfate (115g)

Following the general procedure, the title compound was prepared from 3-bromoquinoline (**67b**) (0.65 mL, 4.81 mmol), Me₂SO₄ (1.14 mL, 12.02 mmol) in CH₃CN (25 mL). After refluxing for 24 hours, workup was carried out according to the general procedure to give the target compound **115g** as a yellow solid (1.47 g, 96%).

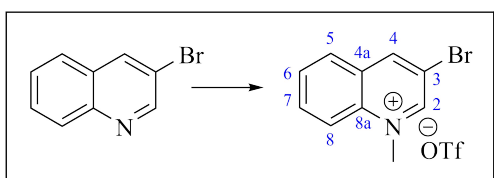
mp: 69-70 °C.

IR (ATR): ν 3145, 3095, 3048, 2945, 1676, 1522, 1218, 999, 734 cm⁻¹.

¹H NMR (400 MHz, DMSO-*d*₆): δ 9.87 (d, *J* = 1.6 Hz, 1H, H-2), 9.63 (d, *J* = 1.6 Hz, 1H, H-4), 8.50 (d, *J* = 8.9 Hz, 1H, H-8), 8.39 (dd, *J* = 8.3 Hz, 1.2 Hz, 1H, H-5), 8.31-8.27 (m, 1H, H-7), 8.09-8.06 (m, 1H, H-6), 4.63 (s, 3H, NCH₃).

¹³C NMR (100 MHz, DMSO-*d*₆): δ 151.4 (C-2), 148.1 (C-4), 137.2 (C-8a), 135.6 (C-4a), 130.8 (C-6), 129.6 (C-5), 129.5 (C-7), 119.3 (C-8), 114.4 (C-3), 45.3 (NCH₃).

HRMS (ESI): sample sent to UiB for analysis.

3-Bromo-*N*-methylquinolinium triflate (115k)

Following the general procedure, the title compound was prepared from 3-bromoquinoline (**67b**) (0.33 mL, 2.40 mmol), MeOTf (0.29 mL, 2.60 mmol) in anhydrous CH₂Cl₂ (10 mL). After 19 hours at rt, workup was carried out according to the general procedure to give the target compound **115k** as a white solid (1.16 g, quant.).

mp: 215-218 °C.

IR (ATR): ν_{\max} 3150, 3100, 3054, 1523, 1258, 1028, 775 cm⁻¹.

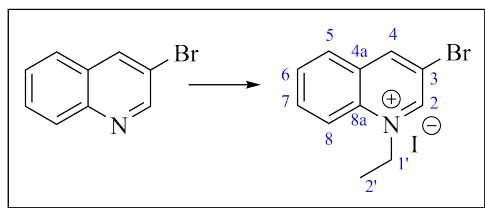
¹H NMR (400 MHz, DMSO-*d*₆): δ 9.88 (d, *J* = 1.6 Hz, 1H, H-2), 9.63 (d, *J* = 1.7 Hz, 1H, H-4), 8.50 (dd, *J* = 8.9 Hz, 0.5 Hz, 1H, H-8), 8.39 (dd, *J* = 8.2 Hz, 1.3 Hz, 1H, H-5), 8.32-8.28 (m, 1H, H-7), 8.11-8.07 (m, 1H, H-6), 4.63 (s, 3H, NCH₃).

^{13}C NMR (100 MHz, DMSO- d_6): δ 151.4 (C-2), 148.1 (C-4), 137.2 (C-8a), 135.6 (C-4a), 130.8 (C-6), 129.6 (C-7), 120.6 (q, $J_{\text{CF}} = 322.9$ Hz, OCF_3), 119.2 (C-8), 114.4 (C-3), 45.3 (NCH $_3$).

^{19}F NMR (376 MHz, DMSO- d_6): δ -77.5.

HRMS (ESI): sample sent to UiB for analysis.

3-Bromo-*N*-ethylquinolinium iodide (115a)



Following the general procedure, the title compound was prepared from 3-bromoquinoline (**67b**) (0.65 mL, 4.81 mmol), EtI (3.85 mL, 48.10 mmol) in CH_3CN (50 mL). After refluxing for 42 hours, workup was carried out according to the general procedure to give the target compound **115a** as a yellow solid (1.47 g, 84%).

mp: 235-237 °C.

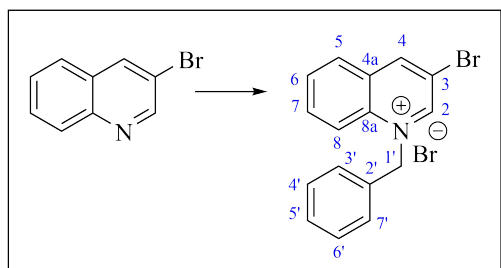
IR (ATR): ν_{max} 2998, 2965, 2928, 1571, 1516, 781 cm^{-1} .

^1H NMR (400 MHz, DMSO- d_6): δ 9.91 (d, $J = 2.1$ Hz, 1H, H-2), 9.64 (d, $J = 1.8$ Hz, 1H, H-4), 8.61 (d, $J = 9.0$ Hz, 1H, H-8), 8.40 (dd, $J = 8.2$ Hz, 1.3 Hz, 1H, H-5), 8.31-8.27 (m, 1H, H-7), 8.10-8.06 (m, 1H, H-6), 5.09 (q, $J = 7.2$ Hz, 2H, H-1'), 1.62 (t, $J = 7.2$ Hz, 3H, H-2').

^{13}C NMR (100 MHz, DMSO- d_6): δ 150.7 (C-2), 148.3 (C-4), 136.1 (C-8a), 135.7 (C-7), 130.6 (C-6), 130.1 (C-4a), 129.9 (C-5), 118.9 (C-8), 114.9 (C-3), 53.4 (C-1'), 15.1 (C-2').

HRMS (ESI): calcd. for $\text{C}_{11}\text{H}_{11}\text{NBr}$ [$\text{M} - \text{I}^-$] 236.0069; 238.0049, found 236.0070; 238.0044.

3-Bromo-*N*-benzylquinolinium bromide (115b)



Following the general procedure, the title compound was prepared from 3-bromoquinoline (**67b**) (0.065 mL, 0.48 mmol), BnBr (0.57 mL, 4.80 mmol) in CH_3CN (5 mL). After refluxing

for 24 hours, workup was carried out according to the general procedure to give the target compound **115b** as an off-white powder (200.0 mg, quant.).

mp: 236 °C.

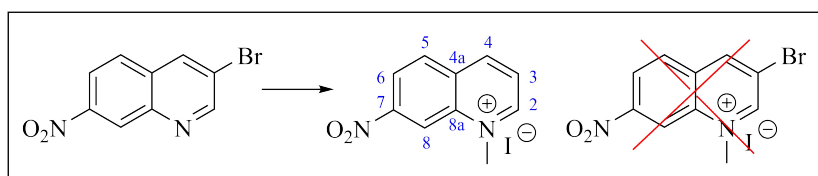
IR (ATR): ν_{\max} 3043, 2922, 2879, 2817, 1522, 1373, 767, 725, 693 cm^{-1} .

^1H NMR (400 MHz, DMSO- d_6): δ 10.23 (d, $J = 2.0$ Hz, 1H, H-2), 9.77 (d, $J = 1.8$ Hz, 1H, H-4), 8.46-8.42 (m, 2H, H-5 and H-8), 8.23-8.18 (m, 1H, H-7), 8.05-8.02 (m, 1H, H-6), 7.46-7.44 (m, 2H, H-3' and H-7'), 7.41-7.35 (m, 3H, H-4', H-5' and H-6'), 6.40 (s, 2H, H-1').

^{13}C NMR (100 MHz, DMSO- d_6): δ 151.5 (C-2), 149.4 (C-4), 136.3 (C-8a), 135.8 (C-7), 133.6 (C-2'), 130.8 (C-6), 130.4 (C-4a), 130.1 (C-5), 128.9 (C-4' and C-6'), 128.7 (C-5'), 127.3 (C-3' and C-7'), 119.4 (C-8), 115.2 (C-3), 60.1 (C-1').

HRMS (ESI): calcd. for $\text{C}_{16}\text{H}_{13}\text{NBr}$ [$\text{M} - \text{Br}^-$] 298.0226; 300.0205, found 298.0229; 300.0210.

7-Nitro-*N*-methylquinolinium iodide (**119**)



Following the general procedure, the title compound was prepared from 3-bromo-7-nitroquinoline (**67bc**) (100.0 mg, 0.39 mmol), CH_3I (2.50 mL, 39.0 mmol) in CH_3CN (5 mL). After refluxing for 17 hours, workup was carried out according to the general procedure to give compound **119** as a red powder (181.5 mg, quant.).

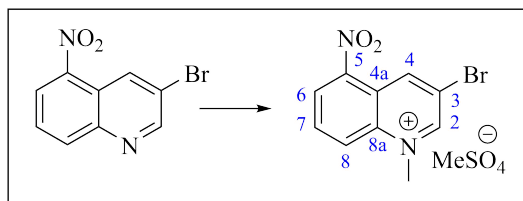
mp: 213-216 °C.

IR (ATR): ν_{\max} 3116, 3047, 2993, 1516, 1335, 812 cm^{-1} .

^1H NMR (400 MHz, DMSO- d_6): δ 9.68 (d, $J = 5.7$ Hz, 1H, H-2), 9.53 (d, $J = 8.9$ Hz, 1H, H-4), 8.92 (d, $J = 9.0$ Hz, 1H, H-8), 8.79-8.77 (m, 1H, H-6), 8.43 (dd, $J = 8.9$ Hz, 7.9 Hz, 1H, H-3), 8.38 (dd, $J = 9.0$ Hz, 5.7 Hz, 1H, H-5), 4.72 (s, 3H, NCH_3).

^{13}C NMR (100 MHz, DMSO- d_6): δ 151.8 (C-2), 146.3 (C-7), 142.3 (C-4), 138.4 (C-8a), 133.8 (C-5), 127.0 (C-6), 125.5 (C-8), 124.5 (C-3), 121.7 (C-4a), 46.7 (NCH_3).

HRMS (ESI): sample sent to UiB for analysis.

3-Bromo-*N*-methyl-5-nitroquinolinium methyl sulfate (115h)

Following the general procedure, the title compound was prepared from 3-bromo-5-nitroquinoline (**67ba**) (500.0 mg, 1.98 mmol), Me₂SO₄ (0.94 mL, 9.92 mmol) in CH₃CN (12 mL). After refluxing for 68 hours, workup was carried out according to the general procedure to give the target compound **115h** as an off-white solid (875.9 mg, quant.).

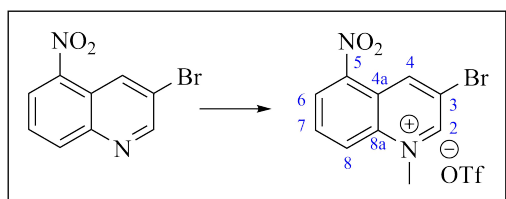
mp: 200-203 °C.

IR (ATR): ν_{\max} 3034, 1670, 1221, 1030 cm⁻¹.

¹H NMR (400 MHz, DMSO-*d*₆): δ 10.07 (d, J = 1.5 Hz, 1H, H-2), 9.67 (d, J = 0.9 Hz, 1H, H-4), 8.92-8.90 (m, 1H, H-6), 8.78 (dd, J = 7.7 Hz, 0.4 Hz, 1H, H-8), 8.42 (dd, J = 9.0 Hz, 7.8 Hz, 1H, H-7), 4.71 (s, 3H, NCH₃).

¹³C NMR (100 MHz, DMSO-*d*₆): δ 153.4 (C-2), 145.3 (C-5), 143.3 (C-4), 137.4 (C-8a), 133.9 (C-7), 127.9 (C-8), 125.7 (C-6), 121.9 (C-4a), 117.7 (C-3), 46.7 (NCH₃).

HRMS (ESI): sample sent to UiB for analysis.

3-Bromo-*N*-methyl-5-nitroquinolinium triflate (115l)

Following the general procedure, the title compound was prepared from 3-bromo-5-nitroquinoline (**67ba**) (200.0 mg, 0.79 mmol), MeOTf (0.10 mL, 0.95 mmol) in anhydrous CH₂Cl₂ (5 mL). After stirring at rt for 22 hours, workup was carried out according to the general procedure to give the target compound **115l** as an off-white solid (349.1 mg, quant.).

mp: 104-107 °C.

IR (ATR): ν_{\max} 3080, 1529, 1247, 1141, 1025, 815, 737 cm⁻¹.

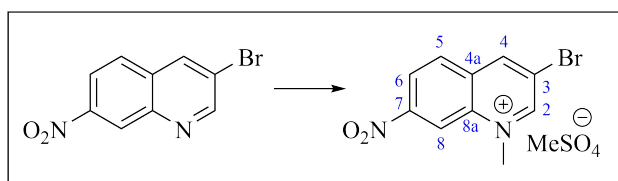
¹H NMR (400 MHz, DMSO-*d*₆): δ 10.09 (d, J = 1.5 Hz, 1H, H-2), 9.70 (d, J = 1.1 Hz, 1H, H-4), 8.90-8.88 (m, 1H, H-6), 8.79 (dd, J = 7.7 Hz, 0.6 Hz, 1H, H-8), 8.43 (dd, J = 8.9 Hz, 7.8 Hz, 1H, H-7), 4.70 (s, 3H, NCH₃).

^{13}C NMR (100 MHz, DMSO- d_6): δ 153.4 (C-2), 145.4 (C-5), 143.4 (C-4), 137.3 (C-8a), 133.9 (C-7), 127.9 (C-8), 125.5 (C-6), 121.9 (C-4a), 120.6 (q, $J_{\text{CF}} = 322.2$ Hz, OCF_3), 117.6 (C-3), 46.6 (NCH_3).

^{19}F NMR (376 MHz, DMSO- d_6): δ -76.9.

HRMS (ESI): calcd. for $\text{C}_{10}\text{H}_8\text{N}_2\text{BrO}_2$ [$\text{M} - \text{OTf}^-$] 266.9764; 268.9743, found 266.9764; 268.9868.

3-Bromo-*N*-methyl-7-nitroquinolinium methyl sulfate (115i)



Following the general procedure, the title compound was prepared from 3-bromo-7-nitroquinoline (**67bc**) (1.00 g, 3.95 mmol), Me_2SO_4 (1.86 mL, 19.76 mmol) in CH_3CN (20 mL). After refluxing for 25 hours, workup was carried out according to the general procedure to give the target compound **115i** as a white solid (1.47 g, quant.).

mp: 199-203 °C.

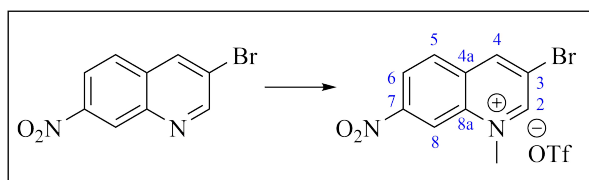
IR (ATR): ν_{max} 3084, 3037, 2955, 1551, 1212, 734 cm^{-1} .

^1H NMR (400 MHz, DMSO- d_6): δ 10.09 (d, $J = 1.5$ Hz, 1H, H-2), 9.77 (d, $J = 1.4$ Hz, 1H, H-4), 9.24 (d, $J = 1.8$ Hz, 1H, H-8), 8.75 (dd, $J = 9.0$ Hz, 2.0 Hz, 1H, H-6), 8.63 (d, $J = 9.1$ Hz, 1H, H-5), 4.76 (s, 3H, NCH_3).

^{13}C NMR (100 MHz, DMSO- d_6): δ 154.7 (C-2), 150.0 (C-7), 148.1 (C-4), 136.7 (C-8a), 132.0 (C-5), 131.9 (C-4a), 124.3 (C-6), 118.2 (C-3), 115.9 (C-8).

HRMS (ESI): calcd. for $\text{C}_{10}\text{H}_8\text{N}_2\text{BrO}_2$ [$\text{M} - \text{MeSO}_4^-$] 266.9764; 268.9743, found 266.9762; 268.9748.

3-Bromo-*N*-methyl-7-nitroquinolinium triflate (115m)



Following the general procedure, the title compound was prepared from 3-bromo-7-nitroquinoline (**67bc**) (500.0 mg, 1.97 mmol), MeOTf (0.24 mL, 2.17 mmol) in anhydrous CH_2Cl_2 (10

mL). After stirring at rt for five days, workup was carried out according to the general procedure to give the target compound **115m** as an off-white solid (768.0 mg, 94%).

mp: 235-236 °C.

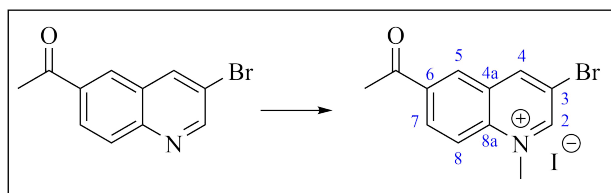
IR (ATR): ν_{\max} 3137, 3084, 3056, 1551, 1249, 1148, 1025, 823, 734 cm^{-1} .

^1H NMR (400 MHz, DMSO- d_6): δ 10.10 (d, $J = 1.4$ Hz, 1H, H-2), 9.77 (d, $J = 1.4$ Hz, 1H, H-4), 9.25 (d, $J = 1.9$ Hz, 1H, H-8), 8.76 (dd, $J = 9.0$ Hz, 2.0 Hz, 1H, H-6), 8.61 (d, $J = 9.0$ Hz, 1H, H-5), 4.75 (s, 3H, NCH₃).

^{13}C NMR (100 MHz, DMSO- d_6): δ 154.7 (C-2), 150.1 (C-7), 148.0 (C-4), 136.6 (C-8a), 131.9 (C-5), 131.8 (C-4a), 124.3 (C-6), 118.2 (C-3), 115.8 (C-8), 45.9 (NCH₃).

HRMS (ESI): sample sent to UiB for analysis.

6-Acetyl-3-bromo-*N*-methylquinolinium iodide (**115d**)



Following the general procedure, the title compound was prepared 6-acetyl-3-bromoquinoline (100.0 mg, 0.40 mmol), CH₃I in CH₃CN (5 mL). After refluxing for 23 hours, workup was carried out according to the general procedure to give the target compound **115d** as a yellow powder (195.1 mg, quant.).

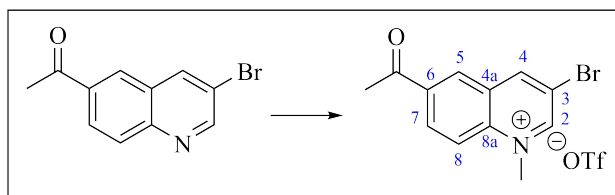
mp: 244-245 °C.

IR (ATR): ν_{\max} 3060, 3009, 2917, 1684 (C=O), 1360, 828 cm^{-1} .

^1H NMR (400 MHz, DMSO- d_6): δ 10.00 (d, $J = 1.8$ Hz, 1H, H-2), 9.75 (d, $J = 1.8$ Hz, 1H, H-4), 9.04 (d, $J = 1.8$ Hz, 1H, H-5), 8.65 (dd, $J = 9.2$ Hz, 1.9 Hz, 1H, H-7), 8.59 (d, $J = 9.2$ Hz, 1H, H-8), 4.65 (s, 3H, NCH₃), 2.79 (s, 3H, CH₃).

^{13}C NMR (100 MHz, DMSO- d_6): δ 196.6 (C=O), 153.1 (C-2), 149.2 (C-4), 138.8 (C-8a), 137.1 (C-6), 133.1 (C-5), 130.6 (C-7), 129.4 (C-8), 120.0 (C-4a), 115.4 (C-3), 45.6 (NCH₃), 27.1 (CH₃).

HRMS (ESI): sample sent to UiB for analysis.

6-Acetyl-3-bromo-*N*-methylquinolinium triflate (115n)

Following the general procedure, the title compound was prepared from 6-acetyl-3-bromoquinoline (500.0 mg, 2.00 mmol), MeOTf (0.26 mL, 2.40 mmol) in anhydrous CH₂Cl₂ (20 mL). After stirring at rt for four days, workup was carried out according to the general procedure to give the target compound **115n** as an off-white powder (836.0 mg, quant.).

mp: 182-185 °C.

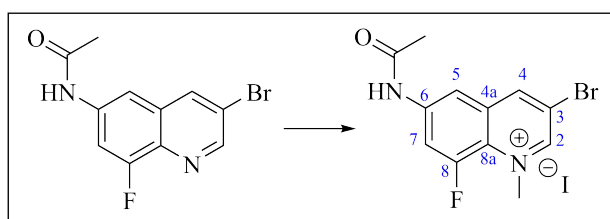
IR (ATR): ν_{\max} 3083, 3052, 1690 (C=O), 1251, 1154, 1025, 827 cm⁻¹.

¹H NMR (400 MHz, DMSO-*d*₆): δ 9.98 (d, *J* = 1.7 Hz, 1H, H-2), 9.73 (d, *J* = 1.5 Hz, 1H, H-4), 9.01 (d, *J* = 1.7 Hz, 1H, H-5), 8.65 (dd, *J* = 9.2 Hz, 1.9 Hz, 1H, H-7), 8.58 (d, *J* = 9.3 Hz, 1H, H-8), 4.64 (s, 3H, NCH₃), 2.78 (s, 3H, CH₃).

¹³C NMR (100 MHz, DMSO-*d*₆): δ 196.6 (C=O), 153.2 (C-2), 149.3 (C-4), 138.9 (C-8a), 137.1 (C-6), 133.1 (C-5), 130.6 (C-7), 129.4 (C-8), 120.0 (C-4a), 115.4 (C-3), 45.5 (NCH₃), 27.0 (CH₃) (OCF₃ was obscured or overlapping).

¹⁹F NMR (376 MHz, DMSO-*d*₆): δ -77.5.

HRMS (ESI): calcd. for C₁₂H₁₁NBrO [M - OTf⁻] 264.0019; 265.9998, found 264.0019; 265.9985.

6-Acetamido-3-bromo-8-fluoro-*N*-methylquinolinium iodide (115e)

Following the general procedure, the title compound was prepared from *N*-(3-bromo-8-fluoroquinolin-6-yl)acetamide (**67bb**) (#) (200.0 mg, 0.71 mmol), CH₃I (0.88 mL, 14.18 mmol) in CH₃CN (15 mL). After refluxing for 3 days, workup was carried out according to the general procedure to give the target compound **115e** as an orange solid (265.7 mg, 88%).

mp: 215-217 °C.

IR (ATR): ν_{\max} 3149, 3090, 3035, 1691 (C=O), 1549, 1255, 878 cm⁻¹.

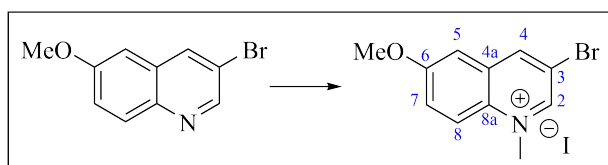
^1H NMR (400 MHz, DMSO- d_6): δ 10.83 (bs, 1H, NH), 9.71 (d, J = 1.2 Hz, 1H, H-2), 9.62-9.61 (m, 1H, H-4), 8.37 (d, J = 1.8 Hz, 1H, H-5), 8.15 (dd, J = 16.2 Hz, 2.1 Hz, 1H, H-7) 4.69 (d, J = 8.3 Hz, 1H, NCH₃), 2.17 (s, 3H, CH₃).

^{13}C NMR (100 MHz, DMSO- d_6): δ 169.7 (C=O), 152.2 (d, J_{CF} = 254.1 Hz, C-8), 150.9 (C-2), 147.0 (d, J_{CF} = 2.2 Hz, C-4), 140.7 (d, J_{CF} = 10.9 Hz, C-6), 132.4 (C-8a), 123.9 (d, J_{CF} = 8.7 Hz, C-4a), 115.8 (C-3), 113.5 (d, J_{CF} = 26.6 Hz, C-7), 111.4 (d, J_{CF} = 3.6 Hz, C-5), 49.6 (d, J_{CF} = 16.0 Hz, NCH₃), 24.2 (CH₃).

^{19}F NMR (376 MHz, DMSO- d_6): δ -111.9.

HRMS (ESI): calcd. for C₁₂H₁₁BrFN₂O [M - I⁻] 297.0033; 299.0013, found 297.0034; 299.0011.

3-Bromo-6-methoxy-*N*-quinolinium iodide (115f)



Following the general procedure, the title compound was prepared from 3-bromo-6-methoxyquinoline (200.0 mg, 0.84 mmol), CH₃I (2.62 mL, 42.19 mmol) in CH₃CN (10 mL). After refluxing for 21 hours, workup was carried out according to the general procedure to give the target compound **115f** as an orange solid (309.2 mg, 97%).

mp: 159-162 °C.

IR (ATR): ν_{max} 2979, 2935, 1614, 1522, 892, 824 cm⁻¹.

^1H NMR (400 MHz, DMSO- d_6): δ 9.70 (d, J = 1.6 Hz, 1H, H-2), 9.43 (d, J = 1.3 Hz, 1H, H-4), 8.42 (d, J = 9.4 Hz, 1H, H-8), 7.92 (dd, J = 9.6 Hz, 2.8 Hz, 1H, H-7), 7.82 (d, J = 2.8 Hz, 1H, H-5), 4.59 (s, 3H, NCH₃), 4.00 (s, 3H, OCH₃).

^{13}C NMR (100 MHz, DMSO- d_6): δ 159.8 (C-6), 148.0 (C-2), 145.9 (C-4), 133.0 (C-8a), 131.7 (C-4a), 127.6 (C-7), 120.9 (C-8), 114.9 (C-3), 107.1 (C-5), 56.4 (OCH₃), 45.4 (NCH₃).

HRMS (ESI): calcd. for C₁₁H₁₁NBrO [M - I⁻] 252.0019; 253.9998, found 252.0020; 254.0025.

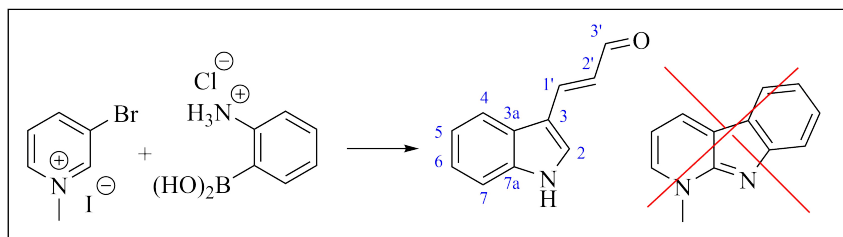
7.2.8 Cascade Suzuki-Miyaura cross coupling and cyclization reactions

General procedure

To a solution of pyridinium halide or quinolinium halide **115** (1 equiv.) in an appropriate amount of DME under an argon atmosphere was added boronic acid (1.2-1.3 equiv.), an aq. solution of Cs₂CO₃ (3.2-4.2 equiv.) and Pd(PPh₃)₄ (5 mol%). The resulting reaction mixture

was stirred at 80 °C until completion as indicated by TLC analysis. The crude mixture was then allowed to cool to rt and the volatiles were removed under reduced pressure. The concentrate was evaporated onto celite and purified by column chromatography using the eluent as indicated in the specific descriptions to give target compounds.

(*E*)-3-(1*H*-Indol-3-yl)acrylaldehyde (**122**)



Following the general procedure, the title compound was prepared from 3-bromo-*N*-methylpyridinium iodide (**121**) (200.0 mg, 0.67 mmol), 2-aminophenylboronic acid hydrochloride (**68**) (139.2 mg, 0.80 mmol), an aq. solution of Cs₂CO₃ (916.8 mg, 2.81 mmol in 2 mL H₂O) and Pd(PPh₃)₄ (38.7 mg, 0.033 mmol) in DME (10 mL). After a reaction time of 27 hours, the crude was purified by silica gel column chromatography (pet. ether/EtOAc/CH₂Cl₂, 6:2:2 v/v) and concentration of the relevant fractions [*R*_f = 0.16 (pet. ether/EtOAc/CH₂Cl₂, 6:2:2 v/v)] gave compound **122** as a dark red solid (29.7 mg, 24%).

mp: 145-146 °C.

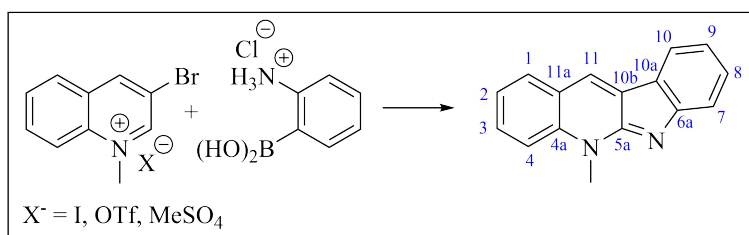
IR (ATR): ν_{\max} 3260, 2955, 2925, 2855, 1608, 1123, 741 cm⁻¹.

¹H NMR (400 MHz, CD₃OD): δ 9.50 (d, *J* = 8.1 Hz, 1H, H-3'), 7.90 (d, *J* = 15.7 Hz, 1H, H-1'), 7.87-7.82 (m, 2H, H-2 and H-4), 7.47-7.45 (m, 1H, H-7), 7.27-7.21 (m, 2H, H-5 and H-6), 6.72 (dd, *J* = 15.7 Hz, 8.1 Hz, 1H, H-2').

¹³C NMR (100 MHz, CD₃OD): δ 196.6 (C-3'), 150.8 (C-1'), 139.4 (C-7a), 133.8 (C-2), 126.5 (C-3a), 124.3 (C-6), 124.0 (C-2'), 122.7 (C-5), 121.0 (C-4), 114.5 (C-3), 113.4 (C-7).

In accordance with previously reported data.^[287]

Neocryptolepine (**24**)



Following the general procedure, the title compound was prepared from 3-bromo-*N*-methylquinolinium iodide (**115**) (200.0 mg, 0.57 mmol), 2-aminophenylboronic acid hydrochloride (**68**) (119.3 mg, 0.69 mmol), an aq. solution of Cs₂CO₃ (780.0 mg, 2.39 mmol in 2 mL H₂O) and Pd(PPh₃)₄ (32.9 mg, 0.028 mmol) in DME (10 mL). After a reaction time of 24 hours, the crude was purified by silica gel column chromatography (EtOAc/CH₂Cl₂, 8:2 v/v) and concentration of the relevant fractions [*R*_f = 0.23 (EtOAc/CH₂Cl₂, 8:2 v/v)] gave the target compound **24** as a pale red solid (106.6 mg, 80%).

Following the general procedure outlined in Section 7.2.6, neocryptolepine (**24**) was prepared from 6*H*-indolo[2,3-*b*]quinoline (**26**) (23.0 mg, 0.10 mmol), iodomethane (0.66 mL, 10.0 mmol) in THF (2 mL). After a reaction time of 24 hours, the crude was purified by silica gel column chromatography (CH₂Cl₂/MeOH, 95:5 v/v) and concentration of the relevant fractions [*R*_f = 0.18 (CH₂Cl₂/MeOH, 95:5 v/v)] gave the hydroiodide salt of neocryptolepine. The free base was obtained according to the general procedure to give the target compound **24** as dark yellow crystals (19.5 mg, 84%).^[153]

mp: 85-86 °C (lit.^[153] 104-105 °C).

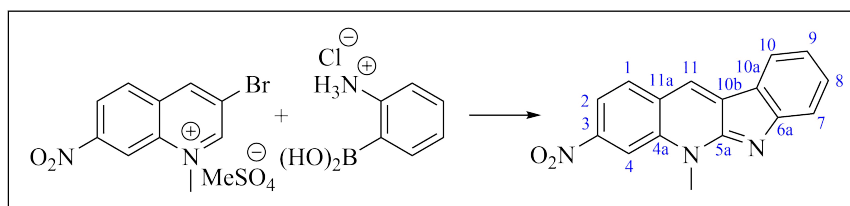
IR (ATR): ν_{\max} 3051, 2961, 2923, 2852, 1494, 1012, 741 cm⁻¹.

¹H NMR (400 MHz, CD₃OD): δ 8.67 (s, 1H, H-11), 8.05-8.02 (m, 2H, H-1 and H-10), 7.90 (d, *J* = 8.6 Hz, 1H, H-4), 7.83-7.78 (m, 1H, H-7), 7.59-7.57 (m, 1H, H-2), 7.50-7.45 (m, 2H, H-3 and H-8), 7.19 (td, *J* = 7.5 Hz, 1.0 Hz, 1H, H-9), 4.23 (s, 3H, NCH₃).

¹³C NMR (100 MHz, CD₃OD): δ 156.9 (C-5a), 155.4 (C-4a), 138.1 (C-6a), 132.0 (C-7), 131.2 (C-1), 130.4 (C-11), 130.1 (C-8), 128.4 (C-10a), 124.9 (C-11a), 123.6 (C-3), 122.4 (C-10b), 122.2 (C-10), 121.2 (C-9), 117.7 (C-2), 115.7 (C-4), 33.7 (NCH₃).

In accordance with previously reported data.^[153]

5-Methyl-3-nitro-5*H*indolo[2,3-*b*]quinoline (**24a**)



Following the general procedure, the title compound was prepared from 3-bromo-*N*-methyl-7-nitroquinolinium methyl sulfate (**115i**) (100.0 mg, 0.27 mmol), 2-aminophenylboronic acid hydrochloride (**68**) (71.5 mg, 0.41 mmol), an aq. solution of K₂CO₃ (130.6 mg, 0.94 mmol in 1 mL H₂O) and PdCl₂(dppf) (9.9 mg, 0.013 mmol) in EtOH (5 mL). After a reaction time of 22 hours, the crude was purified by silica gel column chromatography (pet. ether/EtOAc, 1:1 v/v) and concentration of the relevant fractions [*R*_f = 0.31 (pet. ether/EtOAc, 1:1 v/v)] gave the

target compound **24a** as a dark red gel (10.8 mg, 14%).

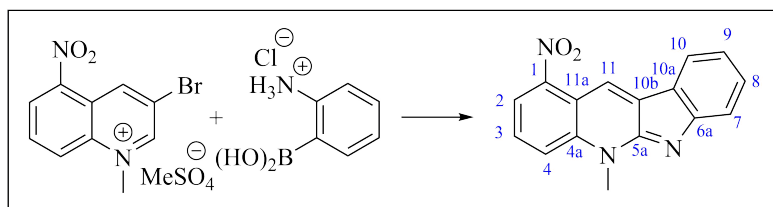
IR (ATR): ν_{\max} 2924, 2854, 1513, 1334 cm^{-1} .

^1H NMR (400 MHz, CDCl_3): δ 8.67 (d, $J = 1.5$ Hz, 1H, H-4), 8.56 (s, 1H, H-11), 8.27 (dd, $J = 8.7$ Hz, 1.7 Hz, 1H, H-2), 8.13 (d, $J = 8.7$ Hz, 1H, H-1), 8.06 (d, $J = 7.6$ Hz, 1H, H-7), 7.76 (d, $J = 8.0$ Hz, 1H, H-8), 7.61 (t, $J = 7.6$ Hz, 1H, H-9), 7.30-7.26 (m, 1H, H-10), 4.47 (s, 3H, NCH_3).

^{13}C NMR (100 MHz, CDCl_3): δ 156.3 (C-5a), 156.3 (C-6a), 148.0 (C-3), 136.5 (C-4a), 132.1 (C-10b), 131.1 (C-9), 130.9 (C-1), 126.2 (C-11), 124.8 (C-11a), 123.7 (C-10a), 121.9 (C-7), 121.1 (C-10), 118.5 (C-8), 116.1 (C-2), 110.2 (C-4), 33.6 (NCH_3).

HRMS (ESI): calcd. for $\text{C}_{16}\text{H}_{12}\text{N}_2\text{O}$ [$\text{M} + \text{H}^+$] 278.0924, found 278.0921.

5-Methyl-1-nitro-5*H*-indolo[2,3-*b*]quinoline (**24b**)



Following the general procedure, the title compound was prepared from 3-bromo-*N*-methyl-5-nitroquinolinium methyl sulfate (**115h**) (100.0 mg, 0.27 mmol), 2-aminophenylboronic acid hydrochloride (**68**) (61.9 mg, 0.36 mmol), an aq. solution of Cs_2CO_3 (290.3 mg, 0.89 mmol in 1 mL H_2O) and $\text{Pd}(\text{PPh}_3)_4$ (15.6 mg, 0.013 mmol) in DME (5 mL). After a reaction time of 24 hours, the crude was purified by silica gel column chromatography (EtOAc) and concentration of the relevant fractions [$R_f = 0.14$ (EtOAc)] gave the target compound **24b** as a red solid (10.0 mg, 13%).

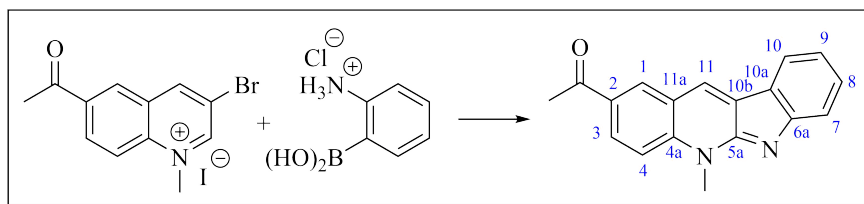
mp: 241-242 $^\circ\text{C}$.

IR (ATR): ν_{\max} 2923, 2852, 1520, 732 cm^{-1} .

^1H NMR (400 MHz, CDCl_3): δ 9.03 (s, 1H, H-11), 8.03 (d, $J = 7.7$ Hz, 1H, H-10) 8.02-7.98 (m, 2H, H-2 and H-7), 7.79 (t, $J = 8.2$ Hz, 1H, H-9), 7.69 (d, $J = 7.9$ Hz, 1H, H-8), 7.58-7.55 (m, 1H, H-3), 7.27-7.24 (m, 1H, H-4), 4.40 (s, 3H, NCH_3).

^{13}C NMR (100 MHz, CDCl_3): δ 155.7 (C-5a), 155.0 (C-4a), 148.3 (C-1), 137.6 (C-11a), 131.0 (C-6a), 130.8 (C-3), 128.8 (C-9), 123.9 (C-10a), 122.0 (C-10), 121.5 (C-11), 121.0 (C-4), 119.2 (C-7), 118.6 (C-2), 118.1 (C-8), 113.8 (C-10b), 34.1 (NCH_3).

HRMS (ESI): sample sent to UiB for analysis.

2-Acetyl-5-methyl-5H-indolo[2,3-b]quinoline (24c)

Following the general procedure, the title compound was prepared from 6-acetyl-3-bromo-*N*-methylquinolinium iodide (**115d**) (100.0 mg, 0.24 mmol), 2-aminophenylboronic acid hydrochloride (**68**) (54.1 mg, 0.31 mmol), an aq. solution of Cs_2CO_3 (258.0 mg, 0.79 mmol in 1 mL H_2O) and $\text{Pd}(\text{PPh}_3)_4$ (13.9 mg, 0.012 mmol) in DME (5 mL). After a reaction time of 24 hours, the crude was purified by silica gel column chromatography (EtOAc) and concentration of the relevant fractions [$R_f = 0.20$ (EtOAc)] gave the target compound **24c** as bright orange crystals (41.4 mg, 62%).

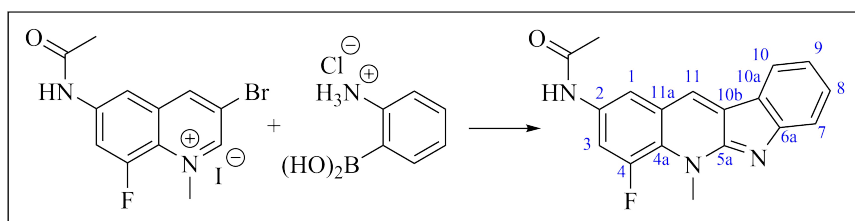
mp: 185-187 °C.

IR (ATR): ν_{max} 3051, 2925, 2854, 1676 (C=O), 1613, 1518, 1184 cm^{-1} .

^1H NMR (400 MHz, CDCl_3): δ 8.74 (d, $J = 2.0$ Hz, 1H, H-1), 8.40 (s, 1H, H-11), 8.25 (dd, $J = 9.0$ Hz, 2.1 Hz, 1H, H-3), 7.98-7.96 (m, 1H, H-10), 7.72-7.70 (m, 1H, H-7), 7.67 (d, $J = 9.0$ Hz, 1H, H-4), 7.56-7.52 (m, 1H, H-8), 7.23 (td, $J = 7.4$ Hz, 0.9 Hz, 1H, H-9), 4.28 (s, 3H, NCH_3), 2.69 (s, 3H, CH_3).

^{13}C NMR (100 MHz, CDCl_3): δ 196.5 (C=O), 156.2 (C-5a), 155.4 (C-6a), 139.5 (C-4a), 131.1 (C-1), 130.7 (C-2), 129.9 (C-8), 129.6 (C-3), 129.1 (C-11a), 128.1 (C-11), 123.9 (C-10a), 121.3 (C-10), 120.7 (C-9), 120.0 (C-10b), 118.2 (C-7), 114.3 (C-4), 33.3 (NCH_3), 26.6 (CH_3).

HRMS (ESI): calcd. for $\text{C}_{18}\text{H}_{14}\text{N}_2\text{O}$ [$\text{M} + \text{H}^+$] 275.1179, found 275.1179.

***N*-(4-Fluoro-5-methyl-5H-indolo[2,3-b]quinolin-2-yl)acetamide (24d)**

Following the general procedure, the title compound was prepared from 6-acetamido-3-bromo-8-fluoro-*N*-methylquinolinium iodide (**115e**) (100.0 mg, 0.23 mmol), 2-aminophenylboronic acid hydrochloride (**68**) (53.2 mg, 0.31 mmol), an aq. solution of Cs_2CO_3 (262.3 mg, 0.80 mmol in 1 mL H_2O) and $\text{Pd}(\text{PPh}_3)_4$ (13.3 mg, 0.011 mmol) in DME (5 mL). After a reaction time of 21 hours, the crude was purified by silica gel column chromatography (EtOAc/MeOH,

99:1 v/v) and concentration of the relevant fractions [$R_f = 0.17$ (EtOAc/MeOH, 99:1 v/v)] gave the target compound **24d** as a bright red solid (48.5 mg, 69%).

mp: 299-300 °C.

IR (ATR): ν_{\max} 3297, 3056, 2960, 2928, 2856, 1654 (C=O), 1582, 1489, 1205, 761 cm^{-1} .

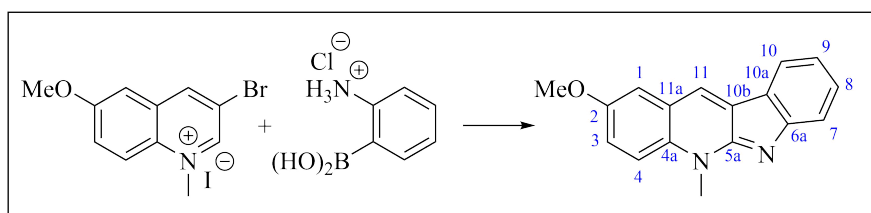
^1H NMR (400 MHz, DMSO- d_6): δ 10.34 (bs, 1H, NH), 8.92 (d, $J = 1.0$ Hz, 1H, H-11), 8.14-8.12 (m, 2H, H-1 and H-10), 7.87 (dd, $J = 17.1$ Hz, 2.1 Hz, 1H, H-3), 7.55 (d, $J = 7.9$ Hz, 1H, H-7), 7.50-7.46 (m, 1H, H-8), 7.19-7.15 (m, 1H, H-9), 4.45 (d, $J = 8.2$ Hz, 3H, NCH₃), 2.11 (s, 3H, CH₃).

^{13}C NMR (100 MHz, DMSO- d_6): δ 168.6 (C=O), 155.7 (C-5a), 155.2 (C-6a), 150.5 (d, $J_{\text{CF}} = 245.2$ Hz, C-4), 133.6 (d, $J_{\text{CF}} = 10.4$ Hz, C-2), 129.2 (C-8), 128.6 (d, $J_{\text{CF}} = 2.8$ Hz, C-11), 128.0 (C-10a), 123.5 (C-11a), 122.9 (d, $J_{\text{CF}} = 3.5$ Hz, C-4a), 121.9 (C-10b), 121.8 (C-10), 119.4 (C-9), 117.1 (C-7), 114.2 (d, $J_{\text{CF}} = 3.1$ Hz, C-1), 109.5 (d, $J_{\text{CF}} = 27.3$ Hz, C-3), 36.5 (d, $J_{\text{CF}} = 15.1$ Hz, NCH₃), 23.9 (CH₃).

^{19}F NMR (376 MHz, DMSO- d_6): δ -120.7.

HRMS (ESI): calcd. for C₁₈H₁₄FN₃O [M + H⁺] 308.1194, found 308.1205.

2-Methoxy-5-methyl-5H-indolo[2,3-b]quinoline (24e)



Following the general procedure, the title compound was prepared from 3-bromo-6-methoxy-*N*-methylquinolinium iodide (**115f**) (100.0 mg, 0.26 mmol), 2-aminophenylboronic acid hydrochloride (**68**) (59.5 mg, 0.34 mmol), an aq. solution of Cs₂CO₃ (279.5 mg, 0.86 mmol) and Pd(PPh₃)₄ (15.0 mg, 0.013 mmol) in DME (5 mL). After a reaction time of 23 hours, the crude was purified by silica gel column chromatography (EtOAc) and concentration of the relevant fractions [$R_f = 0.10$ (EtOAc)] gave the target compound **24e** as a bright red wax (33.3 mg, 49%).

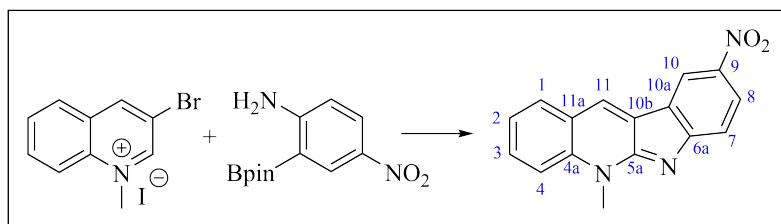
IR (ATR): 2925, 2854, 1576, 1492, 1234 cm^{-1} .

^1H NMR (400 MHz, CDCl₃): δ 8.44 (s, 1H, H-11), 8.01 (d, $J = 7.3$ Hz, 1H, H-10), 7.73 (d, $J = 7.9$ Hz, 1H, H-4), 7.66 (d, $J = 9.2$ Hz, 1H, H-7), 7.55-7.52 (m, 1H, H-8), 7.39 (dd, $J = 9.2$ Hz, 2.8 Hz, 1H, H-3), 7.35 (d, $J = 2.7$ Hz, 1H, H-1), 7.20 (t, $J = 7.4$ Hz, 1H, H-9), 4.33 (s, 3H, NCH₃), 3.94 (s, 3H, OCH₃).

^{13}C NMR (100 MHz, CDCl_3): δ 155.9 (C-5a), 155.6 (C-6a), 154.7 (C-2), 131.9 (C-4a), 129.5 (C-8), 128.6 (C-11a), 127.6 (C-11), 123.8 (C-10a), 121.7 (C-10b), 121.1 (C-10), 120.4 (C-3), 119.6 (C-9), 117.6 (C-4), 115.5 (C-7), 110.4 (C-1), 55.9 (OCH_3), 33.9 (NCH_3).

In accordance with previously reported data.^[186]

5-Methyl-9-nitro-5*H*-indolo[2,3-*b*]quinoline (24f)



Following the general procedure, the title compound was prepared from 3-bromo-*N*-methylquinolinium iodide (**115**) (100.0 mg, 0.29 mmol), 4-nitro-2-(4,4,5,5-tetramethyl-1,3,2-dioxaborolan-2-yl)aniline (**83b**) (98.4 mg, 0.37 mmol), an aq. solution of Cs_2CO_3 (330.7 mg, 1.01 mmol in 1 mL H_2O) and $\text{Pd}(\text{PPh}_3)_4$ (16.7 mg, 0.014 mmol) in DME (5 mL). After a reaction time of 21 hours, the crude was purified by silica gel column chromatography (EtOAc) and concentration of the relevant fractions [$R_f = 0.24$ (EtOAc)] gave the target compound **24f** as a yellow solid (28.9 mg, 36%).

mp: 292-293 °C.

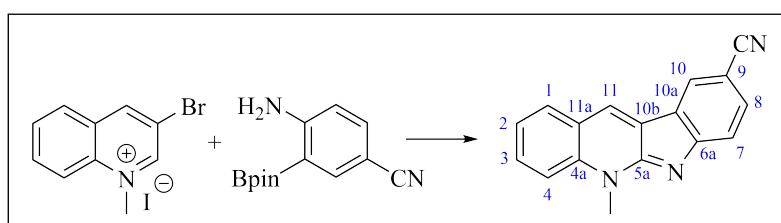
IR (ATR): ν_{max} 2955, 2922, 2854, 1611, 1282, 1074, 738, 737 cm^{-1} .

^1H NMR (400 MHz, $\text{DMSO}-d_6$): δ 9.29 (s, 1H, H-11), 9.06 (d, $J = 2.2$ Hz, 1H, H-10), 8.30 (dd, $J = 8.8$ Hz, 2.3 Hz, 1H, H-8), 8.17 (d, $J = 7.7$ Hz, 1H, H-1), 8.07 (d, $J = 8.7$ Hz, 1H, H-4), 7.95-7.91 (m, 1H, H-3), 7.63-7.58 (m, 2H, H-2 and H-7), 4.36 (s, 3H, NCH_3).

^{13}C NMR (100 MHz, $\text{DMSO}-d_6$): δ 132.7, 131.9, 131.5, 130.5, 128.8, 125.4, 124.2, 123.6, 123.2, 120.9, 118.2, 116.7, 115.9, 33.5. The presence of two signals at roughly 156 and 155 ppm, respectively, determined by ^1H - ^{13}C HMBC. Sample decomposed before more scans could be run.

HRMS (ESI): sample sent to UiB for analysis.

5-Methyl-5*H*-indolo[2,3-*b*]quinoline-9-carbonitrile (24g)



Following the general procedure, the title compound was prepared from 3-bromo-*N*-methylquinolinium iodide (**115**) (100.0 mg, 0.29 mmol), 4-amino-3-(4,4,5,5-tetramethyl-1,3,2-dioxaborolan-2-yl)benzonitrile (**83c**) (90.9 mg, 0.37 mmol), an aq. solution of Cs₂CO₃ (312.8 mg, 0.96 mmol in 1 mL H₂O) and Pd(PPh₃)₄ (16.7 mg, 0.014 mmol) in DME (5 mL). After a reaction time of 22 hours, the crude was purified by silica gel column chromatography (EtOAc) and concentration of the relevant fractions [*R*_f = 0.12 (EtOAc)] gave the target compound **24g** as a bright yellow solid (51.6 mg, 69%).

mp: 257-258 °C (lit.^[260] 258.4 °C).

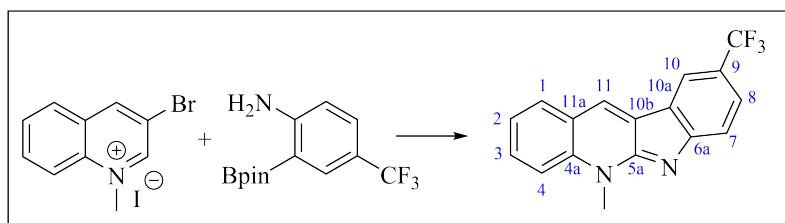
IR (ATR): ν_{\max} 3038, 2922, 2853, 2208 (CN), 1573, 1483, 1249, 831, 738 cm⁻¹.

¹H NMR (400 MHz, DMSO-*d*₆): δ 9.17 (s, 1H, H-11), 8.64 (d, *J* = 1.3 Hz, 1H, H-10), 8.21 (dd, *J* = 7.9 Hz, 1.0 Hz, 1H, H-1), 8.09 (d, *J* = 8.7 Hz, 1H, H-4), 7.96-7.92 (m, 1H, H-3), 7.83 (dd, *J* = 8.3 Hz, 1.6 Hz, 1H, H-8), 7.69 (d, *J* = 8.3 Hz, 1H, H-7), 7.61-7.58 (m, 1H, H-2), 4.38 (s, 3H, NCH₃).

¹³C NMR (100 MHz, DMSO-*d*₆): δ 157.9 (C-6a), 157.0 (C-5a), 136.8 (C-4a), 131.8 (C-8), 131.7 (C-3), 131.7 (C-11), 130.3 (C-1), 126.0 (C-10), 125.0 (C-10b), 124.2 (C-11a), 122.8 (C-2), 120.6 (C-10a), 120.5 (CN), 117.8 (C-7), 115.6 (C-4), 100.1 (C-9), 33.3 (NCH₃).

In accordance with previously reported data.^[260]

5-Methyl-9-(trifluoromethyl)-5*H*-indolo[2,3-*b*]quinoline (**24h**)



Following the general procedure, the title compound was prepared from 3-bromo-*N*-methylquinolinium iodide (**115**) (100.0 mg, 0.29 mmol), 2-(4,4,5,5-tetramethyl-1,3,2-dioxaborolan-2-yl)-4-(trifluoromethyl)aniline (**83d**) (106.2 mg, 0.37 mmol), an aq. solution of Cs₂CO₃ (311.8 mg, 0.96 mmol in 1 mL H₂O) and Pd(PPh₃)₄ (16.7 mg, 0.014 mmol) in DME (5 mL). After a reaction time of 23 hours, the crude was purified by silica gel column chromatography (EtOAc/CH₂Cl₂, 1:1 → 1:0 v/v) and concentration of the relevant fractions [*R*_f = 0.17 (EtOAc/CH₂Cl₂, 1:1 v/v)] gave the target compound **24h** as yellow crystals (50.5 mg, 58%).

mp: 202-205 °C.

IR (ATR): ν_{\max} 2920, 2851, 1654, 1617, 1491, 1281, 1046, 749 cm⁻¹.

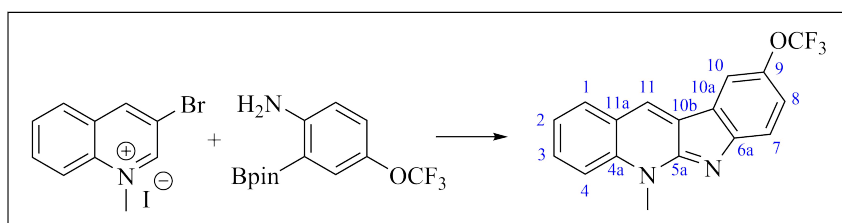
¹H NMR (400 MHz, CDCl₃): δ 8.67 (s, 1H, H-11), 8.32 (s, 1H, H-10) 8.05 (d, *J* = 7.8 Hz, 1H, H-1), 7.87-7.83 (m, 2H, H-3 and H-4), 7.82-7.79 (m, 1H, H-7 and H-8), 7.54-7.50 (m, 1H, H-2), 4.42 (s, 3H, NCH₃).

¹³C NRM (100 MHz, CDCl₃): δ 157.5 (C-5a), 157.3 (C-6a), 137.1 (C-4a), 131.2 (C-3), 130.3 (C-1), 129.6 (C-11), 127.1 (C-10a), 126.1 (q, *J*_{CF} = 3.5 Hz, C-8), 124.1 (C-9), 123.6 (C-10b), 122.7 (C-2), 121.7 (q, *J*_{CF} = 32.5 Hz, CF₃), 120.9 (C-11a), 118.4 (q, *J*_{CF} = 3.8 Hz, C-10), 117.6 (C-7), 114.5 (C-4), 33.4 (NCH₃).

¹⁹F NMR (376 MHz, CDCl₃): δ -60.0.

HRMS (ESI): calcd. for C₁₇H₁₁F₃N₂ [M + H⁺] 301.0947, found 301.0946.

5-Methyl-9-(trifluoromethoxy)-5*H*-indolo[2,3-*b*]quinoline (24i)



Following the general procedure, the title compound was prepared from 3-bromo-*N*-methylquinolinium iodide (**115**) (100.0 mg, 0.29 mmol), 2-(3,3,4,4-tetramethyl-1,3,2-dioxaborolan-1-yl)-4-(trifluoromethoxy)aniline (**83e**) (112.9 mg, 0.37 mmol), an aq. solution of Cs₂CO₃ (290.3 mg, 0.89 mmol in 1 mL H₂O) and Pd(PPh₃)₄ (15.6 mg, 0.013 mmol) in DME (5 mL). After a reaction time of 21 hours, the crude was purified by silica gel column chromatography (EtOAc/CH₂Cl₂, 1:1 → 1:0 v/v) and concentration of the relevant fractions [*R*_f = 0.19 (EtOAc/CH₂Cl₂, 1:1 v/v)] gave the target compound **24i** as an orange solid (57.4 mg, 67%).

mp: 170-172 °C.

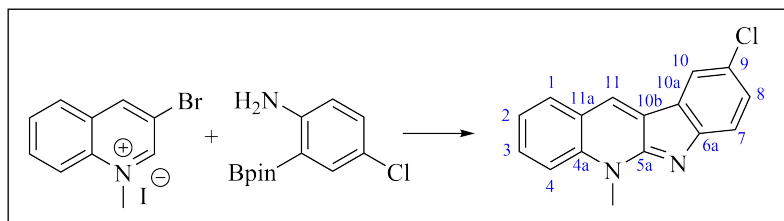
IR (ATR): ν_{max} 2922, 2851, 1645, 1490, 1215, 1150, 761 cm⁻¹.

¹H NMR (400 MHz, CDCl₃): δ 8.52 (s, 1H, H-11), 7.97 (dd, *J* = 8.0 Hz, 1.1 Hz, 1H, H-1), 7.86 (d, *J* = 1.1 Hz, 1H, H-10), 7.81-7.73 (m, 2H, H-3 and H-4), 7.68 (d, *J* = 8.6 Hz, 1H, H-7), 7.48-7.44 (m, 1H, H-2), 7.39 (dd, *J* = 8.6 Hz, 1.5 Hz, 1H, H-8), 4.34 (s, 3H, NCH₃).

¹³C NMR (100 MHz, CDCl₃): δ 156.8 (C-5a), 142.7 (q, *J*_{CF} = 2.4 Hz, C-9), 137.2 (C-4a), 131.1 (C-3), 130.3 (C-1), 129.6 (C-11), 127.5 (C-10a), 124.3 (C-11a), 122.7 (C-8), 122.3 (C-2), 121.1 (q, *J*_{CF} = 255.0 Hz, OCF₃), 120.7 (C-10b), 118.2 (C-7), 114.4 (C-4), 114.1 (C-10), 33.2 (NCH₃).

¹⁹F NMR (376 MHz, CDCl₃): δ -57.9.

HRMS (ESI): sample sent to UiB for analysis.

9-Chloro-5-methyl-5H-indolo[2,3-b]quinoline (24j)

Following the general procedure, the title compound was prepared from 3-bromo-*N*-methylquinolinium iodide (**115**) (100.0 mg, 0.29 mmol), 4-chloro-2-(4,4,5,5-tetramethyl-1,3,2-dioxaborolan-2-yl)benzeneamine (**83f**) (94.3 mg, 0.37 mmol), an aq. solution of Cs_2CO_3 (311.8 mg, 0.96 mmol in 1 mL H_2O) and $\text{Pd}(\text{PPh}_3)_4$ (16.7 mg, 0.014 mmol) in DME (5 mL). After a reaction time of 19 hours, the crude was purified by silica gel column chromatography (EtOAc) and concentration of the relevant fractions [$R_f = 0.19$ (EtOAc)] gave the target compound **24j** as an orange solid (50.0 mg, 65%).

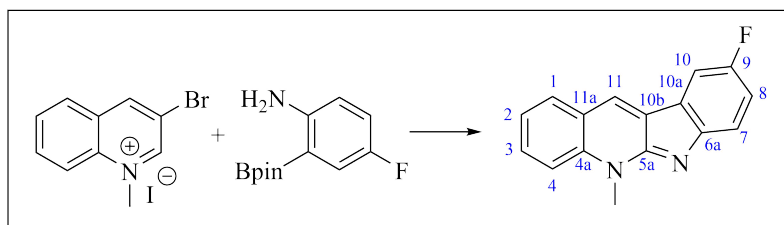
mp: 226-228 °C.

IR (ATR): ν_{max} 3026, 2924, 2852, 1648, 1489, 810, 749 cm^{-1} .

$^1\text{H NMR}$ (400 MHz, CDCl_3): δ 8.47 (s, 1H, H-11), 7.96 (d, $J = 7.9$ Hz, 1H, H-1), 7.94 (d, $J = 2.0$ Hz, 1H, H-10), 7.80-7.72 (m, 2H, H-3 and H-4), 7.62 (d, $J = 8.4$ Hz, 1H, H-8), 7.47-7.44 (m, 2H, H-2 and H-7), 4.33 (s, 3H, NCH_3).

$^{13}\text{C NMR}$ (100 MHz, CDCl_3): δ 156.4 (C-5a), 153.7 (C-6a), 137.2 (C-4a), 131.0 (C-3), 130.3 (C-1), 129.3 (C-11), 129.2 (C-7), 127.2 (C-10a), 125.1 (C-11a), 122.3 (C-2), 120.9 (C-10), 120.8 (C-10b), 118.6 (C-8), 114.3 (C-4), 33.2 (NCH_3). C-9 was obscured or overlapping.

In accordance with previously reported data.^[151]

9-Fluoro-5-methyl-5H-indolo[2,3-b]quinoline (24k)

Following the general procedure, the title compound was prepared from 3-bromo-*N*-methylquinolinium iodide (**115**) (100.0 mg, 0.29 mmol), 4-fluoro-2-(4,4,5,5-tetramethyl-1,3,2-dioxaborolan-2-yl)aniline (**83a**) (81.5 mg, 0.34 mmol), an aq. solution of Cs_2CO_3 (302.4 mg, 0.93 mmol in 1 mL H_2O) and $\text{Pd}(\text{PPh}_3)_4$ (16.7 mg, 0.014 mmol) in DME (5 mL). After a reaction time of 20 hours, the crude was purified by silica gel column chromatography (EtOAc) and

concentration of the relevant fractions [$R_f = 0.20$ (EtOAc)] gave the target compound **24k** as bright orange crystals (44.2 mg, 61%).

mp: 161-164 °C (lit.^[288] 162.3-165.1 °C).

IR (ATR): ν_{\max} 3065, 2920, 1455, 1239, 1117, 740 cm^{-1} .

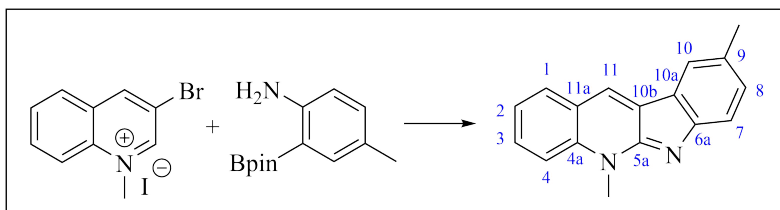
^1H NMR (400 MHz, CDCl_3): δ 8.53 (s, 1H, H-11), 7.99 (d, $J = 8.0$ Hz, 1H, H-1), 7.82-7.77 (m, 2H, H-2 and H-3), 7.70 (dd, $J = 8.3$ Hz, 2.6 Hz, 1H, H-10), 7.66 (dd, $J = 8.7$ Hz, 4.5 Hz, 1H, H-7), 7.48-7.44 (m, 1H, H-4), 7.29-7.24 (m, 1H, H-9), 4.36 (s, 3H, NCH_3).

^{13}C NMR (100 MHz, CDCl_3): δ 157.8 (d, $J_{\text{CF}} = 236.3$ Hz, C-9), 156.4 (d, $J_{\text{CF}} = 1.7$ Hz, C-5a), 151.5 (C-6a), 137.3 (C-4a), 131.0 (C-3), 130.3 (C-1), 129.3 (C-11), 128.0 (d, $J_{\text{CF}} = 4.4$ Hz, C-10b), 124.4 (d, $J_{\text{CF}} = 9.8$ Hz, C-10a), 122.1 (C-4), 120.6 (C-11a), 118.2 (d, $J_{\text{CF}} = 8.7$ Hz, C-7), 116.6 (d, $J_{\text{CF}} = 24.5$ Hz, C-8), 114.3 (C-2), 107.3 (d, $J_{\text{CF}} = 24.6$ Hz, C-10), 33.2 (NCH_3).

^{19}F NMR (376 MHz, CDCl_3): δ -123.7.

In accordance with previously reported data.^[288]

5,9-Dimethyl-5H-indolo[2,3-b]quinoline (24l)



Following the general procedure, the title compound was prepared from 3-bromo-*N*-methylquinolinium iodide (**115**) (100.0 mg, 0.29 mmol), 4-methyl-2-(4,4,5,5-tetramethyl-1,3,2-dioxaborolan-2-yl)aniline (**83g**) (86.9 mg, 0.37 mmol), an aq. solution of Cs_2CO_3 (311.8 mg, 0.96 mmol in 1 mL H_2O) and $\text{Pd}(\text{PPh}_3)_4$ (16.7 mg, 0.014 mmol) in DME (5 mL). After a reaction time of 24 hours, the crude was purified by silica gel column chromatography (EtOAc) and concentration of the relevant fractions [$R_f = 0.17$ (EtOAc)] gave the target compound **24l** as a red oily solid (41.5 mg, 58%).

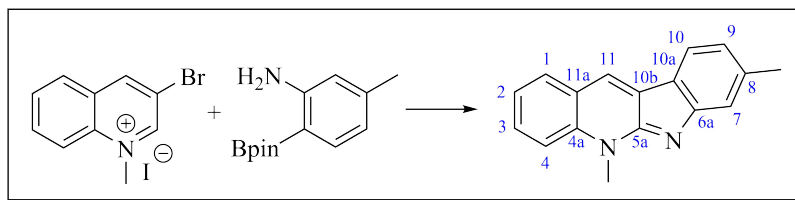
IR (ATR): ν_{\max} 3010, 2971, 2919, 2860, 1562, 1493, 1198, 746 cm^{-1} .

^1H NMR (400 MHz, CDCl_3): δ 8.42 (s, 1H, H-11), 7.93 (dd, $J = 7.9$ Hz, 1.3 Hz, 1H, H-1), 7.82-7.81 (m, 1H, H-10), 7.75-7.68 (m, 2H, H-2 and H-4), 7.63 (d, $J = 8.0$ Hz, 1H, H-7), 7.43-7.39 (m, 1H, H-3), 7.37-7.35 (m, 1H, H-8), 4.31 (s, 3H, NCH_3), 2.52 (s, 3H, CH_3).

^{13}C NMR (100 MHz, CDCl_3): δ 156.1 (C-5a), 153.4 (C-6a), 137.0 (C-4a), 130.5 (C-8), 130.3 (C-2), 130.0 (C-1), 129.3 (C-10a), 128.3 (C-9), 127.9 (C-11), 124.1 (C-11a), 121.8 (C-3), 121.3 (C-10), 120.8 (C-10b), 117.3 (C-7), 114.1 (C-4), 33.0 (NCH_3), 21.6 (CH_3).

In accordance with previously reported data.^[289]

5,8-Dimethyl-5*H*-indolo[2,3-*b*]quinoline (24m)



Following the general procedure, the title compound was prepared from 3-bromo-*N*-methylquinolinium iodide (**115**) (100.0 mg, 0.29 mmol), 5-methyl-2-(4,4,5,5-tetramethyl-1,3,2-dioxaborolan-2-yl)aniline (**83h**) (86.9 mg, 0.37 mmol), an aq. solution of Cs_2CO_3 (406.3 mg, 1.25 mmol in 1 mL H_2O) and $\text{Pd}(\text{PPh}_3)_4$ (16.7 mg, 0.014 mmol) in DME (5 mL). After a reaction time of 23 hours, the crude was purified by silica gel column chromatography (EtOAc) and concentration of the relevant fractions [$R_f = 0.22$ (EtOAc)] gave the target compound **24m** as a bright orange solid (45.9 mg, 64%).

mp: 147-150 °C (lit.^[288] 155-156 °C).

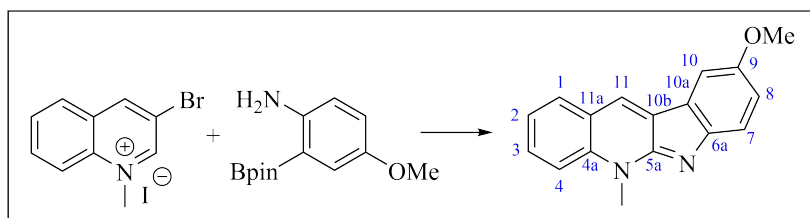
IR (ATR): ν_{max} 3028, 2919, 2850, 1491, 1238, 795, 747 cm^{-1} .

^1H NMR (400 MHz, CDCl_3): δ 8.38 (s, 1H, H-11), 7.92 (d, $J = 7.8$ Hz, 1H, H-10), 7.89 (d, $J = 7.7$ Hz, 1H, H-1), 7.74-7.68 (m, 2H, H-3 and H-4), 7.54 (s, 1H, H-7), 7.42-7.38 (m, 1H, H-9), 7.04 (d, $J = 7.6$ Hz, 1H, H-2), 4.31 (s, 3H, NCH_3), 2.55 (s, 3H, CH_3).

^{13}C NMR (100 MHz, CDCl_3): δ 156.6 (C-5a), 156.0 (C-6a), 139.8 (C-8), 136.8 (C-4a), 130.1 (C-3), 129.9 (C-1), 128.3 (C-10b), 127.1 (C-11), 121.9 (C-9), 121.6 (C-11a), 121.2 (C-2), 120.7 (C-10), 118.3 (C-7), 114.1 (C-4), 33.0 (NCH_3), 22.6 (CH_3).

In accordance with previously reported data.^[288]

9-Methoxy-5-methyl-5*H*-indolo[2,3-*b*]quinoline (24n)



Following the general procedure, the title compound was prepared from 3-bromo-*N*-methylquinolinium iodide (**115**) (100.0 mg, 0.29 mmol), 4-methoxy-2-(4,4,5,5-tetramethyl-1,3,2-dioxaborolan-2-yl)aniline (**83i**) (92.8 mg, 0.37 mmol), an aq. solution of Cs_2CO_3 (311.8 mg, 0.96 mmol in 1 mL H_2O) and $\text{Pd}(\text{PPh}_3)_4$ (16.7 mg, 0.014 mmol) in DME (5 mL). After a reaction time of 24 hours, the crude was purified by silica gel column chromatography (EtOAc) and concentration of the relevant fractions [$R_f = 0.13$ (EtOAc)] gave the target compound **24n** as a

bright red solid (48.6 mg, 64%).

mp: 103-105 °C (lit.^[288] 106.85-108.85 °C).

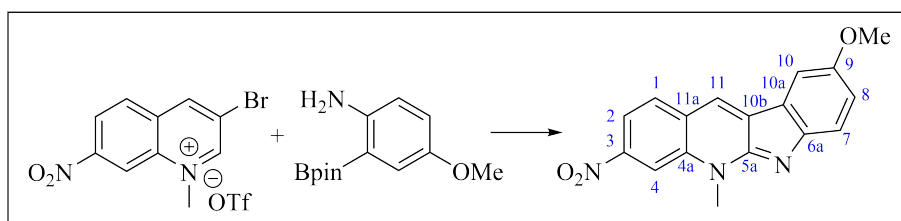
IR (ATR): ν_{\max} 3125, 2984, 2922, 2824, 1459, 1193, 744 cm^{-1} .

¹H NMR (400 MHz, CDCl₃): δ 8.44 (s, 1H), 7.94-7.92 (m, 1H), 7.76-7.68 (m, 2H), 7.63 (d, $J = 8.6$ Hz, 1H), 7.53 (d, $J = 2.5$ Hz, 1H), 7.43-7.39 (m, 1H), 7.16 (dd, $J = 8.6$ Hz, 2.6 Hz, 1H), 4.29 (s, 3H), 3.91 (s, 3H).

¹³C NMR (100 MHz, CDCl₃): δ 155.6, 154.2, 149.6, 137.0, 130.5, 130.0, 128.3, 128.3, 124.3, 121.7, 120.5, 118.0, 117.0, 114.0, 105.4, 56.1, 32.9.

In accordance with previously reported data.^[288]

9-Methoxy-5-methyl-3-nitro-5H-indolo[2,3-*b*]quinoline (24o)



Following the general procedure, the title compound was prepared from 3-bromo-*N*-methyl-7-nitroquinolinium triflate (**115m**) (163.7 mg, 0.39 mmol), 4-methoxy-2-(4,4,5,5-tetramethyl-1,3,2-dioxaborolan-2-yl)aniline (**83i**) (127.5 mg, 0.51 mmol), an aq. solution of Cs₂CO₃ (419.3 mg, 1.29 mmol in 5 mL H₂O) and Pd(PPh₃)₄ (22.5 mg, 0.019 mmol) in DME (5 mL). After a reaction time of 24 hours, the crude was purified by silica gel column chromatography (pet. ether/EtOAc, 1:1 → 0:1 v/v) and concentration of the relevant fractions [$R_f = 0.25$ (pet. ether/EtOAc, 1:1 v/v)] gave the target compound **24o** as a purple solid (60.0 mg, 50%).

mp: 223-224 °C.

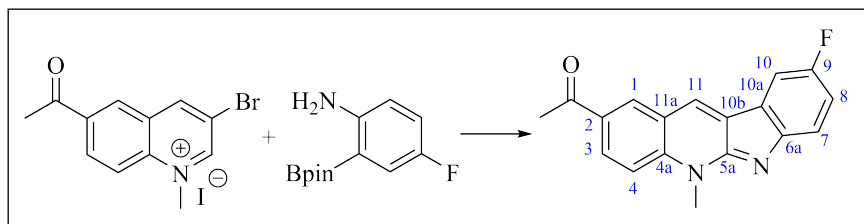
IR (ATR): ν_{\max} 3004, 2935, 2830, 1509, 1476, 1340, 733 cm^{-1} .

¹H NMR (400 MHz, DMSO-*d*₆): δ 8.95 (s, 1H, H-11), 8.59 (d, $J = 1.8$ Hz, 1H, H-4), 8.28 (d, $J = 8.7$ Hz, 1H, H-1), 8.18 (dd, $J = 8.7$ Hz, 2.1 Hz, 1H, H-2), 7.72 (d, $J = 2.5$ Hz, 1H, H-10), 7.49 (d, $J = 8.6$ Hz, 1H, H-7), 7.14 (dd, $J = 8.6$ Hz, 2.6 Hz, 1H, H-8), 4.30 (s, 3H, NCH₃), 3.85 (s, 3H, OCH₃).

¹³C NMR (100 MHz, DMSO-*d*₆): δ 154.7 (C-5a), 153.9 (C-6a), 150.0 (C-9), 147.4 (C-3), 136.1 (C-4a), 131.3 (C-1), 128.8 (C-11a), 127.6 (C-11), 123.9 (C-10b), 123.8 (C-10a), 118.1 (C-7), 117.9 (C-8), 115.2 (C-2), 110.4 (C-4), 106.1 (C-10), 55.6 (OCH₃), 32.9 (NCH₃).

HRMS (ESI): sample sent to UiB for analysis.

2-Acetyl-9-fluoro-5-methyl-5*H*-indolo[2,3-*b*]quinoline (24q)



Following the general procedure, the title compound was prepared from 6-acetyl-3-bromo-*N*-methylquinolinium iodide (**115d**) (100.0 mg, 0.24 mmol), 4-fluoro-2-(4,4,5,5-tetramethyl-1,3,2-dioxaborolan-2-yl)aniline (**83a**) (75.7 mg, 0.32 mmol), an aq. solution of Cs₂CO₃ (258.0 mg, 0.79 mmol in 1 mL H₂O) and Pd(PPh₃)₄ (13.9 mg, 0.012 mmol) in DME (5 mL). After a reaction time of 22 hours, the crude was purified by silica gel column chromatography (EtOAc) and concentration of the relevant fractions [*R*_f = 0.10 (EtOAc)] gave the target compound **24q** as a bright orange solid (44.6 mg, 64%).

mp: 254-256 °C.

IR (ATR): ν_{\max} 3048, 3005, 2922, 1672, 1647, 1492, 1179, 807 cm⁻¹.

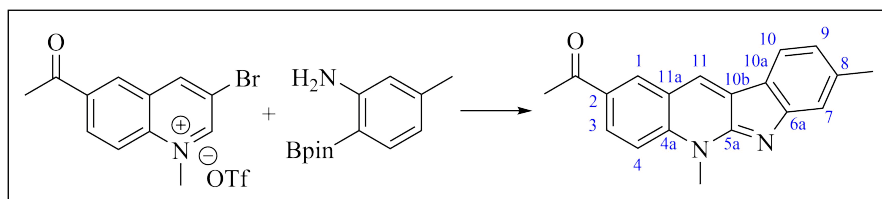
¹H NMR (400 MHz, DMSO-*d*₆): δ 9.08 (s, 1H, H-4), 8.75 (d, *J* = 1.7 Hz, 1H, H-1), 8.32 (dd, *J* = 8.9 Hz, 1.9 Hz, 1H, H-3), 8.04 (d, *J* = 9.0 Hz, 1H, H-4), 7.98 (dd, *J* = 8.6 Hz, 2.5 Hz, 1H, H-10), 7.59 (dd, *J* = 8.6 Hz, 4.5 Hz, 1H, H-7), 7.37-7.32 (m, 1H, H-8), 4.30 (s, 3H, NCH₃), 2.71 (s, 3H, CH₃).

¹³C NMR (100 MHz, DMSO-*d*₆): δ 196.5 (C=O), 157.0 (d, *J*_{CF} = 233.2 Hz, C-9), 155.5 (C-5a), 139.4 (C-4a), 131.6 (C-1), 130.9 (C-11), 130.3 (C-6a), 129.7 (C-3), 127.3 (C-10b), 124.2 (d, *J*_{CF} = 10.0 Hz, C-10a), 122.3 (C-11a), 119.3 (C-2), 118.1 (d, *J*_{CF} = 8.4 Hz, C-7), 116.2 (d, *J*_{CF} = 24.1 Hz, C-8), 115.4 (C-4), 107.8 (d, *J*_{CF} = 24.3 Hz, C-10), 33.1 (NCH₃), 26.6 (CH₃).

¹⁹F NMR (376 MHz, DMSO-*d*₆): δ -77.3.

HRMS (ESI): sample sent to UiB for analysis.

2-Acetyl-5,8-dimethyl-5*H*-indolo[2,3-*b*]quinoline (24r)



Following the general procedure, the title compound was prepared from 6-acetyl-3-bromo-*N*-methylquinolinium triflate (**115n**) (100.0 mg, 0.24 mmol), 5-methyl-2-(4,4,5,5-tetramethyl-

1,3,2-dioxaborolan-2-yl)aniline (**83h**) (74.5 mg, 0.32 mmol), an aq. solution of Cs_2CO_3 (273.7 mg, 0.84 mmol in 1 mL H_2O) and $\text{Pd}(\text{PPh}_3)_4$ (13.9 mg, 0.012 mmol) in DME (5 mL). After a reaction time of 21 hours, the crude was purified by silica gel column chromatography (EtOAc) and concentration of the relevant fractions [$R_f = 0.11$ (EtOAc)] gave the target compound **24r** as a yellow solid (32.0 mg, 46%).

mp: 273-275 °C.

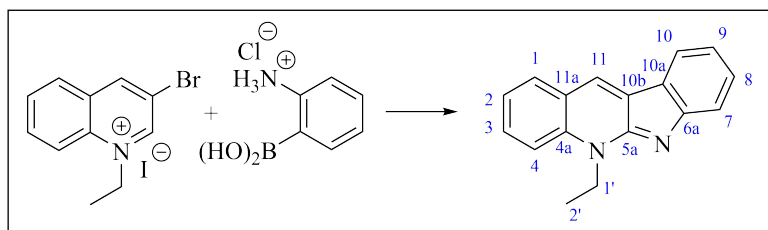
IR (ATR): ν_{max} 2920, 2851, 1685, 1604, 1256, 1169, 1033, 804 cm^{-1} .

^1H NMR (400 MHz, $\text{DMSO}-d_6$): δ 8.94 (s, 1H, H-11), 8.76 (d, $J = 1.7$ Hz, 1H, H-1), 8.29 (dd, $J = 9.0$ Hz, 1.9 Hz, 1H, H-3), 8.04-7.99 (m, 2H, H-4 and H-10), 7.42 (s, 1H, H-7), 7.05 (d, $J = 7.7$ Hz, 1H, H-9), 4.31 (s, 3H, NCH_3), 2.70 (s, 3H, $\text{CO}-\text{CH}_3$), 2.48 (s, 3H, CH_3).

^{13}C NMR (100 MHz, $\text{DMSO}-d_6$): δ 196.5 (C=O), 139.1 (C-4a), 138.9 (C-8), 131.2 (C-1), 130.2 (C-11a), 129.1 (C-3), 128.4 (C-11), 127.6 (C-2), 121.2 (C-4), 121.2 (C-7), 119.7 (C-10a), 119.1 (C-10b), 117.8 (C-9), 115.2 (C-10), 33.1 (NCH_3), 26.6 ($\text{CO}-\text{CH}_3$), 22.0 (CH_3). The presence of C-5a and C-6a were confirmed by $^1\text{H}-^{13}\text{C}$ HMBC. The presence of two carbons at 121.2 ppm was confirmed by $^1\text{H}-^{13}\text{C}$ HSQC.

HRMS (ESI): sample sent to UiB for analysis.

5-Ethyl-5H-indolo[2,3-b]quinoline (24s)



Following the general procedure, the title compound was prepared from 3-bromo-*N*-ethylquinolinium iodide (**115a**) (100.0 mg, 0.27 mmol), 2-aminophenylboronic acid hydrochloride (**68**) (57.3 mg, 0.33 mmol), an aq. solution of Cs_2CO_3 (369.5 mg, 1.13 mmol in 1 mL H_2O) and $\text{Pd}(\text{PPh}_3)_4$ (15.6 mg, 0.013) in DME (5 mL). After a reaction time of 22 hours, the crude was purified by silica gel column chromatography (pet. ether/EtOAc, 1:1 \rightarrow 0:1 v/v) and concentration of the relevant fractions [$R_f = 0.01$ (pet. ether/EtOAc, 1:1 v/v)] gave the target compound **24s** as a red oily solid (46.2 mg, 69%).

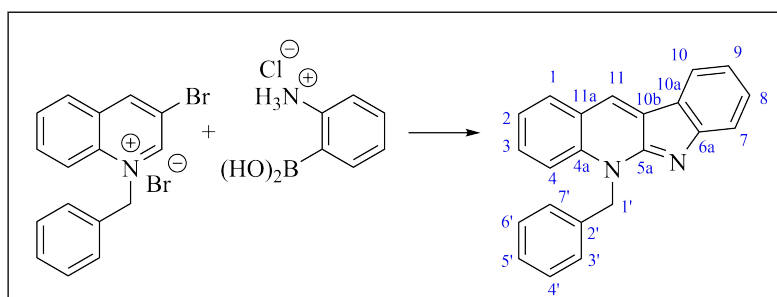
IR (ATR): ν_{max} 3056, 2923, 2852, 1562, 1514, 1495, 1441, 1201, 730 cm^{-1} .

^1H NMR (400 MHz, CDCl_3): δ 8.53 (s, 1H, H-11), 8.05 (d, $J = 7.6$ Hz, 1H, H-1), 7.99 (d, $J = 7.7$ Hz, 1H, H-10), 7.80-7.74 (m, 3H, H-2, H-4 and H-7), 7.57-7.53 (m, 1H, H-9), 7.45-7.41 (m, 1H, H-8), 7.23 (t, $J = 7.4$ Hz, 1H, H-3), 5.02 (q, $J = 7.2$ Hz, 2H, H-1'), 1.62 (t, $J = 7.2$ Hz, 3H, H-2').

^{13}C NMR (100 MHz, CDCl_3): δ 155.6 (C-5a), 155.4 (C-6a), 135.9 (C-4a), 130.4 (C-10), 130.3 (C-7), 129.4 (C-9), 128.3 (C-11), 128.2 (C-10b), 124.1 (C-11a), 121.8 (C-8), 121.2 (C-10a), 121.1 (C-1), 119.9 (C-3), 117.8 (C-2), 114.2 (C-4), 40.9 (C-1'), 13.0 (C-2').

In accordance with previously reported data.^[186]

5-Benzyl-5H-indolo[2,3-b]quinoline (24t)



Following the general procedure, the title compound was prepared from 3-bromo-*N*-benzylquinolinium bromide (**115b**) (100.0 mg, 0.26 mmol), 2-aminophenylboronic acid hydrochloride (**68**) (59.8 mg, 0.34 mmol), an aq. solution of Cs_2CO_3 (279.5 mg, 0.86 mmol in 1 mL H_2O) and $\text{Pd}(\text{PPh}_3)_4$ (15.0 mg, 0.013 mmol) in DME (5 mL). After a reaction time of 23 hours, the crude was purified by silica gel column chromatography (pet. ether/EtOAc, 7:3 v/v) and concentration of the relevant fractions [$R_f = 0.25$ (pet. ether/EtOAc, 7:3 v/v)] gave the target compound **24t** as a red crystalline solid (40.1 mg, 50%).

mp: 215-219 °C (lit.^[186] 184-187 °C).

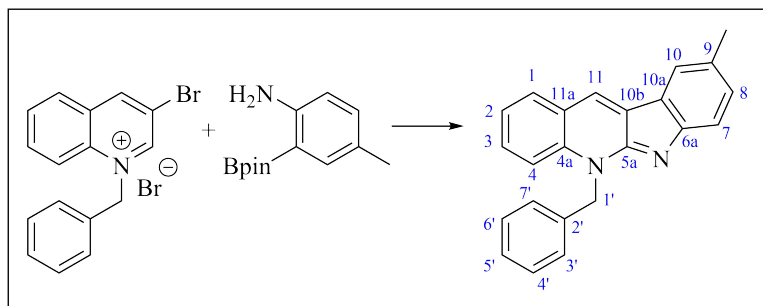
IR (ATR): ν_{max} 3055, 3033, 2926, 2855, 1562, 1497, 1202, 745 cm^{-1} .

^1H NMR (400 MHz, CDCl_3): δ 8.60 (s, 1H, H-11), 8.10 (ddd, $J = 7.7$ Hz, 1.2 Hz, 0.7 Hz, 1H, H-10), 8.06-7.98 (m, 1H, H-1), 7.77-7.75 (m, 1H, H-7), 7.65-7.60 (m, 2H, H-8 and H-9), 7.59-7.54 (m, 1H, H-4), 7.41-7.37 (m, 1H, H-2), 7.29-7.20 (m, 7H, H-3, H-2'-H-7' and residual chloroform), 6.22 (bs, 2H, H' 1).

^{13}C NMR (100 MHz, CDCl_3): δ 156.7 (C-5a), 155.7 (C-6a), 136.5 (C-4a), 135.9 (C-2'), 130.5 (C-9), 130.1 (C-1), 129.5 (C-8), 129.0 (C-4' and C-6'), 128.6 (C-11), 128.5 (C-10a), 127.7 (C-3), 126.8 (C-3' and C-7'), 124.4 (C-11a), 122.1 (C-10), 121.2 (C-7), 121.1 (C-10b), 120.1 (C-5'), 118.1 (C-2), 115.3 (C-4), 49.6 (C-1').

In accordance with previously reported data.^[186]

5-Benzyl-9-methyl-5*H*-indolo[2,3-*b*]quinoline (24u)



Following the general procedure, the title compound was prepared from 3-bromo-*N*-benzylquinolinium bromide (**115b**) (100.0 mg, 0.26 mmol), 4-methyl-2-(4,4,5,5-tetramethyl-1,3,2-dioxaborolan-2-yl)aniline (**83g**) (80.4 mg, 0.34 mmol), an aq. solution of Cs_2CO_3 (296.5 mg, 0.91 mmol in 1 mL H_2O) and $\text{Pd}(\text{PPh}_3)_4$ (15.0 mg, 0.013 mmol) in DME (5 mL). After a reaction time of 23 hours, the crude was purified by silica gel column chromatography (pet. ether/EtOAc, 7:3 \rightarrow 1:1 v/v) and concentration of the relevant fractions [$R_f = 0.31$ (pet. ether/EtOAc, 7:3 v/v)] gave the target compound **24u** as a dark red solid (43.8 mg, 52%).

mp: 223-225 °C.

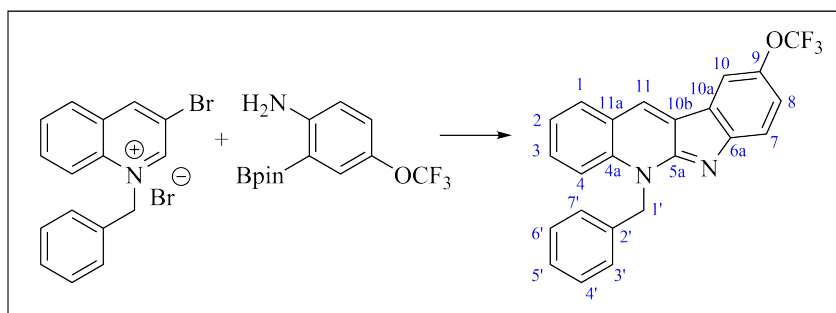
IR (ATR): ν_{max} 3057, 3001, 2915, 2856, 1497, 1453, 1199, 750, 732 cm^{-1} .

^1H NMR (400 MHz, CDCl_3): δ 8.54 (s, 1H, H-11), 7.97 (d, $J = 7.6$ Hz, 1H, H-1), 7.89 (s, 1H, H-10), 7.65 (d, $J = 8.1$ Hz, 1H, H-3), 7.62-7.56 (m, 2H, H-4 and H-7), 7.39-7.35 (m, 2H, H-2 and H-8), 7.25-7.21 (m, 5H, H-3'-H-7'), 6.19 (bs, 2H, H-1'), 2.55 (s, 3H, CH_3).

^{13}C NMR (100 MHz, CDCl_3): δ 156.3 (C-5a), 153.4 (C-6a), 136.5 (C-4a), 135.9 (C-2'), 130.6 (C-8), 130.4 (C-7), 130.1 (C-1), 129.6 (C-9), 129.0 (C-4' and C-6'), 128.5 (C-10b), 128.4 (C-11), 127.6 (C-5'), 126.8 (C-3' and C-7'), 124.3 (C-11a), 121.9 (C-2), 121.4 (C-10), 121.2 (C-10a), 117.6 (C-3), 115.2 (C-4), 49.6 (C-1'), 21.6 (CH_3).

HRMS (ESI): calcd. for $\text{C}_{23}\text{H}_{18}\text{N}_2$ [$\text{M} + \text{H}^+$] 323.1543, found 323.1543.

5-Benzyl-9-(trifluoromethoxy)-5*H*-indolo[2,3-*b*]quinoline (24v)



Following the general procedure, the title compound was prepared from 3-bromo-*N*-benzylquinolinium bromide (**115b**) (100.0 mg, 0.26 mmol), 2-(3,3,4,4-tetramethyl-1,3,2-dioxaborolan-1-yl)-4-(trifluoromethoxy)aniline (**83e**) (104.5 mg, 0.34 mmol), an aq. solution of Cs₂CO₃ (279.5 mg, 0.86 mmol in 1 mL H₂O) and Pd(PPh₃)₄ (15.0 mg, 0.013 mmol) in DME (5 mL). After a reaction time of 20 hours, the crude was purified by silica gel column chromatography (pet. ether/EtOAc, 8:2 → 7:3 v/v) and concentration of the relevant fractions [*R*_f = 0.21 (pet. ether/EtOAc, 8:2 v/v)] gave the target compound **24v** as a bright orange solid (58.9 mg, 58%).

mp: 206-209 °C.

IR (ATR): ν_{\max} 3065, 3029, 2924, 2852, 1494, 1228, 1128, 747 cm⁻¹.

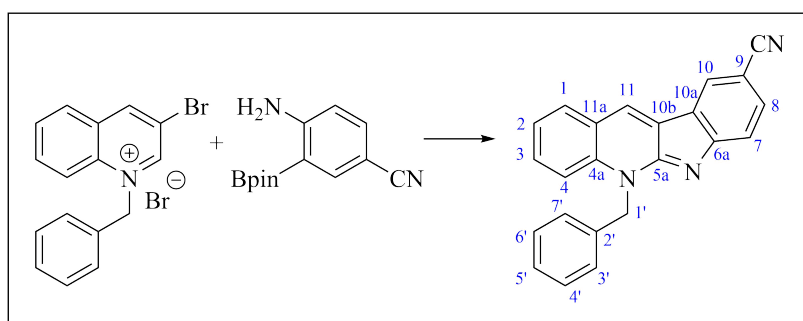
¹H NMR (400 MHz, CDCl₃): δ 8.64 (s, 1H, H-11), 8.01 (d, *J* = 7.8 Hz, 1H, H-1), 7.93 (d, *J* = 1.1 Hz, 1H, H-10), 7.71 (d, *J* = 8.6 Hz, 1H, H-3), 7.66-7.64 (m, 2H, H-4 and H-7), 7.44-7.40 (m, 2H, H-2 and H-8), 7.28-7.20 (m, 5H, H-3'-H-7'), 6.20 (bs, 2H, H-1').

¹³C NMR (100 MHz, CDCl₃): δ 157.1 (C-5a), 153.9 (C-6a), 142.9 (q, *J*_{CF} = 2.0 Hz, C-9), 136.7 (C-4a), 135.6 (C-2'), 131.1 (C-7), 130.4 (C-1), 130.1 (C-11), 129.1 (C-4' and C-6'), 127.8 (C-5'), 127.7 (C-10a), 126.7 (C-3' and C-7'), 124.6 (C-11a), 122.8 (C-8), 122.4 (C-2), 121.0 (C-10b), 120.0 (q, *J*_{CF} = 255.6 Hz, OCF₃), 118.4 (C-3), 115.4 (C-4), 114.2 (C-10), 49.8 (C-1').

¹⁹F NMR (376 MHz, CDCl₃): δ -57.9.

HRMS (ESI): sample sent to UiB for analysis.

5-Benzyl-5*H*-indolo[2,3-*b*]quinoline-9-carbonitrile (**24w**)



Following the general procedure, the title compound was prepared from 3-bromo-*N*-benzylquinolinium bromide (**115b**) (100.0 mg, 0.26 mmol), 4-amino-3-(4,4,5,5-tetramethyl-1,3,2-dioxaborolan-2-yl)benzonitrile (**83c**) (84.2 mg, 0.34 mmol), an aq. solution of Cs₂CO₃ (279.5 mg, 0.86 mmol in 2 mL H₂O) and Pd(PPh₃)₄ (15.0 mg, 0.013 mmol) in DME (10 mL). After a reaction time of 24 hours, the crude was purified by silica gel column chromatography (pet. ether/EtOAc, 7:3 → 1:1 v/v) and concentration of the relevant fractions [*R*_f = 0.33 (pet. ether/EtOAc, 7:3 v/v)] gave the target compound **24w** as a dark orange solid (16.4 mg, 19%).

mp: 307-310 °C.

IR (ATR): ν_{\max} 2949, 2919, 2217, 1485, 1246, 757 cm^{-1} .

^1H NMR (400 MHz, CDCl_3): δ 8.75 (s, 1H, H-11), 8.39 (d, $J = 0.9$ Hz, 1H, H-10), 8.09-8.07 (m, 1H, H-1), 7.81-7.69 (m, 4H, H-3, H-4, H-7 and H-8), 7.51-7.47 (m, 1H, H-2), 7.31-7.21 (m, 6H, H-3'-H-7'), 6.26 (bs, 2H, H-1').

^{13}C NMR (100 MHz, CDCl_3): δ 158.5 (C-5a), 158.2 (C-6a), 136.7 (C-4a), 135.2 (C-2'), 132.7 (C-7), 131.7 (C-8), 130.9 (C-11), 130.6 (C-1), 129.2 (C-4' and C-6'), 128.0 (C-5'), 126.7 (C-3' and C-7'), 126.6 (C-10b), 125.6 (C-10), 124.6 (C-11a), 123.1 (C-2), 121.5 (C-10a), 120.8 (CN), 118.7 (C-3), 115.7 (C-4), 102.3 (C-9), 50.1 (C-1').

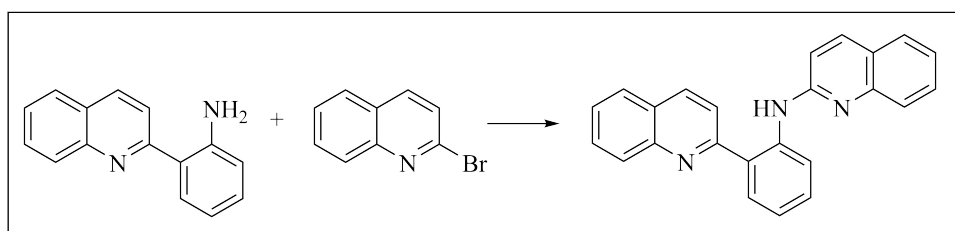
HRMS (ESI): sample sent to UiB for analysis.

7.2.9 Buchwald-Hartwig aminations

General procedure

A suitable round-bottom flask was charged with 2-(quinolin-2-yl)aniline (**70**) (1000.0 mg, 4.54 mmol), the appropriate coupling partner (4.99 mmol), Cs_2CO_3 (2958.4 mg, 9.08 mmol) followed by anhydrous THF (8 mL) and the mixture was thoroughly flushed with argon. $\text{Pd}_2(\text{dba})_3$ (207.9 mg, 0.23 mmol, 5 mol%) and XantPhos (288.9 mg, 0.49 mmol, 11 mol%) were added to the mixture and the flask was then flushed with argon for 5 minutes. The resulting reaction mixture was heated to reflux and stirred until completion as indicated by TLC analysis. The crude mixture was then allowed to cool to rt and the volatiles were removed under reduced pressure. The concentrate was evaporated onto celite and purified by column chromatography using the eluent as indicated in the specific descriptions to give target compounds **L**.

N-(2-(Quinolin-2-yl)phenyl)quinolin-2-amine (**L1**)



Following the general procedure, the title compound was prepared from 2-(quinolin-2-yl)aniline (**70**), 2-bromoquinoline (**67a**) (1.04 g, 4.99 mmol), Cs_2CO_3 , $\text{Pd}_2(\text{dba})_3$, XantPhos and THF. After a reaction time of 4 hours, the crude was purified by silica gel column chromatography (pet. ether/diethyl ether, 8:2 v/v) and concentration of the relevant fractions [$R_f = 0.24$ (pet. ether/diethyl ether, 8:2 v/v)] and further recrystallized using a mixture of pet. ether, diethyl ether and CH_2Cl_2 gave the target compound **L1** as a bright yellow solid (0.81 g, 52%).

mp: 156-158 °C.

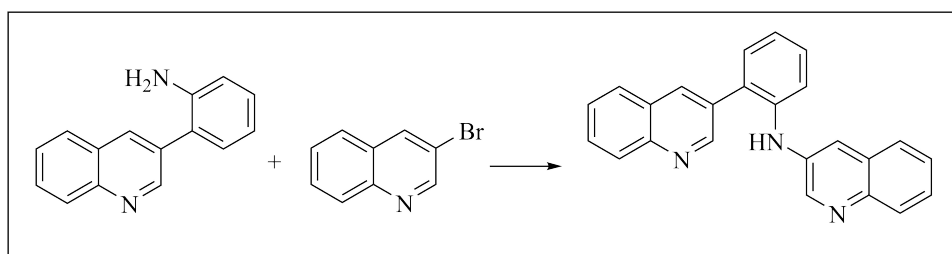
IR (NaCl): ν_{\max} 3460, 3261, 3186, 3052, 2928, 1592, 1443, 1319, 762 cm^{-1} .

^1H NMR (400 MHz, CDCl_3): δ 12.63 (bs, 1H), 9.18 (bs, 1H), 8.26 (d, $J = 8.8$ Hz, 1H), 8.22 (d, $J = 8.2$ Hz, 1H), 7.94-7.91 (m, 2H), 7.88-7.85 (m, 3H), 7.83-7.79 (m, 1H), 7.63 (dd, $J = 7.9$ Hz, 1.1 Hz, 1H), 7.61-7.57 (m, 2H), 7.55-7.51 (m, 1H), 7.31-7.27 (m, 1H), 7.17-7.13 (m, 1H), 7.02 (d, $J = 8.9$ Hz, 1H).

^{13}C NMR (100 MHz, CDCl_3): δ 158.8, 153.9, 147.6, 146.3, 140.9, 137.3, 130.5, 130.2, 129.8, 129.7, 129.6, 128.6, 127.7, 127.4, 127.3, 126.7, 126.5, 124.2, 123.2, 121.2, 121.1, 120.6, 114.8. One carbon was obscured or overlapping.

HRMS (ESI): calcd. for $\text{C}_{24}\text{H}_{17}\text{N}_3$ [$\text{M} + \text{H}^+$] 348.1495, found 348.1502.

***N*-(2-(Quinolin-3-yl)phenyl)quinolin-3-amine (L2)**



Following the general procedure, the title compound was prepared from 2-(quinolin-3-yl)aniline (**69**), 3-bromoquinoline (**67b**) (0.68 mL, 4.99 mmol), Cs_2CO_3 , $\text{Pd}_2(\text{dba})_3$, XantPhos and THF. After a reaction time of 23 hours, the crude was purified by silica gel column chromatography (diethyl ether/MeOH, 100:0 \rightarrow 95:5 v/v) and concentration of the relevant fractions [$R_f = 0.11$ (diethyl ether)] gave the target compound **L2** as a puffy yellow solid (1.48 g, 94%).

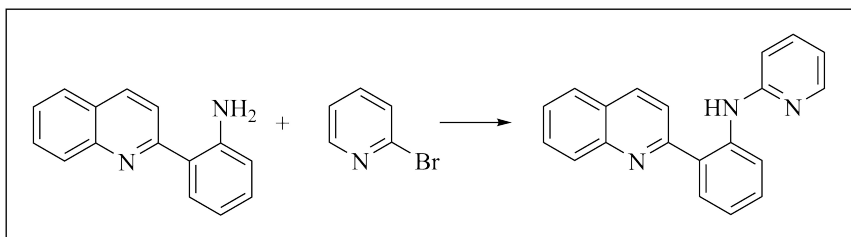
mp: 97-99 °C.

IR (ATR): ν_{\max} 3228, 3037, 2974, 1578, 1490, 694 cm^{-1} .

^1H NMR (400 MHz, CDCl_3): δ 9.00 (d, $J = 2.2$ Hz, 1H), 8.63 (d, $J = 2.7$ Hz, 1H), 8.22 (d, $J = 1.8$ Hz, 1H), 8.08 (d, $J = 8.5$ Hz, 1H), 7.98 (dd, $J = 8.4$ Hz, 0.8 Hz, 1H), 7.78 (dd, $J = 8.2$ Hz, 1.0 Hz, 1H), 7.74-7.71 (m, 1H), 7.67 (d, $J = 2.6$ Hz, 1H), 7.63-7.60 (m, 1H), 7.57-7.39 (m, 6H), 7.21 (dt, $J = 7.7$ Hz, 1.2 Hz, 1H), 5.96 (bs, 1H).

^{13}C NMR (100 MHz, CDCl_3): δ 151.3, 147.3, 144.7, 143.5, 139.6, 137.3, 136.0, 131.9, 131.8, 130.0, 129.9, 129.7, 129.3, 128.9, 128.8, 128.1, 128.0, 127.5, 127.3, 127.0, 126.6, 123.6, 119.6, 118.4.

HRMS (ESI): calcd. for $\text{C}_{24}\text{H}_{17}\text{N}_3$ [$\text{M} + \text{H}^+$] 348.1495, found 348.1503.

***N*-(2-(Quinolin-2-yl)phenyl)pyridine-2-amine (L3)**

Following the general procedure, the title compound was prepared from 2-(quinolin-2-yl)aniline (**70**), 2-bromopyridine (**93**) (0.49 mL, 4.99 mmol), Cs₂CO₃, Pd₂(dba)₃, XantPhos and THF. After a reaction time of 17 hours, the crude was purified by silica gel column chromatography (pet. ether/diethyl ether, 8:2 v/v) and concentration of the relevant fractions [*R*_f = 0.21 (pet. ether/diethyl ether, 8:2 v/v)] gave the target compound **L3** as a bright yellow crystalline solid (0.66 g, 49%).

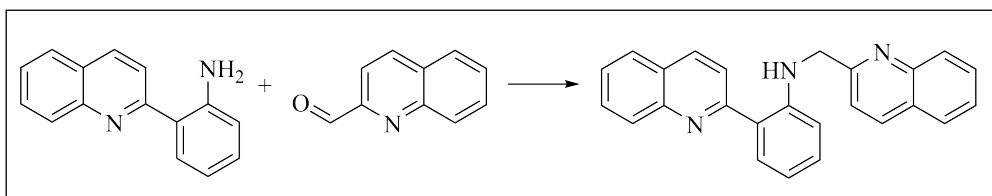
mp: 136-138 °C.

IR (ATR): ν_{\max} 3176, 3055, 3012, 2924, 1590, 1441, 763 cm⁻¹.

¹H NMR (400 MHz, (CD₃)₂CO): δ 8.74-8.72 (m, 1H), 8.46 (d, *J* = 8.6 Hz, 1H), 8.26 (d, *J* = 8.4 Hz, 1H), 8.22 (ddd, *J* = 5.0 Hz, 1.9 Hz, 0.8 Hz, 1H), 8.09 (d, *J* = 8.8 Hz, 1H), 7.99 (dd, *J* = 8.0 Hz, 1.3 Hz, 2H), 7.87-7.83 (m, 1H), 7.66-7.59 (m, 2H), 7.46-7.41 (m, 1H), 7.12-7.07 (m, 1H), 7.06-7.04 (m, 1H), 6.79 (ddd, *J* = 7.1 Hz, 5.0 Hz, 0.9 Hz, 1H).

¹³C NMR (100 MHz, (CD₃)₂CO): δ 159.4, 156.4, 148.3, 147.0, 142.1, 138.4, 138.3, 131.1, 130.9, 130.7, 129.3, 128.6, 127.6, 127.4, 124.8, 121.7, 121.4, 120.6, 115.9, 112.3.

HRMS (ESI): calcd. for C₂₀H₁₅N₃ [M + H⁺] 298.1339, found 298.1348.

7.2.10 Reductive aminations***N*-(2-(Quinolin-2-yl methyl)-2-(quinolin-2-yl)aniline (L4)**

2-Quinolinecarboxaldehyde (**94**) (400.0 mg, 2.54 mmol), 2-(quinolin-2-yl)aniline (**70**) (616.2 mg, 2.80 mmol) and 4 Å MS were mixed in MeOH (20 mL) under an argon atmosphere and stirred at rt for 3 hours until formation of the imine was completed as indicated by TLC and LRMS. The imine was then added AcOH (0.16 mL, 2.80 mmol) and NaBH₃CN (255.4 mg,

4.06 mmol) and stirred at 0 °C for 20 minutes. The crude mixture was then quenched by addition of suitable amounts of 1 M NaOH and the MS were filtered off. The aq. phase was extracted by CH₂Cl₂ (4 x 20 mL). The combined organic phases were washed with water (2 x 20 mL), brine (1 x 20 mL), dried (MgSO₄), filtered and evaporated onto celite. Purification by silica gel column chromatography (pet. ether/EtOAc, 9:1 → 7:3 v/v) and concentration of the relevant fractions [*R_f* = 0.13 (pet. ether/EtOAc, 9:1 v/v)] gave the target compound **L4** as a pale yellow fused mass (720.5 mg, 78%).

mp: 124-126 °C.

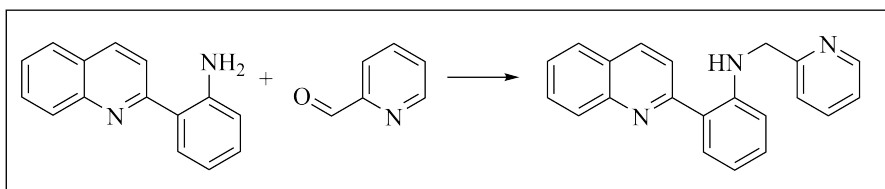
IR (ATR): ν_{\max} 3057, 2926, 2850, 1605, 1505, 1228, 762, 745 cm⁻¹.

¹H NMR (400 MHz, CDCl₃): δ 10.13 (bs, 1H), 8.22 (d, *J* = 8.7 Hz, 1H), 8.16-8.14 (m, 1H), 8.13-8.09 (m, 2H), 7.93 (d, *J* = 8.8 Hz, 1H), 7.84-7.79 (m, 3H), 7.74-7.70 (m, 2H), 7.57 (d, *J* = 8.6 Hz, 1H), 7.55-7.51 (m, 2H), 7.29-7.24 (m, 1H), 6.83-6.78 (m, 2H), 4.87 (d, *J* = 2.4 Hz, 2H).

¹³C NMR (100 MHz, CDCl₃): δ 159.9, 159.5, 148.2, 147.9, 146.7, 136.8, 136.7, 130.9, 130.1, 129.7, 129.6, 129.1 (2C), 127.8, 127.5, 126.4, 126.3, 126.2, 121.2, 120.7, 119.7, 116.1, 112.2, 50.0. One carbon not visible.

HRMS (ESI): calcd. for C₂₅H₁₉N₃ [M + H⁺] 362.1652, found 362.1659.

***N*-(Pyridin-2-yl methyl)-2-(quinolin-2-yl)aniline (L5)**



2-Pyridinecarboxaldehyde (**95**) (0.35 mL, 3.74 mmol) and 2-(quinolin-2-yl)aniline (**70**) (905.1 mg, 4.11 mmol) were mixed in MeOH (10 mL) under an argon atmosphere and stirred at rt for 4 hours until formation of the aldimine was complete as determined by TLC and LRMS. The imine was then added NaBH₄ (226.4 mg, 5.98 mmol) portionwise and the mixture stirred at rt for 15 minutes. The crude mixture was then quenched by addition of suitable amounts of 1 M NaOH and the aq. phase was extracted by CHCl₃ (4 x 20 mL). The combined organic phases were washed with water (1 x 20 mL), brine (1 x 20 mL), dried (MgSO₄), filtered and evaporated onto celite. Purification by silica gel column chromatography (pet. ether/EtOAc, 8:2 → 7:3 v/v) and concentration of the relevant fractions [*R_f* = 0.26 (pet. ether/EtOAc, 8:2 v/v)] gave the target compound **L5** as a bright yellow fused mass (788.6 mg, 68%).

mp: 93-95 °C.

IR (ATR): ν_{\max} 3213, 3055, 3009, 2923, 2851, 1606, 1509, 1225, 759 cm⁻¹.

¹H NMR (400 MHz, CDCl₃): δ 8.66 (d, *J* = 4.3 Hz, 1H), 8.20 (d, *J* = 8.8 Hz, 1H), 8.10 (d, *J* = 8.4 Hz, 1H), 7.92 (d, *J* = 8.8 Hz, 1H), 7.83-7.79 (m, 2H), 7.73-7.69 (m, 1H), 7.64 (dt, *J* = 7.7 Hz, 1.7 Hz, 1H), 7.54-7.50 (m, 1H), 7.44 (d, *J* = 7.8 Hz, 1H), 7.29-7.25 (m, 1H), 7.19 (dd, *J* = 7.1 Hz, 5.6 Hz, 1H), 6.81-6.77 (m, 1H), 6.75 (dd, *J* = 8.3 Hz, 0.7 Hz, 1H), 4.71 (s, 2H).

¹³C NMR (100 MHz, CDCl₃): δ 159.4, 149.3, 148.3, 146.6, 136.8, 136.6, 130.9, 129.9, 129.7, 128.8, 127.5, 126.3, 126.2, 122.1, 121.4, 120.8, 120.5, 116.0, 112.1, 49.3. One carbon was obscured or overlapping.

HRMS (ESI): calcd. for C₂₁H₁₇N₃ [M + H⁺] 312.1495, found 312.1503.

References

- [1] Cox-Singh, J.; Singh, B. *Trends Parasitol.* **2008**, *24*, 406–410.
- [2] World Health Organization, *World Malaria Report 2021*. Available from: www.who.int/malaria/publications/world-malaria-report-2021/en/, Accessed: 7 March 2022.
- [3] Collins, F. H.; Paskewitz, S. M. *Annu. Rev. Entomol.* **1995**, *40*, 195–219.
- [4] Amambua-Ngwa, A. et al. *Science* **2019**, *365*, 813–816.
- [5] Rosenthal, P. J. et al. *Am. J. Trop. Med. Hyg.* **2022**, 1–3.
- [6] Cox, F. E. G. *Parasites Vectors* **2010**, *3*, 1–9.
- [7] King, A. *Nature* **2019**, *575*, 51–54.
- [8] Chemison, A.; Ramstein, G.; Tompkins, A. M.; Defrance, D.; Camus, G.; Charra, M.; Caminade, C. *Nat. Commun.* **2021**, *12*, 1–12.
- [9] Baelen, G. V. et al. *Bioorg. Med. Chem.* **2009**, *17*, 7209–7217.
- [10] van Dorp, L. et al. *Mol. Biol. Evol.* **2020**, *37*, 773–785.
- [11] Fischer, L.; Gültekin, N.; Kaelin, M. B.; Fehr, J.; Schlagenhauf, P. *Travel Med. Infect. Dis.* **2020**, *36*, 101815.
- [12] Hertig, E. *Parasites Vectors* **2019**, *12*, 1–9.
- [13] Anthony, M. P.; Burrows, J. N.; Duparc, S.; Moehrle, J. J.; Wells, T. N. C. *Malar. J.* **2012**, *11*, 1–25.
- [14] Achan, J.; Talisuna, A. O.; Erhart, A.; Yeka, A.; Tibenderana, J. K.; Baliraine, F. N.; Rosenthal, P. J.; D’Alessandro, U. *Malar. J.* **2011**, *10*, 1–12.
- [15] Tse, E. G.; Korsik, M.; Todd, M. H. *Malar. J.* **2019**, *18*, 1–21.
- [16] Wang, N.; Wicht, K. J.; Imai, K.; Wang, M.; Ngoc, T. A.; Kiguchi, R.; Kaiser, M.; Egan, T. J.; Inokuchi, T. *Bioorg. Med. Chem.* **2014**, *22*, 2629–2642.

- [17] Krafts, K.; Hempelmann, E.; Skórska-Stania, A. *Parasitol. Res.* **2012**, *111*, 1–6.
- [18] Nzila, A. *J. Antimicrob. Chemother.* **2006**, *57*, 1043–1054.
- [19] Hurwitz, E. S.; Johnson, D.; Campbell, C. C. *Lancet* **1981**, *317*, 1068–1070.
- [20] Gregson, A.; Plowe, C. V. *Pharmacol. Rev.* **2005**, *57*, 117–145.
- [21] Andersson, J.; Forssberg, H.; Zierath, J. R. Avermectin and Artemisinin - Revolutionary Therapies against Parasitic Diseases. *Nobelförsamlingen* **2015**, 1–11, Available from: www.nobelprize.org/nobel_prizes/medicine/laureates/2015/press.html, Accessed: 11 July 2018.
- [22] Su, X.-Z.; Miller, L. H. *Sci. China Life Sci.* **2015**, *58*, 1175–1179.
- [23] van Agtmael, M. A.; Eggelte, T. A.; van Boxtel, C. J. *Trends Pharmacol. Sci.* **1999**, *20*, 199–205.
- [24] Ansari, M. T.; Saify, Z. S.; Sultana, N.; Ahmad, I.; Saeed-Ul-Hassan, S.; Tariq, I.; Khanum, M. *Mini-Rev. Med. Chem.* **2013**, *13*, 1879–1902.
- [25] Bridgford, J. L.; Xie, S. C.; Cobbold, S. A.; Pasaje, C. F. A.; Herrmann, S.; Yang, T.; Gillett, D. L.; Dick, L. R.; Ralph, S. A.; Dogovski, C.; Spillman, N. J.; Tilley, L. *Nat. Commun.* **2018**, *9*, 1–9.
- [26] Yeung, S.; Vornpinyo, W. P.; Hastings, I. M.; Mills, A. J.; White, N. J. *Am. J. Trop. Med. Hyg.* **2004**, *71*, 179–186.
- [27] Noedl, H.; Se, Y.; Scaecher, K.; Smith, B. L.; Socheat, D.; Fukuda, M. N. *N. Engl. J. Med.* **2008**, *359*, 2619–2620.
- [28] Amato, R.; Pearson, R. D.; Almagro-Garcia, J.; Amaratunga, C.; Lim, P.; Suon, S.; Sreng, S.; Drury, E.; Stalker, J.; Miotto, O.; Fairhurst, R. M.; Kwiatkowski, D. P. *Lancet Infect. Dis.* **2018**, *18*, 337–345.
- [29] Asua, V.; Conrad, M. D.; Aydemir, O.; DuvalSaint, M.; Legac, J.; Duarte, E.; Tumwebaze, P.; Chin, D. M.; Cooper, R. A.; Yeka, A.; Kamya, M. R.; Dorsey, G.; Nsobya, S. L.; Bailey, J.; Rosenthal, P. J. *J. Infect. Dis.* **2021**, *223*, 985–994.
- [30] Bergmann, C.; van Loon, W.; Habarugira, F.; Tacoli, C.; Jäger, J. C.; Savelsberg, D.; Nshimiyimana, F.; Rwamugema, E.; Mbarushimana, D.; Ndoli, J.; Sendegeya, A.; Bayingana, C.; Mockenhaupt, F. P. *Emerg. Infect. Dis.* **2021**, *27*, 294–296.
- [31] Uwimana, A. et al. *Nat. Med.* **2020**, *26*, 1602–1608.
- [32] Uwimana, A. et al. *Lancet Infect. Dis.* **2021**, *21*, 1120–1128.

- [33] Balikagala, B.; Fukuda, N.; Ikeda, M.; Katuru, O. T.; Tachibana, S.-I.; Yamauchi, M.; Opio, W.; Emoto, S.; Anywar, D. A.; Kimura, E.; Palacpac, N. M. Q.; Odongo-Aginya, E. I.; Ogwang, M.; Horii, T.; Mita, T. *N. Engl. J. Med.* **2021**, *385*, 1163–1171.
- [34] Straimer, J.; Gandhi, P.; Renner, K. C.; Schmitt, E. K. *J. Infect. Dis.* **2022**, *225*, 1411–1414.
- [35] Ndwiga, L. et al. *Int. J. Parasitol. Drugs Drug Resist.* **2021**, *16*, 155–161.
- [36] Kumar, S.; Bhardwaj, T. R.; Prasad, D. N.; Singh, R. K. *Biomed. Pharmacother.* **2018**, *104*, 8–27.
- [37] RTS,S Clinical Trial Partnership. *Lancet* **2015**, *386*, 31–45.
- [38] World Health Organization, *WHO Urges Countries to Move Quickly to Save Lives From Malaria in Sub-Saharan Africa*, Available online at: <https://www.who.int/news-room/questions-and-answers/item/malaria-vaccine-implementation-programme>, Accessed: June 7, 2022. 2020.
- [39] Nghochuzie, N. N.; Olwal, C. O.; Udoakang, A. J.; Amenga-Etego, L.; Amambua-Ngwa, A. *Front. Microbiol.* **2020**, *18*, 1–5.
- [40] Mondal, A.; Gandhi, A.; Fimognari, C.; Atanasov, A. G.; Bishayee, A. *Eur. J. Pharmacol.* **2019**, *858*, 172472.
- [41] Qui, S.; Sun, H.; Zhang, A.-H.; Xu, H.-Y.; Yan, G.-L.; Ying, H.; Wang, X.-J. *Chin. J. Nat. Med.* **2014**, *12*, 401–406.
- [42] Newman, D. J.; Cragg, G. M. *J. Nat. Prod.* **2020**, *83*, 770–803.
- [43] Daley, S.-K.; Cordell, G. A. *Molecules* **2021**, *26*, 3800.
- [44] Brook, K.; Bennett, J.; Desai, S. P. *J. Anesth. Hist.* **2017**, *3*, 50–55.
- [45] Tillhon, M.; Oriz, L. M. G.; Lombardi, P.; Scovassi, A. I. *Biochem. Pharmacol.* **2012**, *84*, 1260–1267.
- [46] Abourashed, E. A.; El-Alfy, A. T.; Khan, I. A.; Walker, L. *Phytother. Res.* **2003**, *17*, 703–712.
- [47] Osafo, N.; Mensah, K. B.; Yeboah, O. K. *Adv. Pharmacol. Sci.* **2017**, 1–13.
- [48] Gellért, E.; Schlittler, R.-H. E. *Helv. Chim. Acta* **1951**, *34*, 642–651.
- [49] Grycovà, L.; Dommissse, R.; Pieters, L.; Marek, R. *Magn. Reson. Chem.* **2009**, *47*, 977–981.

- [50] Sofowora, A. *Medicinal Plants and Traditional Medicine in Africa*; John Wiley & Sons: Chichester, 1982; pp 183–256.
- [51] Kirby, G. C.; Paine, A.; Warhurst, D. C.; Noamese, B. K.; Phillipson, J. D. *Phytother. Res.* **1995**, *9*, 359–363.
- [52] Grellier, P.; Ramiamanana, L.; Millerioux, V.; Deharo, E.; Shrèvel, K.; Frappier, F.; Trigalo, F.; Bodo, B.; Pousset, J. L. *Phytother. Res.* **1996**, *10*, 317–321.
- [53] Olajide, O. A.; Heiss, E. H.; Schachener, D.; Wright, C. W.; Vollmar, A. M.; Dirsch, V. M. *Bioorg. Med. Chem.* **2007**, *15*, 43–49.
- [54] Bierer, D. E. et al. *J. Med. Chem.* **1998**, *41*, 894–901.
- [55] Rauwald, H. W.; Kober, M.; Mutschler, E.; Lambrecht, G. *Planta Med.* **1992**, *58*, 486–488.
- [56] Chen, Y.-J.; Liu, H.; Zhang, S.-Y.; Li, H.; Ma, K.-Y.; Liu, Y.-Q.; Yin, X.-D.; Zhou, R.; Yan, Y.-F.; Wang, R.-X.; He, Y.-H.; Chu, Q.-R.; Tang, C. *J. Agric. Food. Chem.* **2021**, *69*, 1259–1271.
- [57] Ablordeppey, S. Y.; Fan, P.; Li, S.; Clark, A. M.; Hufford, C. D. *Bioorg. Med. Chem.* **2002**, *10*, 1337–1346.
- [58] Singh, M.; Singh, M. P. *Drug Dev. Ind. Pharm.* **1996**, *22*, 377–381.
- [59] Paulo, A.; Duarte, A.; Gomes, E. T. *J. Ethnopharmacol.* **1994**, *44*, 127–130.
- [60] Cimanga, K.; Bruyne, T. D.; Lasure, A.; Poel, B. V.; Pieters, L.; Claeys, M.; Berghe, D. V.; Kambu, K.; Tona, L.; Vlietinck, A. *Planta Med.* **1996**, *62*, 22–27.
- [61] Zhao, M.; Kamada, T.; Takeuchi, A.; Nishioka, H.; Kuroda, T.; Takeuchi, Y. *Bioorg. Med. Chem.* **2015**, *25*, 5551–5554.
- [62] Karou, D.; Savadogo, A.; Canini, A.; Yameogo, S.; Montesano, C.; Simpoire, J.; Colizzi, V.; Traore, A. S. *Afr. J. Biotechnol.* **2007**, *5*, 195–200.
- [63] Lu, C.-M.; Chen, Y.-L.; Chen, H.-L.; Chen, C.-A.; Yang, P.-J.; Tzeng, C.-C. *Bioorg. Med. Chem.* **2010**, *18*, 1948–1957.
- [64] Dassonneville, L.; Lansiaux, A.; Wattelet, A.; Watterz, N.; Mahieu, C.; Miert, S. V.; Pieters, L.; Bailly, C. *Eur. J. Pharmacol.* **2000**, *409*, 9–18.
- [65] Zhu, H.; Gooderham, N. J. *Toxicol. Sci.* **2006**, *91*, 132–139.
- [66] Matsui, T.-A.; Sowa, Y.; Murata, H.; Takagi, K.; Nakanishi, R.; Aoki, S.; Kobayashi, M.; Sakabe, T.; Kubo, T.; Sakai, T. *Int. J. Oncol.* **2007**, *31*, 915–922.

- [67] Bonjean, K.; Pauw-Gillet, M. C. D.; Defresne, M. P.; Colson, P.; Houssier, C.; Dasselonneville, L.; Bailly, C.; Greimers, R.; Wright, C. W.; Quetin-Leclercq, J.; Tits, M.; Angenot, L. *Biochemistry* **1998**, *37*, 5136–5146.
- [68] Mimanga, K.; Bruyne, T. D.; Pieters, L.; Vlietinck, A. J.; Turger, C. A. *J. Nat. Prod.* **1997**, *60*, 688–691.
- [69] Pousset, J.-L.; Martin, M.-T.; Jossang, A.; Bodo, B. *Phytochemistry* **1995**, *39*, 735–736.
- [70] Sharaf, M. M. H.; Schiff, P. L.; Tackie, A. N.; Phoebe, C. H.; Martin, G. E. *J. Heterocycl. Chem.* **1996**, *33*, 239–243.
- [71] Sharaf, M. M. H.; Schiff, P. L.; Tackie, A. N.; Phoebe, C. H.; Johnson, R. L.; Minick, D.; Crouch, R. C.; Martin, G. E.; Andrews, C. W. *J. Heterocycl. Chem.* **1996**, *33*, 789–797.
- [72] Lavrado, J.; Moreira, R.; Paulo, A. *Curr. Med. Chem.* **2010**, *17*, 2348–2370.
- [73] Paulo, A.; Gomes, E. T.; Houghton, P. J. *J. Nat. Prod.* **1995**, *58*, 1485–1491.
- [74] Crouch, R. C.; Davis, A. O.; Spitzer, T. D.; Martin, G. E.; Sharaf, M. M. H.; Schiff, P. L.; Phoebe, C. H.; Tackie, A. N. *J. Heterocycl. Chem.* **1995**, *32*, 1077–1080.
- [75] Wright, C. W.; Addae-Kyereme, J.; Breen, A. G.; Brown, J. E.; Cox, M. F.; Croft, S. L.; Gökçek, Y.; Kendrick, H.; Phillips, R. M.; Pollet, P. L. *J. Med. Chem.* **2001**, *44*, 3187–3194.
- [76] Onyeibor, O.; Croft, S. L.; Dodson, H. I.; Feiz-Haddad, M.; Kendrick, H.; Millington, N. J.; Parapini, S.; Phillips, R. M.; Seville, S.; Shnyder, S. D.; Tarameli, D.; Wright, C. W. *J. Med. Chem.* **2005**, *48*, 2701–2709.
- [77] Wang, N.; Świtalska, M.; Wang, L.; Shaban, E.; Hossain, M. I.; Sayed, I. E. T. E.; Wietryzk, J.; Inokuchi, T. *Molecules* **2019**, *24*, 1–12.
- [78] Baker, N. C.; Ekins, S.; Williams, A. J.; Tropsha, A. *Drug Discov.* **2018**, *23*, 661–672.
- [79] PATH, *From Pipeline to Product: Malaria R&D malaria funding needs into the next decade*; WHO Press: Seattle, 2013.
- [80] Hao, Y.; Wang, K.; Wang, Z.; Liu, Y.; Ma, D.; Wang, Q. *J. Agric. Food Chem.* **2020**, *68*, 8764–8773.
- [81] World Health Organization, *World Cancer Report 2020: Cancer Research for Cancer Prevention*. Available from: www.iarc.who.int/cards_page/world-cancer-report/, Accessed: 11 June 2022.

- [82] Sidoryk, K.; Jaromin, A.; Edwards, J. A.; Świtalska, M.; Stefńska, J.; Cmoch, P.; Zagrodzka, J.; Szczepek, Q.; Peczyńska-Czoch, W.; Wietrzyk, J.; Kozubek, A.; Zarnowski, R.; Anders, D. R.; Ł. Kaczmarek, *Eur. J. Med. Chem.* **2014**, *78*, 304–313.
- [83] Carvalho, C.; Santos, R. X.; Cardoso, S.; Correia, S.; Oliveira, P. J.; Santos, M. S.; Moreira, P. I. *Curr. Med. Chem.* **2009**, *16*, 3267–3285.
- [84] Amari, M. R.; Wiraswati, H. L.; Fauziah, N.; Ma'ruf, I. F. *Biomed. & Pharmacol. J.* **2022**, *15*, 313–320.
- [85] Moore, A.; Pinkerton, R. *Pediatr. Blood Cancer* **2009**, *53*, 1180–1187.
- [86] Shaban, E.; Świtalska, M.; Wang, L.; Xiu, F.; Hayashi, I.; Ngoc, T. A.; Nagae, S.; El-Ghlban, S.; Shimoda, S.; Gokha, A. A. A. E.; Sayed, I. E. T. E.; Wietrzyk, J.; Inokuchi, T. *Molecules* **2017**, *22*, 1–11.
- [87] Wang, N.; Świtalska, M.; Wu, M.-Y.; Imai, K.; Ngoc, T. A.; Pang, C.-Q.; Wietrzyk, J.; Inokuchi, T. *Eur. J. Med. Chem.* **2014**, *78*, 314–323.
- [88] Nuthakki, V. K.; Mudududdla, R.; Bharate, S. B. *Eur. J. Med. Chem.* **2022**, *227*, 113938.
- [89] Holmes, A. H.; Moore, L. S. P.; Sundsfjord, A.; Steinbakk, M.; Regmi, S.; Karkey, A.; Guerin, P. J.; Piddock, L. J. V. *Lancet* **2016**, *387*, 176–187.
- [90] Antimicrobial Resistance Collaborators, *Lancet* **2022**, *399*, 629–655.
- [91] Durand, G. A.; Raoult, D.; Dubourg, G. *Int. J. Antimicrob. Agents* **2019**, *53*, 371–382.
- [92] O'Neill, J. Tackling drug-resistant infections globally: final report and recommendations. London: Review on Antimicrobial Resistance. 2016.
- [93] Stamm, A. M.; Long, M. N.; Belcher, B. *Am. J. Infect. Control* **1993**, *21*, 70–74.
- [94] Drenkard, E. *Microb. Infect.* **2003**, *5*, 1213–1219.
- [95] Teng, C. P.; Zhou, T.; Ye, E.; Liu, S.; Koh, L. D.; Low, M.; Loh, X. J.; Win, Y.; Zhang, L.; Han, M.-Y. *Adv. Healthcare Mater.* **2016**, *5*, 2122–2130.
- [96] Ligon, B. L. *Semin. Pediatr. Infect. Dis.* **2004**, *15*, 52–57.
- [97] Rodvold, K. A.; Piscitelli, S. C. *Clin. Infect. Dis.* **1993**, *17*, S192–S199.
- [98] Rehman, A.; Patrick, W. M.; Lamont, I. L. *J. Med. Microbiol.* **2019**, *68*, 1–10.
- [99] Aroonkit, P.; Thongsornkleeb, C.; Tummatorn, J.; Krajangsri, S.; Mungthin, M.; Ruchirawat, S. *Eur. J. Med. Chem.* **2015**, *94*, 56–62.

- [100] Kumar, E. V. K. S.; Etukala, J. R.; Ablordeppey, S. Y. *Mini Rev. Med. Chem.* **2008**, *8*, 538–554.
- [101] Parvatkar, P. T.; Parameswaran, P. S.; Tilve, S. G. *Curr. Org. Chem.* **2011**, *15*, 1036–1057.
- [102] Bracca, A. B. J.; Heredia, D. A.; Larghi, E. L.; Kaufman, T. S. *Eur. J. Org. Chem.* **2014**, 7979–8003.
- [103] Parvatkar, P. T.; Parameswaran, P. S. *Curr. Org. Synth.* **2016**, *13*, 58–72.
- [104] Thongsornkleeb, C.; Tummatorn, J.; Ruchirawat, S. *Chem. Asian J.* **2022**, *17*, 1–19.
- [105] Akitake, M.; Noda, S.; Miyoshi, K.; Sonoda, M.; Tanimori, S. *J. Org. Chem.* **2021**, *86*, 17727–17737.
- [106] Aksenov, A. V.; Aksenov, D. A.; Orazova, N. A.; Aksenov, N. A.; Griaznov, G. D.; Carvalho, A. D.; Kiss, R.; Mathieu, V.; Kornienko, A.; Rubin, M. *J. Org. Chem.* **2017**, *82*, 3011–3018.
- [107] Xu, M.; Wang, Q. H. S.; Wang, H.; Yao, Z.-J. *Synthesis* **2011**, *4*, 626–634.
- [108] Scriven, E.; Ramsden, C. A. *Advances in Heterocyclic Chemistry, Volume 132*; Elsevier: Cambridge, 2020; pp 116–134.
- [109] Dilek, O.; Patir, S.; Tilki, T.; Ertürk, E. *J. Org. Chem.* **2019**, *84*, 7901–7916.
- [110] Miller, C. M.; McCarthy, F. O. *RCS Adv.* **2012**, *2*, 8883–8918.
- [111] Sainsbury, M. *Synthesis* **1977**, 437–448.
- [112] Hewlins, M. J.; Oliveira-Campos, A. M.; Shannon, P. V. *Synthesis* **1984**, 289–302.
- [113] Gribble, G. W.; Saulnier, M. G. *Heterocycles* **1985**, *23*, 1277–1315.
- [114] Kansal, V. K.; Potier, P. *Tetrahedron* **1986**, *42*, 2389–2408.
- [115] Alvares, M.; Joule, J. A. *Alkaloids: Chem. Biol.* **2001**, *57*, 235–273.
- [116] Knölker, H.-J.; Reddy, K. R. *Chem. Rev.* **2002**, *102*, 4303–4428.
- [117] Schmutz, J.; Wittwer, H. *Helv. Chim. Acta* **1960**, *43*, 793–799.
- [118] Liu, B.; Wang, S.; Bian, C.; Liao, H.; Lin, H.-W. *Chin. J. Chem.* **2021**, *39*, 1905–1910.
- [119] Beauchard, A.; Chabane, H.; Sinbandhit, S.; Guenot, P.; Thiéry, V.; Besson, T. *Tetrahedron* **2006**, *62*, 1895–1903.

- [120] Katritzky, A. R.; Lan, X.; Yang, J. Z.; Denisko, O. V. *Chem. Rev.* **1998**, *98*, 409–548.
- [121] Kalinowski, J.; Rykowski, A.; Nantka-Namiriski, P. *Pol. J. Chem.* **1984**, *58*, 125–126.
- [122] Alekseev, R. S.; Kurkin, A. V.; Yurovskaya, M. A. *Chem. Heterocycl. Compd.* **2012**, *48*, 1235–1250.
- [123] Mehra, M. K.; Sharma, S.; Rangan, K.; Kumar, D. *Eur. J. Org. Chem.* **2020**, 2409–2413s.
- [124] Helgeland, I. T. U.; Sydnnes, M. O. *SynOpen* **2017**, *1*, 41–44.
- [125] Heravi, M. M.; Hashemi, E. *Tetrahedron* **2012**, *68*, 9145–9178.
- [126] Melchor, M. G. A. *A Theoretical Study of Pd-Catalyzed C-C Cross-Coupling Reactions*; Springer Science & Business Media: Barcelona, 2013; pp 113–115.
- [127] Suzuki, A. *Organomet. Chem.* **1999**, *576*, 147–168.
- [128] Xia, Y.; Bao, Q.-F.; Li, Y.; Wang, L.-J.; Zhang, B.-S.; Liu, H.-C.; Liang, Y.-M. *Chem. Commun.* **2019**, *55*, 4675–4678.
- [129] Pacchioni, G.; Bagus, P. S. *Inorg. Chem.* **1992**, *31*, 4391–4398.
- [130] Amatore, C.; Jutand, A.; Duc, G. L. *Chem. Eur. J.* **2011**, *17*, 2492–2503.
- [131] Osakada, K.; Yamamoto, T. *Coord. Chem. Rev.* **2000**, *198*, 379–399.
- [132] Håheim, K. S.; Helgeland, I. T. U.; Lindbäck, E.; Sydnnes, M. O. *Tetrahedron* **2019**, *75*, 2949–2957.
- [133] Chakraborty, M.; Umrigar, V.; Parikh, P. A. *Int. J. Chem. React. Eng.* **2008**, *6*, 1–12.
- [134] Charville, H.; Jackson, D. A.; Hodges, G.; Whiting, A.; Wilson, W. R. *Eur. J. Org. Chem.* **2011**, 5981–5990.
- [135] Ciufolini, M. A.; Byrne, N. E. *J. Am. Chem. Soc.* **1991**, *113*, 8016–8024.
- [136] Casadei, M. A.; Galli, C.; Mandolini, L. *J. Am. Chem. Soc.* **1984**, *106*, 1051–1056.
- [137] Bjørsvik, H.-R.; Elumalai, V. *Eur. J. Org. Chem.* **2016**, 5474–5479.
- [138] Landagaray, E.; Ettaoussi, M.; Rami, M.; Boutin, J. A.; Caignard, D.-H.; Delagrangé, P.; Melnyk, P.; Berthelot, P.; Yous, S. *Eur. J. Med. Chem.* **2017**, *127*, 621–631.
- [139] Landagaray, E.; Ettaoussi, M.; Rami, M.; Boutin, J. A.; Caignard, D.-H.; Delagrangé, P.; Melnyk, P.; Berthelot, P.; Yous, S. *Eur. J. Med. Chem.* **2017**, *127*, 621–631.

- [140] Tsang, W. C.; Munday, R. H.; Brasche, G.; Zheng, N.; Buchwald, S. L. *J. Org. Chem.* **2008**, *73*, 7603–7610.
- [141] Lautens, M.; Fang, Y.-Q. *Org. Lett.* **2003**, *5*, 3679–3682.
- [142] Kato, T.; Yosihazawa, K.; Hirao, K. *J. Chem. Phys.* **2002**, *116*, 3420–3429.
- [143] Balaban, A. T. *Pure Appl. Chem.* **1980**, *52*, 1409–1429.
- [144] Fukui, K. *Science* **1982**, *218*, 747–754.
- [145] Cyrański, M. K.; Stępién, B. T.; Krygowski, T. M. *Tetrahedron* **2000**, *56*, 9663–9667.
- [146] Portella, G.; Poater, J.; Bofill, J. M.; Alemany, P.; Solà, M. *J. Org. Chem.* **2005**, *70*, 2509–2521.
- [147] Hemelsoet, K.; Speybroeck, V. V.; Marin, G. B.; Proft, F. D.; Geerlings, P.; Waroquier, M. *J. Phys. Chem. A* **2004**, *108*, 7281–7290.
- [148] Poater, J.; Visser, R.; Solà, M.; Bickelhaupt, F. M. *J. Org. Chem.* **2007**, *72*, 1134–1142.
- [149] Håheim, K. S.; Lindbäck, E.; Tan, K. N.; Albrigtsen, M.; Helgeland, I. T. U.; Lauga, C.; Matringe, T.; Kennedy, E. K.; Andersen, J. H.; Avery, V. M.; Sydnes, M. O. *Molecules* **2021**, *26*, 3268–3290.
- [150] Timàri, G.; Soès, T.; Hajòs, G. *Synlett* **1997**, 1067–1068.
- [151] Hostyn, S.; Tehrani, K. A.; Lemièrre, F.; Smout, V.; Maes, B. U. W. *Tetrahedron* **2011**, *67*, 655–659.
- [152] Nàjera, C.; Beletskaya, I. P.; Yus, M. *Chem. Soc. Rev.* **2019**, *48*, 4515–4618.
- [153] Ho, T.-L.; Jou, D.-G. *Helv. Chim. Acta* **2002**, *85*, 3823–3827.
- [154] Castejon, H.; Wiberg, K. B. *J. Am. Chem. Soc.* **1999**, *121*, 2139–2146.
- [155] Chelucci, G.; Thummel, R. P. *Chem. Rev.* **2002**, *102*, 3129–3170.
- [156] Fache, F.; Schulz, E.; Tommasino, M. L.; Lemaire, M. *Chem. Rev.* **2000**, *100*, 2159–2232.
- [157] Ma, W.-A.; Wang, Z.-X. *Organometallics* **2011**, *30*, 4364–4373.
- [158] Gong, D.-P.; Gao, T.-B.; Cao, D.-K.; Ward, M. D. *Dalton Trans.* **2017**, *46*, 275–286.
- [159] Durand, J.; Milani, B. *Coord. Chem. Rev.* **2006**, *250*, 542–560.

- [160] Trickett, C. A.; Helal, A.; Al-Maythaly, B. A.; Yamani, Z. H.; Cordova, K. E.; Yaghi, O. M. *Nat. Rev.* **2017**, *2*, 17045.
- [161] Qian, J.; Li, Q.; Liang, L.; Li, T.-T.; Hu, Y.; Huang, S. *Dalton Trans.* **2017**, *46*, 14102–14106.
- [162] Busemann, A.; Flaspohler, I.; Zhou, X.-Q.; Schmidt, C.; Goetzfried, S. K.; Rixel, V. H. S.; Ott, I.; Siegler, M. A.; Bonnet, S. *J. Biol. Inorg. Chem.* **2021**, *26*, 667–674.
- [163] Zayat, L.; Filevich, O.; Baraldo, L. M.; Etchenique, R. *Phil. Trans. R. Soc. A* **2013**, *371*, 1–12.
- [164] Lessing, T.; Müller, T. J. *J. Appl. Sci.* **2015**, *5*, 1803–1836.
- [165] Stephens, D. E.; Lakey-Beitia, J.; Burch, J. E.; Arman, H. D.; Larionov, O. V. *Chem. Commun.* **2016**, *52*, 9945–9948.
- [166] Maddess, M. L.; Li, C. *Organometallics* **2019**, *38*, 81–84.
- [167] Dorel, R.; Grugel, C. P.; Haydl, A. M. *Angew. Chem. Int. Ed.* **2019**, *58*, 17118–17129.
- [168] Hartwig, J. F. *Synlett* **1997**, *4*, 329–340.
- [169] Paul, F.; Patt, J.; Hartwig, J. F. *J. Am. Chem. Soc.* **1994**, *116*, 5969–5970.
- [170] Whitesides, G. M.; Gaasch, J. F.; Stedronsky, E. R. *J. Am. Chem. Soc.* **1972**, *94*, 5258–5270.
- [171] Cook, X. A. F.; Gombert, A.; McKnight, J.; Pantaine, L. R. E.; Willis, M. C. *Angew. Chem. Int. Ed.* **2021**, *60*, 11068–11091.
- [172] Salvatore, R. N.; Nagle, A. S.; Jung, K. W. *J. Org. Chem.* **2002**, *67*, 674–683.
- [173] Abdel-Magid, A. F.; Carson, K. G.; Harris, B. D.; Maryanoff, C. A.; Shah, R. D. *J. Org. Chem.* **1996**, *61*, 3849–3862.
- [174] Adkins, H.; Billica, H. R. *J. Am. Chem. Soc.* **1948**, *70*, 695–698.
- [175] Suzuki, Y.; Kaneno, D.; Tomoda, S. *J. Phys. Chem. A* **2009**, *113*, 2578–2583.
- [176] Nadein, O. M.; Aksenov, D. A.; Aksenov, G. M.; Aksenov, N. A.; Voskressensky, L. G.; Aksenov, A. V. *Chem. Heterocycl. Compd.* **2019**, *55*, 905–932.
- [177] C-Thongsornkleeb,; Tummatorn, J.; Ruchirawat, S. *Chem. Asian J.* **2022**, *17*, 1–19.
- [178] Wender, P. A.; Verma, V. A.; Paxton, T. J.; Pillow, T. H. *Acc. Chem. Res.* **2008**, *41*, 40–49.

- [179] Kadam, H. K.; Tilve, S. G. *J. Heterocyclic Chem.* **2016**, *53*, 2066–2069.
- [180] Das, S. K.; Roy, S.; Khatua, H.; Chattopadhyay, B. *J. Am. Chem. Soc.* **2018**, *140*, 8429–8433.
- [181] Proter, T. C.; Smalley, R. K.; Teguique, M.; Purwono, B. *Synthesis* **1997**, *1997*, 773–777.
- [182] Roy, S. K.; Purkait, A.; Aziz, S. M. T.; Jana, C. K. *Chem. Commun.* **2020**, *56*, 3167–3170.
- [183] Yeh, L.-H.; Wang, H.-K.; Pallikonda, G.; Ciou, Y.-L.; Hsieh, J.-C. *Org. Lett.* **2019**, *21*, 1730–1734.
- [184] Aksenov, D. A.; Arutyunov, N. A.; Gasanova, A. Z.; Aksenov, N. A.; Aksenov, A. V.; Lower, C.; Rubin, M. *Tetrahedron Lett.* **2021**, *82*, 153395.
- [185] Akkachairin, B.; Tummatorn, J.; Khamsuwan, N.; Thongsornkleeb, C.; Ruchirawat, S. *J. Org. Chem.* **2018**, *83*, 11254–11268.
- [186] Vecchione, M. K.; Sun, A. X.; Seidel, D. *Chem. Sci.* **2011**, *2*, 2178–2181.
- [187] Kraus, G. A.; Guo, H. A. *Tetrahedron Lett.* **2010**, *51*, 4137–4139.
- [188] Parvatkar, P. T.; Ajay, A. K.; Bhat, M. K.; Parameswaran, P. S.; Tilve, S. G. *Med. Chem. Res.* **2013**, *22*, 88–93.
- [189] Kearney, A. M.; Vanderwal, C. D. *Angew. Chem. Int. Ed.* **2006**, *45*, 7803–7806.
- [190] Sowmiah, S.; Esperança, J. M. S. S.; Rebelo, L. P. N.; Afonso, C. A. M. *Org. Chem. Front.* **2018**, *5*, 453–493.
- [191] Lavilla, R. J. *J. Chem. Soc., Perkin Trans.* **2002**, *1*, 1141–1156.
- [192] Bull, J. A.; Mousseau, J. J.; Pelletier, G.; Charette, A. B. *Chem. Rev.* **2012**, *112*, 2642–2713.
- [193] Bannasar, M.-L.; Alvares, M.; Lavilla, R.; Zulaica, E.; Bosch, J. *J. Org. Chem.* **1990**, *55*, 1156–1168.
- [194] Mayr, H.; Breugst, M.; Ofial, A. R. *Angew. Chem. Int. Ed.* **2011**, *50*, 6470–6505.
- [195] Poddubnyi, I. S. *Chem. Heterocycl. Compd.* **1995**, *31*, 682–714.
- [196] Crowley, J. D.; Steele, I. M.; Bosnich, B. *Chem. Eur. J.* **2006**, *12*, 8935–8951.
- [197] Barré, A.; Țîntaş, M.-L.; Alix, F.; Gembus, V.; Papamicaël, C.; Levacher, V. *J. Org. Chem.* **2015**, *80*, 6537–6544.

- [198] Pattabiraman, V. R.; Bode, J. W. *Nature* **2011**, *480*, 471–479.
- [199] Ullmann, F.; Bielecki, J. *Ber. Dtsch. Chem. Ges.* **1901**, *34*, 2174–2185.
- [200] Hassan, J.; Sévignon, M.; Gozzi, G.; Schulz, E.; Lemaire, M. *Chem. Rev.* **2002**, *102*, 1359–1469.
- [201] Fier, P. S.; Hartwig, J. F. *J. Am. Chem. Soc.* **2012**, *134*, 10795–10798.
- [202] Jana, N.; Nguyen, Q.; Driver, T. G. *J. Org. Chem.* **2014**, *79*, 2781–2791.
- [203] Zhou, F.; Driver, T. G. *Org. Lett.* **2014**, *16*, 2916–2919.
- [204] Murata, M.; Watanabe, S.; Masuda, Y. *J. Org. Chem.* **1997**, *62*, 6458–6459.
- [205] Murata, M.; Oyama, T.; Watanabe, S.; Masuda, Y. *J. Org. Chem.* **2000**, *65*, 164–168.
- [206] Ishiyama, T.; Murata, M.; Miyaura, N. *J. Org. Chem.* **1995**, *60*, 7508–.
- [207] Chow, W. K.; Yuen, O. Y.; Choy, P. Y.; So, C. M.; Lau, C. P.; Wong, W. T.; Kwong, F. Y. *RSC Adv.* **2013**, *3*, 12518–12539.
- [208] Kam, K. C.; Marder, T. B.; Lin, Z. *Organometallics* **2010**, *29*, 1849–1857.
- [209] Nasri, N. S.; Jones, J. M.; Dupont, V. A.; Williams, A. *Energy Fuels* **1998**, *12*, 1130–1134.
- [210] Hao, F.; Nishiwaki, N. *Molecules* **2020**, *25*, 673.
- [211] Zhang, Z.; Pi, C.; Tong, H.; Cui, X.; Wu, Y. *Org. Lett.* **2017**, *19*, 440–443.
- [212] Vanderwal, C. D. *J. Org. Chem.* **2011**, *76*, 9555–9567.
- [213] Zincke, T. *Liebigs Ann. Chem.* **1904**, *330*, 361–374.
- [214] Zincke, T.; Möller, W. *Liebigs Ann. Chem.* **1904**, *333*, 296–345.
- [215] Zincke, T.; Wurker, W. *Liebigs Ann. Chem.* **1905**, *338*, 107–141.
- [216] Kassel, V. M.; Hanneman, C. M.; Delaney, C. P.; Denmark, S. E. *J. Am. Chem. Soc.* **2021**, *143*, 13845–13853.
- [217] Katritzky, A. R.; Lunt, E. *Tetrahedron* **1969**, *25*, 4291–4305.
- [218] Gritsan, N. P.; Platz, M. S. *Chem. Rev.* **2006**, *106*, 3844–3867.
- [219] Rehm, T. H. *Chem. Eur. J.* **2020**, *18*, 16952–16974.
- [220] Hoffmann, N. *Chem. Rev.* **2008**, *108*, 1052–1103.

- [221] Schendera, E.; Unkel, L.-N.; Quyen, P. P. H.; Salkewitz, G.; Hoffmann, F.; Villinger, A.; Brasholz, M. *Chem. Eur. J.* **2020**, *26*, 269–274.
- [222] Meng, Q.-Y.; Gao, X.-W.; Lei, T.; Liu, Z.; Zhan, F.; Li, Z.-J.; Zhong, J.-J.; Xiao, H.; Feng, K.; Chen, B.; Tao, Y.; Tung, C.-H.; Wu, L.-Z. *Sci. Adv.* **2017**, *3*, 1–10.
- [223] Scriven, E. F. V. *Azides and Nitrenes: Reactivity and Utility*; Academic Press INC: Indianapolis, 1984; pp 95–487.
- [224] Borden, W. T.; Gritsan, N. P.; Hadad, C. M.; Karney, W. L.; Kemnitz, C. R.; Platz, M. S. *Acc. Chem. Res.* **2000**, *33*, 765–771.
- [225] Belloli, R. *J. Chem. Edu.* **1971**, *48*, 422–426.
- [226] Karila, D.; Dodd, R. H. *Curr. Org. Chem.* **2011**, *15*, 1507–1538.
- [227] Wang, J.; Burdzinski, G.; Platz, M. S.; Vyas, S.; Winter, A. H.; Hadad, C. M. In *Nitrenes and Nitrenium Ions*; Falvey, D. E., Gudmundsdottir, A. D., Eds.; John Wiley & Sons: Hoboken, 2013; pp 1–33.
- [228] Lindley, J. M.; McRobbie, I. M.; Meth-Cohn, O.; Suschitzky, H. *Tetrahedron Lett.* **1976**, *49*, 4513–4516.
- [229] Sundberg, R. J.; Brenner, M.; Suter, S. R.; Das, B. P. *Tetrahedron Lett.* **1970**, *31*, 2715.
- [230] Sundberg, R. J.; Heintzelman, R. W. *J. Org. Chem.* **1974**, *39*, 2546.
- [231] Klán, P.; Wirz, J. *Photochemistry of Organic Compounds: From Concepts to Practice*; John Wiley & Sons: Wiltshire, 2009; p 25.
- [232] Coyle, J. D. *Introduction to Organic Photochemistry*; John Wiley & Sons: Chichester, 1986.
- [233] Wilkinson, F.; Kelly, G. P. *J. Chem. Soc. Faraday Trans.* **1991**, *87*, 547–552.
- [234] Turro, N. J. *Modern Molecular Photochemistry*; University Science Books: Sausalito, 1991; p 421.
- [235] Schmidt, M. W.; Lee, E. K. C. *J. Am. Chem. Soc.* **1970**, *92*, 3579–3586.
- [236] Feixas, F.; Matito, E.; Poater, J.; Sola, M. *Chem. Soc. Rev.* **2015**, *44*, 6434–6451.
- [237] Peterson, D. B.; Mains, G. J. *J. Am. Chem. Soc.* **1959**, *81*, 3510–3515.
- [238] Ikeda, N.; Nakashima, N.; Yoshihara, K. *J. Chem. Phys.* **1985**, *82*, 5285–5286.
- [239] Tsao, M.-L.; Gritsan, N. P.; James, T. R.; Platz, M. S.; Hrovat, D. A.; Borden, W. T. *J. Am. Chem. Soc.* **2003**, *125*, 9343–9358.

- [240] Miyaura, N.; Suzuki, A. *Chem. Rev.* **1995**, *95*, 2457–2483.
- [241] Miyaura, N.; Yamada, K.; Suzuki, A. *Tetrahedron Lett.* **1979**, *36*, 3437–3440.
- [242] Liu, M.; Tan, L.; Rashid, R. T.; Cen, Y.; Cheng, S.; Botton, G.; Mi, Z.; Li, C.-J. *Chem. Sci.* **2020**, *11*, 7864–7870.
- [243] Kuivila, H. G.; Reuwer, J. F.; Mangravite, J. A. *Can. J. Chem.* **1963**, *41*, 3081–3090.
- [244] Lennox, A. J. J.; Lloyd-Jones, G. C. *Chem. Soc. Rev.* **2014**, *43*, 412–443.
- [245] Hayes, H. L. D.; Wei, R.; Assante, M.; Geogheghan, K. J.; Jin, N.; Tomasi, S.; Noonan, G.; Leach, A. G.; Lloyd-Jones, G. C. *J. Am. Chem. Soc.* **2021**, *143*, 14814–14826.
- [246] Xu, L.; Wang, G.; Zhang, S.; Wang, H.; Wang, L.; Liu, L.; Jiao, J.; Li, P. *Tetrahedron* **2017**, *73*, 7123–7157.
- [247] Jones, R. G. *J. Am. Chem. Soc.* **1947**, *69*, 2346–2350.
- [248] Merritt, J. M.; Andiappan, M.; Pietz, M. A.; Richey, R. N.; Sullivan, K. A.; Kjell, D. P. *Org. Process Res. Dev.* **2016**, *20*, 176–188.
- [249] Lieber, E.; Rao, C. N. R.; Thomas, A. E.; Oftedahl, E.; Minnis, R.; Nambury, C. V. N. *Spectrochim. Acta* **1963**, *19*, 1135–1144.
- [250] Keicher, T.; Löbbecke, S. In *Organic Azides: Syntheses and Applications*; Bräse, S., Banert, K., Eds.; John Wiley & Sons: Chichester, 2010; pp 3–4.
- [251] Kalsi, P. S. *Organic Reactions and Their Mechanisms*; New Age International (P) Limited, Publishers: New Delhi, 1996.
- [252] Butler, R. N.; Fox, A.; Collier, S.; Burke, L. A. *J. Chem. Soc., Perkin Trans. 2* **1998**, 2243–2248.
- [253] Burke, L. A.; Fazen, P. J. *Int. J. Quantum Chem.* **2009**, *109*, 3613–3618.
- [254] Kazakevich, Y. V.; LoBrutto, R. *HPLC for Pharmaceutical Scientists*; John Wiley & Sons: Hoboken, 2007; p 146.
- [255] Kalbag, S. M.; Roeske, R. W. *J. Am. Chem. Soc.* **1975**, *97*, 440–441.
- [256] Tousek, J.; Miert, S. V.; Pieters, L.; Baelen, G. V.; Hostyn, S.; Maes, B. U. W.; Lemiére, G.; Dommissie, R.; Marek, R. *Magn. Reson. Chem.* **2008**, *46*, 42–51.
- [257] Barltrop, J. A.; Bunce, N. J. *J. Chem. Soc. C.* **1968**, 1467–1474.
- [258] Iddon, B.; Meth-Cohn, O.; Scriven, E. F. V.; Suschitzky, H.; Gallagher, P. T. *Angew. Chem. Int. Ed. Engl.* **1979**, *18*, 900–917.

- [259] Reiser, A.; Marley, R. *Trans. Faraday Soc.* **1968**, *64*, 1806–1815.
- [260] Jonckers, T. H. M. et al. *J. Med. Chem.* **2002**, *45*, 3497–3508.
- [261] Whittell, L. R.; Batty, K. T.; Wong, R. P. M.; Bolitho, E. M.; Fox, S. A.; Davis, T. M. E.; Murray, P. E. *Bioorg. Med. Chem.* **2011**, *19*, 7519–7525.
- [262] Lu, W.-J.; Switalska, M.; Wang, L.; Yonezawa, M.; El-Sayed, I. E.-T.; Wietrzyk, J.; Inokuchi, T. *Med. Chem. Res.* **2013**, *22*, 4492–4504.
- [263] Iorio, F.; Bosotti, R.; Scacheri, E.; Belcastro, V.; Mithboakar, P.; Ferriero, R.; Murino, L.; Tagliaferri, R.; Brunetti-Pierri, N.; Isacchi, A.; di Bernardo, D. *Proc. Natl. Acad. Sci. USA* **2012**, *107*, 14621–14626.
- [264] Fulmer, G. R.; Miller, A. J. M.; Sherden, N. H.; Gottlieb, H. E.; Nudelman, A.; Stoltz, B. M.; Bercaw, J. E.; Goldberg, K. I. *Organometallics* **2010**, *29*, 2176–2179.
- [265] Rosenau, C. P.; Jelier, B. J.; Gossert, A. D.; Togni, A. *Angew. Chem. Int. Ed.* **2018**, *57*, 9528–9533.
- [266] Pedersen, D. S.; Rosenbohm, C. *Synthesis* **2001**, *16*, 2431–2434.
- [267] Preshlock, S. M.; Plattner, D. L.; Maligres, P. E.; Krska, S. W.; Maleczka, R. E.; Smith, M. R. *Angew. Chem. Int. Ed.* **2013**, *52*, 12915–12919.
- [268] Smith, M. R.; Bisht, R.; Haldar, C.; Pandey, G.; Dannatt, J. E.; Glaffari, B.; Jr., R. E. M.; Chattopadhyay, B. *ACS Catal.* **2018**, *7*, 6216–6223.
- [269] Bogányiab, B.; Kámána, J. *Tetrahedron* **2013**, *69*, 9512–9519.
- [270] Reddy, Y. P.; Reddy, K. K. *Indian J. Chem.* **1988**, *27B*, 563–564.
- [271] Wippich, J.; Truchan, N.; Bach, T. *Adv. Synth. Catal.* **2016**, *358*, 2083–2087.
- [272] Lescot, E.; Muzard, G.; Markovits, J.; Belleney, J.; Roques, B. P.; LePecq, J.-B. *J. Med. Chem.* **1986**, *63*, 1731–1737.
- [273] Chatterjee, T.; Choi, M. G.; Kim, J.; Chang, S.-K.; Cho, E. J. *Chem. Commun.* **2016**, *52*, 4203–4206.
- [274] Rao, M. S.; Sarkar, S.; Hussain, S. *Tetrahedron Lett.* **2019**, *60*, 1221–1225.
- [275] Bag, S.; Jana, S.; Pradhan, S.; Bhowmich, S.; Goswami, N.; Sinha, S. K. *Nat. Commun.* **2021**, *12*, 1–8.
- [276] Long, C.-Y.; Ni, S.-F.; Su, M.-H.; Wang, X.-Q.; Tan, W. *ACS Catal.* **2020**, *10*, 13641–13649.

- [277] Scarborough, C. C.; M. J. W. Grady, I. A. G.; Gandhi, B. A.; Bunel, E. E.; Stahl, S. S. *Angew. Chem. Int. Ed.* **2005**, *117*, 5403–5406.
- [278] Hostyn, S.; Maes, B. U.; Pieters, L.; Lemièrre, G. L. F.; Mátyus, P.; Hajòs, G.; Dom-misse, R. A. *Tetrahedron* **2005**, *61*, 1571–1577.
- [279] Alajarin, M.; Molina, P.; Vidal, A. *J. Nat. Prod.* **1997**, *60*, 747.
- [280] F.,; Hardesty, J.; Thummel, R. P. *J. Org. Chem.* **1998**, *63*, 4055–4061.
- [281] Kulka, M.; Manske, R. H. F. *Can. J. Med.* **1952**, *30*, 711–719.
- [282] Meyers, C.; Rombouts, G.; Loones, K. T. J.; Maes, B. U. W. *Adv. Synth. Catal.* **2008**, *350*, 465–470.
- [283] Uchuskin, M. G.; Pilipenko, A. S.; Serdyuk, O. V.; Trushkov, I. V.; Butin, A. V. *Org. Biomol. Chem.* **2012**, *10*, 7262–7265.
- [284] He, L.; Chang, H.-X.; Chou, T.-C.; Savaraj, N.; Cheng, C. C. *Eur. J. Med. Chem.* **2003**, *38*, 101–107.
- [285] Meyers, C.; Rombouts, G.; Loones, K. T. J.; Coelho, A.; Maes, B. U. W. *Adv. Synth. Catal.* **2008**, *350*, 465–470.
- [286] Caneque, T.; Cuadro, A. M.; Alvarez-Builla, J.; Pérez-Moreno, J.; Clays, K.; Marcelo, G.; Mendicuti, F.; Castano, O.; Andrés, J. L.; Vaquero, J. J. *Eur. J. Org. Chem.* **2010**, 6323–6330.
- [287] Xiang, S.-K.; Zhang, B.; Cui, Y.; Jiao, N. *Chem. Commun.* **2011**, *47*, 8097–8099.
- [288] Zhu, J.-K.; Gao, J.-M.; Yang, C.-J.; Shang, X.-F.; Zhao, Z.-M.; Lawoe, R. K.; Zhou, R.; Sun, Y.; Yin, X.-D.; Liu, Y.-Q. *J. Agric. Food Chem.* **2020**, *68*, 2306–2315.
- [289] Miller, M.; Vogel, J. C.; Tsang, W.; Merrit, A.; Procter, D. J. *Org. Biomol. Chem.* **2009**, *7*, 589–597.



Mapping the reactivity of the quinoline ring-system – Synthesis of the tetracyclic ring-system of isocryptolepine and regioisomers

Katja S. Håheim, Ida T. Urdal Helgeland, Emil Lindbäck, Magne O. Sydnes*

Faculty of Science and Technology, Department of Chemistry, Bioscience and Environmental Engineering, University of Stavanger, NO-4036, Stavanger, Norway

ARTICLE INFO

Article history:

Received 17 January 2019

Received in revised form

27 March 2019

Accepted 11 April 2019

Available online 17 April 2019

Keywords:

Natural product

Suzuki-Miyaura cross-coupling

Tandem C-H activation/C-N bond formation

ABSTRACT

Bromoquinolines (2-bromoquinoline – 8-bromoquinoline and 5-bromo-3-methoxyquinoline) and 2-aminophenylboronic acid hydrochloride were subjected to Suzuki-Miyaura cross-coupling conditions resulting in formation of the desired biaryl systems in good yields. The resulting biaryls were then subjected to palladium catalyzed C–H activation/C–N bond formation utilizing PdCl₂(dppf). The reactions revealed large differences in reactivity depending on the attachment point for the 2-aminophenyl group on the quinoline. The variation in the reactivity was rationalized based on the electron distribution around the quinoline ring-system.

© 2019 Elsevier Ltd. All rights reserved.

1. Introduction

Nitrogen containing heterocycles are immensely important appearing in 59% of the Food and Drug Administration (FDA) approved small-molecule drugs [1]. Heterocycles containing one or more nitrogen atoms are also commonly found in nature [2], with many of these compounds being based on the quinoline core [2c,2d]. Cryptolepine, neocryptolepine, and isocryptolepine belonging to the indoloquinoline family of natural products represents examples of such compounds (Fig. 1) [3]. The antimalarial activity of these three compounds has made them attractive synthetic targets [4]. In particular isocryptolepine has been the focus of studies in several research groups throughout the world resulting in a range of total syntheses [5,6], including our own synthesis [7]. Lately it has also been found that neocryptolepine has activity towards neglected topical diseases caused by trypanosomatid parasites, increasing the interest for this natural product amongst medicinal chemists [8]. The three mentioned natural products have also been targeted for analogue synthesis with the aim to enhance the antimalarial and anticancer activity [9].

As a continuation of our own synthesis of isocryptolepine [7], we became interested in mapping the reactivity around the quinoline ring-system in terms of the ability to engage in the Suzuki-

Miyaura cross-coupling and the following C–H activation/C–N bond formation leading up to the formation of the core structure of the natural products neocryptolepine and isocryptolepine and regioisomers thereof. Although several of these compounds have been prepared previously (compounds **4a** [10,11], **4b** [7,11], **4c** [10,11], **4d** [12], **4e** [13], **4f** [14], and **4g**¹⁵), in particular the natural product precursors (compound **4a** and **4b**), it is the first time that the same reaction conditions have been utilized in order to study the reactivity around the quinoline ring-system. Herein, we present the results of these studies highlighting the difference in reactivity around the quinoline ring-system in particular towards ring formation.

2. Result and discussion

In our reported synthesis of isocryptolepine, PdCl₂(dppf) was utilized as catalyst in order to facilitate the Suzuki-Miyaura cross-coupling reaction [7]. Naturally, this catalyst was an obvious starting point for our further studies. Treating 2-bromoquinoline (**1a**) and boronic acid **2** with PdCl₂(dppf) under our previously used reaction conditions gave quick conversion (1 h) to the desired product **3a** in 65% isolated yield (Table 1, Entry 1). Prolonging the reaction time only resulted in the formation of unwanted byproducts. The drop in yield compared to the yield obtained for the cross-coupling in C3,^{7a} which gave compound **3b** in 84% yield, prompted us to try Pd(PPh₃)₄ as catalyst. Switching catalyst to Pd(PPh₃)₄ resulted in formation of compound **3a** in 94% yield (Table 1, Entry

* Corresponding author.

E-mail address: magne.o.sydnes@uis.no (M.O. Sydnes).

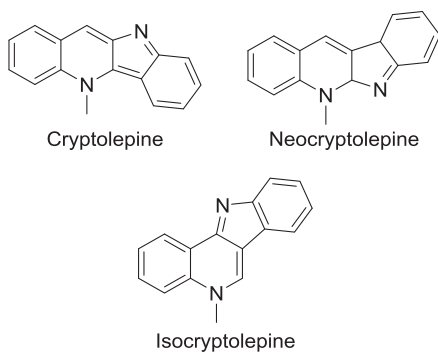


Fig. 1. The structure of cryptolepine, neocryptolepine, and isocryptolepine.

1). The great difference in yields obtained with the two catalysts in these two reactions prompted us to utilize both reaction conditions in the continuation of the work.

The remaining bromoquinolines were subjected to Suzuki-Miyaura cross-coupling reaction using PdCl₂(dppf) (Method A) and Pd(PPh₃)₄ (Method B). Both methods successfully yielded all the desired Suzuki-Miyaura cross-coupling products **3b–g** in predominantly good yields (Table 1). Overall, tetrakis(triphenylphosphine)palladium(0) (Method B) generally resulted in the best yields and the reaction times were mostly shorter (Table 1). In particular, the coupling reaction with 4-bromoquinoline worked remarkably well resulting in the formation of the desired cross-coupling product **3c** in close to quantitative yield (96%) in less than 2 h (Table 1, Entry 3).

Based on the results obtained for the Suzuki-Miyaura cross-coupling reactions it is obvious that the reactivity around the quinoline ring varies. It has been known for some time that the two least electron dense positions of the quinoline ring-system are the C2 and C4 [16,17]. This is clearly demonstrated by electron density calculations by Coulson and Longuet-Higgins (Fig. 2a) [18], however, other calculations suggest that the data for the C2 and C4 should be reversed [10,18]. Indeed, Brower et al. [17] observed lower activation energies at the C2 of quinoline in the aromatic substitution with piperidine (Fig. 2b) and PM3 calculations carried out by Hostyn et al. [10] revealed a significantly higher electron density at the C4 of quinoline.

It was noted by Brower et al. that this deviation in electron density could be the result of the chosen model employed by

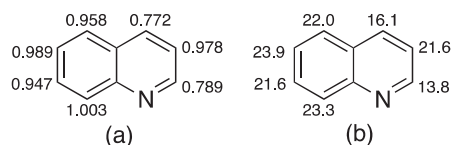


Fig. 2. (a) Electron densities of the quinoline ring-system [18]; (b) Energies of activation (ΔE) for reactions of haloquinolines with piperidine [17].

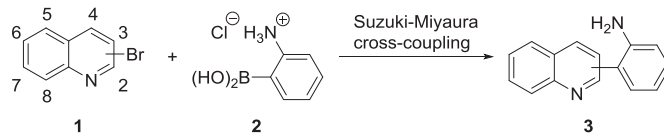
Coulson and Longuet-Higgins, as the calculations are based on the occurrence of a certain substitution reaction being made [17,18]. While there seems to be an agreement that C3 is the least active of the pyridyl carbons [17,19], there is some debate regarding which position is the most active between C2 and C4, as evident by the preceding discussion. Schröter et al. argue that the annelated benzol ring in quinoline makes C2 the only carbon with any significant electrophilicity [20], while Almond-Thynne et al. claims that in dihalogenated quinolines, the electrophilicity is highest at C2, C4 and C3, in decreasing order [19].

In the Suzuki-Miyaura cross-coupling reactions of heteroaryl halides it has been remarked that the oxidative addition step proceeds in a similar mechanistic fashion to S_NAr reactions [19]. From this, it can be inferred that the reaction occurs at the most electrophilic carbon given the choice between multiple reaction sites [19–21]. This trend was not quite representative for our cross-couplings, with the reactions at C5 and C8 performing better than at C3 when Pd(PPh₃)₄ was used as catalyst (Table 1, Entries 2, 4, and 7). As can be seen from Table 1 the reactivity was not only determined by the relative electron density, but also by the employed catalyst.

Keeping the previous discussion in mind, when it came to testing the reactivity of our Suzuki-Miyaura cross-coupling products towards cyclization, we expected that when two positions were available to form a C–N bond it would selectively occur at the most electron deficient carbon. This is based on the assumption that the cyclization proceeds via an oxidative addition-type mechanism with the palladium species, which was proposed by Bjørsvik and Elumalai as a likely reaction pathway for the cyclization of 2-aminobiphenyl to form the carbazole scaffold under conditions similar to the ones used in this work [22].

Rerunning the cyclization of compound **3b** using our previously reported chemistry [7a], proceeded regioselective to give indoloquinoline **4b** in 73% yield (Table 2, Entry 2). The increased yield (62% → 73%) for the cyclization reaction compared to our previous

Table 1
Suzuki-Miyaura cross-coupling of bromoquinoline **1** with 2-aminophenylboronic acid hydrochloride (**2**).



Entry	Substrate	Catalyst PdCl ₂ (dppf) ^a (Reaction time)	Catalyst Pd(PPh ₃) ₄ ^b (Reaction time)
1	2-bromoquinoline (1a)	3a 65% (1 h)	3a 94% (16 h)
2	3-bromoquinoline (1b)	3b 84% ^c (20 h)	3b 53% (20 h)
3	4-bromoquinoline (1c)	3c 91% (21 h)	3c 96% (1.75 h)
4	5-bromoquinoline (1d)	3d 54% (overnight)	3d 90% (overnight)
5	6-bromoquinoline (1e)	3e 81% (overnight)	3e 82% (overnight)
6	7-bromoquinoline (1f)	3f 30% (29 h)	3f 82% (20 h)
7	8-bromoquinoline (1g)	3g 45% (22 h)	3g 87% (16 h)

^a Method A: PdCl₂(dppf) (dppf = 1,1'-bis(diphenylphosphino)ferrocene) (5 mol%), K₂CO₃, EtOH/H₂O (5:1), 60 °C.

^b Method B: Pd(PPh₃)₄ (5 mol%), Cs₂CO₃, DME/H₂O (5:1), 80 °C.

^c Slightly increased yield compared to our previously reported yield is due to optimization of the purification of the crude material.

report [7a] is due to the discovery of a better solvent combination for purification of the crude product by flash chromatography.

Upon cyclization of substrate **3b** no trace of its regioisomer 6*H*-indolo[2,3-*b*]quinoline was observed in the crude reaction mixture despite the resonance forms of compound **3b** bearing a negative charge at both the C2 and C4 as outlined in Scheme 3a. The observed regioselectivity towards C–N bond formation at the C4 over C2 is presumably governed by favorable relative electrostatic effects. Similar observations has also been reported for C–C bond formations, although in those examples small amounts of the product resulting from reaction at C2 was also isolated [10,17].

Much to our disappointment, subjecting biaryls **3a** and **3c** to our standard cyclization conditions did not yield the expected products 7*H*-indolo[2,3-*c*]quinoline (**4a**) and 10*H*-indolo[3,2-*b*]quinoline (**4c**), respectively. Instead, these reactions resulted in acetylation of the starting materials to give **5a** and **5c** in 55% and 54% yield, respectively (Table 2, Entries 1 and 3). The resonance structures of **3a** and **3c** show that the C3 of the quinoline moiety can bear a negative charge and additional inductive effects exhibited by the nuclear nitrogen may make this position particularly unreactive [17]. With the aid of ESI-MS, traces of a mass corresponding to the expected mass of protonated species **4c** was detected, however, ¹H NMR analysis on a minute amount of compound post purification by silica gel column chromatography failed to provide evidence of its formation.

Acetic acid is known to act as an acetylating agent when employed in microwave-assisted syntheses [23]. Efforts were therefore made to avoid the formation of the acetylation product by replacing acetic acid with a more sterically hindered acid, viz. pivalic acid. Attempts to carry out the cyclization of **3a** in pivalic acid unfortunately only lead to the formation of *N*-(2-(quinolin-2-yl)phenyl)pivalamide (**7a**) in 65% yield, thus no further experiments were conducted using this solvent (Scheme 1).

Cyclization of compound **3d** gave only phenanthridine **6d** in 73% yield with no trace of cyclization into C6 (Table 2, Entry 4). It can be seen from the resonance structures of compound **3d** that C6 of quinoline can have a negative charge while C4 cannot (Scheme 3b). Formation of compound **6d** is in agreement with cyclization into the most electron deficient position.

Despite the resonance structures for compound **3d** favoring cyclization into C4 (Scheme 3b), the kinetic preference is to form 5- over 6-membered rings [24] and the regioselective formation of phenanthridine **6d** warranted further exploration. We became interested in altering the electron distribution of biaryl **3d** by introducing a methoxy group at C3 to examine if the electron donating properties of the alkoxide would affect the regioselectivity (Scheme 3b). Following the procedure outlined by Landagaray et al. [25] 5-bromo-3-methoxyquinoline (**1h**) was synthesized starting from 3-bromoquinoline (**1b**) (Scheme 2). Subsequent Suzuki-Miyaura cross-coupling of quinoline **1h** with boronic acid **2** using methods A and B yielded 2-(3-methoxyquinolin-5-yl)aniline (**3h**) in poor yields (method A: 47%; method B: 34%). Unreacted starting material (**1h**) (29%) and 19% of 2,2'-biphenyldiamine was also isolated when method A was used. Method A could be further optimized by adjusting the equivalents of boronic acid **2** from 1.5 eq. to 3 eq., which increased the yield of the desired coupling product **3h** from 47% → 88%. Finally, cyclization of biaryl **3h** surprisingly yielded phenanthridine **6h** in 39% yield in addition to a small quantity of the acetylated product **5h** (<5%) together with several unidentified impurities. Analyzing the crude mixture by ESI-MS, traces of a mass corresponding to the protonated mass of the 5-membered ring product **4h** was detected but this was not verifiable by ¹H NMR. Consequently, it is clear that the inductive effect exhibited by the methoxy moiety affects the system, however, it is not sufficient to completely reverse the

regioselectivity observed for the cyclization of biaryl **3d**.

A literature search revealed no synthetic strategies for the synthesis of systems such as phenanthridines **6d** and **6h** at present time. Hostyn et al. [10] describes the synthesis of 7*H*-indolo[2,3-*c*]quinoline (**4a**) and 7*H*-pyrido[2,3,4-*kl*]acridine by thermal collapse of 4-(2-azidophenyl)quinoline, where the indoloquinoline was the major product and only traces of the acridine was observed. The authors rationalize the selectivity in terms of kinetics, moreover, the cyclization is thought to be the result of a nitrene insertion which presumably plays a role in determining the regioselectivity.

Turning to the cyclization of compounds **3e** and **3f** (Table 2, Entries 5 and 6), it did not seem immediately obvious where the C–N bond would be formed. Unlike the resonance form of compound **3b**, there is no adjacent heteroatom to delocalize the negative charge in these cases (Scheme 3c). Instead, we examined the chemical shifts for the protons adjacent to the tethered aniline to see which of the two protons experienced the most deshielding, a method advocated for by Handy and Zhang for the prediction of regioselectivity in cross-coupling reactions [21]. However, it is noted that when $\Delta\delta_{\text{H}} < 0.03$ ppm this technique should be used with caution as they demonstrated that it failed to accurately predict the selectivity in such cases. In compound **3e**, H-5 has a shift of 7.91 ppm while H-7 is at 7.85 ppm ($\Delta\delta_{\text{H}} = 0.06$ ppm), favoring cyclization into C5, which in fact was the outcome of the reaction resulting in a 65% isolated yield of compound **4e** (Table 2, Entry 5). No trace of the H-7 regioisomer, 10*H*-pyrido[2,3-*b*]carbazole, was observed.

Similarly, cyclization of compound **3f** occurred at H-8, which displayed a higher chemical shift than H-6, to furnish **4f** in 25% yield (Table 2, Entry 6). This reaction was also regioselective towards cyclization at H-8, however, undesired acetylation product **5f** was also formed in 61% yield. The cyclization of biaryl **3g** returned a similar outcome, with target compound **4g** formed in 29% yield while the acetylation product was furnished in 69% yield (Table 2, Entry 7). It seems that acetylation of biaryls **3** is the outcome when the electron flow of the quinoline ring-system is congested, i.e. it is energetically unfavorable to form the tetracyclic ring-system due to high electron densities at the adjacent protons.

3. Conclusion

In conclusion, the reactivity of the quinoline ring-system has been mapped by subjecting bromoquinolines **1a-h** to a Suzuki-Miyaura cross-coupling reaction with 2-aminophenylboronic acid hydrochloride (**2**). The resulting cross-coupling products were then subjected to an intramolecular cyclization via tandem C–H activation and C–N bond formation to furnish tetracyclic ring-systems **4b** and **4e-4g** and **6d** and **6h**. Our findings were congruent with earlier reports that C2 and C4 of the quinoline scaffold is the most active and it appears that the electron densities at the various carbons determined the regioselectivity of the cyclization. Our synthetic efforts also resulted in an improved yield for the formation of the tetracyclic ring-system required for the formation of isocryptolepine.

4. Experimental

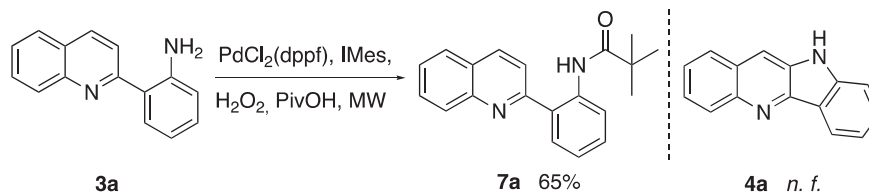
4.1. General experimental

Nuclear magnetic resonance (NMR) spectra were recorded on a Bruker Ascend™ 400 series, operating at 400 MHz for ¹H and 100 MHz for ¹³C, respectively. Chemical shifts (δ) are expressed in ppm relative to residual chloroform (¹H, 7.26 ppm; ¹³C, 77.16 ppm), DMSO-*d*₆ (¹H, 2.50 ppm; ¹³C, 39.52 ppm) or methanol (¹H, 3.31 ppm; ¹³C, 49.00 ppm). The assignments of signals in various

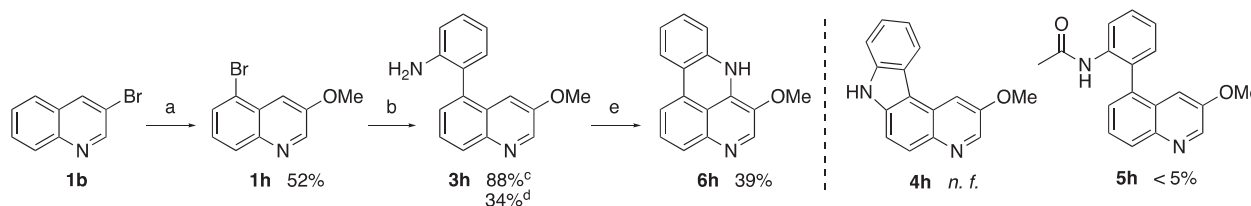
Table 2Summary of the C–H activation/C–N bond formation resulting in the formation of the tetracyclic ring-systems **4b**, **4e**, **4f**, **4g** and **6c**.^a

Entry	Substrate	Cyclization product	Acetylation product
1			
2			
3			
4			
5			
6			
7			

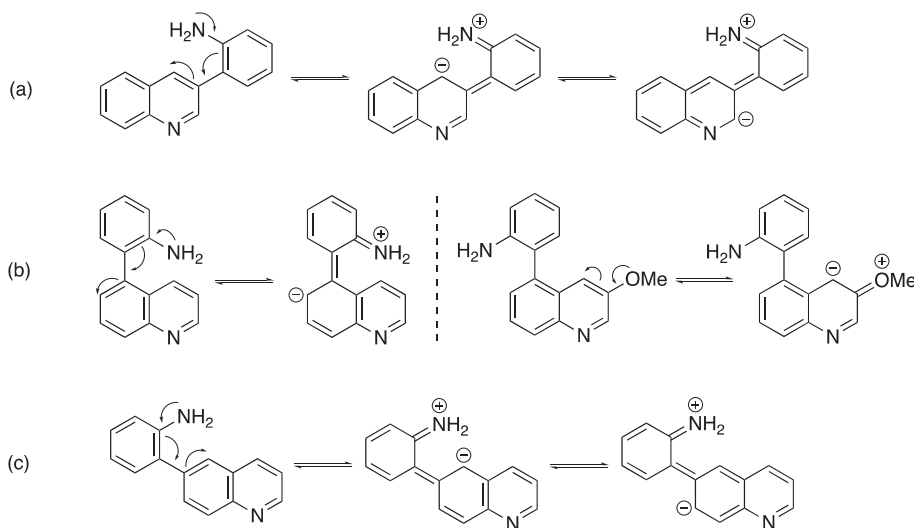
^aConditions: PdCl₂(dppf) (20 mol%), 1,3-bis(2,4,6-trimethylphenyl)-imidazolium (IMes) (5 mol%), H₂O₂ (35 wt%, 29 mol%), AcOH, MW sealed reactor tube 118 °C; ^b*n.f.* = not formed.



Scheme 1. Attempted formation of compound **4a** utilizing pivalic acid as solvent.



Scheme 2. Synthesis of 2-(3-methoxyquinolin-5-yl)aniline (**3h**) and subsequent ring closure to yield 6-methoxy-7H-pyrido[4,3,2-g]phenanthridine (**6h**). Conditions: a) (i) NaOMe (30%), CuI (5 mol%), DMF, reflux, overnight; (ii) NBS, H₂SO₄ (conc.), 0 °C to rt, overnight; b) Method A: **2** (0.48 mmol), PdCl₂(dppf) (5 mol%), K₂CO₃, EtOH/H₂O (5:1), 60 °C, overnight; ^dMethod B: **2** (0.24 mmol), Pd(PPh₃)₄ (5 mol%), Cs₂CO₃, DME/H₂O (5:1), 80 °C, overnight; e) PdCl₂(dppf) (20 mol%), IMes (5 mol%), H₂O₂ (35 wt%, 29 mol%), AcOH, MW 118 °C 1 h.



Scheme 3. Resonance structures for compounds **3b**, **3d/3h** and **3e**.

NMR spectra was often assisted by conducting correlation spectroscopy (COSY), heteronuclear single-quantum correlation spectroscopy (HSQC) and/or heteronuclear multiple bond correlation spectroscopy (HMBC).

Reactions were monitored by thin-layer chromatography (TLC) carried out on 0.25 mm silica gel 60 F₂₅₄ coated aluminium sheets using UV light as visualizing agent. Silica gel 60 (particle size 40–63 μm) was used for silica flash chromatography and alumina gel (particle size 30–48 μm) was used for alumina flash chromatography. Automated flash chromatography was carried out using an Interchim puriFlash[®] 215 chromatography system. The sample was evaporated onto celite and then dry-loaded onto a specialized column which was attached to an SI-HP Interchim column filled with silica gel (particle size 40–50 μm). The appropriate eluent was flushed through the columns using an applied pressure of 22–26 bar.

In addition to TLC, low resolution mass spectrometry (LRMS) was routinely used to monitor and identify the various components of reaction mixtures. The LRMS spectra were obtained on an Advion expression^s CMS mass spectrometer operating at 3.5 kV in

electrospray ionization (ESI) mode.

Infrared spectroscopy (IR) was performed on a Cary 360 FTIR spectrophotometer. Solids were dissolved in CHCl₃ or DCM and absorbed on a NaCl plate, or by placing the sample directly onto the crystal of an attenuated total reflectance (ATR) module. Melting points were measured using a Stuart Scientific SMP3 melting point apparatus and are uncorrected. High resolution mass spectroscopy (HRMS) were conducted externally at the University of Bergen or the University of Tromsø, using electron spray ionization (ESI). The microwave-assisted experiments were performed in a CEM Focused Microwave[™] Synthesis System, model type Discover, operating at 0–300 W at a temperature of 118 °C, a pressure range of 0–290 psi, with reactor vial volumes of either 10 or 35 mL. Commercially chemicals were used as delivered from the supplier unless otherwise noted.

4.2. 5-Bromo-3-methoxyquinoline (**1h**) [25]

Following the procedure reported by Landagaray et al. the title compound **1h** was obtained as off-white crystals (52%), mp

76–77 °C (lit [25], 81–83 °C); IR (ATR): ν_{\max} 3067, 3004, 2995, 2964, 2853, 1599, 1407, 1161, 859 cm^{-1} ; ^1H NMR (400 MHz, CD_3OD): δ 8.61 (d, $J = 2.8$ Hz, 1H), 7.99–7.96 (m, 1H), 7.87 (dd, $J = 7.6$ Hz, 1.0 Hz, 1H), 7.84 (d, $J = 2.6$ Hz, 1H), 7.48 (dd, $J = 8.4$ Hz, 7.6 Hz, 1H), 4.02 (s, 3H); ^{13}C NMR (100 MHz, CD_3OD): δ 155.9, 146.2, 144.6, 132.3, 129.7, 129.3, 128.3, 121.5, 113.2, 56.3. In accordance with previously reported data [25].

4.3. Method A: general method for Suzuki-Miyaura cross-coupling using $[\text{PdCl}_2(\text{dppf})]$ as catalyst

2-Aminophenylboronic acid hydrochloride (**2**) (62.5 mg, 0.36 mmol), an aqueous solution of potassium carbonate (116.1 mg, 0.84 mmol in 0.2 mL H_2O), and $\text{PdCl}_2(\text{dppf})$ (8.9 mg, 0.012 mmol, 5 mol%) was added to a stirred solution of bromoquinoline **1a-h** (0.24 mmol) in EtOH (1 mL) under an argon atmosphere and the reaction mixture was stirred at 60 °C until completion of the reaction as indicated by TLC analysis. The reaction mixture was then allowed to cool to room temperature and the volatiles were removed under reduced pressure. The concentrate was evaporated onto celite and purified by silica gel column chromatography using the chromatographic technique and eluent as indicated for each compound in order to give compound **3a-h**.

4.4. Method B: general method for Suzuki-Miyaura cross-coupling using $\text{Pd}(\text{PPh}_3)_4$ as catalyst

To a solution of bromoquinoline **1a-h** (0.24 mmol) in dime-thoxyethane (2 mL) under an argon atmosphere was added 2-aminophenylboronic acid hydrochloride (**2**) (62.5 mg, 0.36 mmol), an aqueous solution of cesium carbonate (273.7 mg, 0.84 mmol in 0.4 mL H_2O), and tetrakis(triphenylphosphine)palladium(0) (13.9 mg, 0.012 mmol, 5 mol%). The resulting reaction mixture was stirred at 80 °C until completion as indicated by TLC. The reaction mixture was then allowed to cool to room temperature and the volatiles were removed under reduced pressure. The concentrate was evaporated onto celite and purified by silica gel column chromatography using the chromatographic technique and eluent as indicated for each compound in order to give compound **3a-h**.

4.5. 2-(Quinolin-2-yl)aniline (**3a**)

Following methods A and B; the crude was purified by silica gel column chromatography (pet. ether/EtOAc, 9:1 v/v) and concentration of the relevant fractions [$R_f = 0.17$ (pet. ether/EtOAc, 9:1 v/v)] gave the title compound **3a** as bright yellow crystals (method A: 65%; method B: 94%), mp 152–155 °C; IR (ATR): ν_{\max} 2922, 2852, 1718, 1465, 759 cm^{-1} ; ^1H NMR (400 MHz, CDCl_3): δ 8.20 (d, $J = 8.7$ Hz, 1H), 8.06 (d, $J = 8.4$ Hz, 1H), 7.84 (d, $J = 8.7$ Hz, 1H), 7.82–7.80 (m, 1H), 7.73–7.69 (m, 2H), 7.54–7.49 (m, 1H), 7.24–7.19 (m, 1H), 6.85–6.82 (m, 2H); ^{13}C NMR (100 MHz, CDCl_3): δ 159.2, 147.2, 146.9, 136.9, 130.5, 129.9, 129.8, 128.9, 127.5, 126.4, 126.3, 121.8, 120.6, 117.9, 117.7. In accordance with previously reported data [26].

Utilizing method A, the desired product **3a** had to undergo recrystallization (*n*-heptane/EtOAc, 9:1 v/v) to remove overlapping impurities.

4.6. 2-(Quinolin-3-yl)aniline (**3b**)

Following methods A and B; the crude was purified by silica gel column chromatography (pet. ether/EtOAc, 7:3 → 1:1 v/v) and concentration of the relevant fractions [$R_f = 0.27$ (pet. ether/EtOAc, 7:3 v/v)] gave the title compound **3b** as a yellow crystalline solid (method A: 84%; method B: 53%), mp 132–135 °C (lit [7a].

130–132 °C). IR (NaCl): ν_{\max} 3438, 3331, 3208, 3061, 1619, 1575, 1497, 1452 cm^{-1} ; ^1H NMR (400 MHz, CDCl_3) δ 9.03 (d, $J = 2.0$ Hz, 1H), 8.25 (d, $J = 2.0$ Hz, 1H), 8.14 (d, $J = 8.4$ Hz, 1H), 7.83–7.81 (m, 1H), 7.75–7.71 (m, 1H), 7.59–7.55 (m, 1H), 7.25–7.19 (m, 2H), 6.92–6.88 (m, 1H), 6.84–6.82 (m, 1H), 3.80 (bs, 2H); ^{13}C NMR (100 MHz, CDCl_3): δ 151.5, 147.1, 144.1, 135.5, 132.5, 130.9, 129.6, 129.5, 129.2, 127.9, 127.8, 127.1, 123.7, 119.1, 116.0. In accordance with previously reported data [7a].

4.7. 2-(Quinolin-4-yl)aniline (**3c**)

Following methods A and B; the crude was purified by an Interchim puriFlash chromatography system (pet. ether/EtOAc, 95:5 → 55:45 v/v) and concentration of the relevant fractions [$R_f = 0.29$ (pet. ether/EtOAc, 1:1 v/v)] gave the title compound **3c** as a yellow solid (method A: 91%; method B: 96%), mp 128–129 °C (lit [13], 119 °C). IR (NaCl): ν_{\max} 3454, 3328, 3210, 3061, 3033, 1617, 1494, 1451, 752 cm^{-1} ; ^1H NMR (400 MHz, CDCl_3) δ 8.94 (d, $J = 4.4$ Hz, 1H), 8.18–8.15 (m, 1H), 7.74–7.69 (m, 2H), 7.50–7.46 (m, 1H), 7.37 (d, $J = 4.4$ Hz, 1H), 7.28 (ddd, $J = 7.5$ Hz, 1.6 Hz, 0.6 Hz, 1H), 7.12 (dd, $J = 7.5$ Hz, 1.5 Hz, 1H), 6.88 (td, $J = 7.4$ Hz, 1.0 Hz, 1H), 6.83 (dd, $J = 8.1$ Hz, 0.8 Hz, 1H), 3.83 (bs, 2H); ^{13}C NMR (100 MHz, CDCl_3) δ 150.4, 148.7, 146.2, 143.9, 130.6, 129.9, 129.8, 129.7, 126.9, 126.9, 126.1, 122.9, 122.3, 118.5, 115.8. In accordance with previously reported data [13].

4.8. 2-(Quinolin-5-yl)aniline (**3d**)

Following methods A and B; the crude was purified by silica gel column chromatography (pet. ether/EtOAc, 7:3 → 6:4 v/v) and concentration of the relevant fractions [$R_f = 0.23$ (pet. ether/EtOAc, 1:1 v/v)] gave the title compound **3d** as light brown crystals (method A: 54%; method B: 90%), mp 163–166 °C. IR (ATR) ν_{\max} 3410, 3318, 3209, 2924, 1618, 1491, 959, 803, 754 cm^{-1} ; ^1H NMR (400 MHz, CDCl_3): δ 8.93 (dd, $J = 4.1$ Hz, 1.7 Hz, 1H), 8.16–8.14 (m, 1H), 8.02–7.99 (m, 1H), 7.81–7.77 (m, 1H), 7.53 (dd, $J = 6.9$ Hz, 0.9 Hz, 1H), 7.35 (dd, $J = 8.5$ Hz, 4.2 Hz, 1H), 7.30–7.25 (m, 1H), 7.13 (dd, $J = 7.5$ Hz, 1.5 Hz, 1H), 6.88 (td, $J = 7.5$ Hz, 1.1 Hz, 1H), 6.84 (dd, $J = 8.0$ Hz, 0.7 Hz, 1H), 3.44 (bs, 2H); ^{13}C NMR (100 MHz, CDCl_3): δ 150.6, 148.7, 144.4, 137.5, 134.9, 131.4, 129.6, 129.5, 129.3, 128.2, 127.1, 124.4, 121.4, 118.56, 115.6; HRMS (ESI): calcd. for $\text{C}_{15}\text{H}_{12}\text{N}_2\text{H}^+$ 221.1073, found 221.1071.

4.9. 2-(Quinolin-6-yl)aniline (**3e**)

Following methods A and B; the crude was purified by silica gel column chromatography (pet. ether/EtOAc, 4:6 v/v) and concentration of the relevant fractions [$R_f = 0.16$ (pet. ether/EtOAc, 6:4 v/v)] gave the title compound **3e** as an off-white solid (method A: 81%; method B: 82%), mp 130–132 °C. IR (NaCl) ν_{\max} 3462, 3327, 3203, 3020, 2925, 2854, 1618, 1570, 1490 cm^{-1} ; ^1H NMR (400 MHz, CDCl_3): δ 8.93 (d, $J = 2.4$ Hz, 1H), 8.20–8.18 (m, 2H), 7.91 (s, 1H), 7.85 (d, $J = 8.1$ Hz, 1H), 7.45–7.42 (m, 1H), 7.26–7.19 (m, 2H), 6.88–6.81 (m, 1H), 6.82 (d, $J = 8.3$ Hz, 1H), 3.62 (bs, 2H); ^{13}C NMR (100 MHz, CDCl_3) δ 150.5, 147.4, 143.8, 138.1, 136.3, 131.3, 130.8, 129.9, 129.1, 128.6, 127.8, 126.7, 121.6, 119.0, 115.9; HRMS (ESI): calcd. for $\text{C}_{15}\text{H}_{12}\text{N}_2\text{H}^+$ 221.1073, found 221.1072.

4.10. 2-(Quinolin-7-yl)aniline (**3f**)

Following methods A and B; the crude was purified by silica gel column chromatography (pet. ether/EtOAc, 6:4 v/v) and concentration of the relevant fractions [$R_f = 0.21$ (pet. ether/EtOAc, 6:4 v/v)] gave the title compound **3f** as a pale yellow oil (method A: 30%; method B: 82%). IR (ATR): ν_{\max} 3453, 3330, 3200, 3050, 3019, 2923,

2858, 1618, 1488, 1301, 839, 749 cm^{-1} ; ^1H NMR (400 MHz, CDCl_3): δ 8.93 (d, $J = 3.1$ Hz, 1H), 8.22 (s, 1H), 8.17 (d, $J = 8.3$ Hz, 1H), 7.87 (d, $J = 8.4$ Hz, 1H), 7.68 (dd, $J = 8.4$ Hz, 1.6 Hz, 1H), 7.40 (dd, $J = 8.2$ Hz, 4.2 Hz, 1H), 7.24 (dd, $J = 7.6$ Hz, 1.5 Hz, 1H), 7.20 (td, $J = 7.9$ Hz, 1.5 Hz, 1H), 6.87 (td, $J = 7.4$ Hz, 1.0 Hz, 1H), 6.80 (dd, $J = 8.0$ Hz, 0.8 Hz, 1H), 3.73 (bs, 2H); ^{13}C NMR (100 MHz, CDCl_3): δ 150.8, 148.5, 143.7, 141.2, 135.9, 130.7, 129.1, 129.0, 128.4, 128.3, 127.3, 126.6, 121.2, 118.9, 115.9; HRMS (ESI): calcd. for $\text{C}_{15}\text{H}_{12}\text{N}_2\text{H}^+$ 221.1073, found 221.1073.

4.11. 2-(Quinolin-8-yl)aniline (**3g**)

Following methods A and B; the crude was purified by silica gel column chromatography (pet. ether/EtOAc, 9:1 v/v) and concentration of the relevant fractions [$R_f = 0.30$ (pet. ether/EtOAc, 7:3 v/v)] gave the title compound **3g** as an off-white solid (method A: 45%; method B: 87%), mp 103–105 °C (lit [27], 100–102 °C). IR (ATR): ν_{max} 3424, 3330, 3206, 3026, 1615, 1491, 793, 743 cm^{-1} ; ^1H NMR (400 MHz, CDCl_3): δ 8.93 (dd, $J = 4.1$ Hz, 1.8 Hz, 1H), 8.19 (dd, $J = 8.3$ Hz, 1.9 Hz, 1H), 7.83 (dd, $J = 8.1$ Hz, 1.5 Hz, 1H), 7.70 (dd, $J = 7.1$ Hz, 1.5 Hz, 1H), 7.62–7.58 (m, 1H), 7.39 (dd, $J = 8.3$ Hz, 4.2 Hz, 1H), 7.25–7.21 (m, 2H), 6.90 (td, $J = 7.5$ Hz, 1.1 Hz, 1H), 6.85–6.82 (m, 1H), 3.67 (bs, 2H); ^{13}C NMR (100 MHz, CDCl_3): δ 150.6, 146.2, 144.8, 139.4, 136.7, 131.7, 131.6, 128.9, 127.9, 126.8, 121.1, 118.8, 116.4. In accordance with previously reported data [27].

4.12. 2-(3-Methoxyquinolin-5-yl)aniline (**3h**)

Following methods A and B; the crude was purified by silica gel column chromatography (pet. ether/EtOAc, 1:1 v/v) followed by alumina gel column chromatography (CH_2Cl_2 /pet. ether, 8:2 v/v) and concentration of the relevant fractions [$R_f = 0.33$ (CH_2Cl_2 /pet. ether, 8:2 v/v)] gave the title compound **3h** as an orange solid (method A: 88%; method B: 34%) along with recovered starting material (**1h**) (method B: 18%), mp 142–144 °C. IR (ATR): ν_{max} 3059, 3018, 2957, 2933, 2857, 1604, 1249, 819 cm^{-1} ; ^1H NMR (400 MHz, CDCl_3): δ 8.68 (d, $J = 2.9$ Hz, 1H), 8.11–8.08 (m, 1H), 7.62 (dd, $J = 8.4$ Hz, 7.1 Hz, 1H), 7.49 (dd, $J = 7.0$ Hz, 1.2 Hz, 1H), 7.27 (ddd, $J = 7.9$ Hz, 7.5 Hz, 1.6 Hz, 1H), 7.21 (d, $J = 2.8$ Hz, 1H), 7.14 (dd, $J = 7.5$ Hz, 1.5 Hz, 1H), 6.88 (dt, $J = 7.4$ Hz, 1.1 Hz, 1H), 6.84 (dd, $J = 8.0$ Hz, 0.8 Hz, 1H), 3.79 (s, 3H), 3.58 (bs, 2H); ^{13}C NMR (100 MHz, CDCl_3): δ 153.4, 144.3, 143.6, 136.2, 131.3, 129.3, 128.9, 128.8, 127.6, 126.8, 124.6, 118.5, 115.6, 111.4, 55.6; HRMS (ESI): calcd. for $\text{C}_{16}\text{H}_{15}\text{N}_2\text{OH}^+$ 251.1179, found 251.1188.

4.13. Method C: general method for palladium-initiated intramolecular C–H activation/C–N bond formation

The appropriate biaryl (**3a–h**) (0.23 mmol) in acetic acid (0.8 mL) was added to a premixed solution of $\text{PdCl}_2(\text{dppf})$ (33.6 mg, 0.046 mmol), 1,3-bis(2,4,6-trimethylphenyl)-imidazolium (IMes) (3.5 mg, 0.011 mmol), H_2O_2 (35 wt%, 5.6 μL , 0.067 mmol) and acetic acid (0.2 mL). The reaction mixture was placed in a sealed reactor tube and immersed into the cavity of the microwave oven and heated at 118 °C until completion as indicated by TLC. The reaction mixture was then transferred to a 25 mL round bottom flask with the aid of EtOAc/ CHCl_3 and the volatiles were removed under reduced pressure. The reaction mixture was evaporated onto celite and purified by silica gel column chromatography, with the chromatographic technique and eluent gradient as indicated.

4.14. 5H-Indolo[3,2-c]quinoline (**4b**)

Following method C; the crude was purified by silica gel column chromatography (CH_2Cl_2 /EtOAc 8:2 \rightarrow 6:4 v/v) to give the title compound **4b** ($R_f = 0.25$ (CH_2Cl_2 /EtOAc, 1:1 v/v)) as an off-white

solid (73%), mp 333–336 °C (lit [7a], 340–341 °C). IR (NaCl): λ_{max} 3060, 2958, 2854, 1682, 1582, 1515, 1493 cm^{-1} ; ^1H NMR (400 MHz, $\text{DMSO}-d_6$) δ 12.71 (bs, 1H), 9.59 (s, 1H), 8.52 (dd, $J = 7.9$ Hz, 1.1 Hz, 1H), 8.32 (d, $J = 7.9$ Hz, 1H), 8.13 (dd, $J = 8.0$ Hz, 1.1 Hz, 1H), 7.77–7.67 (m, 3H), 7.52–7.48 (m, 1H), 7.36–7.33 (m, 1H); ^{13}C NMR (100 MHz, $\text{DMSO}-d_6$) δ 145.4, 144.8, 139.7, 138.7, 129.4, 128.0, 125.7, 125.5, 122.1, 121.8, 120.6, 120.1, 117.1, 114.3, 111.8. In accordance with previously reported data [7a].

4.15. 11H-Pyrido[3,2-a]carbazole (**4e**)

Following method C; the crude was purified by silica gel column chromatography (CH_2Cl_2 /EtOAc, 8:2 + 5% Et_3N v/v) and concentration of the relevant fractions [$R_f = 0.06$ (pet. ether/EtOAc, 6:4 v/v)] gave the title compound **4e** as an off-white solid (65%) along with recovered starting material (**3e**) (12%), mp 135–139 °C. IR (NaCl): λ_{max} 3133, 3075, 2923, 2852, 1731, 1574, 1372, 808, 776 cm^{-1} ; ^1H NMR (400 MHz, $\text{DMSO}-d_6$): δ 12.48 (bs, 1H), 8.94 (ddd, $J = 8.3$ Hz, 1.6 Hz, 0.6 Hz, 1H), 8.91 (dd, $J = 4.3$ Hz, 1.7 Hz, 1H), 8.46 (d, $J = 8.7$ Hz, 1H), 8.22 (d, $J = 7.8$ Hz, 1H), 7.74 (dd, $J = 8.7$ Hz, 0.5 Hz, 1H), 7.68–7.63 (m, 2H), 7.46–7.42 (m, 1H), 7.29–7.25 (m, 1H); ^{13}C NMR (100 MHz, $\text{DMSO}-d_6$): δ 148.9, 147.2, 139.1, 134.6, 130.1, 124.9, 122.9, 122.7, 120.5, 119.9, 119.5, 117.3, 116.4, 111.5. In accordance with previously reported data [24].

4.16. 11H-Pyrido[2,3-a]carbazole (**4f**)

Following method C; the crude was purified by silica gel column chromatography (pet. ether/EtOAc, 1:1 + 0.2% Et_3N \rightarrow 2/8 v/v) and concentration of the relevant fractions [$R_f = 0.27$ (pet. ether/ CH_2Cl_2 , 1:1 v/v)] gave the title compound **4f** as pale yellow crystals (25%), mp 165–167 °C (lit [14], 164–165 °C). IR (ATR): ν_{max} 3263, 3043, 2923, 2854, 1523, 1369, 820, 734 cm^{-1} ; ^1H NMR (400 MHz, CDCl_3): δ 10.20 (bs, 1H), 8.92 (dd, $J = 4.4$ Hz, 1.5 Hz, 1H), 8.35 (dd, $J = 8.3$ Hz, 1.5 Hz, 1H), 8.24 (d, $J = 8.5$ Hz, 1H), 8.19–8.17 (m, 1H), 7.62–7.60 (m, 2H), 7.51–7.47 (m, 2H), 7.35–7.31 (m, 1H); ^{13}C NMR (100 MHz, CDCl_3): δ 147.8, 139.2, 137.4, 136.8, 134.9, 127.3, 125.9, 123.8, 121.7, 120.8, 120.5, 120.4, 120.2, 118.8, 111.8. In accordance with previously reported data [14].

4.17. 7H-Pyrido[3,2-c]carbazole (**4g**)

Following method C; the crude was purified by silica gel column chromatography (pet. ether/EtOAc, 1:1 + 0.2% Et_3N v/v) and concentration of the relevant fractions [$R_f = 0.06$ (pet. ether/EtOAc, 6:4 v/v)] gave the title compound **4g** as a pale yellow solid (29%), mp 150–152 °C (lit [15], 173–174 °C). IR (ATR): ν_{max} 3207, 2976, 2919, 2850, 2740, 2605, 2499 cm^{-1} ; ^1H NMR (400 MHz, $\text{DMSO}-d_6$): δ 11.92 (bs, 1H), 9.02 (dd, $J = 4.4$ Hz, 1.8 Hz, 1H), 8.90–8.88 (m, 1H), 8.46 (dd, $J = 8.1$ Hz, 1.4 Hz, 1H), 7.92 (d, $J = 8.8$ Hz, 1H), 7.84 (d, $J = 8.8$ Hz, 1H), 7.66–7.64 (m, 1H), 7.49 (dd, $J = 8.0$ Hz, 4.3 Hz, 1H), 7.46–7.42 (m, 1H), 7.33–7.29 (m, 1H); ^{13}C NMR (100 MHz, $\text{DMSO}-d_6$): δ 149.8, 145.3, 139.6, 138.5, 136.5, 126.0, 124.5, 123.1, 122.9, 122.8, 119.7, 118.3, 115.3, 114.2, 111.4.

4.18. N-(2-(Quinolin-2-yl)phenyl)acetamide (**5a**)

Following method C; the crude was purified by silica gel column chromatography (pet. ether/EtOAc, 9:1 \rightarrow 7:3 v/v) and concentration of the relevant fractions [$R_f = 0.24$ (pet. ether/EtOAc, 7:3 v/v)] gave the title compound **5a** as orange crystals (55%), mp 124–125 °C. IR (NaCl): ν_{max} cm^{-1} ; ^1H NMR (400 MHz, CDCl_3): δ 12.97 (bs, 1H), 8.65 (d, $J = 8.2$ Hz, 1H), 8.28 (d, $J = 8.7$ Hz, 1H), 8.06–8.04 (m, 1H), 7.89 (d, $J = 8.7$ Hz, 1H), 7.86 (dd, $J = 8.2$ Hz, 1.0 Hz, 1H), 7.83 (dd, $J = 7.9$ Hz, 1.5 Hz, 1H), 7.80–7.76 (m, 1H),

7.48–7.43 (m, 1H), 7.20 (td, $J = 7.9$ Hz, 1.2 Hz, 1H), 2.26 (s, 3H); ^{13}C NMR (100 MHz, CDCl_3): δ 168.8, 158.2, 146.2, 138.6, 137.7, 130.7, 130.5, 129.4, 128.4, 127.8, 127.1, 126.6, 124.9, 123.4, 121.8, 120.9, 25.5; HRMS (ESI): calcd. for $\text{C}_{17}\text{H}_{14}\text{N}_2\text{OH}^+$ 263.1179, found 263.1182.

4.19. *N*-(2-(Quinolin-4-yl)phenyl)acetamide (**5c**)

Following method C; the crude was purified by silica gel column chromatography (pet. ether/EtOAc, 6:4 \rightarrow 3:7 v/v) and concentration of the relevant fractions [$R_f = 0.44$ (pet. ether/EtOAc, 3:7 v/v)] gave the title compound **5c** as a dark yellow solid (54%), mp 183–185 °C. IR (NaCl): ν_{max} 3253, 3033, 2925, 2853, 1685, 1526, 1295, 850 cm^{-1} ; ^1H NMR (400 MHz, $\text{DMSO}-d_6$): δ 9.08 (bs, 1H), 8.95 (d, $J = 4.4$ Hz, 1H), 8.09–8.07 (m, 1H), 7.78–7.74 (m, 1H), 7.68 (d, $J = 8.0$ Hz, 1H), 7.52–7.49 (m, 3H), 7.38 (d, $J = 4.4$ Hz, 1H), 7.35–7.33 (m, 2H), 1.64 (s, 3H); ^{13}C NMR (100 MHz, $\text{DMSO}-d_6$): δ 168.5, 150.1, 148.0, 145.0, 135.8, 131.4, 130.7, 129.4, 129.2, 128.8, 126.4, 126.3, 126.2, 125.6, 125.2, 122.3, 22.3; HRMS (ESI): calcd. for $\text{C}_{17}\text{H}_{14}\text{N}_2\text{OH}^+$ 263.1179, found 263.1187.

4.20. *N*-(2-(Quinolin-7-yl)phenyl)acetamide (**5f**)

Following method C; the crude was purified by silica gel column chromatography (pet. ether/EtOAc, 1:1 + 0.2% Et_3N v/v) and concentration of the relevant fractions [$R_f = 0.16$ (pet. ether/EtOAc, 8:2 v/v)] gave the title compound **5f** as a red oil (61%). IR (NaCl): ν_{max} 3418, 3249, 3051, 2966, 2924, 2852, 1676, 1526, 1301, 840, 758 cm^{-1} ; ^1H NMR (400 MHz, $\text{CD}_3\text{OD}/\text{CDCl}_3$): δ 8.85 (d, $J = 3.3$ Hz, 1H), 8.36 (d, $J = 8.2$ Hz, 1H), 8.04 (s, 1H), 7.97 (d, $J = 8.5$ Hz, 1H), 7.63 (d, $J = 8.4$ Hz, 1H), 7.55–7.53 (m, 2H), 7.48–7.35 (m, 3H), 1.94 (s, 3H); ^{13}C NMR (100 MHz, $\text{CD}_3\text{OD}/\text{CDCl}_3$): δ 172.1, 151.2, 148.4, 142.4, 138.0, 137.6, 135.3, 131.5, 129.5, 129.2, 128.9, 128.7, 128.5, 128.0, 127.7, 122.4, 22.9; HRMS (ESI): calcd. for $\text{C}_{17}\text{H}_{14}\text{N}_2\text{OH}^+$ 263.1179, found 263.1181.

4.21. *N*-(2-(Quinolin-8-yl)phenyl)acetamide (**5g**)

Following method C; the crude was purified by silica gel column chromatography (pet. ether/EtOAc, 9:1 \rightarrow 4:6 + 1% Et_3N) and concentration of the relevant fractions [$R_f = 0.21$ (pet. ether/EtOAc, 1:1 v/v)] gave the title compound **5g** as dark yellow crystals (69%), mp 128–130 °C. IR (ATR): ν_{max} 3247, 3195, 3059, 3026, 2926, 2854, 1678, 1522, 1439, 1295, 789, 748 cm^{-1} ; ^1H NMR (400 MHz, CDCl_3): δ 8.97 (dd, $J = 3.9$ Hz, 1.4 Hz, 1H), 8.48 (bs, 1H), 8.31 (dd, $J = 8.2$ Hz, 1.3 Hz, 1H), 8.00 (d, $J = 8.1$ Hz, 1H), 7.92 (dd, $J = 7.9$ Hz, 1.3 Hz, 1H), 7.74–7.66 (m, 2H), 7.52–7.45 (m, 2H), 7.35 (dd, $J = 7.7$ Hz, 1.3 Hz, 1H), 7.29–7.25 (m, 1H), 1.77 (s, 3H); ^{13}C NMR (100 MHz, CDCl_3): δ 168.3, 150.7, 145.8, 138.8, 137.7, 135.7, 133.1, 132.9, 131.9, 128.9, 128.6, 128.6, 127.2, 125.3, 124.4, 121.4, 24.4; HRMS (ESI): calcd. for $\text{C}_{17}\text{H}_{14}\text{N}_2\text{OH}^+$ 263.1179, found 263.1183.

4.22. 7*H*-Pyrido[4,3,2-*gh*]phenanthridine (**6d**)

Following method C; the crude was purified by silica gel column chromatography (EtOH/MeOH, 100:0 \rightarrow 8:2 v/v) and concentration of the relevant fractions [$R_f = 0.19$ (EtOH)] gave the title compound **6d** as a yellow gel (73%). IR (NaCl): ν_{max} 3274, 3167, 3112, 3049, 2919, 2851, 2762, 1614, 1576, 1460, 669 cm^{-1} ; ^1H NMR (400 MHz, $\text{DMSO}-d_6$): δ 8.33 (dd, $J = 8.2$ Hz, 0.8 Hz, 1H), 8.27 (d, $J = 6.6$ Hz, 1H), 8.16 (d, $J = 7.8$ Hz, 1H), 7.96 (t, $J = 8.0$ Hz, 1H), 7.66 (dd, $J = 8.4$ Hz, 0.6 Hz, 1H), 7.59–7.55 (m, 1H), 6.78–6.76 (m, 1H); ^{13}C NMR (100 MHz, $\text{DMSO}-d_6$): δ 149.2, 143.3, 141.1, 135.5, 134.1, 131.6, 130.9, 124.9, 123.8, 120.4, 118.1, 117.2, 115.9, 115.0, 99.7; HRMS (ESI): calcd. for $\text{C}_{15}\text{H}_{10}\text{N}_2\text{H}^+$ 219.0917, found 219.0917.

4.23. 6-Methoxy-7*H*-pyrido[4,3,2-*gh*]phenanthridine (**6h**)

Following method C; the crude was purified by silica gel column chromatography ($\text{CH}_2\text{Cl}_2/\text{EtOAc}/\text{EtOH}$, 1:1:0 \rightarrow 1:0:1 \rightarrow 0:0:1 v/v) followed by a second purification by silica gel ($\text{CH}_2\text{Cl}_2/\text{EtOH}$, 7:3 \rightarrow 1:1 v/v) and concentration of the relevant fractions [$R_f = 0.33$ ($\text{CH}_2\text{Cl}_2/\text{EtOH}$, 7:3 v/v)] gave the title compound **6h** as a bright yellow gel (39%). IR (ATR): ν_{max} 2958, 2926, 2860, 1609, 1464, 1278, 764 cm^{-1} ; ^1H NMR (400 MHz, $\text{DMSO}-d_6$): δ 8.42 (bs, 1H), 8.30 (dd, $J = 8.4$ Hz, 1.0 Hz, 1H), 8.08 (d, $J = 7.7$ Hz, 1H), 7.88 (t, $J = 8.0$ Hz, 1H), 7.80 (dd, $J = 8.2$ Hz, 0.8 Hz, 1H), 7.71 (d, $J = 8.4$ Hz, 1H), 7.56–7.52 (m, 1H), 7.38–7.34 (m, 1H), 4.07 (s, 3H); ^{13}C NMR (100 MHz, $\text{DMSO}-d_6$): δ 140.2, 138.3, 135.5, 132.8, 131.0, 130.8, 127.0 (2C), 125.2, 123.6, 120.7, 118.8, 116.5, 115.7, 113.8, 57.8; HRMS (ESI): calcd. for $\text{C}_{16}\text{H}_{13}\text{N}_2\text{OH}^+$ 249.1028, found 249.1029.

4.24. *N*-(2-(Quinolin-2-yl)phenyl)pivalamide (**7a**)

Following method C, take for the solvent being pivalic acid; the crude was purified by silica gel column chromatography (pet. ether/EtOAc, 9/1 v/v) and concentration of the relevant fractions [$R_f = 0.25$ (pet. ether/EtOAc, 9:1 v/v)] gave the title compound **7a** as white crystals (65%), mp 107–108 °C (lit [28], 99–100 °C). IR (ATR): ν_{max} 3181, 2954, 2928, 2865, 1676, 1582, 1501, 1297, 1158, 829, 757 cm^{-1} ; ^1H NMR (400 MHz, CDCl_3): δ 12.28 (bs, 1H), 8.64 (dd, $J = 8.4$ Hz, 1.0 Hz, 1H), 8.28 (d, $J = 8.6$ Hz, 1H), 8.11 (d, $J = 8.5$ Hz, 1H), 7.86 (dd, $J = 8.2$ Hz, 1.1 Hz, 1H), 7.82 (d, $J = 8.8$ Hz, 1H), 7.79–7.75 (m, 1H), 7.73 (dd, $J = 7.9$ Hz, 1.5 Hz, 1H), 7.60–7.56 (m, 1H), 7.47–7.43 (m, 1H), 7.20 (td, $J = 7.8$ Hz, 1.2 Hz, 1H), 1.34 (s, 9H); ^{13}C NMR (100 MHz, CDCl_3): δ 177.7, 158.5, 146.4, 138.1, 137.8, 130.4, 130.3, 129.9, 128.4, 127.9, 126.9, 126.8, 126.7, 123.4, 122.3, 121.5, 40.2, 27.9. In accordance with previously reported data [28].

Acknowledgments

The ToppForsk program and the research program Bioactive at the University of Stavanger is gratefully acknowledged for funding. Dr. Holmelid, University of Bergen, and Dr. Johansen, UiT The Arctic University of Norway, is also thanked for recording HRMS.

Appendix A. Supplementary data

Supplementary data to this article can be found online at <https://doi.org/10.1016/j.tet.2019.04.026>.

References

- [1] E. Vitaku, D.T. Smith, J.T. Njardarson, Analysis of the structural diversity, substitution patterns, and frequency of nitrogen heterocycles among U.S. FDA approved pharmaceuticals, *J. Med. Chem.* 57 (2014) 10257–10274.
- [2] a) E.K. Davidson, J. Sperry, Natural products with heteroatom-rich ring systems, *J. Nat. Prod.* 80 (2017) 3060–3079; b) J.A. Homer, J. Sperry, Mushroom-derived indole alkaloids, *J. Nat. Prod.* 80 (2017) 2178–2187; c) J.P. Michael, Quinoline, quinazoline and acridone alkaloids, *Nat. Prod. Rep.* 25 (2008) 166–187; d) J.P. Michael, Quinoline, quinazoline and acridone alkaloids, *Nat. Prod. Rep.* 20 (2003) 476–493.
- [3] a) J.L. Pousset, M.T. Martin, A. Jossang, A. Bodo, Isocryptolepine from *cryptolepis sanguinolenta*, *Phytochemistry* 39 (1995) 735–736; b) M.H.H. Sharaf, P.L. Schiff, A.N. Tackie Jr., C.H. Phoebe, R.L. Johnson Jr., D. Minick, C.W. Andrews, R.C. Crouch, G.E. Martin, The isolation and structure determination of cryptomisine, a novel indolo[3,2-*b*]quinoline dimeric alkaloid from *cryptolepis sanguinolenta*, *J. Heterocycl. Chem.* 33 (1996) 789–797.
- [4] a) P. Aroonkit, C. Thongsornkleeb, J. Tummatom, S. Karjangsri, M. Mungthin, S. Ruchirawat, Synthesis of isocryptolepine analogues and their structure-activity relationship studies as antiplasmodial and antiproliferative agents, *Eur. J. Med. Chem.* 94 (2015) 56–62; b) N. Wang, K.J. Wicht, K. Imai, M. Wang, T.A. Ngoc, R. Kiguchi, M. Kaiser, T.J. Egan, T. Inokuchi, Synthesis, β -haematin inhibition, and *in vitro*

- antimalarial testing of isocryptolepine analogues: SAR study of indolo[3,2-*c*]quinolones with various substituents at C2, C6, and N11, *Bioorg. Med. Chem.* 22 (2014) 2629–2642;
- c) L.R. Whittell, K.T. Batty, R.P.M. Wong, E.M. Bolitho, S.A. Fox, T.M.E. Davis, P.E. Murray, Synthesis and antimalarial evaluation of novel isocryptolepine derivatives, *Bioorg. Med. Chem.* 19 (2011) 7519–7525.
- [5] For synthesis prior to 2016 see the following three review articles; a) P.T. Parvatkar, P.S. Parameswaran, Indoloquinolines: possible biogenesis from common indole precursors and their synthesis using domino strategies, *Curr. Org. Synth.* 13 (2016) 58–72;
- b) P. Prakash, T. Parash, S.G. Tilve, Bioactivities and synthesis of indoloquinoline alkaloids: cryptolepine, isocryptolepine and neocryptolepine, *Biact. Heterocycl.* (2013) 217–234;
- c) P.T. Parvatkar, P.S. Parameswaran, S.G. Tilve, Isolation, biological activities, and synthesis of indoloquinoline alkaloids: cryptolepine, isocryptolepine, and neocryptolepine, *Curr. Org. Chem.* 15 (2011) 1036–1057.
- [6] a) A.V. Aksenov, D.A. Aksenov, G.D. Griaznov, N.A. Aksenov, L.G. Voskressensky, M. Rubin, Unexpected cyclization of 2-(2-aminophenyl)indoles with nitroalkenes to furnish indolo[3,2-*c*]quinolones, *Org. Biomol. Chem.* 16 (2018) 4325–4332;
- b) T.-Y. Zhang, C. Liu, C. Chen, J.-X. Liu, H.-Y. Xiang, W. Jiang, T.-M. Ding, S.-Y. Zhang, Copper-mediated cascade C-H/N-H annulation of indolocarboxamides with arynes: construction of tetracyclic indoloquinoline alkaloids, *Org. Lett.* 20 (2018) 220–223;
- c) A. Murugan, S. Vidyacharan, R. Ghosh, S.M. Duddu, Metal-Free regioselective dual C-H functionalization in a cascade fashion: access to isocryptolepine alkaloid analogues, *ChemistrySelect* 2 (2017) 3511–3515;
- d) A.V. Aksenov, D.A. Aksenov, N.A. Orazova, N.A. Aksenov, G.D. Griaznov, A. De Carvalho, R. Kiss, V. Mathieu, A. Kornienko, M. Rubin, One-Pot, three-component assembly of indoloquinolines: total synthesis of isocryptolepine, *J. Org. Chem.* 82 (2017) 3011–3018;
- e) P.S. Mahajan, V.T. Humne, S.D. Tanpure, S.B. Mhaske, Radical Beckmann rearrangement and its application in the formal total synthesis of antimalarial natural product isocryptolepine via C-H activation, *Org. Lett.* 18 (2016) 3450–3453;
- f) Z.-W. Hou, Z.-Y. Mao, H.-B. Zhao, Y.Y. Melcamu, X. Lu, J. Song, H.-C. Xu, Electrochemical C-H/N-H functionalization for synthesis of highly functionalized (Aza)indoles, *Angew. Chem., Int. Ed. Engl.* 55 (2016) 9168–9172;
- g) P.S. Volvoikar, S.G. Tilve, Iodine-mediated intramolecular dehydrogenative coupling: synthesis of N-Alkylindole[3,2-*c*] and -[2,3-*c*]quinoline iodides, *Org. Lett.* 18 (2016) 892–895.
- [7] a) I.T.U. Helgeland, M.O. Sydnes, A concise synthesis of isocryptolepine by C-C cross-coupling followed by a tandem C-H activation and C-N bond formation, *SynOpen* 1 (2017) 41–44;
- b) M.O. Sydnes, One-pot strategies for the synthesis of nitrogen-containing heteroaromatics, *Curr. Green Chem.* 5 (2018) 22–39.
- [8] P.E. Cockram, T.K. Smith, Active natural product scaffolds against trypanosomatid parasites: a review, *J. Nat. Prod.* 81 (2018) 2138–2154.
- [9] a) L.R. Whittell, K.T. Batty, R.P.M. Wong, E.M. Bolitho, S.A. Fox, T.M.E. Davis, P.E. Murray, Synthesis and antimalarial evaluation of novel isocryptolepine derivatives, *Bioorg. Med. Chem.* 19 (2011) 7519–7525;
- b) P. Aroonkit, C. Thongsornkleeb, J. Tummatorn, S. Karjansri, M. Mungthin, S. Ruchirawat, Synthesis of isocryptolepine analogues and their structure-activity relationship studies as antiplamodial and antiproliferative agents, *Eur. J. Med. Chem.* 94 (2015) 56–62;
- c) N. Wang, K.J. Wicht, K. Imai, M. Wang, T.A. Ngoc, R. Kiguchi, M. Kaiser, T.J. Egan, T. Inokuchi, Synthesis, β -haematin inhibition, and in vitro antimalarial testing of isocryptolepine analogues: SAR study of indolo[3,2-*c*]quinolines with various substituents at C2, C6, and N11, *Bioorg. Med. Chem.* 22 (2014) 2629–2642.
- [10] S. Hostyn, B.U.W. Maes, L. Pieters, G.L.F. Lemi re, P. Matyus, G. Hajos, R.A. Dommissie, Synthesis of the benzo- β -carboline isoneocryptolepine: the missing indoloquinoline isomer in the alkaloid series cryptolepine, neocryptolepine and isocryptolepine, *Tetrahedron* 61 (2005) 1571–1577.
- [11] T. Dhanabal, R. Sangeetha, P.S. Mohan, Heteroatom directed photoannulation: synthesis of indoloquinoline alkaloids: cryptolepine, cryptotackieine, cryptosanguinentine, and their methyl derivatives, *Tetrahedron* 62 (2006) 6258–6263.
- [12] F.B. Mallory, C.W. Mallory, Photocyclization of stilbenes and related molecules, *Org. React.* 30 (1981) 1–456.
- [13] E. Lescot, G. Muzard, J. Markovits, J. Belleney, B.P. Roques, J.-B. Le Pecq, Synthesis of 11*H*-pyridocarbazoles and derivatives. Comparison of their DNA binding and antitumor activity with those of 6*H*- and 7*H*-pyridocarbazoles, *J. Med. Chem.* 29 (1986) 1731–1737.
- [14] F. Wu, J. Hardesty, R.P. Thummel, Preparation and study of tautomers derived from 2-(2'-pyridyl)indole and related compounds, *J. Org. Chem.* 63 (1998) 4055–4061.
- [15] M. Kulka, R.H.F. Manske, The synthesis of pyridocarbazoles, *Can. J. Chem.* 30 (1952) 711–719.
- [16] H.E. Jansen, J.P. Wibaut, Some reactions of 2-bromo- and 3-bromoquinolines, *Recl. Trav. Chim. Pays-Bas* 56 (1937) 709–713.
- [17] K.R. Brower, W.P. Samuels, J.W. Way, E.D. Amstutz, Halogen reactivities. III. Kinetic study of displacement reactions of haloquinolines with piperidine, *J. Org. Chem.* 18 (1953) 1648–1654.
- [18] C.A. Coulson, H.C. Longuet-Higgins, The electronic structure of conjugated systems II. Unsaturated hydrocarbons and their hetero-derivatives, *Proc. Roy. Soc. Lond.* 192 (1947) 16–32.
- [19] J. Almond-Thynne, D.C. Blakemore, D.C. Pryde, A.C. Spivey, Site-selective Suzuki-Miyaura coupling of heteroaryl halides – understanding the trends for pharmaceutically important classes, *Chem. Sci.* 8 (2017) 40–61.
- [20] S. Schr oter, C. Stock, T. Bach, Regioselective cross-coupling reactions of multiple halogenated nitrogen-, oxygen-, and sulfur-containing heterocycles, *Tetrahedron* 61 (2005) 2245–2267.
- [21] S.T. Handy, Y. Zhang, A simple guide for predicting regioselectivity in the coupling of polyheteroaromatics, *Chem. Commun.* (2006) 299–301.
- [22] H.-R. Bj orsvik, V. Elumalai, Synthesis of the carbazole scaffold directly from 2-aminobiphenyl by means of tandem C-H activation and C-N bond formation, *Eur. J. Org. Chem.* (2016) 5474–5479.
- [23] a) X.-J. Wang, Q. Yang, F. Liu, Q.-D. You, Microwave-assisted synthesis of amide under solvent-free conditions, *Synth. Commun.* 38 (2008) 1028–1035;
- b) M. Chakraborty, V. Umrigar, P.A. Parikh, Microwave irradiated acetylation of *p*-anisidine: a step towards green chemistry, *Int. J. Chem. React. Eng.* 6 (2008) 1–12.
- [24] M.A. Ciufolini, N.E. Byrne, The total synthesis of cystodytins, *J. Am. Chem. Soc.* 113 (1991) 8016–8024.
- [25] E. Landagaray, M. Ettaoussi, M. Rami, J.A. Boutin, D.-H. Caignard, P. Delagrangre, P. Melnyk, P. Berthelot, S. Yous, New quinolinic derivatives as melatonergic ligands: synthesis and pharmacological evaluation, *Eur. J. Med. Chem.* 127 (2017) 621–631.
- [26] J. Wippich, N. Truchan, T. Bach, Rhodium-catalyzed *N*-*tert*-Butyloxycarbonyl (Boc) amination by directed C-H bond activation, *Adv. Synth. Catal.* 358 (2016) 2083–2087.
- [27] T. Chatterjee, M.G. Choi, J. Kim, S.-K. Chang, E.J. Cho, Visible-light-induced regioselective synthesis of polyheteroaromatic compounds, *Chem. Commun.* 52 (2016) 4203–4206.
- [28] D. Csanyi, G. Timari, G. Hajos, An alternative synthesis of quindoline and one of its closely related derivatives, *Synth. Commun.* 29 (1999) 3959–3969.

Article

Synthesis and Evaluation of the Tetracyclic Ring-System of Isocryptolepine and Regioisomers for Antimalarial, Antiproliferative and Antimicrobial Activities

Katja S. Håheim¹, Emil Lindbäck¹, Kah Ni Tan² , Marte Albrigtsen³, Ida T. Urdal Helgeland¹, Clémence Lauga¹, Théodora Matringe¹ , Emily K. Kennedy², Jeanette H. Andersen³ , Vicky M. Avery^{2,4,5} and Magne O. Sydnes^{1,*} 

- ¹ Department of Chemistry, Bioscience and Environmental Engineering, University of Stavanger, NO-4036 Stavanger, Norway; katja.s.haheim@uis.no (K.S.H.); emil.lindback@uis.no (E.L.); ida.t.helgeland@uis.no (I.T.U.H.); clemence.lauga08@gmail.com (C.L.); theodora.matringe@gmail.com (T.M.)
- ² Discovery Biology, Griffith Institute for Drug Discovery, Griffith University, Don Young Road, Nathan, QLD 4111, Australia; kahni.tan@griffith.edu.au (K.N.T.); emily.kennedy@griffith.edu.au (E.K.K.); v.avery@griffith.edu.au (V.M.A.)
- ³ The Norwegian College of Fishery Science, Marbio, UiT—The Arctic University of Norway, Breivika, NO-9037 Tromsø, Norway; marte.albrigtsen@uit.no (M.A.); jeanette.h.andersen@uit.no (J.H.A.)
- ⁴ CRC for Cancer Therapeutics, Griffith University, Nathan, QLD 4111, Australia
- ⁵ School of Environment & Science, Nathan, Griffith University, Nathan, QLD 4111, Australia
- * Correspondence: magne.o.sydnes@uis.no



Citation: Håheim, K.S.; Lindbäck, E.; Tan, K.N.; Albrigtsen, M.; Urdal Helgeland, I.T.; Lauga, C.; Matringe, T.; Kennedy, E.K.; Andersen, J.H.; Avery, V.M.; et al. Synthesis and Evaluation of the Tetracyclic Ring-System of Isocryptolepine and Regioisomers for Antimalarial, Antiproliferative and Antimicrobial Activities. *Molecules* **2021**, *26*, 3268. <https://doi.org/10.3390/molecules26113268>

Academic Editor: Valeria Patricia Sülsen

Received: 28 April 2021
Accepted: 26 May 2021
Published: 30 May 2021

Publisher's Note: MDPI stays neutral with regard to jurisdictional claims in published maps and institutional affiliations.



Copyright: © 2021 by the authors. Licensee MDPI, Basel, Switzerland. This article is an open access article distributed under the terms and conditions of the Creative Commons Attribution (CC BY) license (<https://creativecommons.org/licenses/by/4.0/>).

Abstract: A series of novel quinoline-based tetracyclic ring-systems were synthesized and evaluated in vitro for their antiparasmodial, antiproliferative and antimicrobial activities. The novel hydroiodide salts **10** and **21** showed the most promising antiparasmodial inhibition, with compound **10** displaying higher selectivity than the employed standards. The antiproliferative assay revealed novel pyridophenanthridine **4b** to be significantly more active against human prostate cancer (IC₅₀ = 24 nM) than Puromycin (IC₅₀ = 270 nM) and Doxorubicin (IC₅₀ = 830 nM), which are used for clinical treatment. Pyridocarbazoles **9** was also moderately effective against all the employed cancer cell lines and moreover showed excellent biofilm inhibition (**9a**: MBIC = 100 μM; **9b**: MBIC = 100 μM).

Keywords: indoloquinoline; antiparasmodial activity; antiproliferative activity; antimicrobial activity; biofilm inhibition

1. Introduction

Malaria and cancer are two major health issues affecting millions of lives annually. Malaria is a parasitic blood disease caused by protozoans of the *Plasmodium* genus. Although five *Plasmodium* strains are known to infect humans, namely *P. falciparum*, *P. vivax*, *P. ovale*, *P. knowlesi* and *P. malariae*, infections by *P. falciparum* are responsible for the majority of malaria-related deaths [1,2]. The World Health Organization (WHO) estimated the number of malaria cases to be 229 million in 2019, claiming approximately 409,000 lives [1], despite considerable global efforts to combat the disease. A major obstacle in the battle against malaria has been the rapid appearance and spread of resistant strains across endemic areas [3]. An excess of 90% of all malaria incidents occur in sub-Saharan Africa [1], a region sorely dependent on the availability of affordable treatments. Originally, malaria-endemic regions were primarily limited to the immediate areas surrounding the tropics. The increasing surface air temperatures as a consequence of global warming is predicted to change this, leaving also temperate climates susceptible to the disease, and with it, a larger part of the human population [4]. Following the widespread appearance of chloroquine (CQ)-resistant strains of *P. falciparum*, artemisinin-based therapies have been the gold standard of malaria treatment [5]. However, in 2008, the first reports of

artemisinin-based resistance were observed in Cambodia [6] and ten years later, over 30 independent cases had been documented throughout southeast Asia [7]. Therefore, the development of novel and affordable treatments remains of paramount importance.

Contrary to malaria, which is an infectious disease, cancer is a noncommunicable disease, ranking as the second leading cause of death globally, responsible for approximately 1 in 6 deaths. Estimates from WHO put the number of cancer cases in 2018 at 18.1 million, accompanied by 9.6 million fatalities [8]. The five most diagnosed cancers are lung, breast, colorectal, prostate and stomach. A variety of anti-cancer therapies are currently available, however, those treated suffer from the unwanted side effect of being highly immunosuppressed. Patients suffering from a compromised immune system following cancer treatments are therefore more likely to contract nosocomial infections [9], such as infection caused by drug-resistant *Staphylococcus aureus*, increasing the overall burden of nosocomial infectious diseases [10]. This is further complicated by the increased likelihood of formations of multidrug-resistant biofilms, which are notoriously hard to treat [11,12]. Bacterial infections are also known to be a cause of cancer on their own, and according to the WHO, roughly 13% of all cancers globally occur as a result of chronic infections [8]. Additionally, research in recent years has started to uncover a direct link between the formation of microbial biofilms in the body and the growth of certain cancers [13–15]. The availability of anticancer drugs with the dual capability of inhibiting biofilm growth is severely limited, making the development of such drugs greatly needed.

Natural products have proven to be an invaluable source of lead compounds for medicinal research in the past and present due to their wide array of structural diversity [16–18]. As of 2020, roughly 40% of all Food and Drugs Administration (FDA) approved drugs have natural origins [19], further demonstrating the importance of natural products in drug discovery. Accordingly, discovery and characterization of natural products and their semi-synthetic derivatives remain pivotal in the search for novel drug candidates [20]. The quinoline core represents a versatile structural motif, possessing applications in the fields of material science, the dye industry and moreover constitute an important building block in the design of pharmaceutical compounds [21]. In particular, due to the presence of the quinoline skeleton in numerous natural products displaying a vast array of biological activities, quinoline-based natural products and their derivatives are attractive medicinal targets [22–25].

Almost exclusively found in the West African climbing shrub *Cryptolepis sanguinolenta* [26,27], the indoloquinoline natural products cryptolepine (1), neocryptolepine (2), and isocryptolepine (3a) (Figure 1) represent a unique class of bioactive compounds. These alkaloids are characterized by a fused quinoline and indole moiety [28] and long before the constituents of *C. sanguinolenta* were identified, the extracts were used in herbal remedies to treat malarial fevers among other ailments [29]. The major bioactive component of the shrub was eventually determined to be cryptolepine (1), which has subsequently received the most attention in the literature of the three regioisomeric indoloquinolines 1, 2, and 3a. A host of biological properties have been observed in cryptolepine (1) assays, such as antiplasmodial, antimalarial [30–35], anti-inflammatory [33], antifungal [36–38], antimicrobial [39–42], antiproliferative [43–46] and antiviral [40]. The linearly arranged planar structure of cryptolepine (1) is believed to be related to its high level of undesired cytotoxicity, resulting in its ability to non-specifically intercalate into DNA, inhibiting topoisomerase II [44,47–49]. Neocryptolepine (2) and isocryptolepine (3a) have also been demonstrated to possess similar biological profiles, although inferior to cryptolepine (1) [28,50]. Despite the lower potency, both neocryptolepine (2) and isocryptolepine (3a) were revealed to be significantly less cytotoxic than cryptolepine (1), allowing for the possibility of their derivatives to be developed into new lead compounds [49,51].

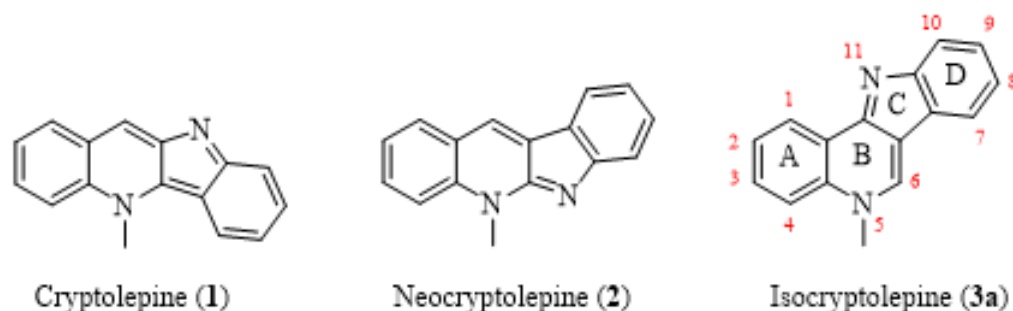


Figure 1. Structures of the major bioactive compounds isolated from *Cryptolepis Sanguinolenta*; cryptolepine (1), neocryptolepine (2) and isocryptolepine (3a).

The biological activities for the core structures of *C. sanguinolenta* have been extensively studied while their regioisomers have been largely undescribed. In particular, the novel pyridophenanthridine scaffold **4a** (Figure 2) unveiled in our previous study [52], represents an interesting target for biological evaluation. The pyridophenanthridine skeleton may be regarded as a regioisomer to the pyridoacridines (the core structure of which is illustrated in compound **5** in Figure 2), a well-studied class of marine alkaloids most notably known for exhibiting potent antiproliferative qualities [53–57]. Similarly, to cryptolepine (1), nearly all naturally occurring pyridoacridines have been shown to act as DNA intercalating agents, resulting in cytotoxic effects in cultured tumor cells [54,55,58]. They also possess the ability to inhibit topoisomerase II [53,58] and further contain biological profiles such as antibacterial, antifungal, antiviral, antiparasitic and insecticidal [53,56,57,59–61]. Consequently, it is postulated that the pyridoacridines and their synthetic derivatives are pivotal for the future generation of medicinal compounds [58].

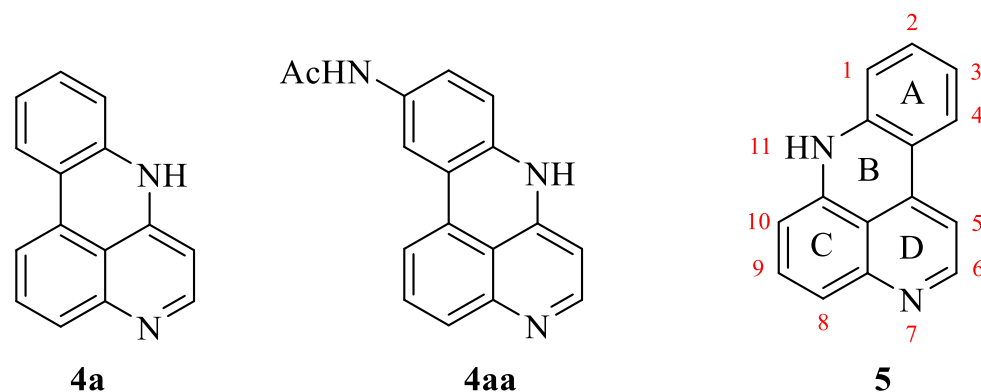


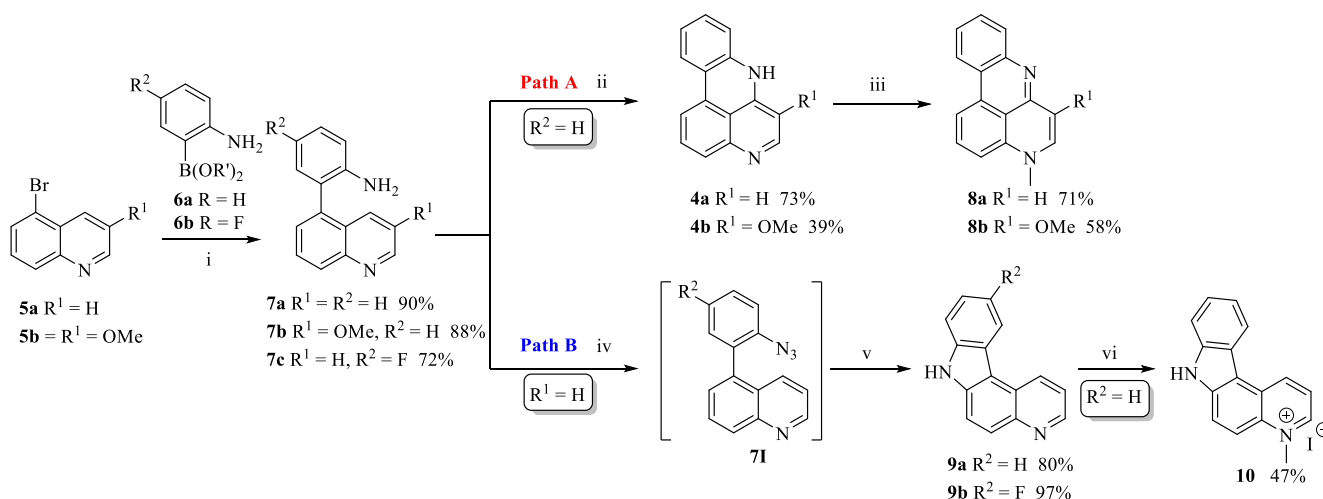
Figure 2. Structures of pyridophenanthridines **4a** and **4aa** along with pyridoacridine **5**.

Recently, we described the preparation of several isocryptolepine regioisomers and certain chemoisomers [52]. In this paper, we present modifications to our previous synthetic strategies which allowed for the realization of novel tetracyclic ring-systems (compounds **4b**, **8**, and **9**) along with the *N*-alkylation of several compounds to furnish new analogues (compounds **3b**, **3c**, **10**, and **21**). Moreover, the newly synthesized compounds, along with our existing library of natural products and analogues, were evaluated for their *in vitro* antiplasmodial activity against *Plasmodium falciparum* 3D7 parasites; cytotoxicity against normal mammalian cell line (HEK293), and three cancer cell lines (HCT116, MDA-MB-231 and PC-3). The compounds were also evaluated as antimicrobial agents against common pathogenic bacteria as well as their ability to inhibit biofilm growth.

2. Results and Discussion

2.1. Chemistry

We recently reported a concise synthesis of isocryptolepine (**3a**) and some regioisomers in which the two key synthetic steps were a Suzuki-Miyaura cross-coupling reaction followed by a palladium-catalyzed intramolecular cyclization [52,62]. The most unexpected result of our previous endeavor was the formation of a pyridophenanthridine scaffold **4a**, when biaryl **7a** was treated with palladium under our intramolecular cyclization conditions (Path A, Scheme 1). Shortly after our report, Kumar and co-workers reported the formation of compound **4a** by a palladium-catalyzed arylation technique utilizing diaryliodonium salts [63]. To the best of our knowledge, these two preparations of pyridophenanthridine **4a** remain the only descriptions in the literature. However, Beauchard and coworkers describe the accidental synthesis of the functionalized pyridophenanthridine **4aa** in 2006 (Figure 2) [64]. This was the result of attempting to synthesize isocryptolepine analogues by a microwave-induced thermal decomposition of a benzotriazole-coupled quinoline.



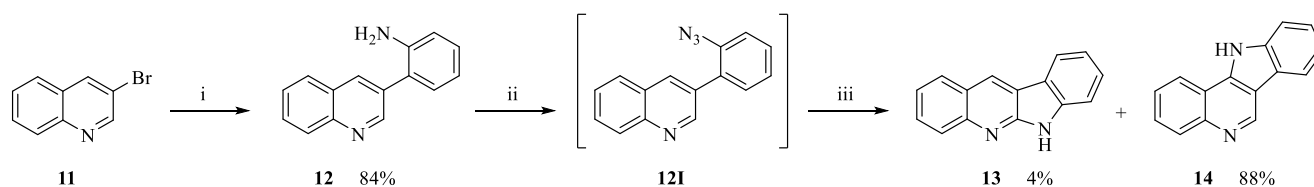
Scheme 1. Synthesis of pyridophenanthridines **8** and pyridocarbazoles **9** from a common starting material. Conditions: (i) coupling partner **6**, Cs_2CO_3 , $\text{Pd}(\text{PPh}_3)_4$ (5 mol%), $\text{DME}/\text{H}_2\text{O}$, 80°C ; Path A: (ii) PdCl_2 (dppf) (20 mol%), IMes (5 mol%), H_2O_2 (35 wt%, 29 mol%), AcOH , 118°C , MW; (iii) CH_3I , CH_3CN , reflux; Path B: (iv) 1) HCl (37%), NaNO_2 (0.4 M), 0°C , 1.5 h; 2) $\text{NaN}_3/\text{NaOAc}$, 0°C , 1 h; (v) 1,2-dichlorobenzene, 180°C , 3 h; (vi) CH_3I , CH_3CN , reflux.

Intrigued by these results, we decided to investigate further and wondered if the regioselectivity would be the same utilizing a different synthetic strategy. Drawing inspiration from Timári et al. [65] in the synthesis of isocryptolepine and further expanded on by Hostyn et al. [66] for the synthesis of isoneocryptolepine, a Suzuki-Miyaura cross-coupling reaction and nitrene insertion approach was undertaken. Standard azidation of biaryl **7a** via installation of a diazonium salt yielded the aryl azide **7I**, which upon thermal decomposition in refluxing 1,2-dichlorobenzene interestingly gave pyridocarbazole **9a** as the only product without any traces of its regioisomer **4a** (Scheme 1, Path B). Thereby, it was concluded that **4a** and **9a** can be achieved from a common starting material by following reaction pathway A and B, respectively, in Scheme 1. A fluoro-substituted analogue of compound **9a**, namely **9b**, was further possible to construct starting from boronic acid **6b**. To conclude the synthetic pathways, compounds **4** and **9a** were finally regioselectively *N*-methylated using excess iodomethane in refluxing acetonitrile [49] to realize tetracycles **8** and **10**.

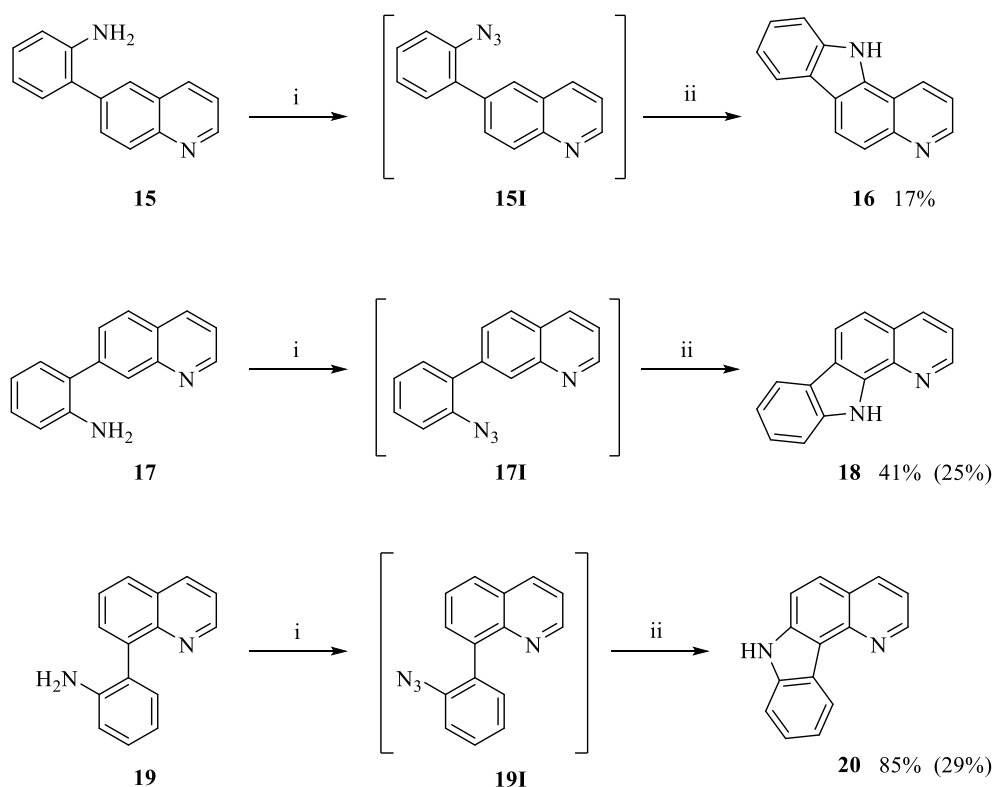
In Timári et al.'s original synthesis of isocryptolepine (**3a**) by means of a thermally induced nitrene insertion, only one regioisomeric product was observed, namely isocryptolepine precursor **14** [65]. Following the same conditions in our laboratories, the approach primarily resulted in the construction of indoloquinoline **14** but its regioisomer **13** was also formed in minor quantities (Scheme 2). Applying the nitrene insertion approach to

biaryls **15**, **17**, and **19**, we were able to significantly improve the yields of tetracycles **18** and **20** compared to our previous endeavors (Scheme 3, previous yields in brackets) [52]. Following a literature procedure, neocryptolepine (**2**) was obtained in good yield starting from its precursor **13** (Scheme 4) [67].

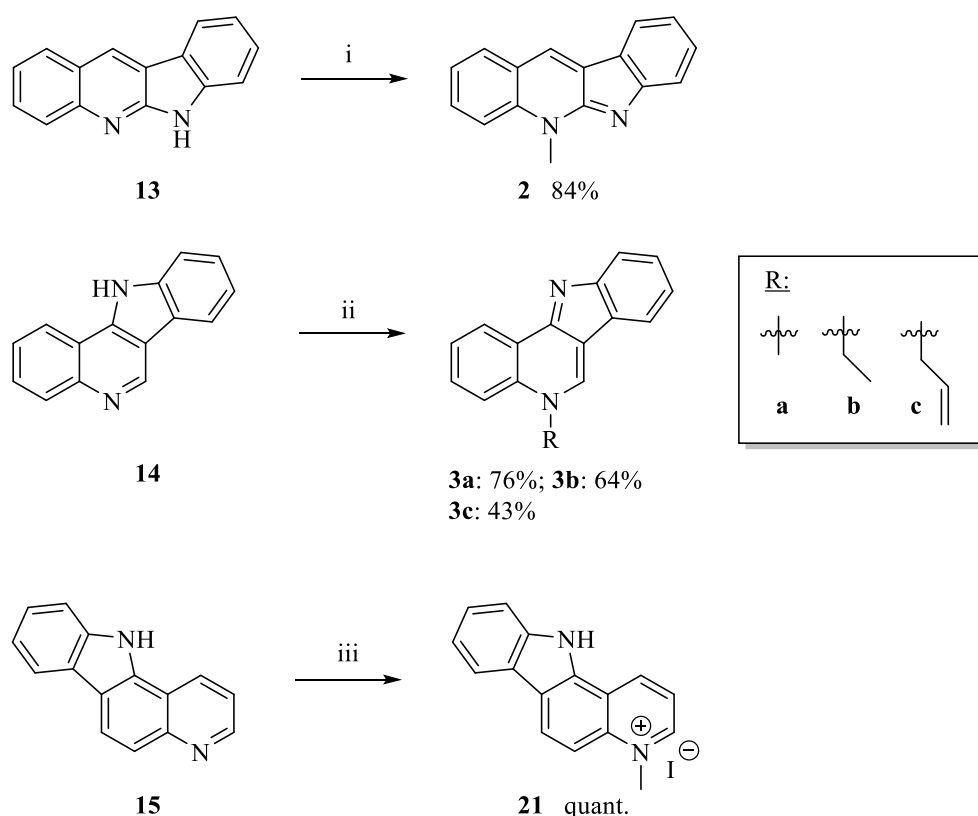
Modification of our previously reported conditions for the *N*-methylation of tetracycle **14** to furnish isocryptolepine (**3a**) [62], allowed the formation of two novel isocryptolepine analogues **3b** and **3c**, albeit in lower yields than the parent alkaloid (Scheme 4). Of the remaining tetracycles, namely compounds **16**, **18**, and **20**, only compound **16** was successfully *N*-methylated using the same conditions as reported in our previous work [62]. Efforts to explain the failure of tetracycles **18** and **20** to undergo *N*-alkylation at the most reactive ring-nitrogen, presumably the quinoline moiety, is currently under way in our laboratories.



Scheme 2. Synthesis of 6*H*-indolo[2,3-*b*]quinoline (**13**) and 11*H*-indolo[3,2-*c*]quinoline (**14**) via a Suzuki-Miyaura cross-coupling and thermally induced nitrene insertion approach. Conditions: (i) boronic acid **6a**, K_2CO_3 , $PdCl_2$ (dppf) (5 mol%), EtOH/H₂O (5:1), 60 °C [52,62]; (ii) 1) HCl (37%), $NaNO_2$ (0.4 M), 0 °C, 1.5 h; 2) $NaN_3/NaOAc$, 0 °C, 1 h; (iii) 1,2-dichlorobenzene, 180 °C, 3 h.



Scheme 3. Synthesis of 11*H*-pyrido[3,2-*a*]carbazole (**16**), 11*H*-pyrido[2,3-*c*]carbazole (**18**) and 7*H*-pyrido[3,2-*c*]carbazole (**20**) using a diazotization-azidation-nitrene insertion approach. In brackets: yields from our previous endeavors [52]. Conditions: (i) HCl (37%), $NaNO_2$ (0.4 M), 0 °C, 1.5 h; (ii) 1,2-dichlorobenzene, 180 °C, 3 h. For the synthesis of compounds **15**, **17**, and **19**, refer to our previous work [52].



Scheme 4. Regioselective *N*-alkylations to synthesize neocryptolepine (**2**), isocryptolepine (**3a**), *N*-alkyl isocryptolepine derivatives (**3b** and **3c**) and 4-methyl-11*H*-pyrido[3,2-*a*]carbazolium iodide (**21**). Conditions: (i) CH₃CN, THF, reflux, 24 h [67]; (ii) a: CH₃I, PhMe, reflux, 3 h [62]; b: CH₃CH₂I, PhMe, reflux, 3 h; c: CH₂=CHCH₂Br, PhMe, reflux, 22 h; (iii) CH₃I, CH₃CN, reflux, 20 h.

2.2. Antiplasmodial Assay

The prepared natural products and their derivatives were evaluated for their *in vitro* antiplasmodial activities against the *Plasmodium falciparum* 3D7 strain. The compounds were further tested for their *in vitro* cytotoxicity against HEK293 cells (human embryonic kidney cells) for the determination of their selectivity indices. Furthermore, to serve as positive controls for our analyses, chloroquine (CQ), dihydroartemisinin (DHA) and puromycin were employed. Results from these studies are summarized in Table 1.

The tested compounds were found to possess diverse activities against the Pf3D7 cell line. Albeit being well documented to have antiplasmodial activity in the literature, the parent alkaloid neocryptolepine (**2**) has thus far not been evaluated for *in vitro* antimalarial activity against Pf3D7 (IC₅₀ = 7249 nM), showing a lower potency compared to isocryptolepine (**3a**) (IC₅₀ = 1211 nM). Out of the two novel isocryptolepine derivatives, allyl variant **3c** showed a marginal improvement compared to the natural product (IC₅₀ = 1198 nM), while ethyl variant **3b** showed a lower activity (IC₅₀ = 1318 nM). Both derivatives were revealed to be notably more cytotoxic than the parent alkaloid **3a**.

The neocryptolepine precursor **13** was revealed to display no antiplasmodial inhibition, which is in accordance with a previous study conducted by Jonckers et al., where they highlighted the importance of the *N*-5 methyl group for activity in certain halogen-substituted indolo[3,2-*b*]quinolines [68]. The regioisomer **15** was also shown to be inactive against Pf3D7. Contrary to this, the isocryptolepine precursor **14** displayed more potent antimalarial activities (IC₅₀ = 977 nM) compared to the parent alkaloid **3a**. For the isocryptolepine precursor **14**, it has been shown through previous work that by introduction of certain basic side chains at C-9, the *in vitro* antimalarial activity against the K-1 strain of *P. falciparum* was dramatically increased compared to isocryptolepine (**3a**). The authors

argued that these observations could be attributed to the basic properties allowing the compound to experience a lower degree of hydrophobicity [69], a quality also observed for CQ [28].

Table 1. In vitro antiplasmodial activities of tetracyclic ring-systems **2–3**, **4**, **8–10**, **13–14**, **16**, **18**, **20**, and **21** against the 3D7 *P. falciparum* strain, cytotoxicity against HEK293 cells and selectivity indices.

Entry	Compound	3D7 IC ₅₀ (nM)	Cytotoxicity IC ₅₀ (nM)	SI ^a
1	Neocryptolepine (2)	7249 ± 6	>20,000	2.8
2	Isocryptolepine (3a)	1211 ± 84	2074 ± 70	1.7
3	3b	1318 ± 5	3078 ± 49	2.3
4	3c	1198 ± 32	3152 ± 40	2.6
5	4a	548 ± 3	2834 ± 92	5.2
6	4b	866 ± 2	3657 ± 2	4.2
7	8a	1698 ± 5	7410 ± 207	4.4
8	8b	1546 ± 27	5057 ± 45	3.3
9	9a	6825 ± 61	>80,000	11.7
10	9b	NT ^b	NT ^b	-
11	10	128 ± 2	NA ^c	213.9
12	13	NA ^c	NA ^c	-
13	14	977 ± 11	18460 ± 183	18.9
14	16	NA ^c	NA ^c	-
15	18	NA ^c	NA ^c	-
16	20	2414 ± 42	NA ^c	16.6
17	21	380 ± 0.5	NA ^c	105.4
18	Chloroquine	24 ± 1	>4000	165
19	DHA	1 ± 0.07	NA ^c	74
20	Puromycin	93 ± 2	3 ± 3	0.03

Data are presented as the mean ± standard deviation from two separate experiments. IC₅₀ values were calculated using non-linear dose-response curves in GraphPad Prism. ^a SI = selectivity index = cytotoxicity in HEK293/activity in 3D7; ^b NT = not tested; ^c NA = not active.

Pyridophenanthridines **4** (a: IC₅₀ = 548 nM; b: IC₅₀ = 866 nM) outperformed both neocryptolepine (**2**) and isocryptolepine (**3a**) in terms of activity and selectivity; however, it displayed an unfavorable increase in cytotoxicity. Keeping in mind the effects observed by Jonckers et al. [68] for the functionalization of the isocryptolepine precursor **14**, addition of appropriate substituents to pyridophenanthridine **4a** could potentially result in increased antiplasmodial activity. Evidently, the presence of the methoxy substituent in compound **4b** negatively impacted both the antiplasmodial activity and cytotoxicity compared to the naked pyridophenanthridine **4a**. Interestingly, the addition of an *N*-methyl group to pyridophenanthridines **4** to furnish compounds **8** (a: IC₅₀ = 1698 nM; b: IC₅₀ = 1546 nM) negatively impacts the antiplasmodial activity. For the indoloquinoline natural products, the *N*-methyl group is considered an instrumental aspect for their parasitic inhibition [28], this is evidently not the case for the pyridophenanthridines, possibly suggesting the presence of a novel mode of action against the parasitic life cycle. As this represents the first case in the literature of the antiplasmodial evaluation of a pyridophenanthridine, other functionalizations of the core scaffold should nonetheless be further researched.

The two most prominent results of our studies were the novel hydroiodide salts **10** (IC₅₀ = 128 nM) and **21** (IC₅₀ = 380 nM), where the latter showed improved selectivity compared to the standards. Their precursors **9a** and **15** showed little to no activity, highlighting the importance of the *N*-methyl functionality. These results are possibly aided by the fact that the salt structure likely promotes increased solubility in aqueous media, further increasing the biological availability of the compounds, a fact which should be carefully considered when exploring new lead compounds.

2.3. Antiproliferative Assay

All prepared samples were evaluated in vitro against a panel of three cancer cell lines, including HCT116 (human colon cancer), MDA-MB-231 (human breast adenocarcinoma)

and PC-3 (human prostate cancer) using a resazurin assay. Puromycin and Doxorubicin were employed as positive controls for the obtained IC₅₀ results, which are summarized in Table 2.

Table 2. In vitro antiproliferative activities and cytotoxicities of tetracyclic ring-systems 2–3, 4, 8–10, 13–14, 16, 18, 20 and 21 against three cancer cell lines.

Entry	Compound	HCT116 IC ₅₀ (nM)	MDA-MB-231 IC ₅₀ (nM)	PC-3 IC ₅₀ (nM)
13	Neocryptolepine (2)	6218 ± 90	10,435 ± 375	27% at 80 µM
14	Isocryptolepine (3a)	667 ± 45	695 ± 130	1821 ± 7
15	3b	742 ± 11	998 ± 300	2440 ± 94
16	3c	1243 ± 80	3064 ± 467	1296 ± 51
1	4a	721 ± 27	594 ± 140	1630 ± 173
2	4b	166 ± 16 ^a	1002 ± 297	24 ± 3 ^b
3	8a	444 ± 52	360 ± 51	2571 ± 114
4	8b	871 ± 172	814 ± 162	4539 ± 361
5	9a	20,015 ± 1665	21,540 ± 2480	17,790 ± 1640
6	9b	NT ^c	NT ^c	NT ^c
7	10	38% at 40 µM	24% at 40 µM	36% at 40 µM
8	13	NA ^d	NA ^d	NA ^d
9	14	3573 ± 309	36% at 80 µM ^e	30% at 80 µM ^f
10	16	82% at 80 µM	80% at 80 µM	NA ^d
11	18	NT ^c	NT ^c	NT ^c
12	20	17,030 ^g	16,415 ± 2305	47% at 40 µM
17	21	NA ^d	NA ^d	NA ^d
18	Puromycin	85	300	270
19	Doxorubicin	150	590	830

Data are presented as the mean ± sem (standard error of the mean) from two separate experiments. IC₅₀ values were calculated using non-linear dose-response curves in GraphPad Prism. ^a 89% metabolic activity at 40 nM; ^b 45% metabolic activity at 40 nM; ^c NT = not tested; ^d NA = not active; ^e 55% metabolic activity at 40 µM; ^f 50% metabolic activity at 40 µM; ^g 12% metabolic activity at 40 µM.

Both parent alkaloids neocryptolepine (2) and isocryptolepine (3a) performed best against the HCT116 cell line (2: 6218 nM; 3a: 667 nM) (Table 2). It is evident that isocryptolepine (3a) had an overall better performance against the tested cancer cell lines than neocryptolepine (2). The same was observed for the isocryptolepine derivatives 3b and 3c; however, the potency was less than for the parent isocryptolepine (3a). Derivatives 3b and 3c were revealed to become less potent with increasing alkyl chain length for the human colon cancer (3b: IC₅₀ = 742 nM; 3c: 1243 nM) and human breast adenocarcinoma (3b: IC₅₀ = 998 nM; 3c: 3064 nM) cell lines. Interestingly, for the human prostate cancer cell line, a different trend was observed (3b: IC₅₀ = 2440 nM; 3c: 1296 nM). The *N*-allyl group outperformed both the methyl and ethyl groups in terms of activity, suggesting that the alkene functionality is somehow important to the mechanism of cell growth inhibition. It is believed that the indoloquinolines inhibit cell growth by direct interactions with DNA, although the exact mechanism(s) remain uncertain [28,44,47,50,70].

Several of the tested compounds were found to display no activity against the panel of cancer cell lines, including novel compounds 10 and 21. Another compound which was observed to be inactive was neocryptolepine precursor 13, being inactive against all three cell lines. The isocryptolepine precursor 14 showed poor activity against all cancer cell lines and further highlights the necessity of the *N*-methyl group for cell growth inhibition.

The importance of incorporating an *N*-methyl is further demonstrated in compounds 4a and its corresponding *N*-methylated product 8a, showing an increase in activity against the HCT116 and MDA-MB-231 cell lines, favoring the inclusion of an *N*-methyl group. In the PC-3 cell lines, the pyridophenanthridines 4 showed a decrease in activity with the addition of an *N*-methyl substituent to give the corresponding compound 8. However, the assay revealed the methoxy pyridophenanthridine 4b to contain potent anticarcinogenic properties (IC₅₀ = 24 nM) against the PC-3 cell line. Compound 4b showed a 10-fold and 35-fold increase in activity compared to the positive controls Puromycin (IC₅₀ = 270 nM)

and Doxorubicin ($IC_{50} = 830$ nM), respectively. The positioning of the methoxy substituent at C-6 of the pyridophenanthridine scaffold appears to be key to the observed increase in activity, as the naked pyridophenanthridine **4a** showed only modest activity against the PC-3 cell line ($IC_{50} = 1630$ nM). A previous study by Lu and coworkers demonstrated the potential of the strategic installation of appropriate ring-substituents to obtain increased antiproliferative activity in various indolo[3,2-*b*]quinolines [71]. Similar to the observations made in this work, Lu et al. noted the potency of C-9 ester substituted indoloquinolines in their screening of several cancer cell lines [71], despite the parent neocryptolepine (**2**) displaying only minor inhibition of cell growth. The *N*-methylated pyridophenanthridine **8a** evaluated in this work was further shown to be more potent against the MDA-MB-231 ($IC_{50} = 360$ nM) cell line than Doxorubicin ($IC_{50} = 590$ nM). Being novel compounds, the mode of action of the pyridophenanthridines against proliferative cancer is naturally unknown. Thus, proceeding studies have the potential to unveil a new mode of action. The discovery of new modes of action is regarded as highly important in the field of drug discovery [72], further illustrating the potential for the novel pyridophenanthridine scaffold as a lead for subsequent development into a new anticancer therapy.

2.4. Antimicrobial and Biofilm Inhibition Assay

The prepared samples were tested for in vitro antimicrobial activity against *E. faecalis*, *E. coli*, *P. aeruginosa*, *S. aureus*, *Streptococcus agalactiae* and *S. epidermis* using gentamycin as a reference compound. The compounds were tested at 100, 75, 50, 25, 12.5, 10, 6.3, 3.1 and 1.6 μ M and the obtained minimal inhibitory concentrations (MIC) and minimal bacterial inhibition concentrations (MBIC) can be seen in Table 3. Several of the screened compounds contained no antibacterial properties against the tested panel of bacteria, including tetracycles **8a**, **10**, **13–14**, **16**, **18**, and **20–21**, while compounds **3b**, **3c**, and **21** were not tested.

Table 3. In vitro antimicrobial activities of tetracyclic ring-systems **2–3**, **4**, and **8–9** against five bacterial cell lines and inhibition of biofilm formation.

Tested Strain	MIC (μ M)							Gentamycin
	2	3a	4a ^a	4b ^a	8a ^a	9a	9b	
<i>E. faecalis</i> (ATCC 29122)	NA ^b	100	100	NA ^b	75	NA ^b	NA ^b	8
<i>E. coli</i> (ATCC 259233)	NA ^b	100	NA ^b	50	NA ^b	NA ^b	NA ^b	0.13
<i>P. aeruginosa</i> (ATCC 27853)	NA ^b	NA ^b	NA ^b	NA ^b	NA ^b	NA ^b	NA ^b	0.25
<i>S. aureus</i> (ATCC 25923)	NA ^b	100	100	NA ^b	75	NA ^b	NA ^b	0.06
<i>Streptococcus agalactiae</i> (ATCC 12386)	100	100	NA ^b	75	NA ^b	100	NA ^b	4
	MBIC (μ M)							
<i>S. epidermis</i> (ATCC 35984)	NA ^b	100	NA ^b	NA ^b	NA ^b	100	100	NT ^c

^a Also tested at concentrations of 100, 75, 50, 25, 12.5, 10, 6.3, 3.1 and 1.6 μ M. Compounds **8b**, **10**, **13–14**, **16**, **18**, and **20** showed no activity against any of the tested strains; ^b NA = not active; ^c NT = not tested. Compounds **3b**, **3c**, and **21** were not tested.

Neocryptolepine (**2**) showed only modest activity against *Streptococcus agalactiae* (MIC = 100 μ M), while its precursor **13** was inactive against all bacterial strains. It has been shown previously that neocryptolepine (**2**) only possesses bacteriostatic properties against Gram-positive bacteria and displays no activity whatsoever against Gram-negative bacteria [40,72–74], which fits well with our observations. With the exception of *P. aeruginosa*, isocryptolepine (**3a**) contained modest activity against all the tested strains and excellent inhibition of biofilm growth.

The novel pyridophenanthridines **4a** and **8a** were both effective against the Gram-positive bacteria *E. faecalis* (**4a**: MIC = 100 μ M; **8a**: MIC = 75 μ M) and *S. aureus* (**4a**: MIC = 100 μ M; **8a**: MIC = 75 μ M) but were inactive against the rest. These results are comparable to previous observations for the indolo[2,3-*b*]quinolines (i.e., neocryptolepines), showing that the presence of an *N*-methyl substituent is essential for antimicrobial inhi-

bition [73]. Methoxy substituted pyridophenanthridine **4b** was proven to be the most successful in the evaluated series, being moderately effective against *E. coli* (MIC = 50 μ M) and *S. aureus* (MIC = 75 μ M). Interestingly, addition of the *N*-methyl functionality to produce pyridophenanthridine **8b**, resulted in a complete loss of activity. Representing unknown scaffolds, the mode of action of the pyridophenanthridines are naturally not known; however, these data indicate that the methoxy substituted **4b** and **8b** could differ from their non-functionalized counterparts **4a** and **8a**.

Novel pyridocarbazoles **9** showed excellent biofilm formation inhibition (**9a**: MBIC = 100 μ M; **9b**: MIC = 100 μ M) and variant **9a** was also active against *Streptococcus agalactiae* (MBIC = 100 μ M). The incorporation of a fluorine into a molecule is usually associated with a significant increase in biological activity [75], which is not the case for compound **9**, having the non-fluorinated **9a** performing better overall. In general, pyridocarbazoles have been primarily studied for their antiproliferative qualities in the past, with natural products such as the ellipticines containing potent anticancer properties [76]. The ellipticines are currently employed clinically as antiproliferative agents, though little is known about the inherent antimicrobial potential of such motifs. Although the antimicrobial activities observed for compound **9** were not particularly significant, this structural motif should be explored in greater detail in future research to uncover its full potential as a dual antimicrobial and antiproliferative agent.

3. Materials and Methods

3.1. Chemistry

3.1.1. General

Nuclear magnetic resonance (NMR) spectra were recorded on a Bruker Ascend™ 400 series (Billerica, MA, USA), operating at 400.13 MHz for ^1H , 376.49 MHz for ^{19}F and 100.61 MHz for ^{13}C , respectively. Chemical shifts (δ) are expressed in ppm relative to residual chloroform-*d* (^1H , 7.26 ppm; ^{13}C , 77.16 ppm), DMSO-*d*₆ (^1H , 2.50 ppm; ^{13}C , 39.52 ppm), methanol-*d*₄ (^1H , 3.31 ppm; ^{13}C , 49.00 ppm), acetone-*d*₆ (^1H , 2.09 ppm; ^{13}C , 30.60 ppm), dichloromethane-*d*₂ (^1H , 5.32 ppm; ^{13}C , 53.84 ppm) or α,α,α -trifluorotoluene (^{19}F , -62.61 ppm) [77] as an external reference. The assignment of signals in various NMR spectra were often assisted by conducting correlation spectroscopy (COSY), heteronuclear single-quantum correlation spectroscopy (HSQC), heteronuclear multiple bond correlation spectroscopy (HMBC) and nuclear Overhauser effect spectroscopy (NOESY).

Reactions were monitored by thin-layer chromatography (TLC) carried out on 0.25 mm silica gel F254 coated aluminum sheets using UV light as a visualizing agent. Silica gel 60 (particle size 40–63 μ m) was used for flash chromatography.

In addition to TLC, low resolution mass spectrometry (LRMS) was routinely used to monitor and identify the various components of reaction mixtures. The LRMS spectra were obtained using an Advion expressions CMS mass spectrometer operating at 3.5 kV in electrospray ionization (ESI) mode.

Infrared spectroscopy (IR) was performed on a Agilent Technologies Cary 360 FTIR spectrophotometer (Santa Clara, CA, USA). Solids were dissolved in CHCl_3 or CH_2Cl_2 and adsorbed on a NaCl plate, or by placing the sample directly onto the crystal of an attenuated total reflectance (ATR) module. Melting points were measured using a Stuart Scientific SMP3 melting point apparatus and are uncorrected. High resolution mass spectrometry (HRMS) were conducted externally at the University of Bergen (UiB) or the University of Tromsø, using ESI mode. The microwave-assisted experiments were performed in a CEM Focused Microwave™ Synthesis System (Charlotte, NC, USA), model type Discover, operating at 0–300 W, a pressure of 0–290 psi, at a temperature of 118 °C, using reactor vial volumes of either 10 or 35 mL. Commercially available chemicals were used as delivered from the supplier unless otherwise noted.

Detailed experimental procedures and full characterizations for compounds **3a**, **4**, **5b**, **7**, **15**, **17**, and **19** are available through our previous works [52,62].

3.1.2. 4-Fluoro-2-(4,4,5,5-tetramethyl-1,3,2-dioxaborolan-2-yl)aniline (**6b**)

To a mixture of 2-bromo-4-fluoroaniline (1000.0 mg, 5.26 mmol), anhydrous Et₃N (2.93 mL, 21.04 mmol), PdCl₂(PPh₃)₂ (369.2 mg, 0.53 mmol, 10 mol%) in 20 mL anhydrous dioxane, was added 4,4,5,5-tetramethyl-1,3,2-dioxaborolane (2.30 mL, 15.79 mmol) dropwise. The resulting mixture was refluxed for 22 h and then allowed to cool to rt before being quenched by addition of suitable amounts of sat. aq. NH₄Cl. The crude was subsequently extracted using CH₂Cl₂ (3 × 20 mL) and the combined organic phases were washed with water (1 × 20 mL), brine (1 × 20 mL), dried (MgSO₄), filtered and concentrated in vacuo. The concentrate was then evaporated onto celite and purification by silica gel column chromatography (pet. ether/EtOAc, 9:1 *v/v*) and concentration of the relevant fractions [*R*_f = 0.33 (pet. ether/EtOAc, 9:1 *v/v*)] gave the target compound **6b** as a red solid (975.7 mg, 78%), mp 49–50 °C (lit. [78] 50–52 °C); IR (ATR): ν_{\max} 3481, 3388, 2978, 2931, 1621, 1431, 1137, 854 cm⁻¹; ¹H NMR (400 MHz, CDCl₃): δ 7.28 (dd, *J* = 9.1 Hz, 3.1 Hz, 1H), 6.92 (ddd, *J* = 8.6 Hz, 8.3 Hz, 3.1 Hz, 1H), 6.53 (dd, *J* = 8.8 Hz, 4.3 Hz, 1H), 4.55 (bs, 2H), 1.34 (s, 12H); ¹³C NMR (100 MHz, CDCl₃): δ 155.3 (d, *J*_{CF} = 235.0 Hz), 149.9, 121.6 (d, *J*_{CF} = 20.3 Hz), 119.8 (d, *J*_{CF} = 23.0 Hz), 116.1 (d, *J*_{CF} = 6.9 Hz), 83.9, 25.0 (one carbon was obscured or overlapping); ¹⁹F NMR (376 MHz, CDCl₃): δ -129.0. The spectroscopic data are in accordance with previously reported data [78].

3.1.3. 4-Fluoro-2-(quinolin-5-yl)aniline (**7c**)

To a solution of 5-bromoquinoline (**5a**) (512.3 mg, 2.46 mmol) in 25 mL 1,2-dimethoxyethane (DME) under an argon atmosphere was added 4-fluoro-2-(4,4,5,5-tetramethyl-1,3,2-dioxaborolan-2-yl)aniline (**6b**) (875.7 mg, 3.69 mmol), an aqueous solution of Cs₂CO₃ (2805.3 mg, 8.61 mmol in 5 mL H₂O) and Pd(PPh₃)₄ (142.1 mg, 0.12 mmol). The resulting mixture was stirred at 80 °C for 17 h before being allowed to cool to rt. The volatiles were then removed under reduced pressure and the concentrate was evaporated onto celite. Purification by silica gel column chromatography (pet. ether/EtOAc, 1:1 *v/v*) and concentration of the relevant fractions [*R*_f = 0.10 (pet. ether/EtOAc, 1:1 *v/v*)] gave the target compound **7c** as an orange solid (419.5 mg, 72%), mp 196–197 °C; IR (ATR): ν_{\max} 3041, 2921, 2852, 1635, 1490, 1192, 900, 792 cm⁻¹; ¹H NMR (400 MHz, CD₂Cl₂): δ 8.90 (dd, *J* = 4.1 Hz, 1.7 Hz, 1H), 8.14–8.12 (m, 1H), 7.96 (ddd, *J* = 8.5 Hz, 1.6 Hz, 0.8 Hz, 1H), 7.79 (dd, *J* = 8.5 Hz, 7.1 Hz, 1H), 7.51 (dd, *J* = 7.0 Hz, 1.1 Hz, 1H), 7.36 (dd, *J* = 8.5 Hz, 4.2 Hz, 1H), 7.00 (td, *J* = 8.6 Hz, 3.0 Hz, 1H), 6.88 (dd, *J* = 9.0 Hz, 3.0 Hz, 1H), 6.79 (dd, *J* = 8.8 Hz, 4.8 Hz, 1H), 3.42 (bs, 2H) (Figure S3.1); ¹³C NMR (100 MHz, CD₂Cl₂): δ 156.4 (d, *J*_{CF} = 235.8 Hz), 151.0, 149.1, 141.4, 136.8, 134.5, 130.1, 129.6, 128.3, 127.0, 125.7 (d, *J*_{CF} = 7.2 Hz), 121.8, 117.7 (d, *J*_{CF} = 22.1 Hz), 116.6 (d, *J*_{CF} = 8.0 Hz), 115.9 (d, *J*_{CF} = 22.1 Hz) (Figure S3.2); ¹⁹F NMR (376 MHz, CD₂Cl₂): δ -128.0 (Figure S3.3); HRMS (ESI): calcd. for C₁₅H₁₁FN₂ [M + H⁺] 239.0979, found 239.0988.

3.1.4. Intramolecular Cyclization to Form Tetracycles **9**, **13**, **14**, **18** and **20**

General Procedures

Method 1—palladium-catalyzed intramolecular C-H activation/C-N bond formation: The appropriate biaryl (1 equiv.) in a suitable amount of glacial acetic acid was added to a premixed solution of PdCl₂(dppf) (10 mol%), 1,3-bis(2,4,6-trimethylphenyl)imidazolium (IMes) (5 mol%), H₂O₂ (35 wt%, 29 mol%) and a suitable amount of glacial acetic acid. The reaction mixture was then placed in a sealed reactor tube and immersed into the cavity of a microwave oven and heated at 118 °C until completion as indicated by TLC analysis. The reaction mixture was then transferred to a round-bottom flask with the aid of EtOAc/CHCl₃ and the volatiles were removed under reduced pressure. The reaction mixture was finally evaporated onto celite and purified by column chromatography with the eluents as indicated in order to give the target compounds.

Method 2—diazotization-azidation-nitrene insertion: The appropriate biaryl (1 equiv.) was dissolved in a suitable amount of aq. HCl (37%) and the mixture was cooled to 0 °C using an ice bath. Next, to ice-cooled aq. NaNO₂ (0.4 M) was added the solution

dropwise and the resulting mixture was stirred at 0 °C for 1.5 h. An ice-cooled aq. solution of $\text{NaN}_3/\text{NaOAc}$ (2.1 equiv./14 equiv. in an appropriate amount of H_2O) was added dropwise and the mixture stirred for 1 h while keeping the temperature at 0 °C. The reaction mixture was quenched by addition of appropriate amounts of sat. aq. K_2CO_3 and subsequently extracted with CH_2Cl_2 (3×20 mL). The combined organic phases were washed with water (1×20 mL), brine (1×20 mL), dried (MgSO_4), filtered and concentrated in vacuo. The obtained residue was dissolved in a suitable amount of 1,2-dichlorobenzene and flushed with argon. The resulting mixture was stirred at 180 °C for 3 h under an argon atmosphere before being cooled to rt. The solvent was removed under reduced pressure and the concentrate was evaporated onto celite and purified by column chromatography using the eluents as indicated in order to give the target compounds.

7H-Pyrido[2,3-c]carbazole (9a)

Method 2: Following the general procedure, the title compound was prepared from 2-(quinolin-5-yl)aniline (7a) (100.0 mg, 0.45 mmol), HCl (37%, 3 mL), NaNO_2 (82.9 mg, 1.20 mmol in 3 mL H_2O), NaN_3 (61.4 mg, 0.94 mmol) and NaOAc (516.8 mg, 6.30 mmol in 5 mL H_2O). After formation of the azide was confirmed by IR, the cyclization was carried out using 3 mL of 1,2-dichlorobenzene. The crude was purified by silica gel column chromatography ($\text{CH}_2\text{Cl}_2/\text{EtOAc}$, 95:5 \rightarrow 9:1 v/v) and concentration of the relevant fractions [$R_f = 0.22$ ($\text{CH}_2\text{Cl}_2/\text{EtOAc}$, 95:5 v/v)] gave the target compound 9a as a light brown solid (78.8 mg, 80%), mp 204–205 °C; IR (ATR): ν_{max} 3045, 2919, 2842, 1523, 1274, 956, 804, 728 cm^{-1} ; ^1H NMR (400 MHz, $\text{DMSO}-d_6$): δ 11.92 (bs, 1H), 9.17 (dd, $J = 8.4$ Hz, 1.4 Hz, 1H), 8.84 (dd, $J = 4.1$ Hz, 1.4 Hz, 1H), 8.60 (d, $J = 8.0$ Hz, 1H), 8.03–7.98 (m, 2H), 7.69–7.65 (m, 2H), 7.47–7.44 (m, 1H), 7.34–7.31 (m, 1H) (Figure S6.1, S6.3, and S6.4); ^{13}C NMR (100 MHz, $\text{DMSO}-d_6$): δ 146.4, 144.3, 139.0, 136.9, 130.8, 127.7, 124.5, 124.3, 122.9, 121.6, 121.5, 119.8, 116.8, 113.6, 111.9 (Figure S6.2, S6.5, and S6.6); HRMS (ESI): calcd. for $\text{C}_{15}\text{H}_{10}\text{N}_2$ [$\text{M} + \text{H}^+$] 219.0917, found 219.0927.

10-Fluoro-7H-pyrido[2,3-c]carbazole (9b)

Method 2: Following the general procedure, the title compound was prepared from 4-fluoro-2-(quinolin-5-yl)aniline (7c) (419.5 mg, 1.76 mmol), HCl (37%, 8 mL), NaNO_2 (137.9 mg, 2.00 mmol), NaN_3 (240.5 mg, 3.70 mmol) and NaOAc (2021.2 mg, 24.64 mmol in 15 mL H_2O). The crude was essentially pure by ^1H NMR and 100.0 mg of the azide was dissolved in 2 mL 1,2-dichlorobenzene and reacted without any further purification. The cyclization yielded a reaction crude which was also pure by NMR and the target compound 9b was obtained as a dark green solid (87.3 mg, 97%), mp 256–257 °C; IR (ATR): ν_{max} 3137, 2974, 2746, 1460, 1149, 789 cm^{-1} ; ^1H NMR (400 MHz, CD_3OD): δ 9.07 (ddd, $J = 8.4$ Hz, 1.6 Hz, 0.8 Hz, 1H), 8.74 (dd, $J = 4.4$ Hz, 1.6 Hz, 1H), 8.18–8.15 (m, 1H), 7.98 (dd, $J = 9.1$ Hz, 0.7 Hz, 1H), 7.91 (d, $J = 9.1$ Hz, 1H), 7.67 (dd, $J = 8.4$ Hz, 4.4 Hz, 1H), 7.58 (ddd, $J = 8.8$ Hz, 4.5 Hz, 0.5 Hz, 1H), 7.25–7.20 (m, 1H) (Figure S7.1, S7.4, and S7.5); ^{13}C NMR (100 MHz, CD_3OD): δ 159.2 (d, $J_{\text{CF}} = 234.5$ Hz), 146.9, 145.1, 139.8, 137.3, 132.9, 127.9, 126.4, 124.7 (d, $J_{\text{CF}} = 9.5$ Hz), 122.7, 118.3, 115.1 (d, $J_{\text{CF}} = 5.3$ Hz), 113.7 (d, $J_{\text{CF}} = 24.0$ Hz), 113.5 (d, $J_{\text{CF}} = 7.2$ Hz), 107.6 (d, $J_{\text{CF}} = 24.8$ Hz) (Figure S7.2, S7.6, and S7.7); ^{19}F NMR (376 MHz, CD_3OD): δ -123.6 (Figure S7.3); HRMS (ESI): calcd. for $\text{C}_{15}\text{H}_9\text{FN}_2$ [$\text{M} + \text{H}^+$] 237.0823, found 237.0830.

6H-Indolo[2,3-b]quinoline (13) and 11H-indolo[3,2-c]quinoline (14)

Method 2: Following the general procedure, the title compounds were prepared starting from 2-(quinolin-3-yl)aniline (12) (100.0 mg, 0.45 mmol), HCl (37%, 3 mL), NaNO_2 (82.8 mg, 1.20 mmol in 3 mL H_2O), NaN_3 (61.4 mg, 0.94 mmol) and NaOAc (516.8 mg, 6.30 mmol in 5 mL H_2O). After formation of the azide was confirmed by IR, the cyclization was carried out using 3 mL 1,2-dichlorobenzene. The crude was purified by silica gel column chromatography ($\text{CH}_2\text{Cl}_2/\text{EtOAc}$, 8:2 \rightarrow 0:1 v/v) and concentration of the relevant

fractions [$R_f = 0.56$ ($\text{CH}_2\text{Cl}_2/\text{EtOAc}$, 2:8 v/v)] gave compound **13** as off-white crystals (4.2 mg, 4%) along with compound **14** as an off-white solid (86.4 mg, 88%).

Characterization of Compound **13**

mp 341–342 °C (lit. [79] 342–346 °C); IR (ATR): ν_{max} 3139, 2923, 2849, 1402, 725 cm^{-1} ; ^1H NMR (400 MHz, $\text{DMSO-}d_6$): δ 11.72 (bs, 1H), 9.06 (s, 1H), 8.26 (d, $J = 7.7$ Hz, 1H), 8.11 (dd, $J = 8.1$ Hz, 1.3 Hz, 1H), 7.99–7.97 (m, 1H), 7.75–7.70 (m, 1H), 7.55–7.46 (m, 3H), 7.29–7.25 (m, 1H); ^{13}C NMR (100 MHz, $\text{DMSO-}d_6$): δ 152.7, 146.1, 141.4, 128.7, 128.6, 128.2, 127.7, 126.8, 123.6, 122.8, 121.8, 120.3, 119.7, 118.0, 110.9. The spectroscopic data are in accordance with previously reported data [79].

Characterization of Compound **14**

mp 333–335 °C (lit. [62] 340–341 °C); IR (NaCl): ν_{max} 3060, 2958, 2854, 1682, 1582, 1515, 1493 cm^{-1} ; ^1H NMR (400 MHz, $\text{DMSO-}d_6$): δ 12.74 (bs, 1H), 9.60 (s, 1H), 8.52 (dd, $J = 7.8$ Hz, 1.1 Hz, 1H), 8.33–8.31 (m, 1H), 8.14 (dd, $J = 8.4$ Hz, 1.1 Hz, 1H), 7.77–7.68 (m, 3H), 7.52–7.48 (m, 1H), 7.37–7.33 (m, 1H); ^{13}C NMR (100 MHz, $\text{DMSO-}d_6$): δ 145.3, 144.7, 139.8, 138.8, 129.4, 128.1, 125.7, 125.6, 122.1, 121.9, 120.6, 120.1, 117.1, 114.3, 111.9. The spectroscopic data are in accordance with previously reported data [62].

11*H*-Pyrido[2,3-*a*]carbazole (**18**)

Method 2: Following the general procedure, the title compound was prepared from 2-(quinolin-7-yl)aniline (**17**) (100.0 mg, 0.45 mmol), HCl (37%, 3 mL), NaNO_2 (82.8 mg, 1.20 mmol in 3 mL H_2O), NaN_3 (61.4 mg, 0.94 mmol) and NaOAc (516.8 mg, 6.30 mmol in 3 mL H_2O). After formation of the azide was confirmed by IR, the cyclization was carried out using 3 mL 1,2-dichlorobenzene. The crude was purified by silica gel column chromatography ($\text{CH}_2\text{Cl}_2/\text{EtOAc}$, 9:1 v/v) and concentration of the relevant fractions [$R_f = 0.36$ ($\text{CH}_2\text{Cl}_2/\text{EtOAc}$, 9:1 v/v)] gave the target compound **18** as off-white crystals (40.0 mg, 41%), mp 164 °C (lit. [52] 165–167 °C); IR (ATR): ν_{max} 3263, 3043, 2923, 2854, 1523, 1369, 820, 734 cm^{-1} ; ^1H NMR (400 MHz, CDCl_3): δ 10.20 (bs, 1H), 8.92 (dd, $J = 4.4$ Hz, 1.5 Hz, 1H), 8.35 (dd, $J = 8.3$ Hz, 1.5 Hz, 1H), 8.24 (d, $J = 8.5$ Hz, 1H), 8.19–8.17 (m, 1H), 7.62–7.60 (m, 2H), 7.51–7.47 (m, 2H), 7.35–7.31 (m, 1H); ^{13}C NMR (100 MHz, CDCl_3): δ 147.8, 139.2, 137.4, 136.8, 134.9, 127.3, 125.9, 123.8, 121.7, 120.8, 120.5, 120.4, 120.2, 118.8, 111.8. The spectroscopic data are in accordance with previously reported data [52].

7*H*-Pyrido[3,2-*c*]carbazole (**20**)

Method 2: Following the general procedure, the title compound was prepared from 2-(quinolin-8-yl)aniline (**19**) (450.0 mg, 2.04 mmol), HCl (37%, 10 mL), NaNO_2 (137.9 mg, 2.00 mmol in 5 mL H_2O), NaN_3 (278.5 mg, 4.28 mmol) and NaOAc (2342.8 mg, 28.56 mmol in 10 mL H_2O). After formation of the azide was confirmed by IR, the cyclization was carried out using 5 mL 1,2-dichlorobenzene. The crude was purified by silica gel column chromatography (pet. ether/ EtOAc , 1:1 v/v) and concentration of the relevant fractions [$R_f = 0.85$ (pet. ether/ EtOAc , 1:1 v/v)] gave the target compound **20** as a dark red oil (195.9 mg, 44%). IR (ATR): ν_{max} 3207, 2976, 2919, 2850, 2740, 2605, 2499 cm^{-1} ; ^1H NMR (400 MHz, $\text{DMSO-}d_6$): δ 11.92 (bs, 1H), 9.02 (dd, $J = 4.4$ Hz, 1.8 Hz, 1H), 8.90–8.88 (m, 1H), 8.46 (dd, $J = 8.1$ Hz, 1.4 Hz, 1H), 7.92 (d, $J = 8.8$ Hz, 1H), 7.84 (d, $J = 8.8$ Hz, 1H), 7.66–7.64 (m, 1H), 7.49 (dd, $J = 8.0$ Hz, 4.3 Hz, 1H), 7.46–7.42 (m, 1H), 7.33–7.29 (m, 1H); ^{13}C NMR (100 MHz, $\text{DMSO-}d_6$): δ 149.8, 145.3, 139.6, 138.5, 136.5, 126.0, 124.5, 123.1, 122.9, 122.8, 119.7, 118.3, 115.3, 114.2, 111.4. The spectroscopic data are in accordance with previously reported data [52].

3.1.5. Neocryptolepine (**2**)

To a solution of 6*H*-indolo[2,3-*b*]quinoline (**13**) (23.0 mg, 0.10 mmol) in 2 mL THF, iodomethane (0.66 mL, 10.0 mmol) was added and the resulting mixture refluxed for 24 h. The volatiles were then removed under reduced pressure and the concentrate was

evaporated onto celite. Purification by silica gel column chromatography ($\text{CH}_2\text{Cl}_2/\text{MeOH}$, 95:5 *v/v*) and concentration of the relevant fractions [$R_f = 0.18$ ($\text{CH}_2\text{Cl}_2/\text{MeOH}$, 95:5 *v/v*)] gave the hydroiodide salt of neocryptolepine. To obtain the free base, the hydroiodide salt was dissolved in a 20 mL 1:1 mixture of CH_2Cl_2 and $\text{NH}_3(\text{aq})$ (20%) and stirred at rt for 30 min. The organic layer was then separated and the aqueous layers were extracted with CH_2Cl_2 (3×10 mL) and the combined organic layers were washed with water (1×10 mL), brine (1×10 mL), dried (MgSO_4), filtered and concentrated in vacuo to give neocryptolepine (**2**) as a dark yellow solid (19.5 mg, 84%), mp 85–86 °C (lit. [67] 104–105 °C); IR (ATR): ν_{max} 3051, 2961, 2923, 2852, 1494, 1012, 741 cm^{-1} ; ^1H NMR (400 MHz, CD_3OD): δ 8.67 (s, 1H), 8.05–8.02 (m, 2H), 7.90 (d, $J = 8.6$ Hz, 1H), 7.83–7.78 (m, 1H), 7.59–7.57 (m, 1H), 7.50–7.45 (m, 2H), 7.19 (td, $J = 7.5$ Hz, 1.0 Hz, 1H), 4.23 (s, 3H); ^{13}C NMR (100 MHz, CD_3OD): δ 156.9, 155.4, 138.1, 132.0, 131.2, 130.4, 130.1, 128.4, 124.9, 123.6, 122.4, 122.2, 121.2, 117.7, 115.7, 33.7. The spectroscopic data are in accordance with previously reported data [67].

3.1.6. 5-Ethyl-5*H*-indolo[3,2-*c*]quinoline (**3b**)

To a solution of 11*H*-indolo[3,2-*c*]quinoline (**14**) (15.0 mg, 0.068 mmol) in 3 mL toluene, ethyl iodide (1.1 mL, 13.68 mmol) was added and the resulting mixture was refluxed for 3 h. The volatiles were then removed under reduced pressure and the concentrate was evaporated onto celite. Purification by silica gel column chromatography ($\text{CHCl}_3/\text{MeOH}$, 9:1 *v/v*) and concentration of the relevant fractions [$R_f = 0.21$ ($\text{CHCl}_3/\text{MeOH}$, 9:1 *v/v*)] gave the hydroiodide salt of compound **3b**. To obtain the free base, the hydroiodide salt was dissolved in a 40 mL 1:1 mixture of CH_2Cl_2 and NH_3 (aq) (20%) and stirred at rt for 5 min. The organic layer was then separated and the aqueous layers were extracted with CH_2Cl_2 (2×10 mL) and the combined organic layers were washed with brine (1×10 mL), dried (MgSO_4), filtered and concentrated in vacuo to give the target compound **3b** as a yellow solid (11.0 mg, 64%), mp 198 °C. IR (NaCl): ν_{max} 3371, 3049, 2960, 2927, 2856, 1731, 1640, 1598, 1455, 1392, 1353 cm^{-1} ; ^1H NMR (400 MHz, $\text{DMSO}-d_6$): δ 9.59 (s, 1H), 8.84 (dd, $J = 8.1$ Hz, 1.3 Hz, 1H), 8.23 (d, $J = 8.7$ Hz, 1H), 8.20–8.18 (m, 1H), 7.93–7.89 (m, 1H), 7.81 (d, $J = 8.1$ Hz, 1H), 7.79–7.75 (m, 1H), 7.51–7.47 (m, 1H), 7.34–7.30 (m, 1H), 4.81 (q, $J = 7.1$ Hz, 2H), 1.56 (t, $J = 7.1$ Hz, 3H) (Figure S1.1, S1.3, and S1.4); ^{13}C NMR (100 MHz, $\text{DMSO}-d_6$): δ 151.2, 150.5, 138.6, 134.3, 130.1, 126.1, 125.8, 124.7, 124.4, 120.5, 120.2, 119.9, 117.8, 117.2, 115.9, 49.7, 15.0 (Figure S1.2, S1.5, and S1.6); HRMS (ESI): calcd. for $\text{C}_{17}\text{H}_{14}\text{N}_2$ [$\text{M} + \text{H}^+$] 247.1235, found 247.1238.

3.1.7. 5-Allyl-5*H*-indolo[3,2-*c*]quinoline (**3c**)

To a solution of 11*H*-indolo[3,2-*c*]quinoline (**14**) (30.0 mg, 0.14 mmol) in 5 mL toluene, allyl bromide (1.14 mL, 13.76 mmol) was added and the resulting mixture was refluxed for 22 h. The volatiles were then removed under reduced pressure and the concentrate was evaporated onto celite. Purification by silica gel column chromatography ($\text{CHCl}_3/\text{MeOH}$, 95:5 \rightarrow 9:1 *v/v*) and concentration of the relevant fractions [$R_f = 0.18$ ($\text{CHCl}_3/\text{MeOH}$, 9:1 *v/v*)] gave the hydroiodide salt of compound **3c**. To obtain the free base, the hydroiodide salt was dissolved in a 20 mL 1:1 mixture of CH_2Cl_2 and NH_3 (aq) (20%) and stirred at rt for 45 min. The organic layer was then separated and the aqueous layers were extracted with CH_2Cl_2 (3×10 mL) and the combined organic layers were washed with water (1×10 mL), brine (1×10 mL), dried (MgSO_4), filtered and concentrated in vacuo to give the target compound **3c** as a yellow viscous oil (15.5 mg, 43%). IR (ATR): ν_{max} 2924, 2723, 1596, 1349, 1204, 927, 743 cm^{-1} ; ^1H NMR (400 MHz, $\text{DMSO}-d_6$): δ 9.67 (s, 1H), 8.84 (dd, $J = 8.0$ Hz, 1.3 Hz, 1H), 8.22–8.20 (m, 1H), 8.15 (d, $J = 8.7$ Hz, 1H), 7.92–7.88 (m, 1H), 7.84–7.77 (m, 2H), 7.55–7.51 (m, 1H), 7.37–7.34 (m, 1H), 6.26–6.17 (m, 1H), 5.46–5.44 (m, 2H), 5.31–5.28 (m, 1H), 5.15–5.11 (m, 1H) (Figure S2.1, S2.3, and S2.4); ^{13}C NMR (100 MHz, $\text{DMSO}-d_6$): δ 150.0, 149.9, 139.6, 134.9, 132.8, 130.3, 126.5, 126.1, 124.4, 124.3, 121.0, 120.1, 119.7, 118.5, 118.2, 116.8, 115.7, 56.5 (Figure S2.2 and S2.5); HRMS (ESI): calcd. for $\text{C}_{18}\text{H}_{14}\text{N}_2$ [$\text{M} + \text{H}^+$] 259.1230, found 259.1232.

3.1.8. 4-Methyl-4*H*-pyrido[4,3,2-*gh*]phenanthridine (**8a**)

To a solution of 7*H*-pyrido[4,3,2-*gh*]phenanthridine (**4a**) (70.0 mg, 0.32 mmol) in 2 mL acetonitrile, iodomethane (2.0 mL, 32.0 mmol) was added and the resulting mixture was refluxed for 2 h. The volatiles were then removed under reduced pressure and the concentrate was evaporated onto celite. Purification by silica gel column chromatography (CHCl₃/MeOH, 95:5 + 0.3% NH₃ (aq) *v/v*) and concentration of the relevant fractions [*R*_f = 0.33 (CHCl₃/MeOH, 95:5 + 0.3% NH₃(aq) *v/v*)] gave the hydroiodide salt of compound **8a**. To obtain the free base, the hydroiodide salt was dissolved in a 20 mL 1:1 mixture of CH₂Cl₂ and NH₃ (aq) (20%) and stirred at rt for 20 min. The organic layer was separated and the aqueous layers were extracted with Et₂O (2 × 20 mL) and the combined organic layers were washed with water (1 × 10 mL), brine (1 × 10 mL), dried (MgSO₄), filtered and concentrated in vacuo to give the target compound **8a** as dark yellow crystals (52.8 mg, 71%), mp 182–183 °C; IR (ATR): ν_{\max} 3485, 3051, 2922, 2851, 2574, 1601, 1327, 820, 748 cm⁻¹; ¹H NMR (400 MHz, DMSO-*d*₆): δ 8.29 (dd, *J* = 8.1 Hz, 1.1 Hz, 1H), 7.97 (d, *J* = 7.9 Hz, 1H), 7.71 (t, *J* = 8.1 Hz, 1H), 7.56 (dd, *J* = 8.2 Hz, 1.2 Hz, 1H), 7.51–7.47 (m, 2H), 7.30–7.26 (m, 1H), 7.05 (d, *J* = 8.1 Hz, 1H), 6.18 (d, *J* = 7.6 Hz, 1H), 3.45 (s, 3H) (Figure S4.1, S4.3, and S4.4); ¹³C NMR (100 MHz, DMSO-*d*₆): "δ" 152.9, 145.9, 141.0, 140.9, 133.8, 131.6, 129.2, 127.0, 123.2, 122.9, 121.3, 119.6, 112.2, 108.8, 106.2, 39.6 (Figure S4.2, S4.5, and S4.6); HRMS (ESI): calcd. for C₁₆H₁₂N₂ [M + H⁺] 233.1073, found 233.1073.

3.1.9. 6-Methoxy-4-methyl-4*H*-pyrido[4,3,2-*gh*]phenanthridine (**8b**)

To a solution of 6-methoxy-7*H*-pyrido[4,3,2-*gh*]phenanthridine (**4b**) (90.0 mg, 0.36 mmol) in 10 mL acetonitrile, iodomethane (2.25 mL, 36.3 mmol) was added and the resulting mixture refluxed for 2 h. The volatiles were then removed under reduced pressure and the concentrate was evaporated onto celite. Purification by silica gel column chromatography (EtOH + 0.1 → 5% NH₃ (aq) *v/v*) and concentration of the relevant fractions [*R*_f = 0.23 (EtOH)] gave the hydroiodide salt of compound **8b**. To obtain the free base, the hydroiodide salt was dissolved in a 20 mL 1:1 mixture of CH₂Cl₂ and NH₃ (aq) (20%) and stirred at rt for 20 min. The organic layer was separated and the aqueous layers were extracted with CH₂Cl₂ (4 × 20 mL) and the combined organic layers were washed with water (1 × 20 mL), brine (1 × 20 mL), dried (MgSO₄), filtered and concentrated in vacuo to give the target compound **8b** as a dark yellow gel (55.1 mg, 58%). IR (ATR): ν_{\max} 2918, 2850, 1600, 1255, 1059, 745 cm⁻¹; ¹H NMR (400 MHz, CD₂Cl₂): δ 8.19 (dd, *J* = 8.2 Hz, 1.3 Hz, 1H), 7.79 (dd, *J* = 8.2 Hz, 1.0 Hz, 1H), 7.72 (d, *J* = 7.9 Hz, 1H), 7.57–7.51 (m, 2H), 7.34–7.30 (m, 1H), 6.74–6.72 (m, 2H), 3.85 (s, 3H), 3.34 (s, 3H) (Figure S5.1, S5.3 and S5.4); ¹³C NMR (100 MHz, CD₂Cl₂): δ 148.1, 146.3, 140.8, 139.9, 134.8, 130.9, 129.4, 128.6, 124.1, 122.7, 122.5, 119.9, 110.6, 107.7, 57.1, 40.4 (one carbon was obscured or overlapping) (Figure S5.2, S5.5 and S5.6); HRMS (ESI): calcd. for C₁₇H₁₄N₂O 263.1179, found 263.1188.

3.1.10. 4-Methyl-7*H*-pyrido[2,3-*c*]carbazolium Iodide (**10**)

To a solution of 7*H*-pyrido[2,3-*c*]carbazole (**9a**) (40.7 mg, 0.19 mmol) in 5 mL acetonitrile, iodomethane (1.20 mL, 19.6 mmol) was added and the resulting mixture refluxed for 20 h. The volatiles were then removed under reduced pressure and the concentrate was evaporated onto celite. Purification by alumina gel column chromatography (CHCl₃/MeOH, 9:1 *v/v* + 1% NH₃ (aq)) and concentration of the relevant fractions [*R*_f = 0.12 (CHCl₃/MeOH, 9:1 *v/v* + 2% NH₃ (aq))] gave the target compound **10** as a bright yellow solid (20.9 mg, 47%), mp 284–286; IR (ATR): ν_{\max} 3353, 3043, 3006, 2960, 2921, 2853, 1556, 1370, 1326, 741 cm⁻¹; ¹H NMR (400 MHz, DMSO-*d*₆): δ 12.84 (bs, 1H), 9.99 (d, *J* = 8.4 Hz, 1H), 9.39 (d, *J* = 5.6 Hz, 1H), 8.76 (d, *J* = 8.1 Hz, 1H), 8.50 (d, *J* = 9.3 Hz, 1H), 8.43 (d, *J* = 9.4 Hz, 1H), 8.22 (dd, *J* = 8.5 Hz, 5.7 Hz, 1H), 7.82 (d, *J* = 8.2 Hz, 1H), 7.64–7.60 (m, 1H), 7.48–7.44 (m, 1H), 4.74 (s, 3H) (Figure S8.1, S8.3, and S8.4); ¹³C NMR (100 MHz, DMSO-*d*₆): δ 145.0, 140.8, 139.8, 137.5, 134.5, 126.6, 125.8, 122.4, 122.1, 121.9, 121.6, 121.1, 116.0, 114.3, 112.8, 46.3 (Figure S8.2, S8.5 and S8.6); HRMS (ESI): calcd. for C₁₆H₁₃N₂I [M – I⁻] 233.1073, found 233.1073.

3.1.11. 4-Methyl-11*H*-pyrido[3,2-*a*]carbazolium Iodide (**21**)

To a solution of 11*H*-pyrido[3,2-*a*]carbazole (**15**) (32.1 mg, 0.15 mmol) in 5 mL acetonitrile, iodomethane (0.92 mL, 14.72 mmol) was added and the resulting mixture stirred at reflux for 20 h. The volatiles were then removed under reduced pressure and the obtained yellow crystals were thoroughly washed with *n*-hexanes and dried in vacuo to give the target compound **21** as a dark orange crystalline solid (47.6 mg, quant.), mp 279–280 °C; IR (ATR): ν_{\max} 3416, 3165, 3077, 2997, 2905, 1599, 1452, 1371, 740 cm^{-1} ; ^1H NMR (400 MHz, CD_3OD): δ 9.64 (d, $J = 8.6$ Hz, 1H), 9.28 (d, $J = 5.7$ Hz, 1H), 8.99 (d, $J = 9.1$ Hz, 1H), 8.35–8.33 (m, 1H), 8.15–8.10 (m, 2H), 7.79–7.77 (m, 1H), 7.65–7.61 (m, 1H), 7.46–7.42 (m, 1H), 4.76 (s, 3H) (Figure S9.1, S9.3, and S9.4); ^{13}C NMR (100 MHz, CD_3OD): δ 148.2, 141.7, 141.6, 139.1, 136.1, 131.1, 128.4, 123.6, 122.4, 122.3, 121.6, 121.1, 119.9, 113.1, 109.0, 46.9 (Figure S9.2, S9.5 and S9.6); HRMS (ESI): calcd. for $\text{C}_{16}\text{H}_{13}\text{N}_2\text{I}$ [$\text{M} - \text{I}$] 233.1073, found 233.1075.

3.2. Biological Testing Assay

3.2.1. General

All compounds for antimicrobial testing were diluted to a final assay concentration of 40 μL , 0.4% DMSO, and tested in full dose-response using three concentrations per log dose (16 points with a concentration range of 0.33 nM–40 μM , for reference compounds: 21 points with a concentration of 0.01 nM–40 μM).

All compounds for antiplasmodial testing were diluted to a final assay concentration of 40 μL , 0.4% DMSO, and tested in full dose-response using three concentrations per log dose (16 points with a concentration range of 0.4 nM–40 μM , for reference compounds: 16 points with a concentration range of 0.4 nM–40 μM for chloroquine and puromycin: 0.001 nM–0.1 μM for artemisinin). Compounds tested in the antiproliferative assays were tested in 11 dilution points (0.02 μM –40 μM or 0.04 μM –80 μM).

Antiplasmodial Imaging Assay

Antiplasmodial activity was determined as previously described by Duffy and Avery [80]. Briefly, compounds were incubated with 2% parasitemia in 0.3% hematocrit, in an assay volume of 50 μL for 72 h at 37 °C and 5% CO_2 in CellCarrier Ultra 384-well PDL-imaging plates. After incubation, plates were stained with 4',6-diamidino-2-phenylindole (DAPI) in a permeabilization buffer for 5 h at rt in the dark. Plates were imaged on the Opera confocal microplate image reader (PerkinElmer). Parasite inhibition was calculated using the minimum (0.4% DMSO) and maximum (5 μM puromycin) controls, and IC_{50} values determined using GraphPad Prism software.

Cytotoxicity Assay

The cytotoxicity of compounds was determined using a resazurin-based viability assay in HEK293 (ATCC[®], CRL-1573), as described by Fletcher and Avery [81]. Compounds were added to TC-treated 384-well plates (Greiner, Kremsmünster, AT) containing 2500 HEK293 cells per well, total assay volume of 50 μL and incubated for 72 h at 37 °C, 5% CO_2 . After incubation, media was removed, replaced with 44 μM resazurin and plates incubated 6 h under the same experimental conditions. Fluorescence was measured using an EnSight plate reader (PerkinElmer, Waltham, MA, USA). Cell viability was calculated using positive (45 μM puromycin) and negative (0.4% DMSO) controls, and the IC_{50} values determined using GraphPad Prism software.

Antiproliferative Assay

Antiproliferative activity was assessed in HCT116 (ATCC[®] CCL-247; 1000 cells/well), MDA-MB-231 (ATCC[®] HTB-26; 2000 cells/well) and PC-3 (ATCC[®] CRL-1435; 1000 cells/well) cells. HCT116 cells were maintained in McCoy's 5A media (Life Technologies, CA, USA), MDA-MB-231 cells were cultured in DMEM media (Life Technologies) with 10 mM HEPES (Life Technologies), whilst PC-3 cells were maintained in RPMI media (Life Technologies). All media were supplemented with 10% heat-inactivated fetal bovine serum (Australian

source; Corning, CA, USA) and all cells were incubated at 37 °C in a humidified incubator with 5% CO₂.

Cells were seeded in 384-well plates (Greiner Bio-One, NC, USA) using the respective complete media. After 24 h cell seeding, compounds were added and antiproliferative activity was determined using the resazurin assay after 72 h compound incubation. Briefly, cells were incubated with 60 µM resazurin (Cayman, MI, USA) for 6 h at 37 °C and fluorescence signals were measured using a microplate reader (EnSight, PerkinElmer, Waltham, MA, USA). Fluorescence signals were normalized to 0.4% DMSO and 50 µM puromycin and IC₅₀ values were calculated from non-linear dose-response curves using GraphPad Prism 7 software (La Jolla, CA, USA).

3.2.2. Growth Inhibition Assay

To determine and quantify antimicrobial activity, a bacteria growth inhibition assay in liquid media was executed. Compounds **2–3**, **4**, **8–10**, **13–14**, **16**, **18**, and **20** were tested against *Staphylococcus aureus* (ATCC 25923), *Escherichia coli* (ATCC 25923), *Enterococcus faecialis* (ATCC 29122), *Pseudomonas aeruginosa* (ATCC 27853) and *Streptococcus agalactiae* (ATCC 12386); all strains from LGC Standards (Teddington, UK). *S. aureus*, *E. coli*, and *P. aeruginosa* were grown in Muller Hinton broth (275730, Becton, Franklin Lakes, NJ, USA). *E. faecialis* and *S. agalactiae* were cultured in brain heart infusion broth (53286, Sigma, St Louise, MO, USA). Fresh bacterial colonies were transferred in the respective medium and incubated at 37 °C overnight. The bacterial cultures were diluted to a culture density representing the log phase and µL/well were pipetted into a 96-well microtiter plate (734–2097, Nunclon™, Thermo Scientific, Waltham, MA, USA). The final cell density was 1500–15,000 colony forming units/well. The compound was diluted in 2% (v/v) DMSO in ddH₂O, providing a final assay concentration of 50% of the prepared sample, since 50 µL of sample in DMSO/water were added to 50 µL bacterial culture. After adding the samples to the plates, they were incubated overnight at 37 °C and the growth was determined by measuring the optical density at λ = 600 nm (OD₆₀₀) with a 1420 Multilabel Counter VICTOR3™ (Perkin Elmer, Waltham, MA, USA). A water sample was used as a reference control, growth medium without bacteria was used as a negative control and dilution series of gentamycin (A2712, Merck, Darmstadt, DE) from 32 to 0.01 µg/mL was used as positive control and visually inspected for bacterial growth. The positive control was used as a system suitability test and the results of the antimicrobial assay were only considered valid when positive control was passed. The final concentration of DMSO in the assays was ≤2% (v/v) and was known to have no effect in the tested bacteria. The data was processed using GraphPad Prism 8.

3.2.3. Biofilm Formation Inhibition Assay

For testing the inhibition of biofilm formation, the biofilm-producing *Staphylococcus epidermidis* (ATCC 35984) was grown in Tryptic Soy Broth (TSB, 105459, Merck, Kenilworth, NJ, USA) overnight at 37 °C. The overnight culture was diluted in fresh medium with 1% glucose (D9434, Sigma) before being transferred to a 96-well microtiter plate; 50 µL/well were incubated overnight with 50 µL of the test compound dissolved in 2% (v/v) DMSO aq. added in duplicates. The bacterial culture was removed from the plate and the plate was washed with tap water. The biofilm was fixed at 65 °C for 1 h before 70 µL 0.1% crystal violet (115940, Millipore, Burlington, MA, USA) was added to the wells for 10 min of incubation and 70 µL of 70% ethanol was then added to each well and the plate incubated on a shaker for 5–10 min. Biofilm formation inhibition was assessed by the presence of violet color and measured at 60 nm absorbance using a 1420 Multilabel Counter VICTOR3™; 50 µL of a non-biofilm forming *Staphylococcus haemolyticus* (clinical isolate 8-7A, University Hospital of North Norway Tromsø, Norway) mixed in 50 µL autoclaved Milli-Q water was used as a control; 50 µL *S. epidermidis* mixed in 50 µL autoclaved Milli-Q water was used as the control for biofilm formation; and 50 µL TSB with 50 µL autoclaved Milli-Q water was used as a medium blank control.

4. Conclusions

In conclusion, a series of quinoline-based tetracyclic ring-systems were prepared and evaluated for their in vitro antiplasmodial, antiproliferative and antimicrobial activities against selected strains. Through these studies, it was determined that the ionic pyridocarbazoles **10** and **21** showed the best antiplasmodial activity against the *Plasmodium falciparum* 3D7 strains (**10**: IC₅₀ = 128 nM; **21**: IC₅₀ = 380 nM) of the evaluated compounds. The antiproliferative assay revealed that the novel pyridophenanthridine scaffold **4** was the most active. In particular, compound **4b** showed excellent potency against the PC-3 cell line (IC₅₀ = 24 nM), significantly outperforming Puromycin (IC₅₀ = 270 nM) and Doxorubicin (IC₅₀ = 830 nM). The pyridophenanthridines **4** were also active against certain strains of Gram-positive and Gram-negative bacteria, with compound **4b** being moderately active against *E. coli* (MIC = 50 µM) and *Streptococcus agalactiae* (MIC = 75 µM). The antimicrobial studies further demonstrated pyridocarbazoles **9** to be highly potent against biofilm growth (**9a**: MBIC = 100 µM; **9b**: MBIC = 100 µM). Overall, this study has highlighted the potential for the novel pyridophenanthridine motif **4** and the studied pyridocarbazoles **9** to be developed into future drug candidates, with emphasis on the formulation of a dual antimicrobial and antiproliferative agent.

Supplementary Materials: Figure S1.1: ¹H NMR of 5-ethyl-5*H*-indolo[3,2-*c*]quinoline (**3b**), Figure S1.2: ¹³C NMR of 5-ethyl-5*H*-indolo[3,2-*c*]quinoline (**3b**), Figure S1.3: COSY of 5-ethyl-5*H*-indolo[3,2-*c*]quinoline (**3b**), Figure S1.4: NOESY of 5-ethyl-5*H*-indolo[3,2-*c*]quinoline (**3b**), Figure S1.5: HSQC of 5-ethyl-5*H*-indolo[3,2-*c*]quinoline (**3b**), Figure S1.6: HMBC of 5-ethyl-5*H*-indolo[3,2-*c*]quinoline (**3b**), Figure S2.1: ¹H NMR of 5-allyl-5*H*-indolo[3,2-*c*]quinoline (**3c**), Figure S2.2: ¹³C NMR of 5-allyl-5*H*-indolo[3,2-*c*]quinoline (**3c**), Figure S2.3: COSY of 5-allyl-5*H*-indolo[3,2-*c*]quinoline (**3c**), Figure S2.4: NOESY of 5-allyl-5*H*-indolo[3,2-*c*]quinoline (**3c**), Figure S2.5: HMBC of 5-allyl-5*H*-indolo[3,2-*c*]quinoline (**3c**), Figure S3.1: ¹H NMR of 4-fluoro-2-(quinolin-5-yl)aniline (**7c**), Figure S3.2: ¹³C NMR of 4-fluoro-2-(quinolin-5-yl)aniline (**7c**), Figure S3.3: ¹⁹F NMR of 4-fluoro-2-(quinolin-5-yl)aniline (**7c**), Figure S4.1: ¹H NMR of 4-methyl-4*H*-pyrido[4,3,2-*gh*]phenanthridine (**8a**), Figure S4.2: ¹³C NMR of 4-methyl-4*H*-pyrido[4,3,2-*gh*]phenanthridine (**8a**), Figure S4.3: COSY of 4-methyl-4*H*-pyrido[4,3,2-*gh*]phenanthridine (**8a**), Figure S4.4: NOESY of 4-methyl-4*H*-pyrido[4,3,2-*gh*]phenanthridine (**8a**), Figure S4.5: HSQC of 4-methyl-4*H*-pyrido[4,3,2-*gh*]phenanthridine (**8a**), Figure S4.6: HMBC of 4-methyl-4*H*-pyrido[4,3,2-*gh*]phenanthridine (**8a**), Figure S5.1: ¹H NMR of 6-methoxy-4-methyl-4*H*-pyrido[4,3,2-*gh*]phenanthridine (**8b**), Figure S5.2: ¹³C NMR of 6-methoxy-4-methyl-4*H*-pyrido[4,3,2-*gh*]phenanthridine (**8b**), Figure S5.3: COSY of 6-methoxy-4-methyl-4*H*-pyrido[4,3,2-*gh*]phenanthridine (**8b**), Figure S5.4: NOESY of 6-methoxy-4-methyl-4*H*-pyrido[4,3,2-*gh*]phenanthridine (**8b**), Figure S5.5: HSQC of 6-methoxy-4-methyl-4*H*-pyrido[4,3,2-*gh*]phenanthridine (**8b**), Figure S5.6: HMBC of 6-methoxy-4-methyl-4*H*-pyrido[4,3,2-*gh*]phenanthridine (**8b**), Figure S6.1: ¹H NMR of 7*H*-pyrido[2,3-*c*]carbazole (**9a**), Figure S6.2: ¹³C NMR of 7*H*-pyrido[2,3-*c*]carbazole (**9a**), Figure S6.3: COSY of 7*H*-pyrido[2,3-*c*]carbazole (**9a**), Figure S6.4: NOESY of 7*H*-pyrido[2,3-*c*]carbazole (**9a**), Figure S6.5: HSQC of 7*H*-pyrido[2,3-*c*]carbazole (**9a**), Figure S6.6: COSY of 7*H*-pyrido[2,3-*c*]carbazole (**9a**), Figure S7.1: ¹H NMR of 10-fluoro-7*H*-pyrido[2,3-*c*]carbazole (**9b**), Figure S7.2: ¹³C NMR of 10-fluoro-7*H*-pyrido[2,3-*c*]carbazole (**9b**), Figure S7.3: ¹⁹F NMR of 10-fluoro-7*H*-pyrido[2,3-*c*]carbazole (**9b**), Figure S7.4: COSY of 10-fluoro-7*H*-pyrido[2,3-*c*]carbazole (**9b**), Figure S7.5: NOESY of 10-fluoro-7*H*-pyrido[2,3-*c*]carbazole (**9b**), Figure S7.6: HSQC of 10-fluoro-7*H*-pyrido[2,3-*c*]carbazole (**9b**), Figure S7.7: HMBC of 10-fluoro-7*H*-pyrido[2,3-*c*]carbazole (**9b**), Figure S8.1: ¹H NMR of 4-methyl-7*H*-pyrido[2,3-*c*]carbazolium iodide (**10**), Figure S8.2: ¹³C NMR of 4-methyl-7*H*-pyrido[2,3-*c*]carbazolium iodide (**10**), Figure S8.3: COSY of 4-methyl-7*H*-pyrido[2,3-*c*]carbazolium iodide (**10**), Figure S8.4: NOESY of 4-methyl-7*H*-pyrido[2,3-*c*]carbazolium iodide (**10**), Figure S8.5: HSQC of 4-methyl-7*H*-pyrido[2,3-*c*]carbazolium iodide (**10**), Figure S8.6: HMBC of 4-methyl-7*H*-pyrido[2,3-*c*]carbazolium iodide (**10**), Figure S9.1: ¹H NMR of 4-methyl-11*H*-pyrido[3,2-*a*]carbazolium iodide (**21**), Figure S9.2: ¹³C NMR of 4-methyl-11*H*-pyrido[3,2-*a*]carbazolium iodide (**21**), Figure S9.3: COSY of 4-methyl-11*H*-pyrido[3,2-*a*]carbazolium iodide (**21**), Figure S9.4: NOESY of 4-methyl-11*H*-pyrido[3,2-*a*]carbazolium iodide (**21**), Figure S9.5: HSQC of 4-methyl-11*H*-pyrido[3,2-*a*]carbazolium iodide (**21**), Figure S9.6: HMBC of 4-methyl-11*H*-pyrido[3,2-*a*]carbazolium iodide (**21**).

Author Contributions: Conceptualization, M.O.S.; methodology, K.S.H., E.L., J.H.A., V.M.A. and M.O.S.; synthesis, K.S.H., I.T.U.H., C.L. and T.M.; antiplasmodial imaging assay, K.N.T., E.K.K. and V.M.A.; cytotoxicity assay, K.N.T., E.K.K. and V.M.A.; antiproliferative assay, K.N.T., E.K.K. and V.M.A.; growth inhibition assay, M.A. and J.H.A.; biofilm formation inhibition assay, M.A. and J.H.A.; writing—original draft preparation, K.S.H.; writing—review and editing, K.S.H., E.L., M.A., J.H.A., V.M.A. and M.O.S.; supervision, J.H.A., V.M.A. and M.O.S.; project administration, M.O.S.; funding acquisition, J.H.A., V.M.A. and M.O.S. All authors have read and agreed to the published version of the manuscript.

Funding: The authors acknowledge the ToppForsk program at the University of Stavanger for financial support and the provision of a PhD fellowship for K.S.H. (PR-10550). K.N.T is funded by a Griffith University Postdoctoral Fellowship.

Institutional Review Board Statement: Not applicable.

Informed Consent Statement: Not applicable.

Data Availability Statement: The data presented in this study are contained within the article and Supplementary Material.

Acknowledgments: B Holmelid, University of Bergen is thanked for recording HRMS analysis. K. B. Jørgensen is sincerely thanked for his help operating and maintaining the NMR instrument. The authors would like to acknowledge the Australian Red Cross Blood Bank for providing fresh human erythrocytes.

Conflicts of Interest: The authors declare no conflict of interest.

Sample Availability: Samples of the compounds are available from the authors.

References

1. World Health Organization. World Malaria Report. 2020. Available online: <https://www.who.int/publications/i/item/9789240015791> (accessed on 11 January 2021).
2. Collins, F.H.; Paskewitz, S.M. Malaria: Current and future prospects for control. *Annu. Rev. Entomol.* **1995**, *40*, 195–219. [[CrossRef](#)]
3. Achan, J.; Talisuna, A.O.; Erhart, A.; Yeka, A.; Tibenderana, J.K.; Baliraine, F.N.; Rosenthal, P.J.; D’Alessandro, U. Quinine, an old anti-malarial drug in a modern world: Role in the treatment of malaria. *Malar. J.* **2011**, *10*, 1–12. [[CrossRef](#)]
4. Van Baelen, G.; Hostyn, S.; Dhooche, L.; Tapolcsányi, P.; Mátyus, P.; Lemièrre, G.; Dommissé, R.; Kaiser, M.; Brun, R.; Cos, P.; et al. Structure-activity relationship of antiparasitic and cytotoxic indoloquinoline alkaloids, and their tricyclic and bicyclic analogues. *Bioorg. Med. Chem.* **2009**, *17*, 7209–7217. [[CrossRef](#)] [[PubMed](#)]
5. Tse, E.G.; Korsik, M.; Todd, M.H. The past, present and future of anti-malarial medicines. *Malar. J.* **2019**, *18*, 1–21. [[CrossRef](#)] [[PubMed](#)]
6. Noedl, H.; Se, Y.; Scaecher, K.; Smith, B.L.; Socheat, D.; Fukuda, M.M. Evidence of artemisinin-resistant malaria in western Cambodia. *N. Engl. J. Med.* **2008**, *359*, 2619–2620. [[CrossRef](#)]
7. Amato, R.; Pearson, R.D.; Almagro-Garcia, J.; Amaratunga, C.; Lim, P. Origins of the current outbreak of multidrug-resistant malaria in southeast Asia: A retrospective genetic study. *Lancet Infect. Dis.* **2018**, *18*, 337–345. [[CrossRef](#)]
8. World Health Organization. World Cancer Report 2020: Cancer Research for Cancer Prevention. Available online: www.iarc.fr/cards_page/world-cancer-report/ (accessed on 24 August 2020).
9. Sidoryk, K.; Jaromin, A.; Edward, J.A.; Świtalska, M.; Stefanska, J.; Cmoch, P.; Zagrodzka, J.; Szczepek, W.; Peczyńska-Czoch, W.; Wietrzyk, J.; et al. Searching for new derivatives of neocryptolepine: A synthesis, antiproliferative, antimicrobial and antifungal activities. *Eur. J. Med. Chem.* **2014**, *78*, 304–313. [[CrossRef](#)]
10. Stamm, A.M.; Long, M.N.; Belcher, B. Higher overall nosocomial infection rate because of increased attack rate of methicillin-resistant *Staphylococcus aureus*. *Am. J. Infect. Control* **1993**, *21*, 70–74. [[CrossRef](#)]
11. Drenkard, E. Antimicrobial resistance of *Pseudomonas aeruginosa* biofilms. *Microb. Infect.* **2003**, *5*, 1213–1219. [[CrossRef](#)]
12. Teng, C.P.; Zhou, T.; Ye, E.; Liu, S.; Koh, L.D.; Low, M.; Loh, X.J.; Win, Y.; Zhang, L.; Han, M.-Y. Effective Targeted Photothermal Ablation of Multidrug Resistant Bacteria and Their Biofilms with NIR-Absorbing Gold Nanocrosses. *Adv. Healthcare Mater.* **2016**, *5*, 2122–2130. [[CrossRef](#)]
13. Rizzato, C.; Torres, J.; Kasamatsu, E.; Carmorlinga-Ponce, M.; Bravo, M.M.; Canzian, F.; Kato, I. Potential role of biofilm formation in the development of digestive tract cancer with special reference to *Helicobacter pylori* infection. *Front Microbiol.* **2019**, *10*, 1–21. [[CrossRef](#)] [[PubMed](#)]
14. Johnson, C.H.; Dejea, C.M.; Edler, D.; Hoang, L.T.; Santidrian, A.F.; Felding, B.H.; Ivanisevic, J.; Cho, K.; Wick, E.C.; Hechenbleikner, E.M.; et al. Metabolism links bacterial biofilms and colon carcinogenesis. *Cell Metab.* **2015**, *21*, 891–897. [[CrossRef](#)]

15. Drewes, J.L.; White, J.R.; Dejea, C.M.; Fathi, P.; Iyadorai, T.; Vadivelu, J.; Roslani, A.C.; Wick, E.C.; Mongodin, E.F.; Loke, M.F.; et al. High-resolution bacterial 16S rRNA gene profile meta-analysis and biofilm status reveal common colorectal cancer consortia. *NPJ Biofilms Microbiomes* **2017**, *3*, 1–34. [[CrossRef](#)] [[PubMed](#)]
16. Lee, K.H. Discovery and development of natural product-derived chemotherapeutic agents based on a medicinal chemistry approach. *J. Nat. Prod.* **2010**, *73*, 500–516. [[CrossRef](#)] [[PubMed](#)]
17. Newman, D.J.; Cragg, G.M. Natural products as sources of new drugs over the last 25 years. *J. Nat. Prod.* **2007**, *70*, 461–477. [[CrossRef](#)] [[PubMed](#)]
18. Vuorela, P.; Leinonen, M.; Saikku, P.; Tammela, P.; Rauhala, J.-P.; Wennberg, T.; Vuorela, H. Natural products in the process of finding new drug candidates. *Curr. Med. Chem.* **2004**, *11*, 1375–1389. [[CrossRef](#)]
19. Newman, D.J.; Cragg, G.M. Natural products as sources of new drugs over the nearly four decades from 01/1981 to 09/2019. *J. Nat. Prod.* **2020**, *83*, 770–803. [[CrossRef](#)] [[PubMed](#)]
20. Bracca, A.B.J.; Heredia, D.A.; Larghi, E.L.; Kaufman, T.S. Neocryptolepine (cryptotackieine), a unique bioactive natural product: Isolation, synthesis, and profile of its biological activity. *Eur. J. Med. Chem.* **2014**, *2014*, 7979–8003. [[CrossRef](#)]
21. Madapa, S.; Tusi, Z.; Batra, S. Advances in the syntheses of quinoline and quinoline-annulated ring systems. *Curr. Org. Chem.* **2008**, *12*, 1116–1183. [[CrossRef](#)]
22. Sydnes, M.O. Recent progress in the synthesis of antimalarial indoloquinoline natural products and analogues. In *Studies in Natural Products Chemistry: Bioactive Natural Products*; Rahman, A., Ed.; Elsevier: Karachi, Pakistan, 2020; pp. 59–84.
23. Sydnes, M.O. Synthetic Strategies for the Synthesis of Indoloquinoline Natural Products. In *Targets in Heterocyclic Systems*; Attanasi, O.A., Merino, P., Spinelli, D., Eds.; Italian Society of Chemistry: Rome, Italy, 2019; Volume 23, pp. 201–219.
24. Wang, N.; Wicht, K.J.; Imai, K.; Wang, M.-Q.; Ngoc, T.A.; Kiguchi, R.; Kaiser, M.; Egan, T.J.; Inokuchi, T. Synthesis, β -haematin inhibition, and in vitro antimalarial testing of isocryptolepine analogues: SAR study of indolo[3,2-*c*]quinolines with various substituents at C2, C6 and N11. *Bioorg. Med. Chem.* **2014**, *22*, 2629–2642. [[CrossRef](#)]
25. Aroonkit, P.; Thongsornkleeb, C.; Tummatorn, J.; Krajangsri, S.; Mungthin, M.; Ruchirawat, S. Synthesis of isocryptolepine analogues and their structure-activity relationship studies as antiplasmodial and antiproliferative agents. *Eur. J. Med. Chem.* **2015**, *94*, 56–62. [[CrossRef](#)] [[PubMed](#)]
26. Pousset, J.L.; Martin, M.T.; Jossang, A.; Bodo, A. Isocryptolepine from *Cryptolepis sanguinolenta*. *Phytochemistry* **1995**, *39*, 735–736. [[CrossRef](#)]
27. Sharaf, M.H.H.; Schiff, P.L.; Tackie, J.A.N.; Phoebe, C.H.; Johnson, J.R.L.; Minick, D.; Andrews, C.W.; Crouch, R.C.; Martin, G.E. The isolation and structure determination of cryptomisine, a novel indolo[3,2-*b*]quinoline dimeric alkaloid from *cryptolepis sanguinolenta*. *J. Heterocycl. Chem.* **1996**, *33*, 789–797. [[CrossRef](#)]
28. Lavrado, J.; Moreira, R.; Paulo, A. Indoloquinolines as scaffolds for drug discovery. *Curr. Med. Chem.* **2010**, *17*, 2348–2370. [[CrossRef](#)] [[PubMed](#)]
29. Cimanga, K.; De Bruyne, T.; Pieters, L.; Vlietinck, A.J. In Vitro and in Vivo Antiplasmodial Activity of Cryptolepine and Related Alkaloids from *Cryptolepis sanguinolenta*. *J. Nat. Prod.* **1997**, *60*, 688–691. [[CrossRef](#)] [[PubMed](#)]
30. Sofowora, A. *Medicinal Plants and Traditional Medicine in Africa*; John Wiley & Sons: Chichester, UK, 1982; pp. 183–256.
31. Kirby, G.C.; Paine, A.; Warhurst, D.C.; Noamese, B.K.; Phillipson, J.D. In vitro and in vivo antimalarial activity of cryptolepine, a plant-derived indoloquinoline. *Phytother. Res.* **1995**, *9*, 359–363. [[CrossRef](#)]
32. Grellier, P.; Ramiaramanana, L.; Millerioux, V.; Deharo, E.; Shrével, J.; Frappier, F.; Trigalo, F.; Bodo, B.; Pousset, J.L. Antimalarial Activity of Cryptolepine and Isocryptolepine, Alkaloids Isolated from *Cryptolepis sanguinolenta*. *Phytother. Res.* **1996**, *10*, 317–321. [[CrossRef](#)]
33. Olajide, O.A.; Heiss, E.H.; Schachner, D.; Wright, C.W.; Vollmar, A.M.; Dirsch, V.M. Synthetic cryptolepine inhibits DNA binding of NF- κ B. *Bioorg. Med. Chem.* **2007**, *15*, 43–49. [[CrossRef](#)]
34. Bierer, D.E.; Fort, D.M.; Mendez, C.D.; Luo, J.; Imbach, P.A.; Dubenko, L.G.; Jolad, S.D.; Gerber, R.E.; Litvak, J.; Lu, Q.; et al. Ethnobotanical-Directed Discovery of the Antihyperglycemic Properties of Cryptolepine: Its Isolation from *Cryptolepis sanguinolenta*, Synthesis, and in Vitro and in Vivo Activities. *J. Med. Chem.* **1998**, *41*, 894–901. [[CrossRef](#)]
35. Rauwald, H.W.; Kober, M.; Mutschler, E.; Lambrecht, G. *Cryptolepis sanguinolenta*: Antimuscarinic properties of cryptolepine and the alkaloid fraction at M1, M2 and M3 receptors. *Planta Med.* **1992**, *58*, 486–488. [[CrossRef](#)] [[PubMed](#)]
36. Chen, Y.-J.; Liu, H.; Zhang, S.-Y.; Li, H.; Ma, K.-Y.; Liu, Y.-Q.; Yin, X.-D.; Zhou, R.; Yan, Y.-F.; Wang, R.-X.; et al. Design, Synthesis, and Antifungal Evaluation of Cryptolepine Derivatives against Phytopathogenic Fungi. *J. Agric. Food Chem.* **2021**, *69*, 1259–1271. [[CrossRef](#)] [[PubMed](#)]
37. Ablordeppey, S.Y.; Fan, P.; Li, S.; Clark, A.M.; Hufford, C.D. Substituted indoloquinolines as new antifungal agents. *Bioorg. Med. Chem.* **2002**, *10*, 1337–1346. [[CrossRef](#)]
38. Singh, M.; Singh, M.P.; Ablordeppey, S. In vitro studies with liposomal cryptolepine. *Drug Dev. Ind. Pharm.* **1996**, *22*, 377–381. [[CrossRef](#)]
39. Paulo, A.; Duarte, A.; Gomes, E.T. In vitro antibacterial screening of *Cryptolepis sanguinolenta* alkaloids. *J. Ethnopharmacol.* **1994**, *44*, 127–130. [[CrossRef](#)]
40. Cimanga, K.; De Bruyne, T.; Lasure, A.; Van Poel, B.; Pieters, L.; Claeys, M.; Berghe, D.V.; Kambu, K.; Tona, L.; Vlietinck, A. In vitro biological activities of alkaloids from *Cryptolepis sanguinolenta*. *Planta Med.* **1996**, *62*, 22–27. [[CrossRef](#)]

41. Zhao, M.; Kamada, T.; Takeuchi, A.; Nishioka, H.; Kuroda, T.; Takeuchi, Y. Structure-activity relationship of indoloquinoline analogs anti-MRSA. *Bioorg. Med. Chem.* **2015**, *25*, 5551–5554. [[CrossRef](#)]
42. Karou, D.; Savadogo, A.; Canini, A.; Yameogo, S.; Montesano, C.; Simpore, J.; Colizzi, V.; Traore, A.S. African ethnopharmacology and new drug discovery. *Afr. J. Biotechnol.* **2007**, *5*, 195–200.
43. Lu, C.-M.; Chen, Y.-L.; Chen, H.-L.; Chen, C.-A.; Lu, P.-J.; Yang, C.-N.; Tzeng, C.-C. Synthesis and antiproliferative evaluation of certain indolo[3,2-c]quinoline derivatives. *Bioorg. Med. Chem.* **2010**, *18*, 1948–1957. [[CrossRef](#)]
44. Dassonneville, L.; Lansiaux, A.; Wattlelet, A.; Watterz, N.; Mahieu, C.; Van Miert, S.; Pieters, L.; Bailly, C. Cytotoxicity and cell cycle effects of the plant alkaloids cryptolepine and neocryptolepine: Relation to drug-induced apoptosis. *Eur. J. Pharmacol.* **2000**, *409*, 9–18. [[CrossRef](#)]
45. Zhu, H.; Gooderham, N.J. Mechanisms of induction of cell cycle arrest and cell death by cryptolepine in human lung adenocarcinoma A549 cells. *Toxicol. Sci.* **2006**, *91*, 132–139. [[CrossRef](#)]
46. Matsui, T.-A.; Sowa, Y.; Murata, H.; Takagi, K.; Nakanishi, R.; Aoki, S.; Yoshikawa, M.; Kobayashi, M.; Sakabe, T.; Kubo, T.; et al. The plant alkaloid cryptolepine induced p21WAF1/CIP1 and cell cycle arrest in a human osteosarcoma cell line. *Int. J. Oncol.* **2007**, *31*, 915–922. [[PubMed](#)]
47. Bonjean, K.; De Pauw-Gillet, M.C.; Defresne, M.P.; Colson, P.; Houssier, C.; Dassonneville, L.; Bailly, C.; Greimers, R.; Wright, C.W.; Quetin-Leclercq, J.; et al. The DNA intercalating alkaloid cryptolepine interferes with topoisomerase II and inhibits primarily DNA synthesis in B16 melanoma cells. *Biochemistry* **1998**, *37*, 5136–5146. [[CrossRef](#)]
48. Dassonneville, L.; Bonjean, K.; De Pauw-Gillet, M.C.; Colson, P.; Houssier, C.; Quetin-Leclercq, J.; Angenot, L.; Bailly, C. Stimulation of topoisomerase II-mediated DNA cleavage by three DNA-intercalating plant alkaloids: Cryptolepine, matadine and serpentine. *Biochemistry* **1999**, *38*, 7719–7726. [[CrossRef](#)]
49. Whittel, L.R.; Batty, K.T.; Wong, R.P.M.; Bolitho, E.M.; Fox, S.A.; Davis, T.M.E.; Murray, P.E. Synthesis and antimalarial evaluation of novel isocryptolepine derivatives. *Bioorg. Med. Chem.* **2011**, *19*, 7519–7525. [[CrossRef](#)] [[PubMed](#)]
50. Van Miert, S.; Hostyn, S.; Maes, B.U.W.; Cimanga, K.; Brun, R.; Kaiser, M.; Mátyus, P.; Dommissie, R.A.; Lemièrre, G.; Vlietinck, A.; et al. Isonocryptolepine, a synthetic indoloquinoline alkaloid, as an antiplasmodial lead compound. *J. Nat. Prod.* **2005**, *68*, 674–677. [[CrossRef](#)] [[PubMed](#)]
51. Bailly, C.; Laine, W.; Baldeyrou, B.; De Pauw-Gillet, M.C.; Colson, P.; Houssier, C.; Cimanga, K.; Van Miert, S.; Vlietinck, A.J.; Pieters, L. DNA intercalation, topoisomerase II inhibition and cytotoxic activity of the plant alkaloid neocryptolepine. *Anti-Cancer Drug Des.* **2000**, *15*, 191–201.
52. Håheim, K.S.; Helgeland, I.T.U.; Lindbäck, E.; Sydnes, M.O. Mapping the reactivity of the quinoline ring-systems—Synthesis of the tetracyclic ring-system of isocryptolepine and regioisomers. *Tetrahedron* **2019**, *75*, 2924–2957. [[CrossRef](#)]
53. Schmitz, F.J.; Deguzman, F.S.; Hossain, M.B.; Vanderhelm, D. Cytotoxic aromatic alkaloids from the ascidian *Amphicarpa meridiana* and *Leptoclinides* sp.: Meridine and 11-hydroxyascididemin. *J. Org. Chem.* **1991**, *56*, 804–808. [[CrossRef](#)]
54. Gunawardana, G.P.; Koehn, F.E.; Lee, A.Y.; Clardy, J.; Hee, H.Y.; Faulkner, D.J. Pyridoacridine alkaloids from deep-water marine sponges of the family Pacchastrellidae: Structure revision of dercitin and related compounds and correlation with the kuanoniamines. *J. Org. Chem.* **1992**, *57*, 1523–1526. [[CrossRef](#)]
55. Molinski, T.F. Marine pyridoacridine alkaloids: Structure, synthesis, and biological chemistry. *Chem. Rev.* **1993**, *93*, 1825–1838. [[CrossRef](#)]
56. Eder, C.; Schupp, P.; Proksch, P.; Wray, V.; Steube, K.; Müller, C.E.; Frobenius, W.; Herderich, M.; van Soest, R.W.M. Bioactive Pyridoacridine Alkaloids from the Micronesian Sponge *Oceanapia* sp. *J. Nat. Prod.* **1998**, *61*, 301–305. [[CrossRef](#)]
57. Marshall, K.M.; Barrows, L.R. Biological activities of pyridoacridines. *Nat. Prod. Rep.* **2004**, *61*, 731–751. [[CrossRef](#)] [[PubMed](#)]
58. Delfourne, E.; Bastide, J. Marine pyridoacridine alkaloids and synthetic analogues as antitumor agents. *Med. Res. Rev.* **2003**, *23*, 234–252. [[CrossRef](#)] [[PubMed](#)]
59. De Guzman, F.S.; Carte, B.; Troupe, N.; Faulkner, D.J.; Harper, M.K.; Concepcion, G.P.; Mangalindan, G.C.; Matsumoto, S.S.; Barrows, L.R.; Ireland, C.M. Neoamphimedine: A new pyridoacridine topoisomerase II inhibitor which catenates DNA. *J. Org. Chem.* **1999**, *64*, 1400–1402. [[CrossRef](#)]
60. Feng, Y.R.; Davis, A.; Sykes, M.L.; Avery, V.M.; Carroll, A.R.; Camp, D.; Quinn, R.J. Antitrypanosomal pyridoacridine alkaloids from the Australian ascidian *Polysyncraton echinatum*. *Tetrahedron Lett.* **2010**, *51*, 2477–2479. [[CrossRef](#)]
61. Fuente, J.A.D.L.; Martin, M.J.; Blanco, M.D.M.; Alfonso, E.P.; Avendano, C.; Mendez, J.C. A C-Ring regioisomer of the marine alkaloid meridine exhibits selective in vitro cytotoxicity for solid tumors. *Bioorg. Med. Chem.* **2001**, *9*, 1807–1814. [[CrossRef](#)]
62. Helgeland, I.T.U.; Sydnes, M.O. A Concise Synthesis of Isocryptolepine by C-C Cross-Coupling Followed by a Tandem C-H Activation and C-N Bond Formation. *SynOpen* **2017**, *1*, 41–44. [[CrossRef](#)]
63. Mehra, M.K.; Sharma, S.; Rangan, K.; Kumar, D. Substrate of Solvent-Controlled PdII-Catalyzed Regioselective Arylation of Quinolin-4(1H)-ones Using Diaryliodonium Salts: Facile Access to Benzoxocine and Aaptamine Analogues. *Eur. J. Org. Chem.* **2020**, *2020*, 2409–2413. [[CrossRef](#)]
64. Beauchard, A.; Chabane, H.; Sinbandhit, S.; Guenot, P.; Thiéry, V.; Besson, T. Synthesis of original thiazoloindolo[3,2-c]quinoline and novel 8-N-substituted-11H-indolo[3,2-c]quinoline derivatives from benzotriazoles. Part I. *Tetrahedron* **2006**, *62*, 1895–1903. [[CrossRef](#)]
65. Timári, G.; Soós, T.; Hajós, G. A convenient synthesis of two new indoloquinoline alkaloids. *Synlett* **1997**, *1997*, 1067–1068. [[CrossRef](#)]

66. Hostyn, S.; Maes, B.U.W.; Pieters, L.; Lemière, G.L.F.; Mátyus, P.; Hajós, G.; Dommissie, R.A. Synthesis of the benzo- β -carboline isoneocryptolepine: The missing indoloquinoline isomer in the alkaloid series cryptolepine, neocryptolepine and isocryptolepine. *Tetrahedron* **2005**, *61*, 1571–1577. [[CrossRef](#)]
67. Miller, M.; Vogel, J.C.; Tsang, W.; Merrit, A.; Procter, D.J. Formation of N-heterocycles by the reaction of thiols with glyoxamides: Exploring a connective Pummerer-type cyclisation. *Org. Biomol. Chem.* **2009**, *7*, 589–597. [[CrossRef](#)]
68. Jonckers, T.H.M.; van Miert, S.; Cimanga, K.; Bailly, C.; Colson, P.; De Pauw-Gillet, M.C.; van den Heuvel, H.; Claeys, M.; Lemière, F.; Esmans, E.L.; et al. Synthesis, cytotoxicity, and antiplasmodial and antitrypanosomal activity of new neocryptolepine derivatives. *J. Med. Chem.* **2002**, *45*, 3497–3508. [[CrossRef](#)]
69. Go, M.L.; Koh, H.L.; Ngiam, T.L.; Phillipson, J.D.; Kirby, G.C.; Oneill, M.J.; Warhurst, D.C. Synthesis and in vitro antimalarial activity of some indolo[3,2-*c*]quinolines. *Eur. J. Med. Chem.* **1992**, *27*, 391–394. [[CrossRef](#)]
70. Ansah, C.; Gooderham, N.J. The Popular Herbal Antimalarial, Extract of *Cryptolepis sanguinolenta*, Is Potently Cytotoxic. *Toxicol. Sci.* **2002**, *70*, 245–251. [[CrossRef](#)] [[PubMed](#)]
71. Lu, W.-J.; Switalska, M.; Wang, L.; Yonezawa, M.; El-Sayed, I.E.-T.; Wietrzyk, J.; Inokuchi, T. In vitro antiproliferative activity of 11-aminoalkylamino-substituted 5H-indolo[2,3-*b*]quinolines; improving activity of neocryptolepines by installation of ester substituent. *Med. Chem. Res.* **2013**, *22*, 4492–4504. [[CrossRef](#)]
72. Iorio, F.; Bosotti, R.; Scacheri, E.; Belcastro, V.; Mithbaokar, P.; Ferrero, R.; Murino, L.; Tagliaferri, R.; Brunetti-Pierri, N.; Isacchi, A.; et al. Discovery of drug mode of action and drug repositioning from transcriptional responses. *Proc. Natl. Acad. Sci. USA* **2012**, *107*, 14621–14626. [[CrossRef](#)]
73. Peczynska-Czoch, W.; Pognan, F.; Kaczmarek, L.; Boratynski, J. Synthesis and structure-activity relationship of methyl-substituted indolo[2,3-*b*]quinolines: Novel cytotoxic, DNA topoisomerase II inhibitors. *J. Med. Chem.* **1994**, *37*, 3503–3510. [[CrossRef](#)]
74. Cimanga, K.; De Bruyne, T.; Pieters, L.; Totte, J.; Tona, L.; Kambu, K.; Vanden Berghe, D.; Vlietinck, A.J. Antibacterial and antifungal activities of neocryptolepine, biscryptolepine and cryptoquinoline, alkaloids isolated from *Cryptolepis sanguinolenta*. *Phytochemistry* **1998**, *5*, 209–214. [[CrossRef](#)]
75. Shah, P.; Westwell, A.D. The role of fluorine in medicinal chemistry. *J. Enzyme Inhib. Med. Chem.* **2007**, *22*, 527–540. [[CrossRef](#)]
76. Miller, C.M.; McCarthy, F.O. Isolation, biological activity and synthesis of the natural product ellipticine and related pyridocarbazoles. *RSC Adv.* **2012**, *2*, 8883–8918. [[CrossRef](#)]
77. Rosenau, C.P.; Jelier, B.J.; Gossert, A.D.; Togni, A. Exposing the origins of irreproducibility in fluorine NMR spectroscopy. *Angew. Chem. Int. Ed.* **2018**, *57*, 9528–9533. [[CrossRef](#)] [[PubMed](#)]
78. Zhou, F.; Driver, T.G. Efficient Synthesis of 3H-Indoles Enabled by the Lead-Mediated α -Arylation of β -Ketoesters or γ -Lactams Using Aryl Azides. *Org. Lett.* **2014**, *16*, 2916–2919. [[CrossRef](#)]
79. Alajarin, M.; Molina, P.; Vidal, A. Formal total synthesis of the alkaloid cryptotackieine (neocryptolepine). *J. Nat. Prod.* **1997**, *60*, 747–748. [[CrossRef](#)]
80. Duffy, S.A.; Avery, V.M. Development and optimization of a novel 384-well anti-malarial imaging assay validated for high-throughput screening. *Am. J. Trop. Med. Hyg.* **2012**, *86*, 84–92. [[CrossRef](#)]
81. Fletcher, S.; Avery, V.M. A novel approach for the discovery of chemically diverse anti-malarial compounds targeting the *Plasmodium falciparum* Coenzyme A synthesis pathway. *Malar. J.* **2014**, *13*, 343. [[CrossRef](#)]